



**HAL**  
open science

# Deep eutectic solvents: characterization, interaction with synthetic and biological membranes, and solubilization of bioactive volatile compounds

Tracy El Achkar

## ► To cite this version:

Tracy El Achkar. Deep eutectic solvents: characterization, interaction with synthetic and biological membranes, and solubilization of bioactive volatile compounds. Organic chemistry. Université du Littoral Côte d'Opale; Université Libanaise, 2020. English. NNT: 2020DUNK0562 . tel-03119851

**HAL Id: tel-03119851**

**<https://theses.hal.science/tel-03119851>**

Submitted on 25 Jan 2021

**HAL** is a multi-disciplinary open access archive for the deposit and dissemination of scientific research documents, whether they are published or not. The documents may come from teaching and research institutions in France or abroad, or from public or private research centers.

L'archive ouverte pluridisciplinaire **HAL**, est destinée au dépôt et à la diffusion de documents scientifiques de niveau recherche, publiés ou non, émanant des établissements d'enseignement et de recherche français ou étrangers, des laboratoires publics ou privés.



Université Libanaise

École Doctorale  
Sciences et Technologies

Doyen



UNIVERSITÉ  
DU LITTORAL  
CÔTE D'OPALE

## Doctoral Thesis

Under the joint supervision of the

**Lebanese University**

and

**Université du Littoral Côte d'Opale**

Discipline: Organic, mineral and industrial chemistry

# Deep eutectic solvents: characterization, interaction with synthetic and biological membranes, and solubilization of bioactive volatile compounds

Presented by

**Tracy El Achkar**

December 11, 2020

## Jury Members

Mr. Farid Chemat, Pr., Université d'Avignon

Reviewer

Mr. Dimitris Makris, Pr., University of Thessaly

Reviewer

Mrs. Alia Jraij, Pr., Lebanese University

Examiner

Mrs. Aida Habib Abdul Karim, Pr., American University of Beirut

Examiner

Mr. Jérôme Lecomte, Dr., CIRAD

Examiner

Mrs. Hélène Greige Gerges, Pr., Lebanese University

Thesis supervisor

Mrs. Sophie Fourmentin, Pr., Université du Littoral Côte d'Opale

Thesis supervisor



Université Libanaise

École Doctorale  
Sciences et Technologies

Doyen



**Thèse de Doctorat**

En cotutelle entre

**L'Université Libanaise**

et

**L'Université du Littoral Côte d'Opale**

Discipline : Chimie organique, minérale, industrielle

**Solvants eutectiques profonds : caractérisation, interaction avec des membranes synthétiques et biologiques, et solubilisation de composés bioactifs volatils**

Présentée par

**Tracy El Achkar**

Le 11 décembre 2020

### **Membres du Jury**

M. Farid Chemat, Pr., Université d'Avignon

M. Dimitris Makris, Pr., University of Thessaly

Mme Alia Jraij, Pr., Université Libanaise

Mme Aida Habib Abdul Karim, Pr., American University of Beirut

M. Jérôme Lecomte, Dr., CIRAD

Mme Hélène Greige Gerges, Pr., Université Libanaise

Mme Sophie Fourmentin, Pr., Université du Littoral Côte d'Opale

Rapporteur

Rapporteur

Examineur

Examineur

Examineur

Directeur de thèse

Directeur de thèse

# Acknowledgments

*Foremost, I would like to express my deepest gratitude to my supervisors Professor Sophie Fourmentin and Professor H el ene Greige Gerges for their continuous support and guidance during the past three years. This thesis would not have been possible without your help and dedication.*

*I would also like to express my appreciation to all the members of the jury Professor Farid Chemat, Professor Dimitris Makris, Professor Alia Jraij, Professor Aida Habib Abdul Karim, and Doctor J er me Lecomte for spending the time to read and judge this manuscript. I would also like to thank the committee members Professor Ana Rita Duarte and Doctor Fran ois-Xavier Legrand for their useful comments and suggestions.*

*I also wish to thank Professor David Landy for his valuable contribution and constructive advice.*

*I'd like to acknowledge the assistance of Doctor Maya Kayouka. It has been a pleasure working with you again.*

*My sincere appreciation to Professor Alia Jraij and my colleague Jad Eid for their help with the AFM studies.*

*I also wish to thank Steven Ruellan for always willing to help with the NMR experiments, and Tarek Moufawad for the effort he put into the characterization studies.*

*Many thanks to Professor Aline Hamade and Professor Fadia Najjar as well as the CCM and UDSMM members for welcoming me into their laboratories.*

*Special thanks to all the friends that I met along the way in France and Lebanon and with whom I made some unforgettable memories, especially Lamia, Nancy, Eliane, Rebecca, Muriel, St ephanie, Marc, Sarah, Justine, Somenath, Myriam, Ghenwa, and Sanaa.*

*I am extremely grateful for my family that made me who I am today. Thank you for believing in me and encouraging me. Thank you for always being there to lift me up. I am even more thankful for this experience because it brought me closer to you.*

*Lastly, I would like to extend my gratitude to my fianc e Imad who has been there for me since day one. Thank you for being my number one supporter and for pushing me to always do my best.*

# Abstract

Deep eutectic solvents (DES) recently emerged as a novel class of green solvents with a high potential to replace common organic solvents. Despite their novelty, DES were extensively explored in the past years owing to their remarkably interesting properties. Yet, a lot remains to be uncovered given the limitless number of possible DES and their versatility. The current study aimed to examine the effect of DES on liposomes, adopted as model membranes, and on cell membranes. It also sought to evaluate the solubilizing ability of DES toward bioactive volatile compounds. Therefore, a group of selected DES along with new solvents were first prepared and characterized. Density, viscosity, and polarity measurements were mainly carried out and showed that DES' properties can be tuned depending on their composition. The organization of phospholipids and liposomes within the DES was then investigated using optical- and atomic force microscopies. Phospholipids self-assembled into vesicles in choline chloride-based DES while liposomes converted to lipid bilayers before their reconstitution into vesicles. Moreover, cytotoxicity studies and morphological examinations were combined to evaluate the impact of some DES on MDA-MB-231, a human breast cancer cell line. Results showed that the effect is highly dependent on the DES' composition. On the other hand, the solubilizing ability of the DES toward bioactive volatile compounds was tested using static headspace-gas chromatography. The influence of the presence of water and some encapsulation systems such as liposomes and cyclodextrins on the overall DES' solubilization efficiency was further analyzed. At last, the release of *trans*-anethole from the DES was monitored via multiple headspace extraction. DES were able to greatly solubilize the bioactive volatile compounds and to control their release when compared with water. Altogether, this work highlights the potential use of DES-based systems as solubilization vehicles for bioactive compounds.

**Keywords:** Deep eutectic solvents; hydrogen bond acceptor; hydrogen bond donor; phospholipids; liposomes; biological membranes; solubilization; bioactive volatile compounds; cyclodextrins.

# Résumé

Les solvants eutectiques profonds (DES) sont récemment apparus comme une nouvelle classe de solvants verts présentant un potentiel élevé pour remplacer les solvants organiques usuels. Bien que découverts récemment, les DES ont fait l'objet de nombreuses recherches au cours des dernières années en raison de leurs propriétés intéressantes. Cependant, il reste encore beaucoup à découvrir étant donné le nombre quasiment illimité de DES potentiels et de leur polyvalence. Notre étude vise à examiner l'effet des DES sur les liposomes, adoptés comme modèles membranaires, et sur les membranes cellulaires. Elle a également cherché à évaluer la capacité de solubilisation des DES envers des composés bioactifs volatils. Ainsi, une sélection de DES ainsi que de nouveaux solvants ont été tout d'abord préparés et caractérisés. Des mesures de densité, de viscosité et de polarité ont été effectuées et ont montré que les propriétés des DES pouvaient être ajustées en fonction de leur composition. L'organisation des phospholipides et des liposomes au sein des DES a ensuite été étudiée à l'aide de microscopies optique et à force atomique. Les phospholipides s'auto-assemblent en vésicules dans les DES à base de chlorure de choline tandis que les liposomes se convertissent en bicouches lipidiques avant leur reconstitution en vésicules. De plus, des études de cytotoxicité et des examens morphologiques ont été combinés afin d'évaluer l'impact de quelques DES sur MDA-MB-231, une lignée cellulaire de cancer du sein humain. Les résultats ont montré que l'effet dépendait fortement de la composition du DES. D'autre part, la capacité de solubilisation des DES envers des composés bioactifs volatils a été testée par chromatographie en phase gazeuse couplée à un espace de tête. L'influence de la présence d'eau et de certains systèmes d'encapsulation tels que les liposomes et les cyclodextrines sur la capacité de solubilisation des DES ont été analysés. Enfin, la libération du *trans*-anéthole à partir des DES a été suivie par extraction multiple de l'espace de tête. Les DES ont été capables de mieux solubiliser les composés bioactifs volatils et de contrôler leur libération par rapport à l'eau. Dans l'ensemble, ces travaux mettent en évidence l'utilisation potentielle des systèmes à base de DES comme véhicules de solubilisation de composés bioactifs.

**Mots-clés :** Solvants eutectiques profonds ; accepteur de liaison hydrogène ; donneur de liaison hydrogène; phospholipides ; liposomes ; membranes biologiques ; solubilisation ; composés bioactifs volatils ; cyclodextrines.

# Table of Contents

List of Tables .....	1
List of Figures.....	2
List of Abbreviations .....	5
Introduction.....	7
I. Literature Review .....	9
1. Deep Eutectic Solvents .....	9
1.1. Definition.....	9
1.2. Classification.....	10
1.3. Methods of preparation.....	13
1.4. Physicochemical properties.....	14
1.4.1. Phase behavior .....	14
1.4.2. Density .....	16
1.4.3. Viscosity.....	17
1.4.4. Ionic conductivity.....	18
1.4.5. Surface tension .....	18
1.4.6. Polarity .....	18
1.5. Effect of water.....	22
1.5.1. Effect on DES' physicochemical properties .....	22
1.5.2. Effect on DES' network.....	25
2. Impact of DES on living systems.....	38
2.1. <i>In vitro</i> toxicity studies .....	38
2.1.1. Microorganisms.....	38
2.1.2. Invertebrates, plants, and fish.....	39
2.1.3. Cell lines.....	39
2.1.4. Effect of DES composition on the overall toxicity .....	40
2.1.5. Importance of the studied organism .....	41
2.1.6. Mechanism of action .....	41
2.1.7. Related uses .....	42
2.2. <i>In vivo</i> toxicity studies .....	43

2.3. Biodegradability .....	44
3. Applications .....	47
3.1. Reaction medium.....	47
3.2. Biomass processing .....	48
3.3. Electrochemistry .....	49
3.4. Extraction.....	49
3.5. Solubilization.....	52
3.6. Drug delivery.....	58
4. Encapsulation systems.....	59
4.1. Cyclodextrins .....	59
4.2. Combination of DES and cyclodextrins .....	60
4.3. Liposomes .....	62
4.4. Amphiphilic self-assembly in DES .....	62
II. Solvents' preparation and characterization .....	71
1. Tested solvents .....	71
2. Characterization .....	74
2.1. Density .....	74
2.2. Viscosity.....	76
2.3. Polarity .....	80
2.4. Differential scanning calorimetry .....	81
2.5. Thermogravimetric analysis.....	83
2.6. Rheological measurements .....	84
III. Phospholipids self-assembly in DES .....	86
1. Organization of E80 phospholipids.....	86
2. DES-based methods for liposomes preparation .....	90
2.1. Ethanol injection method .....	91
2.2. Thin film-DES dissolution method .....	94
IV. Effect of DES on synthetic and biological membranes .....	97
1. Effect on preformed liposomes.....	97
1.1. Exposure of adsorbed liposomes to the studied systems .....	97
1.2. Time-dependent behavior of liposomes suspended in the studied systems.....	101

2. Effect on human cells .....	105
V. The solubilizing ability of DES toward natural volatiles and essential oils .....	133
1. Solubilization of volatile compounds by DES .....	133
1.1. Determination of the partition coefficient $K$ .....	134
1.1.1. The phase ratio variation method .....	134
1.1.2. The vapor phase calibration method .....	135
2. Solubilization of essential oils by DES .....	138
3. Effect of water on DES' solubilization ability .....	140
4. Nuclear magnetic resonance spectroscopy study .....	142
5. Effect of cyclodextrin's addition .....	146
6. Effect of lipids .....	148
7. Effect of surfactant's addition .....	148
8. Release study .....	149
Conclusion and perspectives .....	151
List of publications and communications .....	153
References .....	155
Appendices .....	171

# List of Tables

Table 1. Overview of the reported studies related to the polarity of deep eutectic solvents .....	19
Table 2. Summary of the studies examining the effect of water on deep eutectic solvents' systems (in chronological order) .....	27
Table 3. Summary of the reported studies on deep eutectic solvents' biodegradability.....	45
Table 4. Selected examples of deep eutectic solvent-based extractions .....	51
Table 5. Investigations of the deep eutectic solvents' solubilization mechanism .....	54
Table 6. Investigations of surfactants' self-assembly in deep eutectic solvents.....	64
Table 7. Composition of the tested deep eutectic solvents .....	71
Table 8. Composition of the SUPRADES .....	73
Table 9. Experimental values of the densities of the studied solvents at 30 °C .....	75
Table 10. Comparison of the viscosity values of choline chloride-based DES at 30 °C with available literature sources.....	78
Table 11. Effect of the hydrogen bond donor on the viscosity of polyalcohol-based SUPRADES at 30 °C.....	80
Table 12. Polarity parameter values of the studied deep eutectic solvents.....	81
Table 13. Degradation temperatures of the SUPRADES and their individual compounds .....	84
Table 14. Mean diameter D and height H values of the vesicles formed in ChCl:U, ChCl:G, ChCl:EG, and ChCl:Lev, at 4, 24, and 48h, obtained by the AFM cross-section tool.....	89
Table 15. Mean diameter D and mean height H of Egg PC liposomes following 30 min exposure to ChCl:U, ChCl:G, ChCl:EG, ChCl:Lev, aqueous solution of ChCl + U, an aqueous solution of ChCl + G, an aqueous solution of ChCl + EG, and an aqueous solution of ChCl + Lev, determined by AFM using the cross-section t .....	100
Table 16. Mean diameter D and mean height H of Egg PC liposomes suspended in water, ChCl:U, ChCl:G, ChCl:EG, ChCl:Lev, aqueous solution of ChCl + U, an aqueous solution of ChCl + G, an aqueous solution of ChCl + EG, and an aqueous solution of ChCl+ Lev, at different time points determined by AFM using the cross-section tool.....	104
Table 17. Partition coefficient values of <i>trans</i> -anethole in water and the different solvents and $K_{\text{water}}/K_{\text{solvent}}$ ratio at 30 °C .....	136
Table 18. Partition coefficient values of L-Carvone in water and the different solvents and $K_{\text{water}}/K_{\text{solvent}}$ ratio at 30 °C .....	137
Table 19. Percentage of retention of the essential oils by the studied solvents at 30 °C .....	139
Table 20. Percentage of retention of <i>trans</i> -anethole by aqueous solutions of preformed DES (DES aq) and by aqueous solutions of the forming compounds (HBA + HBD) aq at a concentration equivalent to 70 wt% DES .....	142
Table 21. Diffusion coefficient values of RAMEB, levulinic acid, and <i>trans</i> -anethole, separately dissolved in water in the absence or presence of RAMEB .....	146

# List of Figures

Figure 1. The four types of deep eutectic solvents based on the general formula $Cat^+ X^- zY$ .....	11
Figure 2. Commonly used HBA and HBD compounds in deep eutectic solvents' preparation .....	12
Figure 3. Major events marking the development of deep eutectic solvents throughout the years.....	13
Figure 4. General solid-liquid phase diagram of a binary mixture .....	14
Figure 5. Solid-liquid phase diagram representing a simple ideal eutectic mixture (red line) and a deep eutectic mixture (green line) (Adapted from Martins et al. 2019).....	15
Figure 6. Effect of the hydrogen bond donor on the densities of some choline chloride-based deep eutectic solvents (yellow: 1:3 choline chloride:ethanolamine; light blue: 1:1 choline chloride:oxalic acid; grey: 1:1 choline chloride:malonic acid; black: 1:2 choline chloride:urea; dark blue: 1:2 choline chloride:glycerol; purple: 1:1 choline chloride:glutaric acid; orange: 1:3 choline chloride:2,2,2-trifluoroacetamide; red: 1:2 choline chloride:ethylene glycol; green: 1:3 choline chloride:phenol). Reprinted with permission from (García et al., 2015). Copyright (2015) American Chemical Society .	17
Figure 7. Variation of the freezing point of 1:2 ChCl:U deep eutectic solvent with the added mole fraction of water. Reprinted with permission from (P. J. Smith et al., 2019). Copyright (2019) American Chemical Society) .....	23
Figure 8. Snapshots from molecular dynamics simulations of ChCl:G (left) and ChCl:G-water system (right) at 0.9 mole fraction of water. Purple, dark blue and green points represent the carbon, nitrogen and chlorine atoms of choline chloride, respectively. Orange points represent the carbon atoms of glycerol. Red and light blue points represent oxygen atoms and water molecules, respectively. Reproduced from (Ahmadi, Hemmateenejad, Safavi, Shojaeifard, Shahsavari, et al., 2018) with permission from the PCCP Owner Societies .....	38
Figure 9. Classification of hydrogen bond donor types according to their toxicity level as per the multitasking quantitative structure-toxicity relationship model (adapted from Halder & Cordeiro, 2019). .....	43
Figure 10. Three possible ways to apply deep eutectic solvents in biocatalysis (Pätzold et al., 2019)48	
Figure 11. Distribution of the adopted extraction techniques using deep eutectic solvents. The dark blue color represents the liquid-phase microextraction techniques (based on Scopus database; May 2020) .....	52
Figure 12. Compounds considered for the deep eutectic solvents' solubilization studies .....	53
Figure 13. Illustration of the possible localization of 4-aminophthalimide (AP), coumarin 153 (C153), and anthracene (ATN) in the heterogeneous domain-like structure of ChCl:alcohol deep eutectic system Reproduced from (Hossain & Samanta, 2018) with permission from the PCCP Owner Societies. ....	58
Figure 14. Examples of reported deep eutectic solvents comprising active pharmaceutical ingredients .....	59
Figure 15. Illustration of the three native cyclodextrins.....	60
Figure 16. Structures of SUPRADES' constituents. a) General structure of $\beta$ -CD derivatives: HP- $\beta$ -CD (degree of substitution (DS) = 4.34), R = -H or $-\text{CH}_2\text{-CH(OH)-CH}_3$ ; RAMEB (DS = 12.9), R = -H or $-\text{CH}_3$ ; CRYSMEB (DS = 4.9), R = -H or $-\text{CH}_3$ ; Captisol® (DS = 6.5), R = -H or $-(\text{CH}_2)_4\text{-SO}_3^- \text{Na}^+$ ; b) levulinic acid; c) glycerol; d) ethylene glycol; e) 1,3-propanediol; f) 1,3-butanediol.....	72
Figure 17. Experimental viscosities of the studied deep eutectic solvents (A) and the levulinic acid-containing systems (B) as a function of temperature ranging between 30 and 60 °C. The lines represent the fitted values following the Vogel-Fulcher-Tammann model .....	77

Figure 18. Experimental viscosities of the polyalcohol-based (glycerol- (A), ethylene glycol- (B), 1,3-propanediol- (C), and 1,3-butanediol- (D) based systems as a function of temperature ranging between 30 and 60 °C. The lines represent the fitted values following the Vogel-Fulcher-Tammann model.....	79
Figure 19. Some deep eutectic solvents in presence of Nile Red. From left to right: TBABr:Dec, ChCl:U, ChCl:EG, ChCl:G, ChCl:Lev and TBPBr:Lev.....	81
Figure 20. Differential scanning calorimetry curves of the SUPRADES .....	82
Figure 21. Thermogravimetric analysis curves of the SUPRADES .....	83
Figure 22. Log-log scale representation of the viscosity vs shear rate for SUPRADES at 30 °C.....	85
Figure 23. Schematic diagram of atomic force microscopy (Grobelyny et al., 2011) .....	86
Figure 24. 4x4 $\mu\text{m}^2$ AFM 2D images of Lipoid E80 within ChCl:U, ChCl:G, ChCl:EG, and ChCl:Lev obtained in contact mode at 4, 24, and 48h.....	88
Figure 25. $\lambda_{\text{max}}$ values of Nile Red reflecting the polarity of the DES in the absence or presence of lipid E80 at t = 48h.....	90
Figure 26. Observation of the preparations of DES-based ethanol injection method via optical microscopy .....	92
Figure 27. General structure of Triton X-100 (n = 9-10) .....	93
Figure 28. DES-based ethanol injection method: observation of ChCl-based DES in presence of lipids (left column), in presence of both lipids and Triton X-100 (middle column), and in presence of Triton X-100 (right column) .....	93
Figure 29. Thin lipid film obtained following the organic phase evaporation .....	94
Figure 30. DES-based thin film dissolution method: observation of ChCl-based DES in presence of lipids (left column), in presence of both lipids and Triton X-100 (middle column), and in presence of Triton X-00 (right column) .....	95
Figure 31. Size distribution plots of lipid particles formed in ChCl:G- or ChCl:EG-based thin film dissolution preparations .....	96
Figure 32. AFM contact mode 2D images of Egg PC liposomes following 30 min exposure to A- ultrapure water, B- ChCl:U, C- ChCl:G, D- ChCl:EG, E, E' ChCl:Lev F- aqueous solution of ChCl + U, G- aqueous solution of ChCl + G, H- aqueous solution of ChCl + EG, I- aqueous solution of ChCl + Lev.....	99
Figure 33. AFM 2D 4 x 4 $\mu\text{m}^2$ images of EggPC liposomes suspended in ChCl:U, ChCl:G, ChCl:EG, and ChCl:Lev DES obtained in contact mode at different time points .....	102
Figure 34. AFM 2D 4x4, and 2x2 $\mu\text{m}^2$ images of EggPC liposomes suspended in an aqueous solution of ChCl + U, an aqueous solution of ChCl + G, an aqueous solution of ChCl + EG, and an aqueous solution of ChCl + Lev, obtained in contact mode at different time points.....	103
Figure 35. Principle of static headspace-gas chromatography .....	133
Figure 36. The general structure of (A) <i>trans</i> -anethole and (B) L-carvone.....	134
Figure 37. Chromatogram of star anise essential oil in water and RAMEB:Lev .....	139
Figure 38. Percentage of retention of <i>trans</i> -anethole by DES, in the absence (pure <i>trans</i> -anethole) or presence of other compounds found in star anise or fennel essential oils .....	140
Figure 39. Variation of the chromatographic peak area of <i>trans</i> -anethole in binary DES-water mixtures with varying DES content .....	141

Figure 40. Retention of <i>trans</i> -anethole by aqueous solutions of preformed DES (DES aq), aqueous solutions of the forming compounds (HBA + HBD) aq, and aqueous solutions of the individual compounds (HBA aq or HBD aq) at a concentration equivalent to 20 wt% DES .....	142
Figure 41. The general structure of a) randomly methylated- $\beta$ -cyclodextrin (RAMEB, DS = 12.9 and R= -H or -CH <sub>3</sub> ), b) levulinic acid and c) <i>trans</i> -anethole .....	143
Figure 42. <sup>1</sup> H NMR spectra of RAMEB:Lev in the absence (top) or presence of <i>trans</i> -anethole (bottom). Blue, orange, and green boxes respectively represent peaks related to RAMEB, levulinic acid, and <i>trans</i> -anethole .....	144
Figure 43. ROESY spectrum of RAMEB:Lev in presence of <i>trans</i> -anethole.....	145
Figure 44. Variation of the diffusion coefficients of RAMEB:Lev SUPRADES' components and <i>trans</i> -anethole in different SUPRADES-water binary mixtures .....	146
Figure 45. Variation of the chromatographic peak area of <i>trans</i> -anethole in mixtures of ChCl:U and increasing amounts of cyclodextrins. Glucopyranose was added at 10 wt% as a reference .....	147
Figure 46. The chromatographic peak area of the studied volatile compounds in presence of DES or thin film-DES dissolution preparations .....	148
Figure 47. The chromatographic peak area of <i>trans</i> -anethole in ChCl-based DES in the presence or absence of Triton X-100 surfactant.....	149
Figure 48. Release of <i>trans</i> -anethole from water and studied solvents at 60 °C.....	150

# List of Abbreviations

2D ROESY	Two-dimensional rotating frame Overhauser enhancement Spectroscopy
A	Chromatographic peak area
AAD	Average absolute deviation
AFM	Atomic force microscopy
AN	<i>Trans</i> -anethole
ATPS	Aqueous two-phase system
BA	Butyric acid
BD	Butanediol
BMIIm	1-butyl-3 methylimidazolium
CA	Caprylic acid
Carv	L-carvone
ChAc	Choline Acetate
ChCl	Choline chloride
cmc	Critical micelle concentration
COSMO-RS	Conductor-like screening model for real solvents
DEG	Diethylene glycol
DES	Deep eutectic solvent(s)
DLLME	Dispersive liquid-liquid microextraction
DLS	Dynamic light scattering
DMPC	1,2- dimyristoyl-sn-glycero-3-phosphocholine
DPPC	1,2-dipalmitoylsn- glycero-3 phosphocholine
DSPC	1,2-distearoylsn-glycero-3- phosphocholine
DMU	N,N'-dimethylurea
DS	Degree of substitution
DSC	Differential scanning calorimetry
EAC	N,N-diethyl ethanol ammonium chloride
EG	Ethylene glycol
EMIImCl	1-ethyl-3 methylimidazolium chloride
EO	Essential oil(s)
FTIR	Fourier-transform infrared spectroscopy
G	Glycerol
HBA	Hydrogen bond acceptor
HBD	Hydrogen bond donor
Hc	Henry's law constant
HPLC-MS	High performance liquid chromatography- mass spectrometry
SH-GC	Static headspace-gas chromatography
K	Partition coefficient

LA	Lactic acid
LD50	Lethal dose 50 or median lethal dose
Lev	Levulinic acid
MA	Malonic acid
MD	Molecular dynamics
MHE	Multiple headspace extraction
NADES	Natural deep eutectic solvent(s)
NMR	Nuclear magnetic resonance
OA	Oxalic acid
PC	Phosphatidylcholine
PD	Propanediol
PEG	Polyethylene glycol
PFG	Pulsed field gradient
POPC	1-palmitoyl-2-oleoylphosphatidylcholine
RAMEB	Randomly methylated $\beta$ -cyclodextrin
ROS	Reactive oxygen species
SANS	Small-angle neutron scattering
SAXS	Small-angle X-ray scattering
SDS	Sodium dodecyl sulfate
SLB	Supported lipid bilayer(s)
TBABr	Tetrabutylammonium bromide
TBACl	Tetrabutylammonium chloride
TBMACl	Tributylmethylammonium chloride
TBPBr	Tetrabutylphosphonium bromide
TEG	Triethylene glycol
TEM	Transmission electron microscopy
TGA	Thermogravimetric analysis
THEDES	Therapeutic deep eutectic solvents
TMA	Trimethylammonium
U	Urea
VA	Valeric acid

# Introduction

The quest for green solvents constitutes one of the major concerns in green chemistry. The discovery of deep eutectic solvents (DES) was a real milestone in this field. DES represent a new generation of solvents that caught the researchers' attention in recent years. First reported in 2003, DES are defined as a mixture of two or three compounds that results in a clear and homogenous liquid with a much lower melting point than its forming compounds (Abbott et al., 2003; Q. Zhang et al., 2012). The temperature's depression is often attributed to the hydrogen bonding interactions taking place between the DES' starting compounds. Subsequently, DES can be prepared from a large variety of compounds generating a plethora of possible combinations. In addition to their easy preparation from widely accessible and cheap starting materials, DES hold interesting physicochemical properties. Furthermore, the natural counterparts of DES made of primary metabolites were raised a few years later and were called natural deep eutectic solvents (NADES) (Choi et al., 2011). These solvents were extensively applied in various domains to replace and bypass some of the conventional organic solvents' limitations. Indeed, DES and NADES have shown promising outcomes in chemical, biological, biomedical, and pharmaceutical sectors, among others (Mbous, Hayyan, Hayyan, et al., 2017). Despite the exponentially growing number of publications on this topic, a lot of information and implementations of DES remain to be uncovered.

The present study aims to examine three main points. The first one consists of determining the physicochemical properties of DES and evaluating the influence of their composition on the resulting properties, which may help in the design of DES for specific applications. The second part focuses on investigating the interaction between DES and phospholipids. Phospholipids represent the most abundant class of lipids in cell membranes. Owing to their amphiphilic nature, these molecules tend to self-assemble into lipid vesicles whenever present in an aqueous medium. The resulting lipid vesicles, known as liposomes, are one of the most studied and applied encapsulation systems, given their ability to encapsulate molecules of a wide polarity range (Anwekar et al., 2011). To date, the studies involving DES and phospholipids or liposomes are very limited (Bryant et al., 2016, 2017; M. C. Gutiérrez et al., 2009; R. McCluskey et al., 2019). Therefore, studying the behavior of phospholipids within DES may not only clarify the effect of DES on animal cells and their subsequent biocompatibility but may also open up the possibility to create novel DES-based encapsulation systems. The third goal of the study revolves around the solubilizing ability of DES and DES-based systems, incorporating different encapsulation systems like phospholipids and cyclodextrins, toward bioactive volatile compounds. The combination of DES with safe encapsulating agents can lead to the formation of potentially promising and economic drug delivery systems with unique properties.

This study focuses, more precisely, on four main objectives:

- The preparation and characterization of DES;
- The investigation of the organization of phospholipids within DES;
- The impact of DES on liposomes and human cells;

- The evaluation of the solubilizing ability of DES-based systems toward natural volatile compounds.

This thesis comprises five chapters. The **first** one provides a literature review of deep eutectic solvents: definition, classification, methods of preparation, physicochemical properties, the effect of water on both their properties and network, their toxicity, and biodegradability. Moreover, this chapter overviews some of the main applications of DES, namely organic synthesis, catalysis, biomass processing, electrochemistry, extraction, solubilization, and drug delivery. The last section of the chapter involves the studies dealing with the self-assembly of phospholipids or surfactants within DES, and the combination of DES and cyclodextrins.

The **second** chapter presents the composition of the solvents that were considered in this study, their preparation, and their characterization. The latter mainly involves density, viscosity, and polarity measurements.

The **third** chapter covers the investigation of the phospholipid organization within the DES using both optical- and atomic force microscopies, as well as dynamic light scattering.

The behavior of liposomes in presence of DES, monitored by atomic force microscopy, was described in the **fourth** chapter. Furthermore, this chapter includes the effect of some DES on human cells which was evaluated via cytotoxicity and morphological studies.

In the **fifth** and last chapter, we studied the solubilization of plant volatiles and some related essential oils by DES using static headspace- gas chromatography. We further evaluated the effect of the incorporation of water or some encapsulation systems on the solubilization performance of DES. At last, we were interested in monitoring the release of a volatile compound from the DES via multiple headspace extraction.

# I. Literature Review

## 1. Deep Eutectic Solvents

### 1.1. Definition

The discovery of the deep eutectic solvents (DES) was a major breakthrough in the world of green chemistry. DES are frequently defined as binary or ternary mixtures of compounds that are able to associate mainly via hydrogen bonds. Combining these compounds at a certain molar ratio results in a eutectic mixture (Q. Zhang et al., 2012). The word “eutectic” comes from the Ancient Greek εὐτήκτος or *eútēktos* which means easily melted and a eutectic point represents the chemical composition and temperature at which a mixture of two solids becomes fully molten at the lowest melting temperature, relative to that of either compounds. However, defining a DES is still a controversial subject and there are various reported definitions that do not really distinguish DES from other mixtures, since all the mixtures of immiscible solid compounds present an eutectic point and considering that numerous compounds are able to form hydrogen bonds when put together (Coutinho & Pinho, 2017). Given that the presence of an eutectic point or hydrogen bonding between components are not sufficient conditions to define a “deep eutectic solvent” and in order to clarify what a DES is and what makes it special compared to other mixtures, Martins *et al.* recently defined DES as “a mixture of two or more pure compounds for which the eutectic point temperature is below that of an ideal liquid mixture, presenting significant negative deviations from ideality ( $\Delta T_2 > 0$ )”, where  $\Delta T_2$  stands for the temperature depression which is the difference between the ideal and the real eutectic point (Martins et al., 2019). The same authors stated that it is important that the temperature depression results in a liquid mixture at operating temperature, regardless of the mixture composition. The fact that there is no fixed composition offer an even greater tunability for these systems.

Although DES were extensively studied, especially in the past decade, there is still a lack of understanding the principle behind DES' formation and properties. It all started almost twenty years ago, when Abbott *et al.* were looking for liquids that can overcome the moisture sensitivity and high cost of some common ionic liquids (Abbott et al., 2001). In this study, numerous mixtures based on different quaternary ammonium salts and metal salts were tested and it turned out that choline chloride (ChCl) mixed with zinc chloride in a 1:2 molar ratio presents the lowest freezing point (23-25 °C). Thereafter, the same authors investigated eutectic mixtures of quaternary ammonium salts and hydrogen bond donors (HBD) and named them “deep eutectic solvents” (Abbott et al., 2003). The lowest freezing point (12 °C) was obtained with 1:2 ChCl:urea. This significant depression of the freezing point, compared to that of ChCl (302 °C) or urea (U) (133 °C), is due to hydrogen bonding between urea molecules and chloride ion as proved by nuclear magnetic resonance (NMR) spectroscopy. What is interesting about these solvents is that they are not only liquid at ambient temperature but also tunable and highly

solubilizing. After that, other DES based on ChCl and carboxylic acids were characterized and were also shown to have important solubilizing ability toward some metal oxides (Abbott, Boothby, et al., 2004). Other liquids were also obtained when mixing ChCl with a hydrated metal salt like chromium (III) chloride hexahydrate (Abbott, Capper, et al., 2004). Later on, an additional class of ambient temperature solvents based on metal salts and HBD such as amides (urea and acetamide) and diols (ethylene glycol and 1,6-hexanediol) were reported, but it turned out that only a restricted number of metal salts and HBD can lead to their formation (Abbott, Barron, et al., 2007).

Few years later, Choi *et al.* coined the term “natural deep eutectic solvents” (NADES) (Choi et al., 2011). This category covers the DES that are made of primary metabolites such as organic acids, amino acids, sugars, polyols and choline derivatives (Choi et al., 2011; Dai et al., 2013). Besides, water can also be part of NADES' composition. They were introduced as a way to explain the omnipresence of metabolites in high concentrations in cells. Since different combinations of these candidates led to the formation of liquids which also succeeded in the solubilization of some natural compounds, NADES were proposed as a new cellular phase, together with water and lipids. These mixtures might be engaged in the biosynthesis, storage and transport of some poorly water-soluble compounds as well as some other processes like dehydration, drought resistance and cryoprotection. Further, their consideration is highly encouraged owing to the advantages that they provide from an environmental and economic point of view.

## 1.2. Classification

In order to differentiate between the possible eutectics, DES were classified into four types based on the general formula  $Cat^+ X^- zY$ , where  $Cat^+$  is generally an ammonium, phosphonium or sulfonium, while  $X^-$  is a Lewis base (usually a halide anion).  $Y$  represents a Lewis or Brønsted acid and  $z$  is the number of  $Y$  molecules that interact with the corresponding anion (Figure 1) (Abbott, Barron, et al., 2007; E. L. Smith et al., 2014). Type III eutectics are the most studied in literature and are usually based on ChCl and various HBD. ChCl has been extensively adopted since it is relatively cheap, non-toxic and biodegradable, considering it is approved as a natural additive for several animal species (“Scientific Opinion on Safety and Efficacy of Choline Chloride as a Feed Additive for All Animal Species,” 2011). In fact, the first type III DES was primarily based on ChCl. Since then, a plethora of compounds has been successfully used in DES formation. The hydrogen bond acceptors (HBA) mainly include quaternary ammonium or phosphonium salts, whereas the most common HBD are amides, alcohols and carboxylic acids. In addition, compounds like sugars, sugar alcohols and amino acids are also considered for NADES preparation (Dai et al., 2013). More recently, hydrophobic DES were introduced and they are based on the use of hydrophobic compounds such as tetrabutylammonium bromide (TBABr), menthol, thymol and fatty acids as hydrogen bond acceptors together with long alkyl chain alcohols and carboxylic acids as HBD (Florindo et al., 2019; Osch et al., 2015). Furthermore, DES can be made of active pharmaceutical ingredients like ibuprofen, lidocaine and phenylacetic acid. In that event, the solvents are named therapeutic deep eutectic solvents (THEDES) (Duarte et al., 2017; Paiva

et al., 2014). Some of the frequently used HBA and HBD counterparts described in the literature are illustrated in Figure 2.

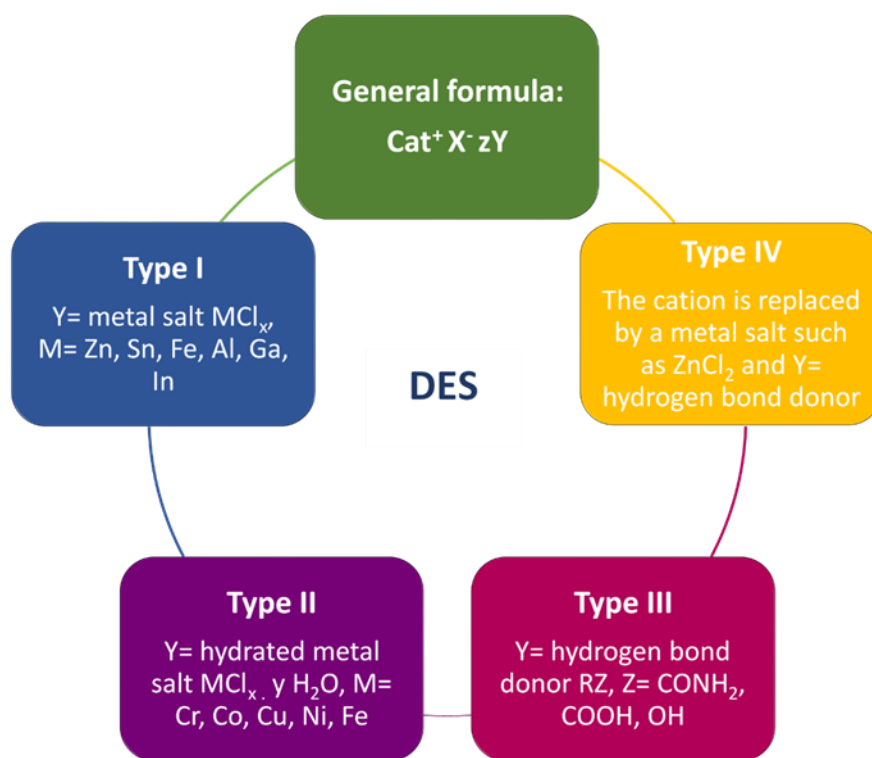


Figure 1. The four types of deep eutectic solvents based on the general formula  $Cat^+ X^- zY$

On the other hand, although NADES can sometimes be considered as type III DES, it is not always the case. That said, NADES were recently classified into five main groups (Dai et al., 2013; González et al., 2018):

- Ionic liquids, made of an acid and a base;
- Neutral, made of only sugars or sugars and other polyalcohols;
- Neutral with acids, made of sugar/polyalcohols and organic acids;
- Neutral with bases, made of sugar/polyalcohols and organic bases;
- Amino acids-containing NADES, made of amino acids and sugars/ organic acids.

Nevertheless, the reported DES do not certainly fall into one of the above-mentioned classes given their versatility and the myriad of the considered starting compounds. As a result, Coutinho and coworkers proposed a type V DES composed of non-ionic species. In their study, they proved that mixing thymol with menthol led to severe negative deviations to ideality due to a strong interaction between the components. The latter is attributed to resonance effects related to the structure of phenolic compounds which acted as strong hydrogen bond donors (Abranches et al., 2019). On another note, two recent studies reported the use of cyclodextrins, which are non-toxic cyclic oligosaccharides, as hydrogen

bond acceptors resulting in the formation of liquid supramolecular mixtures at room temperature (El Achkar, Moufawad, et al., 2020; El Achkar, Moura, et al., 2020). The important events marking the development of deep eutectic solvents so far are presented in Figure 3 (Abbott et al., 2001, 2003; Abbott, Capper, et al., 2004; Abbott, Boothby, et al., 2004; Abbott, Barron, et al., 2007; Choi et al., 2011; El Achkar, Moufawad, et al., 2020; Osch et al., 2015).

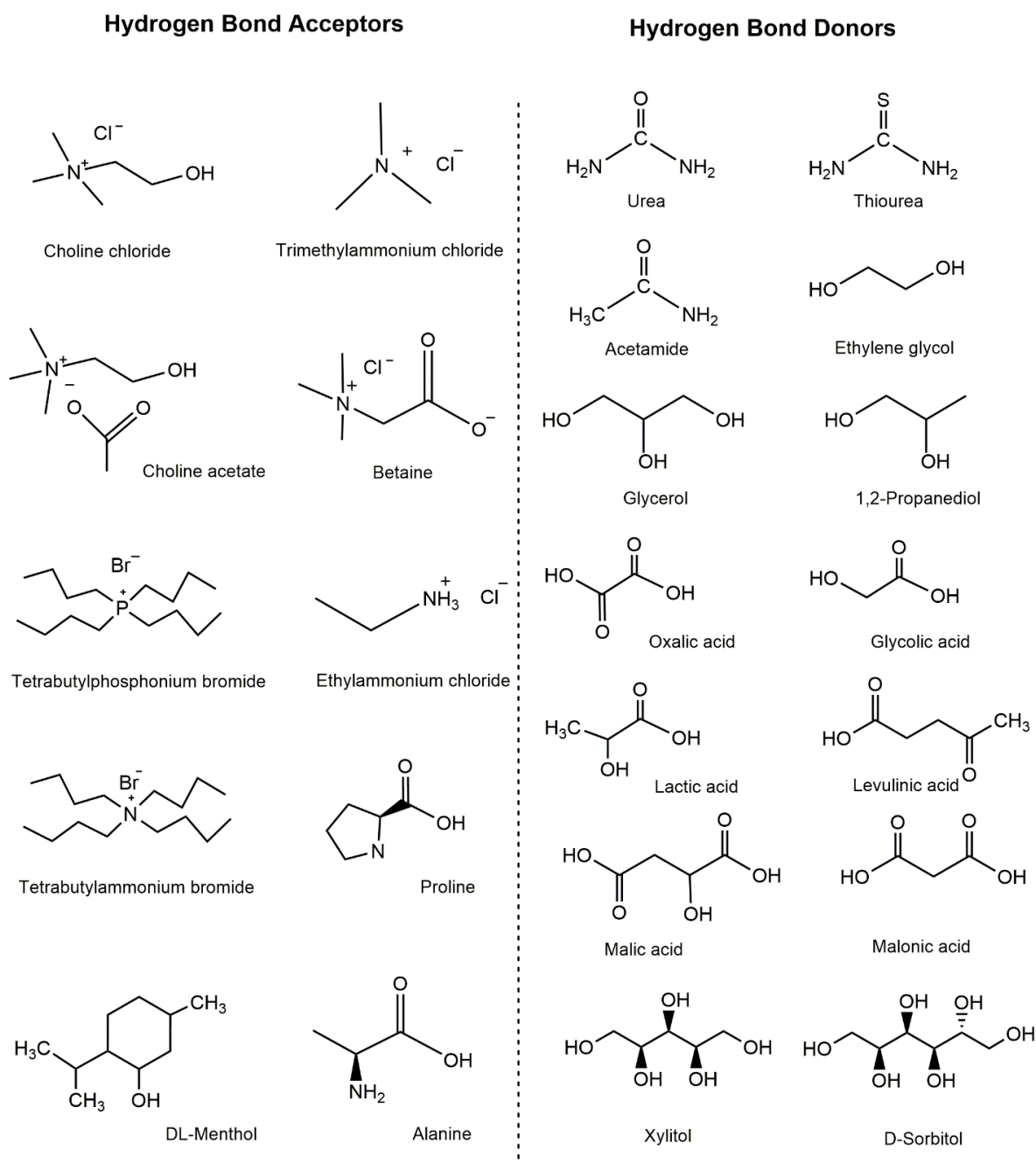


Figure 2. Commonly used HBA and HBD compounds in deep eutectic solvents' preparation

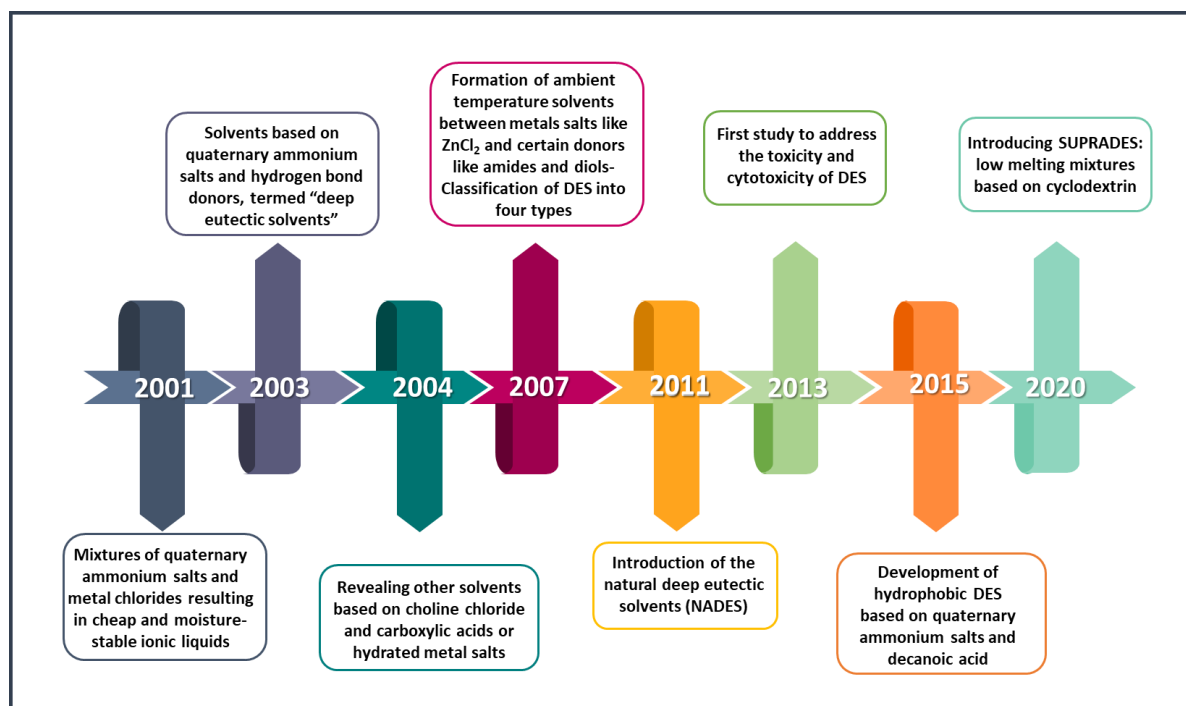


Figure 3. Major events marking the development of deep eutectic solvents throughout the years

### 1.3. Methods of preparation

As mentioned above, DES are obtained by mixing two or more compounds capable of associating through hydrogen bonds, thus forming a eutectic mixture at a well-defined molar ratio. Researchers generally use one of the two main methods to prepare DES: the heating method and the grinding method. The heating method consists on mixing and heating the compounds, under constant stirring, until a homogeneous liquid is formed (Abbott, Boothby, et al., 2004). The heating temperature usually ranges between 50 and 100 °C. However, a high temperature may potentially lead to a degradation of the deep eutectic solvent due to an esterification reaction regardless of the preparation method, as demonstrated by Rodriguez et al. for solvents based on ChCl and carboxylic acids (Rodriguez Rodriguez et al., 2019). The grinding method is based on mixing the compounds at room temperature and crushing them in a mortar with a pestle, until a clear liquid is formed (Florindo et al., 2014). Another method based on the freeze-drying of the aqueous solutions of the components of DES was also revealed by Gutierrez *et al.* (M. C. Gutiérrez et al., 2009). Indeed, separate aqueous solutions of ChCl and urea (or thiourea) were mixed to form an aqueous solution of 1:2 ChCl:U (or ChCl:thiourea), having 5 wt% solute contents. The obtained solutions were then frozen and freeze-dried, resulting in the formation of clear and viscous liquids. However, water was detected in the freeze-dried mixture because it can interact with DES' components and be part of the DES' network (Choi et al., 2011; Dai et al., 2013). That said, different DES are obtained when using different methods of preparation. An evaporation method was also reported by Dai *et al.*, consisting on dissolving the components of DES in water, followed by an evaporation at 50 °C. The resulting liquid is then placed in a desiccator in presence of silica gel (Dai et al., 2013). Considering the optimization of time and energy consumption,

a greener microwave-assisted approach was proposed for the preparation of NADES within seconds (Gomez et al., 2018). Lastly, an ultrasound-assisted synthesis of NADES was recently introduced (Santana et al., 2019).

## 1.4. Physicochemical properties

The physicochemical properties of DES are one of the main reasons behind the rising researchers' interest in these solvents. Besides having a low volatility, non-flammability, low vapor pressure and chemical and thermal stability, DES are chemically tunable meaning they can be designed for specific applications given the wide variety of the possible DES forming compounds. All these properties encouraged the scientists to explore DES and apply them as a good alternative to conventional solvents. Herein, the main physicochemical properties of DES namely their phase behavior, density, viscosity, ionic conductivity, surface tension and polarity are presented and discussed.

### 1.4.1. Phase behavior

As mentioned above, DES are not pure compounds but mixtures of two or more pure compounds. This system is represented by a solid-liquid phase diagram, which shows the melting temperature in function of the mixture composition. Therefore, if we consider a binary mixture of compounds A and B, the eutectic point represents the composition and the minimum melting temperature at which the melting curves of both compounds meet (Figure 4).

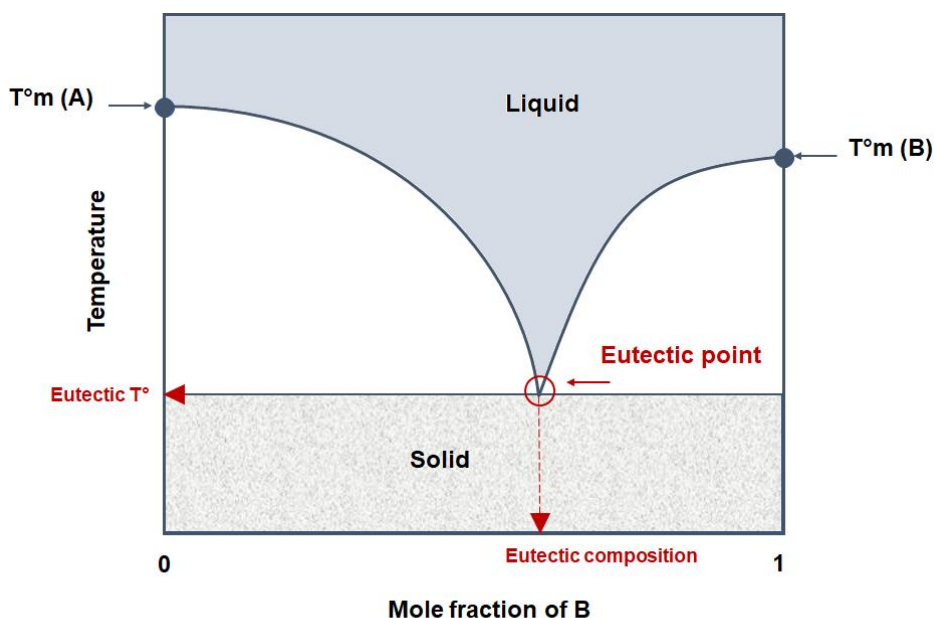


Figure 4. General solid-liquid phase diagram of a binary mixture

According to Martins *et al.*, the DES appellation should only cover mixtures with a melting point lower than the ideal eutectic temperature, otherwise DES would not be called “deep” and could not be differentiated from other mixtures (Martins *et al.*, 2019). In addition, they stated that a DES must be liquid at operating temperature even if this requires a different composition than the eutectic one. Consequently, having a phase diagram is essential and knowing the melting properties of the pure compounds is necessary to determine the ideal solubility curve. Nevertheless, very little is reported about the thermodynamic behavior of the DES to date. The freezing points of most of the DES usually range between  $-69$  and  $149$  °C (Q. Zhang *et al.*, 2012). A number of DES with a melting point lower than  $60$  °C were summarized by García *et al.* (García *et al.*, 2015). The choice of the HBD (Abbott, Boothby, *et al.*, 2004; Abbott *et al.*, 2003), the nature of the organic salt and its anion (Abbott *et al.*, 2003) and the organic salt/HBD molar ratio (Shahbaz *et al.*, 2011b) can all affect the freezing point of the mixture. The method of preparation can also influence the value of the freezing point, but not the eutectic composition which must remain unchanged no matter the method used (Abbott *et al.*, 2006). On the other hand, no correlation was found between the freezing point of a DES and the melting points of its pure components (Abbott, Boothby, *et al.*, 2004; Q. Zhang *et al.*, 2012). The HBD did however affect the freezing point depression  $\Delta T$  (Abbott, Boothby, *et al.*, 2004; E. L. Smith *et al.*, 2014). For instance, Abbott *et al.* found that the lower the HBD’s molecular weight, the greater is the depression of the freezing point (Abbott, Boothby, *et al.*, 2004). But unlike Abbott and coworkers who considered the temperature depression as the difference between the linear combination of the melting points of the pure components and the real eutectic point ( $\Delta T_1$ ), Martins *et al.* thought it would be more appropriate to define the temperature depression as the difference between the ideal and the real eutectic point ( $\Delta T_2$ ), otherwise any mixture of compounds would be referred as a DES (Figure 5) (Martins *et al.*, 2019).

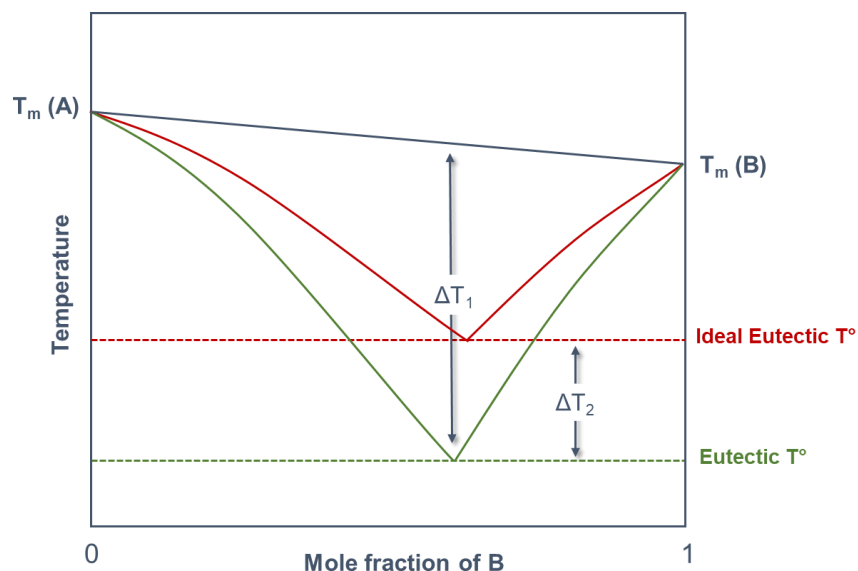


Figure 5. Solid-liquid phase diagram representing a simple ideal eutectic mixture (red line) and a deep eutectic mixture (green line) (Adapted from Martins *et al.* 2019)

Nevertheless, several other reported mixtures presented only a glass transition and no melting point was detected (Dai et al., 2013; Florindo et al., 2014; Francisco et al., 2012; Savi, Carpiné, et al., 2019; Savi, Dias, et al., 2019).

### 1.4.2. Density

Density is one of the fundamental physical properties of liquids. Most of the reported DES present higher densities than water with values ranging between 1.0 and 1.3 g.cm<sup>-3</sup> at 25 °C, while DES based on metal salts have densities in the 1.3- 1.6 g.cm<sup>-3</sup> range (Tang & Row, 2013). Contrarily, lower densities than water are obtained for hydrophobic deep eutectics (Florindo et al., 2019). The DES' density shows a temperature-dependent behavior, it decreases linearly with the increasing temperature (Cui et al., 2017; Florindo et al., 2014; Ibrahim et al., 2019; Shahbaz, Baroutian, et al., 2012). Moreover, the density depends on the choice of the HBD (Abbott, Harris, et al., 2007; Cui et al., 2017; Florindo et al., 2014; García et al., 2015), and the molar ratio (Abbott et al., 2011). According to Shahbaz *et al.*, a higher HBD mole fraction lowers the density of DES whenever the HBD's density is lower than that of the corresponding DES and vice versa (Shahbaz et al., 2011a; Shahbaz, Baroutian, et al., 2012). In addition, when the HBD contains hydroxyl groups, the density of the ChCl-based DES increases with the number of hydroxyl groups but decreases with the addition of aromatic groups. Also, when the DES is made of an acid its density decreases when the chain length is increased (Florindo et al., 2014; García et al., 2015; Mitar et al., 2019). The effect of the HBD type on the density of some ChCl-based DES obtained by different studies is represented in Figure 6. These results were in accordance with Yusof *et al.* who also proved that TBABr:alcohol DES present a higher density when a HBD with a higher number of hydroxyl groups is adopted. The same group also noticed a decrease in density as the HBD's chain length increased (Yusof et al., 2014).

The DES' density is weakly affected by the alkyl chain length of the ammonium salt (Z. Chen et al., 2017). However, looking at results from different studies reviewed by García *et al.*, one can clearly see that the organic salt and its anion affect the density of DES. Indeed, phosphonium salts and bromide salts result in denser DES than ammonium salts and chloride salts, respectively (García et al., 2015). On another note, Florindo *et al.* proved that there is no significant difference in density values whether the heating method or the grinding method was used for the preparation of DES (Florindo et al., 2014). Yet, differences of up to 4% were detected between the available literature sources when it comes to the density of the most studied 1:2 ChCl:U DES (García et al., 2015). A series of studies aiming to efficiently predict the density of DES were conducted by Mjalli *et al.* via several theoretical approaches (Mjalli, 2016; Mjalli et al., 2015; Shahbaz et al., 2011a, 2013; Shahbaz, Mjalli, et al., 2012). The mass connectivity index-based correlation, taking into account the molecular structures of DES' forming compounds, allowed the prediction of the density of different type III DES as a function of temperature with a very high efficiency (Mjalli, 2016).

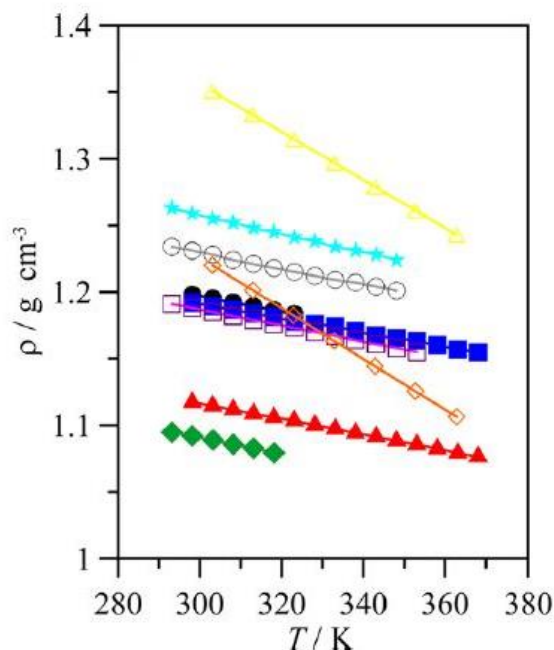


Figure 6. Effect of the hydrogen bond donor on the densities of some choline chloride-based deep eutectic solvents (yellow: 1:3 choline chloride:ethanolamine; light blue: 1:1 choline chloride:oxalic acid; grey: 1:1 choline chloride:malonic acid; black: 1:2 choline chloride:urea; dark blue: 1:2 choline chloride:glycerol; purple: 1:1 choline chloride:glutaric acid; orange: 1:3 choline chloride:2,2,2-trifluoroacetamide; red: 1:2 choline chloride:ethylene glycol; green: 1:3 choline chloride:phenol). Reprinted with permission from (García et al., 2015). Copyright (2015) American Chemical Society

### 1.4.3. Viscosity

The viscosity is another important and extensively studied property of DES. Most of the reported DES to date are highly viscous at room temperature ( $\eta > 100$  mPa.s) which is mainly ascribed to the extensive hydrogen bond network taking place between DES' components. In addition, they present a very broad viscosity range. In fact, ChCl:EG (1:2) is known to have a very low viscosity (37 mPa.s at 25 °C), while sugar-based DES present extremely large viscosities (12730 mPa.s for 1:1 ChCl:sorbitol at 30°C and 34400 mPa.s for 1:1 ChCl:glucose at 50°C) and even higher viscosities were recorded for metal salts-based DES (85000 mPa.s for 1:2 ChCl:zinc chloride at 25 °C) (Q. Zhang et al., 2012). Yet, very low viscosities were recorded for hydrophobic DES based on DL-menthol (7.61 mPa.s at 25 °C for 1:3 DL-menthol:octanoic acid) (Nunes et al., 2019; Ribeiro et al., 2015). The viscosity of a eutectic mixture is clearly affected by the nature of its components (Abbott, Barron, et al., 2007; D'Agostino et al., 2011), their molar ratio (Abbott et al., 2011), the temperature (Abbott, Boothby, et al., 2004; Abbott et al., 2003, 2006; Dai et al., 2015; Kareem et al., 2010) and the water content (D'Agostino et al., 2015; Dai et al., 2015; Du et al., 2016; Florindo et al., 2014; Shah & Mjalli, 2014). The effect of water will be discussed in details in the upcoming sections. Moreover, the viscosity not only depends on the intermolecular forces between the HBD and the ion but also on the steric effects which can be quantified by the hole theory. The latter considers the existence of holes or voids in the fluid which affects the fluid's viscosity and ionic conductivity (Abbott et al., 2006). The distribution of holes of radius  $r$  is

influenced by the HBD and the salt. It also seems that DES containing large holes are less viscous because they allow a certain ionic motion (García et al., 2015). On a separate note, it is worthy to mention that large differences were noticed when comparing the viscosity data obtained by different researchers for the same DES (e.g., 152 mPa.s vs 527.28 mPa.s for 1:2 ChCl:U at 30 °C and 202 mPa.s vs 2142 mPa.s for 1:1 ChCl:oxalic acid at 40 °C) (García et al., 2015). These major differences can be attributed not only to the preparation method as stated by Florindo *et al.* (Florindo et al., 2014), but to the experimental method and the impurities as well (García et al., 2015).

#### 1.4.4. Ionic conductivity

Since the viscosity is the main controller of the conductivity, most of the DES tend to have poor ionic conductivities ( $\kappa < 2 \text{ mS cm}^{-1}$  at room temperature). Therefore, increasing the temperature results in a decrease in the viscosity and an increase in the conductivity (Lapeña et al., 2019a; Q. Zhang et al., 2012). This property is also affected by the HBA/HBD molar ratio (Abbott, Boothby, et al., 2004), the nature of both the organic salt and the HBD as well as the salt's anion (García et al., 2015) and of course the water addition (Dai et al., 2015).

#### 1.4.5. Surface tension

The studies related to the surface tension of DES are quite limited compared to the studies dealing with other physicochemical properties. Yet, it is an essential property since it is highly dependent on the intensity of the intermolecular forces taking place between the HBD and the corresponding salt. That said, highly viscous liquids present high surface tensions. The values relative to the reported DES generally vary between 35 and 75 mN m<sup>-1</sup> at 25 °C (García et al., 2015; Ibrahim et al., 2019). Once again remarkable high values were recorded for sugar-based DES such as ChCl:D-glucose (A. Hayyan et al., 2013) and ChCl:D-fructose (A. Hayyan et al., 2012), reflecting their extensive hydrogen-bond network (Ibrahim et al., 2019). Besides, the surface tension is influenced by the salt mole fraction and the cation type since an additional hydroxyl group or a longer alkyl chain in the quaternary ammonium salt leads to higher surface tensions. Also, the surface tension linearly decreases with increasing temperature (García et al., 2015; Lapeña et al., 2019a; Nunes et al., 2019).

#### 1.4.6. Polarity

Polarity is a key property since it reflects the overall solvation capability of solvents. Despite its significance, the polarity of the DES was not considerably studied and was not addressed until recently. This property is often estimated via the solvatochromic parameters which consider the hypsochromic (blue) shift or bathochromic (red) shift of UV-vis bands for the negatively solvatochromic dyes (e.g. Reichardt's betaine dye) or the positively solvatochromic dyes (e.g. Nile red), respectively, as a function of the solvent's polarity (Reichardt, 1994). The most frequently used scales are the polarity scales of Dimroth and Reichardt ( $E_T$  and  $E_TN$ ) (Reichardt, 1994) and the multiparameter scale of Kamlet and Taft (the hydrogen bond donating ability  $\alpha$ , the hydrogen bond accepting ability  $\beta$  and dipolarity/polarizability  $\pi^*$ ) (Kamlet et al., 1977; Kamlet & Taft, 1976). The common probes adopted for the establishment of Dimroth and Reichardt's scale include Reichardt's betaine dyes and Nile red. While molecules like 4-

nitroaniline and *N,N*-diethyl-4-nitroaniline are used to determine the parameters following the Kamlet and Taft multiparameter scale. However, it is worthy to mention that the polarity scales are not universal and are probe-dependent which means that we cannot compare polarity parameters obtained by different solvatochromic probes (Valvi et al., 2017). A general overview on the studies conducted on DES' polarity is presented in Table 1 following a chronological order.

Table 1. Overview of the reported studies related to the polarity of deep eutectic solvents

Deep eutectic solvent(s)	Solvatochromic probe(s)	Main results	References
ChCl:G (1:1, 1:1.5, 1:2 and 1:3)	Reichardt's dye 30; 4-nitroaniline; <i>N,N</i> -dimethyl-4-nitroaniline	The studied DES at different molar ratios make up polar fluids with the $E_T(30)$ values increasing with the increase in ChCl in a nearly linear trend.	(Abbott et al., 2011)
Numerous NADES based on ChCl, sugars, alcohols, organic acids, amino acids and water	Nile red	The organic acid-based NADES are the most polar, followed by amino acids- and sugar-based NADES. While the sugar- and polyalcohol-based ones seem to be the least polar.	(Dai et al., 2013)
ChCl:U; ChCl:G; ChCl:EG; ChCl:MA (1:2)	Several solvatochromic probes such as betaine dye 33 and Nile red	All the DES are considered highly polar. The structure of the HBD clearly affects the solvent's polarity which is highest with alcohol-based DES followed by those having urea and malonic acid.	(Pandey et al., 2013)
13 Binary or ternary ChCl-based DES using urea, glycerol, ethylene glycol, thiourea or formamide as HBD	Reichardt's dye 30; 4-nitroaniline; <i>N,N</i> -diethyl-4-nitroaniline	The polarity of the studied DES highly depends on the polarity of the HBD. A correlation was also found between the solvatochromic parameters and the influence of DES on the activity or stability of lipase.	(Kim et al., 2016)

Table 1. (continued)

Deep eutectic solvent(s)	Solvatochromic probe(s)	Main results	References
4 DES using different N-oxides as HBA and phenylacetic acid as HBD	Nile red	Four N-oxides were adopted as HBA (three amphiphilic and one non-amphiphilic) along with phenylacetic acid as HBD. The non-amphiphilic HBA gives rise to a more polar DES than the ones based on amphiphilic HBA.	(Germani et al., 2017)
19 DES based on ammonium salts as HBA and carboxylic acids as HBD	4-nitroaniline; <i>N,N</i> -diethyl-4-nitroaniline	Increasing the alkyl chain length of both HBA and HBD results in a decrease in the hydrogen-bond acidity and an increase in the hydrogen-bond basicity. While the dipolarity/polarizability is mainly affected by the HBD given that it decreases when the HBD's alkyl chain length is increased.	(Teles et al., 2017)
ChCl:U; ChCl:EG (1:2)	Several molecular probes	The studied DES present an overall higher polarity than most of the organic solvents. The HBD type might extremely affect the polarity response of the probe. Some polarity parameters displayed different temperature-dependence trends when comparing the 3 studied DES and the polarity did not always decrease with the increasing temperature thus revealing a possible "nonclassical" nature of DES compared to other solvents.	(Valvi et al., 2017)
7 DES based on ChCl; 4 DES based on TBACl; 4 DES based on DL-Menthol	Reichardt's betaine dye; 4-nitroaniline; <i>N,N</i> -diethyl-4-nitroaniline	The HBA seems to play a major role in the polarity of the DES, especially the hydrophobic ones that are based on TBACl or DL-menthol as HBA. While for the hydrophilic ChCl-based DES, a diacid HBD like malonic acid generates a more polar DES than a monoacid-based one.	(Florindo et al., 2018)

Table 1. (continued)

Deep eutectic solvent(s)	Solvatochromic probe(s)	Main results	References
12 DES based on thymol and (L)-menthol as HBA and 6 different monocarboxylic acids as HBD	4-nitroaniline; <i>N,N</i> -diethyl-4-nitroaniline; Pyridine- <i>N</i> -oxide	Thymol-based DES present higher polarity and hydrogen-bond acidity character than (L)-menthol-based ones. On the other hand, a more pronounced hydrogen-bond basicity character is seen with (L)-menthol with a slight positive correlation with the alkyl chain length of the acid.	(Martins et al., 2018)
17 ChCl-based DES using polyalcohols (ethylene glycol, glycerol, propanediols and butanediols) as HBD at molar ratios 1:1, 1:2 and 1:3	Nile red	Polarity is affected by the molecular structure of the HBD. Polarity is also an important property to consider while using DES as an extraction solvent.	(Mulia et al., 2019)
9 DES based on PEG as HBD and carboxylic acids or amides or ammonium salts as HBA	Nile red	The HBA controls the DES' polarity since acid-based DES are more polar than the amide- and ammonium-based DES. A negative correlation was also detected between the pH values and the polarity of these PEGylated DES.	(W. Chen et al., 2019)
9 ternary DES based on ChCl, 1-ethyl-3-methylimidazolium chloride or tributylmethylammonium chloride as HBA and a binary mixture of 3-hydroxycarboxylic acids as HBD at a 1:1 or 1:2 HBA:HBD molar ratio	Nile red	Similar polarities were obtained for all the studied DES. The DES based on 3-hydroxycarboxylic acids were slightly more polar than the ones based on their aliphatic carboxylic acid analogues. No difference was detected between the two adopted molar ratios.	(Haražna et al., 2019)
ChCl:BA; ChCl:VA; ChCl:CA at both 1:2 and 1:3 molar ratios	Nile red; 4-nitroaniline; <i>N,N</i> -diethyl-4-nitroaniline	Increasing the alkyl chain length of the HBD results in a decrease in DES' polarity. Yet, no significant effect was observed when changing the HBA:HBD molar ratio.	(Dwamena & Raynie, 2020)

Table 1. (continued)

Deep eutectic solvent(s)	Solvatochromic probe(s)	Main results	References
ChCl:Lev and ChCl:LA (1:2)	Nile red	ChCl:LA is more polar than ChCl:Lev, which is mainly ascribed to the difference in the HBD's polarity. While the two DES were more polar compared with some alkyl cholinium lactate and alkyl cholinium levulinate ionic liquids.	(Fahri et al., 2020)

**BA:** butyric acid; **CA:** caprylic acid; **ChCl:** choline chloride; **EG:** ethylene glycol; **G:** glycerol; **HBA:** hydrogen bond acceptor; **HBD:** hydrogen bond donor; **LA:** lactic acid; **Lev:** levulinic acid; **MA:** malonic acid; **PEG:** polyethylene glycol; **TBACl:** tetrabutylammonium chloride; **U:** urea; **VA:** valeric acid.

## 1.5. Effect of water

Given the omnipresence of water and the hygroscopic character of some DES and their forming compounds, the water uptake by the eutectic solvents is inevitable (Du et al., 2016; Florindo et al., 2014). While traces of water in DES are usually considered as impurities, a plethora of papers intentionally added water to their solvents in order to fine-tune their properties so they can respond to the requirements of some desired applications and water allowed, in many cases, to improve the performance of DES. On the other hand, the presence of water not only affects the physicochemical properties but may also jeopardize the integrity of DES (El Achkar et al., 2019), which explains the inconsistency in the literature given that DES are prepared in different operating conditions. Therefore, studying the effect of water on the eutectic systems is of utmost importance. This section highlights the impact of water on the physicochemical properties of DES and the characteristics of their supramolecular organizations.

### 1.5.1. Effect on DES' physicochemical properties

Herein, the effect of water on the main physicochemical properties (melting point, density, viscosity, conductivity, surface tension and polarity) will be discussed according to the reported studies so far. Some investigated the effect of low water content that can naturally be present in the DES and others considered a full range of water content. After being in contact with the atmosphere for three weeks, ChCl:U DES absorbed up to 20 wt% water. That said, Meng *et al.* tested the effect of water (up to 10 wt%), that can be naturally absorbed by the DES, on the melting point of ChCl:U. The latter was determined via three different and complementary techniques: a thermostated bath, optical microscopy and differential scanning calorimetry (DSC). A linear decrease of the melting point was observed as a function of the water content. The melting point of the mixture dropped from 30 °C for the dry DES to 15 °C in the presence of 5 wt% of water. This tremendous water effect can explain the dissimilarities obtained by different studies for the same

DES (Meng et al., 2016). These results were somehow in accordance with the findings of Smith *et al.* who also followed the variation of the melting point of the same DES but with a full range of water content. Though a similar linear trend was obtained up until 10 wt% of water by the two studies, further increase in the water content yields a minimum melting point of  $-48 \pm 2$  °C at 0.67 mole fraction of water. Above this point, the melting temperature linearly increased as shown in Figure 7. Owing to the behavior of the studied mixture, the authors proposed that 1:2:6 ChCl:U:water makes a ternary deep eutectic solvent (P. J. Smith et al., 2019). Nevertheless, this behavior of ChCl:U was not observed by the study of Shah *et al.* in which the melting point only decreased as a function of water content studied in full range (Shah & Mjalli, 2014). Contrarily, the addition of up to 10 wt% water slightly increased the melting point of 1:1 ChCl:boric acid which was explained by a possible reaction between water and boric acid (Häkkinen, Willberg-Keyriläinen, et al., 2019). On the other hand, all the studies have agreed that unlike the density, both viscosity and conductivity are highly sensitive to the presence of water in DES. Agieienko *et al.* noticed a slight decrease of 0.14% in the density of ChCl:U at around 0.008 mass fraction of water while 0.005 water mass fraction decreased its viscosity by around 22%. Authors stated that different water contents along with the chosen experimental method and associated instrument calibration may be the reasons behind the poor agreement between the reported viscosity values of ChCl:U (Agieienko & Buchner, 2019). Du *et al.* showed that both viscosity and conductivity of ChCl:U are highly sensitive to water. In fact, the viscosity and the conductivity were 13 times lower and 10 times higher in the hydrated DES, respectively, at only 6 wt% water content (Du et al., 2016).

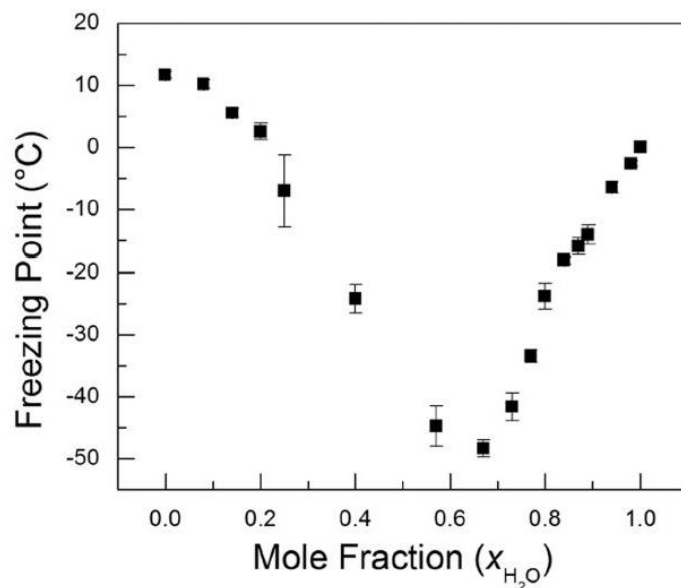


Figure 7. Variation of the freezing point of 1:2 ChCl:U deep eutectic solvent with the added mole fraction of water. Reprinted with permission from (P. J. Smith et al., 2019). Copyright (2019) American Chemical Society)

Likewise, Shah *et al.* found that within 10 wt% of water, the viscosity of ChCl:U was reduced by more than 80% and the conductivity was 3 times higher compared to the dried DES. In contrast, the presence of water only gradually decreased the melting point and the density of the mixture (Shah & Mjalli, 2014). According to Silva *et al.*, the addition of 3 to 9 wt% water to ChCl:sugars DES decreased their melting point, making them liquid at room temperature. The presence of water also contributes to a slight density reduction of 0.82 to 2.22%, a substantial drop in viscosity values and an increase in the liquid's polarizability (L. P. Silva *et al.*, 2018). For ChCl:carboxylic acids, a 5% difference in density was detected between a dried and water-saturated DES (the water content of the hydrated DES varied between 9.88 and 19.40 wt% depending on the DES following their exposition to air) at the same temperature which proves once again that this property is not very sensitive to the amount of water present in the sample. On the other hand, viscosity was strongly decreased in the hydrated DES with 10 to 200 times lower values than the dried ones (Florindo *et al.*, 2014). The presence of water (up to 5 wt%) also significantly decreased the viscosity and increased the conductivity of NADES based on ChCl and betaine as HBA and sugars and carboxylic acids as HBD (Aroso *et al.*, 2017). Increasing the water content from 2 to 22 wt% in ChCl:lactic acid decreased the viscosity by two orders of magnitude and increased the electrical conductivity in a similar trend (Alcalde *et al.*, 2019). Another study noticed a 3-fold and a 10-fold decrease in the viscosity of glucose:ChCl:water NADES after the addition of 5 and 10% water (v/v), respectively (Dai *et al.*, 2013). A significant decrease in the viscosity and a linear decrease in the density of several NADES were also observed in the presence of water, while the conductivity of five selected ternary NADES made of choline chloride, organic acids, sugars and water firstly increased with the increasing water content and then decreased after reaching a peak value of around 10-100 times higher than that of pure NADES at 60-80 wt% water (Dai *et al.*, 2015). Similar water effects on the density and viscosity of some organic acids-based NADES were obtained by Mitar *et al.* However, though clearly higher conductivities were seen in ChCl:organic acid based NADES compared to sugar:organic acid in the studies of both Dai *et al.* and Mitar *et al.*, no rise and fall was obtained by Mitar's group when studying the NADES conductivity as a function of water content. The ionic conductivities simply increased with the water content and this difference can be attributed to the narrower water range that was considered by Mitar *et al.* (10-50 wt%) (Mitar *et al.*, 2019). The viscosity and conductivity of ChCl-based DES with different glycols as HBD were also massively affected by the water content. In fact, the viscosity value was halved after the addition of about 7–10 wt% water. On the other hand, the conductivity of DES firstly increased with the increasing of water content, reached a maximum at 60 wt% water, at which values were 6–15 times higher than that of pure DESs, and then decreased. The ionic dissociation of DES' components caused the initial increase in the conductivity which was later decreased owing to the dilution of the electrolytes at higher water content. The polarity linearly increased with the increasing water content for all three DES (Gabriele *et al.*, 2019). A similar non-monotonic behavior of the ionic conductivity was observed with aqueous solutions of ChCl:U and ChCl:EG via molecular dynamics (MD) simulations. The values reached the maximum also at 60 wt% water (Celebi *et al.*, 2019). When varying the water content from 16 to 30 wt% in citric acid:sucrose NADES, a linear decrease of the density was observed. While a

major impact was seen on the viscosity which decreased by up to 99.73% at the maximum studied water content (30 wt%) (Savi, Dias, et al., 2019). Likewise, the addition of 10 wt% water resulted in a 85.9% decrease in the viscosity of lactic acid:glucose NADES (Savi, Carpiné, et al., 2019).

Rublova *et al.* conducted an in-depth study about the effect of water on the surface tension of binary mixtures of “ChCl + water”, “ChCl + ethylene glycol”, “ethylene glycol + water” and a ternary mixture of “ChCl + ethylene glycol + water”. The interpretation of the variation of the surface tension and the thermodynamic characteristics of adsorption at the interface “solution/air” led to some interesting findings. When comparing the aqueous solution of ChCl to that of EG, stronger adsorption of choline cation was obtained owing to the choline cation- water hydrophobic interactions. The ternary mixture results revealed interactions between DES’ constituents in an adsorbed surface layer formed at the interface air/diluted solution of ChCl:EG which explains the way higher values of equilibrium adsorption constants for the ternary mixture compared to those related to “ChCl + water” and “ethylene glycol + water” mixtures (Rublova et al., 2020). When studying the effect of water on the surface tension of DL-menthol:octanoic acid DES, Nunes *et al.* detected two consecutive behaviors: a decrease of the surface tension while increasing the water content reaching a minimum value at around 4000 ppm of water, followed by an increase of the surface tension (Nunes et al., 2019). The same behavior was observed by Sanchez-Fernandez *et al.* when studying the surface tension of ChCl:malonic acid as a function of water (Sanchez-Fernandez et al., 2017).

The papers dealing with the effect of water on the DES’s polarity are rather limited. The polarity of ChCl:U, ChCl:G and ChCl:EG was investigated through the solvatochromic behavior of different absorbance and fluorescence probes in DES-water mixtures. This approach would inform us about the interactions dominating these mixtures. The water addition happens to increase the dipolarity/polarizability and decrease the hydrogen bond- basicity of all three DES. The behavior of the fluorescent probes further revealed more relevant hydrogen-bond interactions between added water and DES constituents for ChCl:G and ChCl:EG when compared to ChCl:U. The structural differences between the adopted HBD as well the interstitial accommodation of water molecules within ChCl:U would explain the greater influence of water addition on ChCl:G and ChCl:EG, rather than ChCl:U (Pandey & Pandey, 2014).

### **1.5.2. Effect on DES’ network**

As discussed above, water clearly impacts the physicochemical properties of the DES, whether present in low or large amounts. Furthermore, investigating DES-water interactions is crucial especially that binary mixtures of DES and water have been commonly adopted in many applications already. In fact, the presence of water allows the circumvention of some of the shortcomings of DES like their relative high viscosity while maintaining their unique and appealing properties, which explains the rising interest in DES-water mixtures over the past few years. However, the high polarity of water and its propensity to interact with the hygroscopic components of the eutectic system makes it of paramount importance to check out if and how water affects the intra- and intermolecular bonds lying behind the supramolecular network of DES. Despite their relevance, the investigations of the effect of water on DES’ system are rather restricted and

mostly cover ChCl-based eutectics. Table 2 provides an overview of the reported studies dealing with the effect of water on various DES systems. This effect was examined via multiple techniques mainly NMR, Brillouin spectroscopies and neutron total scattering, not to mention the MD simulations. Some studies proposed a passage from DES to an aqueous solution of its individual components while adding water and others suggested that a transition from “water-in-DES” to a “DES-in-water” system occurs at a certain hydration level. In the former system, water is seen as another HBD (Hammond, Bowron, Jackson, et al., 2017; López-Salas et al., 2019; Zhekenov et al., 2017), thus integrating into the DES's network and subsequently strengthening the hydrogen bonds taking place between the HBA and the HBD at a low water content (Hammond, Bowron, & Edler, 2017; Weng & Toner, 2018). However, further dilution results in the weakening of the interactions that usually dominate in a DES supramolecular structure owing to the tendency of water to interact with the DES' forming compounds. The preferential hydration of chloride anions was reported in numerous papers dealing with different ChCl-based DES like ChCl:U, ChCl:G, ChCl:EG and ChCl:LA (Alcalde et al., 2019; Fetisov et al., 2018; Kaur et al., 2020; Kumari et al., 2018; Weng & Toner, 2018). Yet, when it comes to the hydration level at which the transition happens, the values are not always consistent for the same DES. For instance, the transition point varied between 15 and 51 wt% for ChCl:U (Hammond, Bowron, & Edler, 2017; Kumari et al., 2018; Posada et al., 2017; Shah & Mjalli, 2014). There are not enough studies to compare between the transition points of other DES. Few studies also proved that temperature does not affect the structure of DES-water mixtures (Celebi et al., 2019; Weng & Toner, 2018). Further studies must be conducted on other DES because although this transition is likely to occur in all the aqueous mixtures of DES, the changeover water content obviously depends on the HBA and HBD types as well as their molar ratio (Gabriele et al., 2019). Besides, a deep understanding of the impact of water on the DES' structural arrangement will surely expand the possibility of tuning the DES-water mixtures according to the desired applications.

Table 2. Summary of the studies examining the effect of water on deep eutectic solvents' systems (in chronological order)

Studied system(s)	Water content	Technique(s)	Comments	References
ChCl:U ChCl:thiourea 1:2	14- 57- 90 and 95 wt%	NMR	The characteristic chloride-HBD complex was maintained at 14 wt% water. Yet, a disruption was noticed at or above 57 wt% water content.	(M. C. Gutiérrez et al., 2009)
ChCl:U 1:2	0- 90 wt%	MD simulations	The water addition caused a decrease in the number of urea-urea and urea-Cl hydrogen bonds owing to the preferential binding of chloride anions to water and an increase in the ions diffusion. The effect of water became notable beyond 25- 30 wt% water.	(Shah & Mjalli, 2014)
ChCl:U ChCl:EG ChCl:G 1:2	2.5- 20 wt%	Pulsed field gradient NMR	Unlike the case of ChCl:G, a difference between the diffusion coefficients of the aliphatic and hydroxyl groups of choline or the HBD was observed when adding water to both ChCl:U and ChCl:EG, suggesting an interaction with water.	(D'Agostino et al., 2015)
1,2-propanediol:ChCl:water 1:1:1	0-100% (v/v)	NMR	At a water content below 50% (v/v), the NADES structure is maintained. However, further dilution leads to an aqueous solution of the free components of the NADES.	(Dai et al., 2015)
ChCl:G 1:3	25 and 50 wt%	NMR	The interactions between DES' components are weakened up to 25 wt% water and new interactions with water are observed. However, in the presence of 50 wt% water the interactions between ChCl and glycerol are completely disrupted.	(Hadj-Kali et al., 2015)

Table 2. (continued)

Studied system(s)	Water content	Technique(s)	Comments	References
ChCl:U 1:2	0.25 wt% (initial water content)	Measurement of water absorption as a function of the exposure time to the open air by Karl Fisher titration method at a temperature of $298 \pm 2$ K and a humidity of 60%	The water uptake by the DES is very high during the first hours with a rate of around 6.8 wt% per day. The rate decreased to 3.4 wt% after 10 hours then was zeroed after 65 days exposure to air with 40 wt% water content. On the other hand, water content can be easily tailored through heating. It went down from 40 wt% to 1.5 wt% after heating for 6 to 18 h.	(Du et al., 2016)
ChCl:U ChCl:EG ChCl:G 1:2	0- 1 mole fraction	MD simulations	Water molecules are integrated within the DES' network below 30 % mole fraction of water, while retaining the intermolecular interactions occurring in the three DES. However, important changes were observed in fluidity of the different species and the number of hydrogen bonds above 50% mole fraction.	(Zhekenov et al., 2017)
ChCl:U 1:2	0- 100 wt%	Brillouin and NMR spectroscopies	Both techniques perfectly agreed on the dilution range at which structural rearrangements occur in DES-water mixtures. Two distinct regions intersecting at 85 wt% DES were observed for sound propagation via Brillouin spectroscopy, while hydroxyl protons of choline were completely exchanged with water at the same hydration level, as proved by NMR.	(Posada et al., 2017)

Table 2. (continued)

Studied system(s)	Water content	Technique(s)	Comments	References
ChCl:U 1:2	ChCl:U:water mixtures at molar ratios 1:2:1, 1:2:2, 1:2:5, 1:2:10, 1:2:15 and 1:2:20 (corresponding to 6.48-67.53 wt% water)	Neutron total scattering and empirical potential structure refinement	The hydrogen bonds between choline and urea are slightly reinforced at low water levels ( $\leq 1$ mole fraction). The DES then resisted hydration between 2 and 10 mole fractions of water. At 15 mole fraction of water (83 mole % or 51 wt%), a transition from "water in DES" to "DES in water" is witnessed since the DES structural motifs disappeared and the system is rather considered as an aqueous solution of the DES components.	(Hammond, Bowron, & Edler, 2017)
ChCl:malic acid 1:1	2 mole equivalents of water (11.62 wt%)	Neutron total scattering and quasi-elastic neutron scattering	Water contributes to the hydrogen bonding structure of the DES by acting as a second smaller HBD at this hydration level. Water is sequestered into the DES by mostly interacting with the ammonium group of choline whilst preserving the interactions between the DES' components.	(Hammond, Bowron, Jackson, et al., 2017)
ChCl:U 1:2  ChCl:U:water 1:2:3	17 wt% for the hydrated DES	MD simulations	The anhydrous DES mainly consists of hydrogen bonds between urea and the chloride anions. These hydrogen bonds were disrupted in the hydrated DES since water tends to interact with chloride ions. In addition, some of urea-chloride hydrogen bonds are replaced by urea-water hydrogen bonds.	(Fetisov et al., 2018)

Table 2. (continued)

Studied system(s)	Water content	Technique(s)	Comments	References
Binary systems of 1:2 ChCl:G DES/water or glycerol/water	0-100% mole fraction (in 5% intervals) Or 0.9 mole fraction for MD simulations	FTIR and Raman spectroscopies and MD simulations	Results analysis by a multivariate method detected five species in the DES-water mixture: pure water, DES, DES-water association, glycerol and glycerol-water association. The DES-water interactions dominate over DES-DES interactions at 0.9 mole fraction of water. Yet, DES was identified as a highly stable distinct solvent from its constituents. MD simulations pictured the mixture of DES-water at 0.9 mole fraction of water as three different regions: a similar structure to that of pure DES, ChCl solvated by water and self-assembled glycerol molecules (Figure 8).	(Ahmadi, Hemmateenejad, Safavi, Shojaeifard, Shahsavari, et al., 2018)
ChCl:U 1:2	0-100% mole fraction	MD simulations	The ion pairing and ionic hydration within the (DES + water) mixtures were evaluated. Results showed that both choline and chloride ions were not completely hydrated even at 0.9 mole fraction of water. However, the interactions between chloride anion and the surrounding water molecules are stronger than those between choline and water. Besides, the ion pairing between choline and chloride and the ionic hydration coexist in the studied mixtures. While the ion pairing decreases with the increasing water content, the ionic hydration increases and the curves meet at 0.8 mole fraction of water.	(Gao et al., 2018)

Table 2. (continued)

Studied system(s)	Water content	Technique(s)	Comments	References
ChCl:G 1:2	0- 73.6 wt%	MD simulations	Water played both destructuring and structuring roles in ChCl:G DES. The water decreases the major type of interactions in the DES network which is the ChCl:G complex, with chloride anion serving as a bridge between the cation and the HBD. This effect was observed owing the tendency of water to solvate chloride anions. On the other hand, the direct choline-glycerol hydrogen bonds were enhanced at low water content (10.1 wt%) compared to the anhydrous DES. Water molecules were also able to replace Cl <sup>-</sup> by linking choline and glycerol. These types of interactions (choline-water-glycerol) reached a maximum at 35.8 wt% water. Overall, the chloride-bridged interactions between choline and glycerol were predominant below 21.8 wt% water.	(Weng & Toner, 2018)
ChCl:U 1:2	3.4- 58.1 wt%	MD simulations	The DES' structure is qualitatively preserved below 41 wt% of water. Above this water content, water tends to solvate chloride anions as well as choline cations, thus leading to a transition from DES to an aqueous solution of ChCl and urea.	(Kumari et al., 2018)

Table 2. (continued)

Studied system(s)	Water content	Technique(s)	Comments	References
ChCl:U ChCl:methylurea ChCl:EG ChCl:G 1:2  ChCl:glucose ChCl:xylitol 2:1  ChCl:OA ChCl:glutaric acid 1:1	Measured water absorption from air as a function of time (up to 4-8h) at a temperature of $22 \pm 2$ °C and a humidity of 32%	Attenuated total reflectance infrared spectroscopy (ATR- IR) and perturbation- correlation moving- window two- dimensional correlation IR spectra techniques (PCMW2D-COS)	All the studied DES are hygroscopic but their order for the absorption capacity is not in line with that of the absorption rate. Thus, a high absorption rate does not necessarily mean a high capacity. ChCl:glucose and ChCl:xylitol were considered for the investigation of the water absorption process. Results have shown that water molecules are attracted into the bulk of DES first, followed by their surface absorption. The early water absorption increases with the number of hydrophilic groups. Further water absorption depends on the strength of the hydrogen bonds between DES' components. This explains why ChCl:glucose, with a higher number of hydrophilic groups, presents a higher rate but a lower absorption capacity when compared to ChCl:xylitol.	(Y. Chen et al., 2019)

Table 2. (continued)

Studied system(s)	Water content	Technique(s)	Comments	References
Resorcinol:Hexylresorcinol:Tetraethylammonium bromide 1.25:1:1	0-100 wt%	Brillouin and NMR spectroscopies	Both techniques led to the observation of two distinct behaviors, below and above 70 wt% DES, thus reflecting the presence of two hydrogen bond networks: a DES network at low water content and another water network at high water content.	(Posada et al., 2019)
ChCl:malic acid 1:1	4- 60 wt%	Brillouin and NMR spectroscopies	Two different behaviors were observed when varying the ratio of ChCl:malic acid to water. These two regimes are explained by the transition from "water-in-DES" to "DES-in-water" system. This transition point occurred at 60- 70 wt% DES, as supported by Brillouin spectroscopy results, chemical shifts, self-diffusion coefficients and the relaxation times obtained via NMR.	(Roldán-Ruiz et al., 2019)

Table 2. (continued)

Studied system(s)	Water content	Technique(s)	Comments	References
<p>ChCl:U:water 1:1.95:1.67 (equivalent to 10.5 wt% water)</p> <p>ChCl:EG:water 1:1.89:1.33 (equivalent to 8.5 wt% water)</p> <p>ChCl:G:water 1:1.96:0.97 (equivalent to 5.3 wt% water)</p>	Further addition of 10 wt% or 90 wt% of water to the ternary DES	NMR	The most marked hydrogen bonds in urea-based DES are the ones between hydroxyl protons of choline and water as well as between methyl groups of choline and urea. No correlation has been detected between urea and water. On the other hand, interactions between all species were observed in ChCl:G:water, but glycerol-water interactions were the weakest. In ChC:EG:water, and unlike the other two DES, strong ethylene glycol-water interactions were detected. After 10 wt% dilution, the DES' structures were preserved. However, after 90 wt% dilution the mixtures are best described as aqueous solutions of individual compounds.	(Delso et al., 2019)
ChCl:LA 1:1; 1:1.5; 1:2; 1:2.5	1 ChCl: 1 lactic acid: $j$ H <sub>2</sub> O ( $j = 1-10$ ) for DFT and up to 22 wt% for MD simulations	DFT calculations and MD simulations	The DES consists of HBA:HBD clusters which are diluted upon water absorption. Water tends to interact with Cl and to a lesser extent with choline and lactic acid. Yet, the presence of water in the studied composition range does not disrupt the HBA:HBD hydrogen bonding of the DES.	(Alcalde et al., 2019)

Table 2. (continued)

Studied system(s)	Water content	Technique(s)	Comments	References
ChCl:DEG (n=2) ChCl:TEG (n=3) ChCl:PEG 200 (n~4) 1:3  (with n the number of ethylene glycol units)	0-75 wt% D <sub>2</sub> O	FTIR and NMR	Both NMR and FTIR results showed that the interactions between DES' components are gradually weakened by the addition of up to 50 wt% water but the supramolecular structures were somehow maintained. Further dilution led to the complete dissociation and hydration of the DES at 75 wt%.	(Gabriele et al., 2019)
Resorcinol:U:ChCl 3:2:1	0-75 wt%	Brillouin spectroscopy, NMR, neutron scattering, MD simulations and DSC	Water acts as another HBD or HBA at 75wt% DES by strongly interacting with the compounds forming the ternary DES resorcinol:ChCl:U without highly affecting the hydrogen bonds between them. At this point, the system is known as "water in DES" with the lowest DES content or highest dilution point. Further, this mixture results in a new deeper quaternary eutectic, presenting a lower melting point than the corresponding ternary DES and water.	(López-Salas et al., 2019)
ChCl:U ChCl:EG 1:2	0-100 wt%	MD simulations	Slight changes in hydrogen bonds numbers and radial distribution functions were observed at a water content lower than 5 wt%. While the microscopic structure of both DES is massively affected between 5 and 40 wt% of water. Above 40 wt%, both DES lose their intermolecular structure due to dissolution in water and thus the studied parameters barely change. Besides, the structure of DES-water is not affected by the temperature.	(Celebi et al., 2019)

Table 2. (continued)

Studied system(s)	Water content	Technique(s)	Comments	References
RAMEB:Lev 1:27	2.5- 60 wt%	NMR	The diffusion coefficients of the mixture's components revealed two well differentiated behaviors, at a cross-over composition of 72 wt% DES, as the water content varied. This was explained by the predominance of the "water-in-DES" system above 72 wt% DES and a prevalence of the "DES-in-water" system below that same composition.	(El Achkar, Mofawad, et al., 2020)
ChCl:EG 1:2	3.7- 60.3 wt%	MD simulations	The nanostructure of ChCl:EG DES is maintained up to 40 mol% water (13.2 wt%). Between 27.6 and 43.2 wt%, a transition from DES-like structure to water-like structure is noticed. This transition is accompanied by the preferred hydration of chloride, the tendency of water to interact with choline's ammonium group and the increased hydrogen bonding between ethylene glycol molecules.	(Kaur et al., 2020)

Table 2. (continued)

Studied system(s)	Water content	Technique(s)	Comments	References
ChCl:EG 1:2 and 1:3	0-87 wt%	DSC	When studying the phase behavior of ChCl:EG as a function of water content, two distinct thermal phase behaviors were detected at a cross-over composition of 30 wt% water content. When the latter is below 30 wt%, no water crystallization is observed and the glassy phase behavior of the pure DES is preserved. However, when the water content is above 30 wt%, there is a coexistence of ice which is reflected by the crystallization and a residual liquid phase, made of water and rich in DES components, called maximally freeze-concentrated solution. In this latter case, water is thought to be trapped via strong interactions between water and DES components.	(Jani et al., 2020)

**ChCl:** choline chloride; **DEG:** diethylene glycol; **DSC:** differential scanning calorimetry; **EG:** ethylene glycol; **FTIR:** Fourier-transform infrared spectroscopy; **G:** glycerol; **HBA:** hydrogen bond acceptor; **HBD:** hydrogen bond donor; **LA:** lactic acid; **Lev:** levulinic acid; **MD:** molecular dynamics; **NMR:** nuclear magnetic resonance spectroscopy; **OA:** oxalic acid; **PEG:** polyethylene glycol; **RAMEB:** randomly methylated  $\beta$ -cyclodextrin; **TEG:** triethylene glycol; **U:** urea.

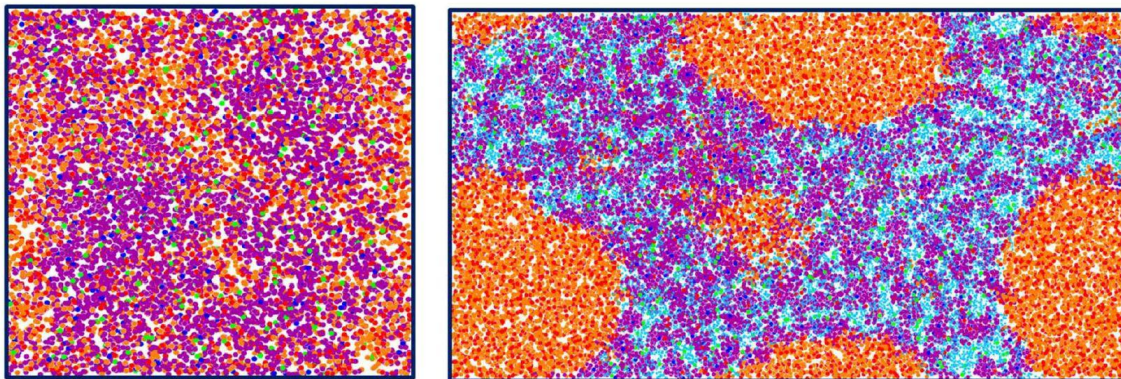


Figure 8. Snapshots from molecular dynamics simulations of ChCl:G (left) and ChCl:G-water system (right) at 0.9 mole fraction of water. Purple, dark blue and green points represent the carbon, nitrogen and chlorine atoms of choline chloride, respectively. Orange points represent the carbon atoms of glycerol. Red and light blue points represent oxygen atoms and water molecules, respectively. Reproduced from (Ahmadi, Hemmateenejad, Safavi, Shojaeifard, Shahsavari, et al., 2018) with permission from the PCCP Owner Societies

## 2. Impact of DES on living systems

Despite their appealing features, namely their green and simple preparation from accessible and low-cost materials, low melting point, non-flammability, thermal and chemical stability, and mostly tunability, a major DES issue remains to be addressed: their safety. Ever since their emergence, DES were always presumed to be non-toxic owing to the well-known safety of their forming compounds. Yet, their toxicity and biodegradability must be investigated to refer to them as biocompatible and environmentally friendly solvents. In 2013, Hayyan *et al.* were the first to directly tackle this issue by reporting a short communication under the title “Are deep eutectic solvents benign or toxic?” (M. Hayyan, Hashim, Hayyan, et al., 2013). Surprisingly, it was found that the studied ChCl-based DES were even more cytotoxic than their individual components towards brine shrimp but were non-toxic towards Gram-positive and Gram-negative bacteria. Thereafter, several toxicity studies, mostly dealing with ChCl-based DES and NADES, were performed toward different biological systems. The upcoming sections highlight and discuss the results of the reported *in vitro* and *in vivo* toxicity studies.

### 2.1. *In vitro* toxicity studies

Various organisms were considered for the *in vitro* toxicity studies of DES notably Gram-positive and Gram-negative bacteria, yeast, fungi, plants along with human, mouse, and fish cell lines.

#### 2.1.1. Microorganisms

Microorganisms were strongly adopted as models for DES' toxicity related studies. Dealing with the most studied DES that are based on ChCl, some studies found no bacteria inhibition (M. Hayyan, Hashim,

Hayyan, et al., 2013; Y. Huang et al., 2017) while antibacterial and antifungal activities were reported by other studies at high concentrations (EC50 ranging between 275 and 532 mM toward *E.coli*) (Juneidi et al., 2015; Wen et al., 2015). Zhao et al. highlighted the important effect of the HBD on the overall toxicity of DES by examining the antibacterial effect of twenty different ChCl-based DES and revealed the toxicity of DES comprising an organic acid (B.-Y. Zhao et al., 2015). Likewise, most of the NADES tested by Radošević's group inhibited the growth of microorganisms and the most antimicrobial activity was observed with citric acid-based ones. This effect might be linked to the acidity of organic acid-based NADES and to the organic acids which are toxic but to a lesser extent, compared to their corresponding DES (Radošević et al., 2018). Whereas DES exhibited lower toxicity than their forming compounds towards four fungi strains (Juneidi et al., 2016).

### 2.1.2. Invertebrates, plants, and fish

The effect of DES on invertebrates like brine shrimp (*Artemia salina* Leach), plants like wheat and garlic, as well as *Cyprinus carpio* fish was evaluated by a limited number of studies. It is worth mentioning that the brine shrimp cytotoxicity assay is considered for preliminary assessment of cytotoxicity. When testing the cytotoxic effect of DES on brine shrimp, both ChCl- and methyltriphenylphosphonium-based DES turned out to be much more cytotoxic than the individual compounds forming the DES suggesting a possible synergistic effect between DES' components (M. Hayyan, Hashim, Al-Saadi, et al., 2013; M. Hayyan, Hashim, Hayyan, et al., 2013). On the other hand, although being toxic to hydras and garlic, ChCl- and ChAc-based DES were less toxic than their forming compounds (Wen et al., 2015). Likewise, both ChCl- and N,N-diethyl ethanol ammonium chloride (EAC)-based DES were less toxic on *Cyprinus carpio* fish than their forming compounds (Juneidi et al., 2015, 2016). DES based on ChCl did not inhibit wheat seed germination (Radošević et al., 2015).

### 2.1.3. Cell lines

The majority of the DES' biocompatibility studies rely on the use of human, fish, and mice cell lines. Besides, these studies almost solely cover the effect of ChCl-based DES. For instance, ChCl:glucose and ChCl:G DES presented a low cytotoxicity (EC50 > 5mM), while ChCl:OA showed a moderate cytotoxicity (0.1 mM < EC50 < 5mM) toward CCO fish cell line and MCF-7 human tumor cell line (Radošević et al., 2015). Similarly, the only NADES having an organic acid like malonic acid as an HBD and not having water as a third component was the most lethal among the ChCl-based NADES (having sugar or glycerol as HBD) tested towards human and mice cancer cell lines (M. Hayyan et al., 2016). Four ChCl-based DES, tested toward 6 human cell lines, turned out to be relatively toxic and the effect was cell line-dependent (M. Hayyan et al., 2015). Contrarily, ChCl:U, ChCl:G, and ChCl:EG exhibited low cytotoxicity toward both CCO fish and MCF-7 human cell lines (Cvjetko Bubalo, Jurinjak Tušek, et al., 2015). Moreover, ChCl:glucose and ChCl:fructose presented lower cytotoxicity toward several human cell lines when compared with N,N-diethyl ethanol ammonium chloride:triethylene glycol (EAC:TEG) whose toxicity is attributed to its acidic pH compared to

the neutral sugar-based DES. The cytotoxicity of EAC:TEG is also driven by its redox stress inducement and its higher capacity to perforate the cell membranes, owing to the possible interactions of its constituents with the cell membrane. However, in this same study, similar EC50 values were obtained for pure DES/NADES and their aqueous solutions. Yet, lower EC50 values were observed with the aqueous solutions of the individual components. Thus, the authors suggested the spontaneous intracellular association of the components to form the DES may minimize the toxic effects of the individual components present in the cells (Mbous, Hayyan, Wong, et al., 2017).

#### **2.1.4. Effect of DES composition on the overall toxicity**

The toxicity studies reported to date do not actually provide a straightforward answer about whether DES are toxic or not. It is a rather complex matter and yet so many insights can be drawn from examining these studies. In fact, several factors can affect the overall toxicity of DES, such as the choice of the HBD. Many studies linked the high toxicity of some DES to the use of organic acids as HBD (Halder & Cordeiro, 2019; M. Hayyan et al., 2015, 2016; Radošević et al., 2015; Radošević, Železnjak, et al., 2016; Radošević et al., 2018; B.-Y. Zhao et al., 2015). As mentioned earlier, Zhao *et al.* who tested 20 different ChCl-based DES on bacteria concluded that amine-, alcohol- and sugar-based DES did not inhibit bacterial growth, but organic acid-based DES showed a significant inhibitory effect due to the acidic pH (B.-Y. Zhao et al., 2015). Contrarily, Mitar *et al.* tested 8 organic acid-containing NADES in presence of 10 wt% water, and no growth inhibition was noticed in three human cell lines in the studied concentration range (500- 2000 mg/mL) (Mitar et al., 2019). When testing the first three types of DES, it turned out that type III which is the most commonly used is the least toxic while type I based on an organic salt and a metal salt is the most toxic (Juneidi et al., 2015). The type of HBA also impacts the overall toxicity of DES. Haražna *et al.* tested the cytotoxicity of ternary DES based on ChCl, 1-ethyl-3-methylimidazolium chloride, or tributylmethylammonium chloride as HBA and a binary mixture of microorganism-derived 3-hydroxycarboxylic acids as HBD. Cytotoxicity test showed moderate toxicity of the DES towards MEF 3T3 mouse embryonic fibroblast cells, except for ChCl-based DES which were non-toxic at the studied concentration range (100- 500 µg/mL) (Haražna et al., 2019). Similarly, Juneidi *et al.* concluded that ChCl-based DES were less toxic than EAC-based DES (Juneidi et al., 2015). In their study, Macário *et al.* adopted different tetraalkylammonium chloride as HBA and ethylene glycol or propanol as HBD. Although all the DES and their starting materials were not considered to be hazardous to the aquatic environment, increased toxicity with the increase of the alkyl side chain length was noticed explained by a higher reactivity with biological membranes and their proteins (Macário, Jesus, et al., 2018). The same group highlighted once more the important contribution of the HBA since the cytotoxicity of tetrabutylammonium chloride resulted in the cytotoxicity of all the corresponding DES, regardless of the HBD type used (Macário et al., 2019). Some studies also revealed how the HBA:HBD molar ratio affects the toxicity of DES (Ahmadi, Hemmateenejad, Safavi, Shojaeifard, Mohabbati, et al., 2018; Macário, Ventura, et al., 2018). For instance, the transition from 1:3 to 1:1 ChCl:HBD DES transformed the effect on *E. coli* from non-toxic (M. Hayyan, Hashim, Hayyan, et al., 2013) to lethal (Wen

et al., 2015). Few studies consider that the presence of water leads to a decrease in the cytotoxic profile of the DES (M. Hayyan et al., 2016; Mbous, Hayyan, Wong, et al., 2017).

### 2.1.5. Importance of the studied organism

Different toxicity responses can result from different organisms when exposed to the same solvents (Radošević et al., 2018). As mentioned earlier, ChCl-based DES showed no toxicity against bacteria but were lethal to brine shrimp (M. Hayyan, Hashim, Hayyan, et al., 2013). Likewise, despite their non-inhibitory effect on bacteria (M. Hayyan, Hashim, Hayyan, et al., 2013) and fungi (Juneidi et al., 2015, 2016), ChCl-based DES showed a toxic effect on *Arthrobacter simplex* (Mao et al., 2018). The toxicity of DES may thus be species-dependent and linked to different effects owing to the structural differences between various organisms. It is also worthy to mention that the adopted concentrations in the toxicity studies are questionable since researchers consider different ways for the determination of the DES' molecular weight (Florindo et al., 2014; Mitar et al., 2019) and the related equation that is taken into account is not even mentioned in most of the papers.

### 2.1.6. Mechanism of action

Few studies considered exploring the mechanism of action of DES. Cardellini *et al.* examined the *Saccharomyces cerevisiae* cells in presence of pure trimethylglycine:carboxylic acid DES. A rapid decrease in the cells' viability was explained by the cell dehydration since the mechanism of action of DES was highly correlated to that of the well-known non-toxic dehydrating agent  $\text{CaCl}_2$  (Cardellini et al., 2014). Hayyan *et al.* confirmed the rupture of the cell membrane when LDH levels increased with the DES concentration tested on MCF7 human breast cancer cells. In addition, it was found that DES did not cause DNA damage but enhanced the production of reactive oxygen species (ROS) and induced apoptosis in treated cancer cells (M. Hayyan et al., 2015). Radošević *et al.* also noticed an accumulation of ROS accompanied by a decrease in the antioxidant enzymes in plants following exposure to DES (Radošević et al., 2015). It has been assumed that when DES dissociate in cellular media, cholinium cations aggregate and disrupt the cellular membranes (Wen et al., 2015). Mao *et al.* observed a reduction in the bacterial cell membrane integrity of *A. simplex* due to the damaging effect of ChCl salt (Mao et al., 2018). Hayyan *et al.* examined the interactions between NADES and some phospholipids using a computational model. Cellular aggregation was proposed as a mechanism of NADES' cytotoxicity given their tendency to interact with HBD and HBA sites and the non-polar surfaces of phospholipids (M. Hayyan et al., 2016). A molecular dynamics study investigated the effect of aqueous solutions of eleven ChCl-based DES on 1-palmitoyl-2-oleoylphosphatidylcholine (POPC) model lipid bilayer. After being dissociated in water, chlorine ions were not inserted and the choline cation was inserted in minor quantities for some solvents whereas the hydrogen-bond donor molecules were incorporated in the lipidic bilayer. The number of inserted HBD depends on their hydrophobicity. However, the structure of the POPC lipidic bilayer does not suffer large

changes upon the insertion of the HBD (Atilhan et al., 2017). Also, the toxicity of DES was sometimes attributed to their physicochemical properties such as their viscosity and acidity.

Furthermore, some unclear results can sometimes be obtained. When studying the effect of eleven NADES (1:1 ChCl:glucose; 1:1 ChCl:citric acid; 2:1 ChCl:citric acid; 4:1 ChCl:sucrose; 1:1 ChCl:sucrose; 2:1 ChCl:tartaric acid; 2:1 ChCl:xylose; 3:1 ChCl:xylose; 1:1 citric acid:sucrose; 1:1 citric acid:glucose; 1:1 glucos:tartaric acid) on L929 fibroblast-like cells, Paiva *et al.* found some inconsistent results. For instance, ChCl:tartaric acid and ChCl:citric acid were the most toxic among tested NADES while tartaric acid:sucrose and ChCl:glucose were the least toxic. Such results underline the importance of choosing the right combination of compounds for the preparation of DES (Paiva et al., 2014). Huang *et al.* tested 13 different NADES based on ChCl or glycerol and all the solvents did not inhibit bacterial growth except for L-arginine:glycerol despite the non-toxicity of their individual compounds (Y. Huang et al., 2017). Besides, DES showed higher toxicity than their individual components in bacteria (M. Hayyan, Hashim, Al-Saadi, et al., 2013; Radošević et al., 2018; B.-Y. Zhao et al., 2015) but an opposite trend was observed in marine organisms and plants (Wen et al., 2015) as well as in some human cell lines (Mbous, Hayyan, Wong, et al., 2017). In fact, possible synergistic interactions between DES' counterparts resulting in more or less toxic DES were suggested by several studies (M. Hayyan et al., 2015, 2016; Juneidi et al., 2015; Mao et al., 2018; J. M. Silva et al., 2019). Considering DES as mixtures rather than single compounds, Macário *et al.* successfully assessed the toxicity results of some DES by the classical models of mixtures' toxicity and revealed the importance of the synergistic or antagonistic interactions between DES' components (Macário, Jesus, et al., 2018; Macário, Ventura, et al., 2018). When it comes to modeling, a highly accurate and predictive multitasking Quantitative Structure-Toxicity Relationship model was reported with a data set of 498 DES and their components under multiple experimental conditions (different measures of toxic effects, different biological targets, and presence of water). The interpretation of various molecular descriptors underlines the importance of HBD, polarizability, electronegativity as well as DES' topological properties to the overall toxicity of DES. Regarding the HBD, it was found that sugar alcohols (e.g. sorbitol and xylitol) and straight-chain alcohols (e.g. glycerol, ethylene glycol, and 1,2-propanediol) are the least toxic HBD, followed by amides (e.g. urea). While sugars (e.g. xylose, fructose, maltose, and glucose) present intermediate toxicity and the use of organic acids (e.g. oxalic acid, phenylacetic acid, citric acid, and malic acid) contributed the most to DES' toxicity (Halder & Cordeiro, 2019). Very recently, Torregrosa-Crespo *et al.* conducted the first study that considered testing pre-adapted *E. coli* cells, suggesting the need to implement new guidelines for testing DES toxicity given the limitations of the commonly adopted approaches such as the high density and viscosity of DES as well as their hydrolysis and possible interactions with the nutrients and salts present in the culture media (Torregrosa-Crespo et al., 2020).

### 2.1.7. Related uses

The relative safety of some DES pushed the researchers to consider applying these systems in various domains. The study by Macário *et al.* reveals the promising integration of DES in the pharmaceutical and

cosmetic sectors. In this study, different DES prepared using ChCl, tetramethylammonium chloride or tetrabutylammonium chloride as HBA and hexanoic acid, butanoic acid, ethylene glycol, 1-propanol, or urea as HBD, were tested on two normal and cancer human skin cell lines. Except for the toxic tetrabutylammonium chloride-based DES, the other DES were not only non-toxic but some of them even enhanced the cell viability of the normal cells (Macário et al., 2019). Having lower toxicity than dimethyl sulfoxide, trehalose:glycerol was adopted as a cryoprotective agent because of its wide thermal stability and ability to prevent crystallization at low temperatures (Castro et al., 2018). Some authors even exploited the toxic effect of some DES towards microorganisms and used them as antimicrobial solvents in biomedical applications (J. M. Silva et al., 2019; Wikene et al., 2017). While Radošević *et al.* made it clear that a promising DES for a certain application may not necessarily be environmentally friendly (Radošević, Čurko, et al., 2016).

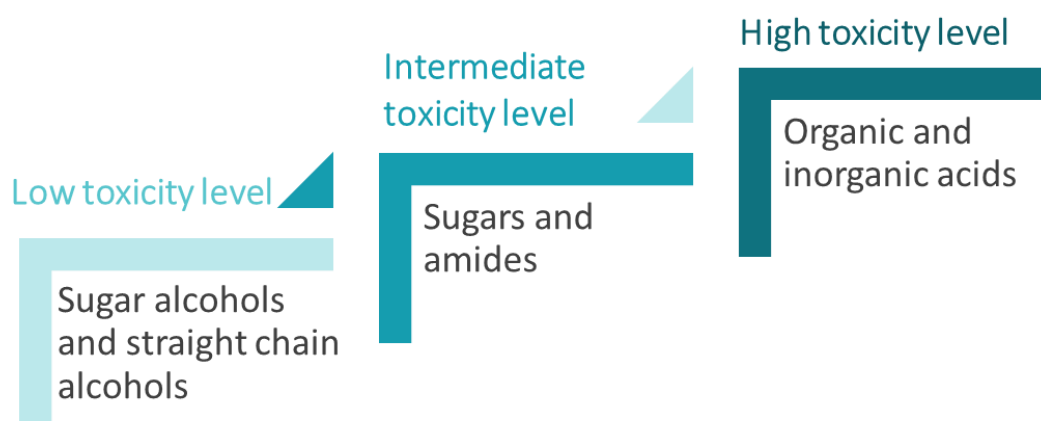


Figure 9. Classification of hydrogen bond donor types according to their toxicity level as per the multitasking quantitative structure-toxicity relationship model (adapted from Halder & Cordeiro, 2019).

## 2.2. *In vivo* toxicity studies

Owing to the novelty of this topic, the *in vivo* toxicity studies of DES are still scarce and they all consist of an oral administration of DES. The first *in vivo* study conducted on mice by Hayyan *et al.* showed a lethal effect of ChCl-based DES (using urea, glycerol, ethylene glycol, and triethylene glycol as HBD) at high concentrations with an LD50 of around 5-6 g/kg. Besides, as with bacteria, the DES was more toxic than its individual compounds (M. Hayyan et al., 2015). Chen *et al.* were aiming to use 1:2 ChCl:G DES as a drug carrier, so they tested its acute toxicity on mice. The authors considered the DES as relatively safe

with an LD50 of 7.733 g/kg (J. Chen et al., 2017). This value is somehow close to that obtained by Hayyan *et al.* for 1:3 ChCl:G (LD50= 6.39 g/kg) although different ChCl:G molar ratios were used. Moreover, despite their low *in vitro* toxicity, NADES based on ChCl and sugars were highly toxic on mice with an LD50 of around 1g/kg, which was probably ascribed to their high viscosity (Mbous, Hayyan, Wong, et al., 2017). According to Benlebna *et al.* who conducted an *in vivo* study on rats by testing a glycerol:betaine NADES extract rich in phenolic compounds, it is a question of finding the right dose and the appropriate combination of the compounds forming the NADES. Although various detrimental effects were observed in rats after an approximative daily dose of 36 g/kg (2 out of 6 rats died), this effect was better than those observed by Hayyan *et al.* and Chen *et al.* who found much lower LD50 of ChCl:G on mice. In addition, the administration of NADES extract induced dietary restriction, weight loss, adipose tissue loss, excessive water consumption, hepatomegaly, plasma oxidative stress, and increased blood lipid levels. Once more, dehydration and high viscosity are thought to cause some of these effects. The overall results might be due to a balance between the positive anti-oxidant properties of both phenolic compounds and betaine and the deleterious effects of glycerol (Benlebna et al., 2018).

### 2.3. Biodegradability

The emergence of DES has come in the first place to replace the traditional organic solvents and to overcome their environmental issues. Finding new eco-friendly solvents is a very important subject in green chemistry. This chemistry section “deals with the design of chemical products and processes that reduce or eliminate the use or generation of substances hazardous to humans, animals, plants, and the environment”, according to the International Union of Pure and Applied Chemistry (IUPAC) (Vert et al., 2012). Therefore, realizing the environmental impact and fate of DES is crucial. In other words, the biodegradability of the DES is required to define them as green systems. Only a few studies have investigated the biodegradability of DES so far. Most of these studies, presented in chronological order in Table 3, have used the closed bottle test to measure the biodegradability level. According to the Organization for Economic Cooperation and Development (OECD), chemicals are considered readily biodegradable if they reach a biodegradation level of 60% in a 10-day window within the 28-day period of the OECD 301 test (OECD, 1992). The majority of the studied DES, mainly based on ChCl, were proved to be readily biodegradable. This was attributed to the biodegradability of their forming compounds. In some cases, lower biodegradability levels were obtained and these dissimilarities between different studies can be ascribed to differences in reaction conditions, sources of microorganisms, DES concentrations, and molar ratios, as well as different time periods.

Table 3. Summary of the reported studies on deep eutectic solvents' biodegradability

Deep eutectic solvents	Initial DES concentration	Method	Time period	Source of microorganisms	Results	References
ChCl:Glucose (2:1); ChCl:OA (1:1); ChCl:G (1:2)	100 mg/L	OECD 301D- Closed bottle test	28 days	Effluent from an urban wastewater treatment plant	The biodegradability ranged between 68 and 96% thus allowing the classification of these DES as readily biodegradable. Order of biodegradability: ChCl:G > ChCl:glucose > ChCl:OA.	(Radošević et al., 2015)
8 DESs using ChCl or ChAc as HBA; and urea, acetamide, glycerol, or ethylene glycol as HBD at 1:1 molar ratio	4 mg/L	OECD 301D- Closed bottle test	28 days	Activated sludge from a wastewater treatment plant	2 out of 8 DES are biodegradable: ChCl:U and ChCl:acetamide. The other DES presented a biodegradability level lower than the pass level (<60%).	(Wen et al., 2015)
ChCl:EG (1:2); ChCl:G (1:2); ChCl:U (1:2); EAC:EG (1:2); EAC:G (1:2); EAC:MA (1:1); EAC:zinc nitrate hexahydrate (1:1); EAC: zinc chloride (1:2)	5 mg/L	OECD 301D- Closed bottle test	28 days	A secondary effluent treatment plant	All the DES are biodegradable with levels ranging between 61 and 91% observed for ChCl:G and EAC:MA DES, respectively. ChCl-based DES were clearly more biodegradable than EAC-based ones.	(Juneidi et al., 2015)
20 ChCl-based DES	3 mg/L	OECD 301D- Closed bottle test	28 days	Fresh lake water	All the tested DES are readily biodegradable with a minimum of 69.3% biodegradability after 28 days. Order of biodegradability: amine-based DES ~ sugar-based DES > alcohol-based DES > acid-based DES.	(B.-Y. Zhao et al., 2015)

Table 3. (continued)

Deep eutectic solvents	Initial DES concentration	Method	Time period	Source of microorganisms	Results	References
13 ChCl- and glycerol-based NADES using alcohols, sugars, and amino acids as HBD	3 mg/L	OECD 301D- Closed bottle test	28 days	Fresh lake water	All the NADES are biodegradable with a minimum of 70.5% for arginine:G and a maximum of 94.8% for ChCl:G.	(Y. Huang et al., 2017)
10 ChCl-based DES	5 mg/L or 43.8 µL	Winkler method or new automated chemiluminescence method	5 days or 7.5 min	Bacteria or Saccharomyces cerevisiae yeast	The DES showed higher biodegradability levels compared to ILs with values ranging between 49.2% and 71.6% for ChCl:MA and ChCl:U, respectively, in the studied time period.	(Costa et al., 2018)
9 ternary DES based on ChCl, EMImCl, or TBMACl as HBA and a binary mixture of 3 hydroxycarboxylic acids as HBD at a 1:1 or 1:2 HBA:HBD molar ratio	50 mg/L	OECD 301	21 days	Activated sludge	The analysis by HPLC-MS showed that ChCl and the HBD were fully degraded within 5- 6 days. While TBMACl and EMImCl were not degraded during the studied period of 21 days.	(Haražna et al., 2019)

**ChAc:** Choline Acetate; **ChCl:** choline chloride; **EAC:** N,N-diethyl ethanol ammonium chloride; **EG:** ethylene glycol; **EMImCl:** 1-ethyl-3-methylimidazolium chloride; **G:** glycerol; **HBA:** hydrogen bond acceptor; **HBD:** hydrogen bond donor; **HPLC-MS:** High Performance Liquid Chromatography- Mass Spectrometry; **MA:** malonic acid; **OA:** oxalic acid; **TBMACl:** tributylmethylammonium chloride; **U:** urea.

### 3. Applications

In addition to the remarkable and tunable properties of DES, the growing need for eco-friendly processes and the urge to replace conventional organic solvents led the researchers to consider these new solvents in diverse fields of application. Since their discovery, DES have been perused in organic synthesis, catalysis, electrochemistry, solubilization, and extraction, among others. This upcoming section provides a general overview of the major reported applications while focusing on the solubilization and extraction studies.

#### 3.1. Reaction medium

The environmental impact of the hazardous organic solvents can be fortunately minimized by the use of DES given the atom economy of their synthesis, their high biodegradability, and their possible recyclability and reusability, among others. That said, DES were considered in organic synthesis and can be divided into two groups depending on their role: innocent and active DES. In the former group, DES simply act as a reaction medium. Whereas in the latter, DES can have an intrinsic reagent character depending on its forming compounds or can act as a catalyst in the organic reaction. Either way, DES were successfully involved in numerous types of reactions namely redox, esterification, cyclization, condensation, and multicomponent reactions (Alonso et al., 2016). Moreover, catalysis represents a tremendously important field since it is involved in the processing of over 80% of the manufactured products. Catalysis can not only save time and energy but can also reduce the production of waste thus supporting the objectives of green chemistry. However, finding a suitable solvent in catalyzed reactions is critical since a solvent must allow better contact between reactants and catalysts and must provide an easy separation and recycling procedure. Due to their peculiar properties and the diversified nature of their possible forming compounds, DES were fruitfully applied in several acid-, base- and metal-catalyzed reactions, which were clearly covered by a comprehensive and illustrating review by Zhang *et al.* (Q. Zhang et al., 2012). When it comes to biocatalysis, water is the most used solvent. Nevertheless, the polar nature of water limits its ability to solubilize some substrates. That's why researchers were looking for non-aqueous media to be employed in biocatalytic transformations. DES were first applied as solvents in a lipase-catalyzed reaction in 2008 by Gorke et al. (Gorke et al., 2008). Since then, DES were mostly evaluated for lipase- and protease-catalyzed esterification and transesterification reactions, among others. The use of DES in both enzymatic and whole-cell biocatalysis led to promising results. There are three application principles of DES in biocatalysis: a DES can serve as a solvent, as a co-solvent or as a combined solvent and substrate, as illustrated in Figure 10. In this 2-in-1 approach, some compound(s) can act as DES component(s) and as substrate(s) at the same time. The enzyme activity and stability and the possible side reactions with DES' components must be taken into consideration when choosing the right DES for the right catalytic reaction. On a separate note, the addition of water to the DES showed considerable effects on the resulting enzymatic reaction, since

higher yields were obtained when a certain optimized water content was added, compared with pure DES (Pätzold et al., 2019).

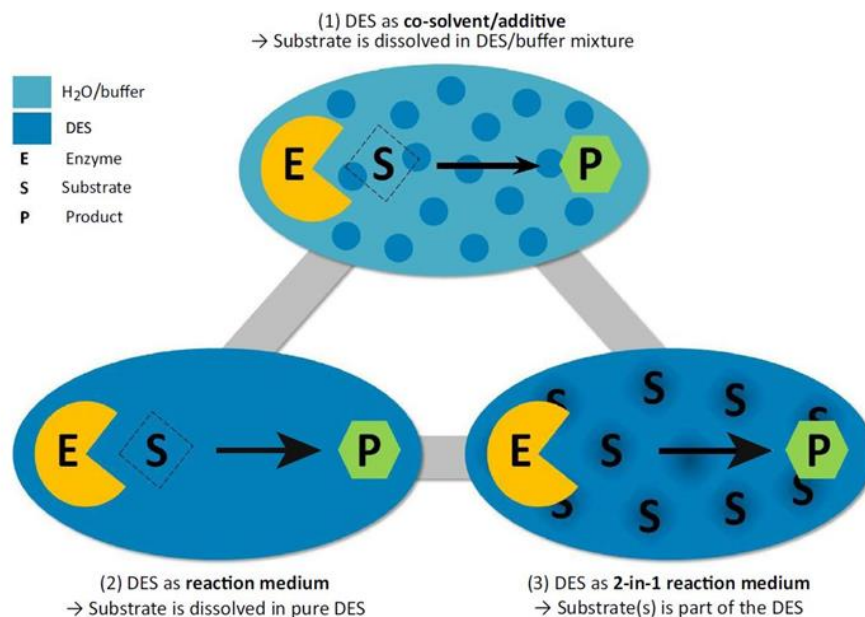


Figure 10. Three possible ways to apply deep eutectic solvents in biocatalysis (Pätzold et al., 2019)

### 3.2. Biomass processing

Biomass consists of renewable, biocompatible, and biodegradable materials derived from food crops, animal and plant wastes, forest products, and industrial residues. The conversion of biomass into valuable materials, energy, and biofuels requires a processing step. Aiming to lower the environmental impact of the traditional solvents and to improve their properties, DES are recently being explored for a greener biomass valorization. DES have been showing encouraging findings when used as solvents or cosolvents in the biomass processing due to their important solubilizing and extracting abilities. DES, mostly based on ChCl, were tested for the pretreatment of biomass and the dissolution, separation, or extraction of biomass compounds. The latter include carbohydrates (cellulose, chitin, starch), lignin (which makes 20 to 30% of the biomass), and some lignin monomeric model compounds, phenolic compounds along with some proteins, lipids, and vitamins. Besides, DES contributed to the biomass conversion by acting as solvents or catalysts (Y. Chen & Mu, 2019).

### 3.3. Electrochemistry

Electrochemistry is the first explored field of the reported DES applications. DES were considered for electrochemical applications to avoid the limitations related to the use of aqueous solutions and ionic liquids. Because of their water tolerance and their redox potential, DES were successfully applied in metal and alloy electrodeposition, electropolishing, metal separation, and electrolytes preparation (Q. Zhang et al., 2012).

### 3.4. Extraction

Conventional organic solvents and water were long considered for extraction-related applications. Nevertheless, the toxicity of the organic solvents and the exclusive selectivity of water toward polar compounds pushed the researchers to explore DES as extraction solvents owing to their greener character, tunable properties, and remarkable solubilizing ability (Fernández et al., 2018). During the past few years, DES and their natural counterparts NADES were successfully applied for the extraction of diverse compounds which mostly include natural bioactive compounds namely flavonoids, isoflavones, phenolic compounds, terpenoids, anthraquinones, and alkaloids (Chemat et al., 2019; J. Huang et al., 2019; LAVAUD et al., 2020). Some studies related to the extraction of proteins, polysaccharides, and nucleic acids were also reported (El Achkar et al., 2019). Further, the development of the hydrophobic DES in the last five years expanded DES' applications as they allowed the extraction of non-polar compounds (Florindo et al., 2019). Table 4 presents some selected examples providing a general overview of DES applications as extraction solvents. DES were considered for the extraction of various compounds from different matrices, at different water contents, and using different extraction techniques. DES have been adopted in modern extraction techniques that can overcome the limitations of conventional ones (e.g. maceration and percolation). Indeed, conventional methodologies impose the use of large volumes of hazardous solvents, long extraction periods, low extraction yields, and poor disposal and recycling practices (Zainal-Abidin et al., 2017). Several methods have been employed while using DES as extraction solvents and they mainly involve liquid-phase microextraction, ultrasound-assisted microextraction, and microwave-assisted extraction. The distribution of the used extraction techniques is illustrated in Figure 11. Liquid-phase microextraction occupies the majority (41%) of DES' extraction studies and it mainly comprises dispersive liquid-liquid microextraction (DLLME), DES-based aqueous two-phase system (ATPS), hollow-fiber liquid-phase microextraction and single drop microextraction. On the other hand, ultrasound- and microwave-assisted extractions are considered in 34% and 11% of DES extraction studies, respectively. In liquid-phase microextraction techniques, few microliters of the extracting solvent are placed in direct contact with the aqueous sample or in its headspace, thus favoring a higher degree of concentration and a lower solvent consumption (Cunha & Fernandes, 2018). The dispersive liquid-liquid microextraction consists on the dispersion of the extracting solvent in the aqueous sample solution, enabling a faster extraction of analytes present in the aqueous sample. The dispersion is usually aided by a dispersive solvent that is miscible with both extracting and aqueous phases. In some other cases, dispersion can be formed by the injection of air

bubbles, vortex-mediated bubbles formation or by the syringe sucking-injecting mechanic action (Cunha & Fernandes, 2018). The ATPS or aqueous two-phase system, used in liquid-liquid extraction processes, is usually based on two aqueous solutions that are immiscible above certain concentrations. DES-based ATPS recently emerged by replacing some phase-forming compounds with DES for a greener and more effective process. The DES-based ATPS generally involves the combined use of a DES and an aqueous solution of an inorganic salt, in the view of extraction and purification of biomolecules. However, the mechanism behind the phase formation of this system is still a controversial subject (Farias et al., 2020).

Ultrasound-assisted microextraction promotes the contact between the sample and the extracting solvent via the ultrasonic energy. It also requires low volumes of DES and short extraction times. On the other hand, microwave-assisted extraction increases the extraction kinetics by heating the solvent and the sample through non-ionizing electromagnetic irradiation (Cunha & Fernandes, 2018).

Gonzalez *et al.* recently discussed the requirements of an optimal extraction method (Gonzalez et al., 2020). These include the use of green solvents, compatibility between the extracting solvent and the method, a high efficiency, reproducibility, and sensitivity as well as maintenance of the extracts' stability. When it comes to the choice of the DES, there are important properties like the polarity and the viscosity that can affect the extraction capacity of the solvent. The high versatility of the DES and their adjustable properties offer promising extraction abilities towards various compounds. Consequently, the extracting solvent can be designed according to the choice of its forming compounds and its molar composition. Although the common high viscosity of DES might come in the way by hindering the mass transfer, it can be reduced by simply adding the right amount of water to relative hydrophilic DES. This addition may also help in changing their polarity in a way to meet the polarities of the target compounds thus enhancing their selective extraction ability. Yet, predicting the appropriate DES for a certain extraction application remains a challenge since a solvent that can highly solubilize the pure target compounds is not necessarily able to extract them most probably due to a matrix effect (Gonzalez et al., 2020). That said, different DES-related parameters must be optimized along with several other external factors to reach the maximum extraction capacity (Zainal-Abidin et al., 2017). The external factors possibly include the water content, the temperature, the extraction time, the sample to the DES ratio, among others (J. Huang et al., 2019).

Table 4. Selected examples of deep eutectic solvent-based extractions

Target compound(s)	Matrix	Deep eutectic solvent(s)	Water content	Extraction method	References
Phenolic acids (ferulic, caffeic and cinnamic acids)	Olive, almond, sesame and cinnamon oils	ChCl:EG and ChCl:G 1:2	No added water	Ultrasound-assisted microextraction	(Khezeli et al., 2016)
Rutin (flavonoid)	Tartary buckwheat hull	13 ChCl- and glycerol-based NADES; best solvent type: ChCl:G 1:1	0- 50 wt%	Ultrasound-assisted extraction	(Y. Huang et al., 2017)
Isoflavones	Soy-containing food products	17 NADES; best solvent type: ChCl: citric acid 1:1	10- 75 wt%	Ultrasound-assisted microextraction	(Bajkacz & Adamek, 2017)
Phenolic acids and tanshinone IIA	Radix <i>Salviae miltiorrhizae</i>	25 ChCl-based DES	0- 80% (v/v)	Microwave-assisted extraction	(J. Chen et al., 2016)
Terpenoids	<i>Chamaecyparis obtusa</i> leaves	ChCl:EG 1:2, 1:3, 1:4 and 1:5	No added water	Headspace solvent microextraction	(Tang et al., 2014)
Phytocannabinoids	<i>Cannabis sativa</i> plant	10 Menthol:carboxylic acids DES	No added water	Ultrasound-assisted microextraction	(Křížek et al., 2018)
Bovine serum albumin and trypsin	–	ChCl:G 1:1	No added water	ATPS	(Xu et al., 2015)
Chitin	Lobster shells	ChCl:U (1:2) ChCl:thiourea (1:1) ChCl:G (1:2) ChCl:MA (1:2)	No added water	Heating and stirring	(Zhu et al., 2017)

**ATPS:** aqueous two-phase system; **ChCl:** choline chloride; **EG:** ethylene glycol; **G:** glycerol; **MA:** malonic acid; **U:** urea.

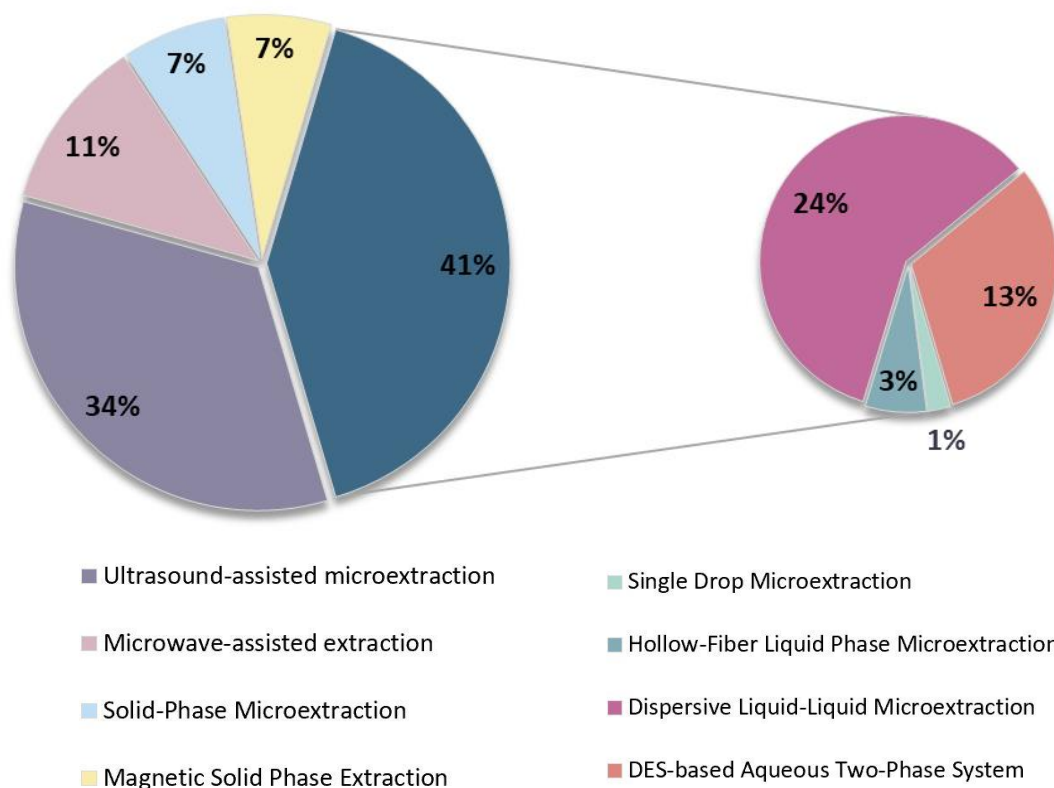


Figure 11. Distribution of the adopted extraction techniques using deep eutectic solvents. The dark blue color represents the liquid-phase microextraction techniques (based on Scopus database; May 2020)

### 3.5. Solubilization

The solubilizing ability of DES constitutes a highly attractive feature that strongly contributed to their consideration in diverse fields of applications namely organic synthesis, biocatalysis, extraction, drug delivery, and biomass processing. Indeed, DES conferred a remarkable solubility to various compounds including metal oxides (Abbott et al., 2003), gas (X. Li et al., 2008), drugs (Morrison et al., 2009), along with biological macromolecules and natural compounds (Choi et al., 2011).

In this section, we will mainly focus on the solubilization of drugs and biomolecules. Morrison and coworkers were the first to evaluate the solubility of five poorly water-soluble drugs in DES and aqueous DES mixtures. They tested ChC:U and ChCl:MA DES which were able to improve the solubility of the compounds by 5 to 22000 fold compared with their solubility in water (Morrison et al., 2009). Thereafter, the solubility of various drugs was explored by many researchers who mainly adopted ChCl-based DES and proved the potential of DES as solvents for pharmaceutical formulations (Emami & Shayanfar, 2020). On another note, Choi's group perused the solubility of some bioactive compounds and biological macromolecules in NADES to

understand the role of the newly discovered solvents at that time. They noticed a significant solubility of some bioactive compounds like rutin, paclitaxel, and ginkgolide B as well as some biomolecules such as salmon DNA, starch, and proteins (albumin and amylase), thus suggesting the engagement of the naturally occurring NADES in various biochemical reactions and physiological functions (Choi et al., 2011; Durand et al., 2020).

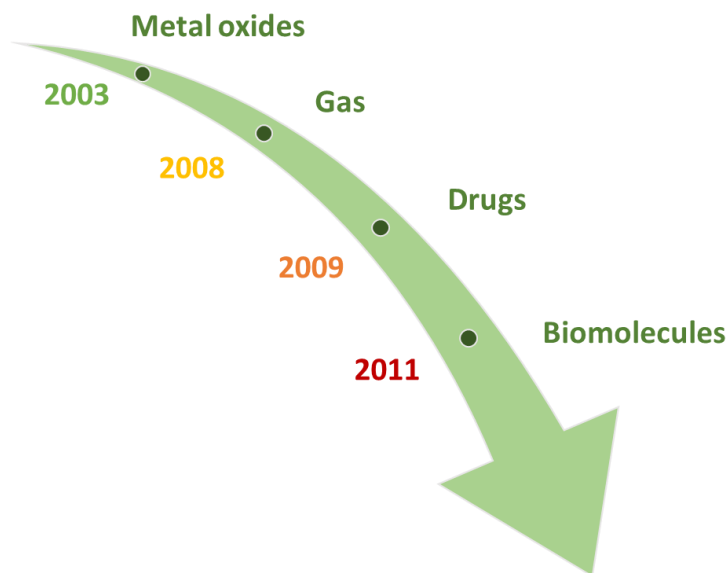


Figure 12. Compounds considered for the deep eutectic solvents' solubilization studies

Despite the number of studies further reporting high solubilization abilities of DES, the ones dealing with solute-solvent interactions as well as the underlying mechanism are still relatively limited. Several methods can be used to study the solubilization mechanism and the interactions lying between the solute and the solvent. These mainly include NMR, infrared and UV-visible spectroscopies, in addition to computational methods like MD simulations. Table 5 presents some studies investigating the dissolution mechanism in DES. The latter mainly involves hydrogen bonding interactions between the solute and the components of the DES. The solute-solvent interactions must be stronger than the solvent-solvent or the solute-solute interactions for dissolution to occur. The dissolution also depends on several factors like the HBA and HBD types, the viscosity and compartmentalized structure of the DES, the solute's polarity, the temperature and the presence of water.

Table 5. Investigations of the deep eutectic solvents' solubilization mechanism

Tested compound(s)	Deep eutectic solvent(s)	Techniques	Mechanism	References
<b>Drugs</b>				
Lidocaine (anesthetic)	ChCl:LA and $\beta$ -alanine:LA 1:1	Density functional theory and MD simulations	The efficient solvation of lidocaine by both studied DES involves a combination of strong van der Waals interactions and hydrogen bonds occurring between lidocaine and DES' components. Upon the addition of lidocaine, the DES undergoes some rearrangements to accommodate the drug, while maintaining its hydrogen bonding network. Important choline-lidocaine van der Waals interactions are observed in ChCl:LA and spatial distribution functions reveal the concentration of choline cations above the phenyl, carbonyl, and amine groups of lidocaine. The dominant hydrogen bonds occur between choline-lidocaine for ChCl:LA and between LA-lidocaine for $\beta$ -alanine:LA. The self-association between lidocaine molecules is discarded.	(A. Gutiérrez et al., 2018)
Indomethacin (a non-steroidal anti-inflammatory drug)	Aqueous solutions of TBABr:G or TBABr:EG 1:4 at a DES weight fraction ranging from 0 to 1	Determination of the Hansen solubility parameters and the thermodynamic properties	Ethylene glycol-containing DES presented a higher indomethacin solubility than glycerol-based one. This experimental result was reflected by the Hansen solubility parameters which can help in the prediction of a solute solubility in a given solvent, thus supporting the "like dissolves like" strategy. The drug dissolution in the aqueous solutions of DES is an endothermic ( $\Delta H > 0$ ) and non-spontaneous process ( $\Delta G > 0$ ). However, a higher DES weight fraction led to a greater indomethacin solubility accompanied by a decrease in $\Delta G$ and $\Delta H$ .	(Mokhtarpour et al., 2019)

Table 5. (continued)

Tested compound(s)	Deep eutectic solvent(s)	Techniques	Mechanism	References
<b>Drugs</b>				
Sulfonamides (antimicrobial)	ChC:G at 2:1, 1:1 and 1:2 molar ratios	COSMO-RS computational model	Being selected as the best solubilizing solvent among other ChCl-based DES toward sulfonamide drugs, ChCl:G solubilizing effect is explained by predominant interactions taking place between ChCl and the sulfonamide drug. The important and stable ChCl-drug interactions are proved by studying the heteromolecular affinities expressed in terms of Gibbs free energy.	(Cysewski & Jeliński, 2019)
Bupivacaine, prilocaine and procaine (anesthetics)	Arginine:glutamic acid; Arginine:OA; Arginine:tartaric acid 1:1	Density functional theory and MD simulations	Strong affinities were observed between the anesthetics and both arginine and the organic acids forming the DES. Hydrogen bonds formation between the anesthetic's carbonyl group and the hydroxyl and amine groups of the HBA and HBD of the DES are the main characteristics of the solvation mechanism.	(A. Gutiérrez et al., 2020)
<b>Biopolymers</b>				
Lignin (technical lignins and lignin monomer model compounds)	14 DES based on ChCl, alkylammonium- and alkylphosphonium chloride or urea as HBA and glycerol, ethylene glycol, urea or carboxylic acids as HBD (both neat DES and their aqueous solutions were tested)	UV-vis spectroscopy and Fourier Transform Infrared spectroscopy-based method for solubility measurements	The solubilization of lignins or lignin monomer model compounds (ferulic acid, vanillic acid, syringaldehyde, and syringic acid) in DES was driven by one of two mechanisms: hydrotropy and cosolvency. Some DES act as hydrotropes when a non-monotonic solubility enhancement is observed as a function of DES concentration. Other DES play the role of cosolvents which induce a monotonic solubility enhancement with increasing DES concentration. However, hydrotropy led to greater solubility enhancement compared with cosolvency.	(Soares et al., 2019)

Table 5. (continued)

Tested compound(s)	Deep eutectic solvent(s)	Techniques	Mechanism	References
<b>Biopolymers</b>				
Cellulose	ChCl:U; ChCl:G; ChCl:citric acid; ChCl:OA 1:2	Scanning electron microscopy and X-Ray diffraction	Although relatively low (up to 2%), the dissolution of cellulose in DES is driven by hydrogen bonding formation between DES' components and the hydroxyl groups of cellulose. The dissolution is also enhanced by the temperature and the solvent's properties such as its low viscosity. ChCl:OA, which is the least viscous exhibited the best cellulose dissolution. The regenerated cellulose presents the same structure but a transition from type I to type II of its crystalline form occurred after dissolution in DES.	(H. Zhang et al., 2020)
<b>Biomolecules</b>				
Quercetin (flavonoid)	Xylitol:ChCl:water 1:2:3	High-resolution magic angle spinning NMR	Being over 400000 times more soluble in NADES than in water, quercetin's high solubility is attributed to the formation of hydrogen bonds between quercetin and NADES' molecules.	(Dai et al., 2013)
Glucose	TBABr:Imidazole 1:2; TBABr:EG and TBABr:G 1:4	Determination of the thermodynamic properties and MD simulations	TBABr:Imidazole presented the highest glucose solubility although an isomerization from glucose to fructose was observed in this DES at high temperatures, in the absence of a catalyst. MD simulations revealed the important role of the anion and the HBD which enhanced the glucose dissolution by forming hydrogen bonds with glucose molecules.	(Mohan et al., 2017)

Table 5. (continued)

Tested compound(s)	Deep eutectic solvent(s)	Techniques	Mechanism	References
<b>Others</b>				
4-aminophthalimide, coumarin 153 and anthracene	ChCl:EG; ChCl:1,3-PD; ChCl:1,4-BD 1:3 ChCl:1,2-BD; ChCl:1,3-BD; ChCl:2,3-BD 1:4	Time-resolved fluorescence anisotropy and fluorescence correlation spectroscopy	A different behavior of the fluorescent solutes was observed in the ChCl:diol DES. Each molecule occupies a certain area of the heterogeneous DES' structure comprising both ionic and molecular regions (Figure 13). The polar 4-aminophthalimide is located in the ionic polar region, the large coumarin 153 at the interface between ionic and molecular regions, and anthracene in the molecular region due to its non-polar nature. The distinct rotational and translational diffusion of 4-aminophthalimide is ascribed to strong solute-solvent hydrogen bonding interactions, which are mostly enhanced with increasing HBD' chain length.	(Hossain & Samanta, 2018)
Glucose, 1-pentanol and phenol	ChCl:EG 1:2	Pulsed-field gradient NMR, 2-dimensional Overhauser effect spectroscopy and DLS	The presence of 10 wt% glucose in ChCl:EG resulted in a homogenous mixture owing to strong solute-solvent hydrogen bonding interactions. On the other hand, 10 wt% 1-pentanol or phenol led to aggregates formation.	(Häkkinen, Alshammari, et al., 2019)
Coumarin 151	ChCl:EG 1:2; ChCl:1,3-PD; ChCl:1,4-BD 1:3; ChCl:1,5-pentanediol 1:3.5	Infrared spectroscopy and MD simulations	Following the electrostatic field exerted by the DES (mostly by ChCl) on coumarin via coumarin's carbonyl group allowed the elucidation of the distribution, orientation, and interactions taking place in ChCl: alcohol DES in presence of a solute. The increase in chain length of the alcohol HBD reduced the hydrogen bonding affinities between alcohols' hydroxyl groups and coumarin's carbonyl group. It also affected the spatial arrangement of choline cations which concentration around the solute increased with the alcohol's chain length.	(Chatterjee et al., 2020)

**BD:** butanediol; **ChCl:** choline chloride; **COSMO-RS:** conductor-like screening model for real solvents; **DLS:** dynamic light scattering; **EG:** ethylene glycol; **G:** glycerol; **HBA:** hydrogen bond acceptor; **HBD:** hydrogen bond donor; **LA:** lactic acid; **MD:** molecular dynamics; **NMR:** nuclear magnetic resonance; **OA:** oxalic acid; **PD:** propanediol; **TBABr:** tetrabutylammonium bromide; **U:** urea

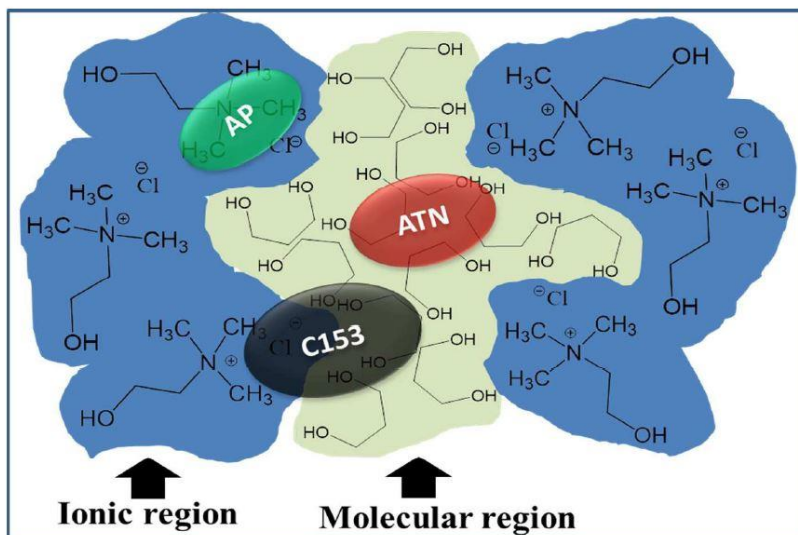


Figure 13. Illustration of the possible localization of 4-aminophthalimide (AP), coumarin 153 (C153), and anthracene (ATN) in the heterogeneous domain-like structure of ChCl:alcohol deep eutectic system Reproduced from (Hossain & Samanta, 2018) with permission from the PCCP Owner Societies.

### 3.6. Drug delivery

Water is the most preferable solvent to be used in pharmaceutical formulations. However, 40% of approved drugs and almost 90% of drugs under development are poorly water-soluble (Pedro et al., 2019). Consequently, new and safe solvents are needed to provide better drug solubility. DES interfere in different ways to overcome the limitations linked with solid drugs namely their low solubility, stability, permeation, bioavailability, and therapeutic action. As mentioned above, DES can act as solvents solubilizing active pharmaceutical ingredients. For instance, Lu *et al.* obtained a 17 to 5477 -fold increase in the solubility of non-steroidal anti-inflammatory drugs in different DES when compared with their solubility in water (Lu et al., 2016). In addition, an active pharmaceutical ingredient can be used as one of the DES' components resulting in the formation of therapeutic DES called THEDES. The concept of THEDES dates back to 1961 when the solubility and absorption of sulfathiazole were improved when using the eutectic mixture comprising sulfathiazole and urea (Sekiguchi & Obi, 1961). The conversion of active pharmaceutical ingredients into liquids may overcome the constraints associated with the use of solid forms. Although an active pharmaceutical ingredient can act as an HBA and/or HBD, most of the reported THEDES to date use it as an HBD. In some other cases, dual-function liquids are prepared by mixing two active pharmaceutical ingredients (Pedro et al., 2019). For instance, the anesthetic cream EMLA<sup>®</sup>, which is the first patented and commercialized eutectic mixture, is composed of prilocaine and lidocaine (Juhlin et al., 1980). However, a dual function DES based on ibuprofen and lidocaine was recently reported and allowed

a faster and stronger lidocaine effect when compared to EMLA (Berton et al., 2017). Furthermore, active pharmaceutical ingredients were combined with skin permeation enhancers (acting as a second DES' component) like menthol and thymol for topical and transdermal delivery. In fact, most of the studies reporting therapeutic DES focus on topical and transdermal delivery (Pedro et al., 2019). Figure 14 provides some examples of DES comprising active pharmaceutical ingredients.

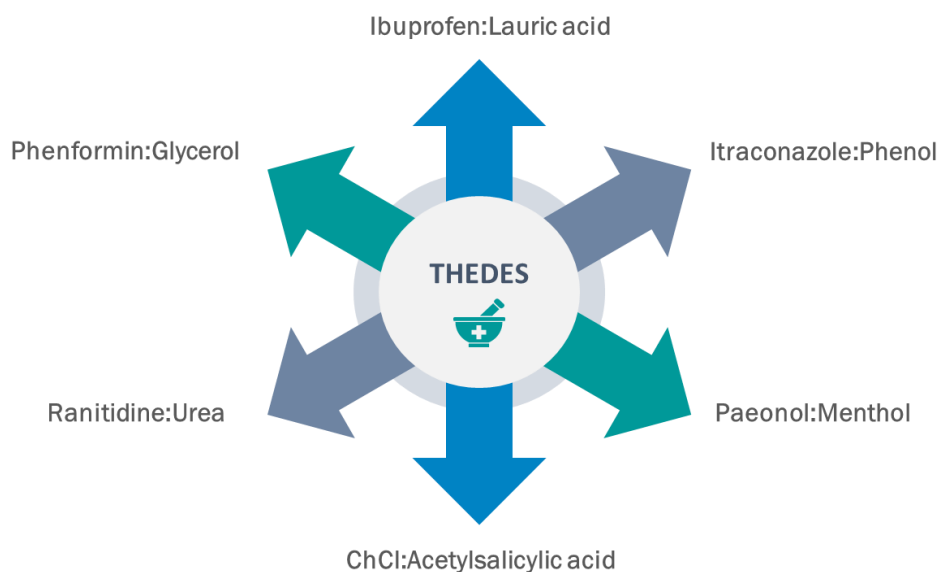


Figure 14. Examples of reported deep eutectic solvents comprising active pharmaceutical ingredients

Also, the therapeutic DES that presents a polymerizable character can contribute to the development of new (bio)polymer-based drug delivery systems while exerting a triple-action by providing the active pharmaceutical ingredient, acting as a monomer and as the synthetic medium. These systems may offer a greater therapeutic effect and a controlled drug release (Pedro et al., 2019). Also, the self-assembly of some amphiphilic molecules like surfactants and lipids in the DES has been investigated by few studies and open up the possibilities to use these self-assembled structures as drug carriers (Emami & Shayanfar, 2020). Further details regarding these studies will be given in the upcoming section.

## 4. Encapsulation systems

### 4.1. Cyclodextrins

Discovered more than 120 years ago, cyclodextrins (CD) are naturally occurring cyclic oligosaccharides resulting from the enzymatic degradation of starch.  $\alpha$ -,  $\beta$ - and  $\gamma$ -CD represent the most common native CD

comprising 6, 7, or 8 (D)- (+) glucopyranose units linked together by  $\alpha$ -1,4 glycosidic bonds. The chair conformation of glucose units gives rise to doughnut-shaped molecules. These molecules present a hydrophilic outer surface characterized by suspended primary and secondary hydroxyl groups on the narrow and wide edges, respectively, alongside a hydrophobic inner cavity marked by C-H groups and glycosidic oxygens (Figure 15). Native CD, especially  $\beta$ -CD, present a poor solubility in water due to the intramolecular hydrogen bonds taking place between hydroxyl groups of adjacent glucose molecules. Consequently, CD derivatives are produced to improve the solubility of native CD by replacing the hydroxyl groups with other polar or apolar moieties. The most adopted CD derivatives include hydroxypropylated, methylated, and sulfobutylated CD. Owing to their amphiphilic nature, CD are fortunately able to selectively encapsulate some molecules of relative low hydrophilicity and appropriate size into their cavity by forming non-covalent host-guest inclusion complexes. This property enabled CD to be involved in numerous application fields like food and aroma, pharmacy and cosmetology (Kfoury et al., 2016).

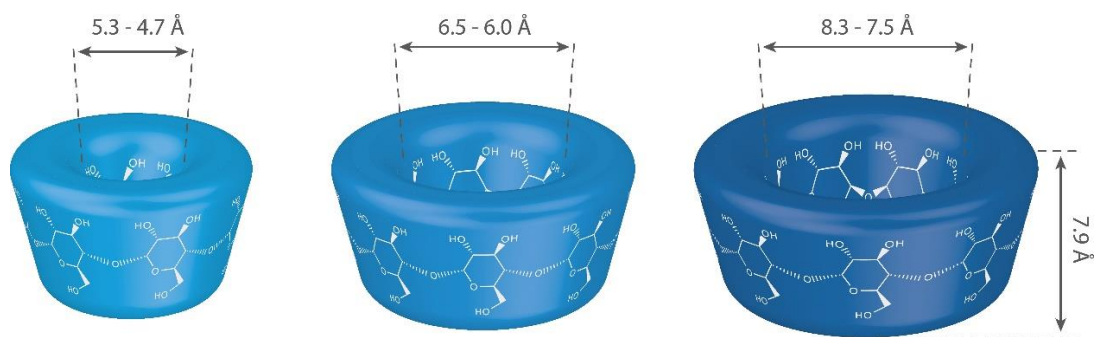


Figure 15. Illustration of the three native cyclodextrins

## 4.2. Combination of DES and cyclodextrins

There are a limited number of studies that considered combining the concept of DES with that of CD. Indeed, CD were dissolved in DES to improve their solubility, to investigate their beneficial properties, and to explore them in several domains. On the other hand, CD were used as one of DES' components in a few studies, given their large number of hydrogen bonding sites. The first CD-based mixture consisted on  $\beta$ -CD:N-methylurea (3:7 mass ratio). This combination resulted in a low melting mixture with a melting point of 80°C and successfully served as a reaction medium for Suzuki-Miyaura and Heck cross-coupling reactions (X. Zhao et al., 2014). Later, Jérôme and coworkers obtained low melting mixtures made of native CD or CD derivatives and N,N'-dimethylurea (DMU) with a melting point around 90°C and high catalytic activities were found when using these mixtures as solvents for hydroformylation and Tsuji-Trost reactions (Ferreira et al., 2015; Jérôme et al., 2014). The high melting point was beneficial in this case allowing, via simple cooling, the recycling of the catalytic system without any loss of catalytic activity. The melting point

was not affected by the size or the chemical modification of the CD. However, modified CD resulted in less viscous liquids, compared with their corresponding native CD, which also led to higher substrate conversion. The idea of complexation between the CD and the substrate was excluded after testing the acyclic CD unit,  $\alpha$ -D-methylglucopyranose (Ferreira et al., 2015; Hapiot et al., 2017). Xiong *et al.* adopted a highly efficient and recyclable catalytic system consisting of ChCl:U DES as a solvent and  $\gamma$ -CD (5 mol%) as a catalyst for the synthesis of 2-amino-4*H*-benzo[b]pyrans and 1,4-dihydropyridines via multi-component reaction (Xiong et al., 2019). After their patent related to the use of DES as an absorbent for volatile organic compounds and after revealing the additional solubilizing effect of the CD when added to ChCl:U, Fourmentin's group proved the ability of native and modified CD to form inclusion complexes in ChCl:U DES medium (Fourmentin et al., 2016; Moufawad et al., 2019). In their study, McCune *et al.* dissolved the three native CD in ChCl:U DES and ended with a solubility enhancement of more than 3 to 55 fold when compared to the solubility in water. They also proved that  $\gamma$ -CD maintains its host-guest properties in the DES (McCune et al., 2017). A recent work conducted an experimental and computational study with the aim of the investigation of the solvation of  $\beta$ -CD in ChCl:U. No aggregation of the CD was detected in the DES medium even at the highest tested concentration (800 mg/mL). The remarkable solvation ability of the DES toward CD is attributed not only to the hydrogen bonding interaction between the DES' moieties and the CD's hydroxyl groups but to the additional effect of urea which allowed the solvation of the hydrophobic walls of the CD. This conclusion also explains why  $\beta$ -CD was highly soluble in ChCl:U but not in ChCl:EG or ChCl:G (Triolo et al., 2020). A recent study considered the molecular examination of a more complex system comprising ChCl:U DES,  $\beta$ -CD, and water. In this system, added water seems to primarily interact with CD hydroxyl groups while preserving the DES' supramolecular network to some extent. The CD mobility conferred by the presence of water allowed CD molecules to form an inclusion complex with a drug within the DES as proved by NMR (Dugoni et al., 2019). Likewise, the same group once again proved the maintenance of  $\beta$ -CD's host-guest properties in neat and hydrated ChCl:U by forming inclusion complexes with volatile organic compounds (Di Pietro et al., 2019). Similarly, the hydrated ChCl:U/  $\beta$ -CD system was tested in presence of two drugs and it was concluded that CD retains both host-guest properties and chiral recognition ability (Di Pietro et al., 2020). Other researchers added  $\beta$ -CD to the aqueous solution of lactic acid-based DES to extract polyphenols. As a result,  $\beta$ -CD showed positive and sometimes negative contribution to polyphenols extraction (Chakroun et al., 2019; Georgantzi et al., 2017). On the other hand, the same group proved that methyl- $\beta$ -CD acted as a booster by enhancing the polyphenol extraction yield and by delaying the chemical degradation of the extracts, such as hydrolysis and oxidation, when added to an aqueous solution of glycine:glycerol:water (Athanasiadis et al., 2018a, 2018b). On another note, the chiral separation of threonine enantiomers was achieved via the biphasic recognition chiral extraction technique while using hydrophilic and hydrophobic DES for the two-phase formation and HP- $\beta$ -CD as one of two chiral selectors. The enantioseparation effect was evaluated by varying different conditions such as the type of DES and the water content of the hydrophilic DES (Wang et al., 2019). In another study, the effect of the addition of ChCl-based DES to the  $\beta$ -CD acting as a chiral selector in a buffer solution was

investigated in an attempt of separation of chiral drugs. The presence of DES (at a concentration of 1% (v/v)), especially ChCl:U, improved the separation efficiency when compared to  $\beta$ -CD alone, thus suggesting a synergy between  $\beta$ -CD and the DES (Mu et al., 2019).

### 4.3. Liposomes

Being one of the most studied encapsulation systems, liposomes are vesicles consisting of an aqueous core surrounded by one or more lipid bilayers (Anwekar et al., 2011). They are mainly composed of phospholipids which present a hydrophobic tail (alkyl chains of fatty acids) and a hydrophilic head (phosphate and polar groups). The amphiphilic nature of phospholipids leads to their spontaneous self-assembly in an aqueous medium. Liposomes, which can be prepared by various techniques, usually range between 20 nm and up to several micrometers. Subsequently, liposomes can be classified according to their size, lamellarity, and preparation method (Immordino et al., 2006). The liposomes' features, namely their mean size, polydispersity index, zeta potential, permeability, encapsulation efficiency, drug release, and stability, largely depend on their lipid composition and method of preparation (Maherani et al., 2011). Furthermore, these lipid vesicles were applied in several domains like pharmaceutical and medical research, food science, and cosmetics given their biocompatibility, their cell membrane-like structures, and their ability to encapsulate drugs of a wide hydrophobicity range. In fact, hydrophilic molecules can be entrapped in the aqueous compartment, hydrophobic ones intercalate in the lipid bilayer while substances with intermediate hydrophobicity can be located at the aqueous-lipid interface (Immordino et al., 2006; Maherani et al., 2011).

### 4.4. Amphiphilic self-assembly in DES

The self-organization of amphiphilic molecules can mainly be driven by the solvophobic effect as well as the solvent's cohesiveness and polarity (Arnold et al., 2015). Though still in its infancy, the use of DES as self-assembly promoting solvents has a great potential given that DES provide a similar hydrogen-bonding environment to that of water (Sanchez-Fernandez, L. Moody, et al., 2018).

Among the few studies related to the phospholipids' self-assembly in DES, a study showed, via solvent penetration experiments, that ChCl:U DES can penetrate and solubilize phosphatidylcholine (PC)- based lipids (1,2- dimyristoyl-sn-glycero-3-phosphocholine (DMPC), 1,2-dipalmitoyl-sn- glycero-3 phosphocholine (DPPC), 1,2-distearoyl-sn-glycero-3- phosphocholine (DSPC), as well as egg PC having 1-palmitoyl-2-oleoyl-sn-glycero-3-phosphocholine (POPC) as major constituent) in the absence of water. As seen in polarizing optical microscopy, the DES swells the lipids above the lipid transition temperature, and a  $\alpha$  lamellar phase spontaneously forms, which transforms into vesicles with time. As in water, the penetration temperature in DES also increases with the increasing lipid alkyl chain length (Bryant et al., 2016). The behavior of the same PC-based phospholipids was investigated in alkylammonium-based DES (HBA: ethylammonium chloride, ethylammonium bromide, propylammonium bromide, butylammonium bromide, and pentylammonium bromide), this time using glycerol and ethylene glycol as HBD. Solvent penetration

experiments revealed that phospholipids form lamellar phases and spontaneously spawn vesicles in all the tested DES. However, higher transition temperatures are required when compared with water, glycerol, or ethylene glycol, which is explained by the electrostatic interactions of the DES' cations with the phospholipids' headgroups, thus stabilizing the ordered acyl chain state and reducing the driving force of the fluid lamellar phase formation. The minimum temperature for fluid lamellar phase formation depends on both cation and anion type of the HBA in the DES but depends less strongly on the HBD used. In fact, the transition temperature first increases (with ethyl- and propylammonium salts) as a result of a competition between the alkyl chains in the DES bulk and the hydrophobic domains in the lipid bilayer. Then the transition temperature decreases with increasing cation chain length (with butyl- and pentylammonium salts) since the cation acts as a cosurfactant for the lipid. Furthermore, a higher chain melting temperature is observed with bromide-containing ethylammonium DES than with chloride-containing ones owing to the stronger binding of bromide ions to the ammonium phospholipid headgroups (Bryant et al., 2017). More recently, McCluskey and coworkers proved the formation of stable phospholipid monolayers at the air-DES interface for the first time, by adopting ChCl:G DES and several PC and one phosphatidylglycerol as phospholipids. They also obtained similar monolayer structures as those obtained at the air-water interface (R. McCluskey et al., 2019). On the other hand, Gutiérrez *et al.* tried to incorporate liposomes in DES by freeze-drying a mixture of preformed DMPC- based liposomes and aqueous solutions of DES individual components (having 20 wt% solute content), after proving that DES can be obtained via freeze-drying the aqueous solutions of their individual components. Cryo-etch SEM showed fence-like structures incorporating vesicles while confocal fluorescence microscopy confirmed the presence of liposomes ranging between 200 and 500 nm and the preservation of their membrane-like structure in DES (M. C. Gutiérrez et al., 2009).

Other papers reported the self-assembly of surfactants in DES and are presented, in chronological order, in Table 6. The surfactants' self-assembly process depends on various factors, namely the type of the surfactant (anionic, cationic, zwitterionic, or non-ionic), headgroup, tail length, charge position, and concentration of the surfactant, as well as the type of DES, its composition, and the water content. For instance, cationic surfactants are insoluble or poorly soluble in ChCl:U while they present an appreciable solubility in ChCl:G (Pal et al., 2015). The aggregation was, in some cases, more favored in pure or hydrated DES than in water which is most probably attributed to the additional electrostatic interactions taking place between DES' components and ionic surfactants.

Table 6. Investigations of surfactants' self-assembly in deep eutectic solvents

Deep eutectic solvent(s)	Surfactant(s)	Technique(s)	Main Results	References
ChCl:U 1:2	SDS (up to 100 mM)	Fluorescence probes experiments; density, viscosity, electrical conductivity, and surface tension measurements; DLS and SAXS	The hydrated ChCl:U (in presence of 5, 15, or 50 wt% water) supports the self-assembly of SDS as proved by a fluorescence dipolarity probe, electrical conductivity, and surface tension measurements, with even lower CMC values than in water. Moreover, the miscibility of non-polar organic solvents like cyclohexane, chloroform, and toluene in the DES was increased in presence of SDS owing to the formation of SDS-assisted oil-in-DES microemulsions as proved with cyclohexane (acting as the oil phase).	(Pal et al., 2014)
ChCl:G 1:2	n-alkyl TMA-based surfactants (n= 10, 12, 14, 16 or 18) (up to 50 mM)	Pyrene fluorescence probe method; electrical conductivity and surface tension measurements; DLS; SAXS; TEM and determination of thermodynamic parameters	Cationic n-alkyltrimethylammonium-based surfactants (n $\geq$ 12) self-aggregate in ChCl:G, although a less favorable aggregation efficiency is observed when compared to water. As in water, a bigger counterion like <i>p</i> -toluenesulfonate (compared with bromide or chloride) facilitates the surfactants' aggregation in the DES. All the techniques confirm the self-aggregation of C16-trimethylammonium bromide, taken as an example, into large (around 36 nm) assemblies with a non-specific shape within ChCl:G.	(Pal et al., 2015)

Table 6. (continued)

Deep eutectic solvent(s)	Surfactant(s)	Technique(s)	Main Results	References
ChCl:U 1:2	SDS (>100 mM)	Surface tension measurements; DSC; SANS; X-Ray reflectivity	The results prove the formation of micelles in pure DES, with a significantly lower CMC than that in water. SDS tends to form cylindrical rather than spherical-shaped micelles, which length increased with increasing SDS mole fraction (from $3.5 \times 10^{-4}$ to $1.7 \times 10^{-3}$ ).	(Arnold et al., 2015)
ChCl:U 1:2 or ChCl:U:water 1:2:1, 1:2:2 and 1:2:4	SDS (up to 449 mM)	SANS and SAXS	The size and shape of the SDS micelles formed in the DES depend on the surfactant concentration and the water content. The length of the micelles first increased (between 8.71 and 42.5 mM) and reached a maximum point at 42.5 mM before decreasing at higher SDS concentration (up to 424 mM). Results highlight the important role of the interaction between choline cation and the negatively charged SDS headgroup which is favored at low surfactant concentration, leading to the formation of longer and packed elongated micelles.	(Sanchez-Fernandez, J. Edler, et al., 2016)
ChCl:G 1:2	1-alkyl-3-methylimidazolium chloride ionic liquid (with n alkyl= 8, 10, 12, 14 and 16)  (up to 30 wt%)	Pyrene fluorescence probe method; SAXS and FT-IR	The solvophobic effect is lying behind the micellization of the ionic liquid in DES since lower CMC values were obtained for the ionic liquid with a longer alkyl chain, as seen in water. Solvent-solute hydrogen-bond interactions are thought to promote micelle formation.	(Tan et al., 2016)

Table 6. (continued)

Deep eutectic solvent(s)	Surfactant(s)	Technique(s)	Main Results	References
ChCl:G 1:2	n-alkyl TMA bromides (n= 12, 14 or 16) (up to 943 mM)	Surface tension measurements; SANS and X-Ray and neutron reflectivity	The cationic surfactants, which were insoluble in ChCl:U, were self-assembled in ChCl:G DES. The micellization process of these cationic surfactants in ChCl:G is similar to that occurring in water since the CMC values in DES are comparable to those in water. The CMC values decrease with the increase of the surfactant chain length, thus suggesting the micellization to be driven by the lyophobic effect. No specific solvent-surfactant headgroup interactions were detected.	(Sanchez-Fernandez, Arnold, et al., 2016)

Table 6. (continued)

Deep eutectic solvent(s)	Surfactant(s)	Technique(s)	Main Results	References
ChCl:MA 1:1 or ChCl:MA:water 1:1:2, 1:1:5, 1:1:10 and 1:1:20	n-alkyl TMA bromides (n= 12, 14 or 16)  (up to 909 mM)	Surface tension measurements and SANS	Although higher than in water, the CMC values in the DES are inversely proportional to the alkyl chain length of the surfactant. However, the presence of water in hydrated DES promotes the surfactant aggregation at lower concentrations compared with pure DES. The CMC value in 1:1:20 ChCl:MA:water was even lower than the CMC in water, which strongly suggests the involvement of DES' individual compounds (after the disruption of DES) in the micellization process. A morphological transition was observed in neat and hydrated DES from globular micelles for C12-surfactant to elongated micelles for C16-surfactant. This transition depends on both the size of the hydrophobic moiety and the type of counterion and its adsorption on the micellar interface. The major contribution is attributed to the interaction between DES' malonate anions and the surfactant's cationic headgroups.	(Sanchez-Fernandez et al., 2017)
Aqueous solutions of 5 wt% ChCl:U or ChCl:G 1:2	BMIm octylsulphate ionic liquid  (up to 120 mM)	Fluorescence probes experiments; DLS; FT- IR and UV-vis spectroscopy	The micellization of the short-chain ionic liquid is favored in the aqueous solutions of both DES, presenting lower CMC and higher aggregation numbers compared with the values in water. This effect is explained by enhanced solvophobicity and electrostatic interactions. Lower CMC and higher binding affinity between the ionic liquid and an antidepressant drug were observed in the aqueous solution of ChCl:U compared with that of ChCl:G.	(Kumar Banjar e et al., 2018)

Table 6. (continued)

Deep eutectic solvent(s)	Surfactant(s)	Technique(s)	Main Results	References
ChCl:U and ChCl:G 1:2	Dodecylsulfate surfactants with different counterions (lithium, cesium, magnesium, EMIm, BMIm, or choline) (up to 196 mM)	Surface tension measurements and SANS	Micelles form in both DES at a lower CMC than in water. The addition of dodecylsulfate surfactants in ChCl:G generates globular micelles while elongated micelles are observed in ChCl:U. The surfactant behavior not only depends on the solvent type but it is mainly driven by the counterion adsorption onto the micelle interface thus reducing the electrostatic repulsion between the headgroups. The concerned counterion may be the native counterion of the surfactant or a counterion in the solvent (choline in this case). The process also depends on the lyophobicity and the solubility of the counterion in the solvent. The latter applies to the case of ChCl:G in which the cation is soluble owing to the glycerol-dominated structure of the DES.	(Sanchez-Fernandez, S. Hammond, et al., 2018)
ChCl:G and ChCl:EG 1:2	Cetylpyridinium bromide (up to 80 wt%)	SAXS; polarized optical microscopy and rheological measurements	Various aggregates were formed in the DES as the surfactant's concentration increased. These include micelles, hexagonal phase, a bicontinuous cubic phase, and lamellar phase. The observed phase diversity is attributed to the relatively large cohesiveness of the DES reflected by the Gordon parameter as well as their charge screening. Both DES present comparable self-assembling ability with water and a better one when compared to an ionic liquid (ethylammonium nitrate).	(Q. Li et al., 2018)
ChCl:G 1:2	1 phosphocholine- and 2 sulfobetaine-based surfactants (up to 312 mM)	Surface tension measurements; X-Ray reflectivity and SANS	Globular micelles are formed in the DES in presence of the surfactants while the structure of the aggregates depends on the surfactant headgroup and tail length as well as the charge positions of the zwitterionic surfactants. The self-assembly of a mixture of two surfactants is also promoted in ChCl:G.	(Sanchez-Fernandez, L. Moody, et al., 2018)

Table 6. (continued)

Deep eutectic solvent(s)	Surfactant(s)	Technique(s)	Main Results	References
Aqueous solutions of ChCl:G 1:2, at DES/water 1/0, 9/1, 7/3, 1/1, and 0/1 weight ratios	A mixture of Tween-80 and span-20 at different weight ratios (at a fixed surfactants: DES/water: oil weight ratio of 20: 4: 76); (Isopropyl myristate is the oil used)	SAXS; TEM and DLS	DES-in-oil microemulsions were successfully formed as potential transdermal drug delivery systems by adopting a mixture of two non-ionic surfactants, while a DES-water mixture constituted the inner phase. At 1/3 tween-80/span-20 weight ratio, spherical microemulsions were obtained which size increased with the increase in DES ratio. On the other hand, a 3/1 surfactants ratio resulted in a transition from spherical to cylindrical structure as the DES ratio increased.	(Sakuragi et al., 2018)
ChCl:U and ChCl:EG 1:2 (in presence or absence of 10, 30, or 50 wt% water)	Sodium dioctyl sulfosuccinate (up to 70 mM approximately)	Conductivity and surface tension measurements; pyrene fluorescence probe method; determination of Kamlet-Taft parameters; NMR spectroscopy and DLS	The surfactant aggregates in both pure and hydrated DES but lower CMC values were obtained with DES-water mixtures and the CMC decreased with the increasing water content. The 30-50 wt% hydrated DES present even lower CMC than in water. When comparing the two DES, the aggregation is better promoted in ChCl:U. The self-assembly depends on the polarity and cohesiveness of the solvent. The additional interaction between cholinium cations and the surfactant's anion explains the favorable aggregation in DES-water mixtures (at 50 wt% water) over water itself.	(Komal et al., 2018)
Benzyltripropylammonium chloride:EG 1:3	Tween-80 (molar ratio DES/Tween-80: 0.3, 0.7, 1.3)	DLS; rheological measurements and Raman spectroscopy	The results prove the formation of reverse micelles using DES as the entrapped polar phase, cyclohexane as the oil phase, and Tween-80 surfactant. This organized system is explained by the formation of hydrogen-bonding interactions between the DES and the surfactant.	(Panda et al., 2019)

**BMIm:** 1-butyl-3 methylimidazolium; **ChCl:** choline chloride; **cmc:** critical micelle concentration; **DLS:** dynamic light scattering; **DSC:** differential scanning calorimetry; **EG:** ethylene glycol; **EMIm:** 1-ethyl-3 methylimidazolium; **FT-IR:** Fourier transform infrared spectroscopy; **G:** glycerol; **MA:** malonic acid; **NMR:** nuclear magnetic resonance; **SANS:** small-angle neutron scattering; **SAXS:** small-angle X-ray scattering; **SDS:** sodium dodecyl sulfate; **TEM:** transmission electron microscopy; **TEM:** transmission electron microscopy; **TMA:** trimethylammonium; **U:** urea.

In the course of our study, DES were first prepared using some common hydrogen bond acceptors like choline chloride, tetrabutylphosphonium bromide, and tetrabutylammonium bromide, and hydrogen bond donors such as urea, glycerol, ethylene glycol, levulinic acid, and decanoic acid. On the other hand, new liquid mixtures based on  $\beta$ -cyclodextrin derivatives, acting as hydrogen bond acceptors, were revealed for the first time. The presence of cyclodextrins could result in some interesting systems with supramolecular properties, thus called SUPRADES. Following their preparation, DES and SUPRADES were characterized by measuring their density, viscosity, and polarity. Owing to their novelty, SUPRADES were further characterized via differential scanning calorimetry, thermogravimetric analysis, and rheological studies.

Thereafter, the organization of egg phospholipids in the solvents was investigated by atomic force microscopy and polarity measurements were conducted using a solvatochromic probe. Moreover, DES were introduced into liposomes' preparation via two conventional methods (ethanol injection method and thin film hydration method), by replacing the aqueous phase with DES. The resulting preparations were then observed by optical microscopy and analyzed by dynamic light scattering.

After studying the behavior of phospholipids within the DES, we examined the effect of the DES on preformed liposomes, prepared via the ethanol injection method and composed of phospholipids and cholesterol, using atomic force microscopy. The first approach consisted of exposing the adsorbed liposomes to DES or aqueous solutions of their components, while the second approach involves suspending the liposomes in DES or aqueous solutions of their components, for different periods before their adsorption and examination. Besides, the impact of two selected choline chloride-based DES on human breast cancer cells was studied by conducting a combination of cytotoxicity and morphological studies. The effects of the DES were also compared to the effect of their individual or combined components.

Lastly, the solubilizing ability of the DES toward volatile compounds, mainly *trans*-anethole, and related essential oils was evaluated using static headspace-gas chromatography. Nuclear magnetic resonance spectroscopy was further used to check if the ability of cyclodextrins to form inclusion complexes is preserved within the SUPRADES. In addition, we assessed the effect of water and some incorporated encapsulating agents namely cyclodextrins, lipids, and surfactants on the DES' solubilization capability. Finally, the release of *trans*-anethole from the studied solvents was monitored via multiple headspace extraction technique.

## II. Solvents' preparation and characterization

### 1. Tested solvents

In the present study, a selection of type III DES was considered using choline chloride (ChCl), tetrabutylphosphonium bromide (TBPBr), and tetrabutylammonium bromide (TBABr) as HBA, along with urea (U), glycerol (G), ethylene glycol (EG), levulinic acid (Lev) and decanoic acid (Dec) as HBD. Table 7 presents the composition of the studied DES which were prepared by simply combining the HBA and HBD at a certain molar ratio, followed by stirring and heating the mixture at 60 °C until the formation of a clear and homogenous liquid. Choline chloride was dried at 60 °C for 2 weeks before use. All the other compounds were used as received. The water content of all the prepared mixtures was determined using the Karl Fisher titration method (Mettler Toledo DL31).

Table 7. Composition of the tested deep eutectic solvents

DES	HBA	HBD	HBA:HBD molar ratio	Water content (%)
ChCl:U	Choline chloride	Urea	1:2	0.33
ChCl:G	Choline chloride	Glycerol	1:2	0.05
ChCl:EG	Choline chloride	Ethylene glycol	1:2	0.06
ChCl:Lev	Choline chloride	Levulinic Acid	1:2	0.05
TBPBr:Lev	Tetrabutylphosphonium bromide	Levulinic Acid	1:6	0.04
TBABr:Dec	Tetrabutylammonium bromide	Decanoic Acid	1:2	0.02
TBPBr:EG	Tetrabutylphosphonium bromide	Ethylene glycol	1:2	0.01

On the other hand, SUPRADES were prepared using different  $\beta$ -CD derivatives as HBA, given their large number of hydrogen bonding sites (Figure 16a). Being natural cyclic oligosaccharides and holding an important encapsulation property, CD-based mixtures could lead to the formation of safe and interesting systems with unusual properties. The combination of four  $\beta$ -CD derivatives (hydroxypropyl- $\beta$ -CD (HPBCD), randomly methylated  $\beta$ -CD (RAMEB), low methylated  $\beta$ -CD (CRYSMEB) and sulfobutylether- $\beta$ -CD (Captisol®)) with levulinic acid was conducted at first and resulted in the formation of clear liquids at room temperature. Thereafter, HPBCD or RAMEB was mixed with different polyalcohols, namely glycerol, ethylene glycol, 1,3-propanediol, or 1,3-butanediol (Figure 16). The selected liquids, named SUPRADES, are presented in Table 8.

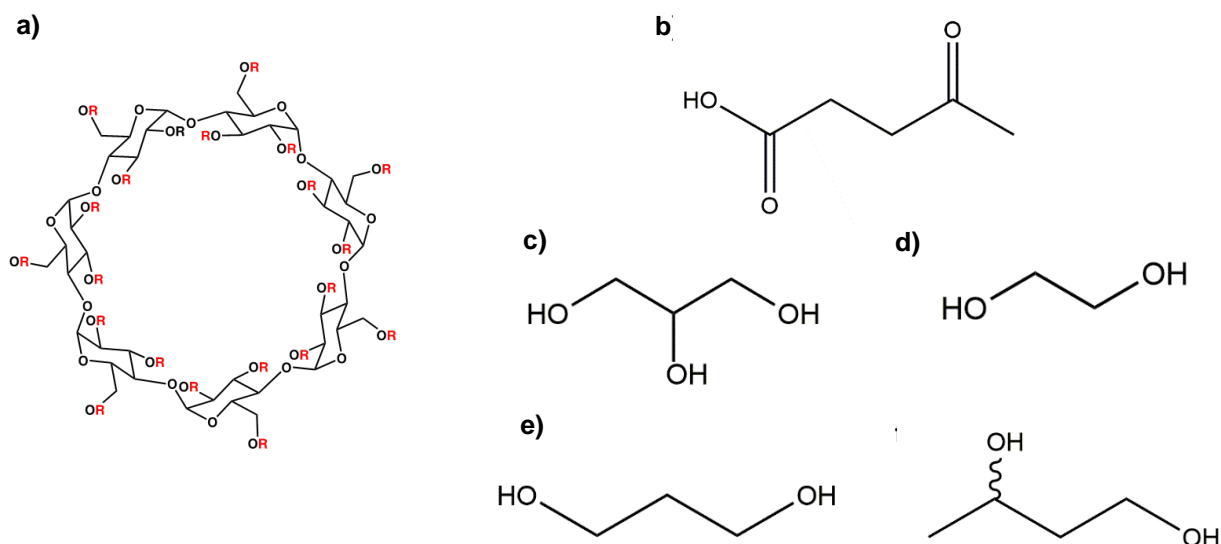


Figure 16. Structures of SUPRADES' constituents. a) General structure of  $\beta$ -CD derivatives: HP- $\beta$ -CD (degree of substitution (DS) = 4.34), R = -H or -CH<sub>2</sub>-CH(OH)-CH<sub>3</sub>; RAMEB (DS = 12.9), R = -H or -CH<sub>3</sub>; CRYSMEB (DS = 4.9), R = -H or -CH<sub>3</sub>; Captisol® (DS = 6.5), R = -H or -(CH<sub>2</sub>)<sub>4</sub>-SO<sub>3</sub><sup>-</sup> Na<sup>+</sup>; b) levulinic acid; c) glycerol; d) ethylene glycol; e) 1,3-propanediol; f) 1,3-butanediol

Table 8. Composition of the SUPRADES

<b>SUPRADES</b>	<b>HBA</b>	<b>HBD</b>	<b>HBA:HBD molar ratio</b>	<b>Water content (%)</b>
HPBCD:Lev	HPBCD	Levulinic acid	1:28	2.7
RAMEB:Lev	RAMEB	Levulinic acid	1:27	2.5
CRYSMEB:Lev	CRYSMEB	Levulinic acid	1:25	3.3
Captisol:Lev	Captisol®	Levulinic Acid	1:44	3.9
HPBCD:G	HPBCD	Glycerol	1:30; 1:40	2.4; 2.0
HPBCD:EG	HPBCD	Ethylene glycol	1:20; 1:30; 1:40	3.7 ; 3.2 ; 2.8
HPBCD:1,3-PD	HPBCD	1,3-propanediol	1:30; 1:40	3.2 ; 2.8
HPBCD:1,3-BD	HPBCD	1,3-butanediol	1:40	2.2
RAMEB:1,3-PD	RAMEB	1,3-propanediol	1:20; 1:30; 1:40	3.7 ; 3.3 ; 2.8
RAMEB:1,3-BD	RAMEB	1,3-butanediol	1:30; 1:40	2.7; 2.3

## 2. Characterization

### 2.1. Density

Density measurements were carried out using a U-shaped vibrating tube densimeter (Anton Paar, model DMA 5000 M) operating in a static mode. The factory calibration was used and verified before and after each measurement with air and tri-distilled degassed water. The DMA 5000 densimeter performs an analysis with an estimated uncertainty in density and temperature of  $\pm 0.1 \text{ kg m}^{-3}$  and  $\pm 0.001 \text{ }^\circ\text{C}$ , respectively. All measurements were performed at atmospheric pressure and temperatures ranging between 30 and 60  $^\circ\text{C}$ . Table 9 presents the experimental density values at 30  $^\circ\text{C}$ . The obtained values at the studied temperature range are all displayed in Table A1. The values were fitted using a linear equation (1) to correlate the density with the temperature and the fitting parameters (a and b) are listed in Table A2. The density decreased linearly as a function of temperature.

$$\rho = a + bT \quad (1)$$

The density values of the tested solvents are all higher than  $1000 \text{ kg m}^{-3}$  and fall in the ( $1000\text{-}1300 \text{ kg m}^{-3}$ ) range observed for the reported DES, except for TBABr:Dec which presents a lower density, following the values reported for hydrophobic DES (Florindo et al., 2019). On the other hand, SUPRADES present similar densities when compared with typical DES although they are slightly denser, most probably owing to the large number of CD hydrogen bonding sites. On another note, the density clearly depends on the choice of the HBD: a higher density is observed when an additional hydroxyl group (e.g.  $1139.0 \text{ kg m}^{-3}$  for 1:40 HPBCD:1,3-PD and  $1290.5 \text{ kg m}^{-3}$  for 1:40 HPBCD:G) or a shorter chain length ( $\rho$  1:40 HPBCD:EG  $>$   $\rho$  1:40 HPBCD:1,3-PD  $>$   $\rho$  1:40 HPBCD:1,3-BD) is considered. Likewise, the density is influenced by the HBA type and the molar ratio.

Table 9. Experimental values of the densities of the studied solvents at 30 °C

DES	$\rho$ (kg m <sup>-3</sup> )	DES	$\rho$ (kg m <sup>-3</sup> )	DES	$\rho$ (kg m <sup>-3</sup> )	DES	$\rho$ (kg m <sup>-3</sup> )
ChCl:U	1193.4	TBPBr:EG	1065.5	HPBCD:G 1:40	1290.5	HPBCD:1,3-BD 1:40	1086.8
ChCl:G	1187.4	HPBCD:Lev	1204.7	HPBCD:EG 1:20	1245.1	RAMEB:1,3-PD 1:20	1160.1
ChCl:EG	1111.9	RAMEB:Lev	1184.5	HPBCD:EG 1:30	1215.9	RAMEB:1,3-PD 1:30	1134.9
ChCl:Lev	1134.5	CRYSMEB:Lev	1207.5	HPBCD:EG 1:40	1197.1	RAMEB:1,3-PD 1:40	1118.6
TBPBr:Lev	1105.7	Captisol:Lev	1234.3	HPBCD:1,3-PD 1:30	1159.8	RAMEB:1,3-BD 1:30	1085.8
TBABr:Dec	965.4	HPBCD:G 1:30	1299.0	HPBCD:1,3-PD 1:40	1139.0	RAMEB:1,3-BD 1:40	1068.7

## 2.2. Viscosity

The viscosity was determined using a falling-ball-based microviscosimeter (Lovis 2000 M/ME from Anton Paar). The temperature was controlled to within 0.005 °C and measured with an accuracy better than 0.02 °C. A capillary tube of 1.8 mm diameter, previously calibrated as a function of temperature and angle of measurement with reference oils, was used for the measurements. The overall uncertainty on the viscosity was estimated to be 2%. All measurements were performed at atmospheric pressure and temperatures ranging between 30 and 60 °C. The results are fitted following the Vogel-Fulcher-Tammann model, described by equation (2), with a maximum average absolute deviation (AAD) of 0.31 %. The equation parameters (A, K, and  $T_0$ ), along with the AAD values, are listed in Table B1.

$$\eta = AT^{1/2} \exp \frac{K}{(T - T_0)} \quad (2)$$

The quaternary ammonium- or phosphonium-based DES present a large viscosity range varying between 33.62 and 919.52 mPa s at 30 °C for ChCl:EG and ChCl:U, respectively (Figure 17A). The viscosity obviously depends on the DES' composition. The obtained viscosity values of ChCl-based DES were compared with those reported in the literature, as shown in Table 10. A remarkable difference is observed between studies, especially with ChCl:U and ChCl:Lev, which may be attributed to the experimental method, the DES' preparation method, and the impurities like water which was previously shown to highly impact the viscosity values. On the other hand, Figure 17 B displays the viscosity of levulinic acid-based systems. CD:Lev mixtures were more viscous than the common DES (ChCl:Lev and TBPBr:Lev), except for RAMEB:Lev which presents a similar viscosity to that of ChCl:Lev (212.9 and 206.2 mPa s at 30 °C, respectively).

Nevertheless, the viscosity values decreased remarkably with increasing temperature. All CD-Lev mixtures, except Captisol:Lev, show relatively low viscosities ( $\leq 80$  mPa.s) at 60 °C. The relatively higher viscosity of Captisol:Lev can be explained by a stronger hydrogen bond network, given the higher number of HBA sites present in Captisol® compared to the other studied  $\beta$ -CD derivatives, due to the presence of the sulfonate groups. In addition, the CD:Lev mixtures were less viscous than the reported mixtures based on  $\beta$ -CD derivatives and N,N'-dimethylurea. Indeed, the latter mixtures present a melting point above 80 °C and their viscosities were at least equal to 205.0 mPa.s at 90 °C (Jérôme et al., 2014).

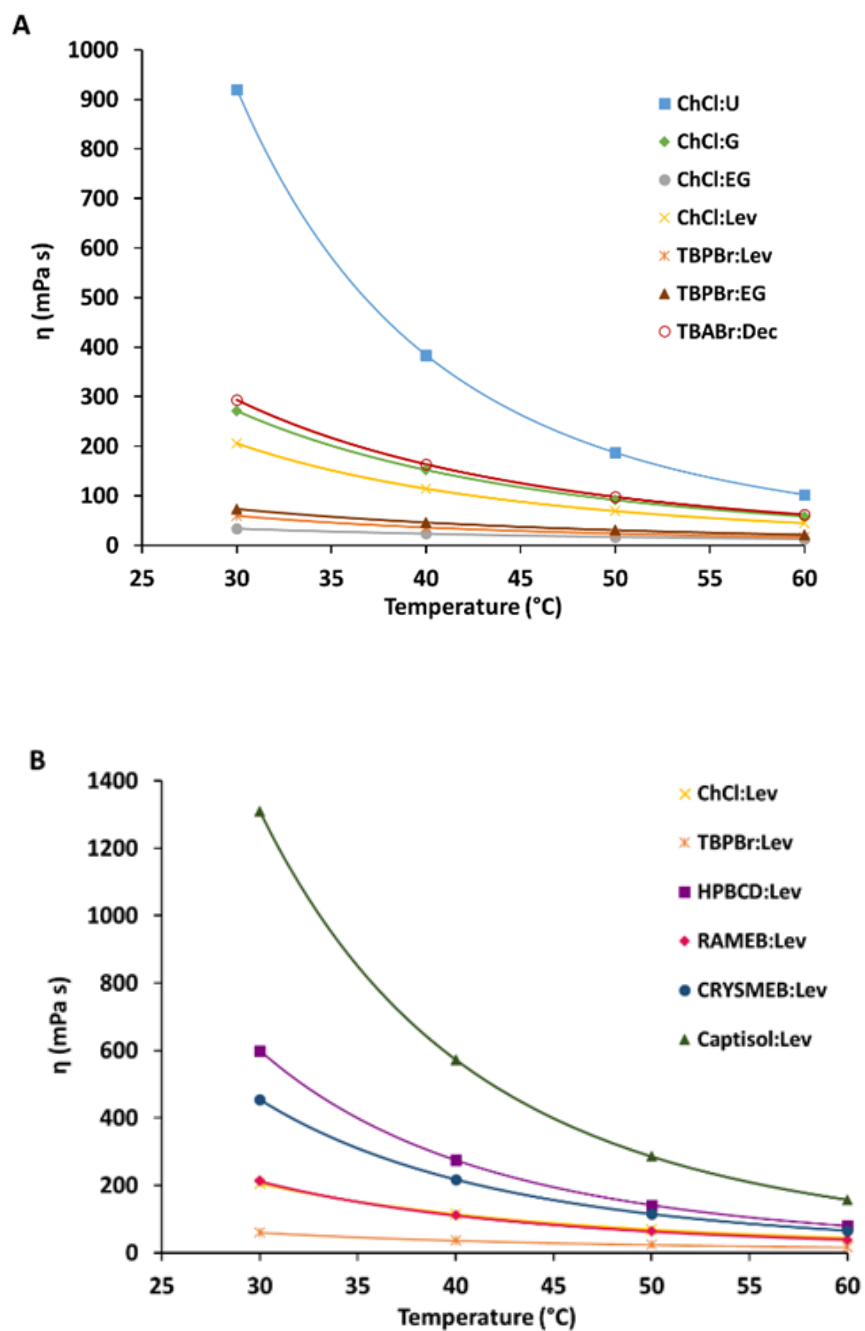


Figure 17. Experimental viscosities of the studied deep eutectic solvents (A) and the levulinic acid-containing systems (B) as a function of temperature ranging between 30 and 60 °C. The lines represent the fitted values following the Vogel-Fulcher-Tammann model

Table 10. Comparison of the viscosity values of choline chloride-based DES at 30 °C with available literature sources

<b>DES</b>	<b>Experimental viscosity (mPa s)</b>	<b>Literature viscosity (mPa s)</b>	<b>References</b>
ChCl:U	919.52	449	(D'Agostino et al., 2011)
1:2		527.28	(Yadav & Pandey, 2014)
ChCl:G	271.73	188	(D'Agostino et al., 2011)
1:2		246.79	(Yadav et al., 2014)
ChCl:EG	33.62	35	(D'Agostino et al., 2011)
1:2		32.40	(Lapeña et al., 2019b)
ChCl:Lev	206.17	164.5	(Florindo et al., 2014)
1:2		79.14	(G. Li et al., 2016)

When looking at the polyalcohol-based systems, Figure 18 reveals the effect of the HBA type on the viscosity of the system since more viscous liquids were obtained with CD compared with those based on ChCl for glycerol- (Figure 18 A) and ethylene glycol- (Figure 18 B) containing systems. Moreover, RAMEB resulted in less viscous systems than HPBCD-based ones (Figure 18 C and D). In addition to the effect of the HBA, the viscosity is affected by the molar ratio since the viscosity decreases when the HBD molar fraction increases ( $\eta$  1:20 >  $\eta$  1:30 >  $\eta$  1:40). Furthermore, Table 11 highlights the influence of the HBD type on the viscosity of the CD:polyalcohol systems. Indeed, the viscosity increases with the alkyl chain length of the HBD ( $\eta$  HPBCD:1,3-BD >  $\eta$  HPBCD:1,3-PD >  $\eta$  HPBCD:EG and  $\eta$  RAMEB:1,3-BD >  $\eta$  RAMEB:1,3-PD). These results are in accordance with those observed by Mulia and coworkers who studied several ChCl-based DES using polyalcohols like ethylene glycol, glycerol, propanediols, and butanediols as HBD (Mulia et al., 2019). Besides, a major rise in the viscosity value was witnessed when an additional hydroxyl group was present. For instance, HPBCD:G 1:40 was 10 times more viscous than HPBCD:1,3-PD 1:40.

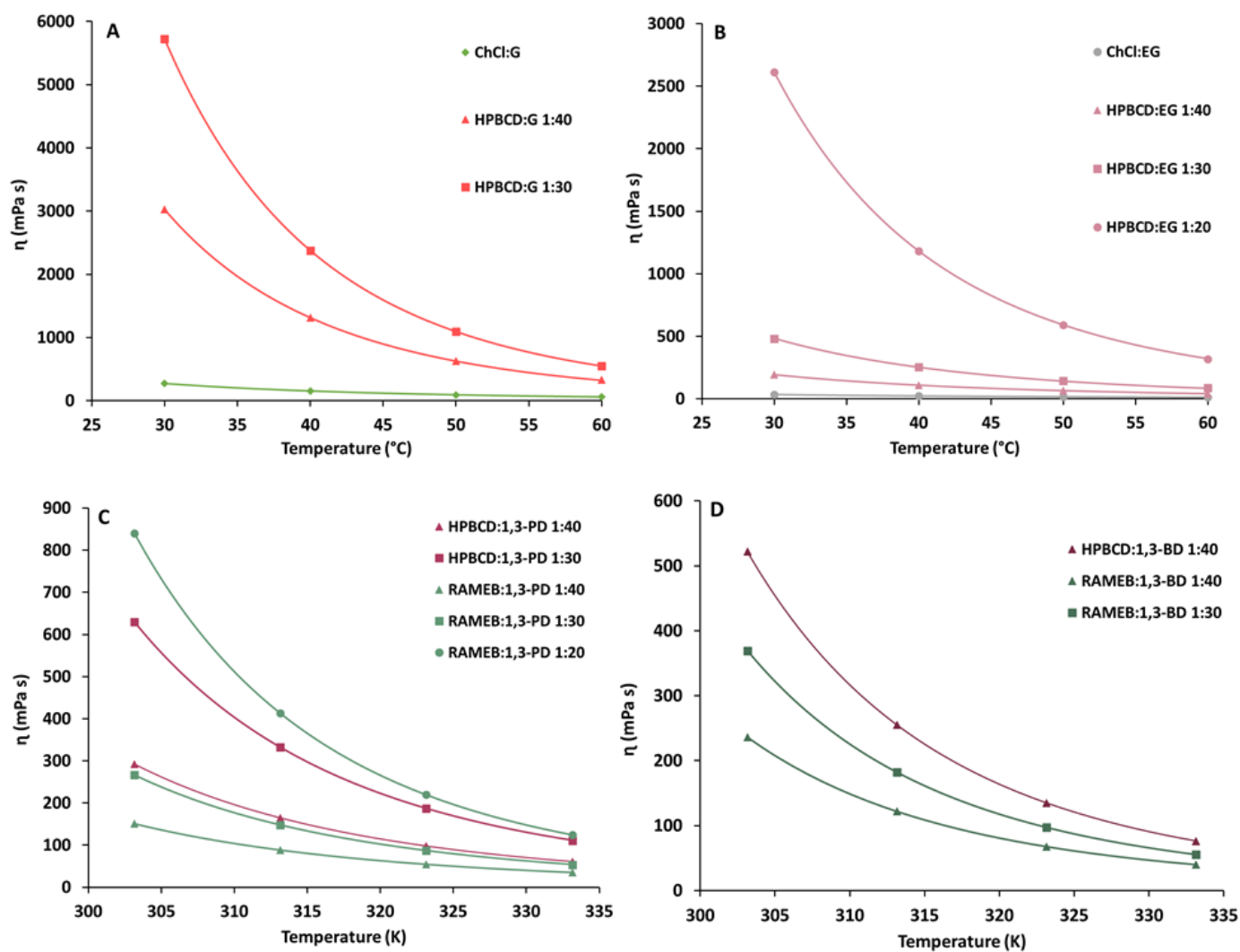


Figure 18. Experimental viscosities of the polyalcohol-based (glycerol- (A), ethylene glycol- (B), 1,3-propanediol- (C), and 1,3-butanediol- (D) based systems as a function of temperature ranging between 30 and 60  $^{\circ}\text{C}$ . The lines represent the fitted values following the Vogel-Fulcher-Tammann model

Table 11. Effect of the hydrogen bond donor on the viscosity of polyalcohol-based SUPRADES at 30 °C

SUPRADES	$\eta$ (mPa s)	SUPRADES	$\eta$ (mPa s)
HPBCD:EG 1:40	192.49	HPBCD:G 1:40	3028.30
HPBCD:1,3-PD 1:40	292.19	RAMEB:1,3-PD 1:40	150.95
HPBCD:1,3-BD 1:40	521.77	RAMEB:1,3-BD 1:40	236.02

### 2.3. Polarity

The polarity of the studied DES was estimated using the solvatochromic probe Nile Red. A stock solution of Nile Red was prepared in ethanol at a concentration of  $10^{-4}$  mol/L. A volume of Nile Red solution (100  $\mu$ L/ 1mL DES) was placed in vials, followed by ethanol evaporation. The studied DES were then added to the vials and stirred at 30 °C for 24 h to ensure the complete solubilization of the probe (Figure 19). UV–Vis spectra were recorded with a Perkin Elmer Lambda 2S spectrophotometer, between 400 and 700 nm with a quartz cell equipped with a thermostatically controlled bath which allows absorbance to be measured at a temperature of 30 °C with an accuracy of  $\pm 0.1$  °C. The wavelength at which the maximum visible-light absorption of Nile Red occurred,  $\lambda_{\max}$ , was determined for each DES and the Nile Red polar parameter  $E_{NR}$  (in kcal/mol) was calculated using equation (3).

$$E_{NR} \text{ (kcal/mol)} = \frac{28591}{\lambda_{\max}(\text{nm})} \quad (3)$$

The values of the polarity parameter of the different DES are listed in Table 12 in descending order of polarity. Since Nile Red is a positively solvatochromic probe, a higher polarity is reflected by a longer wavelength, thus a lower  $E_{NR}$ . The choice of the HBD seems to affect the overall DES polarity since levulinic acid-containing DES are the most polar, followed by glycerol-, ethylene glycol-, urea-, 1,3-PD-, 1,3-BD- and decanoic acid-based ones. Yet, no correlation was found between the DES polarity and logP of the HBD for ChCl-based DES (data not shown). However, the polarity was found to decrease with the increase of the alkyl chain length of the diols used as HBD ( $E_{NR} \text{ ChCl:EG} < E_{NR} \text{ ChCl:1,3-PD} < E_{NR} \text{ ChCl:1,3-BD}$ ), which is in accordance with the findings of Teles *et al.* and Dwamena and Raynie (Dwamena & Raynie, 2020; Teles *et al.*, 2017). Also, the HBA seems to influence the polarity but to a lesser extent given that TBPBr:Lev and TBPBr:EG are slightly more polar than ChCl:Lev and ChCl:EG, respectively.



Figure 19. Some deep eutectic solvents in presence of Nile Red. From left to right: TBABr:Dec, ChCl:U, ChCl:EG, ChCl:G, ChCl:Lev and TBPBr:Lev.

Table 12. Polarity parameter values of the studied deep eutectic solvents

DES	$E_{NR}$ (kcal/mol)
TBPBr:Lev	47.68
ChCl:Lev	48.3
ChCl:G	49.92
TBPBr:EG	49.94
ChCl:U	50.35
ChCl:EG	50.51
ChCl:1,3-PD	50.54
ChCl:1,3-BD	50.93
TBABr:Dec	51.82

The polarity measurements were not conducted on SUPRADES since Nile Red, which is a hydrophobic dye, can form inclusion complexes with CD (Hazra et al., 2004).

## 2.4. Differential scanning calorimetry

DSC measurements were performed in order to understand the thermal behavior of the new CD-based systems. Experiments were carried out using a Q1000 DSC (TA Instruments) with a temperature ranging from  $-100\text{ }^{\circ}\text{C}$  to  $40\text{ }^{\circ}\text{C}$  and at a thermal scanning rate of  $5\text{ }^{\circ}\text{C}\cdot\text{min}^{-1}$ . We chose to focus on the lower temperature range, given that the samples under study were all liquid at room temperature. The CD:Lev systems (HPBCD:Lev, RAMEB:Lev, CRYSMEB:Lev and Captisol:Lev) were encapsulated in aluminum pans (sample weight  $\sim 10\text{--}15\text{ mg}$ ), sealed with hermetic lids, and analyzed. Experiments were performed

under nitrogen flow ( $50 \text{ mL}\cdot\text{min}^{-1}$ ). Interestingly, none of the CD-based mixtures, i.e. HPBCD:Lev, RAMEB:Lev, CRYSMEB:Lev, and Captisol:Lev, showed a melting point in the heating curve. Instead, glass transition curves with  $T_g$  of  $-73.3$ ,  $-74.3$ ,  $-73.5$ , and  $-67.8$  °C were respectively observed for the mixtures (Figure 20). This absence of melting peaks and the presence of glass transition temperature was widely observed in the literature. For example, Francisco *et al.* reported 21 systems showing no melting point but glass transition temperatures ranging between  $-13.64$  and  $-77.73$  °C (Francisco *et al.*, 2012) while Dai *et al.* identified 13 different NADES with a  $T_g < -50$  °C and no melting point (Dai *et al.*, 2013). Likewise, except for glass transition, no other thermal events occur for trehalose:glycerol at a 1:30 molar ratio (Castro *et al.*, 2018). Moreover, the observed  $T_g$  value of  $-75.14$  °C for trehalose:glycerol is interestingly pretty close to the values obtained for our CD-based mixtures. CD generally present a  $T_g$  ranging between  $80$  °C and more than  $200$  °C depending on the CD (Tabary *et al.*, 2011). Therefore, the observed  $T_g$  values could be attributed to the formation of a low melting mixture with levulinic acid.

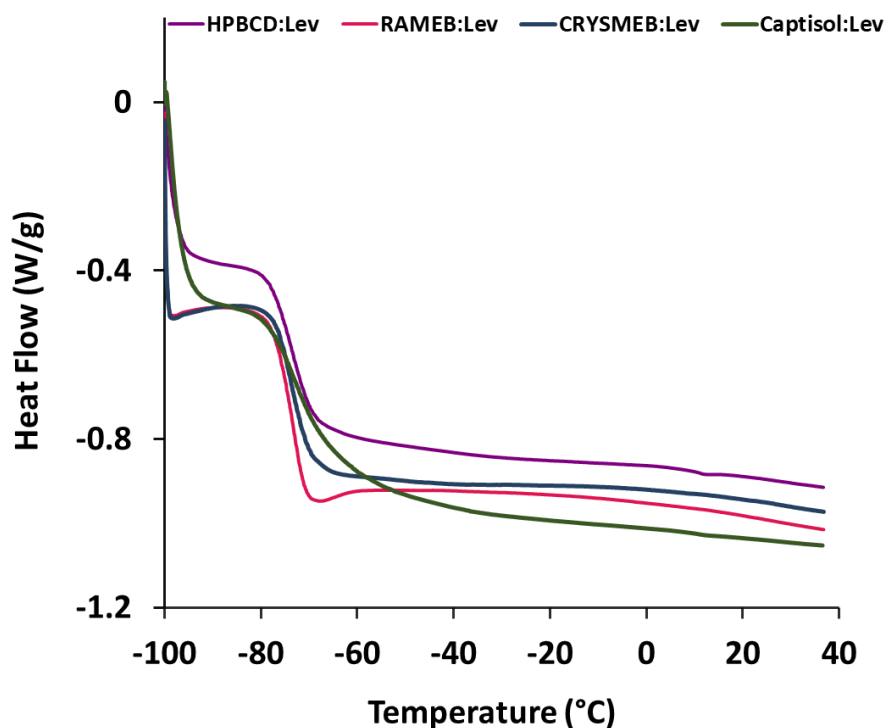


Figure 20. Differential scanning calorimetry curves of the SUPRADES

## 2.5. Thermogravimetric analysis

Dynamic thermogravimetric analysis (TGA) was used to further investigate the thermal stability of the new mixtures. TG measurements were performed with a TGA550 thermogravimetric analyzer (TA Instruments). Samples were placed in an open platinum pan (100  $\mu\text{L}$ ) suspended in the furnace. The initial weight of the sample was around 25–30 mg and nitrogen was used as the purge gas at a fixed flow of 20  $\text{mL}\cdot\text{min}^{-1}$ . The weight of the material was recorded during heating from room temperature to 600  $^{\circ}\text{C}$  at a heating rate of 10  $^{\circ}\text{C}\cdot\text{min}^{-1}$ . As shown in Figure 21, the SUPRADES underwent a progressive decomposition as the temperature increased. Their decomposition showed a two-step weight loss similar to some reported ChCl-based DES (Delgado-Mellado et al., 2018). At around 130  $^{\circ}\text{C}$ , levulinic acid began to decompose while the CD began to degrade at about 325  $^{\circ}\text{C}$ , except in the case of Captisol<sup>®</sup> for which the second decomposition began at around 225  $^{\circ}\text{C}$  and a third decomposition was determined near 350  $^{\circ}\text{C}$ . From the thermogravimetric curves, the results showed that the thermal decomposition temperatures corresponding to the first thermal event of HPBCD:Lev, RAMEB:Lev, CRYSMEB:Lev, and Captisol:Lev were equal to 130.4, 117.6, 137.7, and 127.6  $^{\circ}\text{C}$ , respectively. CRYSMEB:Lev had the best thermal stability and RAMEB:Lev the worst (Table 13). The DSC and TGA results demonstrate that these CD-based mixtures retain a stable liquid state over a wide temperature range.

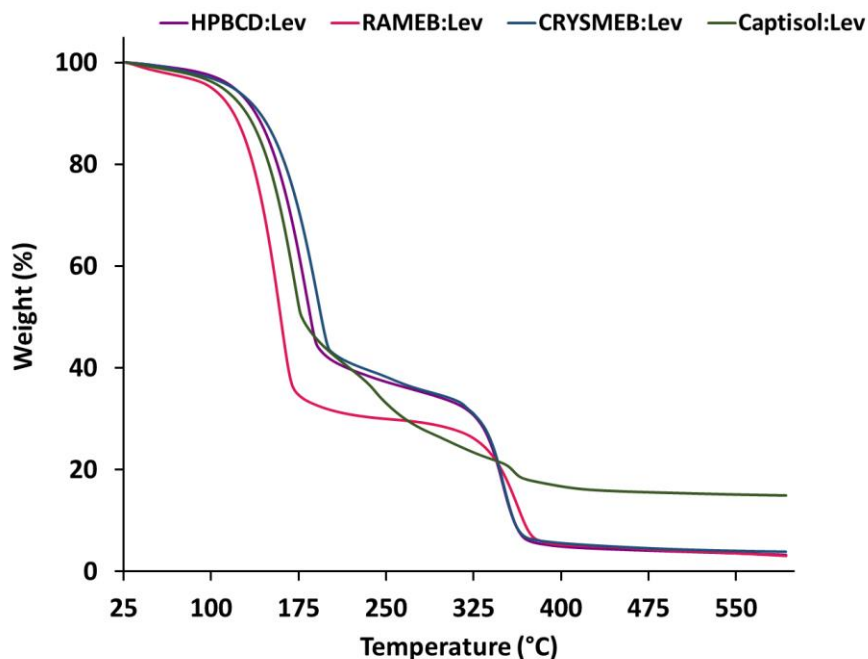


Figure 21. Thermogravimetric analysis curves of the SUPRADES

Table 13. Degradation temperatures of the SUPRADES and their individual compounds

SUPRADES	T <sub>decomposition</sub> (°C)	T <sub>decomposition</sub> (°C)	T <sub>decomposition</sub> (°C)
		Levulinic acid	Cyclodextrins
HPBCD:Lev	130.4		314.8
RAMEB:Lev	117.6		333.7
CRYSMEB:Lev	137.7	139.4	318.8
Captisol:Lev	127.6		267.1

## 2.6. Rheological measurements

In order to investigate the flow behavior of the four CD:Lev mixtures, rheological measurements were performed with an AR-G2 controlled- stress rotational rheometer (TA Instruments) at 30 °C. Flow curves were obtained with an aluminum cone-plate geometry (40 mm diameter, 1° cone angle, 28 μm truncation gap). A three-step shear rate sweep was imposed after a 3-minute equilibration time: 1) increase of the shear rate from 0.1 to 5000 s<sup>-1</sup> over 3 min (upwards curve), 2) peak hold at 5000 s<sup>-1</sup> during 1 min, 3) decrease of the shear rate from 5000 to 0.1 s<sup>-1</sup> over 3 min (downwards curve). The temperature was maintained at 30 °C and controlled with a Peltier plate. Measurements were performed in triplicate at least for each sample, to ensure reproducibility. The statistical analysis was performed by calculating the standard deviation from at least three measurements for each sample. Studying the rheological properties of these mixtures is very important, especially if we are aiming to use them as drug delivery systems for skin application. All the studied mixtures exhibit a Newtonian plateau for shear rates below 1000 s<sup>-1</sup> and a shear-thinning behavior for shear rates above this value (Figure 22). The measured static and dynamic viscosities for the same composition were slightly different (for example, in the case of RAMEB:Lev at 30 °C,  $\eta_{\text{static}} = 212.9$  mPa s vs.  $\eta_{\text{dynamic}} = 245.0$  mPa.s) but the same order was found for the viscosities ( $\eta_{\text{Captisol:Lev}} > \eta_{\text{HPBCD:Lev}} > \eta_{\text{CRYSMEB:Lev}} > \eta_{\text{RAMEB:Lev}}$ ). Moreover, the shear-thinning behavior was more pronounced as the viscosity increased. Indeed, for a high shear rate of 5000 s<sup>-1</sup>, a decrease of around 29% in viscosity was observed for Captisol:Lev, whereas in the case of RAMEB:Lev a smaller decrease (around 8%) was detected. As stated earlier, the most viscous mixtures probably contain a larger number of hydrogen bonds that may be disrupted at high shear rates, leading to a greater decrease in viscosity.

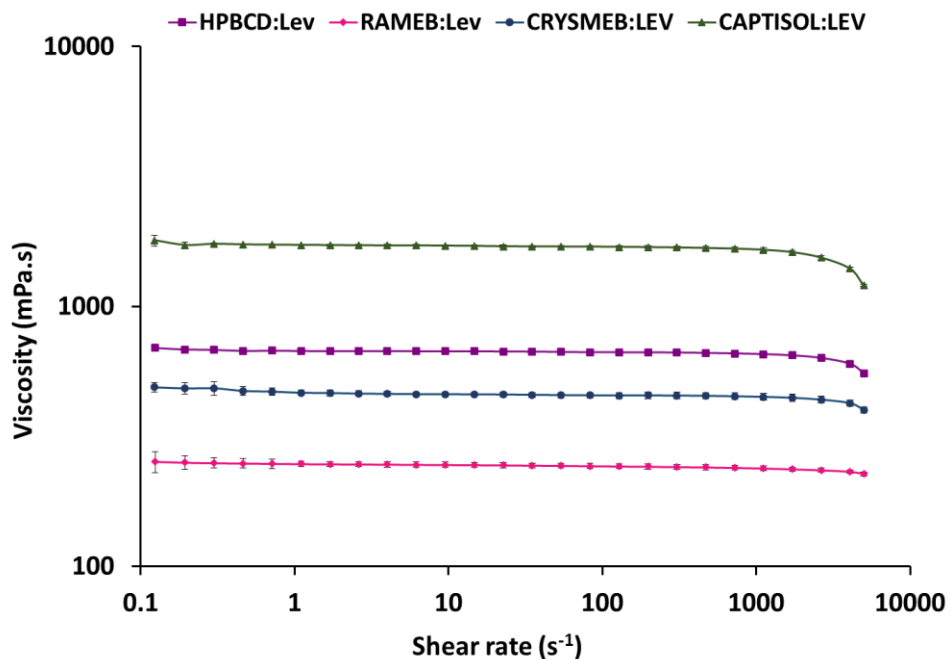


Figure 22. Log-log scale representation of the viscosity vs shear rate for SUPRADES at 30 °C

### III. Phospholipids self-assembly in DES

Owing to their unique properties, DES are recently being explored as self-assembly promoting solvents. Their polarity, cohesiveness, and important hydrogen bond network constitute encouraging factors and important requirements for the self-organization of amphiphilic molecules. DES were found to act as solvents for the self-assembly of ionic surfactants and phospholipids. However, the studies involving the behavior of phospholipids in the DES are quite limited. Therefore, in this section, we aimed to investigate the phospholipid organization in the DES and the new CD-based systems. In addition, DES were introduced as aqueous phase replacement in two typical methods adopted for the preparation of liposomes.

#### 1. Organization of E80 phospholipids

The unexplored organization of phospholipids was investigated in the 7 adopted DES and the new CD:Lev mixtures (HPBCD:Lev, RAMEB:Lev and CRYSMEB:Lev) via atomic force microscopy (AFM) for the first time. AFM is a high-resolution scanning probe microscopy that provides detailed information about the surface of the samples at the nanoscale level. As illustrated in Figure 23, AFM consists of scanning the sample's surface with a sharp tip that is attached to a cantilever. The attractive or repulsive probe-surface interactions result in a deflection of the cantilever. This deflection is measured by monitoring the subsequent deflection of a laser beam that is focused on the back of the cantilever, which is then reflected from a mirrored surface onto a photodiode detector (Grobelyny et al., 2011). AFM provides both imaging and force measurement of soft biomaterial interfaces. It can thus be used to obtain 2D and 3D images of lipid vesicles and to observe their morphology and size distribution. Besides, their surface properties such as their rigidity and viscoelasticity can be determined by this high-resolution technique.

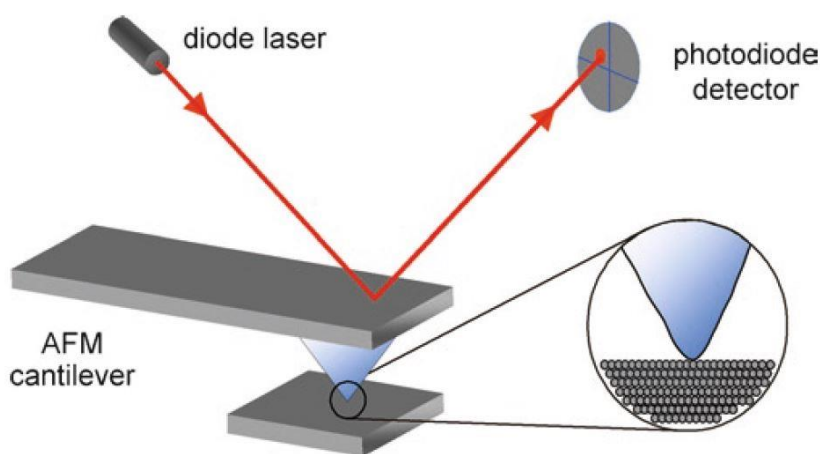


Figure 23. Schematic diagram of atomic force microscopy (Grobelyny et al., 2011)

As mentioned earlier, we aimed to follow the organization of Lipoid E80 phospholipids (80- 85% egg phosphatidylcholine (PC), 7- 9.5% phosphatidylethanolamine, 3% lysoPC, 0.5% lysophosphatidylethanolamine, 2-3% sphingomyelin, 2% water, 0.2% ethanol, iodine value 65-69, obtained from lipoid GmbH (Ludwigshafen, Germany)) within the DES and the newly prepared CD:Lev mixtures. 10 mg of lipoid E80 were dissolved in a mixture of ultrapure water (0.2 ml) and DES or SUPRADES (1.8 mL) (ChCl:U, ChCl:G, ChCl:EG, ChCl:Lev, TBPBr:Lev, TBABr:Dec, TBPBr:EG, HPBCD:Lev, RAMEB:Lev or CRYSMEB:Lev) and were kept under stirring at room temperature. Aliquots of 50  $\mu\text{L}$  were removed at 4, 24, and 48h and deposited on the mica surface for adsorption. The non-adsorbed structures were then removed by rinsing the surface with ultrapure water. Finally, the samples were visualized by AFM and 20 images were recorded for each analysis, and the experiment was repeated at least 2 times. AFM imaging was performed at room temperature using an Agilent 5420 microscope (Key sight, California, USA) and a pyramidal AFM probe with a 0.08 N/m force constant. All samples were imaged in contact mode with a typical scan rate of 1 Hz, a resolution of 512 x 512 pixels per image, a scanning angle of 0°, and a set point typically below 0.1 nN to avoid vesicles damage or displacement. Mica sheets (9 mm diameter and 0.1 mm thickness) were used as a substrate in AFM imaging. Images of 5x5  $\mu\text{m}^2$ , 4x4  $\mu\text{m}^2$ , or 2x2  $\mu\text{m}^2$  were recorded. Figure 24 illustrates AFM 2D images of the evolution of lipoid E80 organization within the four ChCl-based DES (ChCl:U, ChCl:G, ChCl:EG, and ChCl:Lev) as a function of time. At t=4h, supported lipid bilayers (SLB) are formed in presence of the 3 common DES Chl:U, ChCl:G, and ChCl:EG and cover the mica substrate, while the clear formation of aggregated and separated vesicles was detected in ChCl:Lev DES. At t = 24h, spherical vesicles and other structures were seen in the four studied DES. At t = 48h, partial to complete conversion of lipoid E80 to stable spherical cap-shaped structures was observed in all ChCl-based DES. This conversion seems to be complete and faster in ChCl:Lev DES, followed by ChCl:U DES, then the two other solvents. These results are in accordance with those reported by Bryant and coworkers who followed the organization of different PC-based lipids in ChCl:U and observed the spontaneous lamellar phase formation which then transformed into vesicles with time (Bryant et al., 2016). Table 14 shows the mean diameter and height values of the vesicles formed in the four DES as a function of time. The mean size of the lipid vesicles increases with time, accompanied by the simultaneous disappearance of the lipid wires. The distinct behavior of ChCl:Lev could be explained by its higher polarity compared with the 3 other DES (Table 12), resulting in a greater solvophobic effect. It could also be attributed to the interaction between the cationic headgroups of the phospholipids and the levulinate anions originating from the partial deprotonation of levulinic acid, thus promoting the phospholipids self-assembly, as proposed by the group of Karen J. Edler for the surfactant micellization in ChCl:MA DES (Sanchez-Fernandez et al., 2017).

On the other hand, no lipid structures were detected in presence of TBPBr- or TBABr-based DES (TBPBr:Lev, TBPBr:EG and TBABr:Dec), unless these DES induce the formation of small self-assemblies (< 30 nm) that cannot be detected by the AFM. This could also be due to a complete lipid dissolution in the DES. Likewise, no lipid assemblies were observed in the CD:Lev systems, which could be due to the

entrapment of the phospholipids into the CD cavities (Szente & Fenyvesi, 2016). The choice of the HBA has a major effect on the organization of the phospholipids within the DES.

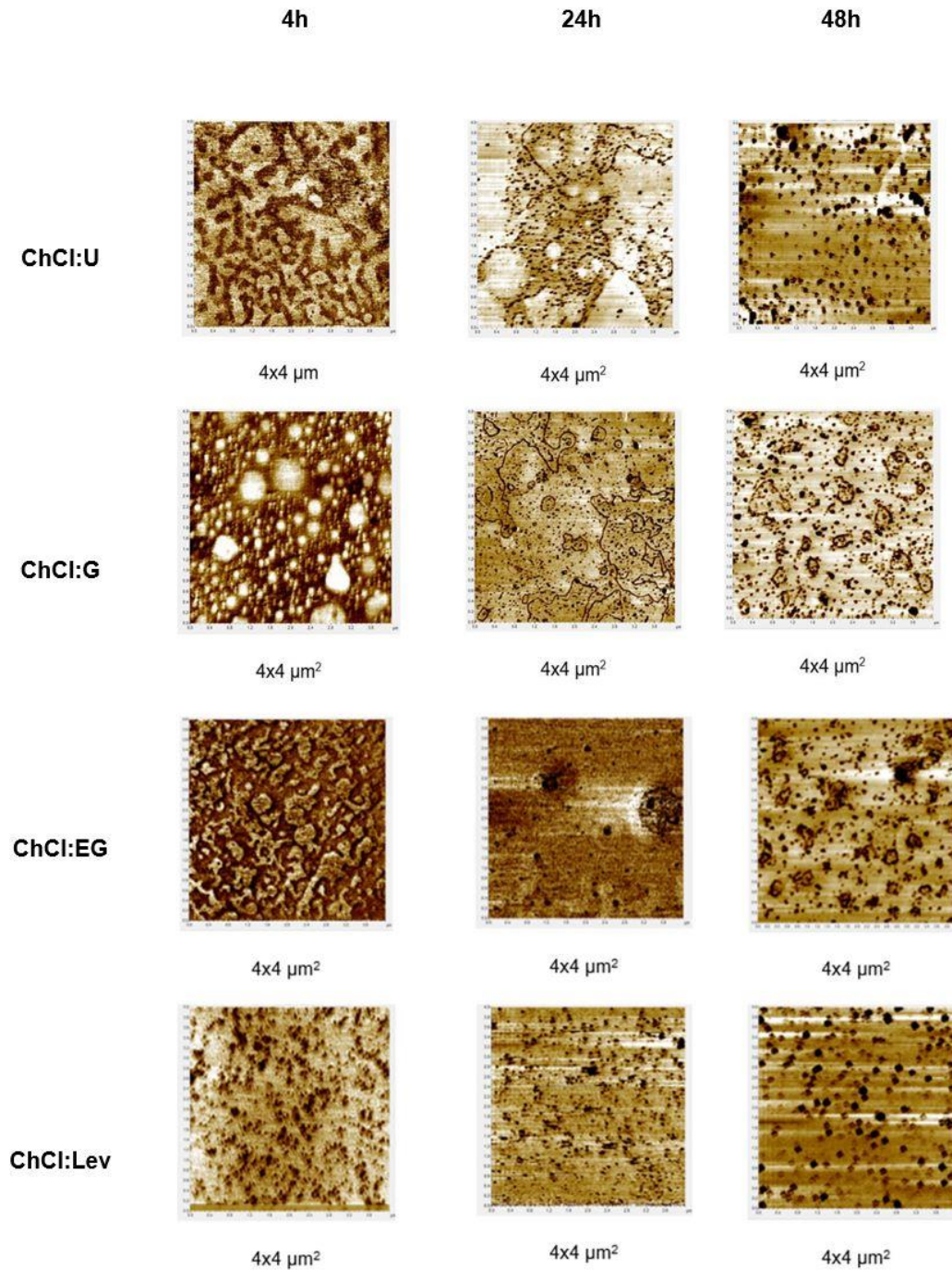


Figure 24. 4x4  $\mu\text{m}^2$  AFM 2D images of Lipoid E80 within ChCl:U, ChCl:G, ChCl:EG, and ChCl:Lev obtained in contact mode at 4, 24, and 48h

Table 14. Mean diameter D and height H values of the vesicles formed in ChCl:U, ChCl:G, ChCl:EG, and ChCl:Lev, at 4, 24, and 48h, obtained by the AFM cross-section tool

DES	Time (h)		
	4	24	48
ChCl:U	SLB	D = 60 ± 12 nm	D = 77 ± 11 nm
		H = 16 ± 3 nm	H = 15 ± 2 nm
ChCl:G	SLB	D = 50 ± 8 nm	D = 78 ± 12 nm
		H = 12 ± 1 nm	H = 16 ± 2 nm
ChCl:EG	SLB	D = 66 ± 25 nm	D = 100 ± 20 nm
		H = 17 ± 3 nm	H = 20 ± 4 nm
ChCl:Lev	D = 60 ± 10 nm	D = 80 ± 12 nm	D = 140 ± 20 nm
	H = 14 ± 2 nm	H = 16 ± 3 nm	H = 25 ± 4 nm

To further investigate the behavior of the phospholipids within these systems, we measured the polarity of 4 selected DES (ChCl:G, ChCl:EG, TBPBr:Lev and TBABr:Dec) in the absence or presence of E80 phospholipids, by determining  $\lambda_{\max}$ , the wavelength that corresponds to the maximum visible-light absorption of the solvatochromic probe Nile Red. The same protocol, described in section II.2.3., was followed herein. After the complete dissolution of Nile Red in the DES, a final lipid E80 concentration of 2.5 mg/ mL was added to the (DES + dye) mixture, stirred at 30 °C, and the polarity measurements were conducted 48h after the phospholipids' addition.

Figure 25 presents the  $\lambda_{\max}$  values of the Nile Red dissolved in the selected DES in the absence or presence of egg phospholipids. The values of  $\lambda_{\max}$  decreased after the addition of the lipids in both ChCl:G and ChCl:EG indicating the transition of the Nile Red to a relatively non-polar environment. This difference can be explained by the possible intercalation of the probe in the lipid bilayer of the vesicles that were formed in the DES, as previously detected by the AFM technique. Contrarily, the  $\lambda_{\max}$  values slightly decreased in TBPBr:Lev and TBABr:Dec DES, where no lipid structures were observed by AFM.

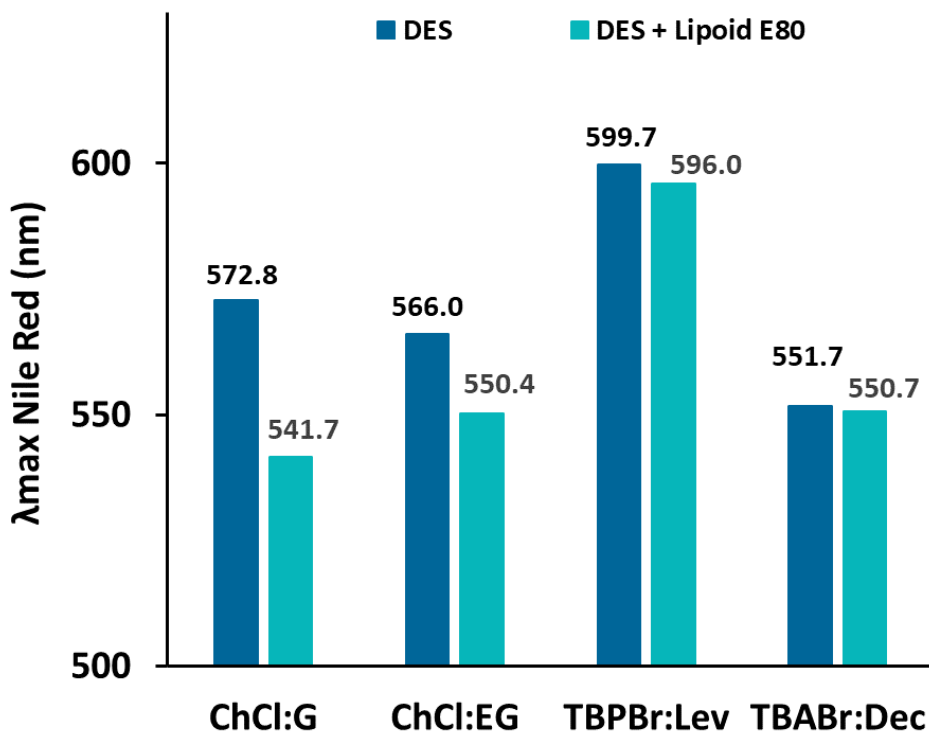


Figure 25.  $\lambda_{\max}$  values of Nile Red reflecting the polarity of the DES in the absence or presence of lipoid E80 at  $t = 48\text{h}$

## 2. DES-based methods for liposomes preparation

In this section, the phospholipid self-assembly was studied using another approach which consists of introducing the DES into liposomes preparation methods. Two conventional methods that are commonly used for the preparation of liposomes were considered: the ethanol injection method and the thin film hydration method. The latter is called “thin film-DES dissolution” in this manuscript since water was not used to dissolve the lipid film. The ethanol injection method, described in 1973 by Batzri and Korn, consists of dissolving the lipids in ethanol, followed by the injection of the ethanolic solution into an aqueous phase and the evaporation of the organic phase, thus leading to the formation of liposomes (Batzri & Korn, 1973). The thin film hydration method also called the Bangham method, on the other hand, requires the dissolution of the lipids in an organic phase before its evaporation which will result in the formation of a thin lipid film. The subsequent hydration of this film generates liposomes (Bangham et al., 1965). The same general procedure was followed herein, except that the aqueous phase was replaced by the DES in both techniques. The obtained preparations were then observed via optical microscopy.

## 2.1. Ethanol injection method

For the ethanol injection method using DES instead of the aqueous phase, lipid S100 (94 % soybean PC, 3 % lysoPC, 0.5 % N-acyl-phosphatidylethanolamine, 0.1 % phosphatidylethanolamine, 0.1 % phosphatidylinositol, 2 % water, 0.2 % ethanol, iodine value 97-107) and cholesterol were dissolved in absolute ethanol (2.5 ml) at a concentration of 10 mg/mL and 5 mg/mL, respectively. The obtained organic phase was then injected, using a syringe pump (Fortuna optima, GmbH-Germany), into 5 ml of DES or SUPRADES, at a flow rate of 1 ml/min, under magnetic stirring at 400 rpm at room temperature. The lipid suspension was kept stirring at 400 rpm for 15 min, followed by the removal of ethanol by rotary evaporation (Heidolph Instruments GmbH and co., Germany) at 40 °C and 60 rpm under reduced pressure. The preparations were stored at 4 °C prior to analysis. Blank samples were prepared following the same protocol in the absence of the lipids, i.e. only ethanol was injected into the preformed DES or SUPRADES. A small sample volume ( $V = 30 \mu\text{L}$ ) of each preparation was deposited on poly-L-lysine coated slides and observed via optical microscopy on a 40x objective. Figure 26 illustrates the images of these preparations for which ChCl-based DES were used instead of water in the ethanol injection method. Different shapes were observed in the 4 ChCl-based DES when compared to the samples prepared without lipids. Long needle-like structures were seen in ChCl:U, small circular aggregates in ChCl:G, while square-shaped structures formed in ChCl:EG and ChCl:Lev. Whereas no lipid structures were detected in the other studied DES or SUPRADES (TBPBr:Lev, TBABr:Dec, TBPBr:EG, HPBCD:Lev, RAMEB:Lev and CRYSMEB:Lev). These findings are somehow linked to the previously discussed AFM results concerning the organization of egg phospholipids within the studied systems. It is also worthy to mention that the preparations in ChCl-based DES presented a cloudy appearance, while clear solutions were obtained with the other solvents. This clarity could be explained by the complete dissolution of lipids within these DES where no lipid structures were observed by AFM and no remarkable changes in the polarity were detected after the lipid addition in both TBPBr:Lev and TBABr:Dec. When it comes to CD:Lev systems, the CD may contribute to the lipid dissolution since  $\beta$ -CD derivatives can form inclusion complexes with both phospholipids and cholesterol (Szente & Fenyvesi, 2016).

Moreover, a non-ionic surfactant Triton X-100 (Figure 27) known for its ability to disrupt lipid vesicles in aqueous media was added at 10 % (v/v) concentration to the DES-based preparations. Nevertheless, giant spherical assemblies surprisingly formed after the addition of Triton X-100 to ChCl:U, ChCl:G, and ChCl:EG. The surfactant was then added to the DES in the absence of any lipid and the large self-assemblies appeared once again indicating that the surfactant is clearly behind their formation (Figure 28). It is also worthy to mention that the lipid structures that were observed in ChCl:U, ChCl:G, and ChCl:EG completely or partially vanished when Triton X-100 was added, which is most probably due to the ability of the surfactant to dissolve the lipids. All the studies, related to the surfactants self-assembly in DES, that were reported to date involve ionic surfactants, except one study dealing with a mixture of 2 non-ionic surfactants (Tween 80 and Span 20) which generated the formation of DES-in-oil microemulsions when

aqueous solutions of ChCl:G DES were put in presence of isopropyl myristate oil (Sakuragi et al., 2018). However, Triton X-100 was never considered and its organization into large vesicles in ChCl-based DES is most probably due to solvophobic interactions taking place between the DES and the hydrophobic chain of the surfactant.

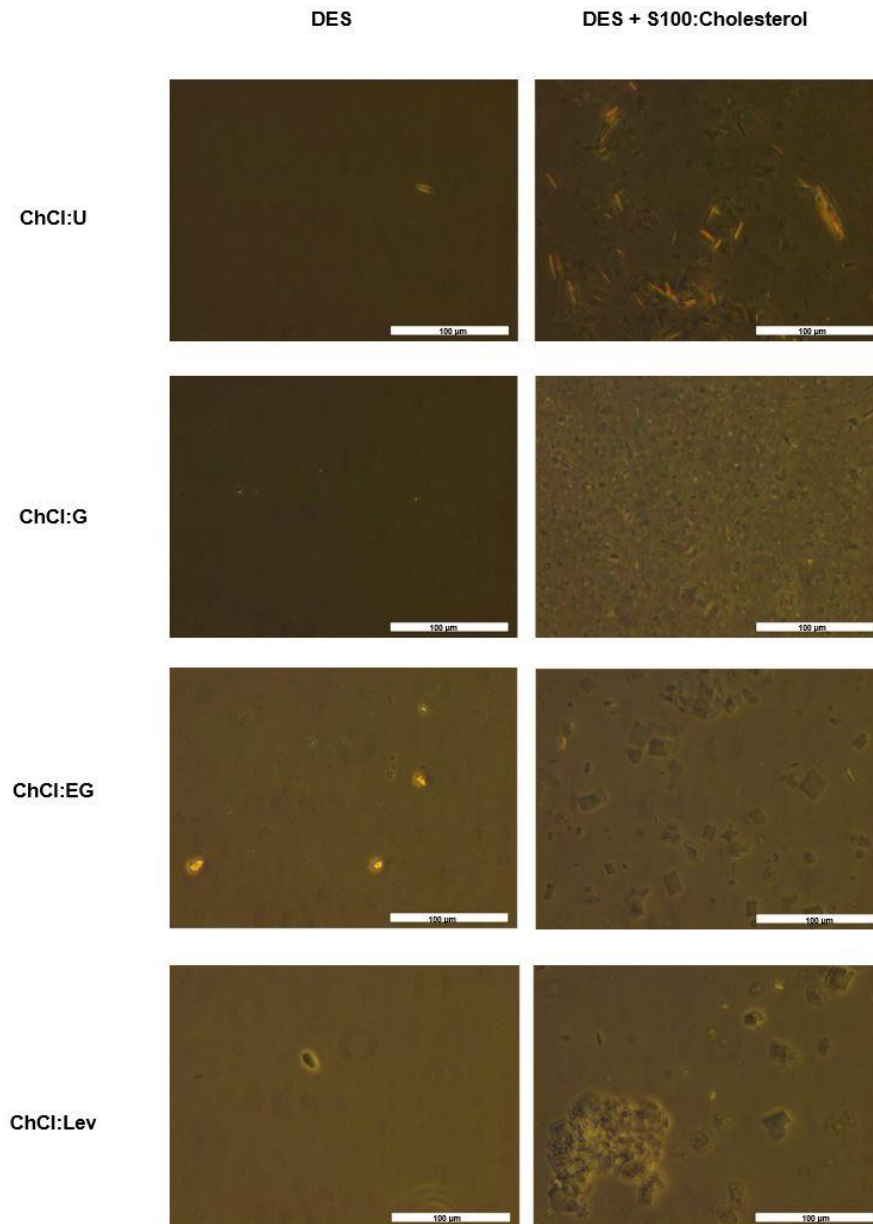


Figure 26. Observation of the preparations of DES-based ethanol injection method via optical microscopy

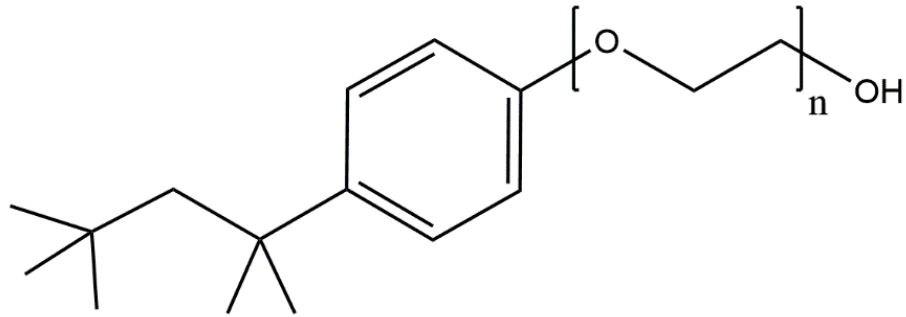


Figure 27. General structure of Triton X-100 (n = 9-10)

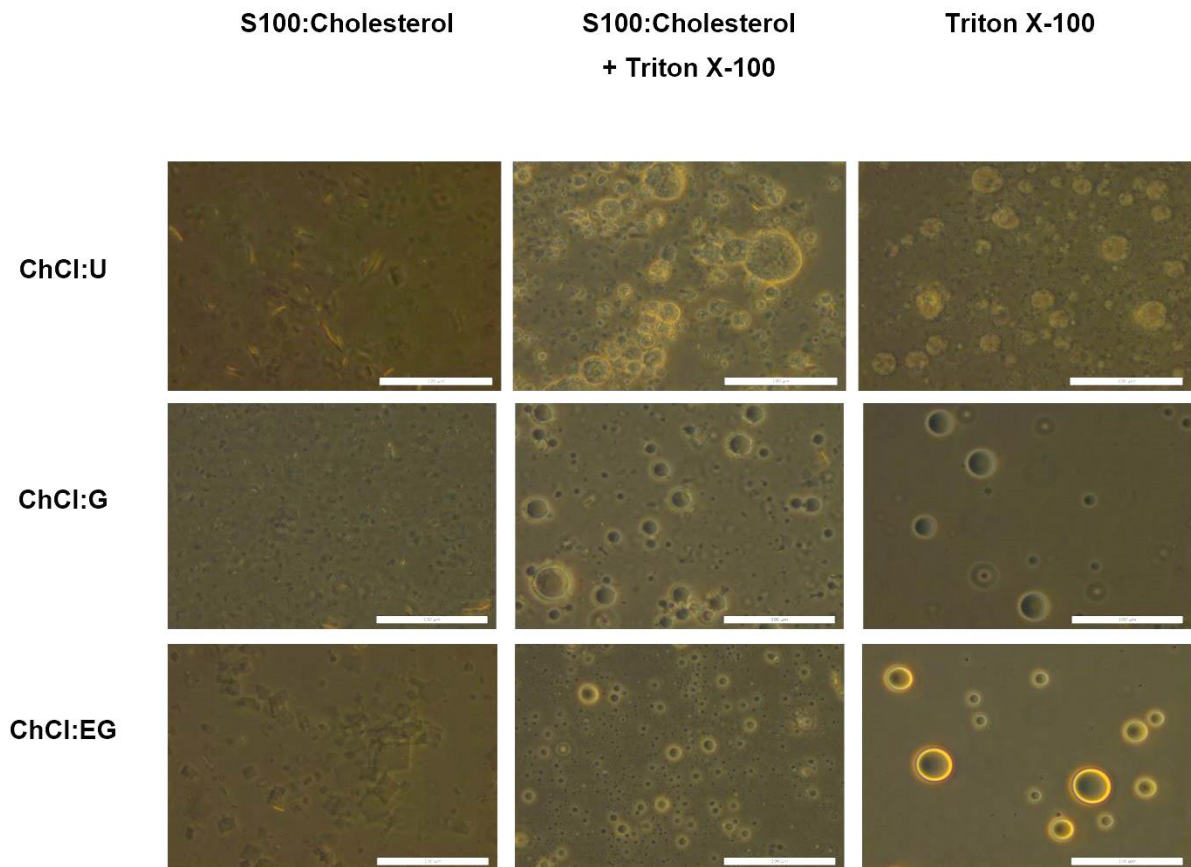


Figure 28. DES-based ethanol injection method: observation of ChCl-based DES in presence of lipids (left column), in presence of both lipids and Triton X-100 (middle column), and in presence of Triton X-100 (right column)

## 2.2. Thin film-DES dissolution method

In the thin film-DES dissolution method, lipid S100 (10 mg/ mL) and cholesterol (5 mg/mL) were dissolved in 3 mL of a chloroform/methanol 2/1 (v/v) mixture. The preparation was then evaporated using a rotary evaporator until the formation of a thin lipid film (Figure 29). Thereafter, the lipid film was dissolved with 1 mL of Tris-HCl buffer (pH 7.4, 0.1 M) (for the preparation of conventional liposomes) or 1 mL of DES or SUPRADES, under mechanical stirring. The preparations were stored at 4 °C prior to analysis. The resulting preparations were then observed via optical microscopy. As shown in Figure 30, lipid structures were again formed in ChCl-based DES (ChCl:G, ChCl:EG, and ChCl:Lev) and no structures were detected in the other studied DES or SUPRADES (figures not shown). Once again, these findings seem to be in accordance with the results of the AFM and ethanol injection method. Yet, the morphology of the self-assemblies was not always the same as in the ethanol injection method: circular- and needle-shaped structures were observed in ChCl:EG and ChCl:Lev, respectively instead of square-shaped ones. Furthermore, Triton X-100 (10 % v/v) was added to the DES or the DES- lipid suspension and led to the formation of large and heterogenous vesicles in ChCl:G and ChCl:EG, unlike ChCl:Lev (Figure 30). These observations are consistent with those of the ethanol injection method, although lipid structures remained in the presence of Triton X-100 probably owing to the highest lipid concentration in the thin film-DES dissolution technique.



Figure 29. Thin lipid film obtained following the organic phase evaporation

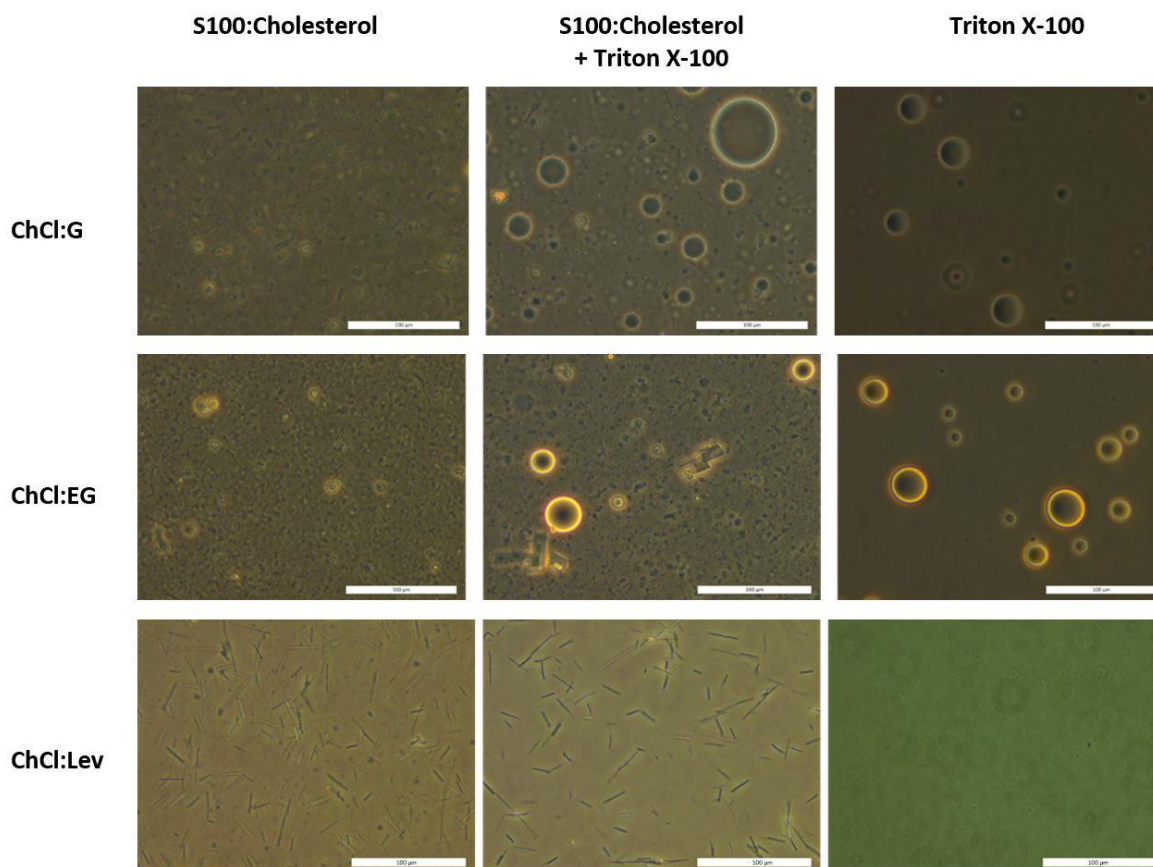


Figure 30. DES-based thin film dissolution method: observation of ChCl-based DES in presence of lipids (left column), in presence of both lipids and Triton X-100 (middle column), and in presence of Triton X-00 (right column)

The dynamic light scattering (DLS) technique was further used to have insight into the size of the lipid assemblies that were observed in ChCl:G and ChCl:EG. The measurements were performed with a Malvern Zetasizer Nano ZS90 operating at a fixed scattered angle of  $90^\circ$  and equipped with a Helium-Neon laser source of a wavelength of 633 nm. An appropriate sample volume (1 mL) was placed in macrocuvettes of a 1-cm optical pathway and four optical faces (Sarstedt). The hydrodynamic diameter  $d(H)$  of the lipid particles was determined at  $25^\circ\text{C}$  using the Stokes-Einstein equation assuming a spherical shape of the nanoparticles and using the viscosity and refractive index values of the corresponding DES. The nanoparticles size profile was obtained from the intensity-weighted distribution and corresponded to the median diameter derived from the cumulative distribution curve. All measurements were performed in triplicate ( $n=3$ ). As shown in Figure 31, one population of lipid particles with an average size of 103 nm was detected in ChCl:G, while two populations were identified in ChCl:EG with average sizes of 267 and 974 nm.

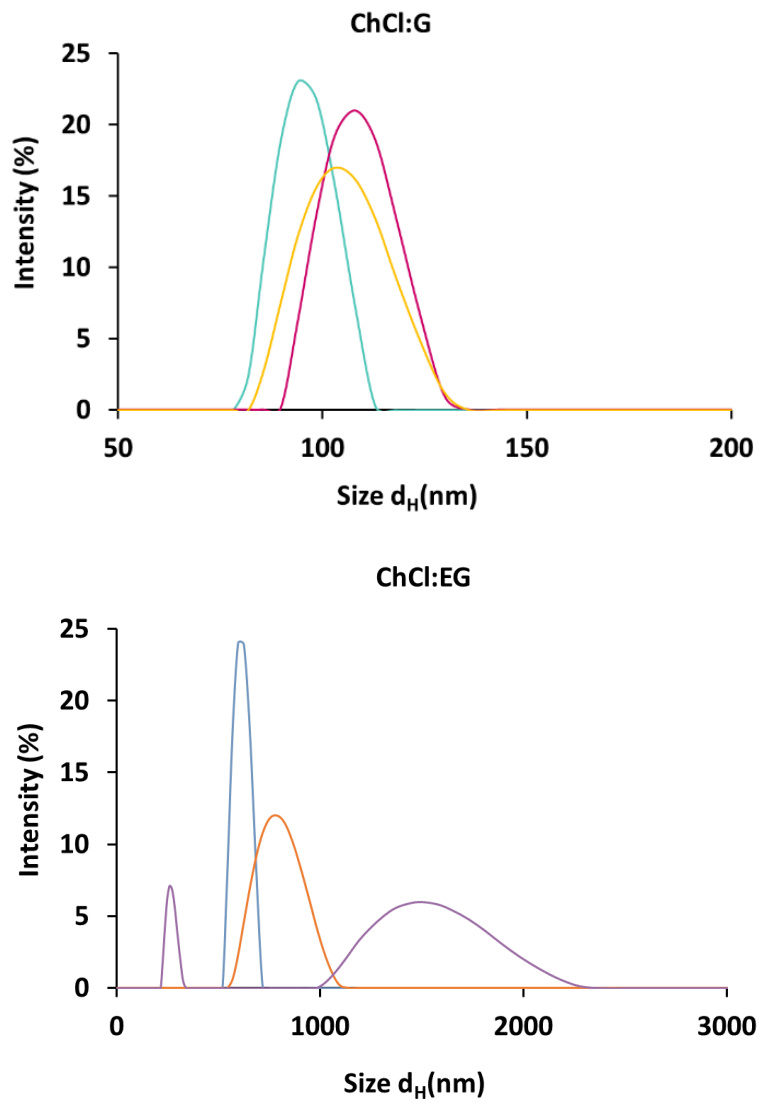


Figure 31. Size distribution plots of lipid particles formed in ChCl:G- or ChCl:EG-based thin film dissolution preparations

## IV. Effect of DES on synthetic and biological membranes

After examining the organization of phospholipids within the studied systems and after proving the formation of self-assemblies in ChCl-based DES, the effect of these DES and the aqueous solutions of their constituents on preformed liposomes was assessed via AFM for the first time. In addition to the liposomes which are considered as models for biological membranes, the effect on human breast cancer cells MDA-MB-231 was also evaluated.

### 1. Effect on preformed liposomes

Liposomes were prepared following the ethanol injection method: 500 mg of lipid E80 were dissolved in 10 mL of ethanol. The obtained organic phase was later injected, using a syringe pump (Fortuna optima, GmbH-Germany), into 20 mL of ultrapure water, at a flow rate of 1 mL/min, under magnetic stirring at 400 rpm at room temperature. The liposomal suspension was then kept under stirring (400 rpm) for 15 min. Finally, ethanol was removed by rotary evaporation (Heidolph Instruments GmbH and co., Germany) at 40 °C and 60 rpm under reduced pressure. The liposomal formulation was stored at 4 °C prior to analysis.

#### 1.1. Exposure of adsorbed liposomes to the studied systems

In a first protocol, an aliquot of the liposomal suspension was diluted 10 times in ultrapure water to obtain a less sticky sample. Then, 50  $\mu$ L of the diluted formulation was deposited on a freshly cleaved mica surface and left for 15 min in the air at room temperature for adsorption. Adsorbed liposomes were directly and separately subjected to 50  $\mu$ L of ultrapure water (used as control), DES (ChCl:U, ChCl:G, ChCl:EG, ChCl:Lev), or aqueous solutions of the individual components of ChCl-based DES added simultaneously in the same ratio of DES. The exposure stands for 30 min in the air for the 15 samples. Every mica sheet was rinsed with ultrapure water to remove the non-adsorbed vesicles, and inserted directly (before drying) for imaging. At least 20 images were taken for each analysis and the experiment was repeated at least 2 times. The average values of the diameter and height of 200 liposomes detected in 20 images were determined using the AFM cross-section tool.

Figure 32 illustrates representative 2D images of the liposomes exposed to water, the four ChCl-based DES, and the aqueous solutions of ChCl and the appropriate HBD. Exposed to water, well-adsorbed vesicles on the mica substrate were obtained, with a spherical cap structure and a diameter ranging from 90 to 220 nm (Figure 32 A), with a mean value of  $150 \pm 30$  nm and a height of  $22 \pm 4$  nm. Exposed to DES (ChCl:U, ChCl:G or ChCl:EG), the adsorbed Egg PC liposomes maintained their spherical cap structures, while their size decreased in comparison with those exposed to water. A different behavior was observed for liposomes exposed to ChCl:Lev, where a clear aggregation of liposomes (Figure 32E), and/or

conversion to supported lipid bilayers of  $\sim 7$  nm height (Figure 32E') were observed. Exposed to the aqueous solutions of DES constituents, liposomes showed the same behavior as when exposed to DES with an additional decrease in the mean dimensions' values; liposomes diameters varied between 30 and 60 nm. The mean diameter  $D$  and height  $H$  values are presented in Table 15. In contrast to liposomes exposed to ChCl:Lev DES, no aggregation or conversion to SLB was observed in the aqueous solution containing ChCl and Lev. Also, the liposomes in the four aqueous solutions of DES' constituents maintain their spherical cap shape. The reduction of the size of the vesicles in presence of the aqueous solutions of ChCl and the HBD can be explained by the osmosis phenomenon. Given that liposomes are prepared in water using the ethanol injection method, the core-shell lipid structures consist of an internal aqueous cavity surrounded by lipid bilayers. That said, in the presence of aqueous solutions of DES components, inner water molecules tend to migrate through the semipermeable membrane. Likewise, a size reduction was detected in presence of the DES which is also related to osmosis. In fact, two recent studies demonstrated the potential of ChCl:G and ChCl:EG DES as efficient, inexpensive, and reusable draw solutions for the enrichment of biomacromolecules or the recovery of water from industrial wastewater, using forward osmosis (Mahto et al., 2017; Mondal et al., 2015). Additionally, Cvjetko Bubalo *et al.* witnessed a decrease in the baker's yeast viability as a result of a high DES content in the medium and explained it by the high osmotic pressure imposed on the yeast cells, leading to the diffusion of water out of the cells (Cvjetko Bubalo, Mazur, et al., 2015). This osmotic potential pushed liposomes to lose their confined water molecules to the surrounding environment, leading to the reduction of their size. On another note, the distinctive effect of ChCl:Lev compared to the three other DES can be explained neither by the density nor the viscosity of the eutectic mixture. However, this effect could be explained by the relatively high polarity and/or acidity of the levulinic acid-containing DES which may lead to a transmembrane pH gradient.

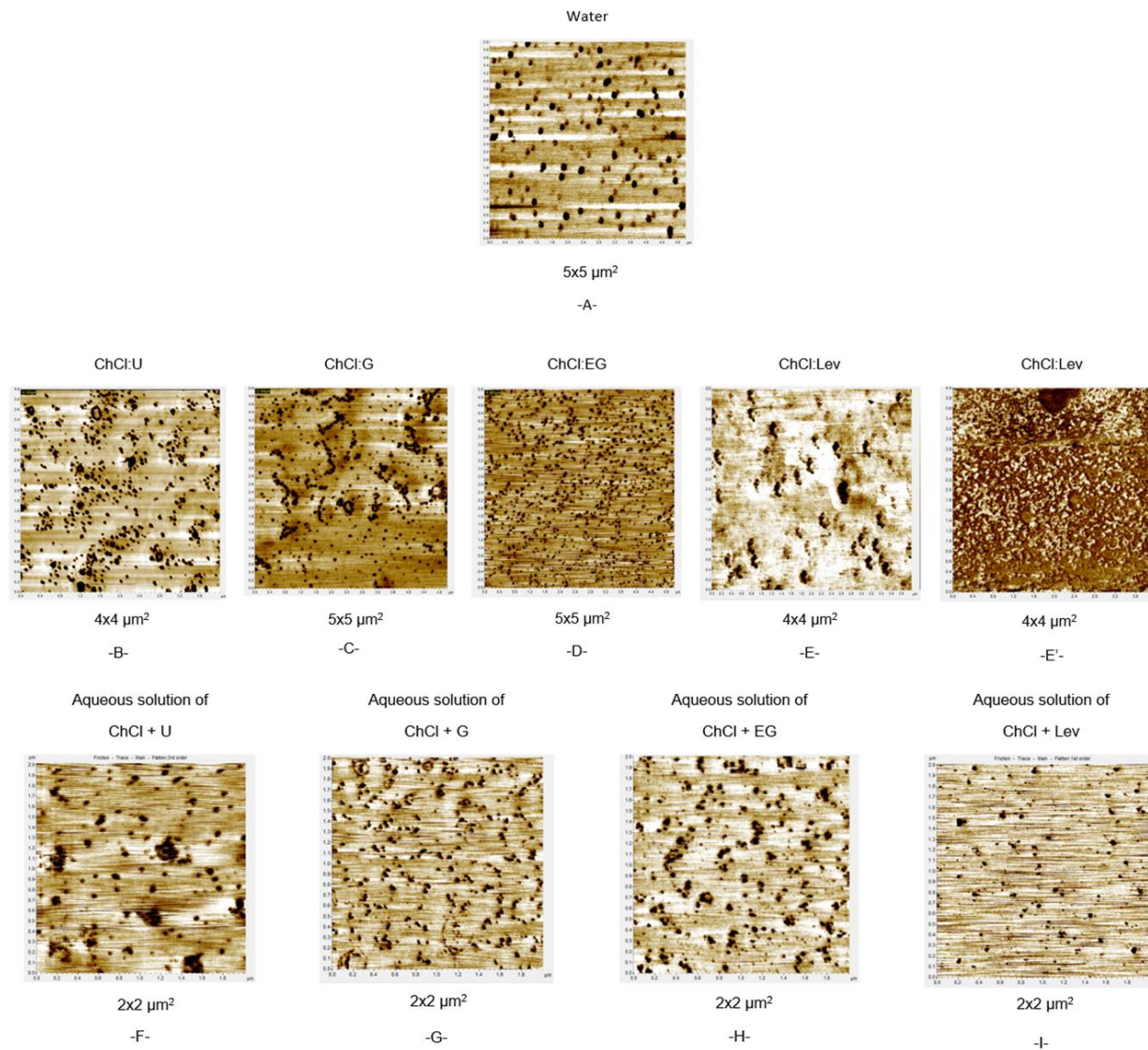


Figure 32. AFM contact mode 2D images of Egg PC liposomes following 30 min exposure to A- ultrapure water, B- ChCl:U, C- ChCl:G, D- ChCl:EG, E, E' ChCl:Lev F- aqueous solution of ChCl + U, G- aqueous solution of ChCl + G, H- aqueous solution of ChCl + EG, I- aqueous solution of ChCl + Lev

Table 15. Mean diameter D and mean height H of Egg PC liposomes following 30 min exposure to ChCl:U, ChCl:G, ChCl:EG, ChCl:Lev, aqueous solution of ChCl + U, an aqueous solution of ChCl + G, an aqueous solution of ChCl + EG, and an aqueous solution of ChCl + Lev, determined by AFM using the cross-section t

Time	DES			
	ChCl:U	ChCl:G	ChCl:EG	ChCl:Lev
30 min	D = $75 \pm 15$ nm H = $17 \pm 3$ nm	D = $80 \pm 20$ nm H = $18 \pm 4$ nm	D = $60 \pm 18$ nm H = $16 \pm 3$ nm	Aggregation and/or SLB
Time	Aqueous solutions			
	Aqueous solution of ChCl + U	Aqueous solution of ChCl + G	Aqueous solution of ChCl + EG	Aqueous solution of ChCl + Lev
30 min	D = $48 \pm 15$ nm H = $14 \pm 2$ nm	D = $45 \pm 7$ nm H = $14 \pm 2$ nm	D = $46 \pm 6$ nm H = $14 \pm 2$ nm	D = $45 \pm 4$ nm H = $14 \pm 2$ nm

## 1.2. Time-dependent behavior of liposomes suspended in the studied systems

In the second approach, an aliquot of the liposomal formulation was diluted 10 times in water, DES (ChCl:U, ChCl:G, ChCl:EG, ChCl:Lev) or the aqueous solutions of the individual components. The dilution in water was considered as a control. After mixing, a volume of 50  $\mu\text{L}$  was removed at different time points, deposited on a freshly cleaved mica surface, and left for 15 min in the air for adsorption at room temperature. Excess vesicles were removed by rinsing the mica surface with ultrapure water, and then the mica sheet was inserted directly for imaging. For a statistical purpose, 20 images were recorded.

Figure 33 and Figure 34 illustrate AFM 2D images of Egg PC liposomes suspended in ChCl-based DES, and in the aqueous solutions of the constituents of ChCl-based DES for 1, 2, 24, and 48h, respectively. The images obtained at other time points (1 h 20 min, 1 h 40 min, and 4 h) are presented in Figure C1. Well adsorbed liposomes on the mica sheets were observed in ChCl-based DES at time  $t = 0$  (Figure 33). However, the images show a non-homogeneous dispersion of vesicles within the ChCl-based DES, compared to liposomes in water (figures not shown). In addition, the mean diameter values of liposomes suspended in these DES are less than those suspended in water, especially at  $t=0$  and  $t=1\text{h}$  (Table 16). Aggregation of vesicles started at  $t=0$  for all the ChCl-based DES and seemed to dominate the images at  $t = 1\text{h}$ . Furthermore, a complete conversion to SLB ( $\sim 7\text{ nm}$  of height) was observed at  $t = 2\text{ h}$ . This indicates that aggregation and/or fusion occurs between  $t = 0$  and  $t = 2\text{ h}$ , and continues till  $4\text{ h}$  (Figure C1). Nevertheless, the SLB formed were not stable and converted into vesicles after  $24\text{ h}$  in all the ChCl-based DES, owing to the solvent encapsulation by the lipid bilayers. The size of the reconstituted liposomes then increased over time. When it comes to liposomes suspended in the aqueous solutions of ChCl-based DES' constituents, AFM images show well-adsorbed liposomes on mica substrates at 0, 1, 2, 24, and 48 h. In contrast to the above-described observations of liposomes suspended in DES, no aggregation or fusion was detected on the mica substrates. We can only notice spherical cap structures of liposomes at the different time points; the SLB structures were seemingly absent. Despite the similarity of liposomes morphology compared to water, we noticed a clear decrease in the size starting from  $t = 0$  reflecting the progression of the osmosis phenomenon; while some vesicles maintained their initial diameter ( $\sim 100\text{ nm}$ ). After  $t=1\text{ h}$ , the mean diameter and height values of the liposomes remain stable, as indicated in Table 16.

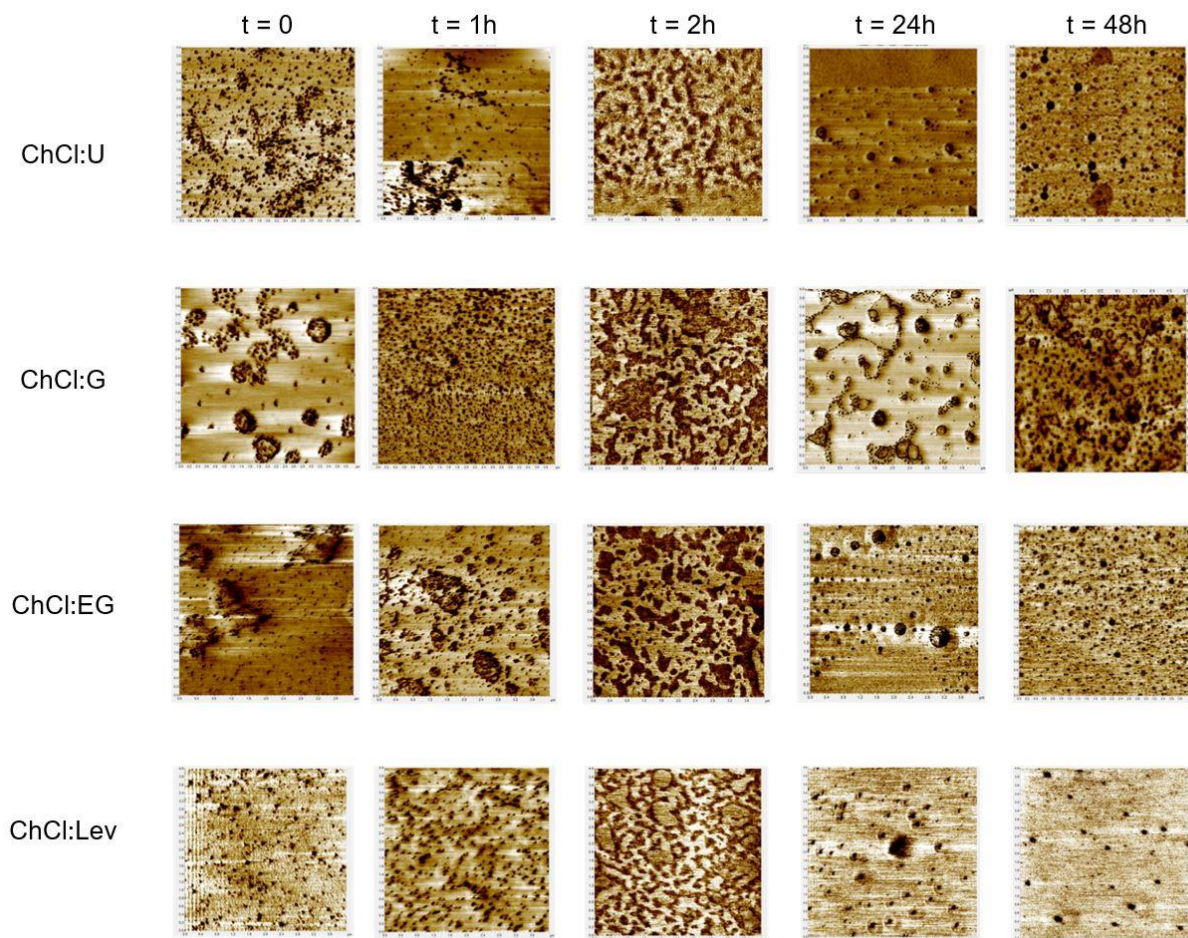


Figure 33. AFM 2D  $4 \times 4 \mu\text{m}^2$  images of EggPC liposomes suspended in ChCl:U, ChCl:G, ChCl:EG, and ChCl:Lev DES obtained in contact mode at different time points

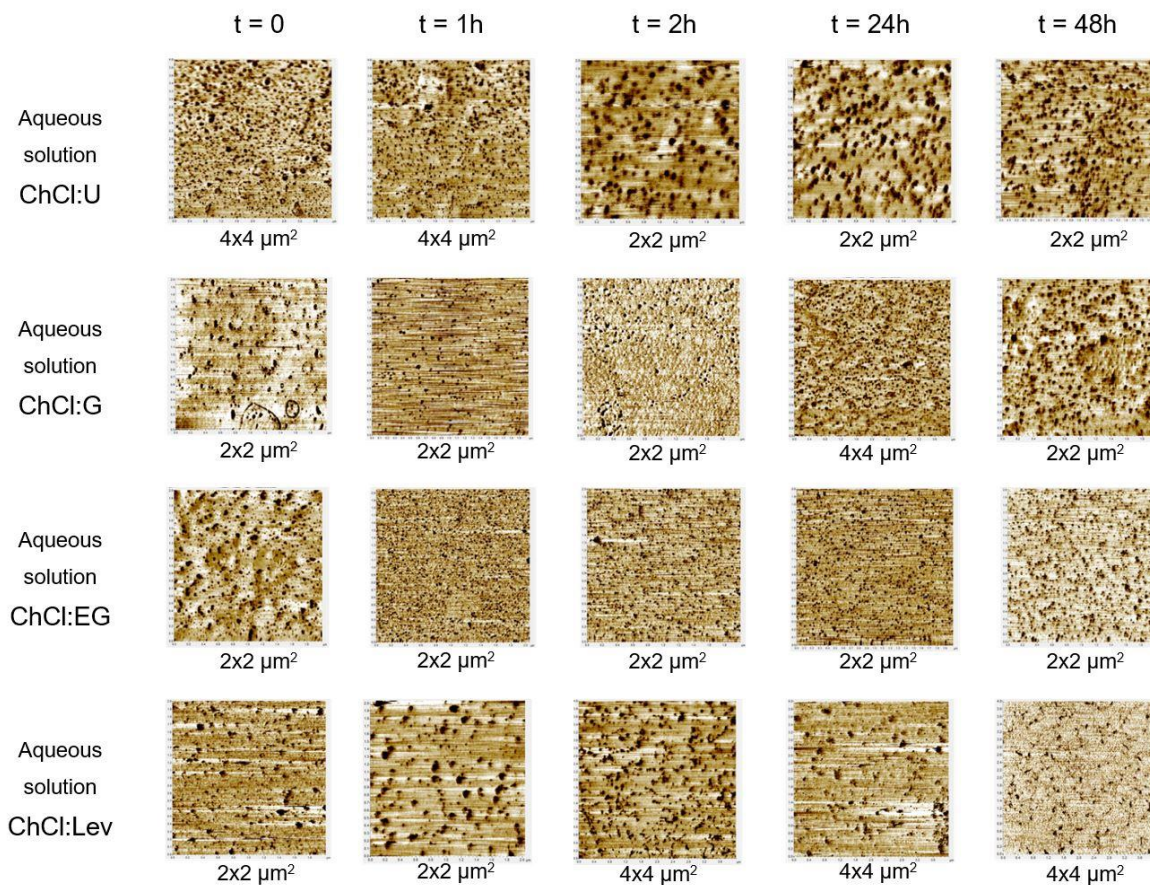


Figure 34. AFM 2D 4x4, and 2x2 μm<sup>2</sup> images of EggPC liposomes suspended in an aqueous solution of ChCl + U, an aqueous solution of ChCl + G, an aqueous solution of ChCl + EG, and an aqueous solution of ChCl + Lev, obtained in contact mode at different time points

Table 16. Mean diameter D and mean height H of Egg PC liposomes suspended in water, ChCl:U, ChCl:G, ChCl:EG, ChCl:Lev, aqueous solution of ChCl + U, an aqueous solution of ChCl + G, an aqueous solution of ChCl + EG, and an aqueous solution of ChCl+ Lev, at different time points determined by AFM using the cross-section tool

Solvent	Time (h)				
	0	1	2	24	48
Water			D = 120 ± 15 nm H = 21 ± 3 nm		
ChCl:U	D = 65 ± 13 nm H = 15 ± 3 nm	D = 60 ± 10 nm H = 14 ± 3 nm	SLB	D = 50 ± 18 nm H = 15 ± 3 nm	D = 80 ± 20 nm H = 17 ± 4 nm
ChCl:G	D = 80 ± 8 nm H = 16 ± 3 nm	D = 67 ± 10 nm H = 15 ± 3 nm	SLB	D = 35 ± 8 nm H = 12 ± 1 nm	D = 75 ± 18 nm H = 14 ± 2 nm
ChCl:EG	D = 65 ± 10 nm H = 14 ± 2 nm	D = 65 ± 8 nm H = 15 ± 3 nm	SLB	D = 66 ± 25 nm H = 17 ± 3 nm	D = 80 ± 18 nm H = 14 ± 2 nm
ChCl:Lev	D = 72 ± 13 nm H = 15 ± 3 nm	D = 60 ± 10 nm H = 14 ± 3 nm	SLB	D = 73 ± 10 nm H = 14 ± 2 nm	D = 90 ± 20 nm H = 18 ± 4 nm
Aqueous solution of ChCl + U	D = 62 ± 10 nm H = 15 ± 2 nm	D = 50 ± 8 nm H = 14 ± 2 nm	D = 47 ± 8 nm H = 14 ± 2 nm	D = 46 ± 6 nm H = 14 ± 3 nm	D = 46 ± 4 nm H = 14 ± 2 nm
Aqueous solution of ChCl + G	D = 55 ± 13 nm H = 15 ± 2 nm	D = 47 ± 6 nm H = 14 ± 2 nm	D = 45 ± 7 nm H = 14 ± 2 nm	D = 44 ± 6 nm H = 14 ± 3 nm	D = 44 ± 4 nm H = 14 ± 2 nm
Aqueous solution of ChCl + EG	D = 58 ± 13 nm H = 15 ± 3 nm	D = 49 ± 8 nm H = 14 ± 2 nm	D = 46 ± 7 nm H = 14 ± 2 nm	D = 45 ± 5 nm H = 14 ± 3 nm	D = 45 ± 4 nm H = 14 ± 2 nm
Aqueous solution of ChCl + Lev	D = 53 ± 11 nm H = 15 ± 2 nm	D = 47 ± 6 nm H = 14 ± 2 nm	D = 45 ± 6 nm H = 14 ± 2 nm	D = 45 ± 5 nm H = 14 ± 3 nm	D = 44 ± 4 nm H = 14 ± 2 nm

## 2. Effect on human cells

After studying the effect of DES on liposomes, known as models for biological membranes, we were interested in evaluating the impact of DES on human cells. As mentioned in section 1.2., DES were always assumed as non-toxic solvents owing to the safety of their forming compounds. Nevertheless, some studies recently reported that DES can have a different toxicity response than their starting compounds. In this section, we examined the effect of two of the most studied and applied DES, ChCl:U and ChCl:EG, on MDA-MB-231, a human breast cancer cell line. To do so, a combination of cytotoxicity studies and morphological assessment was carried out. The cytotoxicity study was performed using the trypan blue exclusion test and by exposing the cells to different concentrations of the DES. On the other hand, the morphological alterations of the cells were monitored via optical microscopy. Furthermore, the effect of the DES was compared with the effect of their individual (ChCl, urea, or ethylene glycol) or combined compounds. The solution of the combined compounds was prepared by separately dissolving the HBA and the HBD in water at the same HBA:HBD molar ratio adopted for the DES. In a second approach, confluent MDA-MB-231 cells were incubated in pure DES, devoid of any culture medium, for the first time. The cells were subsequently observed over time using optical microscopy.

The detailed methodology and the obtained results are presented below, in the form of an article that will be submitted to Chemosphere journal.

# Effect of choline chloride-based deep eutectic solvents on MDA-MB-231 breast cancer cell line: cytotoxicity study and morphological evaluation

Tracy El Achkar<sup>a,b</sup>, H el ene Greige-Gerges<sup>a</sup>, Sophie Fourmentin<sup>b</sup>, Maya Kayouka<sup>a,\*</sup>

<sup>a</sup>*Bioactive Molecules Research Laboratory, Faculty of Sciences, Lebanese University, Lebanon*

<sup>b</sup>*Unit e de Chimie Environnementale et Interactions sur le Vivant (UCEIV, UR 4492), SFR Condorcet FR CNRS 3417, ULCO, F-59140 Dunkerque, France*

\*Corresponding author: maya.kayouka@ul.edu.lb

Bioactive Molecules Research Laboratory, Doctoral School of Sciences and Technologies, Faculty of Sciences, Lebanese University, B.P. 90656, Jdaidet el-Matn, Lebanon

## Abstract

Deep eutectic solvents (DES) represent a new generation of solvents with interesting and tunable physicochemical properties. Despite the rising interest in DES and their multidisciplinary applications, their assumed safety remains a controversial subject. The present work aims to investigate the effect of two common DES, choline chloride:urea and choline chloride:ethylene glycol, on MDA-MB-231 human breast cancer cell line and to compare it with the effect of the aqueous solutions of their individual or combined forming compounds. To this end, the cytotoxicity and the morphological alterations of the cells were evaluated using the trypan blue exclusion test and optical microscopy, respectively. The IC<sub>50</sub> values of the DES lie between the values of the corresponding salt and hydrogen bond donor (HBD). Indeed, DES were mostly more cytotoxic than the aqueous solutions of their combined compounds and presented different behaviors when it comes to the cells' morphology. Choline chloride:ethylene glycol is much more cytotoxic than choline chloride:urea, thus proving the important contribution of the HBD to the overall toxicity of the DES. In another approach, cells were incubated in pure DES medium, devoid of any culture medium, for the first time. As a result, the cells were fixed in a certain state for 12 days.

**Keywords:** deep eutectic solvents, choline chloride, urea, ethylene glycol, cytotoxicity, fixation.

## Introduction

Deep eutectic solvents (DES) constitute a new generation of solvents that was discovered only seventeen years ago [1]. They are mostly defined as a binary or ternary mixture of compounds that are capable of hydrogen bonding. Mixing the hydrogen acceptor (HBA) and the hydrogen bond donor (HBD) at a specific molar ratio will lead to the formation of a homogenous liquid with a very low melting temperature, relative to that of the forming compounds [2]. The point which corresponds to these exact composition and temperature is called the eutectic point. Moreover, the word “deep” comes from the fact that a DES must present a lower eutectic temperature than the ideal one [3]. Given the ease of their preparation and their unique physicochemical properties, DES were successfully applied in numerous domains namely organic synthesis [4], catalysis [2], extraction [5], and drug delivery [6]. Another major reason for the rising interest in DES is that these solvents were long considered non-toxic owing to the safety of their forming compounds, further improving their chances of replacing conventional organic solvents. Yet, the toxicity issue was not directly addressed until recently.

In this first study, Hayyan and coworkers surprisingly found that choline chloride (ChCl)-based DES were more cytotoxic than their individual forming compounds toward brine shrimp and were non-toxic toward Gram-positive and Gram-negative bacteria [7]. Since then, several toxicity studies were conducted toward different biological systems like bacteria, yeast, fungi, along with human, mouse, and fish cell lines [8]. However, the studies reported to date do not provide a clear conclusion about DES' toxicity. It is a complex issue given the countless number of possible DES and the multiple factors that can affect their overall toxicity. These factors include the HBA and HBD types, their molar ratio, and the targeted living system. Indeed, most of the studies highlighted the important role of the HBD in the resulting DES' toxicity [9–14]. A highly accurate and predictive multitasking Quantitative Structure-Toxicity Relationship model using a data set of 498 DES and their components was recently reported and concluded that sugar alcohols (e.g. sorbitol and xylitol) and straight-chain alcohols (e.g. glycerol, ethylene glycol, and 1,2-propanediol) are the least toxic HBD, followed by amides (e.g. urea). While sugars (e.g. xylose, fructose, maltose, and glucose) present intermediate toxicity and the use of organic acids (e.g. oxalic acid, phenylacetic acid, citric acid, and malic acid) contributed the most to DES' toxicity [9]. Some other studies pointed out the impact of the HBA [15,16] and the HBA:HBD molar ratio [17,18]. Moreover, one DES can lead to different toxicity responses when different organisms are considered [7].

Choline chloride:urea (ChCl:U) and choline chloride:ethylene glycol (ChCl:EG) represent two of the most studied and applied DES so far. These solvents were already considered by several toxicity studies and were tested toward different organisms, which mainly include bacteria and various human cell lines. Some papers reported their non-toxicity toward Gram-positive and Gram-negative bacteria [7,14], while others proved their anti-bacterial activity [19,20]. When it comes to the cytotoxicity studies, various profiles are obtained which indicate that DES' cytotoxicity tends to be cell line dependent. For instance, ChCl:U and ChCl:EG were non-toxic toward CCO fish cell line and MCF-7 human breast cancer cell line (at 1- 2000 mg.L<sup>-1</sup> concentration range) [21] and even enhanced the cell viability of two human skin cell lines (at 50 – 500 mg.L<sup>-1</sup> concentration range and 1:1 molar ratio) [22]. On the other

hand, the same DES exhibited relatively high cytotoxicity toward other cell lines, with IC<sub>50</sub> values ranging between 25 and 82 mg.L<sup>-1</sup> [10]. Furthermore, few studies compared the effect of DES with the aqueous solutions of their individual or combined starting compounds. Two studies demonstrated that ChCl:U and ChCl:EG DES presented higher toxicity toward brine shrimp [7] and *Escherichia coli* [19] than a mixture of their individual compounds. In contrast, these DES were less toxic than their forming compounds or their mixtures toward *Arthrobacter simplex* [20]. Likewise, ChCl:U led to a lower toxic effect when tested on several human cancer cell lines [10] or marine bacteria *Aliivibrio fischeri* [18].

In the present study, we aimed to evaluate the effect of ChCl:U and ChCl:EG on the MDA-MB-231 human breast cancer cell line. Hence, we investigated both the cytotoxic effect and the morphological alterations of the cells after their exposure to DES or aqueous solutions of their individual or combined forming compounds. In addition, the cells were incubated in pure DES for the first time and their morphology was subsequently monitored using optical microscopy.

## Experimental section

### Materials

Choline chloride (99%), urea (98%), and ethylene glycol (99.5%) were purchased from Acros Organics (Netherlands). Roswell Park Memorial Institute (RPMI) 1640 medium, fetal bovine serum (FBS), L-glutamine, penicillin-streptomycin, Dulbecco's phosphate-buffered saline (PBS), trypsin, and trypan blue were purchased from Sigma-Aldrich (St Louis, USA).

### Preparation of the deep eutectic solvents

The studied DES, ChCl:U and ChCl:EG, were prepared by combining the two components at a 1:2 ChCl:HBD molar ratio. The mixture was then stirred at 60 °C until the formation of a clear and homogenous liquid. The water content of the prepared solvents was determined using the Karl Fisher titration method (Mettler Toledo DL31) and was found to be 0.33 and 0.06 wt.% for ChCl:U and ChCl:EG, respectively.

### Preparation of the aqueous solutions

The aqueous solutions of the individual components (ChCl, urea or ethylene glycol) were prepared by weighing and dissolving each compound in a total volume of 10 mL of ultrapure water to reach a final concentration of 1.5 M. Likewise, the aqueous solutions of both components, denoted as (ChCl + U) aq or (ChCl + EG) aq, were prepared by dissolving ChCl in ultrapure water at a concentration of 1.5 M, followed by the addition of the corresponding HBD such that a 1:2 ChCl:HBD molar ratio is obtained.

## Cell culture

Highly invasive MDA-MB-231 human breast cancer cells were cultured at 37°C in a humidified atmosphere with 5% CO<sub>2</sub> in RPMI 1640 medium. The medium was supplemented with 10% Fetal Bovine Serum, 1% L-glutamine, and 1% penicillin-streptomycin. The cells were passaged every 3- 4 days: medium removal, PBS wash, cell detachment with trypsin solution, medium addition, centrifugation at 900 rpm for 5 min, and resuspension of the pellet in fresh medium.

## Cell viability assay

The cytotoxicity of DES and the aqueous solutions of their constituents was studied using the trypan blue exclusion test which determines the number of viable cells present in the cell suspension. Trypan blue dye will only be taken up by dead cells since they possess damaged membranes and will be excluded by viable cells. Dead cells will consequently have a blue cytoplasm and viable cells will present a clear one when examined. Briefly, 20000 cells /well were seeded into 24-well culture plates, in a total volume of 500 µL/well of RPMI medium. After overnight incubation to allow cell attachment, the medium was replaced with a fresh medium containing increasing concentrations of DES, an aqueous solution of the individual constituents (ChCl or urea or ethylene glycol), or an aqueous solution of combined HBA and HBD. In other words, the prepared DES and stock solutions of the individual or combined compounds were diluted in the fresh culture medium to reach the desired final concentrations. The molar mass of the DES was calculated according to Florindo *et al.* (MW ChCl:U = 259.74 g.mol<sup>-1</sup> and MW ChCl:EG = 263.76 g.mol<sup>-1</sup>) [24]. Whereas control cells were incubated in a fresh medium. The plates were then incubated for 24, 48, and 72h. After each time point, the medium was removed, the cells were washed with PBS and detached using trypsin. The cell suspension was centrifuged (900 rpm, 5 min) and the resulting pellet was resuspended in fresh medium. The cell suspension was mixed with trypan blue dye at 1:1 dilution (v/v) and 10 µL were slowly deposited on the Neubauer slide and examined on the optical microscope. All measurements were performed in triplicate and each experiment was repeated at least three times. The results are expressed as the percentage of cell viability with respect to the untreated control, which was set as 100%. Corresponding IC<sub>50</sub> values were calculated from the dose-response curves using equations of best-fitted trendlines.

## Morphological assessment

The morphological changes of MDA-MB-231 breast cancer cells following the exposure to different concentrations of DES or the aqueous solutions of their constituents were investigated via optical microscopy. Cells were seeded in a 12-well plate (40000 cells/well) in a total volume of 1 mL/well of RPMI medium. After overnight incubation, cells were subjected to different concentrations of the aqueous solution of the individual components (50 and 100 mM), the aqueous solution of the combined components, or the DES (10; 30; 50 and 100 mM). The cells were then photographed at different time points (1, 3, 6, 24, and 48h) using an inverted microscope (Leica Microsystems, Switzerland). This experiment was repeated 3 times and each concentration was done in duplicate.

## Incubation in pure DES

The effect of DES on human cells was studied by exposing MDA-MB-231 cells to pure DES. Cells were seeded on a 12-well plate (40000 cells/well) in a total volume of 1 mL/well of RPMI medium. 72 hours after seeding, the RPMI medium was removed and replaced with 1 mL of fresh RPMI medium (control) or DES (ChCl:U or ChCl:EG). The cells were then monitored at different time points (1h, 72h, day 6, day 10, and day 12) via optical microscopy on a 10X objective. After 12 days at 37°C, the DES was removed, the well was washed 3 times with PBS buffer ( $V_{\text{PBS}} = 200 \mu\text{L}/\text{well}$ ), and the wells were imaged once again. The cells were then detached using trypsin, centrifuged (900 rpm, 5 min) and the resulting pellet was resuspended in fresh medium. The resulting cell suspension was placed in the wells to check if the cells can recover and proliferate.

## Statistical analysis

Experimental values were expressed as the means  $\pm$  standard deviation (SD) of at least three independent experiments. Statistical analysis was performed using Student's t-test and GraphPad Prism 8 software. Statistical significance was defined when  $P < 0.05$ .

## Results and discussion

### Cytotoxicity and morphological studies

Breast cancer cells (MDA-MB-231) were treated with ChCl:U or ChCl:EG DES, or with aqueous solutions of their separate or combined forming compounds. The cell viability was determined via the trypan blue exclusion test and the cell morphology was observed at different time points following the exposure. Combining these two approaches is interesting since it can provide a better elucidation of the impact of the DES on the cells. Cells were subjected to concentrations ranging between 0.01 and 100 mM of the above-mentioned solutions.

- **Effect of the forming compounds**

In a first step, we evaluated the effect of the individual compounds used for the preparation of the two studied DES on MDA-MB-231 cells. When exposed to choline chloride (ChCl) for 24h, the cell viability decreased from 96.79% to 64.19% when going from 0.01 to 100 mM, respectively (Figure S1a). The viability dropped to 39.67% at the highest concentration (100 mM) after 48h of exposure (Figure 1a). Similar results were obtained after 72h (Figure S2a). On the other hand, the number of viable cells slightly decreased when exposed to urea (Figure 1b), with 69.08% cell viability at the highest concentration and after 72h of exposure (Figure S2b). Conversely, the cell viability significantly dropped in presence of ethylene glycol and reached, after 48h, 42%, and 12.5% at 0.01 and 100 mM, respectively (Figure 1c). A similar effect was also observed following 72h of exposure (Figure S2c). Furthermore, the observations via optical microscopy showed adherent and confluent spindle-shaped cells in control, with few detached cells owing to the full coverage of the wells by the cells. When treated with ChCl, less confluent and elongated MDA-MB-231 cells were observed compared with control cells (Figure 2a). However, no morphological alterations or effect on the cells' proliferation were detected

upon exposure of the cells to urea (Figure 2b). Likewise, no remarkable differences were seen on the microscope when it comes to the cellular morphology or proliferation of ethylene glycol-treated cells (Figure 2c). The IC50 values, displayed in Table 1, prove that ethylene glycol (IC50 = 9.21E-03 mM) is more cytotoxic than ChCl (IC50 = 10.70 mM), which is more cytotoxic than urea (IC50 = 205.60 mM). However, this finding is not in accordance with the studies of Hayyan *et al.* [10] and Macário *et al.* [18] who both agreed on the following toxicity ranking: ChCl > urea > ethylene glycol toward various human cell lines other than MDA-MB-231 and marine bacteria. Consequently, this could be due to the difference in targeted biological systems, type of cell line, or experimental procedure.

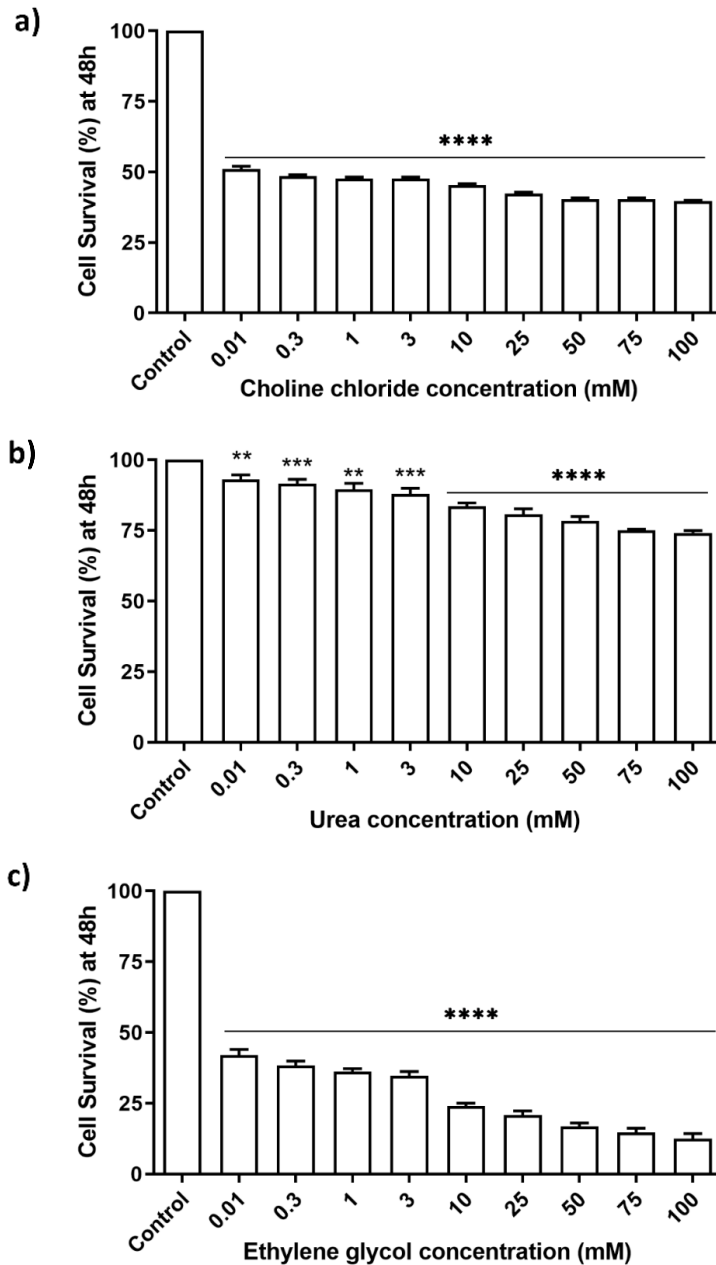


Figure 1. Variation of cell viability of MDA-MB-231 breast cancer cells in function of the concentration of a) choline chloride, b) urea, or c) ethylene glycol following 48h of exposure. Results are expressed as mean ± SD of three independent experiments (\*\* stands for P < 0.01, \*\*\* stands for P < 0.001, and \*\*\*\* stands for P < 0.0001)

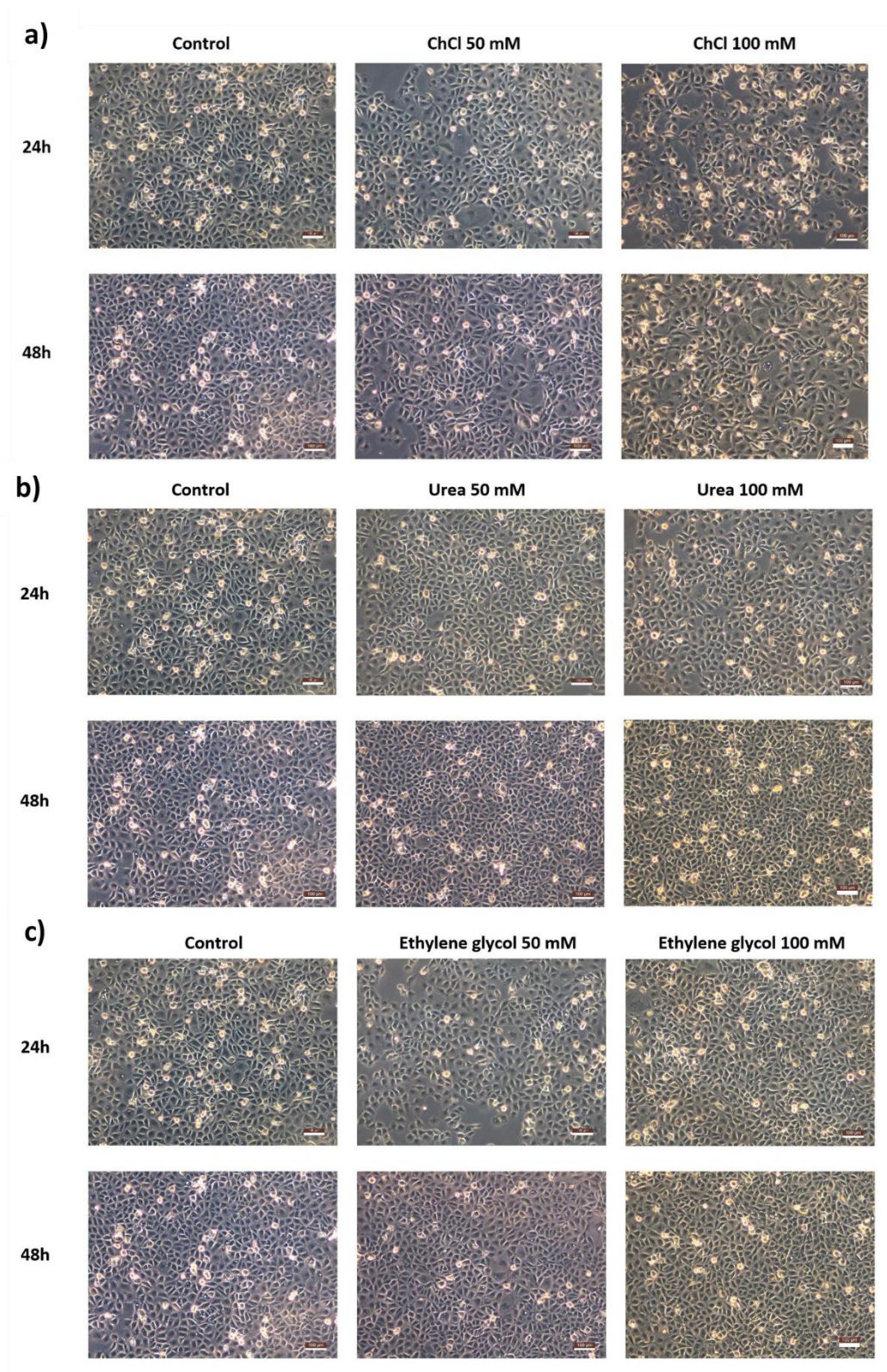


Figure 2. Images of MDA-MB-231 cells untreated (control) or treated with aqueous solutions of a) choline chloride, b) urea or c) ethylene glycol for 24 and 48h

Table 1. IC50 values of DES and the aqueous solutions of their individual or combined forming compounds after 48h of exposure

Solvent	IC50 (mM)			
	HBA	HBD	(HBA + HBD) aq	DES
ChCl:U	10.70	205.60	26.92	32.04
ChCl:EG		9.21E-03	5.47E-01	4.76E-03

- DES vs aqueous mixtures of the forming compounds

Likewise, we evaluated the effect of preformed DES on MDA-MB-231 cells and compared it to the effect of the aqueous solutions of both HBA and HBD denoted as (HBA + HBD) aq. The results of the cell viability assay revealed that ChCl:U DES is less cytotoxic than (ChCl + U) aq after 24 or 48h of exposure. However, this effect was reversed at the highest concentrations (50, 75, and 100 mM) (Figure 3 and Figure S3a). After 72h, the higher cytotoxic effect of ChCl:U compared to (ChCl + U) aq covered a wider concentration range (1- 100 mM) (Figure S3b). Moreover, the IC50 value of ChCl:U (32.04 mM) determined at 48h is very close to that of (ChCl + U) aq (26.92 mM), and lies between the IC50 of ChCl and urea (Table 1). Besides, no clear differences were observed between untreated cells and cells in presence of ChCl:U or (ChCl + U) aq at 10 or 30 mM, as illustrated in Figure 4 and Figure 5. However, at 50 and 100 mM, the number of the cells decreased in presence of the aqueous solution from the first hour of exposure where few round cells were observed at 100 mM. Although the cells were able to recover at 50 mM after 48h of incubation, elongated cells with membrane blebbing were seen at 100 mM (Figure 6). On the other hand, ChCl:U DES does not seem to affect the cell proliferation as much as the aqueous solution but may induce cell death since more floating cells were noticed at high DES concentrations compared with control (Figure 5). In addition, clustered cells were observed at 100 mM DES from  $t = 1h$  (Figure 5), and cell enlargement and elongation, as well as membrane blebbing, were detected at  $t = 48h$  (Figure 6).

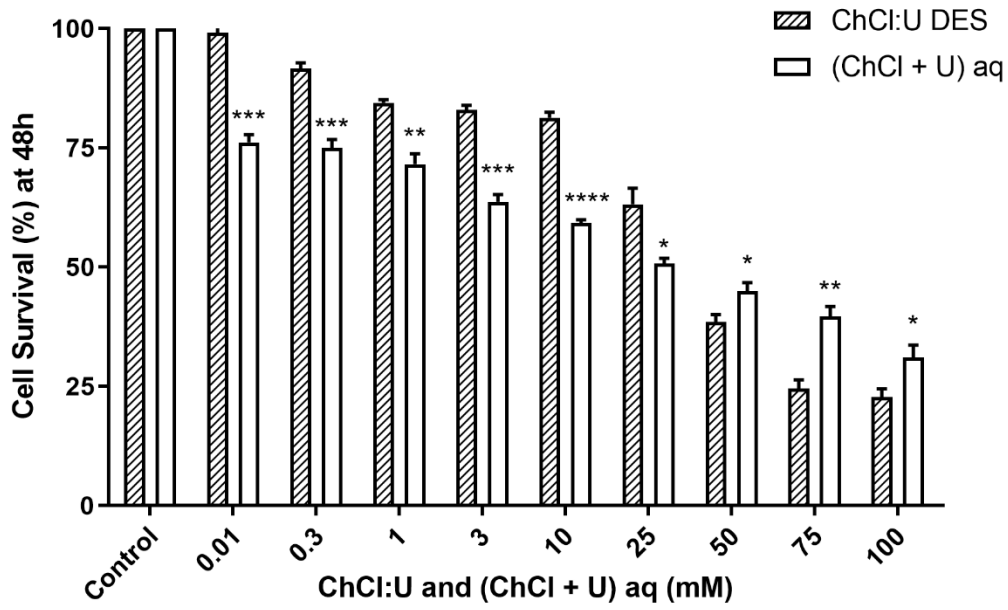


Figure 3. Cytotoxic effect of ChCl:U DES versus the aqueous solution of its components (ChCl + U) aq on MDA-MB-231 breast cancer cells after 48h of exposure. Results are expressed as mean  $\pm$  SD of three independent experiments (\* stands for  $P < 0.1$ , \*\* stands for  $P < 0.01$ , \*\*\* stands for  $P < 0.001$ , and \*\*\*\* stands for  $P < 0.0001$ )

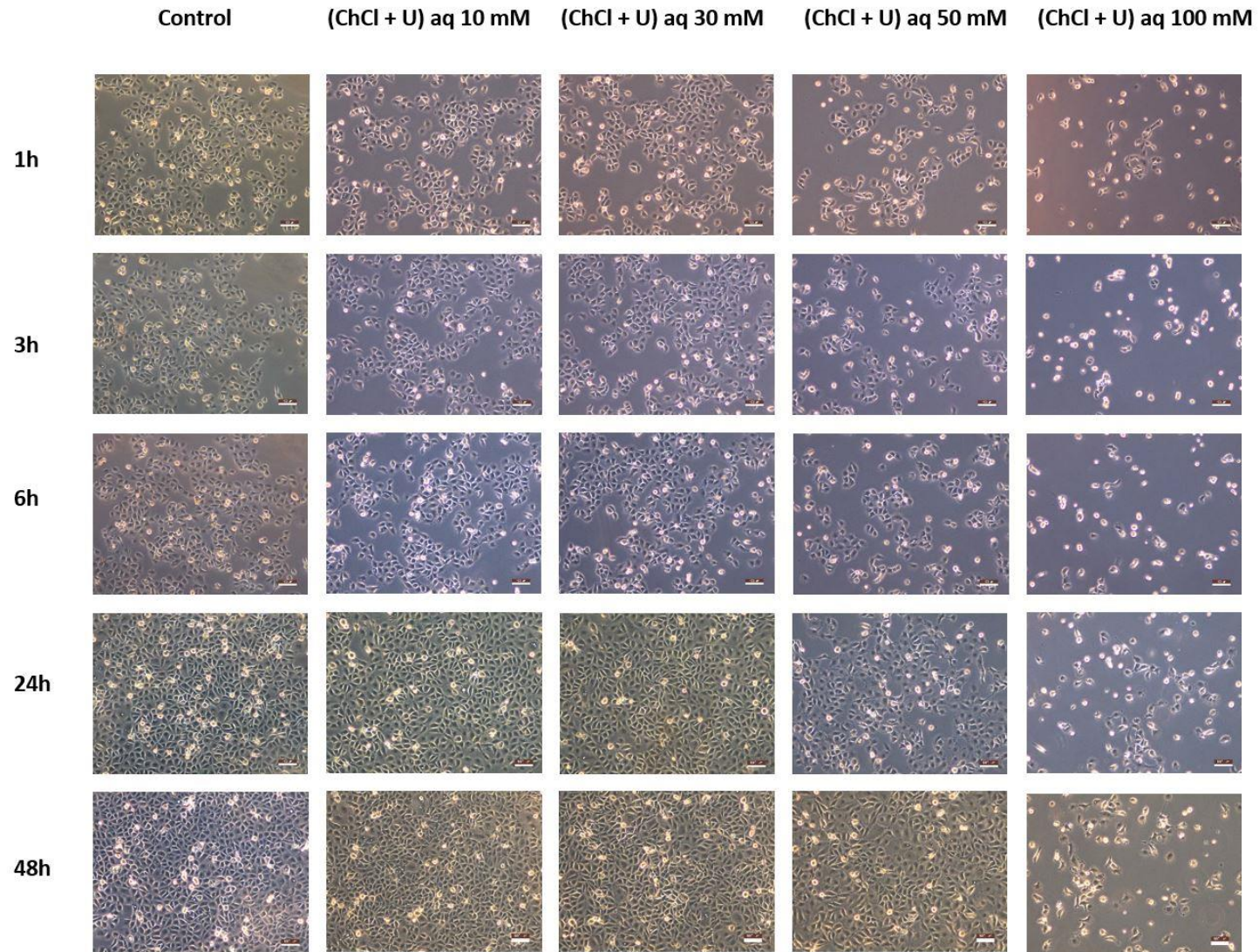


Figure 4. Images of MDA-MB-231 cells untreated (control) or treated with different concentrations of aqueous solutions of choline chloride and urea at different time points

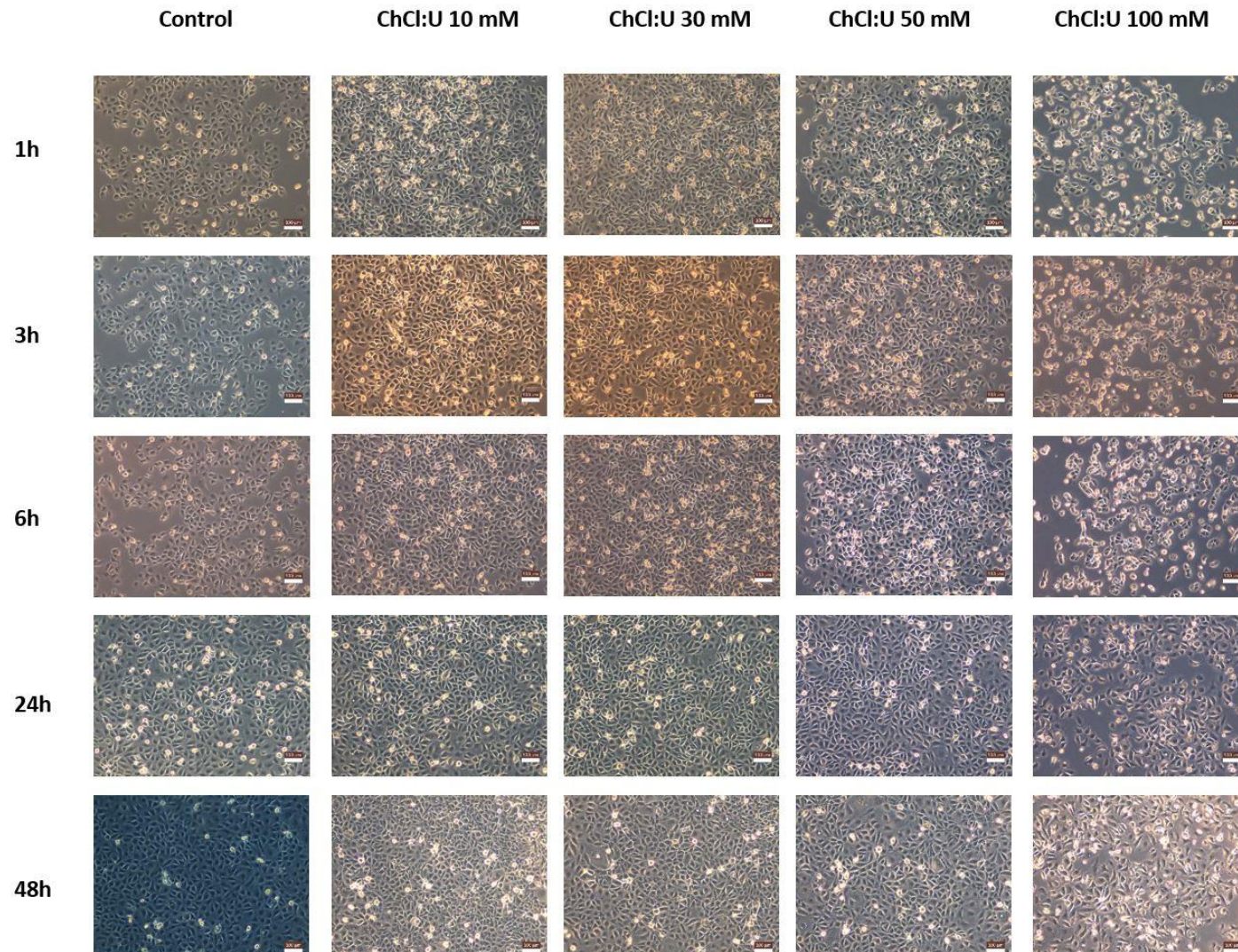


Figure 5. Images of MDA-MB-231 cells untreated (control) or treated with different concentrations of ChCl:U DES at different time points

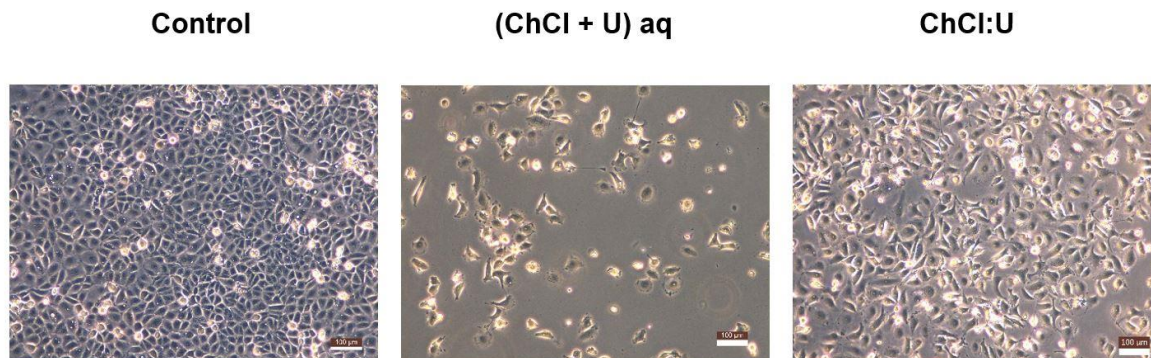


Figure 6. Morphological differences between untreated MDA-MB-231 cells and cells treated with aqueous solutions of choline chloride and urea (ChCl + U) aq or ChCl:U DES at 100 mM for 48h

When it comes to ChCl:EG, DES is significantly more cytotoxic than (ChCl + EG) aq at all tested concentrations. Moreover, no viable cells were obtained in presence of the DES at a concentration  $\geq 10$  mM, following 24h (Figure S5), 48h (Figure 7), or 72h of exposure (Figure S5). Consequently, the IC<sub>50</sub> of ChCl:EG (4.76E-03 mM) is lower than that of (ChCl + EG) aq (5.47E-01 mM). Hayyan and coworkers also found out that aqueous solutions containing the forming compounds of ChCl-based DES are most of the time less cytotoxic than the corresponding DES toward various human cell lines, except for ChCl:U [10]. When it comes to the morphological observations, no remarkable difference was noticed between untreated cells and cells treated with (ChCl + EG) aq (Figure S7) or ChCl:EG DES (Figure S8) at 10 and 30 mM. However, a reduction in the number of cells was clear in presence of the aqueous solution at 50 and 100 mM from the first hour of exposure. Besides, the cells presented a more elongated bipolar shape and a damaged membrane at 50 and 100 mM. A different outcome resulted from the DES' treatment where cells were still confluent at 50 and 100 mM but elongated adherent cells and a higher number of detached dead cells was witnessed especially at 100 mM. The results obtained herein confirm that DES present a different behavior than (HBA + HBD) aq, thus a possibly different mechanism of action. Furthermore, the impact of the DES is not simply caused by the simultaneous presence of the HBA and HBD although the DES, present at a maximum of 2% (v/v), is most probably disrupted in presence of the culture medium [18]. Indeed, many studies have stated that the hydrogen bond network of DES is weakened in presence of high water content since water tends to interact with the DES' forming compounds [25–29]. Furthermore, when comparing the two DES, it can be concluded that ChCl:EG is more cytotoxic than ChCl:U, which is in accordance with the works of Shekaari *et al.* and Mao *et al.* who tested ChCl-based DES on A549 lung cancer cells and *Arthrobacter simplex*, respectively [20,23]. The major difference in the cytotoxicity profile of the studied DES highlights the important role of the HBD in the overall toxicity.

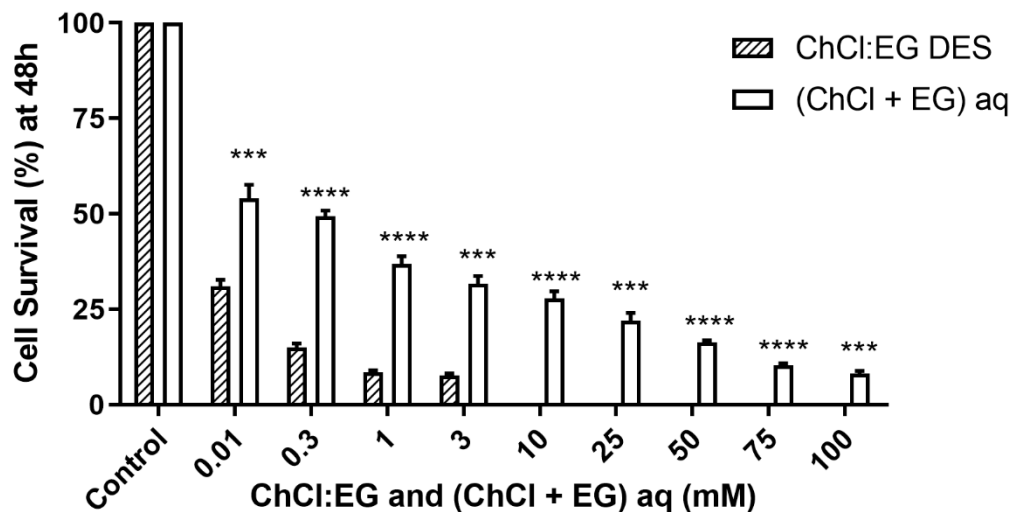


Figure 7. Cytotoxic effect of ChCl:EG DES versus the aqueous solution of its components (ChCl + EG) aq on MDA-MB-231 breast cancer cells after 48h of exposure. Results are expressed as mean  $\pm$  SD of three independent experiments (\*\*\*) stands for  $P < 0.001$ , and \*\*\*\* stands for  $P < 0.0001$ )

### Incubation in pure DES

In another approach, cells were exposed to pure DES for the first time. Figure 8 depicts the images of MDA-MB-231 cells following their incubation in ChCl:U or ChCl:EG for different periods. At  $t = 1$ h, control cells are confluent (72h after seeding) and so are the cells incubated in pure DES, except that cell shrinkage and voids are observed between the cells in both DES. At  $t = 72$ h, floating dead cells were covering the adherent cells in the control given that the rapidly evolving cancer cells did not have enough room to proliferate or enough nutrients from the culture medium. However, no obvious dead cells were seen in both ChCl:U- and ChCl:EG-treated cells. On the other hand, some morphological changes are somehow observed in the cells treated with ChCl:U at  $t = 72$ h, which seemed like a detached monolayer of cells. Twelve days after their exposure, untreated cells are obviously dead but DES-treated cells surprisingly maintained the same state that was observed at earlier time points. Thereafter, the cells were again photographed after DES removal and PBS wash (Figure 9). These results demonstrate that ChCl-based DES somehow fix the cells for at least 12 days. Yet, the cell morphology was altered and the membrane integrity seems to be lost in ChCl:U. Nevertheless, the cells maintained their spindle-like shape in ChCl:EG, although the tight cell to cell junction seemed disrupted (Figure 9). This finding may explain the distinct morphological observations that were noticed when comparing the effect of DES with the aqueous solutions. As discussed earlier, no decrease in the cell number was detected when MDA-MB-231 cells were exposed to both DES, which can be related to the potential cell fixation by DES. The purpose of using a fixative is to physically or chemically fix dynamically changing viable cells or tissues at a certain time point. The physical fixation involves processes

like heating, microwaving, or freeze-drying. On the other hand, chemical fixation consists of using coagulant or non-coagulant chemical fixatives [30]. Coagulant fixatives act by coagulating the proteins which generally maintain the cells or tissues' architecture, whereas non-coagulant fixatives form covalent cross-links between proteins, between nucleic acids, or between proteins and nucleic acids. To the best of our knowledge, this is the first study that highlights the ability of DES in cell fixation. However, liposomal and bacterial preservation in ChCl-based DES has already been demonstrated [31–33]. Understanding the mechanism of DES behind the cells' fixation is quite early but some explanations can be drawn based on the previously reported papers. The exposure to pure DES will induce a high osmotic pressure on the cells which will most probably lead the cells to lose their inner water molecules. Such effects were also obtained when exposing liposomes to ChCl-based DES in our previous study [32]. The removal of water from the cells may destabilize the conformation of the proteins and result in their coagulation. Few studies have already investigated the effect of ChCl-based DES on the activity and structure of proteins and the latter were found to be negatively affected at higher DES concentrations in some cases [34–38].

Thereafter, the cells were partially detached (since complete detachment was not achieved after trypsinization) and resuspended in a fresh medium. Yet, 24h later, the cells did not adhere or proliferate. The preliminary observations presented herein already reveal some interesting information although further investigations must be carried out to understand the behavior of these cells in presence of pure DES.

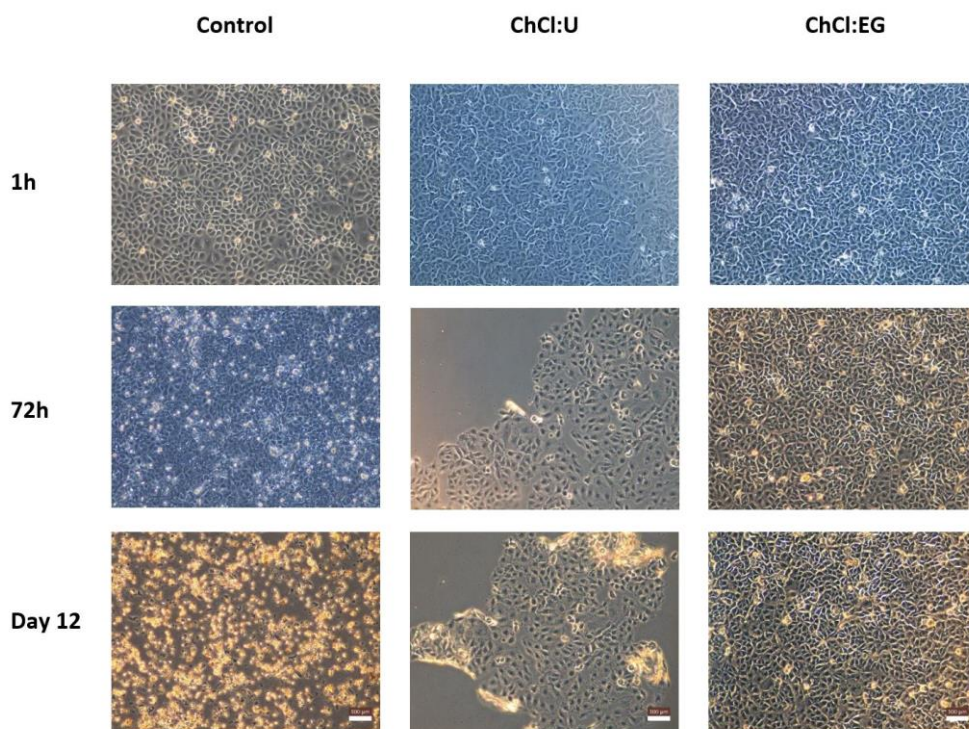


Figure 8. Images of MDA-MB-231 cells exposed to RPMI medium (control) or pure DES for different periods

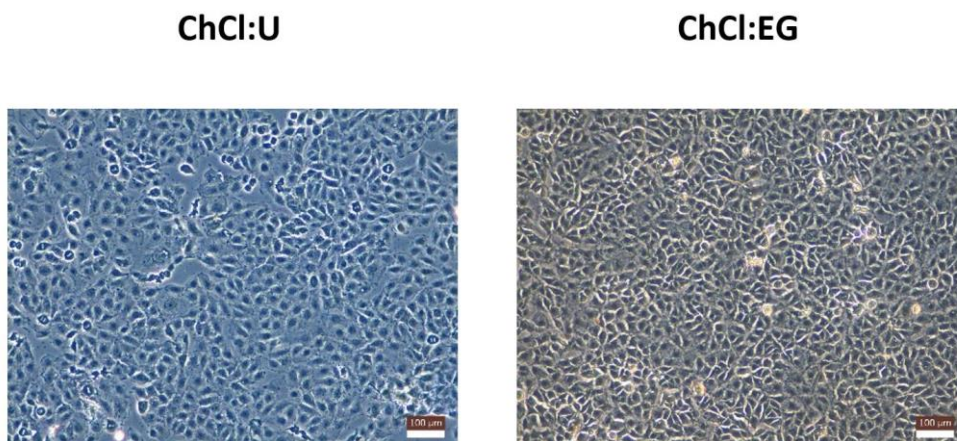


Figure 9. Observations of MDA-MB-231 cells exposed to pure DES for 12 days following DES removal and PBS wash

## Conclusion

DES were long considered non-toxic and green owing to the safety of their starting materials. However, their non-toxicity became questionable when this topic was recently addressed. In this study, we tested two common DES, ChCl:U and ChCl:EG, on MDA-MB-231 human breast cancer cell line and compared their effect to that of their individual or combined forming compounds. The cytotoxicity study conducted via the trypan blue exclusion test revealed that DES are mainly more cytotoxic than the aqueous solution of their compounds. Furthermore, the observation of the cell morphology upon exposure to DES or aqueous solutions of both compounds showed a different behavior which can be explained by a different mechanism of action. The choice of the hydrogen bond donor can highly affect the overall toxicity of a DES, resulting in a relatively harmless DES like ChCl:U or a moderately toxic DES like ChCl:EG. In another approach, cells were incubated in pure DES for the first time and were monitored by optical microscopy. Both DES were able to fix the cells in a certain state for up to 12 days, which can be explained by dehydration of the cells upon exposure to pure DES and subsequent protein coagulation. To the best of our knowledge, this is the first reported case of cell fixation by DES and further studies must be carried out to understand the mechanism behind these observations.

## References

- [1] A.P. Abbott, G. Capper, D.L. Davies, R.K. Rasheed, V. Tambyrajah, Novel solvent properties of choline chloride/urea mixtures, *Chem. Commun.* (2003) 70–71. <https://doi.org/10.1039/B210714G>.
- [2] Q. Zhang, K. De Oliveira Vigier, S. Royer, F. Jérôme, Deep eutectic solvents: syntheses, properties and applications, *Chem. Soc. Rev.* 41 (2012) 7108–7146. <https://doi.org/10.1039/C2CS35178A>.
- [3] M.A.R. Martins, S.P. Pinho, J.A.P. Coutinho, Insights into the nature of eutectic and deep eutectic mixtures, *J. Solut. Chem.* 48 (2019) 962–982. <https://doi.org/10.1007/s10953-018-0793-1>.
- [4] D.A. Alonso, A. Baeza, R. Chinchilla, G. Guillena, I.M. Pastor, D.J. Ramón, Deep eutectic solvents: the organic reaction medium of the century, *Eur. J. Org. Chem.* 2016 (2016) 612–632. <https://doi.org/10.1002/ejoc.201501197>.
- [5] M. de los Á. Fernández, J. Boiteux, M. Espino, F.J.V. Gomez, M.F. Silva, Natural deep eutectic solvents-mediated extractions: The way forward for sustainable analytical developments, *Anal. Chim. Acta.* 1038 (2018) 1–10. <https://doi.org/10.1016/j.aca.2018.07.059>.
- [6] S.N. Pedro, M.G. Freire, C.S.R. Freire, A.J.D. Silvestre, Deep eutectic solvents comprising active pharmaceutical ingredients in the development of drug delivery systems, *Expert Opin. Drug Deliv.* 16 (2019) 497–506. <https://doi.org/10.1080/17425247.2019.1604680>.
- [7] M. Hayyan, M.A. Hashim, A. Hayyan, M.A. Al-Saadi, I.M. AlNashef, M.E.S. Mirghani, O.K. Saheed, Are deep eutectic solvents benign or toxic?, *Chemosphere.* 90 (2013) 2193–2195. <https://doi.org/10.1016/j.chemosphere.2012.11.004>.
- [8] Y.P. Mbous, M. Hayyan, A. Hayyan, W.F. Wong, M.A. Hashim, C.Y. Looi, Applications of deep eutectic solvents in biotechnology and bioengineering—Promises and challenges, *Biotechnol. Adv.* 35 (2017) 105–134. <https://doi.org/10.1016/j.biotechadv.2016.11.006>.
- [9] A.K. Halder, M.N.D.S. Cordeiro, Probing the environmental toxicity of deep eutectic solvents and their components: an in silico modeling approach, *ACS Sustain. Chem. Eng.* 7 (2019) 10649–10660. <https://doi.org/10.1021/acssuschemeng.9b01306>.
- [10] M. Hayyan, C.Y. Looi, A. Hayyan, W.F. Wong, M.A. Hashim, In vitro and in vivo toxicity profiling of ammonium-based deep eutectic solvents, *PLoS ONE.* 10 (2015). <https://doi.org/10.1371/journal.pone.0117934>.
- [11] M. Hayyan, Y.P. Mbous, C.Y. Looi, W.F. Wong, A. Hayyan, Z. Salleh, O. Mohd-Ali, Natural deep eutectic solvents: cytotoxic profile, *SpringerPlus.* 5 (2016) 913. <https://doi.org/10.1186/s40064-016-2575-9>.
- [12] K. Radošević, M. Cvjetko Bubalo, V.G. Srček, D. Grgas, T.L. Dragičević, I.R. Redovniković, Evaluation of toxicity and biodegradability of choline chloride based deep eutectic solvents, *Ecotoxicol. Environ. Saf.* 112 (2015) 46–53. <https://doi.org/10.1016/j.ecoenv.2014.09.034>.
- [13] K. Radošević, I. Čanak, M. Panić, K. Markov, M. Cvjetko Bubalo, J. Frece, V.G. Srček, I.R. Redovniković, Antimicrobial, cytotoxic and antioxidative evaluation of natural deep eutectic solvents, *Environ. Sci. Pollut. Res.* 25 (2018) 14188–14196. <https://doi.org/10.1007/s11356-018-1669-z>.
- [14] B.-Y. Zhao, P. Xu, F.-X. Yang, H. Wu, M.-H. Zong, W.-Y. Lou, Biocompatible deep eutectic solvents based on choline chloride: characterization and application to the extraction of rutin from *Sophora japonica*, *ACS Sustain. Chem. Eng.* 3 (2015) 2746–2755. <https://doi.org/10.1021/acssuschemeng.5b00619>.
- [15] I. Juneidi, M. Hayyan, M.A. Hashim, Evaluation of toxicity and biodegradability for cholinium-based deep eutectic solvents, *RSC Adv.* 5 (2015) 83636–83647. <https://doi.org/10.1039/C5RA12425E>.
- [16] I.P.E. Macário, F. Jesus, J.L. Pereira, S.P.M. Ventura, A.M.M. Gonçalves, J.A.P. Coutinho, F.J.M. Gonçalves, Unraveling the ecotoxicity of deep eutectic solvents using the mixture toxicity theory, *Chemosphere.* 212 (2018) 890–897. <https://doi.org/10.1016/j.chemosphere.2018.08.153>.

- [17] R. Ahmadi, B. Hemmateenejad, A. Safavi, Z. Shojaeifard, M. Mohabbati, O. Firuzi, Assessment of cytotoxicity of choline chloride-based natural deep eutectic solvents against human HEK-293 cells: A QSAR analysis, *Chemosphere*. 209 (2018) 831–838. <https://doi.org/10.1016/j.chemosphere.2018.06.103>.
- [18] I.P.E. Macário, S.P.M. Ventura, J.L. Pereira, A.M.M. Gonçalves, J.A.P. Coutinho, F.J.M. Gonçalves, The antagonist and synergist potential of cholinium-based deep eutectic solvents, *Ecotoxicol. Environ. Saf.* 165 (2018) 597–602. <https://doi.org/10.1016/j.ecoenv.2018.09.027>.
- [19] Q. Wen, J.-X. Chen, Y.-L. Tang, J. Wang, Z. Yang, Assessing the toxicity and biodegradability of deep eutectic solvents, *Chemosphere*. 132 (2015) 63–69. <https://doi.org/10.1016/j.chemosphere.2015.02.061>.
- [20] S. Mao, K. Li, Y. Hou, Y. Liu, S. Ji, H. Qin, F. Lu, Synergistic effects of components in deep eutectic solvents relieve toxicity and improve the performance of steroid biotransformation catalyzed by *Arthrobacter simplex*, *J. Chem. Technol. Biotechnol.* 93 (2018) 2729–2736. <https://doi.org/10.1002/jctb.5629>.
- [21] M. Cvjetko Bubalo, A. Jurinjak Tušek, M. Vinković, K. Radošević, V. Gaurina SrĀek, I. Radojlić Redovniković, Cholinium-based deep eutectic solvents and ionic liquids for lipase-catalyzed synthesis of butyl acetate, *J. Mol. Catal. B Enzym.* 122 (2015) 188–198. <https://doi.org/10.1016/j.molcatb.2015.09.005>.
- [22] I.P.E. Macário, H. Oliveira, A.C. Menezes, S.P.M. Ventura, J.L. Pereira, A.M.M. Gonçalves, J. a. P. Coutinho, F.J.M. Gonçalves, Cytotoxicity profiling of deep eutectic solvents to human skin cells, *Sci. Rep.* 9 (2019) 1–9. <https://doi.org/10.1038/s41598-019-39910-y>.
- [23] H. Shekaari, M.T. Zafarani-Moattar, M. Mokhtarpour, S. Faraji, Exploring cytotoxicity of some choline-based deep eutectic solvents and their effect on the solubility of lamotrigine in aqueous media, *J. Mol. Liq.* 283 (2019) 834–842. <https://doi.org/10.1016/j.molliq.2019.03.079>.
- [24] C. Florindo, F.S. Oliveira, L.P.N. Rebelo, A.M. Fernandes, I.M. Marrucho, Insights into the synthesis and properties of deep eutectic solvents based on cholinium chloride and carboxylic acids, *ACS Sustain. Chem. Eng.* 2 (2014) 2416–2425. <https://doi.org/10.1021/sc500439w>.
- [25] E. Posada, N. López-Salas, R.J.J. Riobóo, M.L. Ferrer, M.C. Gutiérrez, F. del Monte, Reline aqueous solutions behaving as liquid mixtures of H-bonded co-solvents: microphase segregation and formation of co-continuous structures as indicated by Brillouin and <sup>1</sup>H NMR spectroscopies, *Phys. Chem. Chem. Phys.* 19 (2017) 17103–17110. <https://doi.org/10.1039/C7CP02180A>.
- [26] O.S. Hammond, D.T. Bowron, K.J. Edler, The effect of water upon deep eutectic solvent nanostructure: an unusual transition from ionic mixture to aqueous solution, *Angew. Chem. Int. Ed.* 56 (2017) 9782–9785. <https://doi.org/10.1002/anie.201702486>.
- [27] P. Kumari, Shobhna, S. Kaur, H.K. Kashyap, Influence of hydration on the structure of reline deep eutectic solvent: a molecular dynamics study, *ACS Omega*. 3 (2018) 15246–15255. <https://doi.org/10.1021/acsomega.8b02447>.
- [28] S. Kaur, A. Gupta, H.K. Kashyap, How hydration affects the microscopic structural morphology in a deep eutectic solvent, *J. Phys. Chem. B.* 124 (2020) 2230–2237. <https://doi.org/10.1021/acs.jpcc.9b11753>.
- [29] T. El Achkar, S. Fourmentin, H. Greige-Gerges, Deep eutectic solvents: An overview on their interactions with water and biochemical compounds, *J. Mol. Liq.* 288 (2019) 111028. <https://doi.org/10.1016/j.molliq.2019.111028>.
- [30] I. Eltoun, J. Fredenburgh, R.B. Myers, W.E. Grizzle, Introduction to the Theory and Practice of Fixation of Tissues, *J. Histotechnol.* 24 (2001) 173–190. <https://doi.org/10.1179/his.2001.24.3.173>.
- [31] M.C. Gutiérrez, M.L. Ferrer, C.R. Mateo, F. del Monte, Freeze-drying of aqueous solutions of deep eutectic solvents: a suitable approach to deep eutectic suspensions of self-assembled structures, *Langmuir*. 25 (2009) 5509–5515. <https://doi.org/10.1021/la900552b>.

- [32] J. Eid, T. El Achkar, S. Fourmentin, H. Greige-Gerges, A. Jraij, First investigation of liposomes behavior and phospholipids organization in choline chloride-based deep eutectic solvents by atomic force microscopy, *J. Mol. Liq.* 306 (2020) 112851. <https://doi.org/10.1016/j.molliq.2020.112851>.
- [33] M.C. Gutiérrez, M.L. Ferrer, L. Yuste, F. Rojo, F. del Monte, Bacteria Incorporation in Deep-eutectic Solvents through Freeze-Drying, *Angew. Chem. Int. Ed.* 49 (2010) 2158–2162. <https://doi.org/10.1002/anie.200905212>.
- [34] A.R. Harifi-Mood, R. Ghobadi, A. Divsalar, The effect of deep eutectic solvents on catalytic function and structure of bovine liver catalase, *Int. J. Biol. Macromol.* 95 (2017) 115–120. <https://doi.org/10.1016/j.ijbiomac.2016.11.043>.
- [35] A. Sanchez-Fernandez, K.J. Edler, T. Arnold, D. Alba Venero, A.J. Jackson, Protein conformation in pure and hydrated deep eutectic solvents, *Phys. Chem. Chem. Phys.* 19 (2017) 8667–8670. <https://doi.org/10.1039/C7CP00459A>.
- [36] Y.H. Choi, J. van Spronsen, Y. Dai, M. Verberne, F. Hollmann, I.W.C.E. Arends, G.-J. Witkamp, R. Verpoorte, Are natural deep eutectic solvents the missing link in understanding cellular metabolism and physiology?, *Plant Physiol.* 156 (2011) 1701–1705. <https://doi.org/10.1104/pp.111.178426>.
- [37] D. Lindberg, M. de la Fuente Revenga, M. Widersten, Deep eutectic solvents (DESs) are viable cosolvents for enzyme-catalyzed epoxide hydrolysis, *J. Biotechnol.* 147 (2010) 169–171. <https://doi.org/10.1016/j.jbiotec.2010.04.011>.
- [38] A.A. Papadopoulou, E. Efstathiadou, M. Patila, A.C. Polydera, H. Stamatis, Deep Eutectic Solvents as Media for Peroxidation Reactions Catalyzed by Heme-Dependent Biocatalysts, *Ind. Eng. Chem. Res.* 55 (2016) 5145–5151. <https://doi.org/10.1021/acs.iecr.5b04867>.

## Supplementary Material

### Effect of choline chloride-based deep eutectic solvents on MDA-MB-231 breast cancer cell line: cytotoxicity study and morphological evaluation

Tracy El Achkar<sup>a,b</sup>, H el ene Greige-Gerges<sup>a</sup>, Sophie Fourmentin<sup>b</sup>, Maya Kayouka<sup>a,\*</sup>

<sup>a</sup>*Bioactive Molecules Research Laboratory, Faculty of Sciences, Lebanese University, Lebanon*

<sup>b</sup>*Unit e de Chimie Environnementale et Interactions sur le Vivant (UCEIV, UR 4492), SFR Condorcet FR CNRS 3417, ULCO, F-59140 Dunkerque, France*

\*Corresponding author: maya.kayouka@ul.edu.lb

Bioactive Molecules Research Laboratory, Doctoral School of Sciences and Technologies, Faculty of Sciences, Lebanese University, B.P. 90656, Jdaidet el-Matn, Lebanon

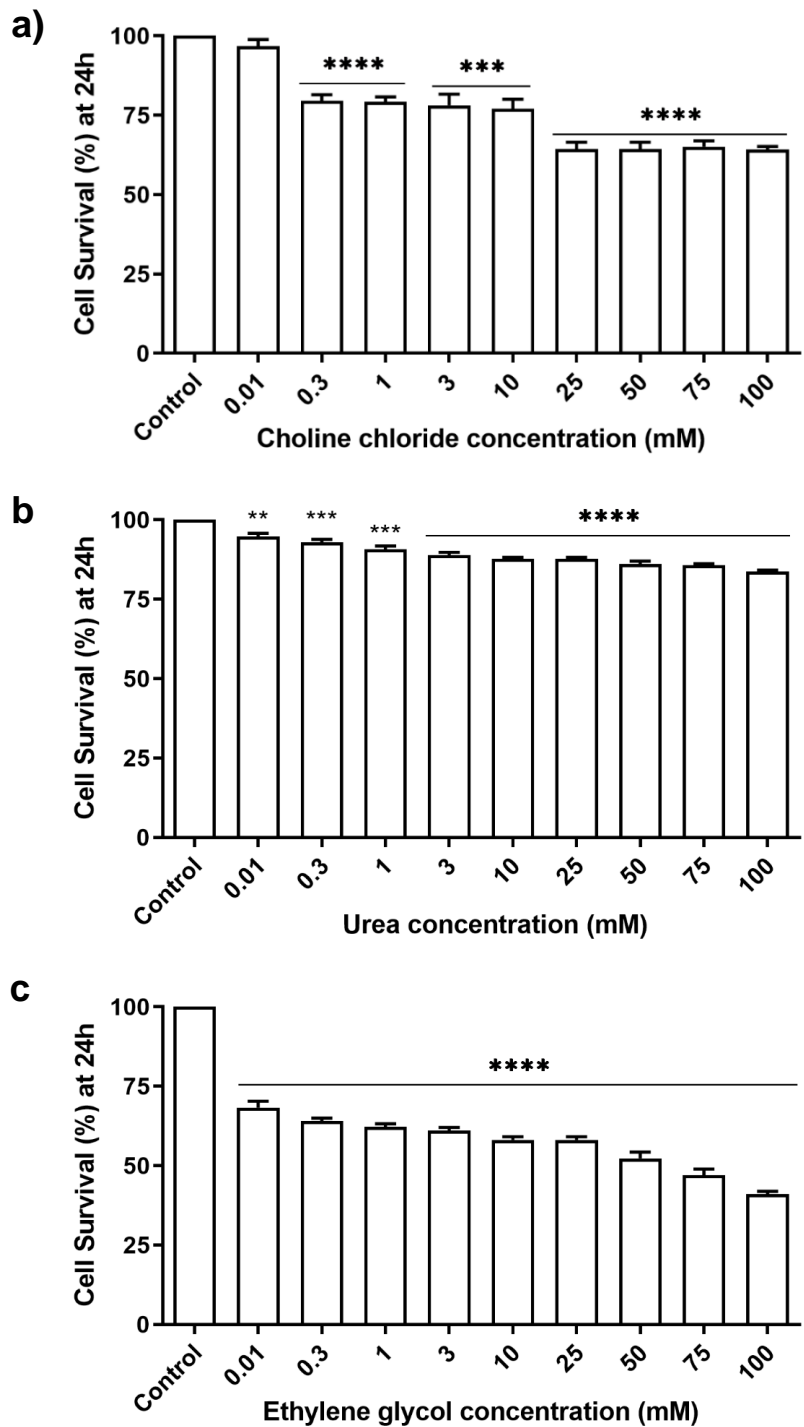


Figure S1. Variation of cell viability of MDA-MB-231 breast cancer cells in function of the concentration of a) choline chloride, b) urea, or c) ethylene glycol following 24h of exposure. Results are expressed as mean  $\pm$  SD of three independent experiments (\*\* stands for  $P < 0.01$ , \*\*\* stands for  $P < 0.001$ , and \*\*\*\* stands for  $P < 0.0001$ )

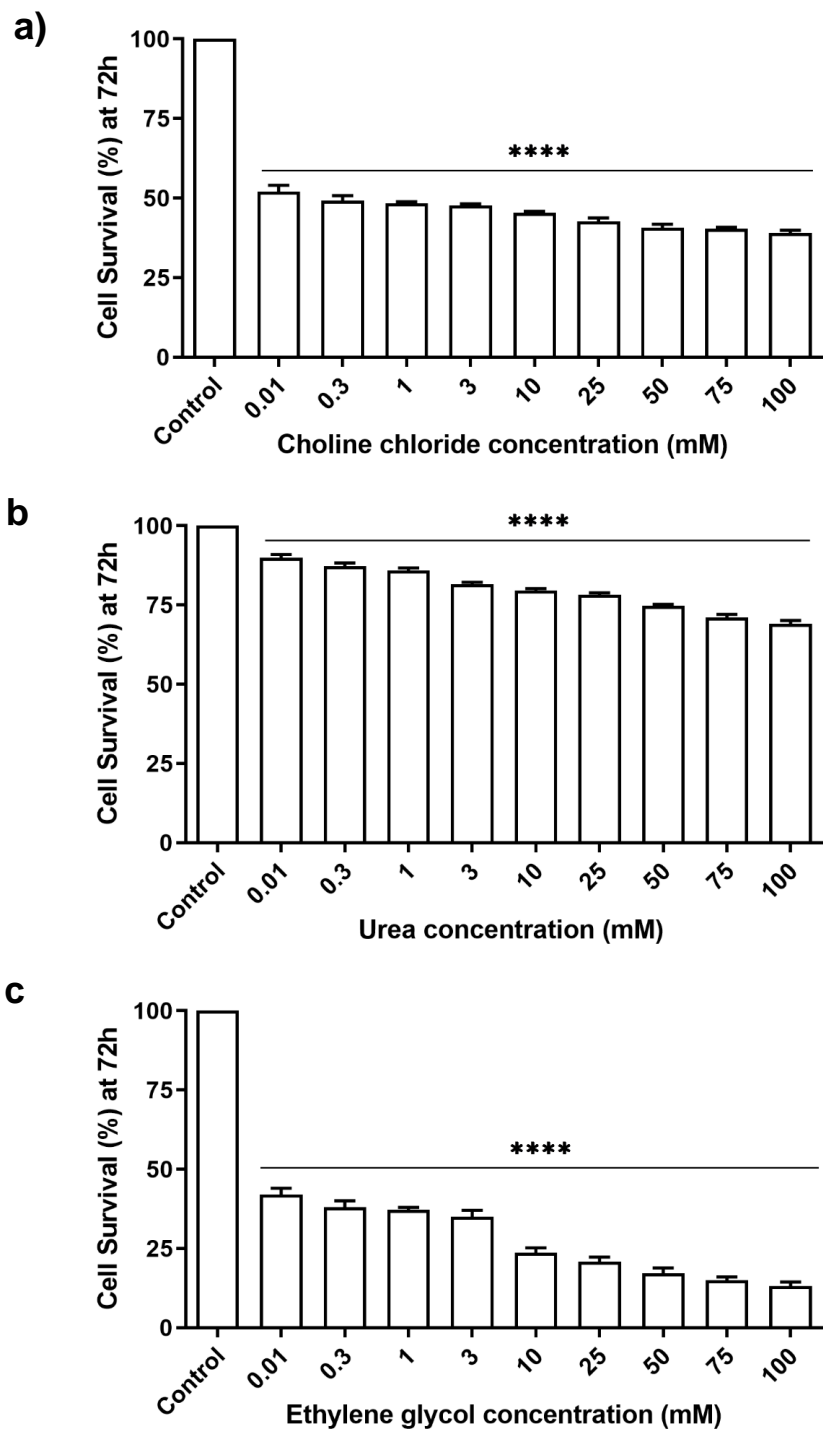
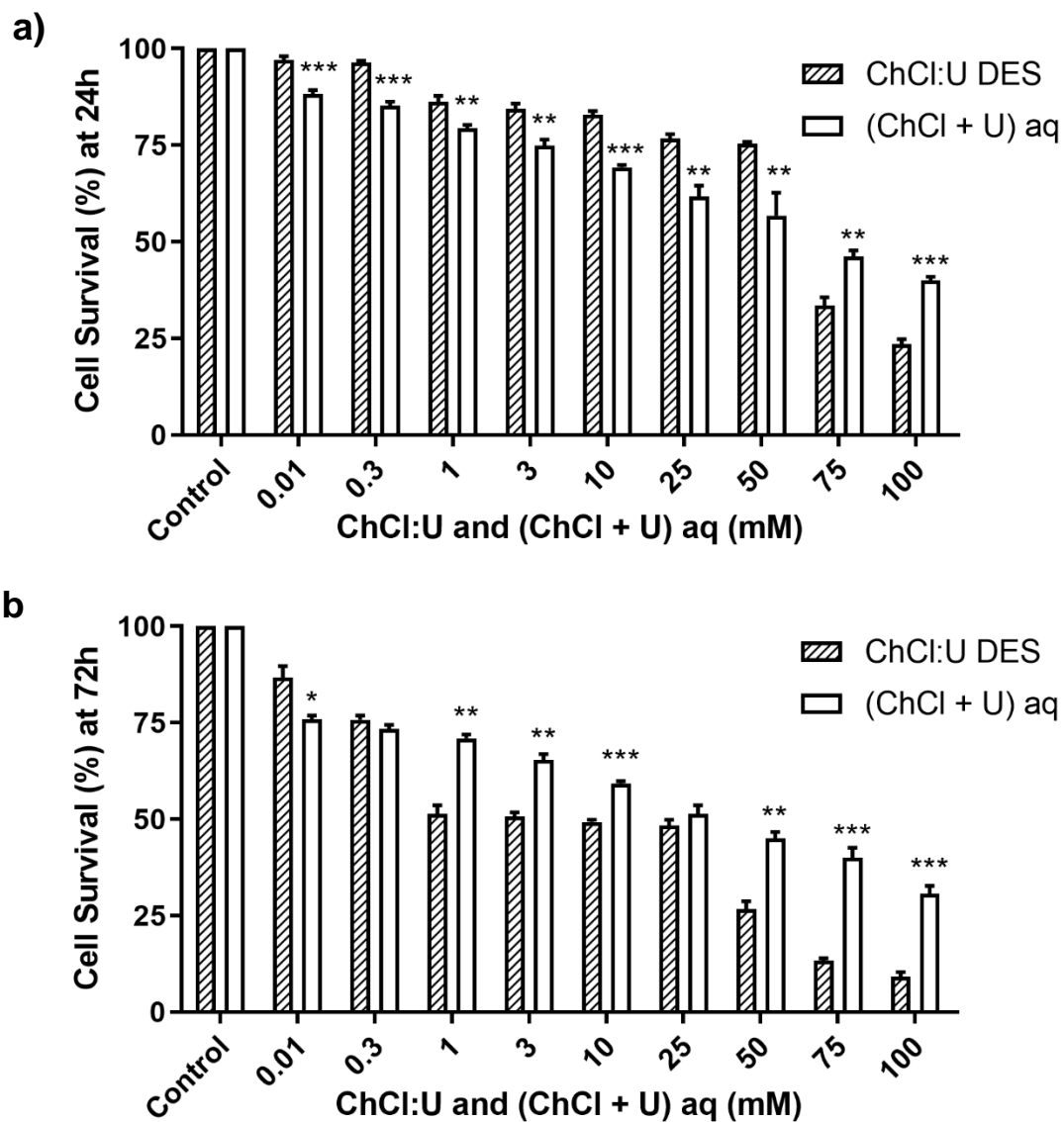


Figure S2. Variation of cell viability of MDA-MB-231 breast cancer cells in function of the concentration of a) choline chloride, b) urea, or c) ethylene glycol following 72h of exposure. Results are expressed as mean  $\pm$  SD of three independent experiments (\*\*\*\* stands for  $P < 0.0001$ )



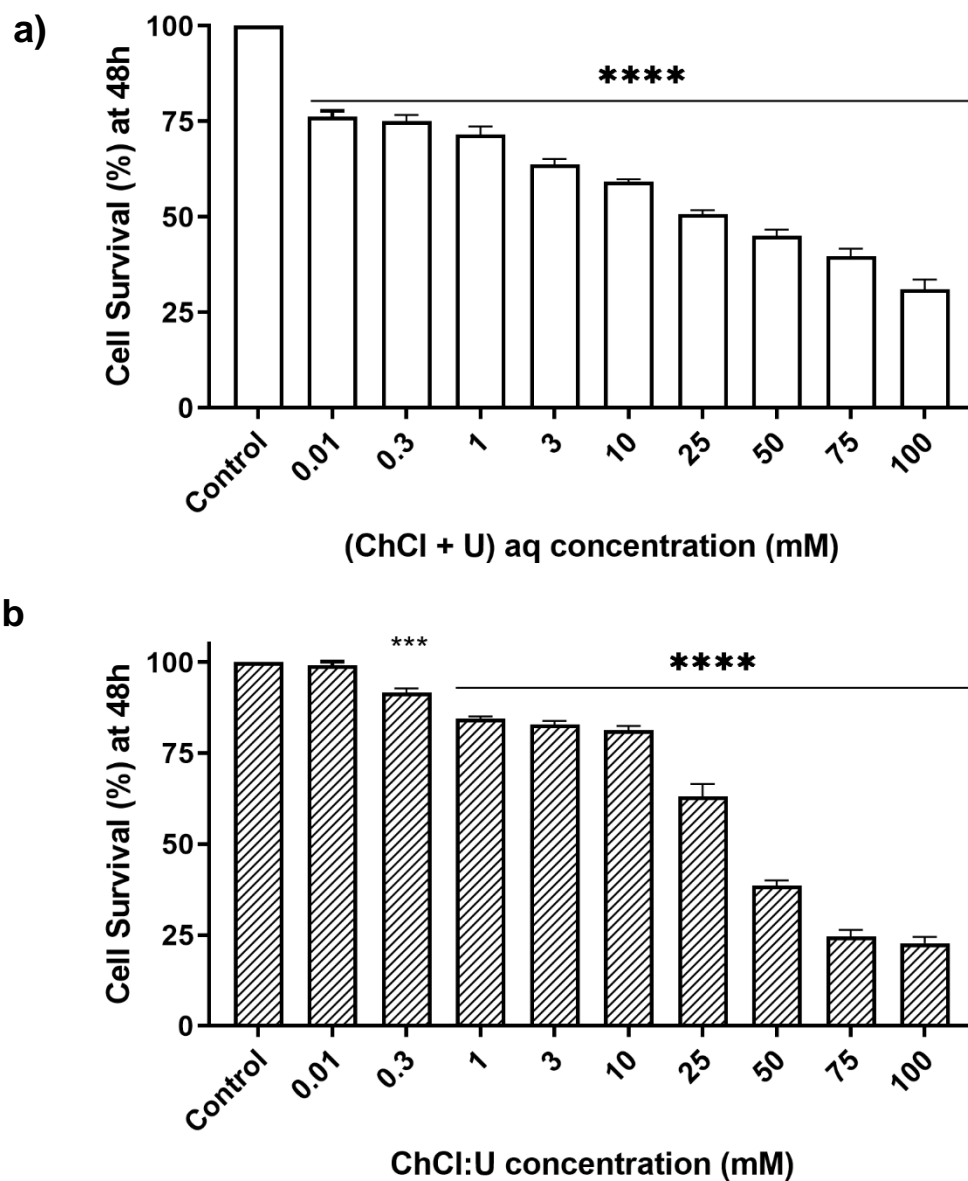


Figure S4. Variation of cell viability of MDA-MB-231 breast cancer cells in function of the concentration of a) aqueous solution of choline chloride and urea (ChCl + U) aq or b) ChCl:U DES following 48h of exposure. Results are expressed as mean  $\pm$  SD of three independent experiments (\*\*\*) stands for  $P < 0.001$  and \*\*\*\* stands for  $P < 0.0001$ )

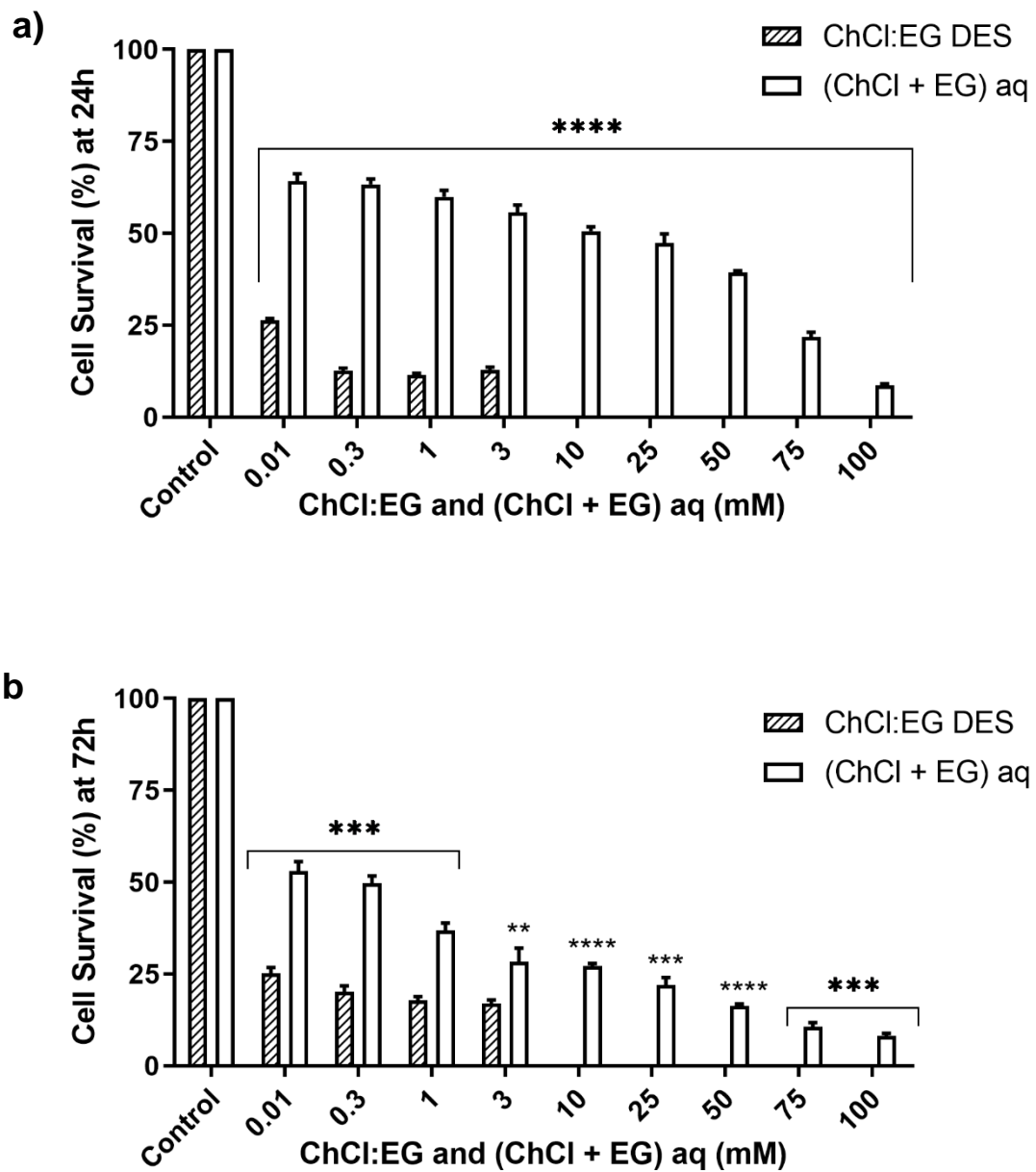


Figure S5. Cytotoxic effect of ChCl:EG DES versus the aqueous solution of its components (ChCl + EG) aq on MDA-MB-231 breast cancer cells after a) 24h and b) 72h of exposure. Results are expressed as mean  $\pm$  SD of three independent experiments (\*\* stands for  $P < 0.01$ , \*\*\* stands for  $P < 0.001$ , and \*\*\*\* stands for  $P < 0.0001$ )

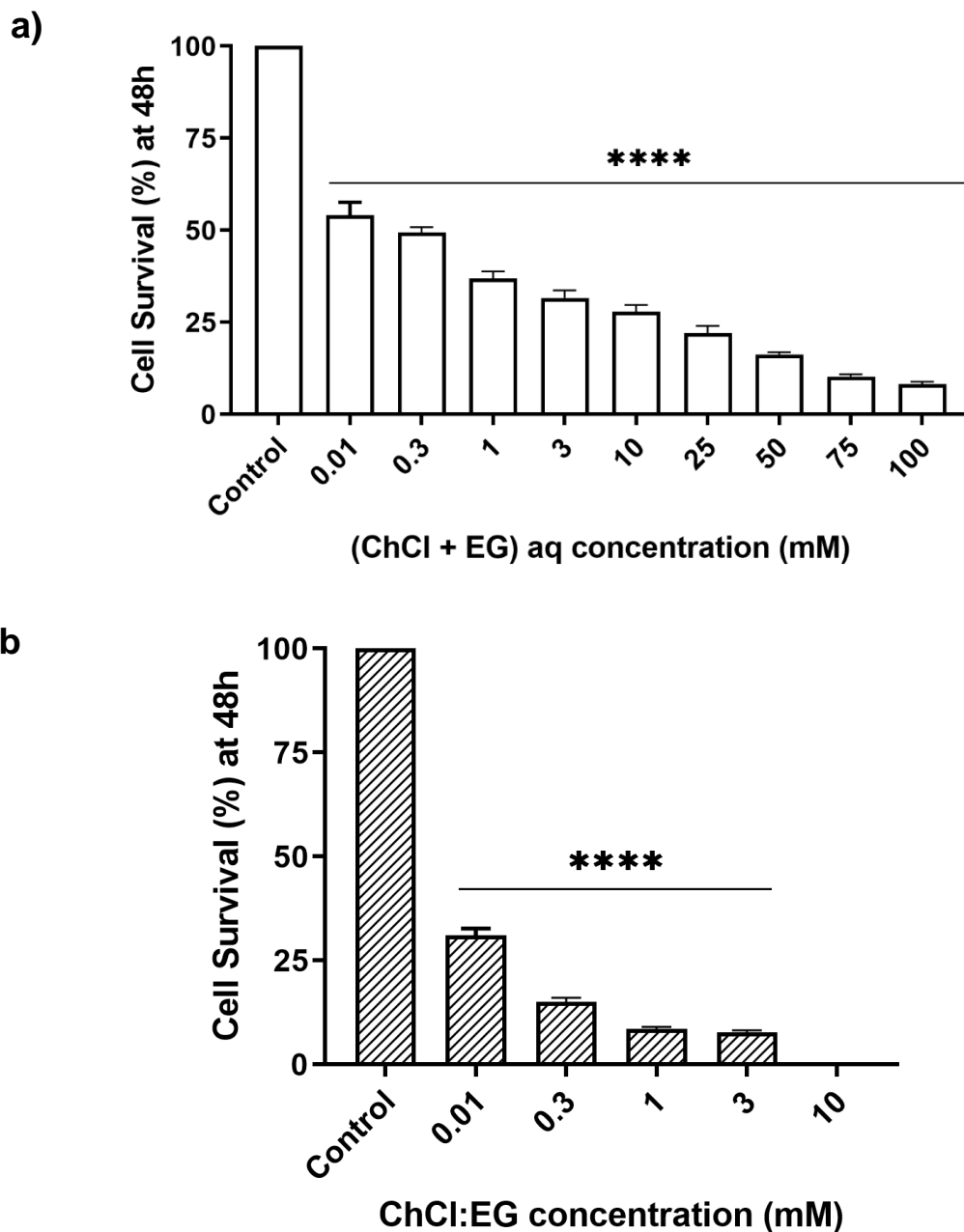


Figure S6. Variation of cell viability of MDA-MB-231 breast cancer cells in function of the concentration of a) aqueous solution of choline chloride and ethylene glycol (ChCl + EG) aq or b) ChCl:EG DES following 48h of exposure. Results are expressed as mean  $\pm$  SD of three independent experiments (\*\*\*\* stands for  $P < 0.0001$ )

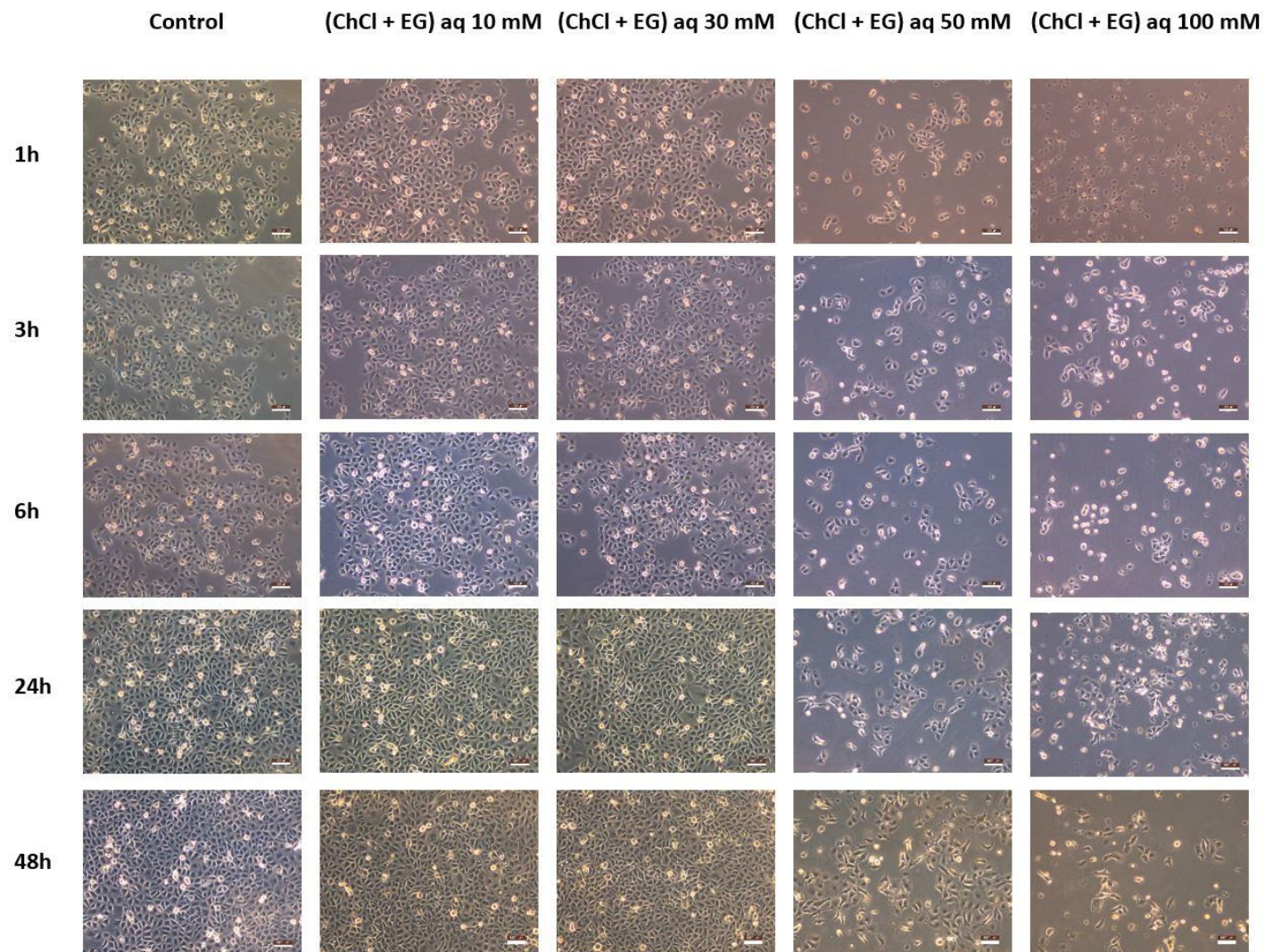


Figure S7. Images of MDA-MB-231 cells untreated (control) or treated with different concentrations of aqueous solutions of choline chloride and ethylene glycol at different time points

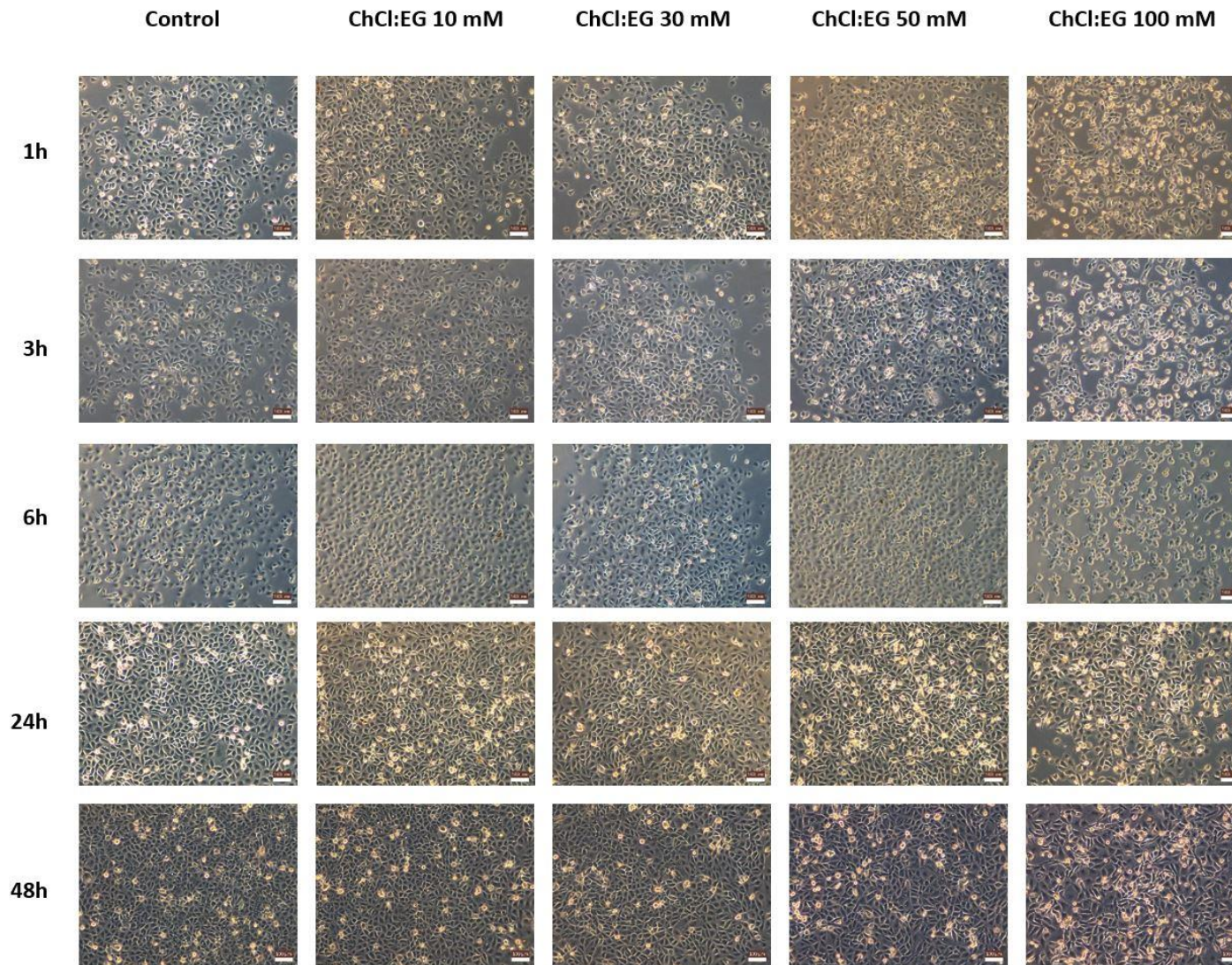


Figure S8. Images of MDA-MB-231 cells untreated (control) or treated with different concentrations of ChCl:EG DES at different time points

## V. The solubilizing ability of DES toward natural volatiles and essential oils

In this chapter, we evaluated the ability of the DES to solubilize plant volatiles like *trans*-anethole (AN) and L-carvone (Carv) and related essential oils. In addition, we investigated the impact of the incorporation of water or some encapsulating agents like cyclodextrins (CD), phospholipids, and surfactants on the overall DES' solubilization efficiency. Finally, we monitored the release of *trans*-anethole from the DES over time.

### 1. Solubilization of volatile compounds by DES

The solubilization studies were conducted using static headspace-gas chromatography (SH-GC). In this technique, the sample (liquid or solid) is generally placed in a closed vial which will then be thermostated at a constant temperature. Thereafter, an equilibrium between the sample phase and the gas phase above it will be reached and the concentration of the volatile compound in the gas phase will be constant. The gas phase is called the headspace and the type of analysis is static since the two phases present in the vial are under static conditions. In a second step, the gas phase is analyzed by gas chromatography: an aliquot of the headspace is transferred to the column (stationary phase) via the carrier gas stream (mobile phase) (Figure 35). The distribution of the studied volatile compound between the two phases is represented by a parameter known as the partition coefficient  $K$  which represents herein the ratio of the analyte's concentration in the gas phase over its concentration in the sample phase. When water constitutes the sample phase, we talk about Henry's law constant  $H_c$ . These parameters reflect the solubility of the analyte in the considered sample (Kolb & Ettre, 2006).

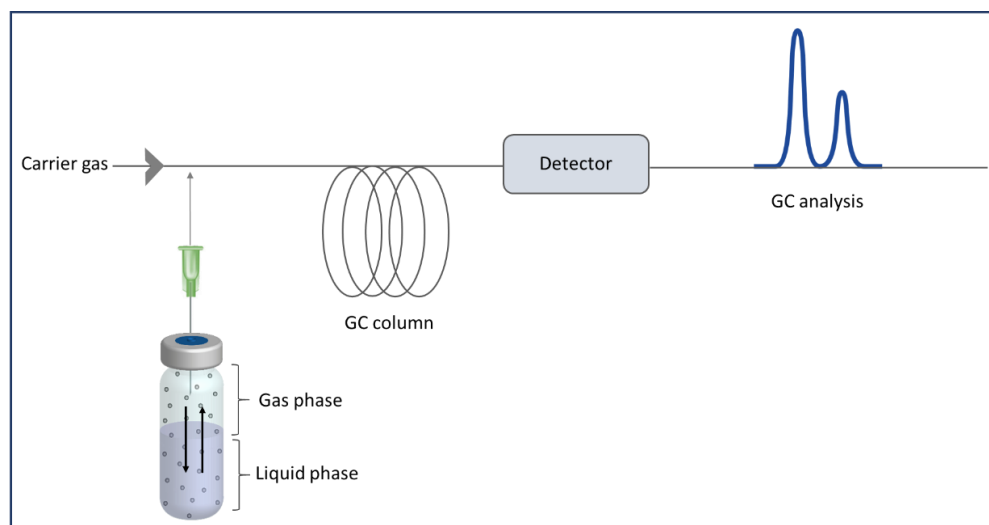


Figure 35. Principle of static headspace-gas chromatography

In the present study, we evaluated the solubility of *trans*-anethole (AN) (Figure 36A) and L-Carvone (Carv) (Figure 36B) in the different DES and compared it to their solubility in water. *Trans*-anethole is a major component of star anise and fennel essential oils, while L-Carvone is found at high concentrations in spearmint oil. They are both mainly used as flavoring agents and applied in food, cosmetics, and pharmaceutical industries due to their numerous biological properties. However, their wider applications are hampered by their high volatility, low water solubility, and chemical instability (de Carvalho & da Fonseca, 2006; Gharib et al., 2018).

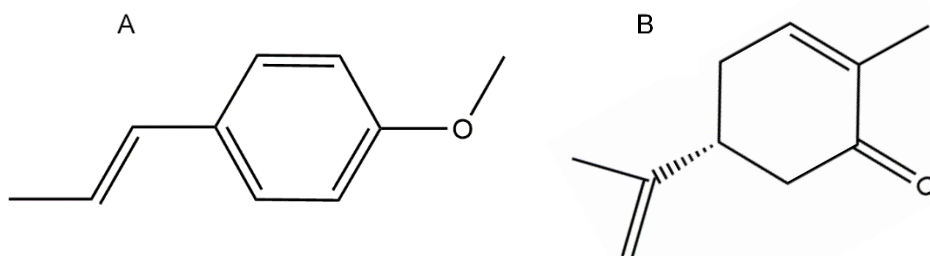


Figure 36. The general structure of (A) *trans*-anethole and (B) L-carvone

## 1.1. Determination of the partition coefficient *K*

The values of the vapor-liquid partition coefficient *K* of the studied volatiles in DES were determined at 30 °C and were compared to the partition coefficients of the same volatiles in water using two complementary methods: the phase ratio variation method and the vapor phase calibration method (Kolb & Ette, 2006). It is noteworthy that the partition coefficient *K* will be considered as the ratio of the concentration in the gas phase over the concentration in the liquid phase to simplify the comparison with the partition coefficient in water.

### 1.1.1. The phase ratio variation method

In the phase ratio variation method, several vials containing different amounts of water and the same amount of the volatile compound are analyzed at 30 °C. Subsequently, Henry's law constant *H<sub>c</sub>* of the considered volatile in water can be determined by plotting the curve relating  $1/AV_L$  to the  $V_G/V_L$  ratio as shown in equation (4):

$$\frac{1}{AV_L} = \frac{1}{\alpha} \frac{V_G}{V_L} + \frac{1}{\alpha H_c} \quad (4)$$

where  $A$  is the chromatographic peak area,  $\alpha$  is a constant, and  $V_L$  and  $V_G$  are the volumes of the liquid phase and the gas phase, respectively.

### 1.1.2. The vapor phase calibration method

The vapor phase calibration method was further applied to determine the partition coefficient of the volatile compounds in the different DES. In a first step, several vials containing the same amount of water and different amounts of the volatile compound are analyzed by SH-GC. A calibration curve  $A = f(C_{total})$  relating the chromatographic peak area to the total concentration of the volatile compound in water is thus obtained. After determining  $H_c$  using the phase ratio variation method, the concentration of the volatile in the gas phase  $C_G$  can be calculated following equation (5):

$$C_G = \frac{n_{total}}{(V_G + \frac{V_L}{H_c})} \quad (5)$$

Where  $n_{total}$  is the number of moles of the analyte, initially added to the vial.

Knowing the concentration in the gas phase, the calibration curve  $A = f(C_G)$  relating the peak area to concentration in the gas phase can thus be drawn.

In the second step, several vials containing the same amount of DES (3 mL) and different amounts of the volatile compound (1- 200 mg) are analyzed by SH-GC. The concentration of the volatile compound in the gas phase  $C_G$  can be determined from the experimental chromatographic peak area, using the parameters of the calibration curve  $A = f(C_G)$  obtained earlier. Subsequently, the vapor-liquid partition coefficient of the volatile compound in the DES which is the ratio of its concentration in the gas phase over its concentration in the liquid phase can be obtained.

Before analysis, the volatile compound was added to the DES placed in 22 mL headspace glass vials. Vials were then sealed and thermostated at 30 °C under stirring for 24 h to reach equilibrium between liquid and gas phases. The vials were then put in the headspace oven at 30 °C for an additional 2 hours. Subsequently, 1 mL of the headspace was withdrawn from the vial and injected in the chromatographic column for analysis via a heated transfer line (250 °C). All measurements were carried out with an Agilent G1888 headspace sampler coupled with a PerkinElmer Autosystem XL gas chromatography equipped with a flame ionization detector and a DB624 column using nitrogen as carrier vector. The GC column temperature was set at 160 °C for both *trans*-anethole and L-carvone.

Table 17 presents the values of the partition coefficient of *trans*-anethole in water or the solvents. A clear decrease in  $K$  occurs when *trans*-anethole is added to all the studied solvents compared with water. A

reduction in  $K$  means an increase in  $C_L$ , which in turn means that the volatile compound is more soluble in the considered solvent than in water.  $K$  of *trans*-anethole was reduced at least 13 times and up to 4200 times in ChCl:U and TBABr:Dec, respectively. The DES based on TBABr or TBPBr as HBA seem to present a greater solubilizing effect than ChCl-based DES. On another note, SUPRADES presented an intermediate solubilizing ability. The SUPRADES based on levulinic acid showed a greater  $K$  reduction when compared with other SUPRADES. The molar ratio also affects the solubilization since a lower partition coefficient is obtained when a lower HBD molar fraction is used (1:20 > 1:30 > 1:40), which can be explained by the higher amount of CD. However, no correlation was detected between the  $K$  reduction and the density or the viscosity of the tested solvents.

Table 17. Partition coefficient values of *trans*-anethole in water and the different solvents and  $K_{\text{water}}/K_{\text{solvent}}$  ratio at 30 °C

Solvent	Partition coefficient $K$	$K_{\text{water}}/K_{\text{solvent}}$
Water	1.29E-02	1
ChCl:U	9.55E-04	13.51
ChCl:G	5.23E-04	24.67
ChCl:EG	2.38E-04	54.20
ChCl:Lev	3.40E-05	379.41
TBPBr:Lev	2.18E-05	591.74
TBABr:Dec	3.05E-06	4229.51
TBPBr:EG	8.70E-06	1482.76
HPBCD:Lev	1.04E-05	1240.38
RAMEB:Lev	9.60E-06	1343.75
CRYSMEB:Lev	1.08E-05	1194.44
Captisol:Lev	2.18E-05	591.74
HPBCD:G 1:30	8.87E-04	14.55
HPBCD:G 1:40	1.12E-04	115.07
HPBCD:EG 1:20	2.55E-05	506.44
HPBCD:EG 1:30	3.21E-05	401.83
HPBCD:EG 1:40	3.49E-05	369.64
HPBCD:1,3-PD 1:30	3.95E-05	326.57

Table 17. (continued)

Solvent	Partition coefficient $K$	$K_{\text{water}}/K_{\text{solvent}}$
RAMEB:1,3-PD 1:20	1.56E-05	828.63
RAMEB:1,3-PD 1:30	2.70E-05	477.75
RAMEB:1,3-PD 1:40	3.14E-05	410.21
RAMEB:1,3-BD 1:30	2.87E-05	450.18
RAMEB:1,3-BD 1:40	3.81E-05	338.52
HPBCD:1,3-PD 1:40	3.91E-05	330.29
HPBCD:1,3-BD 1:40	3.04E-05	424.69

When it comes to L-carvone, a decrease in the partition coefficient is also witnessed in presence of the DES and the levulinic acid-containing SUPRADES but to a lesser extent than with *trans*-anethole, as shown in Table 18.  $K$  is 1.9 to 126 times lower in the tested solvents than in water. Likewise, TBABr:Dec presented the highest solubilization ability and the SUPRADES resulted in better solubilization than ChCl-based DES.

Table 18. Partition coefficient values of L-Carvone in water and the different solvents and  $K_{\text{water}}/K_{\text{solvent}}$  ratio at 30 °C

Solvent	Partition coefficient $K$	$K_{\text{water}}/K_{\text{solvent}}$
Water	3.56E-03	1
ChCl:U	1.91E-03	1.86
ChCl:G	1.85E-03	1.92
ChCl:EG	1.92E-03	1.85
ChCl:Lev	1.13E-04	31.50
TBPBr:Lev	3.75E-05	94.91
TBABr:Dec	2.82E-05	126.18
TBPBr:EG	6.76E-05	52.66
HPBCD:Lev	4.22E-05	84.31
RAMEB:Lev	3.09E-05	115.18
CRYSMEB:Lev	3.55E-05	100.38
Captisol:Lev	5.48E-05	64.94

## 2. Solubilization of essential oils by DES

The solubilizing ability of the DES was also evaluated toward two essential oils (EO): star anise (*Illicium verum*) and fennel (*Foeniculum vulgare*). These EO were chosen for having *trans*-anethole as a major component (91.07% for star anise and 75.30% for fennel). A certain volume of EO (10  $\mu\text{L}$  for star anise and 5  $\mu\text{L}$  for fennel, at a concentration of 0.1  $\text{g}\cdot\text{mL}^{-1}$ ) was added to the DES (3 mL) placed in 22 mL headspace glass vials. Vials were then sealed and thermostated at 30  $^{\circ}\text{C}$  under stirring for 24 h to reach equilibrium between liquid and gas phases. Subsequently, 1 mL of the headspace was withdrawn from the vial and injected in the chromatographic column for analysis via a heated transfer line (250  $^{\circ}\text{C}$ ). The GC column temperature conditions were set as follows: initial temperature of 50  $^{\circ}\text{C}$  for 2 min, increased to 200  $^{\circ}\text{C}$  at 5  $^{\circ}\text{C}\cdot\text{min}^{-1}$ , then hold for 2 min, giving a total runtime of 34 min. The retention of *trans*-anethole, star anise, and fennel EO in the solvents was estimated according to procedures developed for aromas (Decock et al., 2008) and EO (Kfoury et al., 2015), respectively. The percentage of retention of *trans*-anethole and EO by the DES was determined by SH-GC at 30  $^{\circ}\text{C}$  following equations (6) and (7), respectively.

$$\%Retention = \left(1 - \frac{A_{DES}}{A_W}\right) \times 100 \quad (6)$$

Where  $A_{DES}$  and  $A_W$  stand for the peak area of *trans*-anethole in presence of the DES or water, respectively.

$$\%Retention = \left(1 - \frac{\Sigma A_{DES}}{\Sigma A_W}\right) \times 100 \quad (7)$$

Where  $\Sigma A_{DES}$  and  $\Sigma A_W$  stand for the sum of peak areas of the EO's components in presence of the DES or water, respectively.

Figure 37 depicts the chromatogram of star anise EO obtained by SH-GC in presence of RAMEB: Lev, taken as an example and in presence of water as a reference solvent. The peaks corresponding to the volatile compounds found in star anise are obvious in water but almost disappear in presence of the SUPRADES. Table 19 displays the percentage of retention of star anise and fennel EO in DES and levulinic acid-containing SUPRADES. All the tested solvents exhibited a high retention ability ( $\geq 80.39\%$ ) toward both star anise and fennel EO, except for  $\text{ChCl}$ -based DES which retention ability ranged between 61.80 and 83.77%. Moreover, the  $\text{CD}:\text{Lev}$  systems presented a remarkable solubilizing effect.

In addition, we assessed the retention of *trans*-anethole as one of the components of star anise and fennel EO. As shown in Figure 38, similar results were obtained whether *trans*-anethole is in its pure form or in presence of other EO's compounds. Therefore, the ability of the DES to solubilize *trans*-anethole is maintained even with the simultaneous presence of other volatile compounds.

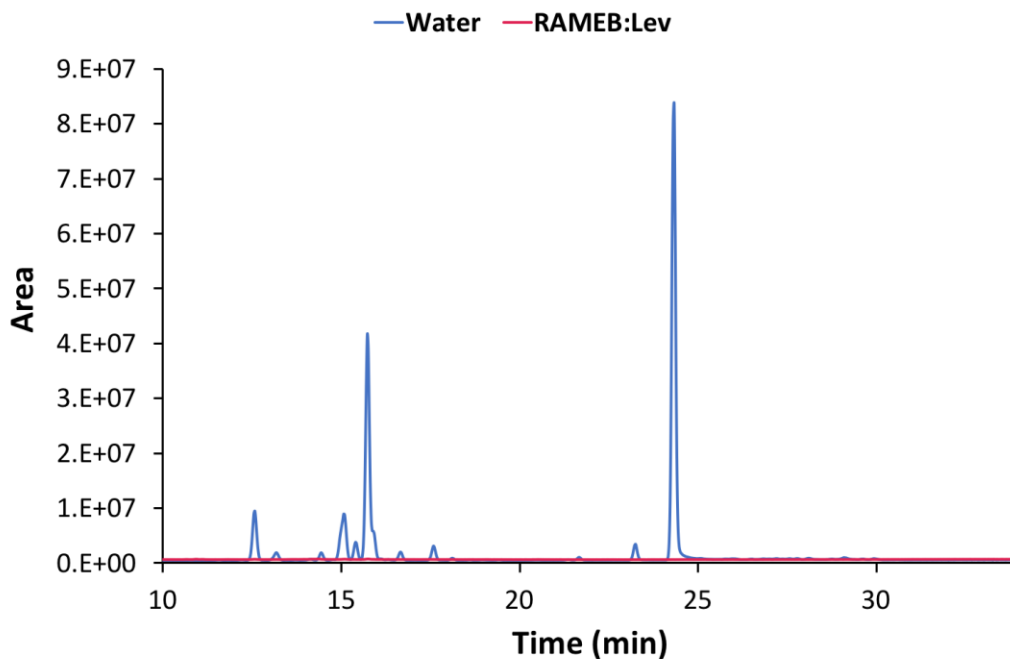


Figure 37. Chromatogram of star anise essential oil in water and RAMEB:Lev

Table 19. Percentage of retention of the essential oils by the studied solvents at 30 °C

DES	% Retention	
	Star anise	Fennel
ChCl:U	65.37	63.99
ChCl:G	76.03	61.80
ChCl:EG	83.77	68.04
ChCl:Lev	99.22	98.16
TBPBr:Lev	99.63	99.55
TBABr:Dec	100.00	99.52
TBPBr:EG	80.39	94.24
HPBCD:Lev	99.67	99.74
RAMEB:Lev	99.35	99.58
CRYSMEB:Lev	99.91	99.73
Captisol:Lev	98.89	99.97

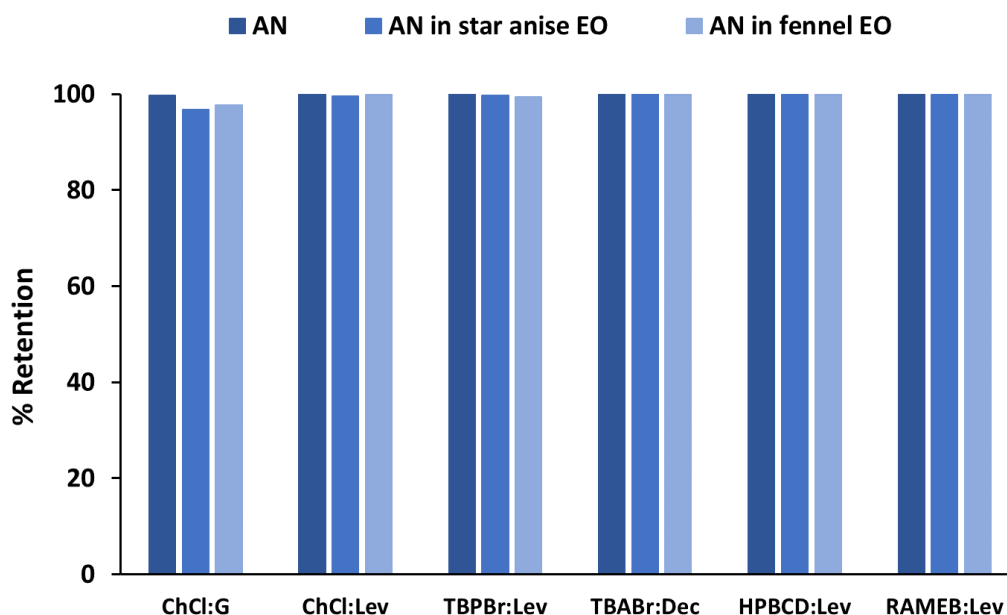


Figure 38. Percentage of retention of *trans*-anethole by DES, in the absence (pure *trans*-anethole) or presence of other compounds found in star anise or fennel essential oils

### 3. Effect of water on DES' solubilization ability

As previously detailed in section 1.5, water has a major impact on DES' physicochemical properties, as well as their hydrogen bond network. Therefore, it is interesting to investigate the effect of water on DES' solubilizing ability. Aqueous solutions of DES were prepared by mixing preformed DES (ChCl:Lev, TBPBr:Lev, HPBCD:Lev or RAMEB:Lev) and ultrapure water at various DES concentrations ranging between 20 and 100 wt%. The same amount of *trans*-anethole (5  $\mu\text{L}$  of 0.1  $\text{g}\cdot\text{mL}^{-1}$ ) was then added to the aqueous solutions of DES (3 g) placed in headspace vials. The mixtures were then homogenized, equilibrated at 30  $^{\circ}\text{C}$  for 24h and analyzed by SH-GC. As demonstrated in Figure 39, the concentration of *trans*-anethole in the gas phase gradually decreases as the DES weight fraction increases. In other words, the addition of water weakens the solubilizing efficiency of the 4 levulinic acid-containing DES. However, the extent of the solubilization reduction by water is lowered in presence of CD, especially in the case of RAMEB:Lev at 20 wt% DES. Besides, two different behaviors were detected below and above 40 wt% DES, which could be explained by a transition from an aqueous DES (above 40 wt% DES) to an aqueous solution of the individual components that form the DES (below 40 wt% DES), as seen in section I.1.5.2.

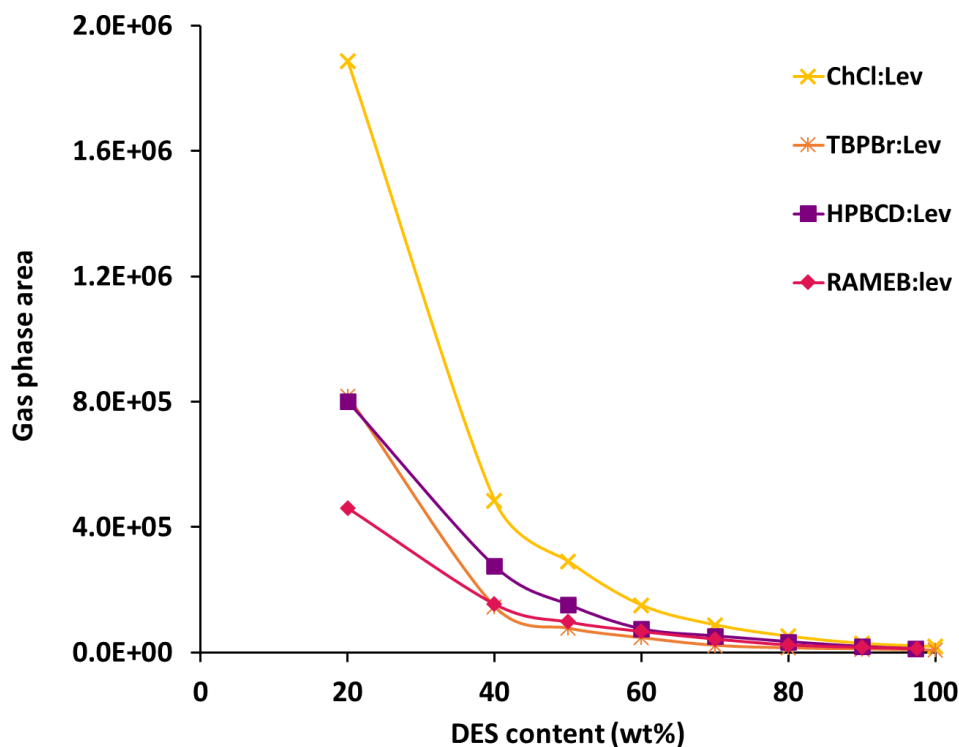


Figure 39. Variation of the chromatographic peak area of *trans*-anethole in binary DES-water mixtures with varying DES content

This behavior was further investigated by comparing the solubilizing ability of the aqueous preformed DES (denoted by DES aq) with that of the aqueous solution of both forming compounds (denoted by (HBA+HBD) aq), or the aqueous solution of each individual compound (denoted by HBA aq or HBD aq), at a concentration equivalent to 20 wt% DES content. Consequently, DES aq and (HBA+HBD) aq result in the same retention capacity (Figure 40). Moreover, the retention of *trans*-anethole seems to arise from the effect of both HBA and HBD. In the cases of ChCl:Lev and TBPBr:Lev, only levulinic acid can retain *trans*-anethole. However, in the case of the CD:Lev systems, both HBA and HBD contribute to the overall retention ability. On the other hand, DES aq and (HBA+HBD) aq were compared at a higher DES content (70 wt%) and they also led to the same percentage of *trans*-anethole retention (Table 20). This means that there is no difference between an aqueous solution of a preformed DES and an aqueous solution of the DES' forming compounds when added separately, even at a high DES content.

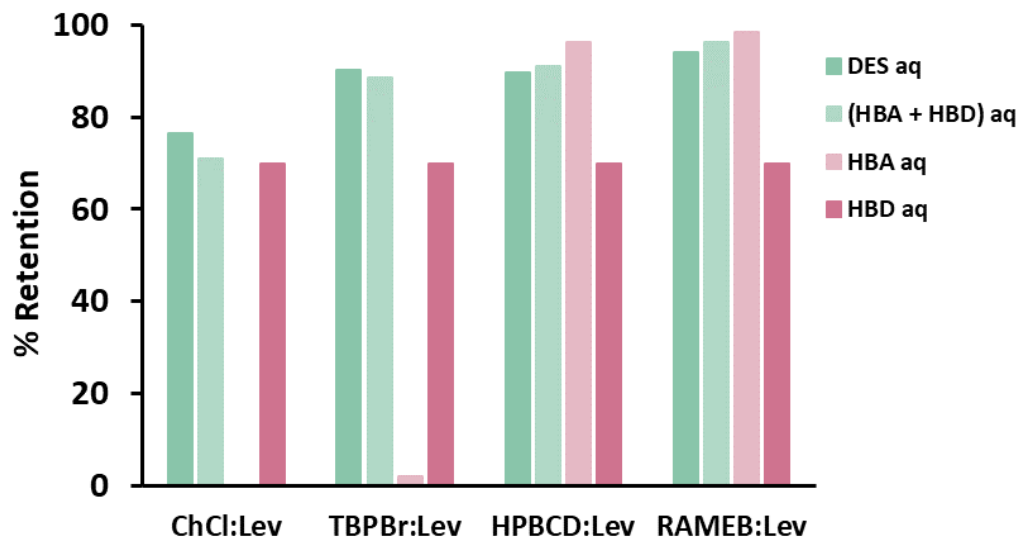


Figure 40. Retention of *trans*-anethole by aqueous solutions of preformed DES (DES aq), aqueous solutions of the forming compounds (HBA + HBD) aq, and aqueous solutions of the individual compounds (HBA aq or HBD aq) at a concentration equivalent to 20 wt% DES

Table 20. Percentage of retention of *trans*-anethole by aqueous solutions of preformed DES (DES aq) and by aqueous solutions of the forming compounds (HBA + HBD) aq at a concentration equivalent to 70 wt% DES

% Retention of <i>trans</i> -anethole				
	ChCl:Lev	TBPBr:Lev	HPBCD:Lev	RAMEB:Lev
DES aq	98.95	99.77	99.59	99.55
(HBA + HBD) aq	98.95	99.78	99.41	99.42

#### 4. Nuclear magnetic resonance spectroscopy study

To further explore the new CD-based mixtures, we selected RAMEB:Lev and investigated the interactions taking place in the presence of *trans*-anethole. It was previously reported that *trans*-anethole can form an inclusion complex with RAMEB in aqueous solutions (Kfoury et al., 2014). Therefore, we were curious to know if the complexation ability of RAMEB is preserved in the SUPRADES form. The possibility of inclusion complex formation in aqueous solutions is usually studied by titration experiments with increasing CD concentrations using techniques like UV-visible spectroscopy, isothermal titration calorimetry, and nuclear magnetic resonance spectroscopy (NMR), or by two-dimensional Rotating Frame Overhauser Enhancement Spectroscopy (2D ROESY) NMR. In the present study, the SUPRADES was first characterized by <sup>1</sup>H NMR. Then, to check if a CD/ *trans*-anethole complexation occurs in SUPRADES, 2D

ROESY NMR was adopted given that the CD consists one of the SUPRADES components. This NMR method was followed by a complementary 2D DOSY NMR which allows tracking of the variation of the diffusion coefficients  $D$  of the involved compounds (Figure 41).

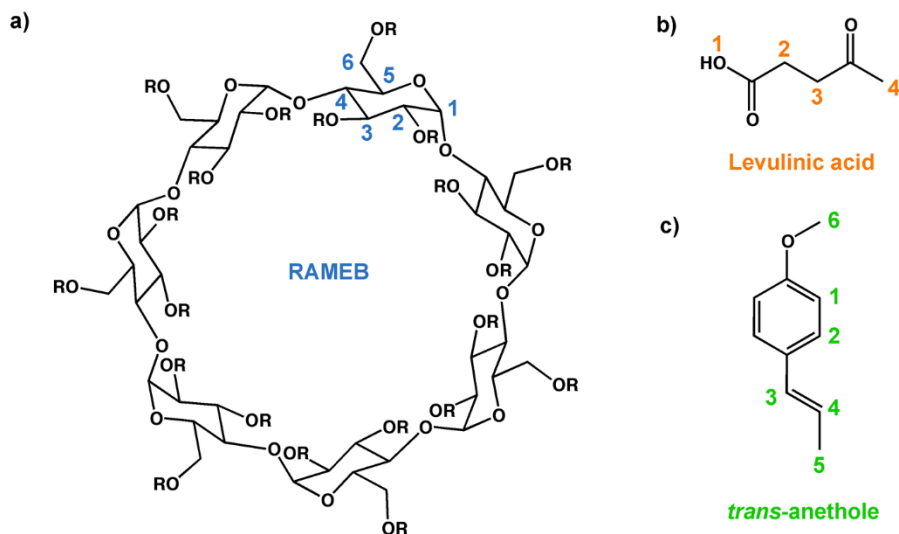


Figure 41. The general structure of a) randomly methylated- $\beta$ -cyclodextrin (RAMEB, DS = 12.9 and R= -H or -CH<sub>3</sub>), b) levulinic acid and c) *trans*-anethole

All NMR experiments were performed on a Bruker Avance III spectrometer operating at 400 MHz for the proton nucleus, equipped with a multinuclear z-gradient BBFO probe head. In all experiments, the probe temperature was maintained at 30 °C and standard 5 mm NMR tubes with D<sub>2</sub>O insert were used. The <sup>1</sup>H spectra were recorded with the following acquisition parameters: time-domain 55 K with a digital resolution of 0.20 Hz, relaxation delay: 2 s, and 16 scans. 2D ROESY spectrum was obtained with a mixing time of 800 ms during spin-lock, using off-resonance pulse program troesyph, and States-TPPI method with a 2048 K time domain in F2 and 512 experiments in F1 with 200 scans. 2D-DOSY spectra have been conducted using the bipolar longitudinal eddy current delay (BPPLIED – Bipolar Pulsed Field Gradient Longitudinal Eddy Delay) pulse sequence. In each DOSY experiment, a series of 16 spectra with 20 K points were collected, with 16 scans. The pulse gradients have been incremented in 16 steps from 2 to 98 % of the maximum gradient strength in a linear ramp. Diffusion times ( $\Delta$ ) and gradient pulse durations ( $\delta$ ) were optimized for each experiment in order to achieve a 95 % decrease in resonance intensity at the largest gradient amplitude; typically,  $\delta$  between 3 and 1.4 ms,  $\Delta$  between 300 and 75 ms. After Fourier transformation, phase, and baseline correction, the diffusion dimension of the 2D-DOSY spectra was processed using MestRenova software (version 11.0.2). The diffusion constants were calculated by the Peak Heights Fit method with 128 points in the diffusion dimension.

The preformed SUPRADES was studied before and after the addition of *trans*-anethole. The corresponding  $^1\text{H}$  NMR spectra, shown in Figure 42, display several peaks relative to each compound. Although the SUPRADES' viscosity hampers the acquisition of well-defined NMR spectra, the peaks could be identified by comparison with the NMR spectrum of RAMEB in  $\text{D}_2\text{O}$  (Fenyvesi et al., 2014).

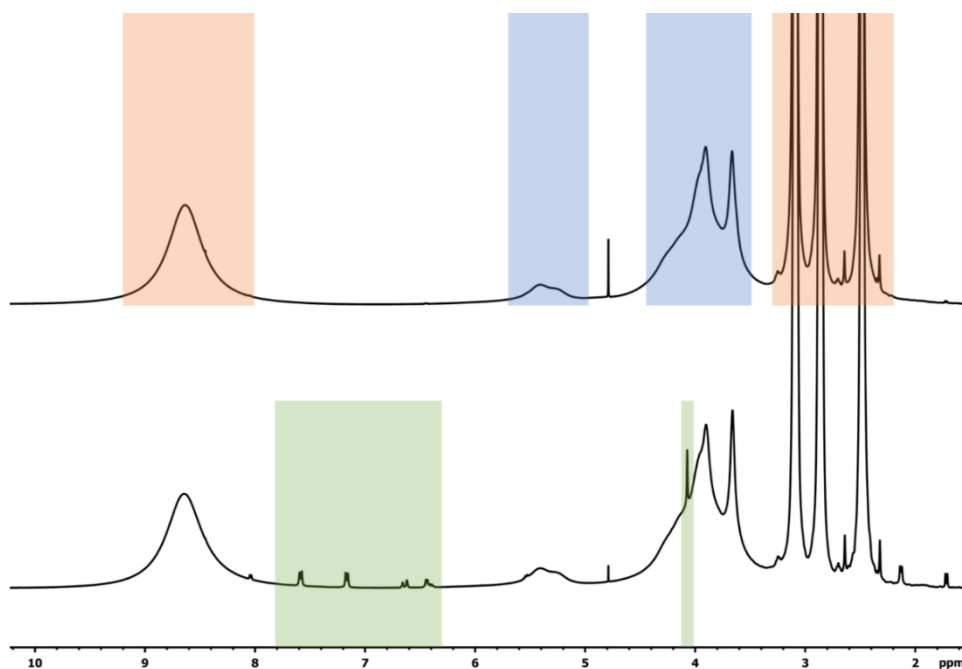


Figure 42.  $^1\text{H}$  NMR spectra of RAMEB:Lev in the absence (top) or presence of *trans*-anethole (bottom). Blue, orange, and green boxes respectively represent peaks related to RAMEB, levulinic acid, and *trans*-anethole

On the other hand, a section of the ROESY spectrum of RAMEB:Lev and *trans*-anethole reveals an important correlation between H1 and H2 of *trans*-anethole and  $-\text{OCH}_3$ , H3, and H5 of RAMEB (Figure 43). Such correlation proves the formation of a CD/ *trans*-anethole inclusion complex, given that H3 and H5 are located inside the CD cavity. Furthermore, the diffusion coefficients (D) of the SUPRADES' components, as well as *trans*-anethole (solubilized in the SUPRADES) were determined by NMR spectroscopy in different SUPRADES-water binary mixtures. Figure 44 shows the variation of the diffusion coefficients of the three compounds in function of SUPRADES content. Two different behaviors were detected at a cut-off value of 72 wt% DES. Above 72 wt% DES, levulinic acid, and *trans*-anethole present similar diffusion coefficients but a lower value was obtained for RAMEB, which is in accordance with the higher molecular weight of the CD. Below 72 wt% DES, the diffusion coefficient of levulinic acid drastically increased, while the diffusion of *trans*-anethole followed the diffusion of RAMEB. In addition, the diffusion coefficients of the

separate compounds in water were determined in the absence or presence of RAMEB. As shown in Table 21, the diffusion coefficient of levulinic acid does not vary much when RAMEB is added. Yet, the diffusion value of *trans*-anethole is greatly lowered in presence of RAMEB, thus confirming the formation of RAMEB/*trans*-anethole inclusion complex and explaining the different behavior of *trans*-anethole and levulinic acid below 72 wt% DES in Figure 44.

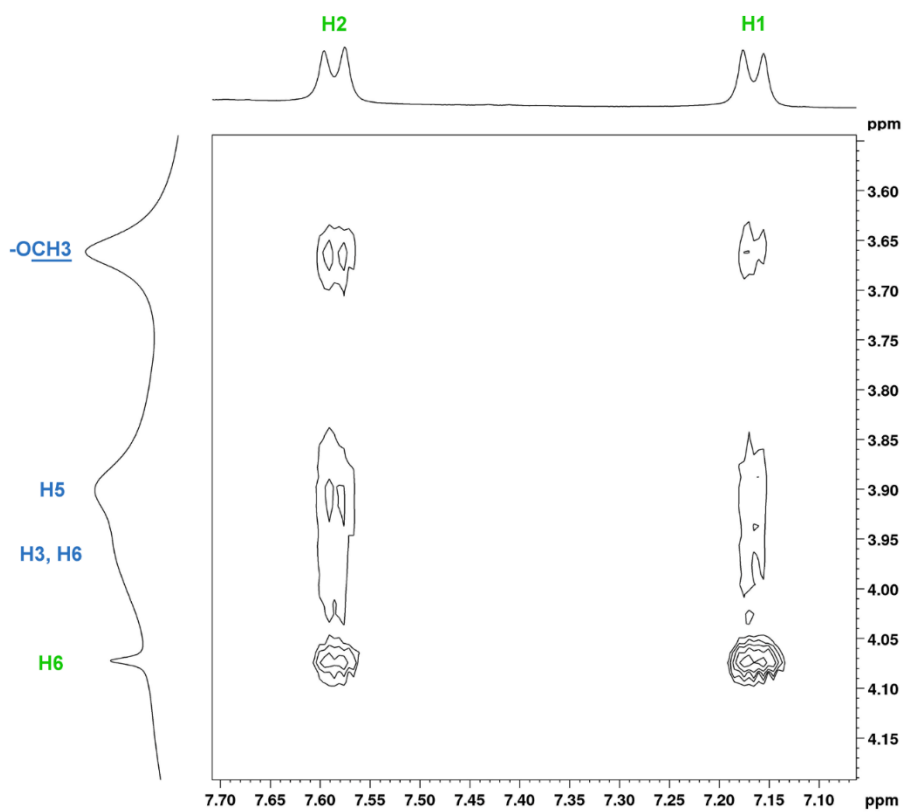


Figure 43. ROESY spectrum of RAMEB:Lev in presence of *trans*-anethole

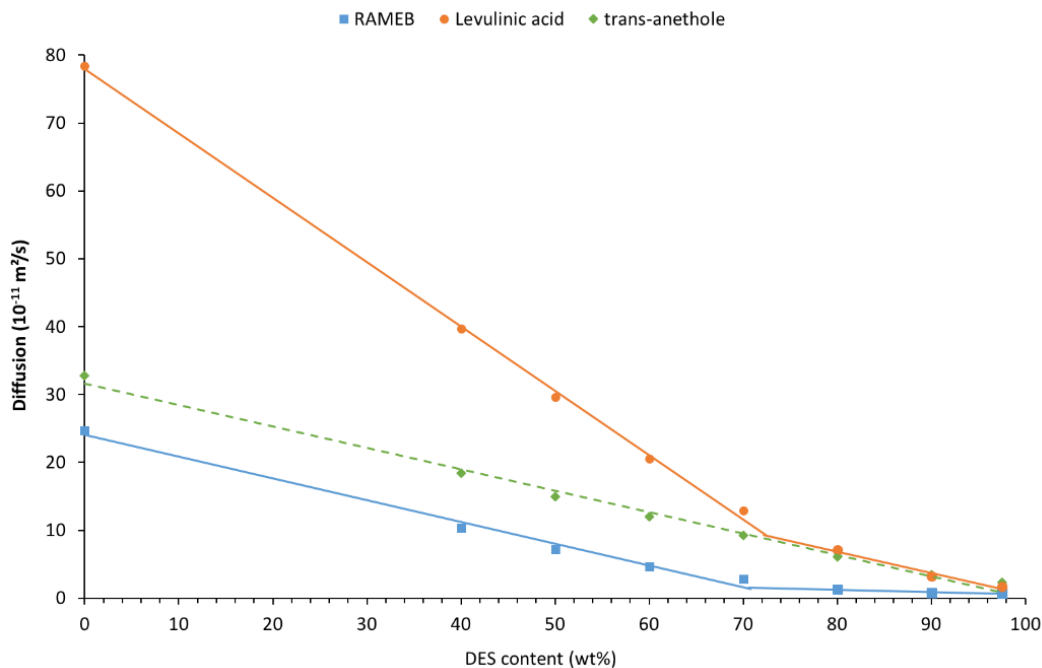


Figure 44. Variation of the diffusion coefficients of RAMEB:Lev SUPRADES' components and *trans*-anethole in different SUPRADES-water binary mixtures

Table 21. Diffusion coefficient values of RAMEB, levulinic acid, and *trans*-anethole, separately dissolved in water in the absence or presence of RAMEB

Diffusion coefficient (10 <sup>-11</sup> m <sup>2</sup> /s)	RAMEB	Levulinic acid	<i>trans</i> -Anethole
Water	24.7	82.7	73.6
Water + RAMEB		78.4	32.8

Altogether, these results prove that RAMEB maintains its ability to form inclusion complexes, even when present as one of the SUPRADES' components. Therefore, SUPRADES constitute promising low-melting mixtures with supramolecular properties.

## 5. Effect of cyclodextrin's addition

Aiming to study the effect of CD on DES' solubilizing ability, ChCl:U or ChCl:Lev DES (3 mL) were put in headspace vials to which increasing amounts (2, 4, 6, and 10 wt%) of different CD ( $\alpha$ -CD,  $\beta$ -CD,  $\gamma$ -CD, HP-

$\beta$ -CD, CRYSMEB, and Captisol®) were added. After CD dissolution and homogenization, the same amount of *trans*-anethole (5  $\mu$ L of 0.1 g.mL<sup>-1</sup>) was added to the (DES + CD) mixtures. Vials were then sealed and thermostated at 30 °C under stirring for 24h prior to analysis by SH-GC. Figure 45 shows the peak area of *trans*-anethole in ChCl:U as a function of CD concentration. The chromatographic peak area, which is proportional to the concentration of *trans*-anethole in the gas phase, decreases as the CD concentration increases. In other words, the addition of CD improves the solubilization of *trans*-anethole by ChCl:U. This result could be explained by the formation of a CD/ *trans*-anethole inclusion complex within ChCl:U DES, especially that it was recently proven that CD maintain their complexation ability in ChCl:U (Di Pietro et al., 2019; Moufawad et al., 2019). Moreover, no significant decrease in the peak area was observed when 10 wt% of glucopyranose was added to ChCl:U (Figure 45). This point confirms that the improved solubilization ability is not related to the sugar effect but most probably to the complexation of *trans*-anethole in the CD cavity. When it comes to ChCl:Lev, no effect was detected when the CD was added, even at the highest CD concentration. This means that unlike ChCl:U, no complexation occurs between CD and *trans*-anethole in ChCl:Lev DES.

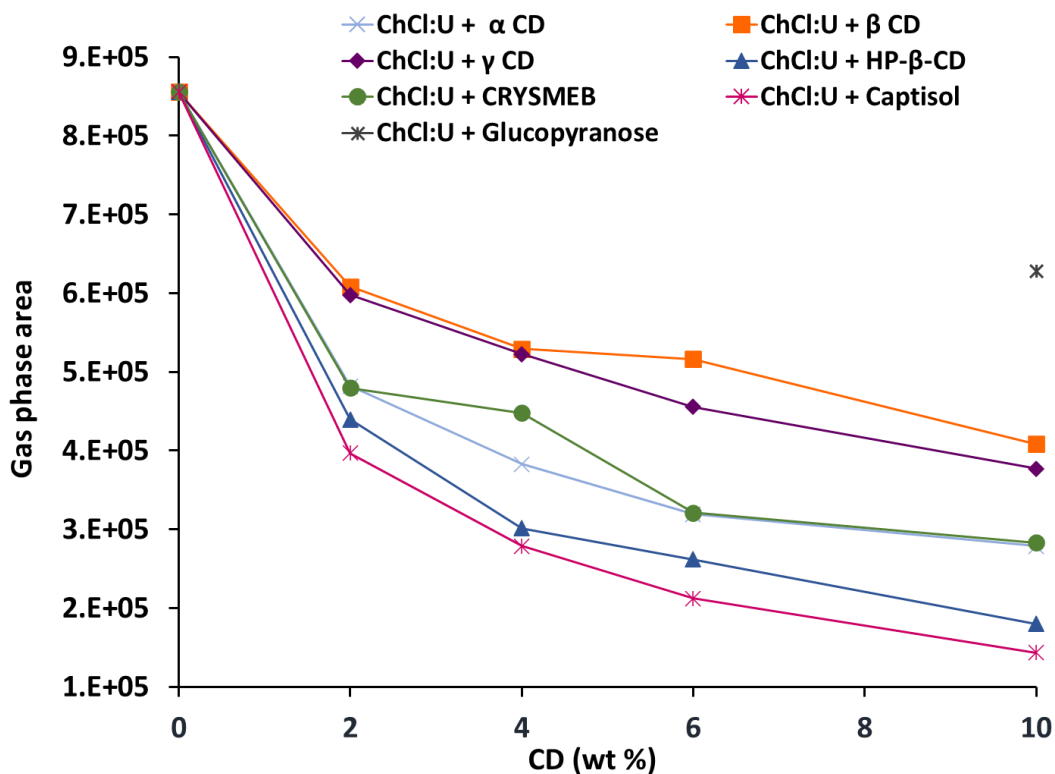


Figure 45. Variation of the chromatographic peak area of *trans*-anethole in mixtures of ChCl:U and increasing amounts of cyclodextrins. Glucopyranose was added at 10 wt% as a reference

## 6. Effect of lipids

In this section, we evaluated the solubilizing ability of the thin film-DES dissolution preparations, previously described in Section 2.2., in which DES were used to solubilize the lipid film in order to form lipid vesicles. ChCl:G and ChCl:EG were chosen since lipid structures were observed in these DES by optical microscopy (Figure 30). The preformed preparations based on the DES, lipid S100, and cholesterol were placed in the headspace vials. The same amount (25  $\mu\text{L}$  at a concentration of 0.1  $\text{g}\cdot\text{mL}^{-1}$ ) of *trans*-anethole, L-carvone, or D-menthol was then added to the vials which were then sealed and thermostated at 30 °C under stirring for 24 h prior to analysis by SH-GC. Menthol, found in peppermint oil (*Mentha piperita*), is known as an important flavoring agent, used in various consumer products like oral hygiene products and over-the-counter medications, as well as topical formulations (Kamatou et al., 2013). The solubilizing ability of both ChCl:G and ChCl:EG toward *trans*-anethole, L-carvone, and D-menthol was improved in presence of the lipids given that a lower gas phase area was obtained when compared with neat DES (Figure 46). The gas phase area of *trans*-anethole decreased by 39.9% and 22.2%, the area of L-carvone decreased by 21.8% and 30.5%, while that of D-menthol was reduced by 51.5% and 16.6% in ChCl:G and ChCl:EG, respectively. These results could be due to the encapsulation of the aroma compounds in the lipid structures that were formed in the DES.

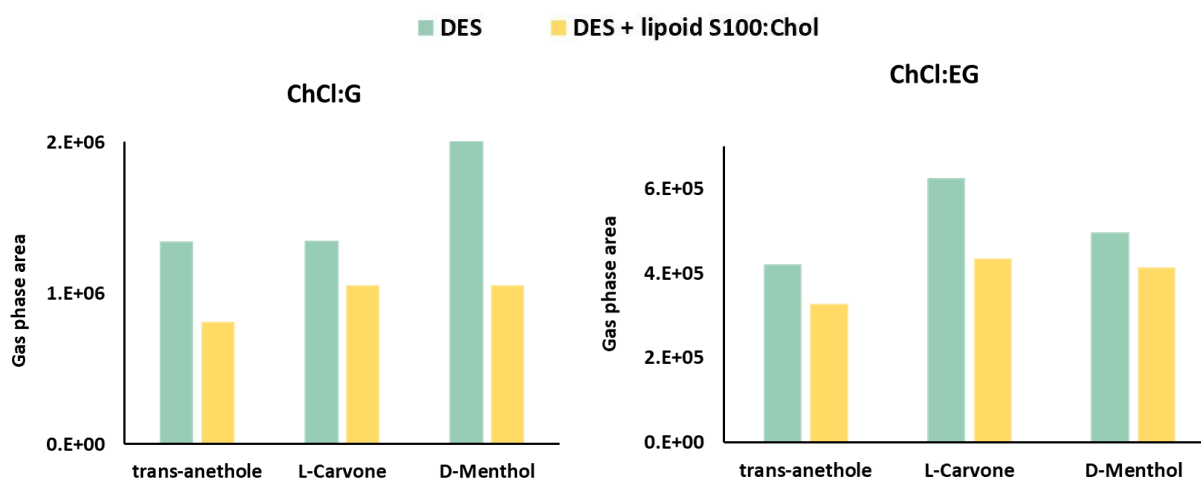


Figure 46. The chromatographic peak area of the studied volatile compounds in presence of DES or thin film-DES dissolution preparations

## 7. Effect of surfactant's addition

After observing large spherical self-assemblies in some ChCl-based DES in the presence of Triton X-100, a non-ionic surfactant, the solubilizing ability of the DES was evaluated in presence of the surfactant and

compared to that of neat DES. *Trans*-anethole (10  $\mu\text{L}$  at a concentration of 0.1  $\text{g}\cdot\text{mL}^{-1}$ ) was added to headspace vials containing 3 mL of DES (ChCl:U, ChCl:G, or ChCl:EG) or a mixture of DES and 10% (v/v) Triton X-100. The vials were sealed, thermostated at 30  $^{\circ}\text{C}$  for 24 h, and analyzed by SH-GC. The solubilization of *trans*-anethole was clearly improved in the presence of triton X-100 in all 3 studied DES (Figure 47). The gas phase area of *trans*-anethole was reduced by 69.3%, 81.2%, and 46.8% in ChCl:U, ChCl:G, and ChCl:EG, respectively. These findings are somehow in line with the optical microscopy observations, where the large self-assemblies formed by the surfactant could result in a greater *trans*-anethole solubility in DES.

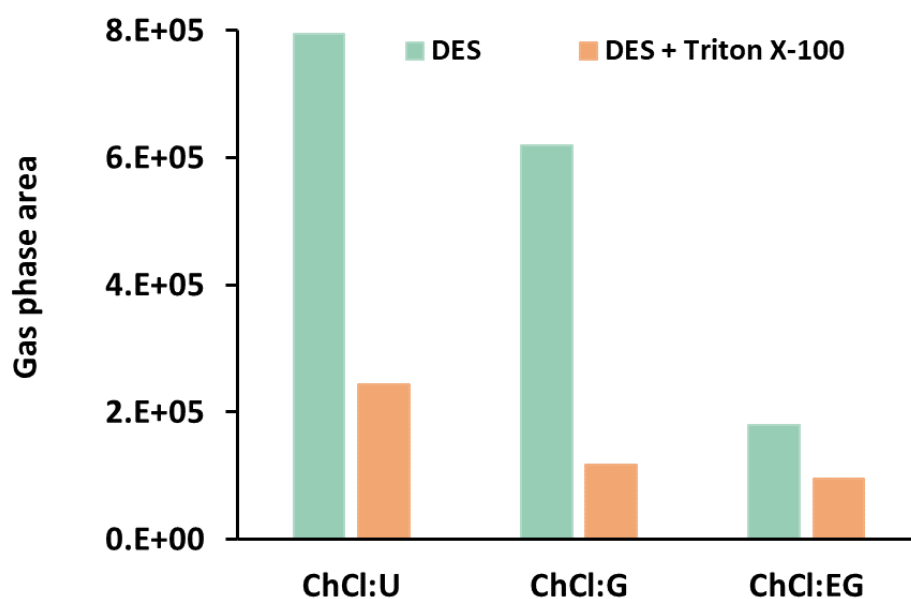


Figure 47. The chromatographic peak area of *trans*-anethole in ChCl-based DES in the presence or absence of Triton X-100 surfactant

## 8. Release study

The release of *trans*-anethole from the DES and the CD:Lev mixtures was monitored by multiple headspace extraction (MHE). This technique is a dynamic gas extraction that consists of successive headspace extractions from the same vial (Kolb & Ettre, 2006). In order to study the release kinetics of *trans*-anethole from the above-mentioned solvents at 60  $^{\circ}\text{C}$  and compare it with the release from water, samples were prepared similarly to the previous experiments but, once equilibrium was reached, vials were subjected to 10 headspace extractions at 1-hour intervals. The amount of *trans*-anethole present in the vial after each extraction could be determined from the chromatographic peak area. The release profiles of *trans*-anethole

from DES, SUPRADES, and water are shown in Figure 48. The results indicate that the studied solvents can not only solubilize *trans*-anethole but also delay its release over time. Indeed, 70% of *trans*-anethole was released from water after 10 extractions at 60 °C, while only 18 to 43% was released from the DES. These results seem to be related to the viscosity of the solvents since the most viscous solvents (Captisol:Lev and ChCl:U) release less AN.

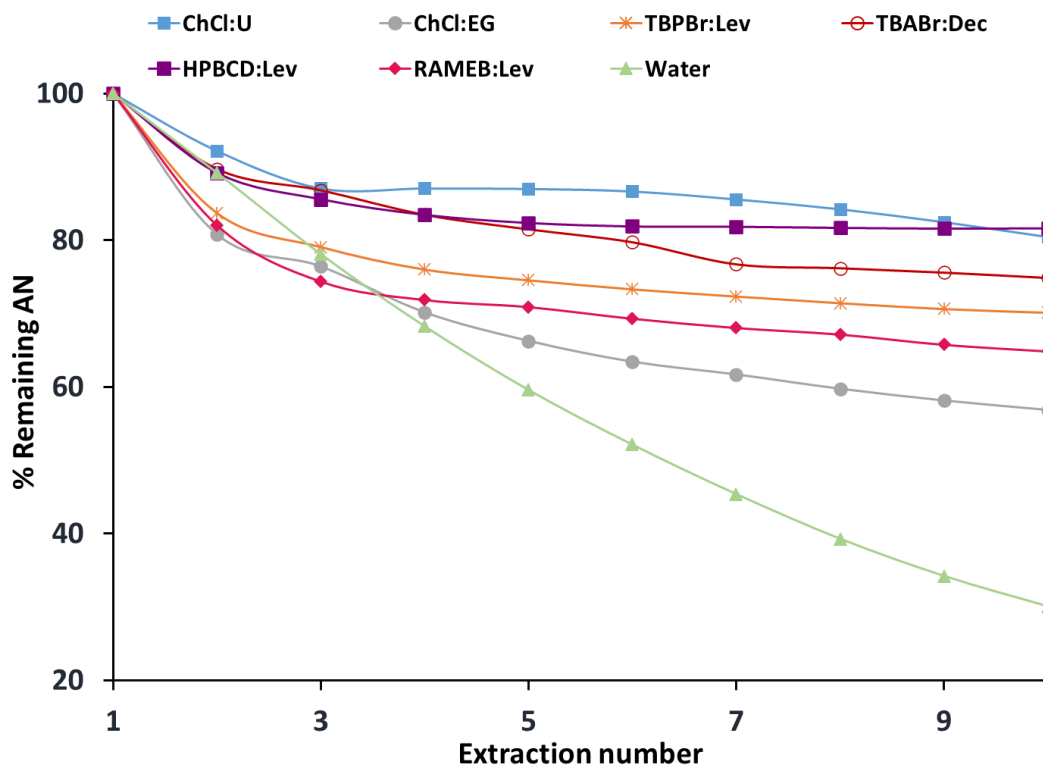


Figure 48. Release of *trans*-anethole from water and studied solvents at 60 °C

## Conclusion and perspectives

The present study aimed to characterize deep eutectic solvents (DES), to explore the behavior of liposomes and biological membranes within these solvents, and to evaluate the solubilizing ability of the rising solvents toward bioactive volatile compounds.

A group of DES was selected and prepared using different hydrogen bond acceptors and hydrogen bond donors. The hydrogen bond acceptors involve choline chloride, tetrabutylphosphonium bromide, and tetrabutylammonium bromide. On the other hand, several hydrogen bond donors namely urea, glycerol, ethylene glycol, levulinic acid, and decanoic acid were considered. The physicochemical characterization studies showed that the density, viscosity, and polarity of the DES can be tuned depending on the choice of the hydrogen bond acceptor, the hydrogen bond donor, and their molar ratio. New solvents were prepared using  $\beta$ -cyclodextrin derivatives as hydrogen bond acceptors and were called SUPRADES for having potential supramolecular properties. Interestingly, SUPRADES have shown similar physicochemical properties to DES and were found to be stable and liquid over a wide temperature range.

Following their characterization, the studied solvents were investigated as potential media for the self-assembly of phospholipids via atomic force microscopy. It was found that phospholipids tend to organize into vesicles in ChCl-based DES. Conversely, no lipid structures were observed in TBABr- or TBPBr- based DES or SUPRADES. DES were also introduced in two common methods adopted for liposomes preparation in aqueous media: ethanol injection method and thin film hydration. The replacement of the aqueous phase with the DES phase in both techniques generated lipid structures with different shapes in the ChCl-based DES. Moreover, the addition of the non-ionic surfactant Triton X-100 led to the formation of large circular assemblies in ChC:U, ChCl:G, and ChCl:EG.

In the next step, we sought to investigate the effect of DES on lipid membranes by exposing or incubating liposomes or human cells in ChCl-based DES. When exposed to DES or aqueous solutions of their components, preformed liposomes preserved their self-assembled structures although they decreased in size due to their probable dehydration. Similar observations were obtained when liposomes were incubated in the aqueous solutions of DES' compounds for different periods. However, when incubated in ChCl-based DES, liposomes converted into lipid bilayers before their reconstitution into vesicles. Moreover, the effect of ChCl:U, ChC:EG, and the aqueous solutions of their forming compounds on human cells was assessed through a combination of cytotoxicity and morphological studies. Results showed that DES are more cytotoxic than the corresponding (HBA + HBD) aqueous solutions toward MDA-MB-231, a human breast cancer cell line. The study also highlights the relevance of the choice of the HBD to DES' cytotoxicity since it can result in a relatively harmless DES like ChCl:U or a moderately toxic DES like ChCl:EG. The incubation of the cells in pure DES medium led to their fixation for up to 12 days.

The last part of the study focuses on the solubilization of bioactive volatile compounds by DES and other complex DES-based systems. DES showed a high solubilizing ability toward *trans*-anethole and L-carvone when compared with water. TBABr:Dec presented the greatest solubilizing capability, followed by TBPBr-based DES, and ChCl-based DES. SUPRADES exhibited an intermediate efficiency. Furthermore, all the tested solvents highly retained star anise and fennel essential oils, with more than 61% retention relative to water. The solubilization of *trans*-anethole by binary DES-water mixtures decreased with the increasing water content. Besides, an NMR study of RAMEB:Lev in presence of *trans*-anethole revealed some important interactions between the volatile compound and the CD cavity, thus suggesting that CD maintains its complexation ability in the SUPRADES form. Besides, the addition of CD to ChCl:U improved the solubility of *trans*-anethole by the DES. Likewise, the solubilizing performance of the DES was improved in presence of lipids or Triton X-100. Lastly, DES provided a controlled release of *trans*-anethole over time when compared with water.

Altogether, the obtained results pointed out the tunability of the DES and the prospect of designing new solvents with unique properties like SUPRADES. They also disclosed the behavior of phospholipids within the DES and the potential of these solvents as media for the self-assembly of amphiphilic molecules or the preservation of liposomes. These findings also contributed to elucidate the impact of the DES on biological membranes and their questionable safety. As proved by the solubilization studies, the main results of this research could also open up the possibility of forming new safe and economic DES-based systems for the encapsulation of bioactive molecules.

Based on this work, future investigations may be carried out to further elucidate some of the key findings of this research. Therefore, we encourage considerations to:

- Study the phase behavior of the new solvents that are based on CD and polyalcohols;
- Characterize the phospholipid self-assemblies formed in ChCl-based DES;
- Determine the critical micelle concentration of Triton X-100 in ChCl-based DES;
- Explore the organization of phospholipids at higher concentrations in TBPBr- and TBABr-based DES;
- Follow the effect of TBPBr- and TBABr-based DES on preformed liposomes;
- Track the long-term stability of self-assembled structures in DES;
- Evaluate the toxicity of the DES and SUPRADES toward a normal cell line;
- Appraise the solubility of other volatiles compounds by DES to understand the mechanism of solubilization;
- Examine the CD complexation ability in other DES than ChCl:U.

# List of publications and communications

## Publications

1. **El Achkar, T.**, Fourmentin, S., & Greige-Gerges, H. (2019). Deep eutectic solvents: An overview on their interactions with water and biochemical compounds. *Journal of Molecular Liquids*, 288, 111028. <https://doi.org/10.1016/j.molliq.2019.111028>
2. **El Achkar, T.**, Moufawad, T., Ruellan, S., Landy, D., Greige-Gerges, H., & Fourmentin, S. (2020). Cyclodextrins: From solute to solvent. *Chemical Communications*. <https://doi.org/10.1039/D0CC00460J>
3. Eid, J., **El Achkar, T.**, Fourmentin, S., Greige-Gerges, H., & Jraij, A. (2020). First investigation of liposomes behavior and phospholipids organization in choline chloride-based deep eutectic solvents by atomic force microscopy. *Journal of Molecular Liquids*, 306, 112851. <https://doi.org/10.1016/j.molliq.2020.112851>
4. **El Achkar, T.**, Moura, L., Moufawad, T., Ruellan, S., Panda, S., Longuemart, S., Legrand, F.-X., Costa Gomes, M., Landy, D., Greige-Gerges, H., & Fourmentin, S. (2020). New generation of supramolecular mixtures: Characterization and solubilization studies. *International Journal of Pharmaceutics*, 119443. <https://doi.org/10.1016/j.ijpharm.2020.119443>

### ▪ Book chapter

1. **El Achkar, T.**, Greige-Gerges, H. & Fourmentin, S. (2020). Understanding the basics and properties of deep eutectic solvents in: S. Fourmentin, M. Costa Gomes, E. Lichtfouse (Eds.), *Deep Eutectic Solvents for Medicine, Gas Solubilization and Extraction of Natural Substances*, Springer International Publishing, Cham, 2021: pp. 1–40. [https://doi.org/10.1007/978-3-030-53069-3\\_1](https://doi.org/10.1007/978-3-030-53069-3_1).

## Oral communications

1. **El Achkar, T.**, Moufawad, T., Moura, L., Ruellan, S., Longuemart, S., Landy, D., Costa Gomes, M., Greige-Gerges, H. & Fourmentin, S., SUPRADES: New generation of solvent based on supramolecular entities. The International Symposium on Green Chemistry (ISGC), La Rochelle, France, May 13 - 17, 2019.
2. **El Achkar, T.**, Moura, L., Moufawad, T., Panda, S., Longuemart, S., Landy, D., Costa Gomes, M., Greige-Gerges, H. & Fourmentin, S., New generation of solvent based on supramolecular entities: SUPRADES. 1<sup>st</sup> International Meeting on Deep Eutectic Systems, Lisbon, Portugal, June 24 - 27, 2019.

## Poster communications

1. **El Achkar, T.**, Greige-Gerges, H., & Fourmentin, S., Les solvants eutectiques profonds: un moyen de solubilisation des arômes et des huiles essentielles. Les Journées Condorcet, Calais, France, June 14 - 15, 2018.
2. **El Achkar, T.**, Greige-Gerges, H., & Fourmentin, S., Solubilization of aroma and essential oils using deep eutectic solvents. 4<sup>th</sup> International Conference on Natural Products Utilization (ICNPU), Albena, Bulgaria, May 29 – June 01, 2019.
3. **El Achkar, T.**, Moufawad, T., Longuemart, S., Costa Gomes, M., Landy, D., Greige-Gerges, H. & Fourmentin, S., SUPRADES: new solvents based on cyclodextrins. 4<sup>th</sup> International Summer School on Cyclodextrins, Milano, Italy, June 10 – 12, 2019.

## References

- Abbott, A. P., Barron, J. C., Ryder, K. S., & Wilson, D. (2007). Eutectic-based ionic liquids with metal-containing anions and cations. *Chemistry – A European Journal*, 13(22), 6495–6501. <https://doi.org/10.1002/chem.200601738>
- Abbott, A. P., Boothby, D., Capper, G., Davies, D. L., & Rasheed, R. K. (2004). Deep eutectic solvents formed between choline chloride and carboxylic acids: Versatile alternatives to ionic liquids. *Journal of the American Chemical Society*, 126(29), 9142–9147. <https://doi.org/10.1021/ja048266j>
- Abbott, A. P., Capper, G., Davies, D. L., Munro, H. L., Rasheed, R. K., & Tambyrajah, V. (2001). Preparation of novel, moisture-stable, Lewis-acidic ionic liquids containing quaternary ammonium salts with functional side chains. *Chemical Communications*, 19, 2010–2011. <https://doi.org/10.1039/B106357J>
- Abbott, A. P., Capper, G., Davies, D. L., & Rasheed, R. K. (2004). Ionic liquid analogues formed from hydrated metal salts. *Chemistry – A European Journal*, 10(15), 3769–3774. <https://doi.org/10.1002/chem.200400127>
- Abbott, A. P., Capper, G., Davies, D. L., Rasheed, R. K., & Tambyrajah, V. (2003). Novel solvent properties of choline chloride/urea mixtures. *Chemical Communications*, 1, 70–71. <https://doi.org/10.1039/B210714G>
- Abbott, A. P., Capper, G., & Gray, S. (2006). Design of improved deep eutectic solvents using hole theory. *ChemPhysChem*, 7(4), 803–806. <https://doi.org/10.1002/cphc.200500489>
- Abbott, A. P., Harris, R. C., & Ryder, K. S. (2007). Application of hole theory to define ionic liquids by their transport properties †. *The Journal of Physical Chemistry B*, 111(18), 4910–4913. <https://doi.org/10.1021/jp0671998>
- Abbott, A. P., Harris, R. C., Ryder, K. S., D'Agostino, C., Gladden, L. F., & Mantle, M. D. (2011). Glycerol eutectics as sustainable solvent systems. *Green Chemistry*, 13(1), 82–90. <https://doi.org/10.1039/C0GC00395F>
- Abranches, D. O., Martins, M. A. R., Silva, L. P., Schaeffer, N., Pinho, S. P., & Coutinho, J. A. P. (2019). Phenolic hydrogen bond donors in the formation of non-ionic deep eutectic solvents: The quest for type V DES. *Chemical Communications*, 55(69), 10253–10256. <https://doi.org/10.1039/C9CC04846D>
- Agieienko, V., & Buchner, R. (2019). Densities, viscosities, and electrical conductivities of pure anhydrous reline and its mixtures with water in the temperature range (293.15 to 338.15) K. *Journal of Chemical & Engineering Data*, 64(11), 4763–4774. <https://doi.org/10.1021/acs.jced.9b00145>
- Ahmadi, R., Hemmateenejad, B., Safavi, A., Shojaeifard, Z., Mohabbati, M., & Firuzi, O. (2018). Assessment of cytotoxicity of choline chloride-based natural deep eutectic solvents against human HEK-293 cells: A QSAR analysis. *Chemosphere*, 209, 831–838. <https://doi.org/10.1016/j.chemosphere.2018.06.103>
- Ahmadi, R., Hemmateenejad, B., Safavi, A., Shojaeifard, Z., Shahsavari, A., Mohajeri, A., Dokoohaki, M. H., & Zolghadr, A. R. (2018). Deep eutectic–water binary solvent associations investigated by vibrational spectroscopy and chemometrics. *Physical Chemistry Chemical Physics*, 20(27), 18463–18473. <https://doi.org/10.1039/C8CP00409A>
- Alcalde, R., Gutiérrez, A., Atilhan, M., & Aparicio, S. (2019). An experimental and theoretical investigation of the physicochemical properties on choline chloride – Lactic acid based natural deep eutectic solvent (NADES). *Journal of Molecular Liquids*, 290, 110916. <https://doi.org/10.1016/j.molliq.2019.110916>

- Alonso, D. A., Baeza, A., Chinchilla, R., Guillena, G., Pastor, I. M., & Ramón, D. J. (2016). Deep eutectic solvents: The organic reaction medium of the century. *European Journal of Organic Chemistry*, 2016(4), 612–632. <https://doi.org/10.1002/ejoc.201501197>
- Anwekar, H., Patel, S., & Singhai, A. K. (2011). Liposome-as drug carriers. *International Journal of Pharmacy & Life Sciences*, 2(7), 945–951.
- Arnold, T., Jackson, A. J., Sanchez-Fernandez, A., Magnone, D., Terry, A. E., & Edler, K. J. (2015). Surfactant behavior of sodium dodecylsulfate in deep eutectic solvent choline chloride/urea. *Langmuir*, 31(47), 12894–12902. <https://doi.org/10.1021/acs.langmuir.5b02596>
- Aroso, I. M., Paiva, A., Reis, R. L., & Duarte, A. R. C. (2017). Natural deep eutectic solvents from choline chloride and betaine – Physicochemical properties. *Journal of Molecular Liquids*, 241, 654–661. <https://doi.org/10.1016/j.molliq.2017.06.051>
- Athanasiadis, V., Grigorakis, S., Lalas, S., & Makris, D. P. (2018a). Methyl  $\beta$ -cyclodextrin as a booster for the extraction for *Olea europaea* leaf polyphenols with a bio-based deep eutectic solvent. *Biomass Conversion and Biorefinery*, 8(2), 345–355. <https://doi.org/10.1007/s13399-017-0283-5>
- Athanasiadis, V., Grigorakis, S., Lalas, S., & Makris, D. P. (2018b). Stability effects of methyl  $\beta$ -cyclodextrin on *Olea europaea* leaf extracts in a natural deep eutectic solvent. *European Food Research and Technology*, 244(10), 1783–1792. <https://doi.org/10.1007/s00217-018-3090-8>
- Atilhan, M., Costa, L. T., & Aparicio, S. (2017). On the behaviour of aqueous solutions of deep eutectic solvents at lipid biomembranes. *Journal of Molecular Liquids*, 247, 116–125. <https://doi.org/10.1016/j.molliq.2017.09.082>
- Bajkacz, S., & Adamek, J. (2017). Evaluation of new natural deep eutectic solvents for the extraction of isoflavones from soy products. *Talanta*, 168, 329–335. <https://doi.org/10.1016/j.talanta.2017.02.065>
- Bangham, A. D., Standish, M. M., & Watkins, J. C. (1965). Diffusion of univalent ions across the lamellae of swollen phospholipids. *Journal of Molecular Biology*, 13(1), 238–252. [https://doi.org/10.1016/s0022-2836\(65\)80093-6](https://doi.org/10.1016/s0022-2836(65)80093-6)
- Batzri, S., & Korn, E. D. (1973). Single bilayer liposomes prepared without sonication. *Biochimica et Biophysica Acta (BBA) - Biomembranes*, 298(4), 1015–1019. [https://doi.org/10.1016/0005-2736\(73\)90408-2](https://doi.org/10.1016/0005-2736(73)90408-2)
- Benlebna, M., Ruesgas-Ramón, M., Bonafos, B., Fouret, G., Casas, F., Coudray, C., Durand, E., Cruz Figueroa-Espinoza, M., & Feillet-Coudray, C. (2018). Toxicity of natural deep eutectic solvent betaine:glycerol in rats. *Journal of Agricultural and Food Chemistry*, 66(24), 6205–6212. <https://doi.org/10.1021/acs.jafc.8b01746>
- Berton, P., Di Bona, K. R., Yancey, D., Rizvi, S. A. A., Gray, M., Gurau, G., Shamshina, J. L., Rasco, J. F., & Rogers, R. D. (2017). Transdermal bioavailability in rats of lidocaine in the forms of ionic liquids, salts, and deep eutectic. *ACS Medicinal Chemistry Letters*, 8(5), 498–503. <https://doi.org/10.1021/acsmedchemlett.6b00504>
- Bryant, S. J., Atkin, R., & Warr, G. G. (2016). Spontaneous vesicle formation in a deep eutectic solvent. *Soft Matter*, 12(6), 1645–1648. <https://doi.org/10.1039/C5SM02660A>
- Bryant, S. J., Atkin, R., & Warr, G. G. (2017). Effect of deep eutectic solvent nanostructure on phospholipid bilayer phases. *Langmuir*, 33(27), 6878–6884. <https://doi.org/10.1021/acs.langmuir.7b01561>
- Cardellini, F., Tiecco, M., Germani, R., Cardinali, G., Corte, L., Roscini, L., & Spreti, N. (2014). Novel zwitterionic deep eutectic solvents from trimethylglycine and carboxylic acids: Characterization of their properties and their toxicity. *RSC Advances*, 4(99), 55990–56002. <https://doi.org/10.1039/C4RA10628H>
- Castro, V. I. B., Craveiro, R., Silva, J. M., Reis, R. L., Paiva, A., & C. Duarte, A. R. (2018). Natural deep eutectic systems as alternative nontoxic cryoprotective agents. *Cryobiology*, 83, 15–26. <https://doi.org/10.1016/j.cryobiol.2018.06.010>

- Celebi, A. T., Vlugt, T. J. H., & Moutos, O. A. (2019). Structural, thermodynamic, and transport properties of aqueous reline and ethaline solutions from molecular dynamics simulations. *The Journal of Physical Chemistry B*, *123*(51), 11014–11025. <https://doi.org/10.1021/acs.jpccb.9b09729>
- Chakroun, D., Grigorakis, S., Loupassaki, S., & Makris, D. P. (2019). Enhanced-performance extraction of olive (*Olea europaea*) leaf polyphenols using L-lactic acid/ammonium acetate deep eutectic solvent combined with  $\beta$ -cyclodextrin: Screening, optimisation, temperature effects and stability. *Biomass Conversion and Biorefinery*. <https://doi.org/10.1007/s13399-019-00521-2>
- Chatterjee, S., Haldar, T., Ghosh, D., & Bagchi, S. (2020). Electrostatic manifestation of micro-heterogeneous solvation structures in deep-eutectic solvents: A spectroscopic approach. *The Journal of Physical Chemistry B*, *124*(18), 3709–3715. <https://doi.org/10.1021/acs.jpccb.9b11352>
- Chemat, F., Abert Vian, M., Ravi, H. K., Khadhraoui, B., Hilali, S., Perino, S., & Fabiano Tixier, A.-S. (2019). Review of Alternative Solvents for Green Extraction of Food and Natural Products: Panorama, Principles, Applications and Prospects. *Molecules*, *24*(16), 3007. <https://doi.org/10.3390/molecules24163007>
- Chen, J., Liu, M., Wang, Q., Du, H., & Zhang, L. (2016). Deep eutectic solvent-based microwave-assisted method for extraction of hydrophilic and hydrophobic components from radix *Salviae miltiorrhizae*. *Molecules*, *21*(10), 1383. <https://doi.org/10.3390/molecules21101383>
- Chen, J., Wang, Q., Liu, M., & Zhang, L. (2017). The effect of deep eutectic solvent on the pharmacokinetics of salvianolic acid B in rats and its acute toxicity test. *Journal of Chromatography B*, *1063*, 60–66. <https://doi.org/10.1016/j.jchromb.2017.08.016>
- Chen, W., Bai, X., Xue, Z., Mou, H., Chen, J., Liu, Z., & Mu, T. (2019). The formation and physicochemical properties of PEGylated deep eutectic solvents. *New Journal of Chemistry*, *43*(22), 8804–8810. <https://doi.org/10.1039/C9NJ02196E>
- Chen, Y., & Mu, T. (2019). Application of deep eutectic solvents in biomass pretreatment and conversion. *Green Energy & Environment*, *4*(2), 95–115. <https://doi.org/10.1016/j.gee.2019.01.012>
- Chen, Y., Yu, D., Chen, W., Fu, L., & Mu, T. (2019). Water absorption by deep eutectic solvents. *Physical Chemistry Chemical Physics*, *21*(5), 2601–2610. <https://doi.org/10.1039/C8CP07383J>
- Chen, Z., Ludwig, M., Warr, G. G., & Atkin, R. (2017). Effect of cation alkyl chain length on surface forces and physical properties in deep eutectic solvents. *Journal of Colloid and Interface Science*, *494*, 373–379. <https://doi.org/10.1016/j.jcis.2017.01.109>
- Choi, Y. H., Spronsen, J. van, Dai, Y., Verberne, M., Hollmann, F., Arends, I. W. C. E., Witkamp, G.-J., & Verpoorte, R. (2011). Are natural deep eutectic solvents the missing link in understanding cellular metabolism and physiology? *Plant Physiology*, *156*(4), 1701–1705. <https://doi.org/10.1104/pp.111.178426>
- Costa, S. P. F., Cunha, E., Azevedo, A. M. O., Pereira, S. A. P., Neves, A. F. D. C., Vilaranda, A. G., Araujo, A. R. T. S., Passos, M. L. C., Pinto, P. C. A. G., & Saraiva, M. L. M. F. S. (2018). Microfluidic chemiluminescence system with yeast *Saccharomyces cerevisiae* for rapid biochemical oxygen demand measurement. *ACS Sustainable Chemistry & Engineering*, *6*(5), 6094–6101. <https://doi.org/10.1021/acssuschemeng.7b04736>
- Coutinho, J. A. P., & Pinho, S. P. (2017). Special issue on deep eutectic solvents: A foreword. *Fluid Phase Equilibria*, *448*, 1. <https://doi.org/10.1016/j.fluid.2017.06.011>
- Cui, Y., Li, C., Yin, J., Li, S., Jia, Y., & Bao, M. (2017). Design, synthesis and properties of acidic deep eutectic solvents based on choline chloride. *Journal of Molecular Liquids*, *236*, 338–343. <https://doi.org/10.1016/j.molliq.2017.04.052>
- Cunha, S. C., & Fernandes, J. O. (2018). Extraction techniques with deep eutectic solvents. *TrAC Trends in Analytical Chemistry*, *105*, 225–239. <https://doi.org/10.1016/j.trac.2018.05.001>
- Cvjetko Bubalo, M., Jurinjak Tušek, A., Vinkovič, M., Radošević, K., Gaurina Srlek, V., & Radojčić Redovnikovič, I. (2015). Cholinium-based deep eutectic solvents and ionic liquids for lipase-

- catalyzed synthesis of butyl acetate. *Journal of Molecular Catalysis B: Enzymatic*, 122, 188–198. <https://doi.org/10.1016/j.molcatb.2015.09.005>
- Cvjetko Bubalo, M., Mazur, M., Radošević, K., & Radojčić Redovniković, I. (2015). Baker's yeast-mediated asymmetric reduction of ethyl 3-oxobutanoate in deep eutectic solvents. *Process Biochemistry*, 50(11), 1788–1792. <https://doi.org/10.1016/j.procbio.2015.07.015>
- Cysewski, P., & Jeliński, T. (2019). Optimization, thermodynamic characteristics and solubility predictions of natural deep eutectic solvents used for sulfonamide dissolution. *International Journal of Pharmaceutics*, 570, 118682. <https://doi.org/10.1016/j.ijpharm.2019.118682>
- D'Agostino, C., Gladden, L. F., Mantle, M. D., Abbott, A. P., Ahmed, E., I., Al-Murshedi, A. Y. M., & Harris, R. C. (2015). Molecular and ionic diffusion in aqueous – deep eutectic solvent mixtures: Probing inter-molecular interactions using PFG NMR. *Physical Chemistry Chemical Physics*, 17(23), 15297–15304. <https://doi.org/10.1039/C5CP01493J>
- D'Agostino, C., Harris, R. C., Abbott, A. P., Gladden, L. F., & Mantle, M. D. (2011). Molecular motion and ion diffusion in choline chloride based deep eutectic solvents studied by <sup>1</sup>H pulsed field gradient NMR spectroscopy. *Physical Chemistry Chemical Physics*, 13(48), 21383. <https://doi.org/10.1039/c1cp22554e>
- Dai, Y., van Spronsen, J., Witkamp, G.-J., Verpoorte, R., & Choi, Y. H. (2013). Natural deep eutectic solvents as new potential media for green technology. *Analytica Chimica Acta*, 766, 61–68. <https://doi.org/10.1016/j.aca.2012.12.019>
- Dai, Y., Witkamp, G.-J., Verpoorte, R., & Choi, Y. H. (2015). Tailoring properties of natural deep eutectic solvents with water to facilitate their applications. *Food Chemistry*, 187, 14–19. <https://doi.org/10.1016/j.foodchem.2015.03.123>
- de Carvalho, C. C. C. R., & da Fonseca, M. M. R. (2006). Carvone: Why and how should one bother to produce this terpene. *Food Chemistry*, 95(3), 413–422. <https://doi.org/10.1016/j.foodchem.2005.01.003>
- Decock, G., Landy, D., Surpateanu, G., & Fourmentin, S. (2008). Study of the retention of aroma components by cyclodextrins by static headspace gas chromatography. *Journal of Inclusion Phenomena and Macrocyclic Chemistry*, 62(3), 297–302. <https://doi.org/10.1007/s10847-008-9471-z>
- Delgado-Mellado, N., Larriba, M., Navarro, P., Rigual, V., Ayuso, M., García, J., & Rodríguez, F. (2018). Thermal stability of choline chloride deep eutectic solvents by TGA/FTIR-ATR analysis. *Journal of Molecular Liquids*, 260, 37–43. <https://doi.org/10.1016/j.molliq.2018.03.076>
- Delso, I., Lafuente, C., Muñoz-Embid, J., & Artal, M. (2019). NMR study of choline chloride-based deep eutectic solvents. *Journal of Molecular Liquids*, 290, 111236. <https://doi.org/10.1016/j.molliq.2019.111236>
- Di Pietro, M. E., Colombo Dugoni, G., Ferro, M., Mannu, A., Castiglione, F., Costa Gomes, M., Fourmentin, S., & Mele, A. (2019). Do cyclodextrins encapsulate volatiles in deep eutectic systems? *ACS Sustainable Chemistry & Engineering*, 7(20), 17397–17405. <https://doi.org/10.1021/acssuschemeng.9b04526>
- Di Pietro, M. E., Ferro, M., & Mele, A. (2020). Drug encapsulation and chiral recognition in deep eutectic solvents/ $\beta$ -cyclodextrin mixtures. *Journal of Molecular Liquids*, 311, 113279. <https://doi.org/10.1016/j.molliq.2020.113279>
- Du, C., Zhao, B., Chen, X.-B., Birbilis, N., & Yang, H. (2016). Effect of water presence on choline chloride-2urea ionic liquid and coating platings from the hydrated ionic liquid. *Scientific Reports*, 6(1). <https://doi.org/10.1038/srep29225>
- Duarte, A. R. C., Ferreira, A. S. D., Barreiros, S., Cabrita, E., Reis, R. L., & Paiva, A. (2017). A comparison between pure active pharmaceutical ingredients and therapeutic deep eutectic solvents: Solubility

- and permeability studies. *European Journal of Pharmaceutics and Biopharmaceutics*, 114, 296–304. <https://doi.org/10.1016/j.ejpb.2017.02.003>
- Dugoni, G. C., Di Pietro, M. E., Ferro, M., Castiglione, F., Ruellan, S., Moufawad, T., Moura, L., Costa Gomes, M. F., Fourmentin, S., & Mele, A. (2019). Effect of water on deep eutectic solvent/ $\beta$ -cyclodextrin systems. *ACS Sustainable Chemistry & Engineering*, 7(7), 7277–7285. <https://doi.org/10.1021/acssuschemeng.9b00315>
- Durand, E., Villeneuve, P., Bourlieu-lacanal, C., & Carrière, F. (2020). Natural deep eutectic solvents: Hypothesis for their possible roles in cellular functions and interaction with membranes and other organized biological systems. In *Advances in Botanical Research*. Academic Press. <https://doi.org/10.1016/bs.abr.2020.09.005>
- Dwamena, A. K., & Raynie, D. E. (2020). Solvatochromic parameters of deep eutectic solvents: Effect of different carboxylic acids as hydrogen bond donor. *Journal of Chemical & Engineering Data*, 65(2), 640–646. <https://doi.org/10.1021/acs.jced.9b00872>
- El Achkar, T., Fourmentin, S., & Greige-Gerges, H. (2019). Deep eutectic solvents: An overview on their interactions with water and biochemical compounds. *Journal of Molecular Liquids*, 288, 111028. <https://doi.org/10.1016/j.molliq.2019.111028>
- El Achkar, T., Moufawad, T., Ruellan, S., Landy, D., Greige-Gerges, H., & Fourmentin, S. (2020). Cyclodextrins: From solute to solvent. *Chemical Communications*. <https://doi.org/10.1039/D0CC00460J>
- El Achkar, T., Moura, L., Moufawad, T., Ruellan, S., Panda, S., Longuemart, S., Legrand, F.-X., Costa Gomes, M., Landy, D., Greige-Gerges, H., & Fourmentin, S. (2020). New generation of supramolecular mixtures: Characterization and solubilization studies. *International Journal of Pharmaceutics*, 119443. <https://doi.org/10.1016/j.ijpharm.2020.119443>
- Emami, S., & Shayanfar, A. (2020). Deep eutectic solvents for pharmaceutical formulation and drug delivery applications. *Pharmaceutical Development and Technology*, 0(0), 1–18. <https://doi.org/10.1080/10837450.2020.1735414>
- Fahri, F., Bacha, K., Chiki, F. F., Mbakidi, J.-P., Panda, S., Bouquillon, S., & Fourmentin, S. (2020). Air pollution: New bio-based ionic liquids absorb both hydrophobic and hydrophilic volatile organic compounds with high efficiency. *Environmental Chemistry Letters*. <https://doi.org/10.1007/s10311-020-01007-8>
- Farias, F. O., Pereira, J. F. B., Coutinho, J. A. P., Igarashi-Mafra, L., & Mafra, M. R. (2020). Understanding the role of the hydrogen bond donor of the deep eutectic solvents in the formation of the aqueous biphasic systems. *Fluid Phase Equilibria*, 503, 112319. <https://doi.org/10.1016/j.fluid.2019.112319>
- Fenyvesi, É., Szemán, J., Csabai, K., Malanga, M., & Szente, L. (2014). Methyl-Beta-Cyclodextrins: The Role of Number and Types of Substituents in Solubilizing Power. *Journal of Pharmaceutical Sciences*, 103(5), 1443–1452. <https://doi.org/10.1002/jps.23917>
- Fernández, M. de los Á., Boiteux, J., Espino, M., Gomez, F. J. V., & Silva, M. F. (2018). Natural deep eutectic solvents-mediated extractions: The way forward for sustainable analytical developments. *Analytica Chimica Acta*, 1038, 1–10. <https://doi.org/10.1016/j.aca.2018.07.059>
- Ferreira, M., Jérôme, F., Bricout, H., Manuel, S., Landy, D., Fourmentin, S., Tilloy, S., & Monflier, E. (2015). Rhodium catalyzed hydroformylation of 1-decene in low melting mixtures based on various cyclodextrins and N,N'-dimethylurea. *Catalysis Communications*, 63, 62–65. <https://doi.org/10.1016/j.catcom.2014.11.001>
- Fetisov, E. O., Harwood, D. B., Kuo, I.-F. W., Warrag, S. E. E., Kroon, M. C., Peters, C. J., & Siepmann, J. I. (2018). First-principles molecular dynamics study of a deep eutectic solvent: Choline chloride/urea and its mixture with water. *The Journal of Physical Chemistry B*, 122(3), 1245–1254. <https://doi.org/10.1021/acs.jpcb.7b10422>

- Florindo, C., Branco, L. C., & Marrucho, I. M. (2019). Quest for green-solvent design: From hydrophilic to hydrophobic (deep) eutectic solvents. *ChemSusChem*, 12(8), 1549–1559. <https://doi.org/10.1002/cssc.201900147>
- Florindo, C., Oliveira, F. S., Rebelo, L. P. N., Fernandes, A. M., & Marrucho, I. M. (2014). Insights into the synthesis and properties of deep eutectic solvents based on cholinium chloride and carboxylic acids. *ACS Sustainable Chemistry & Engineering*, 2(10), 2416–2425. <https://doi.org/10.1021/sc500439w>
- Florindo, C., S. McIntosh, A. J., Welton, T., C. Branco, L., & M. Marrucho, I. (2018). A closer look into deep eutectic solvents: Exploring intermolecular interactions using solvatochromic probes. *Physical Chemistry Chemical Physics*, 20(1), 206–213. <https://doi.org/10.1039/C7CP06471C>
- Fourmentin, S., Landy, D., Moura, L. M. C. G. D., Tilloy, S., Bricout, H., & Ferreira, M. (2016). *Procede d'epuration d'un effluent gazeux* (Patent No. FR3058905A1).
- Francisco, M., Bruinhorst, A. van den, & Kroon, M. C. (2012). New natural and renewable low transition temperature mixtures (LTTMs): Screening as solvents for lignocellulosic biomass processing. *Green Chemistry*, 14(8), 2153–2157. <https://doi.org/10.1039/C2GC35660K>
- Gabriele, F., Chiarini, M., Germani, R., Tiecco, M., & Spreti, N. (2019). Effect of water addition on choline chloride/glycol deep eutectic solvents: Characterization of their structural and physicochemical properties. *Journal of Molecular Liquids*, 291, 111301. <https://doi.org/10.1016/j.molliq.2019.111301>
- Gao, Q., Zhu, Y., Ji, X., Zhu, W., Lu, L., & Lu, X. (2018). Effect of water concentration on the microstructures of choline chloride/urea (1:2) /water mixture. *Fluid Phase Equilibria*, 470, 134–139. <https://doi.org/10.1016/j.fluid.2018.01.031>
- García, G., Aparicio, S., Ullah, R., & Atilhan, M. (2015). Deep eutectic solvents: Physicochemical properties and gas separation applications. *Energy & Fuels*, 29(4), 2616–2644. <https://doi.org/10.1021/ef5028873>
- Georgantzi, C., Lioliou, A.-E., Paterakis, N., & Makris, D. P. (2017). Combination of lactic acid-based deep eutectic solvents (DES) with  $\beta$ -cyclodextrin: Performance screening using ultrasound-assisted extraction of polyphenols from selected native greek medicinal plants. *Agronomy*, 7(3), 54. <https://doi.org/10.3390/agronomy7030054>
- Germani, R., Orlandini, M., Tiecco, M., & Del Giacco, T. (2017). Novel low viscous, green and amphiphilic N-oxides/phenylacetic acid based Deep Eutectic Solvents. *Journal of Molecular Liquids*, 240, 233–239. <https://doi.org/10.1016/j.molliq.2017.05.084>
- Gharib, R., Greige-Gerges, H., Fourmentin, S., & Charcosset, C. (2018). Hydroxypropyl- $\beta$ -cyclodextrin as a membrane protectant during freeze-drying of hydrogenated and non-hydrogenated liposomes and molecule-in-cyclodextrin-in- liposomes: Application to trans-anethole. *Food Chemistry*, 267, 67–74. <https://doi.org/10.1016/j.foodchem.2017.10.144>
- Gomez, F. J. V., Espino, M., Fernández, M. A., & Silva, M. F. (2018). A greener approach to prepare natural deep eutectic solvents. *ChemistrySelect*, 3(22), 6122–6125. <https://doi.org/10.1002/slct.201800713>
- Gonzalez, C. G., Choi, Y. H., & Verpoorte, R. (2020). Chapter 19 - Preanalytical treatments: Extraction with deep eutectic solvents. In C. F. Poole (Ed.), *Liquid-Phase Extraction* (pp. 565–590). Elsevier. <https://doi.org/10.1016/B978-0-12-816911-7.00019-0>
- González, C. G., Mustafa, N. R., Wilson, E. G., Verpoorte, R., & Choi, Y. H. (2018). Application of natural deep eutectic solvents for the “green” extraction of vanillin from vanilla pods. *Flavour and Fragrance Journal*, 33(1), 91–96. <https://doi.org/10.1002/ffj.3425>
- Gorke, J. T., Srien, F., & Kazlauskas, R. J. (2008). Hydrolase-catalyzed biotransformations in deep eutectic solvents. *Chemical Communications*, 10, 1235. <https://doi.org/10.1039/b716317g>
- Grobelyny, J., DelRio, F. W., Pradeep, N., Kim, D.-I., Hackley, V. A., & Cook, R. F. (2011). Size measurement of nanoparticles using atomic force microscopy. In S. E. McNeil (Ed.), *Characterization of*

- Nanoparticles Intended for Drug Delivery* (pp. 71–82). Humana Press. [https://doi.org/10.1007/978-1-60327-198-1\\_7](https://doi.org/10.1007/978-1-60327-198-1_7)
- Gutiérrez, A., Atilhan, M., & Aparicio, S. (2018). A theoretical study on lidocaine solubility in deep eutectic solvents. *Physical Chemistry Chemical Physics*, 20(43), 27464–27473. <https://doi.org/10.1039/C8CP05641B>
- Gutiérrez, A., Atilhan, M., & Aparicio, S. (2020). Theoretical study on deep eutectic solvents as vehicles for the delivery of anesthetics. *The Journal of Physical Chemistry B*, 124(9), 1794–1805. <https://doi.org/10.1021/acs.jpcc.9b11756>
- Gutiérrez, M. C., Ferrer, M. L., Mateo, C. R., & del Monte, F. (2009). Freeze-drying of aqueous solutions of deep eutectic solvents: A suitable approach to deep eutectic suspensions of self-assembled structures. *Langmuir*, 25(10), 5509–5515. <https://doi.org/10.1021/la900552b>
- Hadj-Kali, M. K., Al-khidir, K. E., Wazeer, I., El-blidi, L., Mulyono, S., & AlNashef, I. M. (2015). Application of deep eutectic solvents and their individual constituents as surfactants for enhanced oil recovery. *Colloids and Surfaces A: Physicochemical and Engineering Aspects*, 487, 221–231. <https://doi.org/10.1016/j.colsurfa.2015.10.005>
- Häkkinen, R., Alshammari, O., Timmermann, V., D'Agostino, C., & Abbott, A. (2019). Nanoscale clustering of alcoholic solutes in deep eutectic solvents studied by nuclear magnetic resonance and dynamic light scattering. *ACS Sustainable Chemistry & Engineering*, 7(17), 15086–15092. <https://doi.org/10.1021/acssuschemeng.9b03771>
- Häkkinen, R., Willberg-Keyriläinen, P., Ropponen, J., & Virtanen, T. (2019). Effect of composition and water content on physicochemical properties of choline chloride-boric acid low-melting mixtures. *Journal of Molecular Liquids*, 280, 104–110. <https://doi.org/10.1016/j.molliq.2019.02.011>
- Halder, A. K., & Cordeiro, M. N. D. S. (2019). Probing the environmental toxicity of deep eutectic solvents and their components: An in silico modeling approach. *ACS Sustainable Chemistry & Engineering*, 7(12), 10649–10660. <https://doi.org/10.1021/acssuschemeng.9b01306>
- Hammond, O. S., Bowron, D. T., & Edler, K. J. (2017). The effect of water upon deep eutectic solvent nanostructure: An unusual transition from ionic mixture to aqueous solution. *Angewandte Chemie International Edition*, 56(33), 9782–9785. <https://doi.org/10.1002/anie.201702486>
- Hammond, O. S., Bowron, D. T., Jackson, A. J., Arnold, T., Sanchez-Fernandez, A., Tsapatsaris, N., Garcia Sakai, V., & Edler, K. J. (2017). Resilience of malic acid natural deep eutectic solvent nanostructure to solidification and hydration. *The Journal of Physical Chemistry B*, 121(31), 7473–7483. <https://doi.org/10.1021/acs.jpcc.7b05454>
- Hapiot, F., Menuel, S., Ferreira, M., Léger, B., Bricout, H., Tilloy, S., & Monflier, E. (2017). Catalysis in cyclodextrin-based unconventional reaction media: Recent developments and future opportunities. *ACS Sustainable Chemistry & Engineering*, 5(5), 3598–3606. <https://doi.org/10.1021/acssuschemeng.6b02886>
- Haraźna, K., Walas, K., Urbańska, P., Witko, T., Snoch, W., Siemek, A., Jachimska, B., Krzan, M., Napruszewska, B. D., Witko, M., Bednarz, S., & Guzik, M. (2019). Polyhydroxyalkanoate-derived hydrogen-bond donors for the synthesis of new deep eutectic solvents. *Green Chemistry*, 21(11), 3116–3126. <https://doi.org/10.1039/C9GC00387H>
- Hayyan, A., Mjalli, F. S., AlNashef, I. M., Al-Wahaibi, T., Al-Wahaibi, Y. M., & Hashim, M. A. (2012). Fruit sugar-based deep eutectic solvents and their physical properties. *Thermochimica Acta*, 541, 70–75. <https://doi.org/10.1016/j.tca.2012.04.030>
- Hayyan, A., Mjalli, F. S., AlNashef, I. M., Al-Wahaibi, Y. M., Al-Wahaibi, T., & Hashim, M. A. (2013). Glucose-based deep eutectic solvents: Physical properties. *Journal of Molecular Liquids*, 178, 137–141. <https://doi.org/10.1016/j.molliq.2012.11.025>

- Hayyan, M., Hashim, M. A., Al-Saadi, M. A., Hayyan, A., AlNashef, I. M., & Mirghani, M. E. S. (2013). Assessment of cytotoxicity and toxicity for phosphonium-based deep eutectic solvents. *Chemosphere*, *93*(2), 455–459. <https://doi.org/10.1016/j.chemosphere.2013.05.013>
- Hayyan, M., Hashim, M. A., Hayyan, A., Al-Saadi, M. A., AlNashef, I. M., Mirghani, M. E. S., & Saheed, O. K. (2013). Are deep eutectic solvents benign or toxic? *Chemosphere*, *90*(7), 2193–2195. <https://doi.org/10.1016/j.chemosphere.2012.11.004>
- Hayyan, M., Looi, C. Y., Hayyan, A., Wong, W. F., & Hashim, M. A. (2015). In vitro and in vivo toxicity profiling of ammonium-based deep eutectic solvents. *PLoS ONE*, *10*(2). <https://doi.org/10.1371/journal.pone.0117934>
- Hayyan, M., Mbous, Y. P., Looi, C. Y., Wong, W. F., Hayyan, A., Salleh, Z., & Mohd-Ali, O. (2016). Natural deep eutectic solvents: Cytotoxic profile. *SpringerPlus*, *5*(1), 913. <https://doi.org/10.1186/s40064-016-2575-9>
- Hazra, P., Chakrabarty, D., Chakraborty, A., & Sarkar, N. (2004). Intramolecular charge transfer and solvation dynamics of Nile Red in the nanocavity of cyclodextrins. *Chemical Physics Letters*, *388*(1), 150–157. <https://doi.org/10.1016/j.cplett.2004.02.078>
- Hossain, S. S., & Samanta, A. (2018). How do the hydrocarbon chain length and hydroxyl group position influence the solute dynamics in alcohol-based deep eutectic solvents? *Physical Chemistry Chemical Physics*, *20*(38), 24613–24622. <https://doi.org/10.1039/C8CP04859B>
- Huang, J., Guo, X., Xu, T., Fan, L., Zhou, X., & Wu, S. (2019). Ionic deep eutectic solvents for the extraction and separation of natural products. *Journal of Chromatography A*, *1598*, 1–19. <https://doi.org/10.1016/j.chroma.2019.03.046>
- Huang, Y., Feng, F., Jiang, J., Qiao, Y., Wu, T., Voglmeir, J., & Chen, Z.-G. (2017). Green and efficient extraction of rutin from tartary buckwheat hull by using natural deep eutectic solvents. *Food Chemistry*, *221*, 1400–1405. <https://doi.org/10.1016/j.foodchem.2016.11.013>
- Ibrahim, R. K., Hayyan, M., AlSaadi, M. A., Ibrahim, S., Hayyan, A., & Hashim, M. A. (2019). Physical properties of ethylene glycol-based deep eutectic solvents. *Journal of Molecular Liquids*, *276*, 794–800. <https://doi.org/10.1016/j.molliq.2018.12.032>
- Immordino, M. L., Dosio, F., & Cattell, L. (2006). Stealth liposomes: Review of the basic science, rationale, and clinical applications, existing and potential. *International Journal of Nanomedicine*, *1*(3), 297–315.
- Jani, A., Sohier, T., & Morineau, D. (2020). Phase behavior of aqueous solutions of ethaline deep eutectic solvent. *Journal of Molecular Liquids*, *304*, 112701. <https://doi.org/10.1016/j.molliq.2020.112701>
- Jérôme, F., Ferreira, M., Bricout, H., Menuel, S., Monflier, E., & Tilloy, S. (2014). Low melting mixtures based on  $\beta$ -cyclodextrin derivatives and N,N'-dimethylurea as solvents for sustainable catalytic processes. *Green Chemistry*, *16*(8), 3876–3880. <https://doi.org/10.1039/C4GC00591K>
- Juhlin, L., Evers, H., & Broberg, F. (1980). A lidocaine-prilocaine cream for superficial skin surgery and painful lesions. *Acta Dermato-Venereologica*, *60*(6), 544–546. <https://doi.org/10.2340/0001555560544546>
- Juneidi, I., Hayyan, M., & Hashim, M. A. (2015). Evaluation of toxicity and biodegradability for cholinium-based deep eutectic solvents. *RSC Advances*, *5*(102), 83636–83647. <https://doi.org/10.1039/C5RA12425E>
- Juneidi, I., Hayyan, M., & Mohd Ali, O. (2016). Toxicity profile of choline chloride-based deep eutectic solvents for fungi and *Cyprinus carpio* fish. *Environmental Science and Pollution Research International*, *23*(8), 7648–7659. <https://doi.org/10.1007/s11356-015-6003-4>
- Kamatou, G. P. P., Vermaak, I., Viljoen, A. M., & Lawrence, B. M. (2013). Menthol: A simple monoterpene with remarkable biological properties. *Phytochemistry*, *96*, 15–25. <https://doi.org/10.1016/j.phytochem.2013.08.005>

- Kamlet, M. J., Abboud, J. L., & Taft, R. W. (1977). The solvatochromic comparison method. 6. The .pi.\* scale of solvent polarities. *Journal of the American Chemical Society*, *99*(18), 6027–6038. <https://doi.org/10.1021/ja00460a031>
- Kamlet, M. J., & Taft, R. W. (1976). The solvatochromic comparison method. I. The .beta.-scale of solvent hydrogen-bond acceptor (HBA) basicities. *Journal of the American Chemical Society*, *98*(2), 377–383. <https://doi.org/10.1021/ja00418a009>
- Kareem, M. A., Mjalli, F. S., Hashim, M. A., & AlNashef, I. M. (2010). Phosphonium-based ionic liquids analogues and their physical properties. *Journal of Chemical & Engineering Data*, *55*(11), 4632–4637. <https://doi.org/10.1021/je100104v>
- Kaur, S., Gupta, A., & Kashyap, H. K. (2020). How hydration affects the microscopic structural morphology in a deep eutectic solvent. *The Journal of Physical Chemistry B*, *124*(11), 2230–2237. <https://doi.org/10.1021/acs.jpcc.9b11753>
- Kfoury, M., Auezova, L., Greige-Gerges, H., & Fourmentin, S. (2015). Promising applications of cyclodextrins in food: Improvement of essential oils retention, controlled release and antiradical activity. *Carbohydrate Polymers*, *131*, 264–272. <https://doi.org/10.1016/j.carbpol.2015.06.014>
- Kfoury, M., Auezova, L., Greige-Gerges, H., Ruellan, S., & Fourmentin, S. (2014). Cyclodextrin, an efficient tool for trans-anethole encapsulation: Chromatographic, spectroscopic, thermal and structural studies. *Food Chemistry*, *164*, 454–461. <https://doi.org/10.1016/j.foodchem.2014.05.052>
- Kfoury, M., Hădărugă, N. G., Hădărugă, D. I., & Fourmentin, S. (2016). 4—Cyclodextrins as encapsulation material for flavors and aroma. In A. M. Grumezescu (Ed.), *Encapsulations* (pp. 127–192). Academic Press. <https://doi.org/10.1016/B978-0-12-804307-3.00004-1>
- Khezeli, T., Daneshfar, A., & Sahraei, R. (2016). A green ultrasonic-assisted liquid–liquid microextraction based on deep eutectic solvent for the HPLC-UV determination of ferulic, caffeic and cinnamic acid from olive, almond, sesame and cinnamon oil. *Talanta*, *150*, 577–585. <https://doi.org/10.1016/j.talanta.2015.12.077>
- Kim, S. H., Park, S., Yu, H., Kim, J. H., Kim, H. J., Yang, Y.-H., Kim, Y. H., Kim, K. J., Kan, E., & Lee, S. H. (2016). Effect of deep eutectic solvent mixtures on lipase activity and stability. *Journal of Molecular Catalysis B: Enzymatic*, *128*, 65–72. <https://doi.org/10.1016/j.molcatb.2016.03.012>
- Kolb, B., & Ettre, L. S. (2006). *Static Headspace-Gas Chromatography: Theory and Practice*. John Wiley & Sons.
- Komal, Singh, G., Singh, G., & Kang, T. S. (2018). Aggregation behavior of sodium dioctyl sulfosuccinate in deep eutectic solvents and their mixtures with water: An account of solvent's polarity, cohesiveness, and solvent structure. *ACS Omega*, *3*(10), 13387–13398. <https://doi.org/10.1021/acsomega.8b01637>
- Křížek, T., Bursová, M., Horsley, R., Kuchař, M., Tůma, P., Čabala, R., & Hložek, T. (2018). Menthol-based hydrophobic deep eutectic solvents: Towards greener and efficient extraction of phytocannabinoids. *Journal of Cleaner Production*, *193*, 391–396. <https://doi.org/10.1016/j.jclepro.2018.05.080>
- Kumar Banjare, M., Behera, K., L. Satnami, M., Pandey, S., & K. Ghosh, K. (2018). Self-assembly of a short-chain ionic liquid within deep eutectic solvents. *RSC Advances*, *8*(15), 7969–7979. <https://doi.org/10.1039/C7RA13557B>
- Kumari, P., Shobhna, Kaur, S., & Kashyap, H. K. (2018). Influence of hydration on the structure of reline deep eutectic solvent: A molecular dynamics study. *ACS Omega*, *3*(11), 15246–15255. <https://doi.org/10.1021/acsomega.8b02447>
- Lapeña, D., Lomba, L., Artal, M., Lafuente, C., & Giner, B. (2019a). The NADES glyceline as a potential green solvent: A comprehensive study of its thermophysical properties and effect of water inclusion. *The Journal of Chemical Thermodynamics*, *128*, 164–172. <https://doi.org/10.1016/j.jct.2018.07.031>

- Lapeña, D., Lomba, L., Artal, M., Lafuente, C., & Giner, B. (2019b). Thermophysical characterization of the deep eutectic solvent choline chloride:ethylene glycol and one of its mixtures with water. *Fluid Phase Equilibria*, *492*, 1–9. <https://doi.org/10.1016/j.fluid.2019.03.018>
- LAVAUD, A., LAGUERRE, M., Birtic, S., TIXIER, A. S. F., Roller, M., Chemat, F., & Bily, A. C. (2020). *Solvant eutectique d'extraction, procede d'extraction par eutectigenese utilisant ledit solvant, et extrait issu dudit procede d'extraction* (Patent No. FR3034626B1). <https://patents.google.com/patent/FR3034626B1/en?q=FR3034626+english>
- Li, G., Jiang, Y., Liu, X., & Deng, D. (2016). New levulinic acid-based deep eutectic solvents: Synthesis and physicochemical property determination. *Journal of Molecular Liquids*, *222*, 201–207. <https://doi.org/10.1016/j.molliq.2016.07.039>
- Li, Q., Wang, J., Lei, N., Yan, M., Chen, X., & Yue, X. (2018). Phase behaviours of a cationic surfactant in deep eutectic solvents: From micelles to lyotropic liquid crystals. *Physical Chemistry Chemical Physics*, *20*(17), 12175–12181. <https://doi.org/10.1039/C8CP00001H>
- Li, X., Hou, M., Han, B., Wang, X., & Zou, L. (2008). Solubility of CO<sub>2</sub> in a choline chloride + urea eutectic mixture. *Journal of Chemical and Engineering Data*, *53*(2), 548–550. Scopus. <https://doi.org/10.1021/jc700638u>
- López-Salas, N., Vicent-Luna, J. M., Imberti, S., Posada, E., Roldán, M. J., Anta, J. A., Balestra, S. R. G., Madero Castro, R. M., Calero, S., Jiménez-Riobóo, R. J., Gutiérrez, M. C., Ferrer, M. L., & del Monte, F. (2019). Looking at the “water-in-deep-eutectic-solvent” system: A dilution range for high performance eutectics. *ACS Sustainable Chemistry & Engineering*, *7*(21), 17565–17573. <https://doi.org/10.1021/acssuschemeng.9b05096>
- Lu, C., Cao, J., Wang, N., & Su, E. (2016). Significantly improving the solubility of non-steroidal anti-inflammatory drugs in deep eutectic solvents for potential non-aqueous liquid administration. *Medicinal Chemistry Communications*, *7*(5), 955–959. <https://doi.org/10.1039/C5MD00551E>
- Macário, I. P. E., Jesus, F., Pereira, J. L., Ventura, S. P. M., Gonçalves, A. M. M., Coutinho, J. A. P., & Gonçalves, F. J. M. (2018). Unraveling the ecotoxicity of deep eutectic solvents using the mixture toxicity theory. *Chemosphere*, *212*, 890–897. <https://doi.org/10.1016/j.chemosphere.2018.08.153>
- Macário, I. P. E., Oliveira, H., Menezes, A. C., Ventura, S. P. M., Pereira, J. L., Gonçalves, A. M. M., Coutinho, J. a. P., & Gonçalves, F. J. M. (2019). Cytotoxicity profiling of deep eutectic solvents to human skin cells. *Scientific Reports*, *9*(1), 1–9. <https://doi.org/10.1038/s41598-019-39910-y>
- Macário, I. P. E., Ventura, S. P. M., Pereira, J. L., Gonçalves, A. M. M., Coutinho, J. A. P., & Gonçalves, F. J. M. (2018). The antagonist and synergist potential of cholinium-based deep eutectic solvents. *Ecotoxicology and Environmental Safety*, *165*, 597–602. <https://doi.org/10.1016/j.ecoenv.2018.09.027>
- Maherani, B., Arab-Tehrany, E., R. Mozafari, M., Gaiani, C., & Linder, M. (2011). Liposomes: A review of manufacturing techniques and targeting strategies. *Current Nanoscience*, *7*(3), 436–452. <https://doi.org/10.2174/157341311795542453>
- Mahto, A., Mondal, D., Poliseti, V., Bhatt, J., M. R, N., Prasad, K., & Nataraj, S. K. (2017). Sustainable water reclamation from different feed streams by forward osmosis process using deep eutectic solvents as reusable draw solution. *Industrial & Engineering Chemistry Research*, *56*(49), 14623–14632. <https://doi.org/10.1021/acs.iecr.7b03046>
- Mao, S., Li, K., Hou, Y., Liu, Y., Ji, S., Qin, H., & Lu, F. (2018). Synergistic effects of components in deep eutectic solvents relieve toxicity and improve the performance of steroid biotransformation catalyzed by *Arthrobacter simplex*. *Journal of Chemical Technology & Biotechnology*, *93*(9), 2729–2736. <https://doi.org/10.1002/jctb.5629>
- Martins, M. A. R., Crespo, E. A., Pontes, P. V. A., Silva, L. P., Bülow, M., Maximo, G. J., Batista, E. A. C., Held, C., Pinho, S. P., & Coutinho, J. A. P. (2018). Tunable hydrophobic eutectic solvents based

- on terpenes and monocarboxylic acids. *ACS Sustainable Chemistry & Engineering*, 6(7), 8836–8846. <https://doi.org/10.1021/acssuschemeng.8b01203>
- Martins, M. A. R., Pinho, S. P., & Coutinho, J. A. P. (2019). Insights into the nature of eutectic and deep eutectic mixtures. *Journal of Solution Chemistry*, 48(7), 962–982. <https://doi.org/10.1007/s10953-018-0793-1>
- Mbous, Y. P., Hayyan, M., Hayyan, A., Wong, W. F., Hashim, M. A., & Looi, C. Y. (2017). Applications of deep eutectic solvents in biotechnology and bioengineering—Promises and challenges. *Biotechnology Advances*, 35(2), 105–134. <https://doi.org/10.1016/j.biotechadv.2016.11.006>
- Mbous, Y. P., Hayyan, M., Wong, W. F., Looi, C. Y., & Hashim, M. A. (2017). Unraveling the cytotoxicity and metabolic pathways of binary natural deep eutectic solvent systems. *Scientific Reports*, 7(1), 1–14. <https://doi.org/10.1038/srep41257>
- McCune, J. A., Kunz, S., Olesińska, M., & Scherman, O. A. (2017). DESolution of CD and CB Macrocycles. *Chemistry – A European Journal*, 23(36), 8601–8604. <https://doi.org/10.1002/chem.201701275>
- Meng, X., Ballerat-Busserolles, K., Husson, P., & Andanson, J.-M. (2016). Impact of water on the melting temperature of urea + choline chloride deep eutectic solvent. *New Journal of Chemistry*, 40(5), 4492–4499. <https://doi.org/10.1039/C5NJ02677F>
- Mitar, A., Panić, M., Prlić Kardum, J., Halambek, J., Sander, A., Zagajski Kučan, K., Radojčić Redovniković, I., & Radošević, K. (2019). Physicochemical properties, cytotoxicity, and antioxidative activity of natural deep eutectic solvents containing organic acid. *Chemical and Biochemical Engineering Quarterly*, 33(1), 1–18. <https://doi.org/10.15255/CABEQ.2018.1454>
- Mjalli, F. S. (2016). Mass connectivity index-based density prediction of deep eutectic solvents. *Fluid Phase Equilibria*, 409, 312–317. <https://doi.org/10.1016/j.fluid.2015.09.053>
- Mjalli, F. S., Shahbaz, K., & AlNashef, I. M. (2015). Modified Rackett equation for modelling the molar volume of deep eutectic solvents. *Thermochimica Acta*, 614, 185–190. <https://doi.org/10.1016/j.tca.2015.06.026>
- Mohan, M., Naik, P. K., Banerjee, T., Goud, V. V., & Paul, S. (2017). Solubility of glucose in tetrabutylammonium bromide based deep eutectic solvents: Experimental and molecular dynamic simulations. *Fluid Phase Equilibria*, 448, 168–177. <https://doi.org/10.1016/j.fluid.2017.05.024>
- Mokhtarpour, M., Shekaari, H., Martinez, F., & Zafarani-Moattar, M. T. (2019). Effect of tetrabutylammonium bromide-based deep eutectic solvents on the aqueous solubility of indomethacin at various temperatures: Measurement, modeling, and prediction with three-dimensional hansen solubility parameters. *AAPS PharmSciTech*, 20(5), 204. <https://doi.org/10.1208/s12249-019-1373-4>
- Mondal, D., Mahto, A., Veerababu, P., Bhatt, J., Prasad, K., & Nataraj, S. K. (2015). Deep eutectic solvents as a new class of draw agent to enrich low abundance DNA and proteins using forward osmosis. *RSC Advances*, 5(109), 89539–89544. <https://doi.org/10.1039/C5RA20735E>
- Morrison, H. G., Sun, C. C., & Neervannan, S. (2009). Characterization of thermal behavior of deep eutectic solvents and their potential as drug solubilization vehicles. *International Journal of Pharmaceutics*, 378(1), 136–139. <https://doi.org/10.1016/j.ijpharm.2009.05.039>
- Moufawad, T., Moura, L., Ferreira, M., Bricout, H., Tilloy, S., Monflier, E., Costa Gomes, M., Landy, D., & Fourmentin, S. (2019). First evidence of cyclodextrin inclusion complexes in a deep eutectic solvent. *ACS Sustainable Chemistry & Engineering*, 7(6), 6345–6351. <https://doi.org/10.1021/acssuschemeng.9b00044>
- Mu, Y., Wu, X., Huang, Y.-P., & Liu, Z.-S. (2019). Investigation of deep eutectic solvents as additives to  $\beta$ -CD for enantiomeric separations of Zopiclone, Salbutamol, and Amlodipine by CE. *Electrophoresis*, 40(15), 1992–1995. <https://doi.org/10.1002/elps.201900067>
- Mulia, K., Fauzia, F., & Krisanti, E. A. (2019). Polyalcohols as hydrogen-bonding donors in choline chloride-based deep eutectic solvents for extraction of xanthenes from the pericarp of *Garcinia mangostana* L. *Molecules*, 24(3), 636. <https://doi.org/10.3390/molecules24030636>

- Nunes, R. J., Saramago, B., & Marrucho, I. M. (2019). Surface tension of dl-menthol:octanoic acid eutectic mixtures. *Journal of Chemical & Engineering Data*, 64(11), 4915–4923. <https://doi.org/10.1021/acs.jced.9b00424>
- OECD. (1992). OECD Guideline for testing of chemicals. *Organisation for Economic Co-Operation and Development, Paris*, 71.
- Osch, D. J. G. P. van, Zubeir, L. F., Bruinhorst, A. van den, Rocha, M. A. A., & Kroon, M. C. (2015). Hydrophobic deep eutectic solvents as water-immiscible extractants. *Green Chemistry*, 17(9), 4518–4521. <https://doi.org/10.1039/C5GC01451D>
- Paiva, A., Craveiro, R., Aroso, I., Martins, M., Reis, R. L., & Duarte, A. R. C. (2014). Natural deep eutectic solvents – solvents for the 21st century. *ACS Sustainable Chemistry & Engineering*, 2(5), 1063–1071. <https://doi.org/10.1021/sc500096j>
- Pal, M., Rai, R., Yadav, A., Khanna, R., Baker, G. A., & Pandey, S. (2014). Self-aggregation of sodium dodecyl sulfate within (choline chloride + urea) deep eutectic solvent. *Langmuir*, 30(44), 13191–13198. <https://doi.org/10.1021/la5035678>
- Pal, M., Singh, R. K., & Pandey, S. (2015). Evidence of self-aggregation of cationic surfactants in a choline chloride+glycerol deep eutectic solvent. *ChemPhysChem*, 16(12), 2538–2542. <https://doi.org/10.1002/cphc.201500357>
- Panda, S., Kundu, K., Kiefer, J., Umapathy, S., & Gardas, R. L. (2019). Molecular-level insights into the microstructure of a hydrated and nanoconfined deep eutectic solvent. *The Journal of Physical Chemistry B*, 123(15), 3359–3371. <https://doi.org/10.1021/acs.jpcc.9b01603>
- Pandey, A., & Pandey, S. (2014). Solvatochromic probe behavior within choline chloride-based deep eutectic solvents: Effect of temperature and water. *The Journal of Physical Chemistry B*, 118(50), 14652–14661. <https://doi.org/10.1021/jp510420h>
- Pandey, A., Rai, R., Pal, M., & Pandey, S. (2013). How polar are choline chloride-based deep eutectic solvents? *Physical Chemistry Chemical Physics*, 16(4), 1559–1568. <https://doi.org/10.1039/C3CP53456A>
- Pätzold, M., Siebenhaller, S., Kara, S., Liese, A., Syltatk, C., & Holtmann, D. (2019). Deep eutectic solvents as efficient solvents in biocatalysis. *Trends in Biotechnology*, 37(9), 943–959. <https://doi.org/10.1016/j.tibtech.2019.03.007>
- Pedro, S. N., Freire, M. G., Freire, C. S. R., & Silvestre, A. J. D. (2019). Deep eutectic solvents comprising active pharmaceutical ingredients in the development of drug delivery systems. *Expert Opinion on Drug Delivery*, 16(5), 497–506. <https://doi.org/10.1080/17425247.2019.1604680>
- Posada, E., López-Salas, N., Riobóo, R. J. J., Ferrer, M. L., Gutiérrez, M. C., & Monte, F. del. (2017). Reline aqueous solutions behaving as liquid mixtures of H-bonded co-solvents: Microphase segregation and formation of co-continuous structures as indicated by Brillouin and <sup>1</sup>H NMR spectroscopies. *Physical Chemistry Chemical Physics*, 19(26), 17103–17110. <https://doi.org/10.1039/C7CP02180A>
- Posada, E., Roldán-Ruiz, M. J., Jiménez Riobóo, R. J., Gutiérrez, M. C., Ferrer, M. L., & del Monte, F. (2019). Nanophase separation in aqueous dilutions of a ternary DES as revealed by Brillouin and NMR spectroscopy. *Journal of Molecular Liquids*, 276, 196–203. <https://doi.org/10.1016/j.molliq.2018.11.139>
- Radošević, K., Čanak, I., Panić, M., Markov, K., Cvjetko Bubalo, M., Frece, J., Srček, V. G., & Redovniković, I. R. (2018). Antimicrobial, cytotoxic and antioxidative evaluation of natural deep eutectic solvents. *Environmental Science and Pollution Research*, 25(14), 14188–14196. <https://doi.org/10.1007/s11356-018-1669-z>
- Radošević, K., Čurko, N., Gaurina Srček, V., Cvjetko Bubalo, M., Tomašević, M., Kovačević Ganić, K., & Radojčić Redovniković, I. (2016). Natural deep eutectic solvents as beneficial extractants for

- enhancement of plant extracts bioactivity. *LWT - Food Science and Technology*, *73*, 45–51. <https://doi.org/10.1016/j.lwt.2016.05.037>
- Radošević, K., Cvjetko Bubalo, M., Srček, V. G., Grgas, D., Dragičević, T. L., & Redovniković, I. R. (2015). Evaluation of toxicity and biodegradability of choline chloride based deep eutectic solvents. *Ecotoxicology and Environmental Safety*, *112*, 46–53. <https://doi.org/10.1016/j.ecoenv.2014.09.034>
- Radošević, K., Železnjak, J., Cvjetko Bubalo, M., Radojčić Redovniković, I., Slivac, I., & Gaurina Srček, V. (2016). Comparative in vitro study of cholinium-based ionic liquids and deep eutectic solvents toward fish cell line. *Ecotoxicology and Environmental Safety*, *131*, 30–36. <https://doi.org/10.1016/j.ecoenv.2016.05.005>
- Reichardt, C. (1994). Solvatochromic dyes as solvent polarity indicators. *Chemical Reviews*, *94*(8), 2319–2358. <https://doi.org/10.1021/cr00032a005>
- Ribeiro, B. D., Florindo, C., Iff, L. C., Coelho, M. A. Z., & Marrucho, I. M. (2015). Menthol-based eutectic mixtures: Hydrophobic low viscosity solvents. *ACS Sustainable Chemistry & Engineering*, *3*(10), 2469–2477. <https://doi.org/10.1021/acssuschemeng.5b00532>
- R. McCluskey, A., Sanchez-Fernandez, A., J. Edler, K., C. Parker, S., J. Jackson, A., A. Campbell, R., & Arnold, T. (2019). Bayesian determination of the effect of a deep eutectic solvent on the structure of lipid monolayers. *Physical Chemistry Chemical Physics*, *21*(11), 6133–6141. <https://doi.org/10.1039/C9CP00203K>
- Rodriguez Rodriguez, N., van den Bruinhorst, A., Kollau, L. J. B. M., Kroon, M. C., & Binnemans, K. (2019). Degradation of deep-eutectic solvents based on choline chloride and carboxylic acids. *ACS Sustainable Chemistry & Engineering*, *7*(13), 11521–11528. <https://doi.org/10.1021/acssuschemeng.9b01378>
- Roldán-Ruiz, M. J., Jiménez-Riobóo, R. J., Gutiérrez, M. C., Ferrer, M. L., & del Monte, F. (2019). Brillouin and NMR spectroscopic studies of aqueous dilutions of malicine: Determining the dilution range for transition from a “water-in-DES” system to a “DES-in-water” one. *Journal of Molecular Liquids*, *284*, 175–181. <https://doi.org/10.1016/j.molliq.2019.03.133>
- Rublova, Y., Kityk, A., Danilov, F., & Protsenko, V. (2020). Mechanistic study on surface tension of binary and ternary mixtures containing choline chloride, ethylene glycol and water (components of aqueous solutions of a deep eutectic solvent, ethaline). *Zeitschrift Für Physikalische Chemie*, *234*(3), 399–413. <https://doi.org/10.1515/zpch-2019-1492>
- Sakuragi, M., Tsutsumi, S., & Kusakabe, K. (2018). Deep eutectic solvent-induced structural transition of microemulsions explored with small-angle X-ray scattering. *Langmuir*, *34*(42), 12635–12641. <https://doi.org/10.1021/acs.langmuir.8b02565>
- Sanchez-Fernandez, A., Arnold, T., J. Jackson, A., L. Fussell, S., K. Heenan, R., A. Campbell, R., & J. Edler, K. (2016). Micellization of alkyltrimethylammonium bromide surfactants in choline chloride:glycerol deep eutectic solvent. *Physical Chemistry Chemical Physics*, *18*(48), 33240–33249. <https://doi.org/10.1039/C6CP06053F>
- Sanchez-Fernandez, A., Hammond, O. S., Jackson, A. J., Arnold, T., Douth, J., & Edler, K. J. (2017). Surfactant–solvent interaction effects on the micellization of cationic surfactants in a carboxylic acid-based deep eutectic solvent. *Langmuir*, *33*(50), 14304–14314. <https://doi.org/10.1021/acs.langmuir.7b03254>
- Sanchez-Fernandez, A., J. Edler, K., Arnold, T., K. Heenan, R., Porcar, L., J. Terrill, N., E. Terry, A., & J. Jackson, A. (2016). Micelle structure in a deep eutectic solvent: A small-angle scattering study. *Physical Chemistry Chemical Physics*, *18*(20), 14063–14073. <https://doi.org/10.1039/C6CP01757F>
- Sanchez-Fernandez, A., L. Moody, G., C. Murfin, L., Arnold, T., J. Jackson, A., M. King, S., E. Lewis, S., & J. Edler, K. (2018). Self-assembly and surface behaviour of pure and mixed zwitterionic

- amphiphiles in a deep eutectic solvent. *Soft Matter*, 14(26), 5525–5536. <https://doi.org/10.1039/C8SM00755A>
- Sanchez-Fernandez, A., S. Hammond, O., J. Edler, K., Arnold, T., Douth, J., M. Dalgliesh, R., Li, P., Ma, K., & J. Jackson, A. (2018). Counterion binding alters surfactant self-assembly in deep eutectic solvents. *Physical Chemistry Chemical Physics*, 20(20), 13952–13961. <https://doi.org/10.1039/C8CP01008K>
- Santana, A. P. R., Mora-Vargas, J. A., Guimarães, T. G. S., Amaral, C. D. B., Oliveira, A., & Gonzalez, M. H. (2019). Sustainable synthesis of natural deep eutectic solvents (NADES) by different methods. *Journal of Molecular Liquids*, 293, 111452. <https://doi.org/10.1016/j.molliq.2019.111452>
- Savi, L. K., Carpiné, D., Waszczynskyj, N., Ribani, R. H., & Haminiuk, C. W. I. (2019). Influence of temperature, water content and type of organic acid on the formation, stability and properties of functional natural deep eutectic solvents. *Fluid Phase Equilibria*, 488, 40–47. <https://doi.org/10.1016/j.fluid.2019.01.025>
- Savi, L. K., Dias, M. C. G. C., Carpine, D., Waszczynskyj, N., Ribani, R. H., & Haminiuk, C. W. I. (2019). Natural deep eutectic solvents (NADES) based on citric acid and sucrose as a potential green technology: A comprehensive study of water inclusion and its effect on thermal, physical and rheological properties. *International Journal of Food Science & Technology*, 54(3), 898–907. <https://doi.org/10.1111/ijfs.14013>
- Scientific Opinion on safety and efficacy of choline chloride as a feed additive for all animal species. (2011). *EFSA Journal*, 9(9), 2353. <https://doi.org/10.2903/j.efsa.2011.2353>
- Sekiguchi, K., & Obi, N. (1961). Studies on absorption of eutectic mixture. I. A comparison of the behavior of eutectic mixture of sulfathiazole and that of ordinary sulfathiazole in man. *Chemical & Pharmaceutical Bulletin*, 9(11), 866–872. <https://doi.org/10.1248/cpb.9.866>
- Shah, D., & Mjalli, F. S. (2014). Effect of water on the thermo-physical properties of Reline: An experimental and molecular simulation based approach. *Physical Chemistry Chemical Physics*, 16(43), 23900–23907. <https://doi.org/10.1039/C4CP02600D>
- Shahbaz, K., Bagh, F. S. G., Mjalli, F. S., AlNashef, I. M., & Hashim, M. A. (2013). Prediction of refractive index and density of deep eutectic solvents using atomic contributions. *Fluid Phase Equilibria*, 354, 304–311. <https://doi.org/10.1016/j.fluid.2013.06.050>
- Shahbaz, K., Baroutian, S., Mjalli, F. S., Hashim, M. A., & AlNashef, I. M. (2012). Densities of ammonium and phosphonium based deep eutectic solvents: Prediction using artificial intelligence and group contribution techniques. *Thermochimica Acta*, 527, 59–66. <https://doi.org/10.1016/j.tca.2011.10.010>
- Shahbaz, K., Mjalli, F. S., Hashim, M. A., & AlNashef, I. M. (2011a). Prediction of deep eutectic solvents densities at different temperatures. *Thermochimica Acta*, 515(1), 67–72. <https://doi.org/10.1016/j.tca.2010.12.022>
- Shahbaz, K., Mjalli, F. S., Hashim, M. A., & AlNashef, I. M. (2011b). Using deep eutectic solvents based on methyl triphenyl phosphonium bromide for the removal of glycerol from palm-oil-based biodiesel. *Energy & Fuels*, 25(6), 2671–2678. <https://doi.org/10.1021/ef2004943>
- Shahbaz, K., Mjalli, F. S., Hashim, M. A., & AlNashef, I. M. (2012). Prediction of the surface tension of deep eutectic solvents. *Fluid Phase Equilibria*, 319, 48–54. <https://doi.org/10.1016/j.fluid.2012.01.025>
- Silva, J. M., Pereira, C. V., Mano, F., Silva, E., Castro, V. I. B., Sá-Nogueira, I., Reis, R. L., Paiva, A., Matias, A. A., & Duarte, A. R. C. (2019). Therapeutic role of deep eutectic solvents based on menthol and saturated fatty acids on wound healing. *ACS Applied Bio Materials*, 2(10), 4346–4355. <https://doi.org/10.1021/acsabm.9b00598>
- Silva, L. P., Fernandez, L., Conceição, J. H. F., Martins, M. A. R., Sosa, A., Ortega, J., Pinho, S. P., & Coutinho, J. A. P. (2018). Design and characterization of sugar-based deep eutectic solvents using

- conductor-like screening model for real solvents. *ACS Sustainable Chemistry & Engineering*. <https://doi.org/10.1021/acssuschemeng.8b02042>
- Smith, E. L., Abbott, A. P., & Ryder, K. S. (2014). Deep eutectic solvents (DESs) and their applications. *Chemical Reviews*, *114*(21), 11060–11082. <https://doi.org/10.1021/cr300162p>
- Smith, P. J., Arroyo, C. B., Hernandez, F. L., & Goeltz, J. C. (2019). Ternary deep eutectic solvent behavior of water and urea–choline chloride mixtures. *The Journal of Physical Chemistry B*. <https://doi.org/10.1021/acs.jpcc.8b12322>
- Soares, B., Silvestre, A. J. D., Rodrigues Pinto, P. C., Freire, C. S. R., & Coutinho, J. A. P. (2019). Hydrotrophy and cosolvency in lignin solubilization with deep eutectic solvents. *ACS Sustainable Chemistry & Engineering*, *7*(14), 12485–12493. <https://doi.org/10.1021/acssuschemeng.9b02109>
- Szente, L., & Fenyvesi, É. (2016). Cyclodextrin-lipid complexes: Cavity size matters. *Structural Chemistry*, *2*(28), 479–492. <https://doi.org/10.1007/s11224-016-0884-9>
- Tabary, N., Mahieu, A., Willart, J.-F., Dudognon, E., Danède, F., Descamps, M., Bacquet, M., & Martel, B. (2011). Characterization of the hidden glass transition of amorphous cyclomaltoheptaose. *Carbohydrate Research*, *346*(14), 2193–2199. <https://doi.org/10.1016/j.carres.2011.07.010>
- Tan, X., Zhang, J., Luo, T., Sang, X., Liu, C., Zhang, B., Peng, L., Li, W., & Han, B. (2016). Micellization of long-chain ionic liquids in deep eutectic solvents. *Soft Matter*, *12*(24), 5297–5303. <https://doi.org/10.1039/C6SM00924G>
- Tang, B., Bi, W., Zhang, H., & Row, K. H. (2014). Deep eutectic solvent-based HS-SME coupled with GC for the analysis of bioactive terpenoids in *Chamaecyparis obtusa* leaves. *Chromatographia*, *77*(3–4), 373–377. <https://doi.org/10.1007/s10337-013-2607-3>
- Tang, B., & Row, K. H. (2013). Recent developments in deep eutectic solvents in chemical sciences. *Monatshefte Für Chemie - Chemical Monthly*, *144*(10), 1427–1454. <https://doi.org/10.1007/s00706-013-1050-3>
- Teles, A. R. R., Capela, E. V., Carmo, R. S., Coutinho, J. A. P., Silvestre, A. J. D., & Freire, M. G. (2017). Solvatochromic parameters of deep eutectic solvents formed by ammonium-based salts and carboxylic acids. *Fluid Phase Equilibria*, *448*, 15–21. <https://doi.org/10.1016/j.fluid.2017.04.020>
- Torregrosa-Crespo, J., Marset, X., Guillena, G., Ramón, D. J., & María Martínez-Espinosa, R. (2020). New guidelines for testing “Deep eutectic solvents” toxicity and their effects on the environment and living beings. *Science of The Total Environment*, *704*, 135382. <https://doi.org/10.1016/j.scitotenv.2019.135382>
- Triolo, A., Lo Celso, F., & Russina, O. (2020). Structural features of  $\beta$ -cyclodextrin solvation in the deep eutectic solvent, *reline*. *The Journal of Physical Chemistry B*, *124*(13), 2652–2660. <https://doi.org/10.1021/acs.jpcc.0c00876>
- Valvi, A., Dutta, J., & Tiwari, S. (2017). Temperature-dependent empirical parameters for polarity in choline chloride based deep eutectic solvents. *The Journal of Physical Chemistry B*, *121*(50), 11356–11366. <https://doi.org/10.1021/acs.jpcc.7b07754>
- Vert, M., Doi, Y., Hellwich, K.-H., Hess, M., Hodge, P., Kubisa, P., Rinaudo, M., & Schué, F. (2012). Terminology for biorelated polymers and applications (IUPAC Recommendations 2012). *Pure and Applied Chemistry*, *84*(2), 377–410. <https://doi.org/10.1351/PAC-REC-10-12-04>
- Wang, R., Sun, D., Wang, C., Liu, L., Li, F., & Tan, Z. (2019). Biphasic recognition chiral extraction of threonine enantiomers in a two-phase system formed by hydrophobic and hydrophilic deep-eutectic solvents. *Separation and Purification Technology*, *215*, 102–107. <https://doi.org/10.1016/j.seppur.2019.01.022>
- Wen, Q., Chen, J.-X., Tang, Y.-L., Wang, J., & Yang, Z. (2015). Assessing the toxicity and biodegradability of deep eutectic solvents. *Chemosphere*, *132*, 63–69. <https://doi.org/10.1016/j.chemosphere.2015.02.061>

- Weng, L., & Toner, M. (2018). Janus-faced role of water in defining nanostructure of choline chloride/glycerol deep eutectic solvent. *Physical Chemistry Chemical Physics*, *20*(35), 22455–22462. <https://doi.org/10.1039/C8CP03882A>
- Wikene, K. O., Rukke, H. V., Bruzell, E., & Tønnesen, H. H. (2017). Investigation of the antimicrobial effect of natural deep eutectic solvents (NADES) as solvents in antimicrobial photodynamic therapy. *Journal of Photochemistry and Photobiology B: Biology*, *171*, 27–33. <https://doi.org/10.1016/j.jphotobiol.2017.04.030>
- Xiong, X., Yi, C., Liao, X., & Lai, S. (2019). An effective one-pot access to 2-amino-4H-benzo[b]pyrans and 1,4-dihydropyridines via  $\gamma$ -cyclodextrin-catalyzed multi-component tandem reactions in deep eutectic solvent. *Catalysis Letters*, *149*(6), 1690–1700. <https://doi.org/10.1007/s10562-019-02767-x>
- Xu, K., Wang, Y., Huang, Y., Li, N., & Wen, Q. (2015). A green deep eutectic solvent-based aqueous two-phase system for protein extracting. *Analytica Chimica Acta*, *864*, 9–20. <https://doi.org/10.1016/j.aca.2015.01.026>
- Yadav, A., & Pandey, S. (2014). Densities and viscosities of (choline chloride + urea) deep eutectic solvent and its aqueous mixtures in the temperature range 293.15 K to 363.15 K. *Journal of Chemical & Engineering Data*, *59*(7), 2221–2229. <https://doi.org/10.1021/je5001796>
- Yadav, A., Trivedi, S., Rai, R., & Pandey, S. (2014). Densities and dynamic viscosities of (choline chloride+glycerol) deep eutectic solvent and its aqueous mixtures in the temperature range (283.15–363.15)K. *Fluid Phase Equilibria*, *367*, 135–142. <https://doi.org/10.1016/j.fluid.2014.01.028>
- Yusof, R., Abdulmalek, E., Sirat, K., & Rahman, M. B. A. (2014). Tetrabutylammonium bromide (TBABr)-based deep eutectic solvents (DESs) and their physical properties. *Molecules*, *19*(6), 8011–8026. <https://doi.org/10.3390/molecules19068011>
- Zainal-Abidin, M. H., Hayyan, M., Hayyan, A., & Jayakumar, N. S. (2017). New horizons in the extraction of bioactive compounds using deep eutectic solvents: A review. *Analytica Chimica Acta*, *979*, 1–23. <https://doi.org/10.1016/j.aca.2017.05.012>
- Zhang, H., Lang, J., Lan, P., Yang, H., Lu, J., & Wang, Z. (2020). Study on the dissolution mechanism of cellulose by ChCl-based deep eutectic solvents. *Materials*, *13*(2), 278. <https://doi.org/10.3390/ma13020278>
- Zhang, Q., De Oliveira Vigier, K., Royer, S., & Jérôme, F. (2012). Deep eutectic solvents: Syntheses, properties and applications. *Chemical Society Reviews*, *41*(21), 7108–7146. <https://doi.org/10.1039/C2CS35178A>
- Zhao, B.-Y., Xu, P., Yang, F.-X., Wu, H., Zong, M.-H., & Lou, W.-Y. (2015). Biocompatible deep eutectic solvents based on choline chloride: Characterization and application to the extraction of rutin from *Sophora japonica*. *ACS Sustainable Chemistry & Engineering*, *3*(11), 2746–2755. <https://doi.org/10.1021/acssuschemeng.5b00619>
- Zhao, X., Liu, X., & Lu, M. (2014).  $\beta$ -cyclodextrin-capped palladium nanoparticle-catalyzed ligand-free Suzuki and Heck couplings in low-melting  $\beta$ -cyclodextrin/NMU mixtures. *Applied Organometallic Chemistry*, *28*(8), 635–640. <https://doi.org/10.1002/aoc.3173>
- Zhekenov, T., Toksanbayev, N., Kazakbayeva, Z., Shah, D., & Mjalli, F. S. (2017). Formation of type III deep eutectic solvents and effect of water on their intermolecular interactions. *Fluid Phase Equilibria*, *441*, 43–48. <https://doi.org/10.1016/j.fluid.2017.01.022>
- Zhu, P., Gu, Z., Hong, S., & Lian, H. (2017). One-pot production of chitin with high purity from lobster shells using choline chloride–malonic acid deep eutectic solvent. *Carbohydrate Polymers*, *177*, 217–223. <https://doi.org/10.1016/j.carbpol.2017.09.001>

# Appendices

## Appendix A: Density measurements

Table A1. Experimental values of the densities of the studied solvents at 40, 50, and 60°C

DES	$\rho$ (kg m <sup>-3</sup> )		
	40°C	50°C	60°C
ChCl:U	1187.6	1182.2	1177.0
ChCl:G	1181.9	1176.5	1171.1
ChCl:EG	1106.4	1100.9	1095.2
ChCl:Lev	1127.9	1121.4	1114.9
TBPBr:Lev	1098.3	1090.8	1083.3
TBABr:Dec	958.8	952.4	946.0
TBPBr:EG	1058.9	1052.4	1045.8
HPBCD:Lev	1196.7	1188.8	1180.8
RAMEB:Lev	1176.4	1168.2	1159.8
CRYSMEB:Lev	1199.4	1191.6	1183.6
Captisol:Lev	1226.3	1218.4	1210.4
HPBCD:G 1:30	1292.6	1286.2	1280.1
HPBCD:G 1:40	1284.1	1277.9	1271.8
HPBCD:EG 1:20	1238.4	1232.0	1225.4
HPBCD:EG 1:30	1209.1	1202.4	1195.6
HPBCD:EG 1:40	1190.4	1183.6	1176.7
HPBCD:1,3-PD 1:30	1153.6	1147.4	1141.1
HPBCD:1,3-PD 1:40	1132.8	1126.5	1120.2
HPBCD:1,3-BD 1:40	1080.1	1073.4	1066.6
RAMEB:1,3-PD 1:20	1153.6	1147.0	1140.3
RAMEB:1,3-PD 1:30	1128.4	1121.9	1115.3

Table A1. (continued)

DES	$\rho$ (kg m <sup>-3</sup> )		
	40°C	50°C	60°C
RAMEB:1,3-PD 1:40	1112.1	1105.6	1099.1
RAMEB:1,3-BD 1:30	1078.9	1071.9	1064.9
RAMEB:1,3-BD 1:40	1061.8	1054.8	1047.7

Table A2. Fitting parameters (a and b) and average absolute deviation (AAD) of the fitted density measurements of the studied systems at 30- 60 °C temperature range

DES	a (x 10 <sup>2</sup> )	b	AAD (%)
ChCl:U	13.6	-0.546	0.020
ChCl:G	13.5	-0.543	0.003
ChCl:EG	11.8	-0.554	0.010
ChCl:Lev	13.3	-0.651	0.010
TBPBr:Lev	13.3	-0.747	0.003
TBABr:Dec	11.6	-0.643	0.010
TBPBr:EG	12.6	-0.657	0.001
HPBCD:Lev	14.5	-0.797	0.002
RAMEB:Lev	14.3	-0.821	0.011
CRYSMEB:Lev	14.5	-0.796	0.008
Captisol:Lev	14.7	-0.794	0.003
HPBCD:G 1:30	14.9	- 0.630	0.010
HPBCD:G 1:40	14.8	- 0.621	0.006
HPBCD:EG 1:20	14.4	- 0.654	0.006

Table A2. (continued)

DES	a (x 10 <sup>2</sup> )	b	AAD (%)
HPBCD:EG 1:30	14.2	- 0.675	0.003
HPBCD:EG 1:40	14.0	- 0.677	0.005
HPBCD:1,3-PD 1:30	13.5	- 0.623	0.003
HPBCD:1,3-PD 1:40	13.3	- 0.624	0.005
HPBCD:1,3-BD 1:40	12.9	- 0.670	0.008
RAMEB:1,3-PD 1:20	13.6	- 0.660	0.004
RAMEB:1,3-PD 1:30	13.3	- 0.655	0.004
RAMEB:1,3-PD 1:40	13.2	- 0.652	0.003
RAMEB:1,3-BD 1:30	13.0	- 0.698	0.006
RAMEB:1,3-BD 1:40	12.8	- 0.699	0.006

## Appendix B: Viscosity measurements

Table B1. Vogel-Fulcher-Tammann equation parameters (A, K, and T<sub>0</sub>) and average absolute deviation (AAD) of the fitted viscosity measurements of the studied systems at 30- 60 °C temperature range

DES	A (mPa s K <sup>-1/2</sup> )	K (K)	T <sub>0</sub> (K)	AAD (%)
ChCl:U	2.65	796.5	211.66	0.03
ChCl:G	1.27	1127.1	166.26	0.09

Table B1. (continued)

DES	A (mPa s K <sup>-1/2</sup> )	K (K)	T <sub>0</sub> (K)	AAD (%)
ChCl:EG	4.26	649.6	171.21	0.15
ChCl:Lev	3.15	798.2	189.72	0.05
TBPBr:Lev	2.64	675.6	190.39	0.03
TBABr:Dec	0.84	1245.6	160.26	0.07
TBPBr:EG	1.30	997.8	158.28	0.19
HPBCD:Lev	1.15	997.3	193.68	0.16
RAMEB:Lev	1.21	936.6	186.49	0.05
CRYSMEB:Lev	0.66	1133.0	182.49	0.08
Captisol:Lev	2.13	971.6	198.46	0.05
HPBCD:G 1:30	0.09	2100.2	152.08	0.13
HPBCD:G 1:40	0.09	2022.0	150.76	0.22
HPBCD:EG 1:20	0.48	1574.5	165.71	0.29
HPBCD:EG 1:30	0.29	1579.2	149.48	0.26
HPBCD:EG 1:40	0.44	1367.0	150.12	0.31

Table B1. (continued)

<b>DES</b>	<b>A (mPa s K<sup>-1/2</sup>)</b>	<b>K (K)</b>	<b>T<sub>0</sub> (K)</b>	<b>AAD (%)</b>
HPBCD:1,3-PD 1:30	0.13	1957.6	130.98	0.17
HPBCD:1,3-PD 1:40	0.10	1988.0	119.28	0.07
HPBCD:1,3-BD 1:40	0.07	1881.5	144.13	0.14
RAMEB:1,3-PD 1:20	0.12	1847.3	144.93	0.12
RAMEB:1,3-PD 1:30	0.12	1829.9	129.60	0.23
RAMEB:1,3-PD 1:40	0.14	1752.5	124.48	0.20
RAMEB:1,3-BD 1:30	0.08	1718.3	150.21	0.14
RAMEB:1,3-BD 1:40	0.09	1689.0	146.29	0.08

## Appendix C: Time-dependent behavior of liposomes suspended in DES

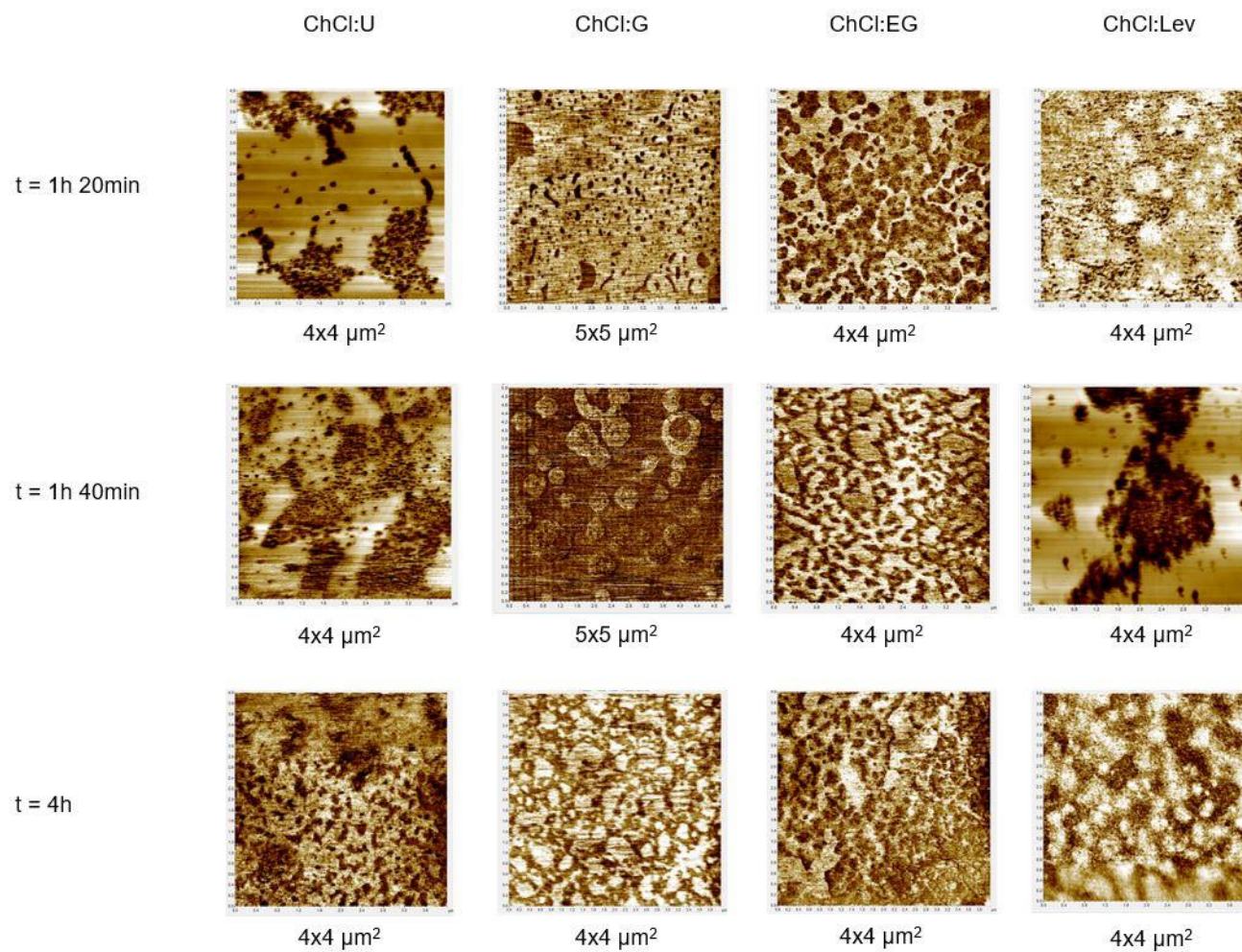
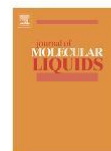


Figure C1. AFM 2D  $4 \times 4 \mu\text{m}^2$  and  $5 \times 5 \mu\text{m}^2$  images of EggPC liposomes suspended in ChCl:U, ChCl:G, ChCl:EG, and ChCl:Lev DES obtained in contact mode at different time points



## Review

## Deep eutectic solvents: An overview on their interactions with water and biochemical compounds

Tracy El Achkar<sup>a,b</sup>, Sophie Fourmentin<sup>b</sup>, H el ene Greige-Gerges<sup>a,\*</sup><sup>a</sup> Bioactive Molecules Research Laboratory, Faculty of Sciences, Lebanese University, Lebanon<sup>b</sup> Unit e de Chimie Environnementale et Interactions sur le Vivant (UCEIV, EA 4492), SFR Condorcet FR CNRS 3417, ULCO, F-59140 Dunkerque, France

## ARTICLE INFO

## Article history:

Received 5 January 2019

Received in revised form 7 May 2019

Accepted 21 May 2019

Available online 23 May 2019

## Keywords:

Biological macromolecules

Deep eutectic solvents

Hydrogen bonding

Solubilization

Water

## ABSTRACT

The search for green solvents that can replace harsh organic solvents and relatively toxic ionic liquids (ILs) has led to the discovery of deep eutectic solvents (DES). DES are now rapidly emerging in numerous applications owing to their green character, biodegradability, tuneability, low cost and simple preparation, compared to other solvents. The possibility that natural DES might play a role as an alternative media to water in living organisms pushed the researchers to investigate their use as solvents for the poorly water soluble macromolecules. However, the addition of water in most of their applications must be controlled to maintain DES' supramolecular structure and properties. This review presents the impact of water on DES, used as solvents for the biological macromolecules mainly phospholipids, proteins, nucleic acids and polysaccharides. The effect of water on the DES' supramolecular network and its physico-chemical properties is discussed and the applications of DES as solvents for the biological macromolecules, in the absence and presence of water, are highlighted.

  2019 Elsevier B.V. All rights reserved.

## Contents

1. Introduction . . . . .	2
2. Synthesis of DES . . . . .	2
3. DES interactions within biological systems . . . . .	3
4. Effect of water on DES. . . . .	3
4.1. DES supramolecular network . . . . .	3
4.2. Physico-chemical properties of DES . . . . .	5
4.2.1. Freezing point . . . . .	5
4.2.2. Viscosity . . . . .	5
4.2.3. Density . . . . .	5
4.2.4. Ionic conductivity . . . . .	5
5. DES applied to biological macromolecules. . . . .	5
5.1. DES - phospholipids . . . . .	6
5.2. DES - proteins . . . . .	7
5.3. DES - nucleic acids . . . . .	11
5.4. DES - polysaccharides . . . . .	11
6. Conclusions . . . . .	15

**Abbreviations:** A, acetamide; ATPS, aqueous two-phase system; Br, bromide; BSA, bovine serum albumin; CA, citric acid; CALB, *Candida Antarctica* lipase B; Ch, choline cation; ChAc, Choline acetate; ChCit, choline citrate; ChCl, choline chloride; cP, centipoise; DES, deep eutectic solvents; DMPC, 1,2-dimyristoyl-sn-glycero-3-phosphocholine; DNA, deoxyribonucleic acid; DPPC, 1,2-dipalmitoyl-sn-glycero-3-phosphocholine; DSPC, 1,2-distearoyl-sn-glycero-3-phosphocholine; EAC, ethylammonium chloride; EG, ethylene glycol; FTIR, Fourier-Transform Infrared spectroscopy; G, glycerol; GCH, glucose:choline chloride:water; HBA, hydrogen bond acceptor; HBD, hydrogen bond donor; HRP, horseradish peroxidase; ILs, ionic liquids; IM, Imidazole; K<sub>2</sub>HPO<sub>4</sub>, dipotassium phosphate; LGH, lactic acid:glucose:water; MA, malic acid; NADES, natural deep eutectic solvent; PC, phosphatidylcholine; PCH, 1,2-propanediol-choline chloride-water; PFG NMR, pulse field gradient nuclear magnetic resonance spectroscopy; POPC, 1-palmitoyl-2-oleoyl-sn-glycero-3-phosphocholine; RC, photosynthetic reaction centers; S, D-Sorbitol; SteH1, *Solanum tuberosum* epoxide hydrolase 1; TBA, tetrabutylammonium; TEM, transmission electron microscopy; TGA, thermogravimetric analysis; Tm, transition temperature; trp, tryptophan; TU, thiourea; U, urea; wt%, weight percent; XoCH, xylitol:xcholine chloride:water; XRD, X-ray diffraction.

\* Corresponding author at: Bioactive Molecules Research Group, Doctoral School of Sciences and Technologies, Faculty of Sciences, Lebanese University, B.P. 90656 Jdaidet el-Matt, Lebanon.

E-mail address: [hgreige@u.edu.lb](mailto:hgreige@u.edu.lb) (H. Greige-Gerges).

<https://doi.org/10.1016/j.molliq.2019.111028>

0167-7322/  2019 Elsevier B.V. All rights reserved.

Contributors . . . . .	15
Acknowledgements . . . . .	15
References . . . . .	15

## 1. Introduction

The search for green solvents is one of the top research activities in green chemistry [1]. Deep eutectic solvents (DES) have been recently described as potential alternative solvents for conventional organic solvents and ionic liquids (ILs) [2,3]. In fact, DES and ILs share many interesting properties such as low volatility, wide liquid range, high thermal stability and conductivity [4], but their difference lies in the chemical formation process and in the source of their starting materials. ILs are formed through ionic bonds between ionic components [5]. Some concerns are linked with the use of ILs like their synthesis and purification requirements, high cost and toxicity [6]. These limitations are somewhat overcome by DES, which are cheap and easy to prepare from numerous and widely available starting materials. First reported by Abbott et al. [2], DES can be defined as mixtures of two or three base components that are able of associating with each other through hydrogen bond interactions [7]. Thus, DES are obtained by mixing a hydrogen-bond acceptor (HBA) (such as a quaternary ammonium salt) and a hydrogen-bond donor (HBD) at an appropriate molar ratio. First introduced by Abbott and co-workers, choline chloride and urea are the most studied DES constituents, among others presented in Fig. 1.

When the compounds that constitute the DES are primary metabolites, namely, amino acids, organic acids, sugars, or choline derivatives, the DES are so called natural deep eutectic solvents (NADES) [3,8]. The term NADES was first introduced by Choi et al. [3]. In that study, they hypothesized that the metabolites, present in high concentrations in cells, may form a new liquid phase, along with water and lipids. NADES might be involved in the biosynthesis, storage and transport of various poorly water-soluble compounds, since NADES were proved

to solubilize some natural compounds and their constituents are ubiquitously found in cells. Furthermore, they showed that different combinations of these natural candidates form liquids [3]. From an environmental and economic perspective, NADES also offer many striking advantages including biodegradability, sustainability, low costs and simple preparation. All these properties make them of interest for applications in analytical chemistry [9] and health-related areas such as pharmaceuticals, foods, and cosmetics [10]. The development of NADES as well as their properties and applications were recently presented and discussed by Vanda et al. [11].

## 2. Synthesis of DES

As mentioned earlier, DES are obtained by combining two or more compounds, able of forming a eutectic mixture via hydrogen bonds, at an adequate molar ratio. Generally, two main methods are used to prepare the DES: the heating method and the grinding method. The heating method is the most commonly used; it consists on mixing and heating the compounds at approximately 100 °C under constant stirring until forming a homogeneous liquid. The grinding method is based on mixing the compounds at room temperature and grinding them in a mortar with a pestle, until a clear liquid is formed [4]. Furthermore, Gutierrez et al. [12] revealed a novel method for DES preparation, based on freeze-drying the aqueous solutions of DES' individual components. As a matter of fact, separated aqueous solutions of choline chloride and urea (or thiourea) were put together to form aqueous solutions of 1:2 choline chloride:urea (or choline chloride:thiourea), having 5 wt% solute contents. These solutions were frozen, freeze-dried and clear viscous liquids were obtained [12]. However, water was detected in the

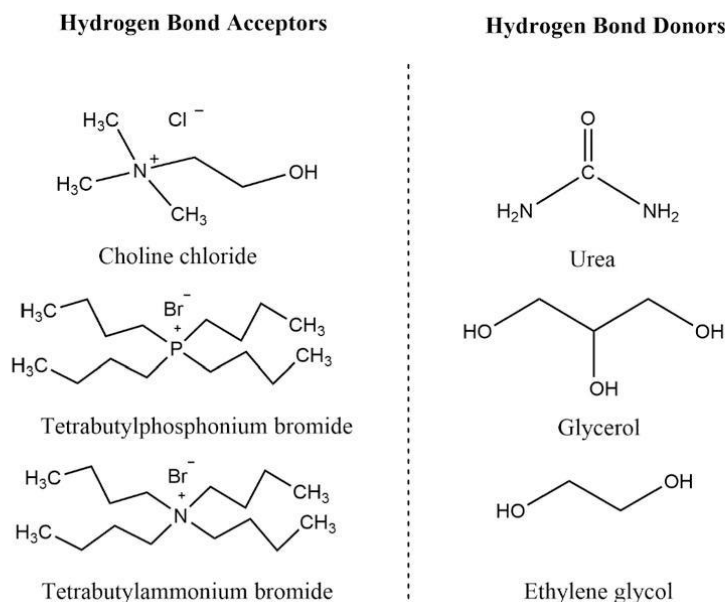


Fig. 1. Representative structures of the most common halide salts and hydrogen bond donors used for DES synthesis (2 column figure).

freeze-dried mixture since it tends to interact with DES' components and eventually be a part of the DES' network [3,8]. Being bound to DES' components, water cannot be removed in this case. Thus, different methods of preparation can lead to different DES.

### 3. DES interactions within biological systems

Biological systems are mainly composed of water and biological macromolecules. Proteins, carbohydrates, lipids and nucleic acids make up the majority of a cell's dry mass. Naturally found and self-organized in water, the structure, activity and stability of these biomolecules were examined in non-aqueous solvents, such as DES. The DES and NADES were applied in catalysis, organic synthesis, electrochemistry, solubilization and extraction of biomolecules. Most of NADES applications were dedicated to the extraction of biological compounds. The use of DES as extraction solvents was first proposed by Dai et al. [13]. Thereafter, the number of publications adopting these solvents for extraction purposes was exponentially growing. Fernandez et al. analyzed the contribution of NADES from a green perspective [14]. Also, a detailed overview of the extraction techniques using DES as extracting solvents was published by Cunha et al. [15]. DES can also be used as storage media for unstable compounds [16]. Recently, many reviews reported the use of DES as solubilizing and extraction solvents for organic molecules such as macromolecules, among others [5,6,11,17,18]. We assume that the water content should be considered in all the DES applications as the presence of water may affect the green solvent's network and properties. Subsequently, this will probably help in understanding the behavior of DES around biological structures and macromolecules, which originally exist in water.

This review is one of its kind, giving insights into the impact of water on DES, used as solvents for the solubilization of biological macromolecules. The studies investigating the effect of water on DES' supramolecular network and physicochemical properties are presented. Furthermore, the applications of DES as solvents for the biological macromolecules, namely proteins, polysaccharides, phospholipids and nucleic acids, together with the presence of water, are highlighted.

### 4. Effect of water on DES

Studying the effect of water on DES is of great importance, since the water uptake by the solvent is inevitable. Water represents one of the few natural substances that act both as a donor and acceptor of hydrogen bonding due to its high polarity. Thus, it probably exhibits strong interactions with hygroscopic DES constituents. In fact, it is possible to prepare DES with the hydrated forms of their constituents, such as hydrated salts or acids. But the hydrated forms do not necessarily form a DES in the same range of molar compositions as anhydrous salts or acids. When eutectic solvents are formed without hydrated constituents, it is possible to add water, which is assumed to form part of the solvent itself through stronger intermolecular bonds [19].

The water content can be determined by the Karl Fischer titration method which is based on a two-step chemical reaction between iodine and sulfur dioxide. Given that water and iodine are consumed in a 1:1 ratio, the amount of water can be determined in the sample [20]. Another parameter related to water content can also be established, which is the water activity, reflecting the amount of water in free and bonded forms in the solvent [8,10]. In addition, the presence of water involved in the hydrogen bonding can be revealed by nuclear magnetic resonance (NMR) spectroscopy [12] and by Fourier transform infrared spectroscopy [21].

#### 4.1. DES supramolecular network

Few studies, listed in chronological order in Table 1, have investigated aqueous DES solutions. Du et al. [22] tested the hygroscopicity of choline chloride:urea DES by measuring the water absorption as a

function of the exposure time to the open air. The water uptake increased at a rate of around 6.8 wt% per day before reaching a plateau of 40 wt% after 65 days exposure to air (Fig. 2A). However, water content can be easily eliminated by heating. Within 6 h at 80 °C, it dropped from 40 wt% to 6 wt% (Fig. 2B). In addition, Fourier-Transform Infrared (FTIR) spectra of choline chloride: urea DES and its individual components were analyzed before and after 6 wt% water absorption. It turned out that water will preferentially bind to urea molecules rather than choline chloride [22].

D'agostino et al. [24] studied the effect of water (2.5–20 wt%) on the molecular mobility of the three most common choline chloride -based DES: Reline, Ethaline and Glyceline (based on the most commonly used HBDs urea, ethylene glycol and glycerol), using pulsed field gradient nuclear magnetic resonance (PFG-NMR). In this technique, the diffusion of a certain species is followed by measuring the signal attenuation of the NMR resonances. In the absence of any interactions with other species, both aliphatic and hydroxyl <sup>1</sup>H resonances of the same molecule present similar diffusion coefficients. On the other hand, a great difference in the diffusion coefficient values is observed in case of important interaction or exchange between hydroxyl protons of different molecules. In Ethaline, the diffusivity values of Ch and ethylene glycol increase when adding water, with values approaching those measured for water. In addition, a strong difference was observed between the diffusivity of the hydroxyl group and the aliphatic group of each molecule with increasing water content, suggesting an interaction between hydroxyl protons of the different molecules. However, a very slight difference was obtained between diffusivity values of Glyceline and these diffusivities were much slower than water, suggesting a strong correlated motion between Ch and glycerol rather than an interaction with water. On the other hand, when adding water to Reline, the diffusivity of the hydroxyl group of Ch starts deviating from the diffusivity of the rest of the molecule and approaching from the value of water. This could be explained by a strong interaction between Ch protons and water protons [24].

Dai et al. [10] also studied the effect of water dilution on the structure and physicochemical properties of different NADES. The eutectic mixture 1,2-propanediol-choline chloride-water (1:1:1) was diluted with deuterium oxide and the diluted NADES was investigated by NMR at 40 °C. The results showed that the structure of NADES was maintained only when the water content was below 50% (v/v). Further dilution produces a solution of the free forms of the individual components in water [10].

As a matter of fact, a mechanism for the transition from hydrated DES to a DES aqueous solution was recently proposed by Hammond et al. [26]. Choline chloride:urea: water mixtures were prepared in different molar ratios (1:2:1, 1:2:2, 1:2:5, 1:2:10, 1:2:15, 1:2:20) to analyze the effect of water on the nanostructure of choline chloride:urea; using neutral total scattering and empirical potential structure refinement. It has been demonstrated that at low water levels ( $\leq 1$  mol fraction), water slightly strengthens the hydrogen bonds between choline and urea. Between 2 and 10 water mole fractions, the DES system resists to hydration by retaining its initial structure. At 15 mol fraction (83 mol % or 51 wt% of water), the DES structural motifs disappeared and the system is described as an aqueous solution of the DES components [26]. A similar limit of water addition was reported by Gutiérrez et al. [12]. The halide anion-hydrogen bond donor supramolecular complexes of ChCl:U and ChCl:TU were preserved at 83 wt% solute content, but were disrupted at a dilution equal or below 43 wt% solute content [12].

On the other hand, molecular dynamics simulations were performed by Shah et al. [23] to investigate the effect of water (0–90 wt%) on the hydrogen bonding pattern of reline. Pure reline and different concentrations of reline aqueous mixtures were tested. Results showed a decrease in the number of hydrogen bonds between urea molecules and between urea and the anion, when adding water. This is clearly due to the fact that the anion will preferentially bind to water rather than urea.

**Table 1**  
Summary of the studies investigating the effect of water addition on Deep Eutectic Solvents.

DES	Water content	Parameters or technique (s)	Comments	Ref
ChCl: U ChCl: TU TU 1:2 ChCl: U 1:2	D <sub>2</sub> O dilutions of ChCl:U and ChCl:TU (5, 10, 43 and 86 wt% solute content)	Characterization of the diluted DES solutions by <sup>1</sup> H NMR	The halide anion-hydrogen bond donor supramolecular complex was preserved at 83 wt% solute content, but was disrupted at a dilution equal or below 43 wt% solute content.	[12]
ChCl: U 1:2	0–90 wt%	Molecular dynamics simulations on different concentrations of reline aqueous mixtures	Results showed a decrease in the number of hydrogen bonds between urea molecules and between urea and the anion, when adding water. This is clearly due to the fact that the anion will preferentially bind to water rather than urea. Moreover, the presence of water strongly increased the diffusion of reline ions. All these changes were remarkable beyond 25–30 wt% of water.	[23]
PCH 1:1:1	0–100% (v/v)	Investigation of the effect of water on PCH structure by NMR at 40 °C, after PCH dilution with deuterium oxide	The structure of NADES was maintained only when the water content was below 50% (v/v). Further dilution produces a solution of the free forms of the individual components in water.	[10]
ChCl: U ChCl: EG ChCl: G 1:2 ChCl: U 1:2	2.5–20 wt%	Measurement of diffusion coefficients of the aliphatic and hydroxyl protons of DES components by Pulsed Field Gradient NMR	In both ChCl:U and ChCl:EG, a difference between the diffusion coefficients of the aliphatic and hydroxyl groups of choline or the HBD (in the case of EG) was observed when adding water, suggesting an interaction with water. This was not the case for ChCl:G.	[24]
ChCl: U 1:2	0.25 wt%	Water absorption as a function of the exposure time to the open air	The water uptake increased at a rate of around 6.8 wt% per day before reaching a plateau of 40 wt% after 65 days exposure to air. However, water content can be easily eliminated by heating.	[22]
ChCl: U EG ChCl: G 1:2 ChCl: U 1:2	0, 0.1, 0.3, 0.5, 0.7, 0.9 and 1 mol fraction of water	Molecular dynamics simulations	The intermolecular interaction network existing in the three DES remains unchanged until 50% mole fraction of water is added, and the water molecules are incorporated between the network. However, beyond 50%, the constituent species of the DES are freed from the interaction network and show higher fluidity and a sharp change in the number of hydrogen bonds.	[25]
ChCl: U 1:2	ChCl:U:Water mixtures (1:2:1; 1:2:2; 1:2:5; 1:2:10; 1:2:15; 1:2:20)	Analysis of the effect of water on the nanostructure of ChCl:U by neutral total scattering and empirical potential structure refinement	At low water levels ( $\leq 1$ mol fraction), water slightly strengthens the hydrogen bonds between choline and urea; Between 2 and 10 water mole fractions, the DES system resists hydration and retains its initial structure; At 15 mol fraction (83 mol% or 51 wt% of water), the DES structural motifs disappeared and the system is described as an aqueous solution of the DES components.	[26]

ChCl: Choline chloride; D<sub>2</sub>O: deuterium oxide; EG: Ethylene glycol; G: Glycerol; NMR: nuclear magnetic resonance; PCH: 1,2-propanediol-choline chloride-water; TU: Thiourea; U: Urea; wt%: weight percent.

Moreover, the presence of water strongly increased the diffusion of reline ions. All these changes were remarkable beyond 25–30 wt% of water [23]. Recently, molecular dynamics simulations were also performed on reline, ethaline and glyceline, along with their water mixtures (0, 0.1, 0.3, 0.5, 0.7, 0.9 and 1.0 mol fraction of the DES). As water was added to the system, the number of hydrogen bonds between the DES components was reduced, and new ones were formed between them and water. Water is incorporated in the hydrogen bond

network of the DES that was preserved until 50% mole fraction of water addition. Nonetheless, further addition of water resulted in free constituents of the DES, thus showing higher fluidity and a remarkable change in the number of hydrogen bonds [25].

Given its high polarity, water can be a part of DES's supramolecular complex by forming hydrogen bonds with DES components. However, above a certain water content, this complex is disrupted and an aqueous solution of DES free components is obtained. Further investigations

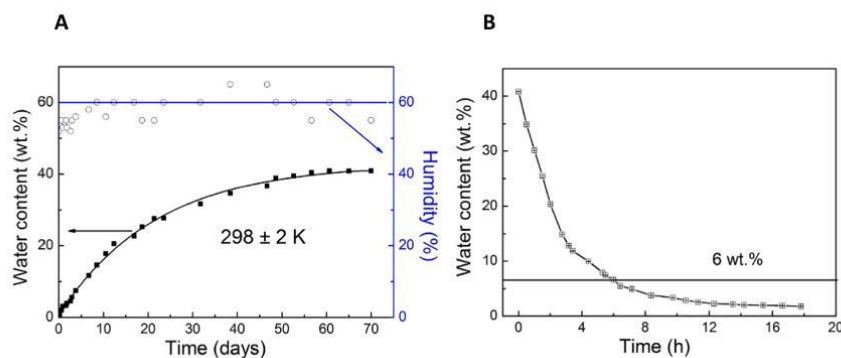


**Fig. 2.** (A) Water absorption by choline chloride:urea DES as a function of the exposure time to open air; (B) Variation of water content of the same DES as a function of heating time (2 column figure) [16].

must be considered to determine the limit of water content, for which DES' network and properties are preserved.

#### 4.2. Physico-chemical properties of DES

The physico-chemical properties of DES can be tailored by properly combining various halide salts with different hydrogen bond donors. Herein, we will present the main physico-chemical properties of DES in absence and presence of water. The latter are given when the literature data are available.

##### 4.2.1. Freezing point

As mentioned earlier, DES are prepared by mixing two solids capable of interacting via hydrogen bonds. As a consequence, a new liquid phase is obtained, with a lower freezing point than that of DES' individual components. For example, the DES consisting on a mixture of choline chloride and urea (choline chloride:urea molar ratio 1:2) presents a freezing point of 12 °C, which is significantly lower than that of pure choline chloride and urea compounds (302 and 133 °C, respectively) [2]. The depression of the freezing point arises from an interaction between the halide anion and the hydrogen bond donor. The freezing points of all studied DES are below 150 °C. Nevertheless, DES with a freezing point lower than 50 °C are very interesting since they can be easily used in various domains. Many factors affect the freezing point such as the choice of HBD [2,27], the nature of the organic salt [2], the anion of the organic salt [2] and the organic salt/HBD molar ratio [28]. No correlation was observed between the freezing point of the eutectic mixture and the melting points of the free components [7].

##### 4.2.2. Viscosity

Most of the DES are highly viscous at room temperature (>100 cP) [7]. This is most probably due to the hydrogen bond network between the components. The viscosity of a eutectic mixture is also affected by the nature of its components [29], the HBA/HBD molar ratio [30], the temperature [2,10,27,31,32] and the water content [4,10,22–24]. For instance, a choline chloride-based DES is much more viscous when a diacid, like oxalic acid, is used as an HBD rather than a monoacid such as levulinic acid. This is likely due to the formation of extra hydrogen bonds [4]. Furthermore, the viscosity decreases significantly when water is added to the system (10–30 times depending on the HBD) [4]. At 25 °C, the viscosity of hydrated choline chloride:urea (with 6 wt% water) was 13 times lower than the viscosity of dry choline chloride:urea [22].

When studying the effect of water (2.5–20 wt%) on three choline chloride-based DES Reline, Ethaline and Glyceline, a decrease in the viscosity is observed with increasing water content in all liquids at 20 °C. However, this is not a steady decrease and there is a pronounced decline at 2.5 wt% for Glyceline and Reline, which corresponds to approximately 1 mol equivalent of water to each chloride anion (Fig. 3). In addition, the effect of water on the viscosity of Reline is greater than for the other two liquids; with a viscosity going from 0.7 to 0.1 Pa·s when water content varied between 0 and 17.5 wt% [24]. Similar effect was observed by Shah et al. [23]; the addition of 10 wt% of water reduced the viscosity of reline by >80% compared to dried DES [23]. Another study showed that the addition of water significantly decreased the viscosity of NADES; after adding 25% water (v/v) to glucose-choline-water and 1,2-propanediol-choline chloride-water, their viscosity values decreased from 397 mm<sup>2</sup> s<sup>-1</sup> to 7.2 mm<sup>2</sup> s<sup>-1</sup> and from 33 mm<sup>2</sup> s<sup>-1</sup> to 6.1 mm<sup>2</sup> s<sup>-1</sup> respectively, which is near the range of water (0.7 mm<sup>2</sup> s<sup>-1</sup>) [8].

##### 4.2.3. Density

The density is one of the most important physical properties of a solvent. Most of DES exhibit higher densities than water. The density values of the most common DES vary between 1.04 and 1.63 g·cm<sup>-3</sup> at 25 °C [31,33,34] and are highly affected by the organic salt/HBD molar

ratio [30,34]. Florindo et al. [4] tested the effect of water on five choline chloride -based DES (HBDs: oxalic acid, glutaric acid, levulinic acid, glycolic acid and malonic acid). The solvents were left in contact with air for one month and the amount of retained water ranged between 14 and 20 wt%. Going from 20 to 80 °C, the density of water-saturated samples was lower than that of the dried samples, with a 5% difference. As a result, the presence of water slightly affects the density of these DES [4]. The same effect was observed when adding up to 65 wt% of water to choline chloride:urea at 30 °C [23]. Whereas the density of glucose-choline-water decreased linearly with the increasing water content [10].

##### 4.2.4. Ionic conductivity

Generally, most of DES present low ionic conductivities (<2 mS cm<sup>-1</sup> at room temperature) due to their high viscosity [7]. So, when increasing the temperature, the viscosity decreases and the ionic conductivity increases. The addition of water also increases the ionic conductivity of DES [10]. The conductivity of reline is increased by >3 folds when adding 10 wt% of water [23].

Hence, the physico-chemical properties of DES are clearly affected by numerous factors: the nature of both organic salt and hydrogen bond donor, the HBA:HBD molar ratio, the temperature and the water content. Consequently, deep eutectic solvents can be tailored according to desired applications.

#### 5. DES applied to biological macromolecules

The use of DES as solubilizing and extraction solvents is strongly encouraged due to their numerous qualities such as sustainability, non-flammability, as well as thermal and chemical stability. Besides, as previously stated, DES offer the advantage to be tailored given the plethora of the possible forming compounds and the plasticity of their properties. This tuneability is one of the greatest advantages of DES since the efficiency of extraction solvents highly depends on their physico-chemical properties, especially polarity. Subsequently, DES polarity can be customized depending on the nature of the target compound. However, the isolation of the target compounds as well as the recovery of the DES can be complicated owing to their low volatility. Some successful and simple methods have been performed to isolate the biological molecules such as polysaccharides [35], DNA [36], RNA [37] and BSA [38]. Moreover, the high viscosity of DES and their questionable safety somehow limit their use as extraction solvents. The high viscosity problem is often overcome by water addition. Thus, water in DES can be either regarded as an impurity when being handled in commercial

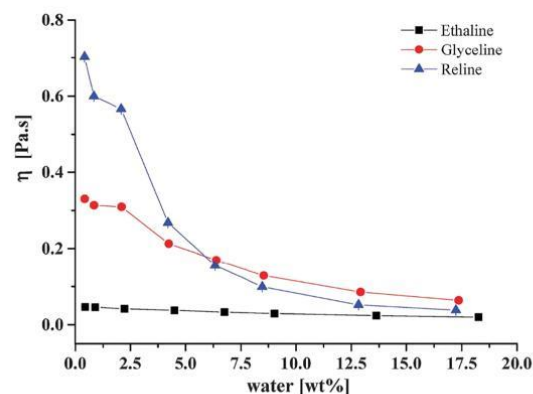


Fig. 3. Effect of water content on the viscosity of the most common choline chloride-based DES Reline (choline chloride:urea), Ethaline (choline chloride:ethylene glycol) and Glyceline (choline chloride:glycerol) at 20 °C [24] (single column figure).

applications, or intentionally added to modulate the physicochemical properties of the solvent [10,25]. In this section, the applications of DES as solvents to the main biological macromolecules will be highlighted and the presence of water will be discussed.

### 5.1. DES - phospholipids

Phospholipids are the most abundant class of lipids that can be found in animal cells. A phospholipid contains two fatty acids, one glycerol and a phosphate esterified by a polar group (Fig. 4A). Having a hydrophobic tail (alkyl chains of fatty acids) and a hydrophilic head (phosphate and polar groups), these amphiphilic molecules spontaneously form a lipid bilayer in an aqueous medium. Furthermore, there are different lipid organization depending on the lipid concentration and the temperature. At the transition temperature ( $T_m$ ), lipids undergo a phase transition from a gel solid-ordered phase ( $L_\beta$ ), where the hydrophobic chains interact with each other resulting in a packed rigid membrane, to a disordered phase ( $L_\alpha$ ) where the chains present a liquid-like organization and thus a fluid membrane (Fig. 4B). The transition temperature is influenced by the hydrocarbon chain length, the saturation of fatty acids, the head group and the charge of the phospholipid [39]. Few studies, summarized in Table 2, investigated the phospholipids organization in DES.

Recently, a study investigated the ability of phospholipids to form vesicles in choline chloride:urea DES using solvent penetration experiments. In this latter, a spot of lipid, was placed on a microscope slide with a cover slip. A drop of the solvent was placed on the outer edge of the cover slip where it was drawn into contact with the lipid via capillary action. This creates a concentration gradient. A heating stage was used to determine the effect of temperature on phase formation [40]. The experiment showed that choline chloride:urea DES is able to penetrate and solubilize phosphatidylcholine (PC)-based lipids (1,2-dimyristoyl-sn-glycero-3-phosphocholine (DMPC), 1,2-dipalmitoyl-sn-glycero-3-phosphocholine (DPPC), 1,2-distearoyl-sn-glycero-3-phosphocholine (DSPC), as well as egg PC having 1-palmitoyl-2-oleoyl-sn-glycero-3-phosphocholine (POPC) as major constituent) in the absence of water. As seen in polarizing optical microscopy, the DES swells the lipids above the penetration temperature and a  $L_\alpha$  lamellar phase spontaneously forms, which transforms to vesicles with time.

As in water, the penetration temperature is affected by the length of the lipid alkyl chain, but higher penetration temperatures were observed in the DES than in water for long alkyl chain lipids (Table 3). This is ascribed to the binding of chloride ions to the lipid membrane [40]. The same PC-based phospholipids were tested in alkylammonium-based DES (HBA: ethylammonium chloride, ethylammonium bromide, propylammonium bromide, butylammonium bromide and pentylammonium bromide), also in the absence of water,

this time using glycerol and ethylene glycol as HBDs. Solvent penetration experiments revealed that phospholipids form lamellar phases and spontaneously spawn vesicles in all the tested DES. However, this phase transition required heating for all the PC-based phospholipids, except for egg PC which formed spawn vesicles at room temperature (23 °C). The minimum temperature for fluid lamellar phase formation depends on the cation and anion type of the HBA in the DES but depends less strongly on the HBDs used. In fact, the transition temperature first increases (with ethyl- and propylammonium salts) as a result of a competition between the alkyl chains in the DES bulk and the hydrophobic domains in the lipid bilayer. Then the transition temperature decreases with increasing cation chain length (with butyl- and pentylammonium salts) since the cation acts as a cosurfactant for the lipid. Furthermore, a higher chain melting temperature is observed with bromide-containing ethylammonium DES than with chloride-containing ones [41].

In 2009, Gutiérrez et al. tested the incorporation of liposomes in choline chloride:urea and choline chloride:thiourea DES [13]. Liposomes are spherical vesicles of phospholipids bilayers with an entrapped aqueous phase and may consist of one or more bilayers (unilamellar or multilamellar, respectively). The combination of DES and liposomes is very challenging since the presence of water is required for liposomes formation, but disrupts the eutectic system as previously discussed. That's why the authors tried to incorporate liposomes in DES by freeze-drying a mixture of preformed liposomes and aqueous solutions of DES individual components (having 20 wt% solute content). First of all, they proved that DES can be obtained via freeze-drying the aqueous solutions of their individual components, by comparing the thermogravimetric analysis of DES prepared via heating and DES prepared via freeze-drying. After that, cryo-etch-scanning electron microscopy allowed the observation of "fence"-like structure in freeze-dried choline chloride:urea and choline chloride:thiourea and confocal fluorescence microscopy proved not only the presence of liposomes ranging between 200 and 500 nm but also the preservation of their membrane-like structure in DES (Fig. 5) [12].

Molecular dynamics simulations were performed to study the interaction of DES components with the lipid membrane at the molecular level. The interaction between eleven choline chloride-based DES (considering different HBDs) and a POPC lipid bilayer was investigated in the presence of 97.6 wt% water. Thus, the DES are clearly disrupted at this stage. The reported results show the presence of HBA's isolated ions and hydrogen bond donors in water solution, and thus interaction of free molecules with lipid bilayers. The insertion of hydrogen bond donor molecules is observed for all the considered solvents, whereas chlorine ions are not inserted and choline cation is inserted in minor quantities, just for some of the studied solvents. The number of inserted molecules increases with the hydrogen bond donor's hydrophobicity since the most important insertion was observed with phenylacetic acid-based solvents. Nevertheless, the structure of the lipid bilayer

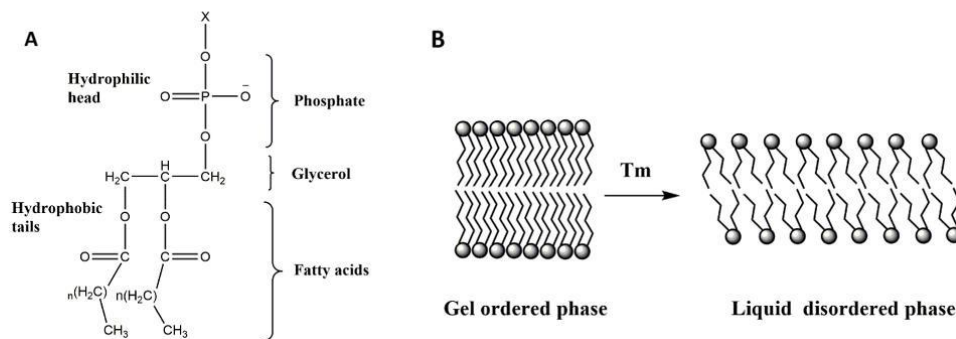


Fig. 4. (A) Phospholipid structure; (B) Phase transition in a lipid bilayer (2 column figure).

**Table 2**  
Summary of the DES-phospholipids studies.

DES	Lipids	Techniques	Comments	Ref
ChCl:U ChCl:TU 1:2	DMPC-based liposomes	Freeze-drying; Confocal fluorescence microscopy; TG; cryo-etch-SEM; <sup>1</sup> H NMR	Freeze-dried liposomes, prepared by thin film hydration were incubated with aqueous solutions of DES individual components.	[12]
ChCl:U 1:2	DMPC, DPPC, DSPC and egg PC phospholipids	Solvent penetration experiments; polarizing optical microscopy; small-angle X-ray scattering	The phospholipids, dissolved in ChCl:U, spontaneously form vesicles above the lipid chain melting temperature. The penetration temperature depends on the length of the lipid alkyl chain.	[40]
Alkylammonium-based DES with G and EG as HBDs (Salt:HBD 1:2)	DMPC, DPPC, DSPC and egg PC phospholipids	Solvent penetration experiments; polarizing optical microscopy; X-ray scattering	The phospholipids form spontaneous vesicles in all tested DES. However, the transition temperature depends on the cation and anion type of the HBA in the DES but depends less strongly on the HBD.	[41]
ChCl:U ChCl:EG ChCl:G ChCl:levulinic acid ChCl:phenylacetic acid ChCl:acetamide 1:2 ChCl:oxalic acid ChCl:malonic acid ChCl:glutaric acid ChCl:malic acid ChCl:citric acid 1:1	POPC lipid bilayer	Molecular dynamics simulations	In the presence of high amount of water (97.6 wt%), DES free molecules interact with the lipid bilayer, especially the HBD. The number of inserted HBD molecules increase with HBD's hydrophobicity.	[42]

<sup>1</sup>H NMR: proton nuclear magnetic resonance spectroscopy; **ChCl**: choline chloride; **DMPC**: 1,2-dimyristoyl-sn-glycero-3-phosphocholine; **DPPC**: 1,2-dipalmitoyl-sn-glycero-3-phosphocholine; **DSPC**: 1,2-distearoyl-sn-glycero-3-phosphocholine; **EG**: Ethylene glycol; **G**: Glycerol; **HBA**: hydrogen bond acceptor; **HBDs**: hydrogen bond donors; **PC**: phosphatidylcholine; **POPC**: 1-palmitoyl-2-oleoyl-sn-glycero-3-phosphocholine; **SEM**: scanning electron microscopy; **TG**: thermogravimetric analysis; **TU**: thiourea; **U**: urea; **wt%**: weight percent.

does not suffer large changes upon hydrogen bond donor's insertion [42].

### 5.2. DES - proteins

Proteins are large molecules composed of amino acids. The sequence of amino acids determines the structure as well as the function of the protein. The catalytic activity is one of the main functions of proteins called enzymes. Besides, biocatalysis in non-aqueous media has been widely investigated because it offers many advantages like a higher substrate solubility, better selectivity and improved enzyme thermostability [43]. Being green and inexpensive, deep eutectic solvents were recently adopted for biocatalytic reactions. All the studies concerning the effect of DES on proteins, mostly enzymes, are displayed in Table 4 in chronological order.

Horseradish peroxidase (HRP) is an ideal model enzyme that catalyzes the oxidation of various organic substrates in presence of hydrogen peroxide. The effect of DES on HRP's activity, stability and structure was examined. A group of 24 DES were prepared using choline

chloride and choline acetate as salts, along with four HBDs urea, glycerol, acetamide and ethylene glycol, at three different HBA:HBD molar ratios (1:2, 1:1, 2:1). Then the DES were dissolved in a phosphate buffer (0.1 M, pH 7.0) at different concentrations (up to 2 M), with the final pH re-adjusted to 7.0 prior to use. The activity and stability of HRP were studied in DES aqueous solutions and compared to pure buffer solution. The activity of HRP was assessed by a colorimetric method and the stability was evaluated by following the time-dependent loss in enzyme's activity and thus determining the half-life of HRP. A higher HRP activity was observed in the presence of choline chloride-based DES, rather than choline acetate-based ones, and at a higher salt/HBD molar ratio. The stability was also improved with most of the studied DES. Increasing DES' concentration resulted in reducing the enzyme's activity on one hand, and stabilizing the protein on the other. Due to the possibility of DES dissociation in aqueous solution, the activity and stability of HRP were also examined in the presence of aqueous solutions of separated components of choline chloride:urea and choline acetate:glycerol. The authors stated that the effect of these DES (choline chloride:urea and choline acetate:glycerol) are due to the DES aqueous solution, rather

**Table 3**  
Temperatures at which vesicles are formed by phosphatidylcholine-based lipids in water and choline chloride:urea DES [40].

Phospholipid	Structure	T <sub>m</sub> in water (°C)	T <sub>m</sub> in ChCl:U (°C)
DMPC (C <sub>14</sub> )		23	26
DPPC (C <sub>16</sub> )		41	52
DSPC (C <sub>18</sub> )		56	62
Egg PC (mainly POPC)		<23	<23

**ChCl**: Choline chloride; **DMPC**: 1,2-dimyristoyl-sn-glycero-3-phosphocholine; **DPPC**: 1,2-dipalmitoyl-sn-glycero-3-phosphocholine; **DSPC**: 1,2-distearoyl-sn-glycero-3-phosphocholine; **PC**: phosphatidylcholine; **POPC**: 1-palmitoyl-2-oleoyl-sn-glycero-3-phosphocholine; **U**: Urea.

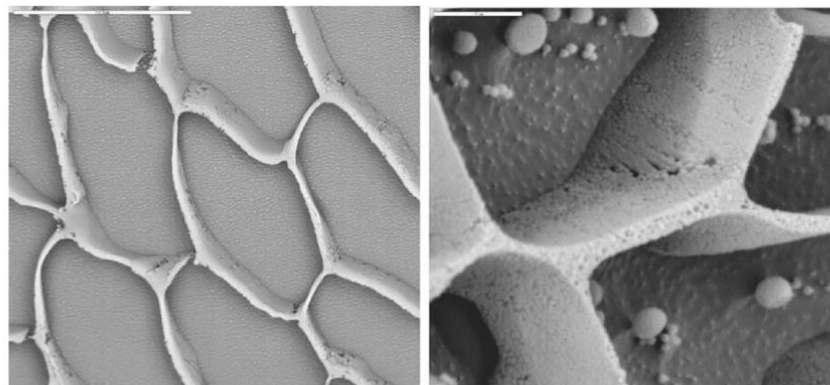


Fig. 5. Cryo-etch-SEM micrographs of liposomes incorporated in choline chloride:urea (left) and choline chloride:thiourea (right) [12] (single column figure).

than the effect of its individual components and are strongly affected by the salt and depends less on the HBD [44]. It is worth noting that at the tested range of concentrations, DES solutions are rather solutions of the individual components in the buffer.

The same group of DES were dissolved in Tris-HCl buffer (50 mM, pH 8.0) at the same concentration (normally up to 2.0 M) and were used to evaluate *Penicillium expansum* lipase (PEL) activity and stability. PEL was successfully used for the production of biodiesel from different oils. This time, choline acetate-based DES were superior to choline chloride-based ones in promoting both activity and stability of PEL. Furthermore, the choice of the HBD seemed very important, glycerol and ethylene glycol showed better enhancing effect than urea and acetamide. A 1.4-fold increase in activity and a 17.4-fold enhancement in stability of PEL were seen in the presence of choline acetate:glycerol, relative to the buffer solution. However, no specific consistency was observed when changing the salt:HBD molar ratio [45]. Laccase activity was also evaluated in ChCl:malic acid (1:1). The enzyme turned out to be soluble but inactive in the NADES. However, its activity is restored after 50% water addition [3]. On the other hand, Khodaverdian et al. examined the laccase activity and stability in different betaine-based and choline-based NADES. Choline-based solvents caused a sudden drop in the enzyme's activity and stability. While betaine-based ones showed even better laccase activity and stability than the aqueous buffer. It should be noted that, when varying the DES concentration from 10 to 50% (v/v), the highest activation was observed at 20% for all the solvents. Moreover, after selecting glycerol:betaine (2:1), the NADES in which laccase demonstrated the highest activity, it was proven that this enzyme behavior is due to the NADES itself. Although the enzyme is stabilized in the aqueous solution of both NADES components, the activity and stability of laccase was even higher in the NADES [46].

Other studies showed that enzymes like *Candida Antarctica* lipase B (CALB) remained active and stable in the presence of choline chloride- and ethylammonium chloride-based deep eutectic mixtures, such as choline chloride:urea having high percentages of urea, although urea is a protein denaturant [47,48]. This was further confirmed by molecular dynamics studies showing that CALB is stable in choline chloride:urea DES (in the presence of about 66% urea), even though a complete denaturation occurred with only 12% urea in water. This is due to the decrease in the diffusion coefficient of urea in the DES, as a result of hydrogen bonding between urea and chloride and chloride ions. Thus, urea molecules are unable to reach the protein domains [49].

Likewise, an increase in the transesterification activity and selectivity of the immobilized subtilisin protease was witnessed in the presence of choline chloride:glycerol with 3% (v/v) water content, even though chloride anion is considered as enzyme-denaturing [50]. It is worthy

to mention that this DES is preserved at 3% water content [24,25]. On the other hand, the activity of potato epoxide hydrolase StEH1 was decreased in the presence of different concentrations of sodium phosphate (0.1 M, pH 7.5) solutions of reline, ethaline and glycerine (v/v: 10–60%). The enzyme activity was least affected by Glycerine, followed by ethaline and reline, with 50% remaining activity in the presence of 60% Glycerine. In addition, the half-life of StEH1 was reduced after prolonged incubation with DES. Besides, the Michaelis constant  $K_m$  was increased, suggesting that the effect of DES is due to an enzyme-substrate destabilization, rather than protein denaturation [51].

Furthermore, bovine liver catalase was mostly inactive in high concentrations (up to 4500 mM) of reline and glycine solutions in phosphate buffer (pH 7.0) [52]. A concentration of 4500 mM is approximately equivalent to 40 wt% of reline and 50 wt% of glycine; with respect to the results discussed in Section 4.1, these DES are probably destructed at this point. According to Xin et al., trehalose:choline chloride DES (at a molar ratio 1:3) at 75 wt% DES retained the intensive hydrogen bonds and improved the thermal stability of a model protein lysozyme and promoted its refolding after heating to 90 °C [53]. This was not the case for bovine serum albumin (BSA) and lysozyme in pure choline chloride:urea and choline chloride:glycerol. In fact, BSA was irreversibly denatured after being heated up to 80 °C in pure choline chloride:glycerol. Thus, no improvement in BSA's thermostability was observed in the DES. In addition, the structures of BSA and lysozyme were partially folded in pure DES, but structures in DES/water mixtures (75 wt% and 50 wt% of DES) at 25 °C were almost similar to those in pure phosphate buffer [54].

The oxidation activity and stability of cytochrome *c* were enhanced in the presence of aqueous solutions of ethylammonium chloride- and choline chloride-based DES, using urea, glycerol and ethylene glycol as HBDs. But a more pronounced effect was observed with ethylammonium chloride-based mixtures compared to the enzyme activity in phosphate buffer, with a 100-fold enhancement in peroxidase activity in the presence of 30% (v/v) aqueous solution of ethylammonium chloride-DES compared to an 8-fold increase at the same concentration of choline chloride-DES. The choice of the HBD and the concentration of the DES also affected the protein's activity. The stability of cytochrome *c* was also improved in all the tested DES at 30% (v/v) aqueous solutions. On the other hand, significant changes occurred in the UV-vis and circular dichroism spectra of the protein, suggesting changes in its microenvironment in the presence of choline chloride:urea and ethylammonium chloride:urea [55]. Changes in the secondary and tertiary structures of cytochrome *c* were also detected in pure guanidine hydrochloride:urea DES. However, cytochrome *c* refolded into its native structure via dialysis, after a long-term storage of the denatured form in this DES [56].

**Table 4**  
Recent applications involving deep eutectic solvents and selected model proteins.

DES	Protein nature	Incubation conditions	Aim	Results	Ref
ChCl:acetamide ChCl:EG ChCl:G ChCl:malonic acid EAC:acetamide EAC:EG EAC:G	iCALB; CALB; CALA; PCL	Not mentioned	Test the activities of different hydrolases in DES	The tested enzymes showed good catalytic activity in DES, even in presence of protein denaturants like urea or in presence of alcohols that can interfere with the enzymatic reactions, like glycerol and ethylene glycol. This is due to the hydrogen-bond network within the DES that makes DES components less active.	[47]
ChCl:U ChCl:G ChCl:EG 1:2	Potato epoxide hydrolase (StEH1)	Sodium phosphate (0.1 M, pH 7.5) solutions of DES at concentrations varying between 10 and 60% (v/v)	Test the DES as cosolvents in enzyme-catalyzed hydrolysis	The enzyme activity decreased and Km increased when increasing DES concentration. But the enzyme was the least sensitive to glycerine, followed by ethaline and reline. This effect is probably due to enzyme-substrate destabilization, rather than protein denaturation.	[51]
ChCl:G (1:2) ChAc:G (1:1.5 and 1:2)	Free and immobilized Subtilisin and $\alpha$ -chymotrypsin proteases	Enzymes were dissolved in phosphate buffer (0.1 M, pH 7.4) before immobilization	Examine the potential use of DES as solvent for protease-catalyzed transformations using immobilized subtilisin and $\alpha$ -chymotrypsin	A higher activity and selectivity was reached with immobilized subtilisin, compared to free subtilisin and in the presence of ChCl:G, having 3% (v/v) water content, rather than ChAc:G. $\alpha$ -chymotrypsin was much less active in the same DES.	[50]
ChCl:malic acid 1:1	Laccase	The DES with 0%, 25% and 50% water	Test the solubility and the activity of laccase in the NADES	Laccase turned out to be soluble but inactive in ChCl:malic acid. The enzyme's activity was restored after the addition of water.	[3]
ChCl:U (1:2) ChCl:G (1:2) ChCl:oxalic acid(1:1) ChCl:malonic acid (1:1) ChCl:EG (1:2) EAC:U (1:2) EAC:G (1:2) PCH (1:1:1) GCH (2:5:5) LGH (5:1:3) XoCH (1:2:3)	iCALB	Pure DES were mixed with crushed iCALB whose water activity was set at 0.44	Analyze CALB-catalyzed reactions in the presence of DES	ChCl:U and ChCl:G allowed the best lipase activity and selectivity, unlike ethylene glycol or dicarboxylic acid-containing DES. These latter HBDs form side reactions by competing with the substrates of alcoholysis reaction.	[48]
24 DES using 2 HBAs: ChCl and ChAc, and 4 HBDs: U, G, EG and A; at three molar ratios (1:2, 1:1 and 2:1)	Gluten	An excess of gluten was put in the different NADES. The mixture was then stirred for 2 h at 40 °C and left 3 h to rest for precipitation	Test the solubility of gluten in different NADES	Being the most polar solvent, LGH presented the highest solubilizing ability towards gluten. The macromolecule was 101 times more soluble in LGH than in water.	[8]
24 DES using 2 HBAs: ChCl and ChAc, and 4 HBDs: U, G, EG and A; at three molar ratios (1:2, 1:1 and 2:1)	<i>Penicillium expansum</i> lipase	DES were dissolved in Tris-HCl buffer (50 mmol L <sup>-1</sup> , pH 8.0) at a concentration of 2.0 M (molar concentration of the ammonium salt)	Study the effect of the DES and their compositions on the activity and stability of <i>Penicillium expansum</i> lipase	ChAc-based DES were superior to ChCl-based ones in promoting both activity and stability of PEL. The choice of the HBD seemed very important, (G) and (EG) showed better enhancing effect than (U) and (A). ChAc:G was the most suitable solvent for PEL.	[45]
24 DES using 2 HBAs: ChCl and ChAc, and 4 HBDs: U, G, EG and A; at three molar ratios (1:2, 1:1 and 2:1)	Horseshadish peroxidase	DES were dissolved in phosphate buffer (0.1 M, pH 7.0) at a concentration of 2.0 M (molar concentration of the ammonium salt)	Examine the impact of the DES and their compositions on the activity, stability and structure of HRP	A higher HRP activity was observed in presence of ChCl-based DES, rather than ChAc-based ones, and at higher salt:HBD molar ratio. HRP's stability was improved with all tested DES. Those effects are caused by DES itself, rather than the synergistic action of its individual components.	[44]
ChCl:U 1:2	Bovine serum albumin	ATPS is composed of ChCl:U DES and an aqueous solution of K <sub>2</sub> HPO <sub>4</sub>	Extract BSA by an aqueous two-phase system based on DES and study the mechanism of extraction	The extraction efficiency is affected by the mass of the DES, concentration of K <sub>2</sub> HPO <sub>4</sub> solution, separation time and extraction temperature. The optimum conditions for BSA extraction were determined. The UV-visible spectra showed that BSA conformations were similar before and after extraction, suggesting that the surrounding of BSA aggregates by DES aggregates is the main reason behind the protein extraction.	[57]
Guanidine hydrochloride:U Guanidine thiocyanate:U 1:2	Cytochrome c and bovine serum albumin	Cytochrome c was tested in a buffer solution, consisting of 10 mM sodium phosphate at pH 7.0 (for the native state) and pH 2.0 (for the denatured state)	Test the solubility of BSA and cyt c in both DES as well as the stability of cyt c in Guanidine HCl:U	BSA and cyt c present higher solubilities in both DES (260 mg/ml for BSA and 18 mg/ml for cyt c) compared to water. Changes in the secondary and tertiary structures of cyt c were detected in the presence of guanidine HCl: U DES. However, cytochrome c refolded into its native structure via dialysis, after 6 months storage of the denatured form in this DES.	[56]
ChCl:U 1:2	CALB	Molecular dynamics simulations of CALB in ChCl:U and 8 M urea	Simulate the enzyme structure, activity and thermal stability of CALB in ChCl:U and in 8 M urea for comparison	The lipase showed a very good conformational stability in ChCl:U with about 66% urea, even though a complete denaturation occurred in 8 M urea with	[49]

(continued on next page)

Table 4 (continued)

DES	Protein nature	Incubation conditions	Aim	Results	Ref
ChCl:G 1:1	Bovine serum albumin and trypsin	ATPS is composed of ChCl:G DES and an aqueous solution of $K_2HPO_4$	Extract BSA and trypsin by ATPS based on DES and study the mechanism of extraction	only 12% urea in water. This could be explained by the formation of hydrogen bonds between the DES components and the surface residues of the enzyme. The extraction efficiency is affected by the mass of the DES, concentration of $K_2HPO_4$ solution, separation time and extraction temperature. The optimum conditions were identified. The conformation of BSA was unchanged before and after extraction. The formation of aggregates is the mechanism behind the protein extraction.	[58]
Betaine:U:water 1:2:1	Bovine serum albumin	ATPS is composed of betaine:U:water DES and an aqueous solution of $K_2HPO_4$	Extract BSA by an aqueous two-phase system based on DES and study the mechanism of extraction	The optimum conditions for BSA extraction were identified. The conformation of BSA did not change after extraction. The extraction is driven by the formation of aggregates.	[38]
ChCl:U ChCl:G ChCl:EG 1:2  EAC:U EAC:G EAC:EG 1:1.5	Cytochrome c and horseradish peroxidase	Protein activity was tested in 0–90% v/v aqueous solutions of DES in 50 mM sodium phosphate buffer pH 7.0 in the case of cyt c, or pH 6.5 in the case of HRP	Study the effect of ChCl- and EAC-based DES on the peroxidase activity and stability of heme-dependent biocatalysts	The catalytic behavior of both proteins is highly affected by the nature of the ammonium salt, the HBD, as well as the concentration of the DES. The activity of HRP was decreased in presence of DES, compared to its activity in buffer. While the peroxidase activity of cytochrome c was strongly enhanced by EAC-based DES, rather than ChCl-based ones, especially at 30% (v/v) EAC-DES aqueous solution. Higher cyt c stability was observed in all tested DES at 30% (v/v) aqueous solutions, compared to buffer.	[55]
Trehalose: ChCl 1:3	Lysozyme	Lysozyme was dissolved in water or in diluted Trehalose:ChCl DES (25, 50 and 75 wt% water)	Examine the thermostability of lysozyme in trehalose:ChCl DES	Diluted Trehalose:ChCl DES, with 25 wt% water, improved the thermostability of a model protein lysozyme and promoted its refolding after heating to 90 °C.	[53]
Fructose: citric acid 1:1	Gluten	Diluted NADES (10–80%) (v/v)	Test the solubilization of gluten in NADES for its determination in food by ELISA	20% (v/v) diluted fructose: citric acid was selected as the NADES with the best gluten solubilizing ability. Combined to an ultrasonic-assisted extraction, the use of NADES allows gluten determination and this method can replace gluten extraction by ethanol-water solution.	[60]
ChCl:U ChCl:G 1:2	Bovine liver catalase	Different concentrations of aqueous solution of DES, prepared in phosphate buffer medium	Evaluate the effect of reline (ChCl:U) and glycine (ChCl:G) on the structure and function of bovine liver catalase	A slight decrease in catalytic activity of bovine liver catalase was observed in low concentrations of phosphate buffer solutions of reline and glycine. Moreover, the 3D- and secondary structure of the enzyme was partially changed. On the other hand, the enzyme was mostly inactive in high concentrations of DES (4500 mM).	[52]
ChCl:U ChCl:G 1:2	Lysozyme and bovine serum albumin	BSA and lysozyme were studied in ChCl:G, and ChCl:G/water mixtures (75 wt% and 50 wt% of DES) and buffer (phosphate buffered saline, 0.01 M, pH = 7.4). Lysozyme was also tested in ChCl:U	Investigate the structure and conformation of two model proteins (lysozyme and BSA) in pure and hydrated DES	BSA was irreversibly denatured after being heated up to 80 °C, in pure ChCl:G. The structures of BSA and lysozyme were partially folded in pure DES, but structures in DES/water mixtures (75 wt% and 50 wt% of DES) were almost similar to those in phosphate buffer.	[54]
ChCl:G ChCl:U ChCl:water 1:2  ChCl:EG 1:3  ChCl:Malonic acid 1:1  ChCl:Lactic acid 2:1  G:Proline 5:2  ChCl:Fructose:water 1:1:1,  ChCl:Glutamic acid:water 1:2:2.7	Photosynthetic Reaction Centers (RC) of <i>Rhodospira rubra</i>	Isolated photosynthetic RC were dissolved in the DES then water was added (final water concentration below 3 M)	Check the stability and activity of RCs in different DES	Photosynthetic RCs integrity and photoactivity are maintained in most of the tested solvents.	[21]
Different ChCl- and betaine- based NADES	Laccase from <i>Bacillus HR03</i>	Citrate phosphate (0.1 M, pH 4.2) solutions of NADES at concentrations	Evaluate the effect of NADES on the activity, stability and	Choline-based solvents caused a sudden drop in the enzyme's activity and stability.	[46]

Table 4 (continued)

DES	Protein nature	Incubation conditions	Aim	Results	Ref
using glycerol, sorbitol, urea, citric, malic and oxalic acids as HBDs		varying between 10 and 50% (v/v)	structure of laccase	While betaine-based ones showed better laccase activity and stability than the aqueous buffer. The highest activity was observed in 20% (v/v) glycerol:betaine (2:1) and the highest stability in sorbitol:betaine:water (1:1:1) and glycerol:betaine (2:1).	

ATPS: aqueous two-phase system; BSA: bovine serum albumin; CALA: *Candida Antarctica* lipase A; ChAc: choline acetate; ChCl: choline chloride; Cyt c: cytochrome c; EAC: ethylammonium chloride; EG: ethylene glycol; G: glycerol; HBA: hydrogen bond acceptor; HBD: hydrogen bond donor; HCl: hydrochloride; HRP: horseradish peroxidase; iCALB: immobilized *Candida Antarctica* lipase B;  $K_2HPO_4$ : dipotassium phosphate; Km: Michaelis constant; PCL: *Pseudomonas cepacia* lipase; PEL: *Penicillium expansum* lipase; U: urea; wt%: weight percent.

Choline chloride:urea was also tested for the extraction of BSA from aqueous buffer using an aqueous two-phase system (ATPS). This system, presented in Fig. 6, is an alternative method for the traditional organic–water solvent extraction system, used for the purification of biomolecules such as proteins. In this case, ATPS consists on putting together choline chloride:urea DES and  $K_2HPO_4$  aqueous solution, before adding the protein. Choline chloride:urea was first selected since it presented the highest extraction efficiency when compared to choline chloride:methylurea, tetramethylammonium chloride:urea, tetrapropylammonium bromide:urea. The extraction efficiency of BSA was influenced by the mass of the DES, concentration of  $K_2HPO_4$  solution, separation time and extraction temperature. The optimum conditions for BSA extraction were 1.6 g,  $0.6 \text{ g}\cdot\text{mL}^{-1}$ , 10 min and  $25^\circ\text{C}$ , respectively. The UV–visible spectra showed that BSA conformations were similar before and after extraction, suggesting that there are no chemical bonds between BSA molecules and DES. The authors proposed that the surrounding of BSA aggregates by DES aggregates is the main reason behind the protein extraction, based on transmission electron microscopy (TEM) images [57]. The same results were obtained when using betaine:urea:water (1:2:1) to extract BSA [38] and choline chloride:glycerol (1:1) to extract BSA and trypsin via ATPS [58].

DES were not only tested for the extraction of protein, but for the extraction of amino acids using supported liquid membranes based on DES. Choline chloride: *p*-toluenesulfonic acid was selected between many choline chloride- and tetrabutylammonium chloride-based DES for having the highest extraction efficiency of tryptophan (Trp) (86.1%). The mechanism behind this extraction is most probably the formation of hydrogen bonds between the DES and Trp [59].

### 5.3. DES - nucleic acids

Given the low stability of nucleic acids in aqueous solutions, researchers are looking for new alternative solvents to provide a stable medium for DNA. DES were first proposed by Mamajanov et al. [61] who showed that choline chloride:urea is able to preserve the native structure of DNA by circular dichroism. However, DNA and RNA duplex were less stable in the DES than in the aqueous solutions since they presented lower melting transition temperatures [61]. Shortly after that, few studies tested the solubility of DNA in several NADES. DNA was more soluble in malic acid: proline (1:1) compared to water [3]. Further, DNA's solubility turned out to be 34 times higher in LGH than in water [8]. Later on, Mondal et al. [36] checked the solubility and long term stability of DNA in different choline chloride-based DES (choline chloride: glycerol, choline chloride:ethylene glycol, choline chloride:levulinic acid, choline chloride:sorbitol and choline chloride:resorcinol). DNA was only soluble in choline chloride:glycerol and choline chloride:ethylene glycol with 2.5% w/w and 5.5% w/w, after 6 and 2 h of stirring, respectively. In addition, no degradation of isolated DNA was detected during the dissolution in both DES, even after six months of storage at room temperature. Choline chloride:ethylene glycol and choline chloride:glycerol could be recycled and reused for DNA dissolution for three consecutive cycles. The solubility and stability of DNA dissolved

in DES are due to interactions between choline cations and DNA phosphate groups (Fig. 7) [36]. Soon after, 1:2 choline chloride:ethylene glycol was used for different DNA applications [62–64]. Zhao and Qu revealed that ChCl:U provided an anhydrous medium for G-quadruplex DNA. The relevance of this DNA structure is ascribed to its biological significance. In addition, G-quadruplex DNA was more soluble in ChCl:U DES than in water [65]. On the other hand, Yusof et al. investigated the mode of interaction between DNA and hydrated tetrabutylammonium bromide-based DES as well as the effect of DES on the DNA structure using fluorescence quenching and circular dichroism spectroscopies [66]. Four different HBDs (ethylene glycol, 1,3-propanediol, 1,5-pentanediol and glycerol) were used to study the effect of the HBD's chain length and the number of OH group. All the DES were able to quench the intercalation of the ethidium bromide that is bound to the DNA due to the hydrophobic interactions between hydrophobic part of DNA bases and hydrocarbon chain of DES, since the highest quenching efficiency followed the order tetrabutylammonium bromide:1,5-pentanediol; tetrabutylammonium bromide:1,3-propanediol; tetrabutylammonium bromide:ethylene glycol and tetrabutylammonium bromide:glycerol. In addition, the presence of an additional OH group in glycerol, reduces the hydrophobicity of the DES. Electrostatic interactions were also formed between tetrabutylammonium cations and the negatively charged phosphate groups of the DNA. The double helical structure of the DNA was maintained in the hydrated tetrabutylammonium bromide:1,5-pentanediol at  $25^\circ\text{C}$ , at a concentration of 25% DES [66]. Zhang et al. proposed the use of aqueous biphasic systems composed of inorganic salts and DES for RNA extraction for the first time [37]. Different DES were tested, based on different quaternary ammonium salts and polyethylene glycol. It turned out that this system was better than the conventional ones used for RNA extraction, with an average extraction efficiency of 92.7%. Electrostatic interaction is the main force behind this efficient RNA extraction, which was also confirmed by the RNA back-extraction.

### 5.4. DES - polysaccharides

Polysaccharides represent an important class of biological polymers. Two main types of polysaccharides are found in living organisms: storage polysaccharides like starch and glycogen, and structure polysaccharides like chitin and cellulose. Besides their natural functions, polysaccharides gained the scientists' attention due to their numerous medicinal properties. Many studies, shown in Table 5, investigated the use of DES as green solvents for solubilization, plasticization or extraction of polysaccharides. Owing to their supramolecular structure and broad polarity range, DES are worthy of further consideration as solvents for poorly water-soluble macromolecules like polysaccharides.

Three choline chloride-based DES (using urea, citric acid and succinic acid as HBDs) were evaluated as plasticizers and solvents for potato starch [67]. Generally, plasticizers are low molecular weight molecules, capable of disrupting the intermolecular bonds of a polysaccharide by forming hydrogen bonds with the hydroxyl groups of the polysaccharide chains, thus leading to a more elastic material [68].

Rheometric curves of DES/dry starch system with mass ratio 30:100 showed a sharp decrease in the system's viscosity between 30 and 70 °C for choline chloride:urea ( $7 \cdot 10^4$ – $3 \cdot 10^2$  Pa·s) and then a sharp increase up to  $10^5$  Pa·s between 70 and 100 °C. While an important drop in the viscosity was observed above 100 °C for the DES based on choline chloride and carboxylic acids. This difference between the systems is possibly due to esterification reaction between the carboxylic groups of citric and succinic acids and the hydroxyl groups of the polysaccharide. In addition, laser scanning microscopy revealed the dissolution of starch (5 wt%) in choline chloride:urea at 118 °C, in choline chloride: citric acid at 120 °C and in choline chloride:succinic acid at 135 °C [67]. According to Dai et al., the solubility of starch at 100 °C was higher in NADES than in water, and precisely in 1,2-propanediol: choline chloride: water (1:1:1), glucose: choline chloride: water (2:5:5) and lactic acid: glucose: water (5:1:3), yielding solutions that remained clear at room temperature [8]. Zdanowicz et al. [69] tested imidazole-based DES (with choline chloride, glycerol, citric acid and malic acid) as solvents and plasticizers for potato starch and high-amylose starch. Choline chloride: imidazole (3:7) and glycerol:imidazole (3:7) were able to dissolve up to 20 wt% of starch after 1-h heating at 100 °C. However, this was not the case for citric acid:imidazole and malic acid:imidazole which did not dissolve the starch even after 90 min heating at 115 °C [69]. When testing the effect of DES on plasticized starch films properties, crosslinking was detected between hydroxyl groups of the polysaccharide and carboxylic groups of choline citrate used as one of DES components [68].

The cellulose accessibility was improved after treating corn stover with DES. Corn stover, composed of cellulose (40–60%), hemicellulose (20–40%) and lignin (10–24%), was pretreated with 7 choline chloride-based DES (using 5 acidic HBDs: formic acid, acetic acid, oxalic acid, malonic acid, citric acid; and 2 neutral HBDs: urea and glycerol) to enhance the accessibility of poorly water-soluble cellulose for subsequent biobutanol fermentation. Acidic DES showed good performance in corn stover pretreatment, unlike choline chloride:urea and choline chloride:glycerol. However, as the number of carboxylic groups and the chain length increased, the concentration of glucose (obtained by cellulose hydrolysis) decreased. Thus, choline chloride:formic acid was the best DES for corn stover pretreatment, improving cellulose accessibility by removing hemicellulose and lignin [70]. On the other hand, lactic acid: choline chloride and lactic acid: betaine NADES were unable to dissolve cellulose and xylan [71].

DES consisting of the mixtures of choline halide (chloride/bromide): urea (1:2), choline chloride: thiourea (1:2), chlorocholine chloride: U

(1:2) and betaine hydrochloride: U (1:4) were able to dissolve  $\alpha$ -chitin by conventional heating (100 °C), heating under microwave (80 °C) and heating assisted by ultrasonication (80 °C).  $\alpha$ -Chitin was best dissolved in choline chloride: thiourea with 9% w/w dissolution upon heating for 6 h at 100 °C. Moreover, optical light microscope confirmed the absence of insoluble particles in the solutions and analysis of  $\alpha$ -chitin by FT-IR, X-ray diffraction (XRD),  $^1\text{H}$  NMR, thermogravimetric analysis (TGA) and rheology revealed that no chemical and structural degradation of the biopolymer occurred during the dissolution process. Surprisingly, chitosan (deacetylated chitin) was not soluble in choline chloride:thiourea suggesting the involvement of acetamide in the dissolution of chitin in DES [72].

When it comes to extraction, polysaccharides are usually extracted with hot water. Since this procedure is energy- and time-consuming, few studies have recently reported the use of DES for the extraction of polysaccharides from sample matrices. Polysaccharides are usually extracted with hot water, but this method requires so much time and energy [73]. Recently, four DES consisting on mixtures of choline chloride as HBA along with ethylene glycol, glycerol, 1,4-butanediol and 1,6-hexanediol as HBDs, were tested for the extraction of polysaccharides from *Dioscorea opposita* Thunb, a popular medicinal plant known as Chinese yam. The experimental factors for the DES-based ultrasound-assisted extraction of polysaccharides were optimized. Choline chloride:1,4-butanediol presented the highest extraction yield, probably because of its high hydrogen bonding ability and electrostatic interactions with the Chinese yam polysaccharides. On the other hand, the lowest extraction yield was obtained with choline chloride:glycerol having three hydroxyl groups, which can weaken the DES-polysaccharides interactions. The HBA:HBD molar ratio, the water content and the temperature also affected the extraction efficiency, since they have an impact on the solvent's viscosity. In fact, the extraction yield increased with the increase of 1,4-butanediol (between a 1,4-butanediol:choline chloride molar ratio of 0.5 to 4), the increase of water content from 0 to 30 wt% (v/v) and the temperature from 50 to 90 °C. This is due to a reduction in DES viscosity and thus the improvement of its diffusivity and the mass transfer of the target compounds. This novel DES-based method turned out to be better than hot water extraction and water-based ultrasound-assisted extraction considering the extraction yield [73].

Similarly, 7 different choline chloride-based DES were screened for the extraction of polysaccharides (alginate and fucoidan) from a brown seaweed, *Saccharina japonica*, combined with subcritical water extraction. The best extraction efficiency was obtained with 1:2 choline

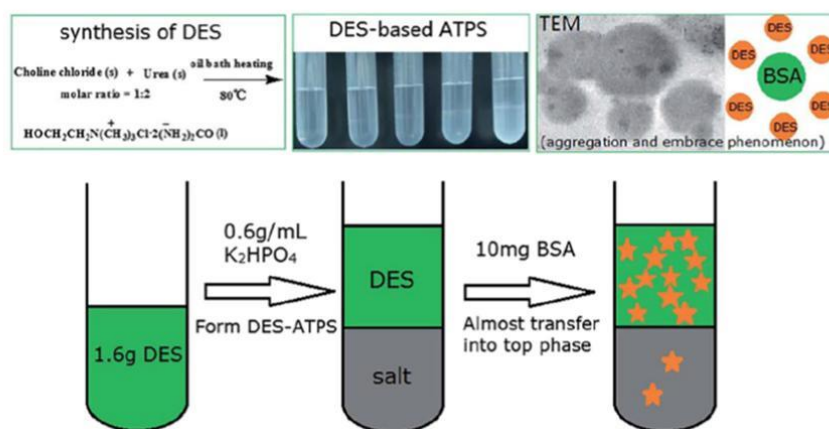


Fig. 6. DES-based aqueous two-phase system for protein extraction [49] (single column figure).

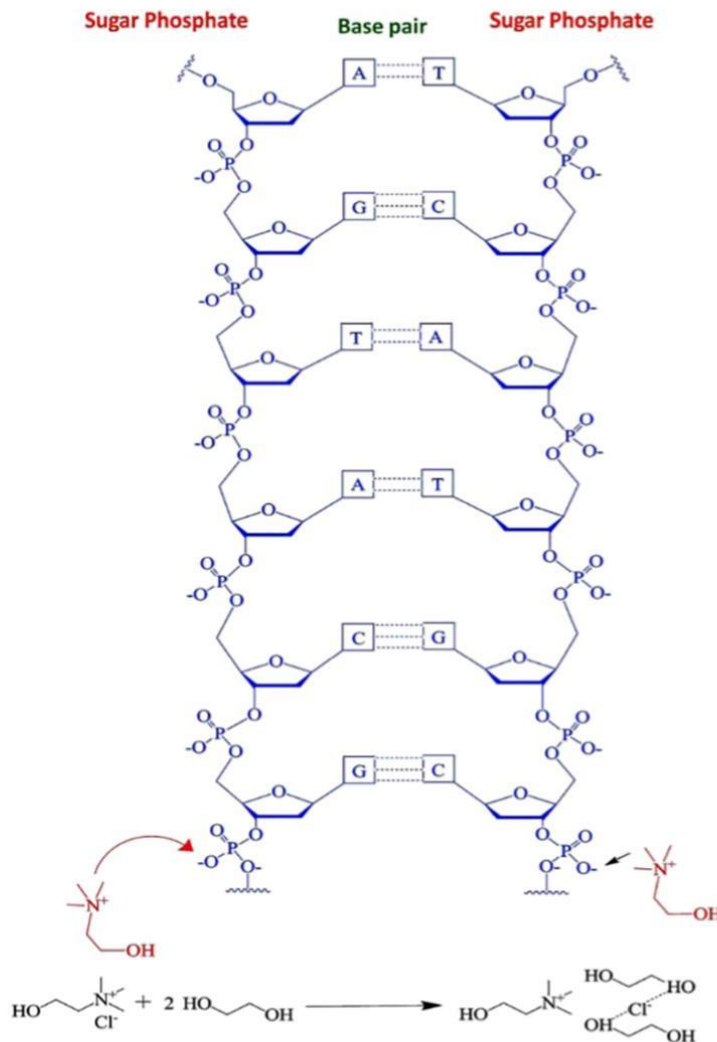


Fig. 7. Dissolution of DNA in choline chloride:ethylene glycol DES via interaction between DNA phosphate and choline cations of DES [36] (single column figure).

chloride:glycerol and the optimal conditions were 150 °C, 19.85 bar and 70% water content [35]. Although the water addition improved the extraction yield of polysaccharides, a high water content like 70% will probably disrupt the DES network. Furthermore, Das et al. succeeded in extracting  $\kappa$ -carrageenan from *Kappaphycus alvarezii*, a polysaccharide present in red seaweed, using the pure and 10% hydrated forms of choline chloride:urea, choline chloride:ethylene glycol and choline chloride:glycerol [74]. In accordance with Saravana et al. [35], higher extraction yields were obtained with the hydrated DES; the yield was highest (60.25%) when 10% hydrated choline chloride:glycerol was used. Given the strong interaction between choline cation and glycerol in choline chloride:glycerol DES, the amount of water added in this case do not affect the DES network, according to D'Agostino et al. [24]. The results obtained with hydrated DES are not clearly due to a difference in viscosity since 10% hydrated choline chloride:ethylene glycol, presented

a marginally lower extraction yield. The extraction efficiency of the hydrated DES is due to choline's high solubility in water, along with electrostatic interactions between the sulfate group attached to the carbon-4 position in the structure of  $\kappa$ -carrageenan and the choline cation present in the DES [74]. Recently, four DES (choline chloride:urea, choline chloride:thiourea, choline chloride:glycerol and choline chloride: malonic acid) were used for the extraction of chitin from lobster shells. Usually, two main steps are followed when extracting chitin from lobster shells: demineralization and deproteinization; since lobster shells contain not only chitin but also proteins, minerals and pigments. There was no effect on the elimination of proteins and minerals for all the DES except for choline chloride: malonic acid (1:2) which showed the most important yield of chitin, with high purity. The extractive potential of choline chloride:malonic acid compared to other tested DES is most probably due to its acidity that helps by removing the proteins [75]. Similar results were obtained by Saravana et al.

**Table 5**  
Recent applications involving DES and polysaccharides.

DES	Polysaccharide	Aim	Results	Ref
ChCl:U (1:2) ChCl: succinic acid (1:1) ChCl: citric acid (2:1)	Potato starch	Evaluation of DES as plasticizers and solvents for potato starch	Different rheometric behavior was observed between ChCl:U and ChCl: carboxylic acid DES. This difference is possibly due to esterification reaction between the carboxylic groups of citric and succinic acids and the hydroxyl groups of the polysaccharide. In addition, starch granules (5 wt%) were fully dissolved in ChCl:U at 118 °C, in ChCl: citric acid at 120 °C and in ChCl: succinic acid at 135 °C.	[67]
PCH (1:1:1) GCH (2:5:5) LGH (5:1:3) XoCH (1:2:3) ChCl:IM (3:7) G:IM (3:7) G:IM (1:1) CA:IM (3:7) Malonic acid:IM (3:7)	Starch	Test the solubilizing ability of NADES towards starch	The solubility of starch at 100 °C was higher in NADES than in water, and precisely in PCH, GCH and LGH, yielding solutions that remained clear at room temperature.	[8]
ChCl:IM (3:7) G:IM (3:7) G:IM (1:1) CA:IM (3:7) Malonic acid:IM (3:7)	Potato starch and high-amylose starch	Examine starch dissolution in imidazole-based DES	ChCl:IM (3:7) and G:IM (3:7) were able to dissolve up to 20 wt% of starch after 1-h heating at 100 °C. CA:IM and Malonic acid:IM did not dissolve the starch even after 90 min heating at 115 °C.	[69]
ChCl:G (1:8, 1:6, 1:4 and 1:2); ChCl:G (1:2); ChCl:U (1:2); ChCl:S (1:2); ChCl:U (1:2); ChCl:U:G (1:2:2); ChCl:U:G (1:2:2); ChCl:U:S (1:1:1)	Native potato starch; hydroxypropylated and oxidized potato starch	Investigate the use of DES as starch plasticizers	When testing the effect of DES on plasticized starch films properties, crosslinking was detected between hydroxyl groups of the polysaccharide and carboxylic groups of choline citrate used as one of DES components.	[68]
26 DES using lactic acid, malic acid and oxalic acid as HBDs and proline, betaine, ChCl, histidine, glycine and alanine as HBAs	Cellulose	Test the suitability of DES as solvents for lignocellulosic biomass processing	Showing high lignin solubility and poor cellulose solubility, most of the tested solvents are highly selective for the separation of lignin	[77]
Lactic acid: betaine (2:1 and 5:1) Lactic acid: ChCl (2:1, 5:1 and 9:1)	Cellulose and xylan	Pretreatment of rice straw biomass with NADES for lignin extraction and subsequent hydrolysis of the residual polysaccharide fraction towards fermentable sugar production (Solubility of cellulose and xylan in NADES)	A selective solubility of lignin in NADES resulted in the extraction of high purity lignin. On the other hand, cellulose and xylan were not soluble in the studied NADES.	[71]
ChCl:U ChCl:G ChCl:Formic acid ChCl:Acetic acid 1:2 ChCl:Oxalic acid ChCl:Malonic acid ChCl:Citric acid 1:1	Cellulose	Pretreating corn stover with DES to improve cellulose accessibility for biobutanol fermentation	Acidic DES showed good performance in corn stover pretreatment, unlike ChCl:U and ChCl:G. However, as the number of carboxylic groups and the chain length both increased, the concentration of glucose (obtained by cellulose hydrolysis) decreased. Thus, ChCl:formic acid was the best DES for corn stover pretreatment, improving cellulose accessibility by removing hemicellulose and lignin.	[70]
ChCl:U (1:2) ChCl:TU (1:2) Choline Bromide:U (1:2) Chlorocholine chloride: U (1: 2) Betaine hydrochloride: U (1: 4)	$\alpha$ -Chitin	Examine $\alpha$ -chitin dissolution in DES via conventional heating, heating under microwave irradiation and heating assisted by ultrasonication	$\alpha$ -Chitin was best dissolved in ChCl:TU with 9% w/w dissolution upon heating for 6 h at 100 °C. Analysis of $\alpha$ -chitin by several techniques revealed that no chemical and structural degradation of the biopolymer occurred during the dissolution process. Chitosan was not soluble in ChCl:TU suggesting the involvement of acetamide in the dissolution of chitin in DES.	[72]
ChCl:U (1: 2) ChCl:TU (1: 1) ChCl:G (1: 2) ChCl:Malonic acid (1: 2)	Chitin	Extraction of chitin from lobster shells using four different ChCl-based DES	The use of DES is a green alternative method for chitin extraction from lobster shells. ChCl:Malonic acid (1:2) presented the best extraction yield (20.63 $\pm$ 3.30%) of pure chitin, compared to other DES and even to the conventional chemical procedure (16.53 $\pm$ 2.35%), due to its acidity.	[75]
14 ChCl-based DES with various HBDs (alcohols, carboxylic acids, amines, ...) at a 1:2 M ratio	Chitin	Extraction of chitin from shrimp shells using 14 different ChCl-based DES	ChCl:Malonic acid was the most suitable DES for the extraction of chitin from shrimp shells. The chitin yield at 80 °C and after 12 h (19.41 $\pm$ 1.35%) was greater than the conventional method at 2 h (16.08 $\pm$ 0.57%).	[76]
ChCl:U ChCl:G ChCl:EG 1:2	$\kappa$ -Carrageenan polysaccharide from <i>Kappaphycus alvarezii</i> (red seaweed)	Extraction of $\kappa$ -carrageenan polysaccharide from red seaweed using three common DES and their hydrated forms	Higher extraction yields were obtained with the hydrated DES; the yield was highest (60.25%) when 10% hydrated ChCl:G was used. The extraction efficiency of the hydrated DES is due to choline's high solubility in water, along with electrostatic interactions between the sulfate group attached to the carbon-4 position in the structure of $\kappa$ -carrageenan and the choline cation present in the DES.	[74]
ChCl:EG ChCl:G ChCl: 1,4-butanediol ChCl: 1,6-hexanediol	Chinese yam polysaccharides	Optimization of the DES-based ultrasound-assisted extraction of polysaccharides from Chinese yam	ChCl: 1,4-butanediol presented the highest extraction yield, probably because of its high hydrogen bonding ability and electrostatic interactions with the polysaccharides. The DES	[73]

Table 5 (continued)

DES	Polysaccharide	Aim	Results	Ref
ChCl:1,2-propanediol ChCl:G ChCl:EG ChCl:1,3-butanediol ChCl:1,4-butanediol ChCl:U ChCl:propanedioic acid 1:2	Alginate and fucoidan from <i>Saccharina japonica</i>	Extraction of fucoidan and alginate from brown seaweed using DES combined with subcritical water extraction	molar ratio, the water content and the temperature also affected the extraction efficiency, since they have an impact on the solvent's viscosity. This DES-based method turned out to be better than hot water extraction and water-based ultrasound-assisted extraction considering the extraction yield. The best extraction efficiency was obtained with 1:2 ChCl:G and the optimal conditions were determined. The structural characterization of crude polysaccharide confirmed the presence of fucoidan and alginate.	[35]

CA: citric acid; ChCl: choline chloride; EG: ethylene glycol; G: glycerol; GCH: glucose:choline chloride:water; HBDs: hydrogen bond donors; IM: imidazole; LGH: lactic acid:glucose:water; NADES: natural deep eutectic solvents; PCH: 1,2-Propanediol:choline chloride:water; S: D-Sorbitol; TU: thiourea; U: urea; wt%: weight percent; XoCH: xylitol:xcholine chloride:water.

[76], when extracting chitin from shrimp shells. Choline chloride: malonic acid (1:2) was the most suitable DES for chitin extraction, compared to 13 other choline chloride-based DES. The chitin yield of choline chloride:malonic acid at 80 °C and after 12 h ( $19.41\% \pm 1.35\%$ ) was greater than the conventional method that is based on demineralization using HCl followed by deproteinization by NaOH after 2 h ( $16.08\% \pm 0.57\%$ ) [76].

Therefore, DES are promising solvents in dissolution and extraction of polysaccharides and the choice of the HBD seems to be very important. Yet, more investigations must be conducted to understand the interactions between these solvents and different biopolymers.

## 6. Conclusions

Being sustainable, cheap and environmentally friendly, deep eutectic solvents have recently gained so much interest compared to highly toxic conventional organic solvents and ionic liquids. Moreover, DES present interesting physico-chemical properties, which can be tailored depending on the choice of DES constituents, the HBA:HBD molar ratio, the temperature and the water content. Hence, numerous applications have been conducted using these solvents. Extraction and solubilization constitute one of the main applications of DES. Since a recent study proved that natural DES might play an important role as a liquid phase for solubilizing poorly water soluble metabolites and macromolecules in living organisms, investigating the use of DES as solvents for biological macromolecules is fundamental. However, the addition of water to the eutectic mixtures must be controlled since water tends to disrupt the DES' network and subsequently change its properties. The effect of water on DES properties and intermolecular network was discussed. DES viscosity and ionic conductivity were highly affected by water addition, unlike their density. Further, water can be a part of DES's supramolecular complex by forming hydrogen bonds with DES components. However, above a certain water content, this complex is disrupted and an aqueous solution of DES free components is obtained. On the other hand, phospholipids form spontaneous vesicles in DES. Besides, promising results were obtained when using DES in biocatalytic reactions, protein and polysaccharide extraction as well as DNA dissolution and stabilization. Although DES are being extensively studied, more investigations must be carried out, given their wide chemical diversity and their potential use as solvents for natural and bioactive molecules.

## Contributors

Tracy El Achkar wrote the manuscript with support from Sophie Fourmentin and Hélène Greige-Gerges. Sophie Fourmentin and Hélène

Greige-Gerges conceived the idea. All authors reviewed the final manuscript.

## Declaration of Competing Interest

Authors declare no conflict of interest.

## Acknowledgements

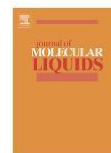
Authors thank the Research Funding Program at the Lebanese University, Lebanon, and the Agence Universitaire de la Francophonie, Moyen-Orient (PCSI project 2018-2020) for funding the project. Tracy El Achkar has received a scholarship from Université du Littoral Côte d'Opale and from Lebanese University.

## References

- [1] A.R.R. Teles, E.V. Capela, R.S. Carmo, J.A.P. Coutinho, A.J.D. Silvestre, M.G. Freire, Solvatochromic parameters of deep eutectic solvents formed by ammonium-based salts and carboxylic acids, *Fluid Phase Equilib.* 448 (2017) 15–21, <https://doi.org/10.1016/j.fluid.2017.04.020>.
- [2] A.P. Abbott, G. Capper, D.L. Davies, R.K. Rasheed, V. Tambyrajah, Novel solvent properties of choline chloride/urea mixtures, *Chem. Commun.* (2003) 70–71, <https://doi.org/10.1039/B210714G>.
- [3] Y.H. Choi, J. van Spronsen, Y. Dai, M. Verberne, F. Hollmann, I.W.C.E. Arends, G.-J. Witkamp, R. Verpoorte, Are natural deep eutectic solvents the missing link in understanding cellular metabolism and physiology? *Plant Physiol.* 156 (2011) 1701–1705, <https://doi.org/10.1104/pp.111.178426>.
- [4] C. Florindo, F.S. Oliveira, L.P.N. Rebelo, A.M. Fernandes, I.M. Marrucho, Insights into the synthesis and properties of deep eutectic solvents based on cholinium chloride and carboxylic acids, *ACS Sustain. Chem. Eng.* 2 (2014) 2416–2425, <https://doi.org/10.1021/sc500439w>.
- [5] Y.P. Mbous, M. Hayyan, A. Hayyan, W.F. Wong, M.A. Hashim, C.Y. Looi, Applications of deep eutectic solvents in biotechnology and bioengineering—promises and challenges, *Biotechnol. Adv.* 35 (2017) 105–134, <https://doi.org/10.1016/j.biotechadv.2016.11.006>.
- [6] M.H. Zainal-Abidin, M. Hayyan, A. Hayyan, N.S. Jayakumar, New horizons in the extraction of bioactive compounds using deep eutectic solvents: a review, *Anal. Chim. Acta* 979 (2017) 1–23, <https://doi.org/10.1016/j.aca.2017.05.012>.
- [7] Q. Zhang, K. De Oliveira Vigier, S. Royer, F. Jérôme, Deep eutectic solvents: syntheses, properties and applications, *Chem. Soc. Rev.* 41 (2012) 7108–7146, <https://doi.org/10.1039/C2CS35178A>.
- [8] Y. Dai, J. van Spronsen, G.-J. Witkamp, R. Verpoorte, Y.H. Choi, Natural deep eutectic solvents as new potential media for green technology, *Anal. Chim. Acta* 766 (2013) 61–68, <https://doi.org/10.1016/j.aca.2012.12.019>.
- [9] M. Espino, M. de los Angeles Fernández, F.J.V. Gomez, M.F. Silva, Natural designer solvents for greening analytical chemistry, *TRAC Trends Anal. Chem.* 76 (2016) 126–136, <https://doi.org/10.1016/j.trac.2015.11.006>.
- [10] Y. Dai, G.-J. Witkamp, R. Verpoorte, Y.H. Choi, Tailoring properties of natural deep eutectic solvents with water to facilitate their applications, *Food Chem.* 187 (2015) 14–19, <https://doi.org/10.1016/j.foodchem.2015.03.123>.
- [11] H. Vanda, Y. Dai, E.G. Wilson, R. Verpoorte, Y.H. Choi, Green solvents from ionic liquids and deep eutectic solvents to natural deep eutectic solvents, *C. R. Chim.* 21 (2018) 628–638, <https://doi.org/10.1016/j.crci.2018.04.002>.

- [12] M.C. Gutiérrez, M.L. Ferrer, C.R. Mateo, F. del Monte, Freeze-drying of aqueous solutions of deep eutectic solvents: a suitable approach to deep eutectic suspensions of self-assembled structures, *Langmuir* 25 (2009) 5509–5515, <https://doi.org/10.1021/la900552b>.
- [13] Y. Dai, J. van Spronsen, G.-J. Witkamp, R. Verpoorte, Y.H. Choi, Ionic liquids and deep eutectic solvents in natural products research: mixtures of solids as extraction solvents, *J. Nat. Prod.* 76 (2013) 2162–2173, <https://doi.org/10.1021/np400051w>.
- [14] M. de los Á. Fernández, J. Boiteux, M. Espino, F.J.V. Gomez, M.F. Silva, Natural deep eutectic solvents-mediated extractions: the way forward for sustainable analytical developments, *Anal. Chim. Acta* 1038 (2018) 1–10, <https://doi.org/10.1016/j.aca.2018.07.059>.
- [15] S.C. Cunha, J.O. Fernandes, Extraction techniques with deep eutectic solvents, *TrAC Trends Anal. Chem.* 105 (2018) 225–239, <https://doi.org/10.1016/j.trac.2018.05.001>.
- [16] K.M. Jeong, J. Ko, J. Zhao, Y. Jin, D.E. Yoo, S.Y. Han, J. Lee, Multi-functioning deep eutectic solvents as extraction and storage media for bioactive natural products that are readily applicable to cosmetic products, *J. Clean. Prod.* 151 (2017) 87–95, <https://doi.org/10.1016/j.jclepro.2017.03.038>.
- [17] F. Pena-Pereira, J. Namieśnik, Ionic liquids and deep eutectic mixtures: sustainable solvents for extraction processes, *ChemSusChem* 7 (2014) 1784–1800, <https://doi.org/10.1002/cssc.201301192>.
- [18] B. Tang, H. Zhang, K.H. Row, Application of deep eutectic solvents in the extraction and separation of target compounds from various samples, *J. Sep. Sci.* 38 (2015) 1053–1064, <https://doi.org/10.1002/jssc.201401347>.
- [19] M. Francisco, A. van den Bruinhorst, M.C. Kroon, Low-transition-temperature mixtures (LTTMs): a new generation of designer solvents, *Angew. Chem. Int. Ed.* 52 (2013) 3074–3085, <https://doi.org/10.1002/anie.201207548>.
- [20] W. Supartono, S. Rückold, H.-D. Isengard, Karl Fischer titration as an alternative method for determining the water content of cloves, *LWT - Food Sci. Technol.* 31 (1998) 402–405, <https://doi.org/10.1006/food.1998.0370>.
- [21] F. Milano, L. Giotta, M.R. Guascito, A. Agostiano, S. Sblendorio, L. Valli, F.M. Perna, L. Cicco, M. Trotta, V. Capriati, Functional enzymes in nonaqueous environment: the case of photosynthetic reaction centers in deep eutectic solvents, *ACS Sustain. Chem. Eng.* 5 (2017) 7768–7776, <https://doi.org/10.1021/acsschemeng.7b01270>.
- [22] C. Du, B. Zhao, X.-B. Chen, N. Birbilis, H. Yang, Effect of water presence on choline chloride-ZnCl<sub>2</sub> ionic liquid and coating platings from the hydrated ionic liquid, *Sci. Rep.* 6 (2016) <https://doi.org/10.1038/srep29225>.
- [23] D. Shah, F.S. Mjalli, Effect of water on the thermo-physical properties of reline: an experimental and molecular simulation based approach, *Phys. Chem. Chem. Phys.* 16 (2014) 23900–23907, <https://doi.org/10.1039/C4CP02600D>.
- [24] C. D'Agostino, L.F. Gladden, M.D. Mantle, A.P. Abbott, E. Ahmed, I. A.Y.M. Al-Murshedi, R.C. Harris, Molecular and ionic diffusion in aqueous – deep eutectic solvents: probing inter-molecular interactions using PGF NMR, *Phys. Chem. Chem. Phys.* 17 (2015) 15297–15304, [doi:https://doi.org/10.1039/C5CP01493J](https://doi.org/10.1039/C5CP01493J).
- [25] T. Zhekenov, N. Toksanbayev, Z. Kazakbayeva, D. Shah, F.S. Mjalli, Formation of type III deep eutectic solvents and effect of water on their intermolecular interactions, *Fluid Phase Equilib.* 441 (2017) 43–48, <https://doi.org/10.1016/j.fluid.2017.01.022>.
- [26] O.S. Hammond, D.T. Bowron, K.J. Edler, The effect of water upon deep eutectic solvent nanostructure: an unusual transition from ionic mixture to aqueous solution, *Angew. Chem. Int. Ed.* 56 (2017) 9782–9785, <https://doi.org/10.1002/anie.201702486>.
- [27] A.P. Abbott, D. Boothby, G. Capper, D.L. Davies, R.K. Rasheed, Deep eutectic solvents formed between choline chloride and carboxylic acids: versatile alternatives to ionic liquids, *J. Am. Chem. Soc.* 126 (2004) 9142–9147, <https://doi.org/10.1021/ja048266j>.
- [28] K. Shahbaz, F.S. Mjalli, M.A. Hashim, I.M. AlNashif, Using deep eutectic solvents based on methyl triphenyl phosphonium bromide for the removal of glycerol from palm-oil-based biodiesel, *Energy Fuel* 25 (2011) 2671–2678, <https://doi.org/10.1021/e12004943>.
- [29] C. D'Agostino, R.C. Harris, A.P. Abbott, L.F. Gladden, M.D. Mantle, Molecular motion and ion diffusion in choline chloride based deep eutectic solvents studied by 1H pulsed field gradient NMR spectroscopy, *Phys. Chem. Chem. Phys.* 13 (2011), 21383, <https://doi.org/10.1039/c1cp22554e>.
- [30] A.P. Abbott, R.C. Harris, K.S. Ryder, C. D'Agostino, L.F. Gladden, M.D. Mantle, Glycerol eutectics as sustainable solvent systems, *Green Chem.* 13 (2011) 82–90, <https://doi.org/10.1039/C0GC00395F>.
- [31] A.P. Abbott, G. Capper, S. Gray, Design of Improved Deep Eutectic Solvents Using Hole Theory, *ChemPhysChem* 7 (2006) 803–806, <https://doi.org/10.1002/cphc.200500489>.
- [32] M.A. Kareem, F.S. Mjalli, M.A. Hashim, I.M. AlNashif, Phosphonium-based ionic liquids analogues and their physical properties, *J. Chem. Eng. Data* 55 (2010) 4632–4637, <https://doi.org/10.1021/jc100104v>.
- [33] A.P. Abbott, R.C. Harris, K.S. Ryder, Application of hole theory to define ionic liquids by their transport properties †, *J. Phys. Chem. B* 111 (2007) 4910–4913, <https://doi.org/10.1021/jp0671998>.
- [34] K. Shahbaz, S. Baroutian, F.S. Mjalli, M.A. Hashim, I.M. AlNashif, Densities of ammonium and phosphonium based deep eutectic solvents: prediction using artificial intelligence and group contribution techniques, *Thermochim. Acta* 527 (2012) 59–66, <https://doi.org/10.1016/j.tca.2011.10.010>.
- [35] P.S. Saravana, Y.-N. Cho, H.-C. Woo, B.-S. Chun, Green and efficient extraction of polysaccharides from brown seaweed by adding deep eutectic solvent in subcritical water hydrolysis, *J. Clean. Prod.* 198 (2018) 1474–1484, <https://doi.org/10.1016/j.jclepro.2018.07.151>.
- [36] D. Mondal, M. Sharma, C. Mukesh, V. Gupta, K. Prasad, Improved solubility of DNA in recyclable and reusable bio-based deep eutectic solvents with long-term structural and chemical stability, *Chem. Commun.* 49 (2013) 9606, <https://doi.org/10.1039/c3cc45849k>.
- [37] H. Zhang, Y. Wang, Y. Zhou, K. Xu, N. Li, Q. Wen, Q. Yang, Aqueous biphasic systems containing PEG-based deep eutectic solvents for high-performance partitioning of RNA, *Talanta* 170 (2017) 266–274, <https://doi.org/10.1016/j.talanta.2017.04.018>.
- [38] N. Li, Y. Wang, K. Xu, Y. Huang, Q. Wen, X. Ding, Development of green betaine-based deep eutectic solvent aqueous two-phase system for the extraction of protein, *Talanta* 152 (2016) 23–32, <https://doi.org/10.1016/j.talanta.2016.01.042>.
- [39] S. Zalba, T.L.M. ten Hagen, Cell membrane modulation as adjuvant in cancer therapy, *Cancer Treat. Rev.* 52 (2017) 48–57, <https://doi.org/10.1016/j.ctrv.2016.10.008>.
- [40] S.J. Bryant, R. Atkin, G.G. Warr, Spontaneous vesicle formation in a deep eutectic solvent, *Soft Matter* 12 (2016) 1645–1648, <https://doi.org/10.1039/C5SM02660A>.
- [41] S.J. Bryant, R. Atkin, G.G. Warr, Effect of deep eutectic solvent nanostructure on phospholipid bilayer phases, *Langmuir* 33 (2017) 6878–6884, <https://doi.org/10.1021/acs.langmuir.7b01561>.
- [42] M. Atilhan, L.T. Costa, S. Aparicio, On the behaviour of aqueous solutions of deep eutectic solvents at lipid biomembranes, *J. Mol. Liq.* 247 (2017) 116–125, <https://doi.org/10.1016/j.molliq.2017.09.082>.
- [43] M.-Y. Lee, J.S. Dordick, Enzyme activation for nonaqueous media, *Curr. Opin. Biotechnol.* 13 (2002) 376–384, [https://doi.org/10.1016/S0958-1669\(02\)00337-3](https://doi.org/10.1016/S0958-1669(02)00337-3).
- [44] B.-P. Wu, Q. Wen, H. Xu, Z. Yang, Insights into the impact of deep eutectic solvents on horseradish peroxidase: activity, stability and structure, *J. Mol. Catal. B Enzym.* 101 (2014) 101–107, <https://doi.org/10.1016/j.molcatb.2014.01.001>.
- [45] Z.-L. Huang, B.-P. Wu, Q. Wen, T.-X. Yang, Z. Yang, Deep eutectic solvents can be viable enzyme activators and stabilizers, *J. Chem. Technol. Biotechnol.* 89 (2014) 1975–1981, <https://doi.org/10.1002/jctb.4285>.
- [46] S. Khodaverdian, B. Dabirmanesh, A. Heydari, E. Dashtban-moghadam, K. Khajeh, F. Ghazi, Activity, stability and structure of lactase in betaine based natural deep eutectic solvents, *Int. J. Biol. Macromol.* 107 (2018) 2574–2579, <https://doi.org/10.1016/j.jbiomac.2017.10.144>.
- [47] J.T. Gorke, F. Srieen, R.J. Kazlauskas, Hydrolase-catalyzed biotransformations in deep eutectic solvents, *Chem. Commun.* (2008) 1235, <https://doi.org/10.1039/b716317g>.
- [48] E. Durand, J. Lecomte, B. Baréa, G. Piombo, E. Dubreucq, P. Villeneuve, Evaluation of deep eutectic solvents as new media for *Candida antarctica* B lipase catalyzed reactions, *Process Biochem.* 47 (2012) 2081–2089, <https://doi.org/10.1016/j.procbio.2012.07.027>.
- [49] H. Monhemi, M.R. Housaindokht, A.A. Moosavi-Movahedi, M.R. Bozorgmehr, How a protein can remain stable in a solvent with high content of urea: insights from molecular dynamics simulation of *Candida antarctica* lipase B in urea: choline chloride deep eutectic solvent, *Phys. Chem. Chem. Phys.* 16 (2014), 14882, <https://doi.org/10.1039/c4cp00503a>.
- [50] H. Zhao, G.A. Baker, S. Holmes, Protease activation in glycerol-based deep eutectic solvents, *J. Mol. Catal. B Enzym.* 72 (2011) 163–167, <https://doi.org/10.1016/j.molcatb.2011.05.015>.
- [51] D. Lindberg, M. de la Fuente Revenga, M. Widersten, Deep eutectic solvents (DESS) are viable cosolvents for enzyme-catalyzed epoxide hydrolysis, *J. Biotechnol.* 147 (2010) 169–171, <https://doi.org/10.1016/j.jbiotec.2010.04.011>.
- [52] A.R. Harifi-Mood, R. Ghobadi, A. Divsalar, The effect of deep eutectic solvents on catalytic function and structure of bovine liver catalase, *Int. J. Biol. Macromol.* 95 (2017) 115–120, <https://doi.org/10.1016/j.jbiomac.2016.11.043>.
- [53] R. Xin, S. Qi, C. Zeng, F.I. Khan, B. Yang, Y. Wang, A functional natural deep eutectic solvent based on trehalose: structural and physicochemical properties, *Food Chem.* 217 (2017) 560–567, <https://doi.org/10.1016/j.foodchem.2016.09.012>.
- [54] A. Sanchez-Fernandez, K.J. Edler, T. Arnold, D. Alba Venero, A.J. Jackson, Protein conformation in pure and hydrated deep eutectic solvents, *Phys. Chem. Chem. Phys.* 19 (2017) 8667–8670, <https://doi.org/10.1039/C7CP00459A>.
- [55] A.A. Papadopoulou, E. Efsthadiou, M. Patila, A.C. Polydera, H. Stamatidis, Deep eutectic solvents as Media for Peroxidation Reactions Catalyzed by Heme-dependent biocatalysts, *Ind. Eng. Chem. Res.* 55 (2016) 5145–5151, <https://doi.org/10.1021/acs.iecr.5b04867>.
- [56] J. Parnica, M. Antalík, Urea and guanidine salts as novel components for deep eutectic solvents, *J. Mol. Liq.* 197 (2014) 23–26, <https://doi.org/10.1016/j.molliq.2014.04.016>.
- [57] Q. Zeng, Y. Wang, Y. Huang, X. Ding, J. Chen, K. Xu, Deep eutectic solvents as novel extraction media for protein partitioning, *Analyst* 139 (2014) 2565, <https://doi.org/10.1039/c3an02235h>.
- [58] K. Xu, Y. Wang, Y. Huang, N. Li, Q. Wen, A green deep eutectic solvent-based aqueous two-phase system for protein extracting, *Anal. Chim. Acta* 864 (2015) 9–20, <https://doi.org/10.1016/j.aca.2015.01.026>.
- [59] Z. Li, Y. Cui, Y. Shen, C. Li, Extraction process of amino acids with deep eutectic solvents-based supported liquid membranes, *Ind. Eng. Chem. Res.* 57 (2018) 4407–4419, <https://doi.org/10.1021/acs.iecr.7b05221>.
- [60] H. Lores, V. Romero, I. Costas, C. Bendicho, I. Lavilla, Natural deep eutectic solvents in combination with ultrasonic energy as a green approach for solubilisation of proteins: application to gluten determination by immunoassay, *Talanta* 162 (2017) 453–459, <https://doi.org/10.1016/j.talanta.2016.10.078>.
- [61] I. Mamajanov, A.E. Engelhart, H.D. Bean, N.V. Hud, DNA and RNA in anhydrous media: duplex, triplex, and G-Quadruplex secondary structures in a deep eutectic solvent, *Angew. Chem.* 122 (2010) 6454–6458, <https://doi.org/10.1002/ange.201001561>.
- [62] J. Bhatt, D. Mondal, G. Bhojani, S. Chatterjee, K. Prasad, Preparation of bio-deep eutectic solvent triggered cephalopod shaped silver chloride-DNA hybrid material having antibacterial and bactericidal activity, *Mater. Sci. Eng. C* 56 (2015) 125–131, <https://doi.org/10.1016/j.msec.2015.06.007>.
- [63] D. Mondal, J. Bhatt, M. Sharma, S. Chatterjee, K. Prasad, A facile approach to prepare a dual functionalized DNA based material in a bio-deep eutectic solvent, *Chem. Commun.* 50 (2014) 3989–3992, <https://doi.org/10.1039/C4CC00145A>.

- [64] C. Mukesh, K. Prasad, Formation of multiple structural formats of DNA in a bio-deep eutectic solvent, *Macromol. Chem. Phys.* 216 (2015) 1061–1066, <https://doi.org/10.1002/macp.201500009>.
- [65] C. Zhao, X. Qu, Recent progress in G-quadruplex DNA in deep eutectic solvent, *Methods* 64 (2013) 52–58, <https://doi.org/10.1016/j.ymeth.2013.04.017>.
- [66] R. Yusof, H. Ahmad, Mohd.B. Abdul Rahman, Studies of interaction between tetrabutylammonium bromide based deep eutectic solvent and DNA using fluorescence quenching method and circular dichroism spectroscopy, *Malays. J. Anal. Sci.* 20 (2016) 1233–1240, <https://doi.org/10.17576/mjas-2016-2006-01>.
- [67] M. Zdanowicz, T. Spychaj, Ionic liquids as starch plasticizers or solvents, *Polimery* (2011) 861–864.
- [68] M. Zdanowicz, C. Johansson, Mechanical and barrier properties of starch-based films plasticized with two- or three component deep eutectic solvents, *Carbohydr. Polym.* 151 (2016) 103–112, <https://doi.org/10.1016/j.carbpol.2016.05.061>.
- [69] M. Zdanowicz, T. Spychaj, H. Mąka, Imidazole-based deep eutectic solvents for starch dissolution and plasticization, *Carbohydr. Polym.* 140 (2016) 416–423, <https://doi.org/10.1016/j.carbpol.2015.12.036>.
- [70] G.-C. Xu, J.-C. Ding, R.-Z. Han, J.-J. Dong, Y. Ni, Enhancing cellulose accessibility of corn stover by deep eutectic solvent pretreatment for butanol fermentation, *Bioresour. Technol.* 203 (2016) 364–369, <https://doi.org/10.1016/j.biortech.2015.11.002>.
- [71] A.K. Kumar, B.S. Parikh, M. Pravakar, Natural deep eutectic solvent mediated pretreatment of rice straw: bioanalytical characterization of lignin extract and enzymatic hydrolysis of pretreated biomass residue, *Environ. Sci. Pollut. Res.* 23 (2016) 9265–9275, <https://doi.org/10.1007/s11356-015-4780-4>.
- [72] M. Sharma, C. Mukesh, D. Mondal, K. Prasad, Dissolution of  $\alpha$ -chitin in deep eutectic solvents, *RSC Adv.* 3 (2013), 18149, <https://doi.org/10.1039/c3ra43404d>.
- [73] L. Zhang, M. Wang, Optimization of deep eutectic solvent-based ultrasound-assisted extraction of polysaccharides from *Dioscorea opposita* Thunb, *Int. J. Biol. Macromol.* 95 (2017) 675–681, <https://doi.org/10.1016/j.jbiomac.2016.11.096>.
- [74] A.K. Das, M. Sharma, D. Mondal, K. Prasad, Deep eutectic solvents as efficient solvent system for the extraction of  $\kappa$ -carrageenan from *Kappaphycus alvarezii*, *Carbohydr. Polym.* 136 (2016) 930–935, <https://doi.org/10.1016/j.carbpol.2015.09.114>.
- [75] P. Zhu, Z. Gu, S. Hong, H. Lian, One-pot production of chitin with high purity from lobster shells using choline chloride–malonic acid deep eutectic solvent, *Carbohydr. Polym.* 177 (2017) 217–223, <https://doi.org/10.1016/j.carbpol.2017.09.001>.
- [76] P.S. Saravana, T.C. Ho, S.-J. Chae, Y.-J. Cho, J.-S. Park, H.-J. Lee, B.-S. Chun, Deep eutectic solvent-based extraction and fabrication of chitin films from crustacean waste, *Carbohydr. Polym.* 195 (2018) 622–630, <https://doi.org/10.1016/j.carbpol.2018.05.018>.
- [77] M. Francisco, A. van den Bruinhorst, M.C. Kroon, New natural and renewable low transition temperature mixtures (LTTMs): screening as solvents for lignocellulosic biomass processing, *Green Chem.* 14 (2012) 2153–2157, <https://doi.org/10.1039/C2GC35660K>.



## First investigation of liposomes behavior and phospholipids organization in choline chloride-based deep eutectic solvents by atomic force microscopy



Jad Eid<sup>a,b</sup>, Tracy El Achkar<sup>a,c</sup>, Sophie Fourmentin<sup>c</sup>, H el ene Greige-Gerges<sup>a</sup>, Alia Jrajaj<sup>a,\*</sup>

<sup>a</sup> Bioactive Molecules Research Laboratory, Faculty of Sciences, Lebanese University, Lebanon

<sup>b</sup> Molecular Microbiology and Structural Biochemistry (MMSB), University of Lyon, CNRS UMR 5086, Lyon, France

<sup>c</sup> Unit e de Chimie Environnementale et Interactions sur le Vivant (UCEIV, EA 4492), SFR Condorcet FR CNRS 3417, ULCO, F-59140 Dunkerque, France

### ARTICLE INFO

#### Article history:

Received 2 December 2019

Received in revised form 13 February 2020

Accepted 4 March 2020

Available online 6 March 2020

#### Keywords:

Atomic force microscopy

Deep eutectic solvents

Liposomes

Phospholipids

### ABSTRACT

Deep eutectic solvents (DES) have gained a lot of attention over the past years due to their numerous interesting properties. Despite being massively explored in various domains, there is still a need to understand the phospholipid self-assembly in these rising solvents. The present work aims to examine the phospholipids organization in four choline chloride-based DES (ChCl-DES) via atomic force microscopy (AFM). The effect of choline chloride: urea, choline chloride:glycerol, choline chloride:ethylene glycol, choline chloride:levulinic acid and the aqueous solutions of their individual components on E80 preformed liposomes was appraised for the first time. Lipid vesicles were formed 24 h after dissolving E80 phospholipids in the studied DES and their mean diameter was dependent on the partition coefficient logP of the hydrogen bond donor (HBD) component. When it comes to the effect on preformed liposomes, the size of the adsorbed liposomes was reduced after exposure to DES or to the aqueous solutions of their constituents. Similar results were observed when studying the dimensions of preformed liposomes in the aqueous solutions of DES components over time. However, when incubated in DES, liposomes were converted into supported lipid bilayers (SLB) before their reconstitution into vesicles.

  2020 Published by Elsevier B.V.

### 1. Introduction

Adopted as alternatives to conventional organic solvents and ionic liquids, DES attracted the researchers' attention for being sustainable, tunable and easy to prepare from widely available and cheap starting materials. DES are obtained by simply combining two or three components that are able to self-associate via hydrogen bonds, resulting in a liquid mixture [1]. After being introduced in 2003 by Abbott and co-workers [2], the physicochemical properties and the potential applications of these systems were extensively explored in various domains [1,3]. Most of the DES are prepared using a quaternary ammonium salt

and hydrogen bond donors (HBD) like sugars, amino acids and alcohols. The majority of the studies consider choline chloride-based DES (ChCl-DES). In fact, choline chloride is not only cheap but also non-toxic and biodegradable, as it is approved as a nutritional additive in all species, for being an effective source of choline [4]. Choline chloride:urea (ChCl:U), choline chloride:glycerol (ChCl:G), choline chloride:ethylene glycol (ChCl:EG) are the most studied eutectic mixtures.

Liposomes are spherical vesicles made of one or more phospholipid bilayers, surrounding aqueous compartments. They have long been used as vehicles for many therapeutic compounds and as models of lipid membranes. Making up most of the membrane lipid fraction, a phospholipid consists of one glycerol, two fatty acids, and a phosphate esterified by a polar group. Owing to their amphiphilic nature, these molecules, above a certain concentration, self-organize into lipid vesicles in aqueous media. The adsorption of liposomes on a solid surface has been investigated in literature [5,6]. Supported lipid bilayers (SLB) with a planar structure can be formed by the direct adsorption of lipids on a solid substrate [7] and by a spontaneous rupture of vesicles on solid surface [8]. The vesicles' rupture may occur via different mechanisms [5,8], such as fusion of vesicles that may lead to the coverage of the surface by lipid bilayers, or interaction of vesicles with a particular substrate [8–11].

*Abbreviations:* AFM, atomic force microscopy; ChCl:EG, choline chloride:ethylene glycol; ChCl:G, choline chloride:glycerol; ChCl:Lev, choline chloride:levulinic acid; ChCl:U, choline chloride:urea; ChCl-DES, choline chloride-based deep eutectic solvents; D, mean diameter; DES, deep eutectic solvents; DMPC, 1,2-dimyristoyl-sn-glycero-3-phosphocholine; DPPC, 1,2-dipalmitoyl-sn-glycero-3-phosphocholine; DSPC, 1,2-distearoyl-sn-glycero-3-phosphocholine; H, mean height; HBA, hydrogen bond acceptor; HBD, hydrogen bond donor; PC, phosphatidylcholine; PNP-TR, pyrene-nitride probes triangular cantilevers; POPC, 1-palmitoyl-2-oleoyl-sn-glycero-3-phosphocholine; SLB, supported lipid bilayers; Tm, melting temperature.

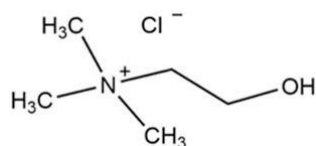
\* Corresponding author at: Department of Physics, Faculty of Sciences, Lebanese University, P.O. Box: 14-6573, Hadath, Lebanon.

E-mail addresses: [ajrajaj@ul.edu.lb](mailto:ajrajaj@ul.edu.lb), [alijrajaj@hotmail.com](mailto:alijrajaj@hotmail.com) (A. Jrajaj).

The phospholipid assembly has been investigated in many non-aqueous but polar solvents, such as glycerol and formamide [12–14]. Few studies investigated the behavior of lipids in DES. They were all presented in our recent review [15]. Bryant et al. investigated the behavior of different phosphatidylcholine lipids in ChCl:U DES. Solvent penetration experiments, paired with polarizing optical microscopy, showed that the DES penetrated the lipids, at ambient temperature (23 °C) and that a non-swelling lamellar phase was formed. Above a certain penetration temperature, a highly swollen and dispersible lamellar phase was formed which spontaneously converted to vesicles few minutes later. Moreover, the chain-melting temperatures increased with the alkyl chain length and saturation of the lipids in the presence of the DES, which is similar to what happens in water. However, the temperature values were higher in DES than in water, which is most probably attributed to the binding of chloride ions to the lipid membrane [16]. After proving that phospholipids self-organize into vesicles in ChCl:U, Bryant et al. tested the behavior of phospholipids, by solvent penetration experiments, in different alkylammonium-based DES using glycerol or ethylene glycol as HBD. The minimum temperature for fluid lamellar phase formation depends on the cation and anion

type in the DES but does not really depend on the HBD type. As in water, melting temperature ( $T_m$ ) in the DES increases with the lipid alkyl chain length. However,  $T_m$  values were higher in DES than in water owing to the stabilization of the ordered phase ( $L_\beta$ ) over the fluid phase ( $L_\alpha$ ) by the cations and anions of the salt [9]. When studying the effect of the anion, alkylammonium bromide-based DES presented higher  $T_m$  than alkylammonium chloride-based ones, owing to a stronger binding of bromide to the quaternary ammonium headgroups of the lipids. The  $L_\alpha$  phase stability strongly depends on the hydrocarbon chain length of the alkylammonium DES cation [17]. Moreover, Gutierrez et al. demonstrated how to go from aqueous chemistry to DES chemistry in order to preserve the membrane-like structure of liposomes in DES (ChCl:U and ChCl:thiourea). Liposomes were prepared by thin film hydration, using 1,2-dimyristoyl-sn-glycero-3-phosphocholine (DMPC) phospholipids. The preformed liposomes were then put in the presence of the aqueous solutions of DES' individual components. Knowing that DES can be obtained by freeze-drying the aqueous solutions of its constituents, the mixture of (water + DES components + liposomes) was freeze-dried. Cryo-etch SEM showed fence-like structures incorporating vesicles. Likewise, vesicles were observed by

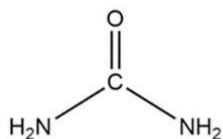
### Hydrogen Bond Acceptor



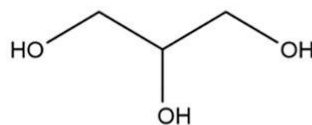
Choline chloride

---

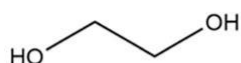
### Hydrogen Bond Donors



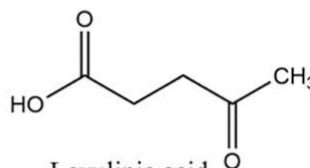
Urea



Glycerol



Ethylene glycol



Levulinic acid

Fig. 1. Structures of the constituents used for DES synthesis (single column figure).

confocal microscopy. These results show that liposomes were incorporated within DES and their membrane-like structure was maintained in these solvents [18].

AFM has been developed mainly as a powerful technique to measure quantitative and qualitative properties by probing different kind of surfaces on the nanometer scale [19]. The application of AFM to biological systems has recently gained a great interest given its ability to image samples in their natural aqueous environment over a wide range of time scales, from milliseconds to hours, and its high resolution performance in visualizing surfaces topologies on the nanometer scale [20–23]. AFM has been used to study the physical characteristics of lipid vesicles [24–26], and visualize 2D and 3D images of the vesicles, to determine their size distribution, their morphology and their stability. AFM allows to image liposomes aggregation and to investigate their surface properties such as rigidity, viscoelasticity, and adhesion [25,27–30]. Furthermore, owing to its high resolution imaging capacity, AFM readily treats the SLB and monolayers [31–33]. Actually, AFM is adopted to assess the instantaneous morphological changes of both liposomes and SLB under various conditions. Several parameters like temperature, pH or salt composition can be modified during the AFM measurements creating defined environments that can modulate the liposomes features [27,34,35].

To the best of our knowledge, no studies regarding the effect of DES or the aqueous solutions of their constituents on the stability of liposomes have been performed to date. In this study, AFM was used to study the behavior of preformed liposomes as well as phospholipids organization in four ChCl-DES and in the aqueous solutions of their constituents. The three most studied DES (ChCl:U, ChCl:G and ChCl:EG) were tested, along with choline chloride:levulinic acid (ChCl:Lev). The structures of the DES' constituents and the main physico-chemical properties are presented in Fig. 1 and Table 1, respectively.

## 2. Materials and methods

### 2.1. Materials

Choline chloride (99%), urea (98%), ethylene glycol (99.5%) and levulinic acid (>98%) were purchased from Acros Organics (Netherlands). Glycerol ( $\geq 99\%$ ) was purchased from Fisher Scientific (UK). Choline chloride was dried at 60 °C for 2 weeks prior to use. All other compounds were used as received. Lipoid E80 (80–85% egg phosphatidylcholine, 7–9.5% phosphatidylethanolamine, 3% lysophosphatidylcholine, 0.5% lysophosphatidylethanolamine, 2–3% sphingomyelin, 2% water, 0.2% ethanol, iodine value 65–69) was obtained from lipoid GmbH (Ludwigshafen, Germany). Ethanol is furnished by Sigma Aldrich (France). Mica sheets (9 mm diameter and 0.1 mm thickness) from Nano and More (France), were used as a substrate in AFM imaging. Pyrex-nitride probes triangular cantilevers PNP-TR, (NanoWord Innovative Technologies, Nano and More, Paris, France) integrating a sharpened pyramidal tip with a radius < 10 nm and a macroscopic half cone 35° angle, were used for liposomes imaging.

### 2.2. Preparation of DES and aqueous solutions of DES constituents

DES were prepared using the heating method, which consists on combining ChCl and the HBD at an appropriate molar ratio, followed

by stirring the mixture at 60 °C until a clear and homogenous liquid is formed. Four ChCl-based solvents were prepared using urea, glycerol, ethylene glycol or levulinic acid as HBD at a HBA:HBD molar ratio of 1:2. The water content of the prepared solvents was determined by a coulometric Karl Fisher titrator (Mettler Toledo DL31). The values of water content vary between 0.05 and 0.33 wt%.

The aqueous solutions of DES constituents were prepared by adding the masses of each individual DES component to water, in which the molar ratio used to prepare the different DES was respected.

### 2.3. Preparation of liposomes

Liposomes were prepared following the ethanol injection method. 500 mg of lipoid E80 were dissolved in 10 ml of ethanol. The obtained organic phase was later injected, using a syringe pump (Fortuna optima, GmbH-Germany), into 20 ml of ultra-pure water, at a flow rate of 1 ml/min, under magnetic stirring at 400 rpm at room temperature. The liposomal suspension was then kept under stirring (400 rpm) for 15 min. Finally, ethanol was removed by rotary evaporation (Heidolph instruments GmbH and co., Germany) at 40 °C and 60 rpm under reduced pressure. The liposomal formulation was stored at 4 °C prior to analysis.

### 2.4. Atomic force microscopy imaging

AFM imaging was performed at room temperature using an Agilent 5420 microscope (Key sight, California, USA) and a pyramidal AFM probe with a 0.08 N/m force constant. All samples were imaged in contact mode with a typical scan rate of 1 Hz, resolution of  $512 \times 512$  pixels per image, scanning angle of 0°, and a set point typically below 0.1 nN to avoid vesicles damage or displacement. Images of  $5 \times 5 \mu\text{m}^2$ ,  $4 \times 4 \mu\text{m}^2$  or  $2 \times 2 \mu\text{m}^2$  were recorded. In this study, the AFM contact mode imaging was used to probe the following samples.

### 2.5. Exposure of adsorbed liposomes to DES and to aqueous solutions of DES components

The liposomal suspension was diluted 10 times in ultrapure water. Then, 50  $\mu\text{l}$  of the diluted suspension was deposited on freshly cleaved mica surface and left for 15 min in air at room temperature; this allows the adsorption of liposomes on the mica surface. The adsorbed liposomes were then exposed to 50  $\mu\text{l}$  of ultrapure water (used as control), 50  $\mu\text{l}$  of each of the studied DES (ChCl:U, ChCl:G, ChCl:EG, ChCl:Lev DES) or 50  $\mu\text{l}$  of the aqueous solutions of DES constituents prepared as described in paragraph 2.2. The exposure stands for 30 min in air for the nine samples. Every mica sheet was rinsed with ultrapure water to remove the non-adsorbed vesicles, and inserted directly (before drying) for imaging. At least 20 images were taken for each analysis and the experiment was repeated at least 2 times.

### 2.6. Incubation of preformed liposomes in DES and in aqueous solutions of DES components

An aliquot of the liposomal suspension was diluted 10 times in water, in DES or in aqueous solutions of DES constituents. The dilution in water was considered as a control. After mixing, 50  $\mu\text{l}$  was removed

**Table 1**  
Main physicochemical properties of the studied DES.

Hydrogen bond acceptor (HBA)	Hydrogen bond donor (HBD)	Abbreviation	Density at 25 °C (g cm <sup>-3</sup> ) [3,36–41]	Viscosity at 25 °C (mPa s) [3,36,38]	Polarity E <sub>T</sub> N [40,42,43]
Choline chloride	Urea	ChCl:U	1.196; 1.240; 1.250	1366; 632; 750	0.81
	Glycerol	ChCl:G	1.190; 1.180; 1.192	360; 376; 259	0.83; 0.84; 0.86
	Ethylene glycol	ChCl:EG	1.115; 1.117; 1.120	40; 36; 37	0.84; 0.82
	Levulinic acid	ChCl:Lev	1.138	270	0.35

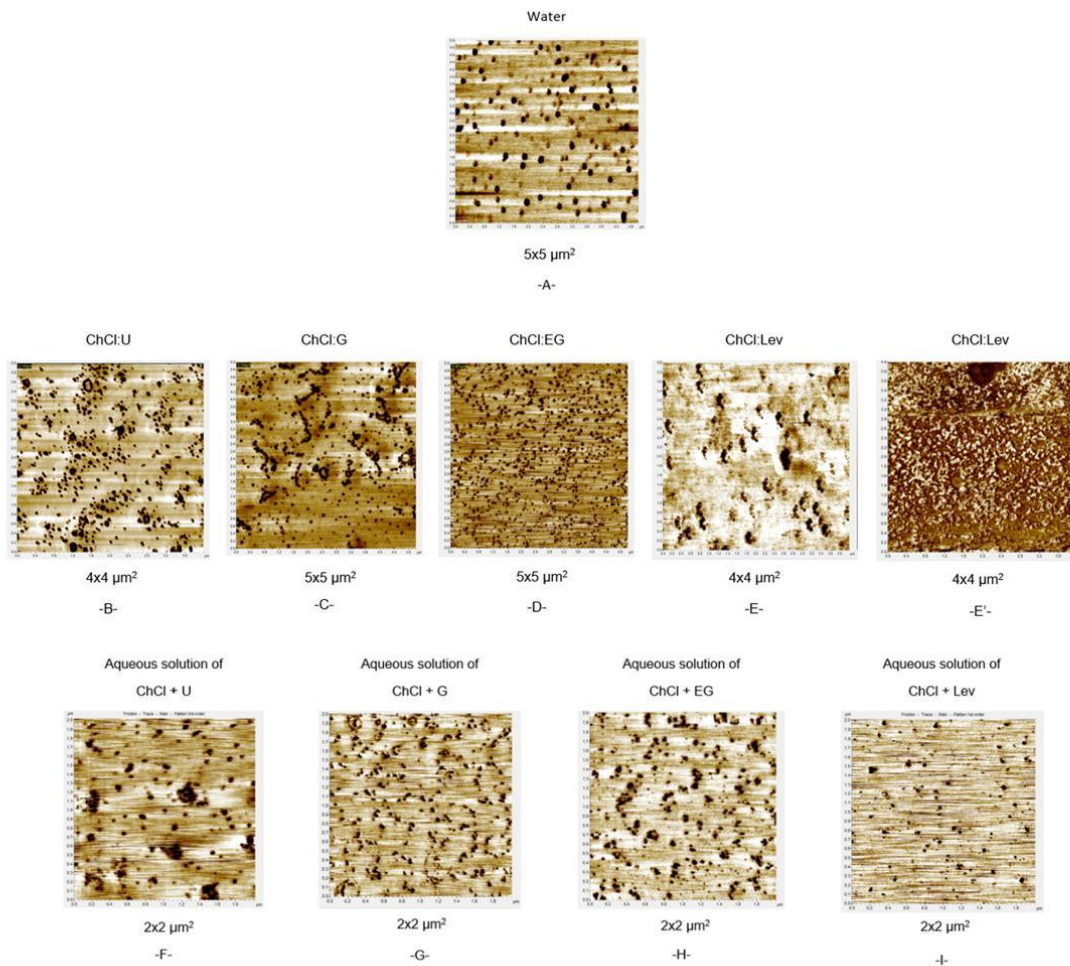


**Fig. 2.** AFM contact mode 2D images of Egg PC liposomes exposed to A- Ultrapure water, B- ChCl:U, C ChCl:G, D- ChCl:EG, E, E' ChCl:Lev F- aqueous solution of ChCl + U, G- aqueous solution of ChCl + G, H- aqueous solution of ChCl + EG, I- aqueous solution of ChCl + Lev (2 column figure).

at different times (5, 60, 80, 100, 120 min, 24 and 48 h), deposited on freshly cleaved mica surface and left for 15 min in air for adsorption at room temperature. Excess vesicles were removed by rinsing the

mica surface with ultrapure water, and then the mica sheet was inserted directly for imaging. For a statistical purpose, 20 images were recorded.

**Table 2**

Mean diameter D and mean height H of Egg PC liposomes exposed to ChCl:U, ChCl:G, ChCl:EG, ChCl:Lev, aqueous solution of ChCl + U, aqueous solution of ChCl + G, aqueous solution of ChCl + EG, and aqueous solution of ChCl + Lev, after 30 min of exposure, determined by AFM using the cross section tool.

Time	DES			
	ChCl:U	ChCl:G	ChCl:EG	ChCl:Lev
30 min	D = 75 ± 15 nm H = 17 ± 3 nm	D = 80 ± 20 nm H = 18 ± 4 nm	D = 60 ± 18 nm H = 16 ± 3 nm	Aggregation and/or SLBs
Time	Aqueous solutions			
	Aqueous solution of ChCl + U	Aqueous solution of ChCl + G	Aqueous solution of ChCl + EG	Aqueous solution of ChCl + Lev
30 min	D = 48 ± 15 nm H = 14 ± 2 nm	D = 45 ± 7 nm H = 14 ± 2 nm	D = 46 ± 6 nm H = 14 ± 2 nm	D = 45 ± 4 nm H = 14 ± 2 nm

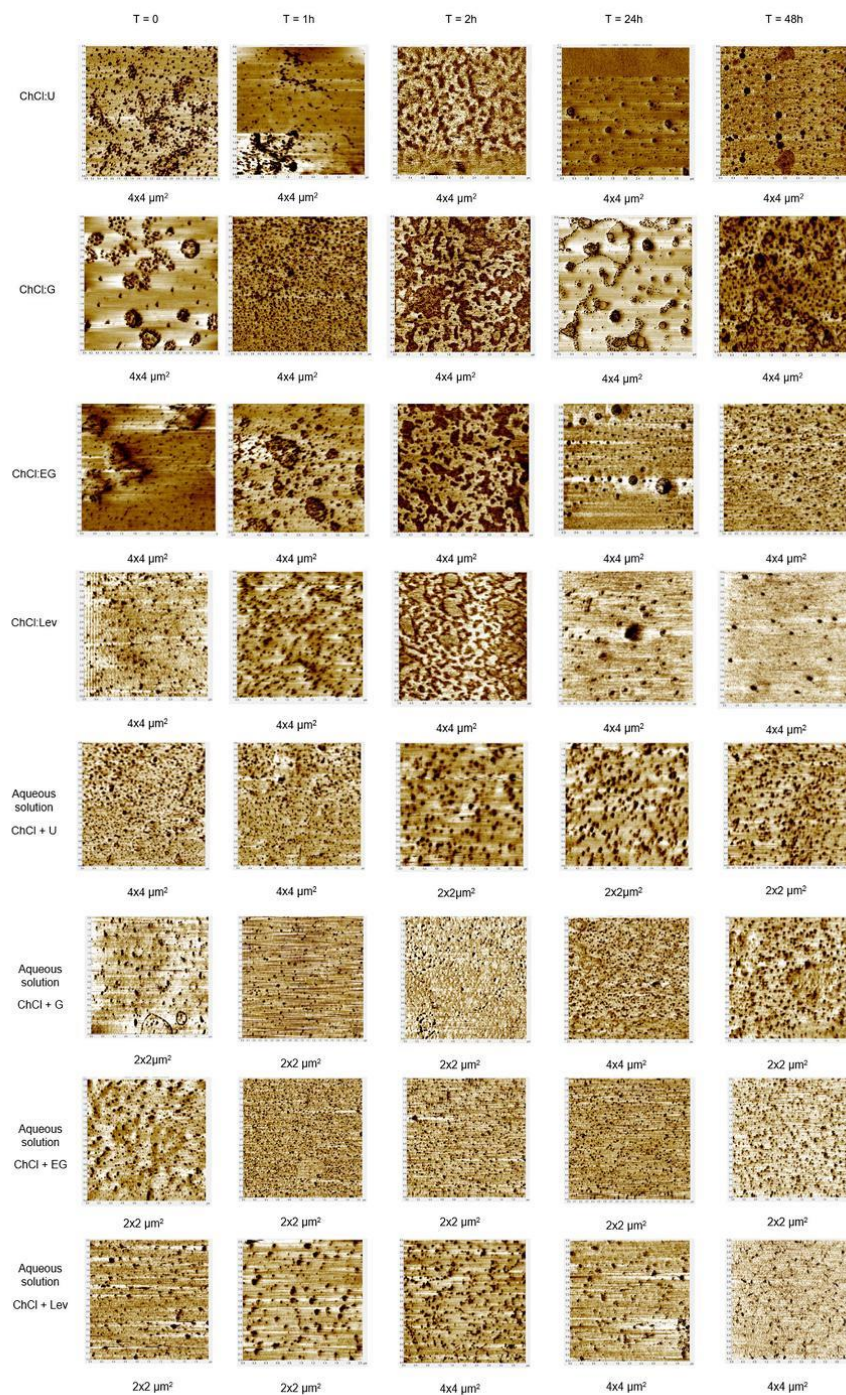


**Fig. 3.** AFM 2D  $4 \times 4$ , and  $2 \times 2$  μm<sup>2</sup> images of EggPC liposomes incubated in ChCl:U, ChCl:G, ChCl:EG, ChCl:Lev, aqueous solution of ChCl + U, aqueous solution of ChCl + G, aqueous solution of ChCl + EG, and aqueous solution of ChCl + Lev, at t = 0, 1, 2, 24, and 48 h, obtained in contact mode (2 column figure).

### 2.7. Phospholipid organization in DES

10 mg of lipid E80 were dissolved in a mixture of DES (1.8 ml) (ChCl:U, ChCl:G, ChCl:EG or ChCl:Lev) and ultrapure water (0.2 ml). Water was added (10% v/v) to imitate the conditions of the experiments executed for preformed liposomes. The obtained mixtures were kept under stirring at room temperature. Aliquots of 50  $\mu$ l were removed at 4, 24 and 48 h and deposited on mica surface for adsorption. The non-adsorbed structures were then removed by rinsing the surface with ultrapure water. Finally, the samples were visualized by AFM, and 20 images were recorded for each analysis and the experiment was repeated at least 2 times.

## 3. Results

### 3.1. Effect of DES on adsorbed liposomes

AFM technique, in contact mode, was first used to study the effect of DES and the aqueous solutions of DES' components on the structure and the morphology of liposomes following their adsorption on mica surface.

Fig. 2 illustrates representative 2D images of the liposomes exposed to water, the four ChCl-DES and the aqueous solutions of ChCl and the appropriate HBD. The average values of the diameter and height of 200 liposomes detected in twenty images were determined using the AFM cross section tool.

Exposed to water, well adsorbed vesicles on the mica substrate were obtained, with a spherical-cap structure and a diameter ranging from 90 to 220 nm (Fig. 2A), with a mean value of  $150 \pm 30$  nm and a height of  $22 \pm 4$  nm.

Exposed to DES (ChCl:U, ChCl:G, ChCl:EG), the adsorbed Egg phosphatidylcholine (Egg PC) liposomes maintained their spherical-cap structures, while their size decreased in comparison with those exposed to water. A different behavior was observed for liposomes exposed to ChCl:Lev. A clear aggregation of liposomes (Fig. 2E), and/or conversion to supported lipid bilayers of  $\sim 7$  nm height (Fig. 2E') were observed.

Exposed to the aqueous solutions of DES constituents, liposomes showed the same behavior as when exposed to DES with additional decrease in the mean dimensions' values; liposomes diameters varied between 30 and 60 nm. The mean diameter D and height H values are presented in Table 2. In contrast to liposomes exposed to ChCl:Lev DES, no aggregation or conversion to SLB was observed for the aqueous

solution containing ChCl and Lev. Also, the liposomes in the four aqueous solutions of DES constituents maintain their spherical-cap shape.

### 3.2. Time-dependent behavior of liposomes in DES media and in aqueous solutions of DES constituents

As mentioned in Section 2.6, the Egg PC liposomal suspension was mixed with water, DES or the aqueous solutions of DES constituents before their deposition on mica surface. The samples were then imaged by AFM in contact mode. The morphology and dimensions (diameter and height) of liposomes were determined after various incubation times (up to 48 h) for the eight samples.

Fig. 3 illustrates AFM 2D images of Egg PC liposomes incubated in the four studied DES, and in the aqueous solutions of DES constituents for 1, 2, 24 and 48 h. The images obtained at other incubation times (1 h 20 min, 1 h 40 min and 4 h) are presented in Fig. S1 (Supplementary material).

AFM images of the suspension composed of DES and liposomes showed well adsorbed liposomes on mica sheets at time  $t = 0$  (Fig. 3). The images present a non-homogeneous dispersion of vesicles on the mica surface. This indicates a non-homogeneity of liposomes distribution within the DES, compared to liposomes in water (figures not shown). In addition, the mean diameter values of liposomes suspended in the studied DES are less than those suspended in water, especially at  $t = 0$  and  $t = 1$  h (Table 3). Aggregation of vesicles started at  $t = 0$  for all the samples and seemed to dominate the images at  $t = 1$  h. Furthermore, complete conversion to SLB ( $\sim 7$  nm of height) was observed at  $t = 2$  h. This indicates that aggregation and/or fusion occurs between  $t = 0$  and  $t = 2$  h, and continues till 4 h (Fig. S1). The time evolution of the liposomes' morphologies in DES between  $t = 1$  h and  $t = 4$  h are shown in Fig. S1 at  $t = 1$  h 20 min, at  $t = 1$  h 40 min, and at  $t = 4$  h. However, a clear reconstitution of liposomes was detected at  $t = 24$  h in all the DES media. The size of the reconstituted liposomes increased over time, and remained stable between 24 and 48 h.

When it comes to liposomes incubated in the aqueous solutions of DES constituents, AFM images show well adsorbed liposomes on mica substrates at 0, 1, 2, 24 and 48 h. In contrast to our findings on liposomes suspended in DES, no aggregation and fusion were detected on the mica substrates. We can only notice spherical-cap structures of liposomes for all the samples at different times; the SLB structures were seemingly absent. Despite the similarity of liposomes morphology compared to water, we noticed a clear decrease in size starting from  $t = 0$  h; while

**Table 3**

Mean diameter D and mean height H of Egg PC liposomes incubated in water, ChCl:U, ChCl:G, ChCl:EG, ChCl:Lev, aqueous solution of ChCl + U, aqueous solution of ChCl + G, aqueous solution of ChCl + EG, and aqueous solution of ChCl + Lev, at  $t = 0, 1, 2, 24,$  and  $48$  h, determined by AFM using the cross section tool.

Solvent	Time (h)				
	0	1	2	24	48
Water	D = $120 \pm 15$ nm H = $21 \pm 3$ nm				
ChCl:U	D = $65 \pm 13$ nm H = $15 \pm 3$ nm	D = $60 \pm 10$ nm H = $14 \pm 3$ nm	SLB	D = $50 \pm 18$ nm H = $15 \pm 3$ nm	D = $80 \pm 20$ nm H = $17 \pm 4$ nm
ChCl:G	D = $80 \pm 8$ nm H = $16 \pm 3$ nm	D = $67 \pm 10$ nm H = $15 \pm 3$ nm	SLB	D = $35 \pm 8$ nm H = $12 \pm 1$ nm	D = $75 \pm 18$ nm H = $14 \pm 2$ nm
ChCl:EG	D = $65 \pm 10$ nm H = $14 \pm 2$ nm	D = $65 \pm 8$ nm H = $15 \pm 3$ nm	SLB	D = $66 \pm 25$ nm H = $17 \pm 3$ nm	D = $80 \pm 18$ nm H = $14 \pm 2$ nm
ChCl:Lev	D = $72 \pm 13$ nm H = $15 \pm 3$ nm	D = $60 \pm 10$ nm H = $14 \pm 3$ nm	SLB	D = $73 \pm 10$ nm H = $14 \pm 2$ nm	D = $90 \pm 20$ nm H = $18 \pm 4$ nm
Aqueous solution of ChCl + U	D = $62 \pm 10$ nm H = $15 \pm 2$ nm	D = $50 \pm 8$ nm H = $14 \pm 2$ nm	D = $47 \pm 8$ nm H = $14 \pm 2$ nm	D = $46 \pm 6$ nm H = $14 \pm 3$ nm	D = $46 \pm 4$ nm H = $14 \pm 2$ nm
Aqueous solution of ChCl + G	D = $55 \pm 13$ nm H = $15 \pm 2$ nm	D = $47 \pm 6$ nm H = $14 \pm 2$ nm	D = $45 \pm 7$ nm H = $14 \pm 2$ nm	D = $44 \pm 6$ nm H = $14 \pm 3$ nm	D = $44 \pm 4$ nm H = $14 \pm 2$ nm
Aqueous solution of ChCl + EG	D = $58 \pm 13$ nm H = $15 \pm 3$ nm	D = $49 \pm 8$ nm H = $14 \pm 2$ nm	D = $46 \pm 7$ nm H = $14 \pm 2$ nm	D = $45 \pm 5$ nm H = $14 \pm 3$ nm	D = $45 \pm 4$ nm H = $14 \pm 2$ nm
Aqueous solution of ChCl + Lev	D = $53 \pm 11$ nm H = $15 \pm 2$ nm	D = $47 \pm 6$ nm H = $14 \pm 2$ nm	D = $45 \pm 6$ nm H = $14 \pm 2$ nm	D = $45 \pm 5$ nm H = $14 \pm 3$ nm	D = $44 \pm 4$ nm H = $14 \pm 2$ nm

some vesicles maintained their initial diameter (~100 nm). Starting from  $t = 1$  h, the decrement of sizes remains stable and liposomes conserve their mean diameter and height values at the different times for all samples, as indicated in Table 3.

### 3.3. Phospholipids organization in the eutectic systems

Lipoid E80 was dissolved in the four ChCl-DES. Aliquots were removed at 4, 24 and 48 h and imaged by AFM in contact mode. Fig. 4

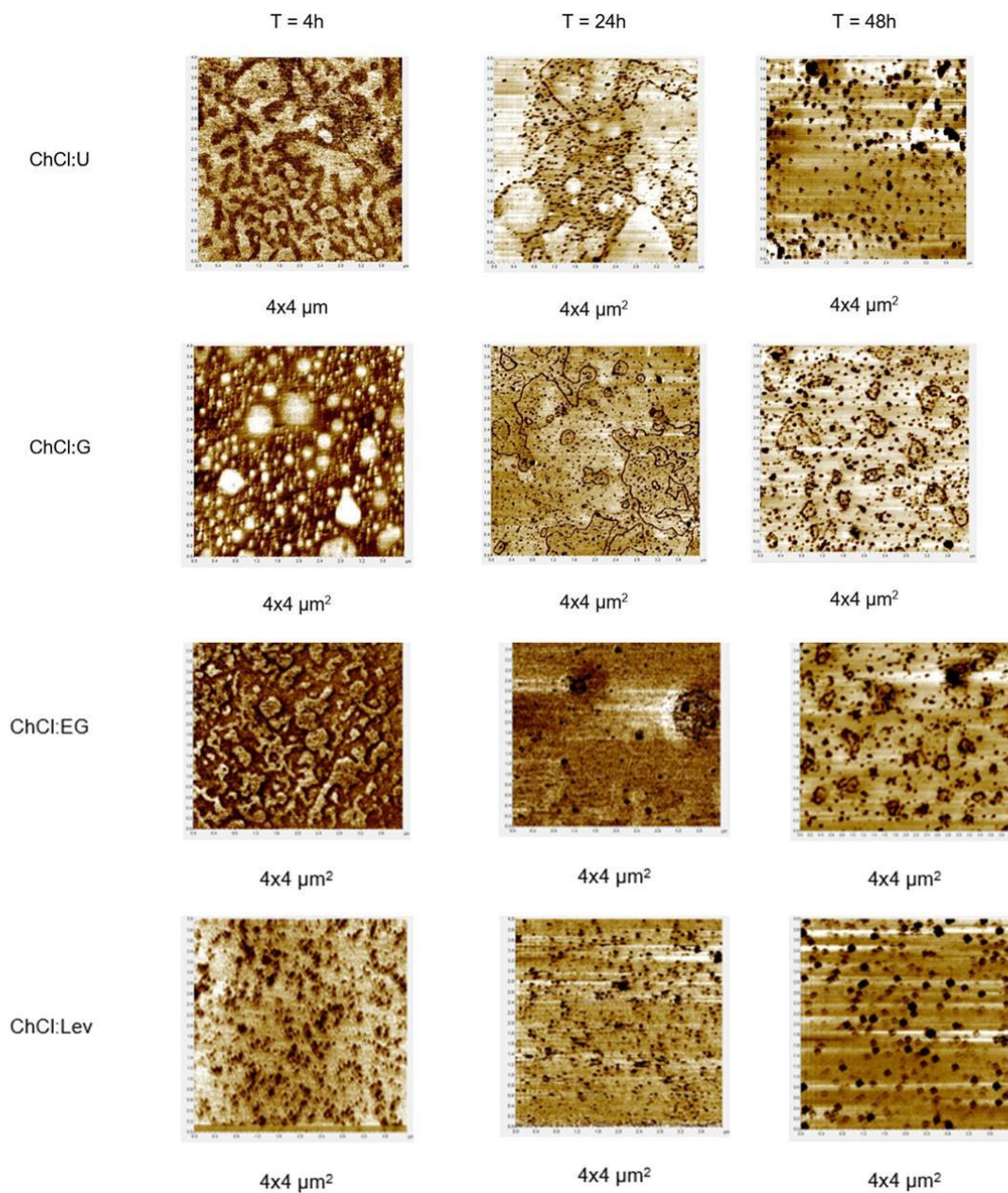


Fig. 4.  $4 \times 4 \mu\text{m}^2$  AFM 2D images of Lipoid E80 within ChCl:U, ChCl:G, ChCl:EG, and ChCl:Lev obtained in contact mode at 4, 24 and 48 h (2 column figure).

illustrates AFM 2D images of the evolution of lipid E80 organization within the four different DES in function of time.

At  $t = 4$  h, lipid bilayers are formed in presence of the three DES ChCl:U, ChCl:G and ChCl:EG and cover the mica substrate, while clear formation of aggregated and separated vesicles was detected in ChCl:Lev DES. At  $t = 24$  h, spherical vesicles and other structures were seen in the four studied DES. At  $t = 48$  h, partial to complete conversion of lipid E80 to stable spherical caps shape was observed in all DES. This conversion seems to be complete and faster in ChCl:Lev DES, followed by ChCl:U DES, then the two other solvents. Such finding is also proven by the increase of the vesicles' diameter with time. Table 4 shows the mean diameter and height values of the vesicles formed in the four DES in function of time.

Taking into account that the size of Egg PC liposomes suspended in water ranged from 80 to 160 nm with a mean size of  $120 \pm 15$  nm and a mean height of  $21 \pm 3$  nm, we can see the formation of Egg PC vesicles in the studied DES (Table 4). Note that the mean size of liposomes formed inside ChCl:Lev or ChCl:U is closer to that of Egg PC liposomes in water. On the other hand, it is obvious that the mean size of the liposomes increases with time; this is accompanied with the simultaneous disappearance of the lipid wires.

#### 4. Discussion

Phospholipids self-assemble in polar solvents due to solvophobic interactions between their hydrocarbon chains and the solvent. For Egg PC, which is a mixture containing 1-palmitoyl-2-oleoyl-sn-glycero-3-phosphocholine (POPC) as its major constituent, the lipid alkyl chain has liquid-like organization at  $23^\circ\text{C}$  [44]. Phospholipids were dissolved within the studied DES, converted into SLB at  $t = 4$  h, then into vesicles at  $t = 24$  h. However, liposomes formation was faster in ChCl:Lev compared to other DES since no SLB were observed at 4 h. Lipid vesicles formation within DES has been also reported by other researchers. Bryant et al. (2016) dissolved four different PC lipids (DMPC, DPPC, DSPC, and EggPC) in ChCl:U, and observed a spontaneous formation of vesicles above the lipid chain melting temperature [16]. The same authors detected the formation of vesicles after dissolving the same phospholipids in alkylammonium-based DES, using G or EG as HBD [45]. The dissolution and organization of lipid molecules within the DES could be explained by an association between chloride and the quaternary ammonium group of phospholipids and between choline of DES salt and the phosphate group of phospholipids. Nevertheless, the viscosity of the solvent does not affect the behavior of phospholipids given that similar results were observed for the most viscous DES (ChCl:U) and the least viscous one (ChCl:EG). The same applies to the density of the tested solvents. In order to understand the rapid formation of vesicles in ChCl:Lev, correlation studies between the mean diameter of the vesicles at 48 h and the DES' or the HBD's properties were conducted, using the experimental values determined in different studies [36,38,42,46]. No correlations were found between the density, viscosity or polarity of the DES and the mean diameter of the vesicles (Fig. S2). However, a correlation was found between the mean diameter of the vesicles and

**Table 4**  
Mean diameter D and height H values of the vesicles formed in ChCl:U, ChCl:G, ChCl:EG, and ChCl:Lev, at 4, 24 and 48 h, obtained by AFM the cross section tool.

DES	Time (h)		
	4	24	48
ChCl:U	SLB	D = $60 \pm 12$ nm H = $16 \pm 3$ nm	D = $77 \pm 11$ nm H = $15 \pm 2$ nm
	SLB	D = $50 \pm 8$ nm H = $12 \pm 1$ nm	D = $78 \pm 12$ nm H = $16 \pm 2$ nm
ChCl:EG	SLB	D = $66 \pm 25$ nm H = $17 \pm 3$ nm	D = $100 \pm 20$ nm H = $20 \pm 4$ nm
		D = $80 \pm 12$ nm H = $14 \pm 2$ nm	D = $140 \pm 20$ nm H = $25 \pm 4$ nm
ChCl:Lev		D = $80 \pm 12$ nm H = $16 \pm 3$ nm	D = $140 \pm 20$ nm H = $25 \pm 4$ nm

$\log P$  of the HBD ( $R^2 = 0.9619$ ) (Fig. 5), unlike the HBD's pKa (Fig. S3). When the HBD is less hydrophilic, larger is the mean diameter of the vesicles.

On the other hand, the effect of DES or the aqueous solutions of DES components was studied on preformed liposomes. Egg PC vesicles showed variations in terms of size and distribution on the mica surface when exposed to DES or aqueous solutions of DES components for 30 min. The reduction of the size of the vesicles in presence of the aqueous solutions of ChCl and the HBD can be explained by the osmosis phenomenon. Given that liposomes are prepared in water using the ethanol injection method, the core-shell lipid structures consist on an internal aqueous cavity surrounded by lipid bilayers. That said, in the presence of aqueous solutions of DES components, inner water molecules tend to migrate through the semipermeable membrane. Likewise, a size reduction was detected in presence of the DES which is also related to osmosis. In fact, two recent studies demonstrated the potential of ChCl:G and ChCl:EG DES as efficient, inexpensive and reusable draw solutions for the enrichment of biomacromolecules or the recovery of water from industrial wastewater, using forward osmosis [47,48]. Additionally, Bubalo et al. (2015) witnessed a decrease in the baker's yeast viability as a result of a high DES content in the medium and explained it by the high osmotic pressure imposed on the yeast cells, leading to the diffusion of water out of the cells [49]. This osmotic potential pushed liposomes to lose their confined water molecules to the surrounding environment, leading to the reduction of their size. Once again, a distinct behavior was noticed for liposomes exposed to ChCl:Lev where a clear aggregation of liposomes and/or conversion to supported lipid bilayers were observed. The distinctive effect of ChCl:Lev compared to the three other DES cannot be explained neither by the density nor the viscosity of the eutectic mixture. Moreover, all four DES are composed of ChCl, the only thing differing is the HBD. That said, if we compare the HBD (urea, glycerol, ethylene glycol and levulinic acid), levulinic acid turns out to be the most hydrophobic one. A hydrophobic compound gives rise to a relatively hydrophobic DES, which probably leads to the dissolution of the bilayer membrane fragments resulting in SLB formation. Thus, in the presence of ChCl:Lev, both osmosis and dissolution may contribute to the SLB formation.

Moreover, the preformed liposomes were also incubated in DES or the aqueous solutions of DES components before their deposition on mica surface and their behavior was followed over time. When incubated in the aqueous solutions of DES constituents, a reduction in the size of the lipid vesicles is detected until  $t = 1$  h, reflecting the progression of the osmosis phenomenon. This behavior was expected since similar observations were seen for adsorbed liposomes exposed to these aqueous solutions. After 2 h in the presence of DES, the mica

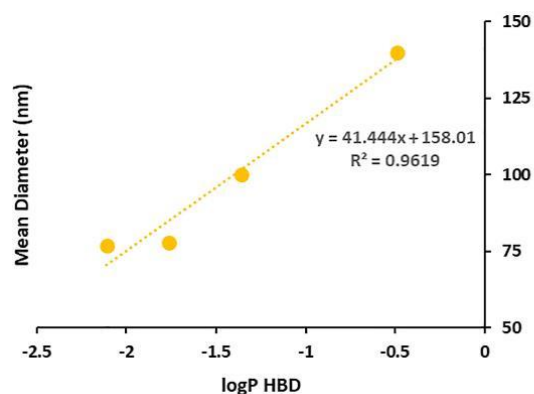


**Fig. 5.** Correlation study between  $\log P$  of the HBD and the mean diameter of the vesicles formed after 48 h of the dissolution of E80 phospholipids in DES (single column figure).

sheets were completely covered by SLB. This is due to osmosis and to eventual aggregation and/or fusion of the vesicles. The SLB formed were not stable and converted into vesicles after 24 h, owing to the solvent encapsulation by the lipid bilayers. The reconstituted liposomes presented an increasing behavior in size with time, which is most probably due to additional lipid molecules joining the liposomal membrane structures. However, no correlation was detected between the mean diameter of the vesicles at 48 h and the properties of the solvents (Fig. S4) or the corresponding HBD (Fig. S5).

## 5. Conclusions

In summary, the present study investigates the organization of phospholipids in four ChCl-DES using AFM technique. It also reveals the effect of DES or the aqueous solutions of their components on preformed liposomes for the first time. The self-assembly of phospholipids in DES leads to the formation of lipid vesicles, that can have a potential application in drug delivery. On the other hand, the size of preformed liposomes decreased after their exposure to the studied DES and their corresponding aqueous solutions due to the osmosis phenomenon. Similar results were obtained when following the effect of the incubation of preformed liposomes in the aqueous solutions of DES components over time. However, when incubated in DES, liposomes converted into SLB after 2 h, preceding their reconstitution into vesicles 24 h later. Once more, results show that DES are promising solvents for the organization of phospholipids. Yet, further studies must be carried out to understand the mechanism behind the phospholipid self-assembly as well as the destruction of preformed liposomes in presence of DES and their reconstitution.

## CRedit authorship contribution statement

**Jad Eid:** Investigation, Writing - original draft. **Tracy El Achkar:** Investigation, Writing - original draft. **Sophie Fourmentin:** Investigation, Writing - original draft. **Hélène Greige-Gerges:** Investigation, Writing - original draft, Conceptualization, Supervision. **Alia Jraji:** Investigation, Writing - original draft, Supervision.

## Declaration of competing interest

The authors declare that they have no known competing financial interests or personal relationships that could have appeared to influence the work reported in this paper.

## Acknowledgements

Authors thank Doctor Luca Monticelli for the valuable suggestions on the manuscript, the Research Funding Program at the Lebanese University and the Agence Universitaire de la Francophonie (PCSI project 2018–2020) for funding the project and providing a scholarship to Jad Eid. We thank also the Lebanese University and the Université du Littoral Côte d'Opale for the scholarship of Tracy El Achkar.

## Appendix A. Supplementary data

Supplementary data to this article can be found online at <https://doi.org/10.1016/j.molliq.2020.112851>.

## References

- [1] Q. Zhang, K. De Oliveira Vigier, S. Royer, F. Jérôme, Deep eutectic solvents: syntheses, properties and applications, *Chem. Soc. Rev.* 41 (2012) 7108–7146, <https://doi.org/10.1039/C2CS3178A>.
- [2] A.P. Abbott, G. Capper, D.L. Davies, R.K. Rasheed, V. Tambyrajah, Novel solvent properties of choline chloride/urea mixtures, *Chem. Commun.* (2003) 70–71, <https://doi.org/10.1039/B210714G>.
- [3] E.L. Smith, A.P. Abbott, K.S. Ryder, Deep eutectic solvents (DESs) and their applications, *Chem. Rev.* 114 (2014) 11060–11082, <https://doi.org/10.1021/cr300162p>.
- [4] Scientific Opinion on safety and efficacy of choline chloride as a feed additive for all animal species, *EFSA J.* 9 (2011) 2353, <https://doi.org/10.2903/j.efsa.2011.2353>.
- [5] L. Habib, A. Jraji, N. Khreich, C. Charcosset, H. Greige-Gerges, Effect of erythrodil, a natural pentacyclic triterpene from olive oil, on the lipid membrane properties, *J. Membr. Biol.* 248 (2015) 1079–1087, <https://doi.org/10.1007/s00232-015-9821-x>.
- [6] I. Reviakine, A. Brisson, Formation of supported phospholipid bilayers from unilamellar vesicles investigated by atomic force microscopy, *Langmuir* 16 (2000) 1806–1815, <https://doi.org/10.1021/la9903043>.
- [7] J. Jass, T. Tjåhage, G. Puu, From liposomes to supported, planar bilayer structures on hydrophilic and hydrophobic surfaces: an atomic force microscopy study, *Biophys. J.* 79 (2000) 3153–3163, [https://doi.org/10.1016/S0006-3495\(00\)76549-0](https://doi.org/10.1016/S0006-3495(00)76549-0).
- [8] R. Richter, A. Mukhopadhyay, A. Brisson, Pathways of lipid vesicle deposition on solid surfaces: a combined QCM-D and AFM study, *Biophys. J.* 85 (2003) 3035–3047, [https://doi.org/10.1016/S0006-3495\(03\)74722-5](https://doi.org/10.1016/S0006-3495(03)74722-5).
- [9] Z. Lv, S. Banerjee, K. Zagorski, Y.L. Lyubchenko, Supported lipid bilayers for atomic force microscopy studies, in: Y.L. Lyubchenko (Ed.), *Nanoscale Imaging Methods Protoc.*, Springer, New York, NY 2018, pp. 129–143, [https://doi.org/10.1007/978-1-4939-8591-3\\_8](https://doi.org/10.1007/978-1-4939-8591-3_8).
- [10] H.M. Seeger, G. Marino, A. Alessandrini, P. Facci, Effect of physical parameters on the main phase transition of supported lipid bilayers, *Biophys. J.* 97 (2009) 1067–1076, <https://doi.org/10.1016/j.bpj.2009.03.068>.
- [11] A. Charrier, F. Thibaudau, Main phase transitions in supported lipid single-bilayer, *Biophys. J.* 89 (2005) 1094–1101, <https://doi.org/10.1529/biophysj.105.062463>.
- [12] R.V. McDaniel, T.J. McIntosh, S.A. Simon, Nonelectrolyte substitution for water in phosphatidylcholine bilayers, *Biochim. Biophys. Acta BBA - Biomembr.* 731 (1983) 97–108, [https://doi.org/10.1016/0005-2736\(83\)90402-9](https://doi.org/10.1016/0005-2736(83)90402-9).
- [13] T.J. McIntosh, A.D. Magid, S.A. Simon, Range of the solvation pressure between lipid membranes: dependence on the packing density of solvent molecules, *Biochemistry* 28 (1989) 7904–7912, <https://doi.org/10.1021/bi00445a053>.
- [14] F. Gayet, J.-D. Marty, A. Brület, N.L. Viguier, Vesicles in ionic liquids, *Langmuir* 27 (2011) 9706–9710, <https://doi.org/10.1021/la2015989>.
- [15] T. El Achkar, S. Fourmentin, H. Greige-Gerges, Deep eutectic solvents: an overview on their interactions with water and biochemical compounds, *J. Mol. Liq.* 288 (2019), 111028, <https://doi.org/10.1016/j.molliq.2019.111028>.
- [16] S.J. Bryant, R. Atkin, G.G. Warr, Spontaneous vesicle formation in a deep eutectic solvent, *Soft Matter* 12 (2016) 1645–1648, <https://doi.org/10.1039/C5SM02660A>.
- [17] S.J. Bryant, R. Atkin, G.G. Warr, Effect of deep eutectic solvent nanostructure on phospholipid bilayer phases, *Langmuir* 33 (2017) 6878–6884, <https://doi.org/10.1021/acs.langmuir.7b01561>.
- [18] M.C. Gutiérrez, M.L. Ferrer, C.R. Mateo, F. del Monte, Freeze-drying of aqueous solutions of deep eutectic solvents: a suitable approach to deep eutectic suspensions of self-assembled structures, *Langmuir* 25 (2009) 5509–5515, <https://doi.org/10.1021/la900552b>.
- [19] G. Binnig, C.F. Quate, Ch. Gerber, Atomic force microscope, *Phys. Rev. Lett.* 56 (1986) 930–933, <https://doi.org/10.1103/PhysRevLett.56.930>.
- [20] B. Ruozzi, G. Tosi, M. Tonelli, L. Bondioli, A. Mucci, F. Forni, M.A. Vandelli, AFM phase imaging of soft-hydrated samples: a versatile tool to complete the chemical-physical study of liposomes, *J. Liposome Res.* 19 (2009) 59–67, <https://doi.org/10.1080/08982100802584071>.
- [21] I. Sokolov, CHAPTER 1 atomic force microscopy in cancer cell research, *Cancer Nanotechnology* 1 (2007) 1–17.
- [22] H. Uehara, T. Osada, A. Ikai, Quantitative measurement of mRNA at different loci within an individual living cell, *Ultramicroscopy* 100 (2004) 197–201, <https://doi.org/10.1016/j.ultramicro.2004.01.014>.
- [23] S. Vahabi, B. Nazemi Salman, A. Javanmard, Atomic force microscopy application in biological research: a review study, *Iran. J. Med. Sci.* 38 (2013) 76–83.
- [24] R.W. Storrs, F.D. Tropper, H.Y. Li, C.K. Song, J.K. Kuniyoshi, D.A. Sipkins, K.C.P. Li, M.D. Bednarski, Paramagnetic polymerized liposomes: synthesis, characterization, and applications for magnetic resonance imaging, *J. Am. Chem. Soc.* 117 (1995) 7301–7306, <https://doi.org/10.1021/ja00133a001>.
- [25] X. Liang, G. Mao, K.Y. Simon Ng, Probing small unilamellar EggPC vesicles on mica surface by atomic force microscopy, *Colloids Surf. B Biointerfaces.* 34 (2004) 41–51, <https://doi.org/10.1016/j.colsurfb.2003.10.017>.
- [26] O. Et-Thakafy, N. Delorme, C. Gaillard, C. Mériadec, F. Artzner, C. Lopez, F. Guyomarç'h, Mechanical properties of membranes composed of gel-phase or fluid-phase phospholipids probed on liposomes by atomic force spectroscopy, *Langmuir* 33 (2017) 5117–5126, <https://doi.org/10.1021/acs.langmuir.7b00363>.
- [27] J. Sitterberg, M.M. Gaspar, C. Ehrhardt, U. Bakowsky, Atomic force microscopy for the characterization of proteoliposomes, *Methods Mol. Biol. Clifton NJ.* 606 (2010) 351–361, [https://doi.org/10.1007/978-1-60761-447-0\\_23](https://doi.org/10.1007/978-1-60761-447-0_23).
- [28] B. Ruozzi, D. Belletti, A. Tombesi, G. Tosi, L. Bondioli, F. Forni, M.A. Vandelli, AFM, ESEM, TEM, and CLSM in liposomal characterization: a comparative study, *Int. J. Nanomedicine* 6 (2011) 557–563, <https://doi.org/10.2147/IJN.S14615>.
- [29] N.H. Thomson, I. Collin, M.C. Davies, K. Palin, D. Parkins, C.J. Roberts, S.J.B. Tendler, P.M. Williams, Atomic force microscopy of cationic liposomes, *Langmuir* 16 (2000) 4813–4818, <https://doi.org/10.1021/la991256p>.
- [30] A.F. Palmer, P. Wingert, J. Nickels, Atomic force microscopy and light scattering of small unilamellar actin-containing liposomes, *Biophys. J.* 85 (2003) 1233–1247, [https://doi.org/10.1016/S0006-3495\(03\)74559-7](https://doi.org/10.1016/S0006-3495(03)74559-7).
- [31] Y. Fang, J. Yang, Role of the bilayer–bilayer interaction on the ripple structure of supported bilayers in solution, *J. Phys. Chem.* 100 (1996) 15614–15619, <https://doi.org/10.1021/jp961054r>.
- [32] L.K. Tamm, C. Böhm, J. Yang, Z. Shao, J. Hwang, M. Edidin, E. Betzig, Nanostructure of supported phospholipid monolayers and bilayers by scanning probe microscopy,

- Thin Solid Films 284–285 (1996) 813–816, [https://doi.org/10.1016/S0040-6090\(95\)08453-3](https://doi.org/10.1016/S0040-6090(95)08453-3).
- [33] S. Singh, D.J. Keller, Atomic force microscopy of supported planar membrane bilayers, *Biophys. J.* 60 (1991) 1401–1410, [https://doi.org/10.1016/S0006-3495\(91\)82177-4](https://doi.org/10.1016/S0006-3495(91)82177-4).
- [34] Y. Takechi-Haraya, K. Sakai-Kato, Y. Abe, T. Kawanishi, H. Okuda, Y. Goda, Observation of liposomes of differing lipid composition in aqueous medium by means of atomic force microscopy, *Microscopy* 65 (2016) 383–389, <https://doi.org/10.1093/jmicro/dfw011>.
- [35] A. Laouini, C. Jaafar-Maalej, I. Limayem-Blouza, S. Sfar, C. Charcosset, H. Fessi, Preparation, characterization and applications of liposomes: state of the art, *J. Colloid Sci. Biotechnol.* 1 (2) (2012) 147–168, <https://doi.org/10.1166/jcsb.2012.1020>.
- [36] L. Moura, T. Moufawad, M. Ferreira, H. Bricout, S. Tilloy, E. Monflier, M.F. Costa Gomes, D. Landy, S. Fourmentin, Deep eutectic solvents as green absorbents of volatile organic pollutants, *Environ. Chem. Lett.* 15 (2017) 747–753, <https://doi.org/10.1007/s10311-017-0654-y>.
- [37] A.P. Abbott, G. Capper, S. Gray, Design of improved deep eutectic solvents using hole theory, *ChemPhysChem* 7 (2006) 803–806, <https://doi.org/10.1002/cphc.200500489>.
- [38] C. D'Agostino, R.C. Harris, A.P. Abbott, L.F. Gladden, M.D. Mantle, Molecular motion and ion diffusion in choline chloride based deep eutectic solvents studied by 1H pulsed field gradient NMR spectroscopy, *Phys. Chem. Chem. Phys.* 13 (2011), 21383, <https://doi.org/10.1039/c1cp22554e>.
- [39] A.P. Abbott, R.C. Harris, K.S. Ryder, Application of hole theory to define ionic liquids by their transport properties<sup>†</sup>, *J. Phys. Chem. B* 111 (2007) 4910–4913, <https://doi.org/10.1021/jp0671998>.
- [40] A.P. Abbott, R.C. Harris, K.S. Ryder, C. D'Agostino, L.F. Gladden, M.D. Mantle, Glycerol eutectics as sustainable solvent systems, *Green Chem.* 13 (2011) 82–90, <https://doi.org/10.1039/C0GC00395F>.
- [41] K. Shahbaz, S. Baroutian, F.S. Mjalli, M.A. Hashim, I.M. AlNashef, Densities of ammonium and phosphonium based deep eutectic solvents: prediction using artificial intelligence and group contribution techniques, *Thermochim. Acta* 527 (2012) 59–66, <https://doi.org/10.1016/j.tca.2011.10.010>.
- [42] C. Florindo, A.J.S. McIntosh, T. Welton, L.C. Branco, I.M. Marrucho, A closer look into deep eutectic solvents: exploring intermolecular interactions using solvatochromic probes, *Phys. Chem. Chem. Phys.* 20 (2018) 206–213, <https://doi.org/10.1039/C7CP06471C>.
- [43] A. Pandey, R. Rai, M. Pal, S. Pandey, How polar are choline chloride-based deep eutectic solvents? *Phys. Chem. Chem. Phys.* 16 (2013) 1559–1568, <https://doi.org/10.1039/C3CP53456A>.
- [44] Y. Takechi-Haraya, K. Sakai-Kato, Y. Abe, T. Kawanishi, H. Okuda, Y. Goda, Atomic force microscopic analysis of the effect of lipid composition on liposome membrane rigidity, *Langmuir* 32 (2016) 6074–6082, <https://doi.org/10.1021/acs.langmuir.6b00741>.
- [45] S.J. Bryant, R. Atkin, G.G. Warr, Effect of deep eutectic solvent nanostructure on phospholipid bilayer phases, *Langmuir ACS J. Surf. Colloids.* 33 (2017) 6878–6884, <https://doi.org/10.1021/acs.langmuir.7b01561>.
- [46] C. Hansch, A. Leo, D. Hoekman, Exploring QSAR - hydrophobic, electronic, and steric constants, Wash. DC Am. Chem. Soc. (1995) 557.
- [47] D. Mondal, A. Mahto, P. Veerababu, J. Bhatt, K. Prasad, S.K. Nataraj, Deep eutectic solvents as a new class of draw agent to enrich low abundance DNA and proteins using forward osmosis, *RSC Adv.* 5 (2015) 89539–89544, <https://doi.org/10.1039/C5RA20735E>.
- [48] A. Mahto, D. Mondal, V. Poliseti, J. Bhatt, N.M. R. K. Prasad, S.K. Nataraj, Sustainable water reclamation from different feed streams by forward osmosis process using deep eutectic solvents as reusable draw solution, *Ind. Eng. Chem. Res.* 56 (2017) 14623–14632, <https://doi.org/10.1021/acs.iecr.7b03046>.
- [49] M. Cijetko Bubalo, M. Mazur, K. Radošević, I. Radojčić Redovniković, Baker's yeast-mediated asymmetric reduction of ethyl 3-oxobutanoate in deep eutectic solvents, *Process Biochem.* 50 (2015) 1788–1792, <https://doi.org/10.1016/j.procbio.2015.07.015>.

## COMMUNICATION



## Cyclodextrins: from solute to solvent†

Cite this: *Chem. Commun.*, 2020, 56, 3385

Received 17th January 2020,  
Accepted 14th February 2020

DOI: 10.1039/d0cc00460j

rsc.li/chemcomm

Tracy El Achkar,<sup>ib ab</sup> Tarek Moufawad,<sup>ib a</sup> Steven Ruellan,<sup>ib a</sup> David Landy,<sup>ib a</sup> H el ene Greige-Gerges,<sup>ib b</sup> and Sophie Fourmentin<sup>ib \*a</sup>

**A supramolecular solvent based on cyclodextrin (CD) is presented here for the first time. Indeed, a low melting mixture was obtained by mixing levulinic acid and a CD derivative, which retained its inclusion ability in the resulting solvent. This new system gives rise to a new family of solvents that could be called SUPRADES (supramolecular deep eutectic solvents).**

Cyclodextrins (CD) are a well-known family of cyclic oligosaccharides obtained from the enzymatic degradation of starch.<sup>1,2</sup> Native CDs typically contain six ( $\alpha$ -CD), seven ( $\beta$ -CD) or eight ( $\gamma$ -CD) D-glucopyranose units, bound by  $\alpha$ -(1–4) linkages. They possess a truncated conical structure with different cavity sizes (Fig. 1).

Their relatively hydrophobic cavity associated to the hydrophilic outer surface, enables them to form inclusion complexes in aqueous solution with a wide range of molecules of low hydrophilicity and suitable geometrical size through noncovalent host–guest interactions. Hence, CD can find applications in numerous domains like pharmaceuticals, cosmetics, food, catalysis or environmental protection.<sup>3–8</sup> Such inclusion complexes have been extensively studied in aqueous solutions.<sup>9–12</sup> However, few examples of inclusion complexes formation were reported in water in combination with a co-solvent<sup>13,14</sup> or in organic solvents.<sup>15</sup>

Deep eutectic solvents (DES) are a new generation of green solvents reported for the first time in 2003.<sup>16</sup> The term DES is commonly used to describe low melting point liquids formed by combining organic salts and hydrogen-bond donor (HBD) components. The most studied salt is choline chloride (ChCl). It is often associated with urea (U) or carboxylic acids (e.g. levulinic acid) or alcohols (e.g. glycerol or ethylene glycol).<sup>17</sup>

Thereafter, DES composed of natural primary metabolites such as sugars, sugar alcohols, organic acids, amino acids and amines were described and named NADES (natural deep eutectic solvents).<sup>18</sup> These NADES could also be obtained from non-ionic compounds.<sup>19,20</sup>

Some recent works investigated the possibility to combine the properties of CD and DES. Namely, we recently patented the use of DES as absorbent for volatile organic compounds (VOC). In this patent, we described for the first time the solubilization of CD in the DES choline chloride:urea (ChCl:U) and its effect on VOC solubility.<sup>21</sup> At the same time, a paper investigated the solubilization of native CD in ChCl:U. Authors were able to solubilize 50 wt% of  $\beta$ -CD (the least water soluble native CD with a solubility of 1.85 g/100 mL) in this DES.<sup>22</sup> Other findings underlined that methyl- $\beta$ -CD acted as a booster for the extraction of polyphenols when incorporated into DES but no evidence of inclusion complexes were reported.<sup>23</sup> Thereafter, we investigated the complexation ability of several native and substituted cyclodextrins solubilized in ChCl:U towards VOC by static-headspace gas chromatography (SH-GC). We observed higher solubilization of the studied VOC in the DES after addition of CD. We were also able to determine the formation constants for the CD/VOC complexes in the DES. These values were lower than the formation constants determined in water. Interestingly, the selectivity of the different CD toward the various guests was preserved in ChCl:U.<sup>24</sup> Additionally, a direct proof of inclusion complexes formation in the DES media was recently obtained by

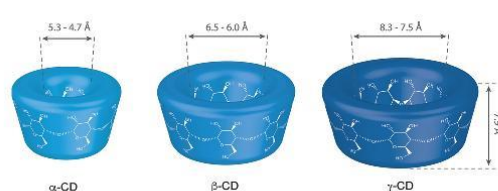


Fig. 1 Representation of chemical structure and dimensions of  $\alpha$ -,  $\beta$ - and  $\gamma$ -cyclodextrins.

<sup>a</sup> Unit e de Chimie Environnementale et Interactions sur le Vivant (UCEIV, UR 4492), SFR Condorcet FR CNRS 3417, ULCO, F-59140 Dunkerque, France.  
E-mail: lamotte@univ-littoral.fr

<sup>b</sup> Bioactive Molecules Research Laboratory, Faculty of Sciences, Lebanese University, Lebanon

† Electronic supplementary information (ESI) available. See DOI: 10.1039/d0cc00460j

## Communication

## ChemComm

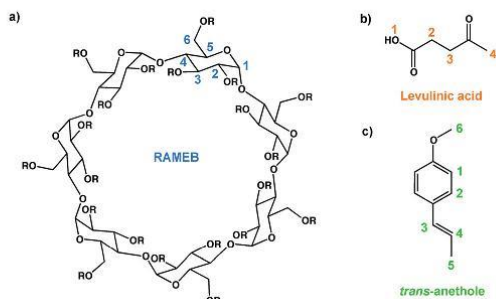


Fig. 2 (a) General structure of randomly methylated- $\beta$ -cyclodextrin (RAMEB, DS = 12.9 and R = -H or -CH<sub>3</sub>), (b) levulinic acid and (c) *trans*-anethole.

NMR for piroxicam<sup>25</sup> and VOC.<sup>26</sup> In all these studies, CD were dissolved in the DES already prepared.

Few studies reported the formation of low melting mixtures (LMM) with CD derivatives and *N,N'*-dimethylurea (DMU). These solvents, based on CD, found applications in hydroformylation, Tsuji–Trost as well as Diels–Alder reactions.<sup>27–29</sup> However, as the melting point of these LMM was superior to 80 °C, they displayed a limited scope of applications apart from catalysis. Melting point values above 60 °C were also obtained in the case of various LMM based on sugar and urea or DMU.<sup>30</sup>

Herein, we report for the first time the preparation of a LMM based on a  $\beta$ -CD derivative (randomly methylated  $\beta$ -CD, RAMEB) and levulinic acid (Fig. 2).

RAMEB is manufactured on an industrial scale and often used in pharmaceutical products<sup>9</sup> while levulinic acid is a renewable platform chemical. Since levulinic acid is known to form DES with ChCl as DMU and U do, we mixed RAMEB and levulinic acid in the same proportion (30% of CD) used for the preparation of the already described LMM to prepare the new solvent.<sup>27</sup> Interestingly, we obtained a clear homogeneous liquid at room temperature. Density, viscosity and water content were then determined at different temperatures (Table 1 and Table S1, ESI<sup>†</sup>). Differential scanning calorimetry (DSC) analysis was also carried out. No melting point was observed for the liquid solvent. However, we obtained a glass transition at a low temperature (Table 1 and Fig. S1, ESI<sup>†</sup>), indicating that this solvent presents a liquid status over a wide temperature range.

The new solvent RAMEB:Lev was used to solubilize *trans*-anethole (AN) chosen as a model compound. Using SH-GC, we could observe a 1300 fold increase in AN solubility when compared to AN solubility in water. It is known that AN can form an inclusion complex with RAMEB in aqueous solution,<sup>10</sup> resulting in a significant, but lower, 17 fold increase in AN solubility.<sup>31</sup>

Table 1 Characterization of the new solvent

Solvent	Viscosity $\eta$ (mPa s) at 30 °C	Density $\rho$ (kg m <sup>-3</sup> ) at 30 °C	%water	$T_g$ (°C)
RAMEB:Lev	212.9	1184.5	2.5	-74.3

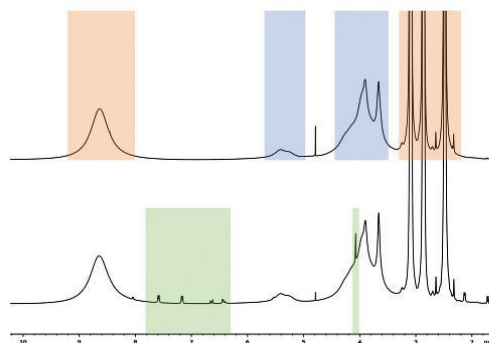


Fig. 3 NMR spectra of RAMEB:Lev (top) and RAMEB:Lev in the presence of *trans*-anethole (bottom). (Blue box, peaks related to RAMEB; orange box, peaks related to levulinic acid and green box, peaks related to *trans*-anethole.)

In order to afford a direct evidence of inclusion complex formation by 2D ROESY NMR spectroscopy, we began by characterizing the solvent by <sup>1</sup>H NMR in order to identify the peaks of each partner. Fig. 3 displays the NMR spectra of RAMEB:Lev (top) and RAMEB:Lev after addition of AN (bottom). Even if the viscosity of the solvent hinders the acquisition of well-defined NMR spectra, peak attribution could be achieved by analogy to the NMR spectrum of RAMEB in D<sub>2</sub>O.<sup>32</sup>

In aqueous solution, the proof of inclusion complex formation could be obtained by titration experiments with various CD concentrations using various analytical techniques (UV-visible, Isothermal Titration Calorimetry or NMR) or by 2D ROESY NMR experiment. Since CD is a component of the solvent in this study, the only way to prove the inclusion of AN in the CD cavity is to perform a 2D ROESY NMR experiment.

Fig. 4 shows a section of the contour plot of the ROESY spectrum of AN in the RAMEB:Lev solvent. Significant correlation

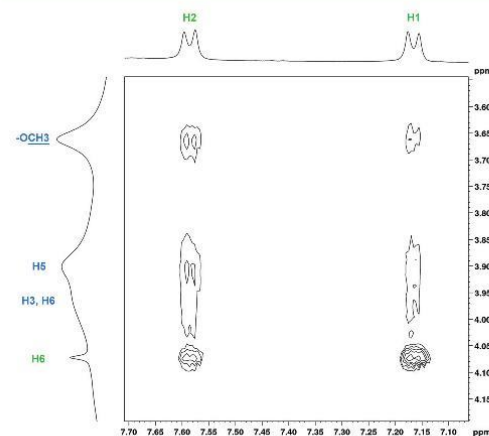


Fig. 4 ROESY spectrum of RAMEB/AN complex in RAMEB:Lev solvent (recorded with a D<sub>2</sub>O insert).

was observed between H1 and H2 of AN and  $-OCH_3$ , H3 and H5 of RAMEB, the two latter protons being located inside the CD cavity while the methoxy groups are hanging at its periphery. Such correlation indicates that the phenyl ring of AN is located inside the RAMEB cavity, therefore proving that CD, although being used as a component of the solvent and not as a solute, is still able to form inclusion complex with guest molecules.

Generally, hydrogen atoms of CD and guest are affected by the inclusion resulting in the displacement of their chemical shifts ( $\delta$ ) and diffusion coefficients ( $D$ ). In this case, as CD is a component of the solvent, we could only follow the diffusion coefficient variation. Moreover, this method might also be used to determine the kind of system ("water-in-DES" or "DES-in-water") that exists at a given amount of water.<sup>33</sup> Therefore we calculated the diffusion coefficients of the different DES components ( $D_{RAMEB}$  and  $D_{Levulinic\ acid}$ ) as well as that of AN ( $D_{AN}$ ) solubilized in RAMEB:Lev, at different water contents (the diffusion of each compound separately in water was also determined).

Concerning the solvent's components (RAMEB and levulinic acid), we found two well differentiated behaviours depending on the dilution range (Fig. S2, ESI<sup>†</sup>). According to a previous work,<sup>33</sup> we can conclude that above 72 ( $\pm 2$ ) DES wt% the "water-in-DES" system is prevailing and below 72 DES wt% the "DES-in-water" system is the most prominent. The presence of AN did not modify these observations for the two components of the solvent (Fig. 5).

Above DES content of 72 wt%, we found similar diffusion values for levulinic acid and AN, while RAMEB presented lower diffusion values. This observation is coherent with the molecular weight of the various compounds. For DES content lower than 72 wt%, the diffusion of AN followed the diffusion of RAMEB, while that of levulinic acid increased more drastically. However, AN present a linear variation of its diffusion coefficient ( $R^2 = 0.992$ ).

Finally, the diffusion coefficient values obtained for the three compounds in water with and without RAMEB are reported in Table 2. As we can see, the diffusion coefficient of AN is strongly impacted by the presence of CD, while only weak difference is observed for levulinic acid. Thus, the formation of a quite stable

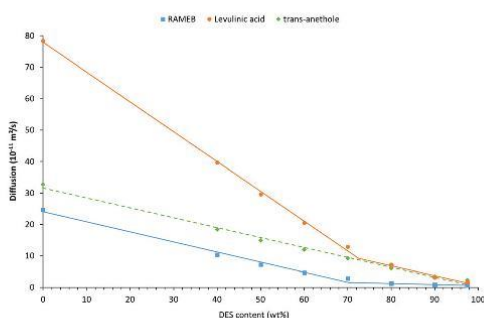


Fig. 5 Plot of diffusion coefficients obtained from NMR spectroscopy versus DES content (in wt%) in DES-H<sub>2</sub>O binary mixtures.

Table 2 Diffusion coefficients ( $D$ ) in water in the absence and in the presence of RAMEB

$D$ ( $10^{-11} \text{ m}^2 \text{ s}^{-1}$ )	RAMEB	Levulinic acid	trans-Anethole
Water	24.7	82.7	73.6
Water + RAMEB		78.4	32.8

inclusion complex RAMEB/AN is proven, while nearly no interaction exists between levulinic acid and RAMEB cavity. Such findings explain the significant difference in the behaviour of AN's and levulinic acid's diffusion coefficient below 72 wt% of DES content.

Therefore, this RAMEB:Lev system is the first example of a LMM solvent with supramolecular properties, thus introducing an emerging class of solvents that could be called SUPRADES. Since the reduction of the use of organic solvents is highly demanded, as it leads to more environmentally benign chemical processes,<sup>34</sup> the high solubilization properties of this new green solvent could be attractive in numerous fields. It can be mainly considered for the extraction of natural products for pharmaceutical and cosmetic applications.

## Conflicts of interest

There are no conflicts to declare.

## Notes and references

- G. Crini, *Chem. Rev.*, 2014, **114**, 10940–10975.
- J. Szejtli, *Chem. Rev.*, 1998, **98**, 1743–1753.
- G. Crini, S. Fourmentin, E. Fenyvesi, G. Torri, M. Fourmentin and N. Morin-Crini, *Environ. Chem. Lett.*, 2018, **16**, 1361–1375.
- P. Blach, S. Fourmentin, D. Landy, F. Cazier and G. Surpateanu, *Chemosphere*, 2008, **70**, 374–380.
- T. Loftsson and M. E. Brewster, *J. Pharm. Sci.*, 1996, **85**, 1017–1025.
- H. M. Cabral-Marques, *Flavour Fragrance J.*, 2010, **25**, 313–326.
- L. Moura, T. Moufawad, M. Ferreira, H. Bricout, S. Tilloy, E. Monflier, M. F. Costa Gomes, D. Landy and S. Fourmentin, *Environ. Chem. Lett.*, 2017, 747–753.
- S. Tilloy, E. Genin, F. Hapiot, D. Landy, S. Fourmentin, J.-P. Genet, V. Michelet and E. Monflier, *Adv. Synth. Catal.*, 2006, **348**, 1547–1552.
- P. Saokham, C. Muankaew, P. Jansook and T. Loftsson, *Molecules*, 2018, **23**, 1–15.
- M. Kfoury, L. Auezova, H. Greige-Gerges, S. Ruellan and S. Fourmentin, *Food Chem.*, 2014, **164**, 454–461.
- M. Kfoury, L. Auezova, H. Greige-Gerges and S. Fourmentin, *Environ. Chem. Lett.*, 2019, **17**, 129–143.
- P. Mura, *J. Pharm. Biomed. Anal.*, 2014, **101**, 238–250.
- C. Rungnim, S. Phunpee, M. Kunaseth, S. Namuangruk, K. Rungsardthong, T. Rungrotmongkol and U. Ruktanonchai, *Beilstein J. Org. Chem.*, 2015, **11**, 2306–2317.
- M. Kfoury, C. Geagea, S. Ruellan, H. Greige-Gerges and S. Fourmentin, *Food Chem.*, 2019, **278**, 163–169.
- T. Kida, T. Iwamoto, Y. Fujino, N. Tohnai, M. Miyata and M. Akashi, *Org. Lett.*, 2011, **13**, 4570–4573.
- A. P. Abbott, G. Capper, D. L. Davies, R. K. Rasheed and V. Tambyrajah, *Chem. Commun.*, 2003, 70–71.
- Z. Maugeri and P. Dominguez de Maria, *RSC Adv.*, 2012, **2**, 421–425.
- Y. H. Choi, J. van Spronsen, Y. Dai, M. Verberne, F. Hollmann, I. W. C. E. Arends, G.-J. Witkamp and R. Verpoorte, *Plant Physiol.*, 2011, **156**, 1701–1705.
- Y. Dai, J. van Spronsen, G.-J. Witkamp, R. Verpoorte and Y. H. Choi, *Anal. Chim. Acta*, 2013, **766**, 61–68.
- B. D. Ribeiro, C. Florindo, L. C. Iff, M. A. Z. Coelho and I. M. Marrucho, *ACS Sustainable Chem. Eng.*, 2015, **3**, 2469–2477.

## Communication

## ChemComm

- 21 S. Fourmentin, D. Landy, L. Moura, S. Tilloy, H. Bricout and M. Ferreira, FR3058905A1, 2016.
- 22 J. A. McCune, S. Kunz, M. Olesińska and O. A. Scherman, *Chem. – Eur. J.*, 2017, **23**, 8601–8604.
- 23 V. Athanasiadis, S. Grigorakis, S. Lalas and D. P. Makris, *Biomass Convers. Biorefin.*, 2018, **8**, 345–355.
- 24 T. Moufawad, L. M. Moura, M. Ferreira, H. Bricout, S. Tilloy, E. Monflier, M. C. Gomes, D. Landy and S. Fourmentin, *ACS Sustainable Chem. Eng.*, 2019, **7**, 6345–6351.
- 25 G. C. Dugoni, M. E. Di Pietro, M. Ferro, F. Castiglione, S. Ruellan, T. Moufawad, L. Moura, M. F. C. Gomes, S. Fourmentin and A. Mele, *ACS Sustainable Chem. Eng.*, 2019, **7**, 7277–7285.
- 26 M. E. Di Pietro, G. C. Dugoni, M. Ferro, A. Mannu, F. Castiglione, M. C. Gomes, S. Fourmentin and A. Mele, *ACS Sustainable Chem. Eng.*, 2019, **7**, 17397–17405.
- 27 F. Jérôme, M. Ferreira, H. Bricout, S. Manuel, E. Monflier and S. Tilloy, *Green Chem.*, 2014, **16**, 3876–3880.
- 28 M. Ferreira, F. Jérôme, H. Bricout, S. Manuel, D. Landy, S. Fourmentin, S. Tilloy and E. Monflier, *Catal. Commun.*, 2015, **63**, 62–65.
- 29 G. Imperato, E. Eibler, J. Niedermaier and B. König, *Chem. Commun.*, 2005, 1170–1172.
- 30 C. Ruß and B. König, *Green Chem.*, 2012, **14**, 2969.
- 31 M. Kfoury, D. Landy, L. Auezova, H. Greige-Gerges and S. Fourmentin, *Beilstein J. Org. Chem.*, 2014, **10**, 2322–2331.
- 32 É. Fenyvesi, J. Szemán, K. Csabai, M. Malanga and L. Szente, *J. Pharm. Sci.*, 2014, **103**, 1443–1452.
- 33 M. J. Roldán-Ruiz, R. J. Jiménez-Riobóo, M. C. Gutiérrez, M. L. Ferrer and F. del Monte, *J. Mol. Liq.*, 2019, **284**, 175–181.
- 34 A. Paiva, R. Craveiro, I. Aroso, M. Martins, R. L. Reis and A. R. C. Duarte, *ACS Sustainable Chem. Eng.*, 2014, **2**, 1063–1071.



Contents lists available at ScienceDirect

International Journal of Pharmaceutics

journal homepage: [www.elsevier.com/locate/ijpharm](http://www.elsevier.com/locate/ijpharm)

## New generation of supramolecular mixtures: Characterization and solubilization studies



Tracy El Achkar<sup>a,b</sup>, Leila Moura<sup>a</sup>, Tarek Moufawad<sup>a,c</sup>, Steven Ruellan<sup>a</sup>, Somenath Panda<sup>a</sup>, Stéphane Longuemart<sup>d</sup>, François-Xavier Legrand<sup>e</sup>, Margarida Costa Gomes<sup>c</sup>, David Landy<sup>a</sup>, H  l  ne Greige-Gerges<sup>b</sup>, Sophie Fourmentin<sup>a,\*</sup>

<sup>a</sup> Unit   de Chimie Environnementale et Interactions sur le Vivant (UCEIV, UR 4492), SFR Condorcet FR CNRS 3417, Universit   du Littoral C  te d'Opale, 59140 Dunkerque, France

<sup>b</sup> Bioactive Molecules Research Laboratory, Faculty of Sciences, Lebanese University, 1202 Jdeidet El Metn, Lebanon

<sup>c</sup> Laboratoire de Chimie, ENS Lyon, UMR CNRS 5182, 46 All  e Italie, 69007 Lyon, France

<sup>d</sup> Unit   Dynamique et Structures des Mat  riaux Mol  culaires (UDSMM, EA 4476), Universit   du Littoral C  te d'Opale, 59140 Dunkerque, France

<sup>e</sup> Institut Gallien Paris-Sud, Universit   Paris-Sud, CNRS, Universit   Paris-Saclay, 92290 Ch  tenay-Malabry, France

### ARTICLE INFO

#### Keywords:

Cyclodextrins  
Static headspace-gas chromatography  
Trans-anethole  
Essential oils  
Low melting mixtures

### ABSTRACT

In this work, a series of novel low melting mixtures (LMM) based on cyclodextrins (CD) and levulinic acid and inspired by the deep eutectic solvents (DES), were prepared. These supramolecular mixtures are the first reported CD-based mixtures that are liquid at room temperature. Density, viscosity and rheological measurements as well as differential scanning calorimetry and thermogravimetric analysis were performed to characterize these new LMM. Nuclear magnetic resonance (NMR) spectroscopy was used to monitor their stability. Furthermore, their ability to solubilize *trans*-anethole (AN) and related essential oils were evaluated by static headspace-gas chromatography (SH-GC), in comparison with water. AN was up to 1300 times more soluble in the CD-based LMM than in water. Finally, multiple headspace extraction (MHE) was used to monitor the release of AN from these LMM. After 10 extractions, 20 to 40% of AN was released from the studied LMM, while 70% was released from water. The new CD-based LMM have potential applications for solubilization and delivery of poorly soluble drugs.

### 1. Introduction

Cyclodextrins (CD) are non-toxic cyclic oligosaccharides obtained from the enzymatic degradation of starch (Crini, 2014; Szejtli, 1998). Native CD, which are produced at an industrial scale, consist of six ( $\alpha$ -CD), seven ( $\beta$ -CD) or eight ( $\gamma$ -CD)  $\alpha$ -(1  $\rightarrow$  4) linked D-glucopyranose units. Due to their hydrophobic internal cavity and hydrophilic external surface, these water-soluble molecules have been extensively used to encapsulate hydrophobic and volatile compounds by forming host-guest inclusion complexes (Ciobanu et al., 2013; Kfoury et al., 2019, 2015; Marques, 2010).

$\beta$ -CD is the most studied and most frequently used CD, because of its cheapness and availability. However, it is the least water-soluble of the three native CD. Therefore, various  $\beta$ -CD derivatives have been synthesized and are commercially available. CD and their derivatives have attracted interest for a wide range of applications such as food, agro-chemistry, environmental chemistry, catalysis, cosmetics and

pharmaceutics (Crini et al., 2018; Kurkov and Loftsson, 2013; Landy et al., 2012; Legrand et al., 2009; Loftsson and Masson, 2001; Nguy  n et al., 2017; Potier et al., 2012).

The discovery of deep eutectic solvents (DES) in 2003 was a turning point in the world of green chemistry (Abbott et al., 2003). Since then the publications in this field have increased exponentially. Being easy to prepare from cheap and widely available starting materials, DES have attracted a lot of attention from researchers in the past few years and have found applications in a wide range of domains: metal processing, synthesis, electrochemistry, solubilization of gas and pollutants, extraction of bioactive compounds and as drug solubilization vehicles (El Achkar et al., 2019; Li and Lee, 2016; Mbous et al., 2017; Morrison et al., 2009; Moura et al., 2017; Zhang et al., 2012). These solvents are obtained by mixing two or three compounds that are able to associate, mainly by the formation of hydrogen bonds, at a particular molar ratio to form a clear homogenous liquid with a lower melting point than that of the individual components (Zhang et al., 2012). Among them, DES

\* Corresponding author.

E-mail address: [lamotte@univ-littoral.fr](mailto:lamotte@univ-littoral.fr) (S. Fourmentin).

<https://doi.org/10.1016/j.ijpharm.2020.119443>

Received 10 April 2020; Received in revised form 14 May 2020; Accepted 15 May 2020

Available online 21 May 2020

0378-5173/   2020 Elsevier B.V. All rights reserved.

based on carbohydrates and other primary metabolites have been described lately (Choi et al., 2011). These DES are called natural deep eutectic solvents (NADES). In this respect, cyclodextrins (CD) are potential NADES-forming compounds.

Only a few studies have investigated the combined use of CD and DES. Some studies have evaluated the possibility of forming low melting mixtures (LMM) with CD and *N,N*-dimethylurea (DMU) (Ferreira et al., 2015; Imperato et al., 2005; Jérôme et al., 2014). A LMM was indeed obtained with various CD derivatives. Hydroformylation, Tsuji-Trost and Diels-Alder reactions were efficiently performed in these new solvents with high catalytic activity. However, the melting point of these LMM was superior to 80 °C, limiting their scope of application. Thereafter, we have patented the use of DES for the absorption of volatile organic compounds (VOC) and described the beneficial effect of adding CD on VOC solubility in a choline chloride:urea (ChCl:U) DES (Fournentin et al., 2016). At the same time, a study showing that the solubility of the three native CD was remarkably enhanced in the same DES was published (McCune et al., 2017). Moreover, it was recently reported that no aggregation of  $\beta$ -CD occurred in ChCl:U up to concentrations of 800 mg/mL (Triolo et al., 2020). Methyl- $\beta$ -CD has also been incorporated into aqueous solutions of a DES based on glycerol and glycine and described to improve the extraction of polyphenols (Athanasiadis et al., 2018). Later, we investigated the advantage of combining ChCl:U and CD to solubilize various volatile compounds and demonstrated that CD maintain their host-guest properties in ChCl:U (Di Pietro et al., 2019; Dugoni et al., 2019; Moufawad et al., 2019). Combinations of DES and CD can potentially give rise to highly attractive materials; however, having a solvent based on CD could be even more useful. To this end, we recently reported the first supramolecular mixture based on randomly methylated- $\beta$ -CD (RAMEB) and levulinic acid and showed that RAMEB retained its inclusion properties (El Achkar et al., 2020).

In the present study, three new supramolecular mixtures were prepared using new  $\beta$ -CD derivatives (HP- $\beta$ -CD, CRYSMEB and Captisol®) in addition to RAMEB as hydrogen bond acceptors (HBA) with levulinic acid (Lev) as hydrogen bond donor (HBD) (Fig. 1). Density, viscosity and rheological measurements, differential scanning calorimetry and thermal gravimetric analysis were carried out to characterize these new liquid mixtures. Moreover, their stability was evaluated as a function of time and temperature by NMR. Finally, their ability to solubilize *trans*-anethole (AN), star anise and fennel essential oils was evaluated by static headspace-gas chromatography (SH-GC) and multiple headspace extraction (MHE) was used to monitor the release of AN from these mixtures.

## 2. Experimental section

### 2.1. Materials

*Trans*-Anethole [1-methoxy-4-(1-propenyl)-benzene] (99%) was purchased from Acros Organics, France. Levulinic acid (98%) was purchased from Sigma-Aldrich, France. Randomly methylated- $\beta$ -CD (RAMEB, DS = 12.9), low methylated- $\beta$ -CD (CRYSMEB, DS = 4.9) and hydroxypropyl- $\beta$ -CD (HPBCD, DS = 5.6) were provided by Roquette Frères (Lestrem, France). Sulfobutylether- $\beta$ -CD (Captisol®, DS = 6.5) was provided by LIGAND Pharmaceuticals (San Diego, CA, USA). All compounds were used as received.

Essential oils of *Illicium verum* (star anise) and *Foeniculum vulgare* (fennel) were provided by Herbes et Traditions (Comines, France). The main constituents (> 1%) of the essential oils are: *trans*-anethole (91.07%) and limonene (3.28%) for star anise; *trans*-anethole (75.30%), estragole (3.10%) and fenchone (2.10%) for fennel (data provided by Herbes et Traditions).

### 2.2. Preparation of the supramolecular mixtures

The LMM were prepared by mixing the HBA and the HBD at a fixed molar ratio (Table 1). The mixtures were then stirred at 60 °C until the formation of a clear homogenous liquid then cooled at room temperature. All the prepared mixtures were liquid at room temperature. As CD possess a large number of HBA sites (35 sites for the native  $\beta$ -CD and 35 to 55 sites for the modified  $\beta$ -CD), we used a large molar excess of levulinic acid. The water content of all the prepared mixtures was determined using Karl Fisher titration method (Mettler Toledo DL31) and was found to vary between 2.5 and 3.9 wt% (Table 1).

We should point out that our attempts to obtain liquid mixtures with the three native CD failed, which tends to emphasize that the density and flexibility of the hydrogen bond network are probably key parameters for the formation of liquid mixtures. It seems that the breakdown of hydrogen bonds from one glucose to another within CD molecules could be a prerequisite, therefore limiting the preparation of such LMM to modified CD.

### 2.3. Stability studies of LMM by NMR

In order to evaluate whether any esterification reaction occurred between the remaining hydroxyl groups of the CD derivatives and levulinic acid, the supramolecular mixtures were prepared at 30 °C and were subjected to gradual heating. Aliquots were withdrawn at

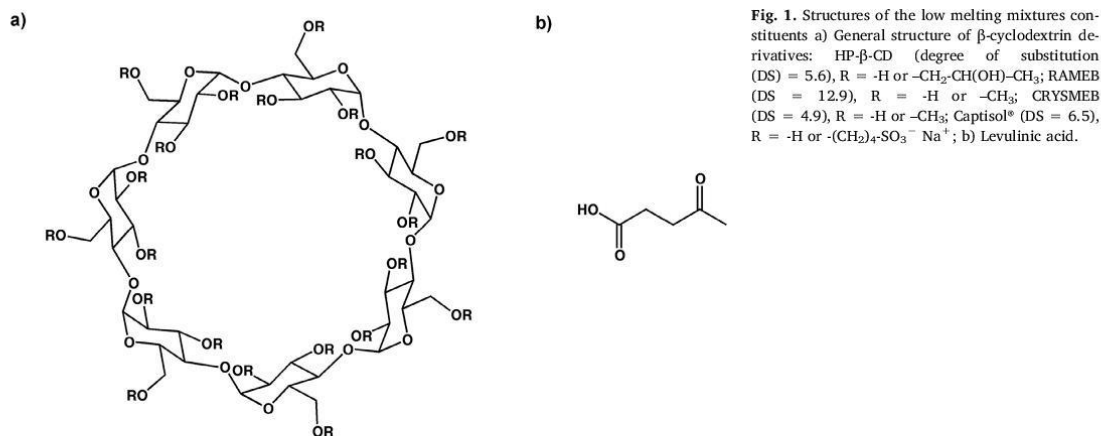


**Table 1**  
Composition and water content of the prepared LMM.

CD:Lev mixture	HBA	HBD	HBA:HBD molar ratio	Water content(wt. %)
HPBCD:Lev	Hydroxypropyl- $\beta$ -CD	Levulinic Acid	1:32	2.7
RAMEB:Lev	Randomly methylated $\beta$ -CD		1:27	2.5
CRYSMEB:Lev	Low methylated $\beta$ -CD		1:25	3.3
Captisol®:Lev	Sulfobutylether- $\beta$ -CD		1:44	3.9

different times and temperatures, then diluted with DMSO- $d_6$ , or CDCl<sub>3</sub>, in the case of Captisol®:Lev, and analyzed by NMR. The first aliquot of the mixture was taken when a clear liquid was formed ( $t_0$ ). The other aliquots were withdrawn at 30, 60, 80 and 100 °C. The mixtures were kept for 24 h at the desired temperature prior to analysis. <sup>13</sup>C NMR experiments were recorded on a Bruker Avance III spectrometer operating at 400 MHz for the proton nucleus, equipped with a multinuclear z-gradient BBFO probe head. The probe temperature was maintained at 30 °C and standard 5 mm NMR tubes were used. <sup>13</sup>C spectra were recorded with the following acquisition parameters: time domain 65 K with a digital resolution of 0.73 Hz, relaxation delay: 2 s and 1536 scans.

#### 2.4. Density and viscosity measurements

Density measurements were carried out using a U-shaped vibrating-tube densimeter (Anton Paar, model DMA 5000 M) operating in a static mode. The factory calibration was used and verified before and after each measurement with air and tri-distilled degassed water. The DMA 5000 densimeter performs an analysis with an estimated uncertainty in density and temperature of  $\pm 0.1 \text{ kg m}^{-3}$  and  $\pm 0.001 \text{ }^\circ\text{C}$ , respectively.

The viscosity was determined using a falling-ball-based microviscosimeter (Lovis 2000 M/ME from Anton Paar). The temperature was controlled to within 0.005 °C and measured with an accuracy better than 0.02 °C. A capillary tube of 1.8 mm diameter, previously calibrated as a function of temperature and angle of measurement with reference oils, was used for the measurements. The overall uncertainty on the viscosity was estimated to be 2%. All measurements were performed at atmospheric pressure and at temperatures ranging between 30 and 60 °C, as previously described (Moufawad et al., 2019).

#### 2.5. Rheological measurements

Rheological measurements were performed with an AR-G2 controlled-stress rotational rheometer (TA Instruments). Flow curves were obtained with an aluminum cone-plate geometry (40 mm diameter, 1° cone angle, 28  $\mu\text{m}$  truncation gap). A three-step shear rate sweep was imposed after a 3-minute equilibration time: 1) increase of the shear rate from 0.1 to 5000  $\text{s}^{-1}$  over 3 min (upwards curve), 2) peak hold at 5000  $\text{s}^{-1}$  during 1 min, 3) decrease of the shear rate from 5000 to 0.1  $\text{s}^{-1}$  over 3 min (downwards curve). The temperature was maintained at 30 °C and controlled with a Peltier plate. Measurements were performed in triplicate at least for each sample, to ensure reproducibility. The statistical analysis was performed by calculating the standard deviation from at least three measurements for each sample.

#### 2.6. Differential scanning calorimetry (DSC)

DSC experiments were carried out using a Q1000 DSC (TA Instruments) with a temperature range from  $-100 \text{ }^\circ\text{C}$  to  $40 \text{ }^\circ\text{C}$  and at a thermal scanning rate of  $5 \text{ }^\circ\text{C}\cdot\text{min}^{-1}$ . All the samples (HPBCD:Lev, RAMEB:Lev, CRYSMEB:Lev and Captisol®:Lev) were encapsulated in aluminum pans (sample weight  $\sim 10\text{--}15 \text{ mg}$ ), sealed with hermetic lids and analyzed. Experiments were performed under nitrogen flow (50  $\text{mL}\cdot\text{min}^{-1}$ ).

#### 2.7. Thermal gravimetric analysis (TGA)

TG measurements were performed with a TGA550 thermogravimetric analyzer (TA Instruments). Samples were placed in an open platinum pan (100  $\mu\text{L}$ ) suspended in the furnace. The initial weight of the sample was around 25–30 mg, and nitrogen was used as the purge gas at a fixed flow of  $20 \text{ mL}\cdot\text{min}^{-1}$ . The weight of material was recorded during heating from room temperature to 600 °C at a heating rate of  $10 \text{ }^\circ\text{C}\cdot\text{min}^{-1}$ .

#### 2.8. Static Headspace-Gas chromatography (SH-GC)

AN, star anise and fennel essential oils (EO) were added to water or to the LMM placed in 22 mL headspace glass vials. Vials were then sealed and thermostated at 30 °C under stirring for 24 h in order to reach equilibrium between liquid and gaseous phases. Subsequently, 1 mL of the gaseous phase was withdrawn from the vial and injected in the chromatographic column for analysis via a heated transfer line.

All experiments were carried out with an Agilent G1888 headspace sampler coupled with a Perkin Elmer Autosystem XL gas chromatography equipped with a flame ionization detector and a DB624 column using nitrogen as carrier gas. The GC column temperature was fixed at 160 °C for AN. For the analysis of EO, temperature conditions were set as follows: initial temperature of 50 °C for 2 min, increased to 200 °C at  $5 \text{ }^\circ\text{C}\cdot\text{min}^{-1}$ , then hold for 2 min, giving a total runtime of 34 min.

##### 2.8.1. Determination of partition coefficient (K)

The vapor–liquid partition coefficient ( $K$ ) is the ratio of the concentration of a substance in vapor phase to its concentration in liquid phase, when the equilibrium is reached (Kolb and Etire, 2006).

$$K = \frac{C_G}{C_L} \quad (1)$$

$K$  of AN was determined in water and in the different supramolecular mixtures at 30 °C by using the phase ratio variation method for AN in water and the vapor phase calibration method for AN in the supramolecular mixtures as reported earlier (Moura et al., 2017).

##### 2.8.2. Retention of AN and essential oils (EO)

The retention of AN, star anise and fennel EO in the formulations was estimated according to procedures developed for aromas (Decock et al., 2008) and EO (Kfoury et al., 2015), respectively. The percentage of retention of AN and EO by the LMM was determined by SH-GC at 30 °C following Eq. (2) for AN and Eq. (3) for EO:

$$\% \text{Retention} = \left(1 - \frac{A_{LMM}}{A_W}\right) \times 100 \quad (2)$$

where  $A_{LMM}$  and  $A_W$  stand for the peak area of AN in presence of LMM and of water, respectively.

$$\% \text{Retention} = \left(1 - \frac{\Sigma A_{LMM}}{\Sigma A_W}\right) \times 100 \quad (3)$$

where  $\Sigma A_{LMM}$  and  $\Sigma A_W$  stand for the sum of peak areas of the EO components in presence of LMM and of water, respectively.

### 2.8.3. Multiple headspace extraction (MHE)

MHE is a quantitative method, consisting of successive headspace extractions (Kolb and Etre, 2006). It was used to study the release kinetics of AN from the prepared LMM at 60 °C. Samples were prepared similarly to the previous experiments but, once equilibrium was reached, vials were subjected to 10 headspace extractions at 1-hour intervals.

## 3. Results and discussion

### 3.1. Stability studies of LMM by NMR

A recent study showed that ChCl:carboxylic acid DES underwent esterification regardless of the method or the temperature employed during their preparation. However, the DES based on levulinic acid was the least affected, with only 6 mol% of the ChCl esterified at 100 °C (Rodríguez Rodríguez et al., 2019). In the present study, the thermal stability of the new supramolecular mixtures was investigated using <sup>13</sup>C NMR, by following the modification of the chemical shift of the carboxylic acid function of levulinic acid. All the supramolecular mixtures were stable after consecutive exposures of 24 h at 30 and 60 °C. After an additional 24 h at 80 °C, a small amount of esterification was observed and identified by the presence of a new broad signal around 173.0 ppm corresponding to the ester function (Fig. S1). No esterification was detected in the case of Captisol®:Lev, which could be due to steric hindrance from the relatively bulky sulfobutyl ether moieties. On the other hand, the most affected LMM was HPBCD:Lev with the relative intensity ratio of the esterified carbon peak being 1.6% of the carboxylic acid carbon peak at 100 °C (Table S1) and could be the result of a higher reactivity of the hydroxyl groups, especially that of the hydroxypropyl moieties. Therefore, the preparation of the LMM was performed at 60 °C for all other experiments, in order to avoid esterification. Furthermore, the long-term stability of the LMM was evaluated after 18 months of storage at room temperature. The mixtures showed no degradation over time. The low esterification ratio observed for these CD-based mixtures compared with ChCl-based DES could be explained by the fact that the remaining hydroxyl groups of the CD derivatives used in this study are sterically hindered since the degree of substitution varied from 4.9 to 12.9.

### 3.2. Physicochemical characterization

The density and viscosity values of the four LMM (HPBCD:Lev, RAMEB:Lev, CRYSMEB:Lev and Captisol®:Lev) were measured from 30 to 60 °C, at 10 °C intervals (Fig. 2 and Tables S2 and S3). CD-based mixtures presented higher density values (ranging between 1184.5 and 1234.3 kg m<sup>-3</sup> at 30 °C) compared with common DES based on

levulinic acid (1134.5 and 1105.7 kg m<sup>-3</sup> at 303.15 K for ChCl:Lev or TBPBr:Lev DES respectively) (Moufawad et al., 2019; Moura et al., 2017). Additionally, the obtained values fall in the 1000–1300 kg m<sup>-3</sup> range of density values observed with most of the reported DES (Tang and Row, 2013). LMM were also more viscous than these common DES, except for RAMEB:Lev which presents similar viscosity to ChCl:Lev (212.9 and 206.2 mPa.s at 30 °C, respectively).

Nevertheless, the viscosity values decreased remarkably with increasing temperature. All CD-based mixtures, except Captisol®:Lev, show relatively low viscosities ( $\leq 80$  mPa.s) at 60 °C. The relatively higher viscosity of Captisol®:Lev can be explained by a stronger hydrogen bond network, given the higher number of HBA sites present in Captisol® compared to the other studied  $\beta$ -CD derivatives due to the presence of the sulfonate groups. In addition, the CD:Lev mixtures were less viscous than the mixtures based on  $\beta$ -CD derivatives and *N,N'*-dimethylurea. Indeed, the latter mixtures present a melting point above 80 °C and their viscosities were at least equal to 205.0 mPa.s at 90 °C (Jérôme et al., 2014).

The flow behavior of the four LMM was then investigated at 30 °C. All the mixtures studied exhibit a Newtonian plateau for shear rates below 1000 s<sup>-1</sup> and shear-thinning behavior for shear rates above this value (Fig. S2). The measured static and dynamic viscosities for the same composition were slightly different (for example, in the case of RAMEB:Lev at 30 °C,  $\eta_{static} = 212.9$  mPa.s vs.  $\eta_{dynamic} = 245.0$  mPa.s) but the same order was found for the viscosities ( $\eta_{Captisol®:Lev} > \eta_{HPBCD:Lev} > \eta_{CRYSMEB:Lev} > \eta_{RAMEB:Lev}$ ). Moreover, the shear-thinning behavior was more pronounced as the viscosity increased. Indeed, for a high shear rate of 5000 s<sup>-1</sup>, a decrease of around 29% in viscosity was observed for Captisol®:Lev, whereas in the case of RAMEB:Lev a smaller decrease (around 8%) was detected. As explained above, the most viscous mixtures probably contain a larger number of hydrogen bonds that may be disrupted at high shear rates, leading to a greater decrease in viscosity.

### 3.3. Thermal properties

DSC measurements were performed over a range of -100 to 40 °C in order to understand the thermal events occurring in this temperature range. We chose to focus on the lower temperature range, given that the samples under study were all liquid at room temperature. Interestingly, none of the CD-based mixtures, i.e. HPBCD:Lev, RAMEB:Lev, CRYSMEB:Lev and Captisol®:Lev, showed any melting point in the heating curve. Instead, glass transition curves with  $T_g$  at -73.3, -74.3, -73.5 and -67.8 °C were observed respectively for the mixtures (Fig. 3a). This absence of melting peaks and presence of glass transition temperature was widely observed in the literature. For example, Francisco et al. reported 21 systems showing no melting point but glass

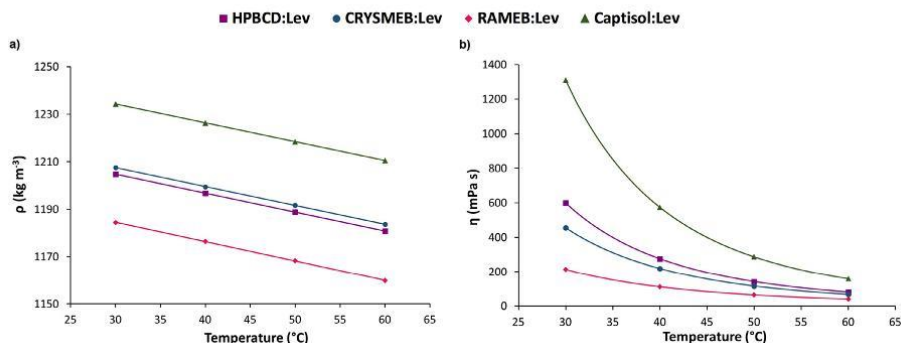


Fig. 2. Experimental values of the density (a) and viscosity (b) of the supramolecular LMM. The lines represent the Vogel-Fulcher-Tammann (VFT) correlation fitting for viscosity and appropriate polynomials in the case of the density.

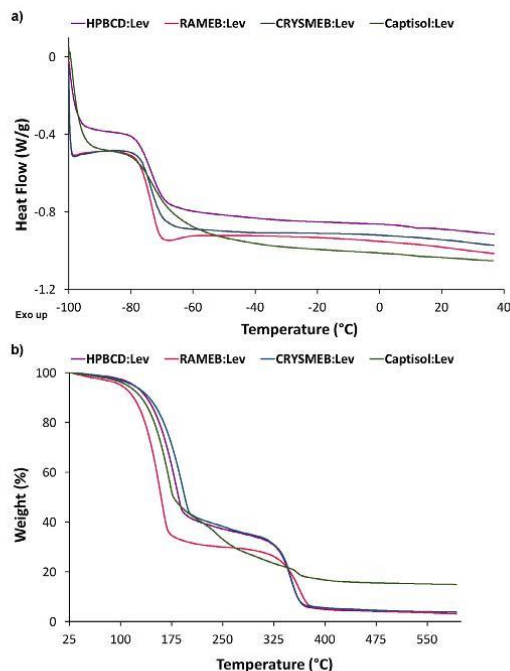


Fig. 3. DSC (a) and thermogravimetric analysis (b) curves of the LMM.

transition temperatures ranging between  $-13.64$  and  $-77.73$  °C (Francisco et al., 2012) while Dai et al. identified 13 different NADES with  $T_g < -50$  °C and no melting point (Dai et al., 2013). Likewise, with the exception of glass transition, no other thermal events occur for trehalose:glycerol at a 1:30 molar ratio (Castro et al., 2018). Moreover, the observed  $T_g$  value of  $-75.14$  °C is interestingly pretty close to the values obtained for our CD-based mixtures. CD generally present a  $T_g$  ranging between 80 °C and more than 200 °C depending on the CD (Tabary et al., 2011). Therefore, the observed  $T_g$  values could be attributed to the formation of a LMM with levulinic acid.

Dynamic thermogravimetric analysis (TGA) was used to further investigate the thermal stability of the new mixtures. As shown in Fig. 3b, they underwent progressive decomposition as the temperature increased. Their decomposition showed a two-step weight loss similar to choline-based DES (Delgado-Mellado et al., 2018). At around 130 °C, levulinic acid began to decompose while the CD began to degrade at about 325 °C, except in the case of Captisol® for which the second decomposition began at around 225 °C and a third decomposition was determined near 350 °C. From the thermogravimetric curve in Fig. 3b, the results showed that the thermal decomposition temperatures corresponding to the first thermal event of HPBCD:Lev, RAMEB:Lev, CRYSMEB:Lev and Captisol®:Lev were equal to 130.4, 117.6, 137.7 and 127.6 °C respectively. CRYSMEB:Lev had the best thermal stability and RAMEB:Lev the worst (Table S3). The DSC and TGA results demonstrate that these CD-based mixtures retain a stable liquid state over a wide temperature range.

### 3.4. Solubilization of AN and essential oils

AN has incited interest from the food, cosmetics and pharmaceutical industries due to its attractive properties. In fact, AN is a major component of star anise and fennel essential oils which are known both as flavoring agents and as medicines owing to their numerous biological

Table 2

Partition coefficient ( $K$ ) values of *trans*-anethole in water and in the tested mixtures and ratio of  $K_{\text{water}}/K_{\text{LMM}}$  at 30 °C.

	$K$	Ratio
Water	$1.29 \times 10^{-2}$	1
HPBCD:Lev	$1.04 \times 10^{-5}$	1240
RAMEB:Lev	$9.60 \times 10^{-6}$	1343
CRYSMEB:Lev	$1.08 \times 10^{-5}$	1194
Captisol®:Lev	$2.18 \times 10^{-5}$	592

properties (Auezova et al., 2020; Diao et al., 2014; Wang et al., 2018). However, its wider applications are hampered by drawbacks related to its high volatility, low water solubility and chemical instability. We have previously investigated the effect of AN complexation with various CD on its solubility and photodegradation and showed that CD were able to improve AN solubility and stability through inclusion complex formation (Kfoury et al., 2014a, 2014b). Therefore, the ability of the LMM to solubilize AN was evaluated by determining the vapor-liquid partition coefficient  $K$  of AN (Table 2) as well as the percentage of AN retention. More than 99% of AN were retained by all the studied mixtures while in aqueous solution CD were able to reduce AN volatility only up to 92% leading to around 20-fold reduction in  $K$  (Kfoury et al., 2014b, 2014a). In the case of the supramolecular mixtures we observed up to 1300 times reduction in  $K$  compared with water (Table 2).

DES have been explored as solvents for the extraction of EO or their components in the past few years (Li et al., 2009; Ozturk et al., 2018), with higher extraction yields observed compared with conventional solvents. However, the majority of the reported studies used diluted DES to improve their extraction efficiency by reducing their viscosity or increasing their polarity (Jeong et al., 2018). To the best of our knowledge, no studies investigating the solubilization or the extraction of AN or star anise EO using DES have been performed to date. Only one publication has reported the use of lactic acid-based NADES for the extraction of polyphenols from fennel EO, among other Greek medicinal plants (Bakirtzi et al., 2016). Subsequently, the ability of the studied LMM to solubilize EO, as well as AN in the presence of other aroma compounds, in two EO was investigated.

Star anise and fennel EO were chosen for having AN as a major component. All the tested mixtures showed high retention ability ( $\geq 98.9\%$ ) toward star anise and fennel EO (Fig. S3). Fig. 4 depicts the chromatogram of star anise EO obtained by SH-GC in presence of RAMEB:Lev and in presence of water as a reference solvent. Clearly, the peaks corresponding to the volatile compounds found in star anise are obvious in water but almost disappear in presence of the CD-based mixture. Fig. S4 shows the chromatograms of star anise EO in the three other mixtures.

Concerning the retention of AN, similar results were obtained regardless of whether AN was added in pure form or as a constituent of

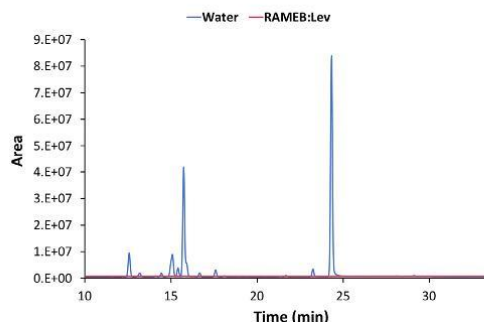


Fig. 4. Chromatogram of star anise essential oil in water and in RAMEB:Lev.

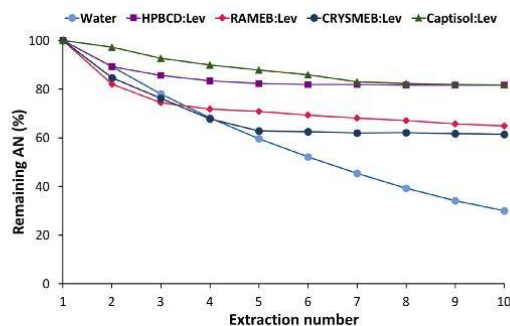


Fig. 5. Release of *trans*-anethole from water and from supramolecular mixtures.

star anise or fennel EO (Fig. S5). Therefore, the ability of the mixtures to retain AN was not affected by the simultaneous presence of other compounds.

### 3.5. Release study

Finally, the release of AN from the LMM was monitored by MHE. As described above, 10 successive headspace extractions were conducted at one-hour intervals. The amount of AN present in the vial after each extraction could be determined using the peak area. The retention ability of the LMM can be monitored and compared to water. The release profiles of AN from LMM and water are shown in Fig. 5. The results indicate that these CD-based mixtures can not only solubilize AN but also delay its release over time. Indeed, 70% of AN was released from water after 10 extractions at 60 °C, while only 20–40% was released from the CD:Lev mixtures.

## 4. Conclusions

New supramolecular mixtures based on  $\beta$ -CD derivatives and levulinic acid were prepared, characterized and studied for their ability to solubilize AN and related essential oils. In addition, their thermal stability was investigated. The physicochemical characterization studies demonstrated that these CD-based mixtures are liquid at room temperature with relatively low viscosity. The stability studies also revealed that they were stable up to 60 °C and that no degradation could be detected after 18 months of storage. These mixtures also presented high solubilizing ability towards AN, star anise and fennel essential oils, when compared with water or aqueous solutions of CD. Furthermore, they were able to delay the release of AN, as shown by MHE experiments. When compared to aqueous CD solutions, these mixtures guarantee the presence of high amounts of CD associated to a liquid state over a wide temperature range, which consequently allow the broadening of CD applications. These mixtures may therefore contribute in the search for greener solvents and result in new promising, safe and economic drug delivery systems. Indeed, due to their peculiar properties (viscosity, stability and encapsulation properties), these supramolecular LMM could solubilize poorly water-soluble drugs and/or protect fragile molecules during topical cutaneous administration. The potential of these LMM is currently being tested for the treatment of cutaneous leishmaniasis with a volatile and poorly water-soluble anti leishmaniasis drug and the results will be communicated in due course.

### CRedit authorship contribution statement

Tracy El Achkar: Methodology, Investigation, Formal analysis, Visualization, Writing - original draft, Writing - review & editing. Leila Moura: Conceptualization, Resources, Methodology, Investigation,

Validation. Tarek Moufawad: Methodology, Investigation, Formal analysis. Steven Ruellan: Methodology, Investigation, Formal analysis. Somenath Panda: Methodology, Investigation, Formal analysis. Stéphane Longuemart: Resources. François-Xavier Legrand: Resources, Methodology, Investigation, Visualization, Formal analysis. Margarida Costa Gomes: Resources, Validation. David Landy: Resources, Methodology, Investigation, Validation, Writing - review & editing. Hélène Greige-Gerges: Supervision, Writing - original draft, Writing - review & editing. Sophie Fourmentin: Conceptualization, Supervision, Methodology, Resources, Formal analysis, Validation, Visualization, Writing - original draft, Writing - review & editing.

### Declaration of Competing Interest

The authors declare that they have no known competing financial interests or personal relationships that could have appeared to influence the work reported in this paper.

### Acknowledgements

The authors thank the Research Funding Program at the Lebanese University, Lebanon, and the Agence Universitaire de la Francophonie, Moyen-Orient (PCSI 2018-2020) for funding the project. Tracy El Achkar is grateful to the Université du Littoral Côte d'Opale and the Lebanese University for providing her a scholarship. Fanny SIMELIERE from Institut Galien Paris-Sud (Châtenay-Malabry, France) and Jacques LOUBENS from TA Instruments (Guyancourt, France) are greatly acknowledged for their generous help. This work partially benefited from the support of the project ParasIDES ANR-19-CE18-0027 of the French National Research Agency (ANR).

### Appendix A. Supplementary data

Supplementary data to this article can be found online at <https://doi.org/10.1016/j.ijpharm.2020.119443>.

### References

- Abbott, A.P., Capper, G., Davies, D.L., Rasheed, R.K., Tambyrajah, V., 2003. Novel solvent properties of choline chloride/urea mixtures. *Chem. Commun.* 70–71. <https://doi.org/10.1039/b210714g>.
- Athanasiadis, V., Grigorakis, S., Lalas, S., Makris, D.P., 2018. Methyl  $\beta$ -cyclodextrin as a booster for the extraction for *Olea europaea* leaf polyphenols with a bio-based deep eutectic solvent. *Biomass Convers. Biorefinery* 8, 345–355. <https://doi.org/10.1007/s13399-017-0283-5>.
- Auezova, L., Najjar, A., Kfoury, M., Fourmentin, S., Greige-Gerges, H., 2020. Antibacterial activity of free or encapsulated selected phenylpropanoids against *Escherichia coli* and *Staphylococcus epidermidis*. *J. Appl. Microbiol.* 128, 710–720. <https://doi.org/10.1111/jam.14516>.
- Bakirtzi, C., Triantafyllidou, K., Makris, D.P., 2016. Novel lactic acid-based natural deep eutectic solvents: Efficiency in the ultrasound-assisted extraction of antioxidant polyphenols from common native Greek medicinal plants. *J. Appl. Res. Med. Aromat. Plants* 3, 120–127. <https://doi.org/10.1016/j.jarmap.2016.03.003>.
- Castro, V.L.B., Craveiro, R., Silva, J.M., Reis, R.L., Paiva, A., Duarte, A.R.C., 2018. Natural deep eutectic systems as alternative nontoxic cryoprotective agents. *Cryobiology* 83, 15–26. <https://doi.org/10.1016/j.cryobiol.2018.06.010>.
- Choi, Y.H., van Spronsen, J., Dai, Y., Verberne, M., Hollmann, F., Arends, I.W.C.E., Witkamp, G.-J., Verpoorte, R., 2011. Are natural deep eutectic solvents the missing link in understanding cellular metabolism and physiology? *Plant Physiol.* 156, 1701–1705. <https://doi.org/10.1104/pp.111.178426>.
- Clobanu, A., Landy, D., Fourmentin, S., 2013. Complexation efficiency of cyclodextrins for volatile flavor compounds. *Food Res. Int.* 53, 110–114. <https://doi.org/10.1016/j.foodres.2013.03.048>.
- Crini, G., 2014. Review: a history of cyclodextrins. *Chem. Rev.* 114, 10940–10975. <https://doi.org/10.1021/cr500081p>.
- Crini, G., Fourmentin, S., Fenyvesi, É., Torri, G., Fourmentin, M., Morin-Crini, N., 2018. Cyclodextrins, from molecules to applications. *Environ. Chem. Lett.* 16, 1361–1375. <https://doi.org/10.1007/s10311-018-0763-2>.
- Dai, Y., van Spronsen, J., Witkamp, G.-J., Verpoorte, R., Choi, Y.H., 2013. Natural deep eutectic solvents as new potential media for green technology. *Anal. Chim. Acta* 766, 61–68. <https://doi.org/10.1016/j.aca.2012.12.019>.
- Decock, G., Landy, D., Surpateanu, G., Fourmentin, S., 2008. Study of the retention of aroma components by cyclodextrins by static headspace gas chromatography. *J. Incl. Phenom. Macrocycl. Chem.* 62, 297–302. <https://doi.org/10.1007/s10847-008->

- 9471-z.
- Delgado-Mellado, N., Larriba, M., Navarro, P., Rigual, V., Ayuso, M., García, J., Rodríguez, F., 2018. Thermal stability of choline chloride deep eutectic solvents by TGA/FTIR-ATR analysis. *J. Mol. Liq.* 260, 37–43. <https://doi.org/10.1016/j.molliq.2018.03.076>.
- Di Pietro, M.E., Dugoni, G.C., Ferro, M., Mannu, A., Castiglione, F., Gomes, M.C., Fourmentin, S., Mele, A., 2019. Do cyclodextrins encapsulate volatiles in deep eutectic systems? *ACS Sustain. Chem. Eng.* 7, 17397–17405. <https://doi.org/10.1021/acssuschemeng.9b04526>.
- Diao, W.R., Hu, Q.P., Zhang, H., Xu, J.G., 2014. Chemical composition, antibacterial activity and mechanism of action of essential oil from seeds of fennel (*Foeniculum vulgare* Mill.). *Food Control* 35, 109–116. <https://doi.org/10.1016/j.foodcont.2013.06.056>.
- Dugoni, G.C., Di Pietro, M.E., Ferro, M., Castiglione, F., Ruellan, S., Moufawad, T., Moura, L., Gomes, M.F.C., Fourmentin, S., Mele, A., 2019. Effect of water on deep eutectic solvent/ $\beta$ -cyclodextrin systems. *ACS Sustain. Chem. Eng.* 7, 7277–7285. <https://doi.org/10.1021/acssuschemeng.9b00315>.
- El Achkar, T., Fourmentin, S., Greige-gerges, H., 2019. Deep eutectic solvents: an overview on their interactions with water and biochemical compounds. *J. Mol. Liq.* 288, 111028. <https://doi.org/10.1016/j.molliq.2019.111028>.
- El Achkar, T., Moufawad, T., Ruellan, S., Landy, D., Greige-Gerges, H., Fourmentin, S., 2020. Cyclodextrins: from solute to solvent. *Chem. Commun.* 56, 3385–3388. <https://doi.org/10.1039/d0cc00460j>.
- Ferreira, M., Jérôme, F., Bricout, H., Menuel, S., Landy, D., Fourmentin, S., Tilloy, S., Monflier, E., 2015. Rhodium catalyzed hydroformylation of 1-decene in low melting mixtures based on various cyclodextrins and N,N'-dimethylurea. *Catal. Commun.* 63, 62–65. <https://doi.org/10.1016/j.catcom.2014.11.001>.
- Fourmentin, S., Landy, D., Moura, L., Tilloy, S., Bricout, H., Ferreira, M., 2016. Procédé d'épuration d'un effluent gazeux. FR3058905A1.
- Francisco, M., van den Bruinhorst, A., Kroon, M.C., 2012. New natural and renewable low transition temperature mixtures (LTTMs): screening as solvents for lignocellulosic biomass processing. *Green Chem.* 14, 2153–2157. <https://doi.org/10.1039/c2gc35660k>.
- Imperato, G., Eibler, E., Niedermaier, J., König, B., 2005. Low-melting sugar-urea-salt mixtures as solvents for Diels-Alder reactions. *Chem. Commun.* 1170–1172. <https://doi.org/10.1039/b414515a>.
- Jeong, K.M., Jin, Y., Yoo, D.E., Han, S.Y., Kim, E.M., Lee, J., 2018. One-step sample preparation for convenient examination of volatile monoterpenes and phenolic compounds in peppermint leaves using deep eutectic solvents. *Food Chem.* 251, 69–76. <https://doi.org/10.1016/j.foodchem.2018.01.079>.
- Jérôme, F., Ferreira, M., Bricout, H., Menuel, S., Monflier, E., Tilloy, S., 2014. Low melting mixtures based on  $\beta$ -cyclodextrin derivatives and N,N'-dimethylurea as solvents for sustainable catalytic processes. *Green Chem.* 16, 3876–3880. <https://doi.org/10.1039/c4gc00591k>.
- Kfoury, M., Auezova, L., Greige-Gerges, H., Fourmentin, S., 2019. Encapsulation in cyclodextrins to widen the applications of essential oils. *Environ. Chem. Lett.* 17, 129–143. <https://doi.org/10.1007/s10311-018-0783-y>.
- Kfoury, M., Auezova, L., Greige-Gerges, H., Fourmentin, S., 2015. Promising applications of cyclodextrins in food: Improvement of essential oils retention, controlled release and antiradical activity. *Carbohydr. Polym.* 131, 264–272. <https://doi.org/10.1016/j.carbpol.2015.06.014>.
- Kfoury, M., Auezova, L., Greige-Gerges, H., Ruellan, S., Fourmentin, S., 2014a. Cyclodextrin, an efficient tool for trans-anethole encapsulation: chromatographic, spectroscopic, thermal and structural studies. *Food Chem.* 164, 454–461. <https://doi.org/10.1016/j.foodchem.2014.05.052>.
- Kfoury, M., Landy, D., Auezova, L., Greige-Gerges, H., Fourmentin, S., 2014b. Effect of cyclodextrin complexation on phenylpropanoids' solubility and antioxidant activity. *Beilstein J. Org. Chem.* 10, 2322–2331. <https://doi.org/10.3762/bjoc.10.241>.
- Kolb, B., Ettre, L.S., 2006. *Static Headspace-Gas Chromatography: Theory and Practice*. John Wiley & Sons Inc, Hoboken, New Jersey.
- Kurkov, S.V., Loftsson, T., 2013. Cyclodextrins. *Int. J. Pharm.* 453, 167–180. <https://doi.org/10.1016/j.ijpharm.2012.06.055>.
- Landy, D., Mallard, J., Ponchel, A., Monflier, E., Fourmentin, S., 2012. Remediation technologies using cyclodextrins: An overview. *Environ. Chem. Lett.* 10, 225–237. <https://doi.org/10.1007/s10311-011-0351-1>.
- Legrand, F.X., Sauthier, M., Flahaut, C., Hachani, J., Elfakir, C., Fourmentin, S., Tilloy, S., Monflier, E., 2009. Aqueous hydroformylation reaction mediated by randomly methylated beta-cyclodextrin: How substitution degree influences catalytic activity and selectivity. *J. Mol. Catal. A Chem.* 303, 72–77. <https://doi.org/10.1016/j.molcata.2008.12.017>.
- Li, J.H., Li, W., Luo, S., Ma, C.H., Liu, S.X., 2019. Alternate ultrasound/microwave digestion for deep eutectic hydro-distillation extraction of essential oil and polysaccharide from schisandra chinensis (Turcz.) Baill. *Molecules* 24. <https://doi.org/10.3390/molecules24071288>.
- Li, Z., Lee, P.L., 2016. Investigation on drug solubility enhancement using deep eutectic solvents and their derivatives. *Int. J. Pharm.* 505, 283–288. <https://doi.org/10.1016/j.ijpharm.2016.04.018>.
- Loftsson, T., Masson, M., 2001. Cyclodextrins in topical drug formulations: theory and practice. *Int. J. Pharm.* 225, 15–30. [https://doi.org/10.1016/S0378-5173\(01\)00761-X](https://doi.org/10.1016/S0378-5173(01)00761-X).
- Marques, H.M.C., 2010. A review on cyclodextrin encapsulation of essential oils and volatiles. *Flavour Fragr. J.* 25, 313–326. <https://doi.org/10.1002/ffj.2019>.
- Mbous, Y.P., Hayyan, M., Hayyan, A., Wong, W.F., Hashim, M.A., Looi, C.Y., 2017. Applications of deep eutectic solvents in biotechnology and bioengineering—Promises and challenges. *Biotechnol. Adv.* 35, 105–134. <https://doi.org/10.1016/j.biotechadv.2016.11.006>.
- McCune, J.A., Kunz, S., Olesifski, M., Scherman, O.A., 2017. DESolution of CD and CB Macrocycles. *Chem. - A Eur. J.* 23, 8601–8604. <https://doi.org/10.1002/chem.201701275>.
- Morrison, H.G., Sun, C.C., Neervannan, S., 2009. Characterization of thermal behavior of deep eutectic solvents and their potential as drug solubilization vehicles. *Int. J. Pharm.* 378, 136–139. <https://doi.org/10.1016/j.ijpharm.2009.05.039>.
- Moufawad, T., Moura, L.M., Ferreira, M., Bricout, H., Tilloy, S., Monflier, E., Gomes, M.C., Landy, D., Fourmentin, S., 2019. First evidence of cyclodextrin inclusion complexes in a deep eutectic solvent. *ACS Sustain. Chem. Eng.* 7, 6345–6351. <https://doi.org/10.1021/acssuschemeng.9b00044>.
- Moura, L., Moufawad, T., Ferreira, M., Bricout, H., Tilloy, S., Monflier, E., Costa Gomes, M.F., Landy, D., Fourmentin, S., 2017. Deep eutectic solvents as green absorbents of volatile organic pollutants. *Environ. Chem. Lett.* 747–753. <https://doi.org/10.1007/s10311-017-0654-y>.
- Nguyễn, C.H., Putaux, J.-L., Santoni, G., Tfaïli, S., Fourmentin, S., Coty, J.-B., Choïnard, L., Gèze, A., Wouessidjewe, D., Barratt, G., Lesieur, S., Legrand, F.-X., 2017. New nanoparticles obtained by co-assembly of amphiphilic cyclodextrins and nonlamellar single-chain lipids: Preparation and characterization. *Int. J. Pharm.* 531, 444–456. <https://doi.org/10.1016/j.ijpharm.2017.07.007>.
- Ozturk, B., Esteban, J., Gonzalez-Miquel, M., 2018. Deterpenation of citrus essential oils using glycerol-based deep eutectic solvents. *J. Chem. Eng. Data* 63, 2384–2393. <https://doi.org/10.1021/acs.jced.7b00944>.
- Potier, J., Menuel, S., Fournier, D., Fourmentin, S., Woisel, P., Monflier, E., Hapiot, F., 2012. Cooperativity in aqueous organometallic catalysis: Contribution of cyclodextrin-substituted polymers. *ACS Catal.* 2, 1417–1420. <https://doi.org/10.1021/cs300254t>.
- Rodriguez Rodriguez, N., Van Den Bruinhorst, A., Kollau, L.J.B.M., Kroon, M.C., Binnemans, K., 2019. Degradation of deep-eutectic solvents based on choline chloride and carboxylic acids. *ACS Sustain. Chem. Eng.* 7, 11521–11528. <https://doi.org/10.1021/acssuschemeng.9b01378>.
- Szejtli, J., 1998. Introduction and general overview of cyclodextrin chemistry. *Chem. Rev.* 98, 1743–1753. <https://doi.org/10.1021/CR970022C>.
- Tabary, N., Mahieu, A., Willart, J.F., Dugonon, E., Dande, F., Descamps, M., Bacquet, M., Martel, B., 2011. Characterization of the hidden glass transition of amorphous cyclomaltoheptaose. *Carbohydr. Res.* 346, 2193–2199. <https://doi.org/10.1016/j.carres.2011.07.010>.
- Tang, B., Row, K.H., 2013. Recent developments in deep eutectic solvents in chemical sciences. *Monatshfte für Chemie - Chem. Mon.* 144, 1427–1454. <https://doi.org/10.1007/s00706-013-1050-3>.
- Triolo, A., Lo Celso, F., Russina, O., 2020. Structural features of  $\beta$ -cyclodextrin solvation in the deep eutectic solvent. *Reline. J. Phys. Chem. B* 124, 2652–2660. <https://doi.org/10.1021/acs.jpcc.0c00876>.
- Wang, B., Zhang, G., Yang, M., Liu, N., Li, Y.X., Ma, H., Ma, L., Sun, T., Tan, H., Yu, J., 2018. Neuroprotective effect of anethole against neuropathic pain induced by chronic constriction injury of the sciatic nerve in mice. *Neurochem. Res.* 43, 2404–2422. <https://doi.org/10.1007/s11064-018-2668-7>.
- Zhang, Q., De Oliveira Vigier, K., Royer, S., Jérôme, F., 2012. Deep eutectic solvents: syntheses, properties and applications. *Chem. Soc. Rev.* 41, 7108–7146. <https://doi.org/10.1039/c2cs35178a>.



Université Libanaise

École Doctorale  
Sciences et Technologies

Doyen



Résumé de thèse de doctorat

En cotutelle entre

**L'Université du Littoral Côte d'Opale**

et

**L'Université Libanaise**

**Solvants eutectiques profonds : caractérisation, interaction avec des membranes synthétiques et biologiques, et solubilisation de composés bioactifs volatils.**

Présentée par

**Tracy El Achkar**

Le 11 décembre 2020

### **Membres du Jury**

M. Farid Chemat, Pr., Université d'Avignon

M. Dimitris Makris, Pr., University of Thessaly

Mme Alia Jraij, Pr., Université Libanaise

Mme Aida Habib Abdul Karim, Pr., American University of Beirut

M. Jérôme Lecomte, Dr., CIRAD

Mme Hélène Greige Gerges, Pr., Université Libanaise

Mme Sophie Fourmentin, Pr., Université du Littoral Côte d'Opale

Rapporteur

Rapporteur

Examineur

Examineur

Examineur

Directeur de thèse

Directeur de thèse

# Introduction

La recherche de solvants verts constitue l'une des préoccupations majeures de la chimie verte. La découverte des solvants eutectiques profonds (DES) a constitué un tournant dans ce domaine. Les DES représentent une nouvelle génération de solvants qui a attiré l'attention des chercheurs au cours de ces dernières années. Décrits pour la première fois en 2003, les DES sont définis comme un mélange de deux ou trois composés qui donne un liquide clair et homogène dont le point de fusion est beaucoup plus bas que ceux de ses composants (Abbott et al., 2003; Zhang et al., 2012). La dépression de la température est souvent attribuée aux interactions de type liaison hydrogène qui ont lieu entre les constituants du DES. Ainsi, ces solvants peuvent être préparés à partir d'une grande variété de composés générant une pléthore de combinaisons possibles. En plus de leur préparation facile à partir de matières premières largement accessibles, les DES possèdent des propriétés physico-chimiques intéressantes. Des homologues naturels des DES constitués de métabolites primaires ont été décrits quelques années plus tard et appelés solvants eutectiques profonds naturels (NADES) (Choi et al., 2011). Ces solvants ont été largement appliqués dans divers domaines pour remplacer et contourner certaines des limitations des solvants organiques conventionnels. En effet, les DES et les NADES ont donné des résultats prometteurs dans les secteurs de la chimie, biologie, du biomédical et pharmaceutique, entre autres (Mbous et al., 2017). Malgré le nombre croissant de publications sur ce sujet, beaucoup d'informations et de mises en œuvre du DES restent à découvrir.

La présente étude vise à examiner trois points principaux. Le premier consiste à déterminer les propriétés physico-chimiques des DES et à évaluer l'influence de leur composition sur les propriétés résultantes, ce qui peut aider à la conception de DES pour des applications spécifiques. La deuxième partie se concentre sur l'étude de l'interaction entre les DES et les phospholipides. Les phospholipides représentent la classe de lipides la plus abondante dans les membranes cellulaires. En raison de leur nature amphiphile, ces molécules ont tendance à s'auto-assembler en vésicules lipidiques lorsqu'elles sont présentes dans un milieu aqueux. Les vésicules lipidiques, connues sous le nom de liposomes, sont l'un des systèmes d'encapsulation les plus étudiés et appliqués, étant donné leur capacité à encapsuler des molécules d'une large gamme de polarité (Anwekar et al., 2011). À ce jour, les études impliquant les DES et les phospholipides ou les liposomes sont très limitées (Bryant et al., 2016, 2017; Gutiérrez et al., 2009; R. McCluskey et al., 2019). Par conséquent, l'étude du comportement des phospholipides dans les DES peut non seulement clarifier l'effet du DES sur les cellules animales et leur biocompatibilité ultérieure, mais peut également ouvrir la possibilité de créer de nouveaux systèmes d'encapsulation basés sur les DES. Le troisième objectif de l'étude repose sur la capacité de solubilisation des DES et de nouveaux systèmes basés sur le DES, incorporant différents systèmes d'encapsulation comme les phospholipides et les cyclodextrines, envers des composés volatils bioactifs. La combinaison des DES avec des agents d'encapsulation peut conduire à la formation de systèmes d'administration de médicaments potentiellement prometteurs et économiques, aux propriétés uniques.

Cette étude se concentre, plus précisément, sur quatre objectifs principaux :

- La préparation et la caractérisation de DES ;
- L'étude de l'organisation des phospholipides au sein des DES ;
- L'impact des DES sur les liposomes et les cellules humaines ;
- L'évaluation de la capacité de solubilisation des systèmes à base de DES envers des composés volatils naturels.

Cette thèse comprend cinq chapitres. Le premier présente une revue bibliographique sur les solvants eutectiques profonds : définition, classification, méthodes de préparation, propriétés physico-chimiques, effet de l'eau sur leurs propriétés et leur réseau, leur toxicité et leur biodégradabilité. En outre, ce chapitre présente quelques-unes des principales applications du DES, tels que la synthèse organique, la catalyse, le traitement de la biomasse, l'électrochimie, l'extraction, la solubilisation et l'administration de médicaments. La dernière section du chapitre concerne les études portant sur l'auto-assemblage de phospholipides ou de tensioactifs dans les DES, et la combinaison des DES et des cyclodextrines.

Le deuxième chapitre présente la composition des solvants qui ont été considérés dans cette étude, leur préparation et leur caractérisation. Cette dernière consiste principalement en des mesures de densité, de viscosité et de polarité.

Le troisième chapitre couvre l'étude de l'organisation des phospholipides dans les DES en utilisant les microscopies optique et à force atomique, ainsi que la diffusion dynamique de la lumière.

Le comportement des liposomes en présence des DES, suivi par microscopie à force atomique, est décrit dans le quatrième chapitre. De plus, ce chapitre inclut l'étude de l'effet de certains DES sur les cellules humaines, évalué par des études de cytotoxicité et de morphologie.

Dans le cinquième et dernier chapitre, nous avons étudié la solubilisation de composés bioactifs volatils et de certaines huiles essentielles par les DES en utilisant la chromatographie en phase gazeuse couplée à un espace de tête. Nous avons ensuite évalué l'effet de la présence d'eau ou de certains systèmes d'encapsulation sur la capacité de solubilisation des DES. Enfin, nous nous sommes intéressés à suivre la libération d'un composé volatil à partir des DES par extraction multiple de l'espace de tête.

# I. Revue bibliographique

## 1. Les solvants eutectiques profonds

### 1.1. Définition

Les DES sont souvent définis comme des mélanges binaires ou ternaires de composés capables de s'associer principalement par des liaisons hydrogène. La combinaison de ces composés à un certain rapport molaire donne un mélange eutectique (Zhang et al., 2012). Le mot "eutectique" vient du grec ancien εὐτηκτος ou eutéktos qui signifie "facilement fondu" et un point eutectique représente la composition chimique et la température auxquelles un mélange de deux solides devient entièrement fondu à la température de fusion la plus basse, par rapport à celle de l'un ou l'autre des composés. Cependant, la définition d'un DES est encore un sujet controversé et il existe plusieurs définitions publiées qui ne distinguent pas vraiment le DES des autres mélanges, puisque tous les mélanges de composés solides non miscibles présentent un point eutectique et compte tenu du fait que de nombreux composés sont capables de former des liaisons hydrogène lorsqu'ils sont mis ensemble (Coutinho & Pinho, 2017). Étant donné que la présence d'un point eutectique ou de liaisons hydrogène entre les composants ne sont pas des conditions suffisantes pour définir un "solvant eutectique profond" et afin de clarifier ce qu'est un DES et ce qui le rend spécial par rapport à d'autres mélanges, Martins *et al.* ont récemment défini le DES comme "un mélange de deux ou plusieurs composés purs pour lequel la température du point eutectique est inférieure à celle d'un mélange liquide idéal, présentant des écarts négatifs importants par rapport à l'idéal ( $\Delta T_2 > 0$ )", où  $\Delta T_2$  représente la dépression de la température qui est la différence entre le point eutectique idéal et le point eutectique réel (Martins et al., 2019). Les mêmes auteurs ont déclaré qu'il est important que la dépression de température se traduise par un mélange liquide à la température de fonctionnement, quelle que soit la composition du mélange. Le fait qu'il n'y ait pas de composition fixe offre une plus grande flexibilité pour ces systèmes.

### 1.2. Classification

Les DES ont été classés en quatre types selon la formule générale  $Cat^+ X^- zY$ , où  $Cat^+$  est généralement un ammonium, un phosphonium ou un sulfonium, tandis que  $X^-$  est une base de Lewis (généralement un anion halogénure).  $Y$  représente un acide de Lewis ou de Brønsted et  $z$  est le nombre de molécules  $Y$  qui interagissent avec l'anion correspondant (Figure 1) (Abbott et al., 2007; Smith et al., 2014). Les eutectiques de type III sont les plus étudiés dans la littérature et sont généralement basés sur le chlorure de choline (ChCl) et divers donneurs de liaison hydrogène (HBD). Le ChCl a été largement adopté car il est relativement bon marché, non toxique et biodégradable, étant donné qu'il est approuvé comme additif naturel pour plusieurs espèces animales ("Scientific Opinion on Safety and Efficacy of Choline Chloride as a Feed Additive for All Animal Species," 2011).

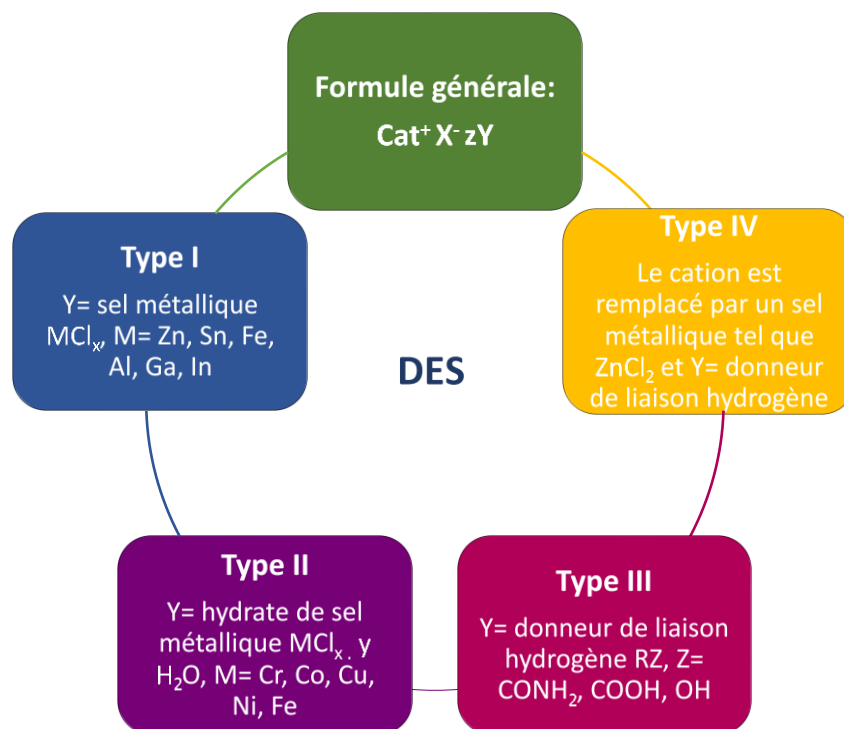


Figure 1. Les quatre types de solvants eutectiques profonds suivant la formule générale  $Cat^+ X^- zY$

Le premier DES de type III décrit était à base de  $ChCl$ . Depuis, une pléthore de composés ont été utilisés pour la préparation des DES. Les accepteurs de liaisons hydrogène (HBA) comprennent principalement des sels d'ammonium ou de phosphonium quaternaires, tandis que les HBD les plus courants sont les amides, les alcools et les acides carboxyliques. Lorsque les DES sont constitués de métabolites primaires tels que les acides organiques, les acides aminés, les sucres, les polyols et les dérivés de la choline, on parle de solvants eutectiques profonds naturels (NADES) (Choi et al., 2011; Dai et al., 2013). En outre, l'eau peut également faire partie de la composition des NADES. Plus récemment, les DES hydrophobes ont été introduits et ils sont basés sur l'utilisation de composés hydrophobes tels que le bromure de tétrabutylammonium (TBABr), le menthol, le thymol et les acides gras comme accepteurs de liaisons hydrogène ainsi que les alcools à longue chaîne alkyle et les acides carboxyliques comme HBD (Florindo et al., 2019; Osch et al., 2015). De plus, les DES peuvent être composés de principes actifs pharmaceutiques comme l'ibuprofène, la lidocaïne et l'acide phénylacétique. Dans ce cas, les solvants sont appelés solvants eutectiques profonds thérapeutiques (THEDES) (Duarte et al., 2017; Paiva et al., 2014). La Figure 2 présente les événements importants qui ont marqué le développement des DES jusqu'à présent (Abbott et al., 2001, 2003; Abbott, Capper, et al., 2004; Abbott, Boothby, et al., 2004; Abbott et al., 2007; Choi et al., 2011; El Achkar, Moufawad, et al., 2020; Osch et al., 2015).

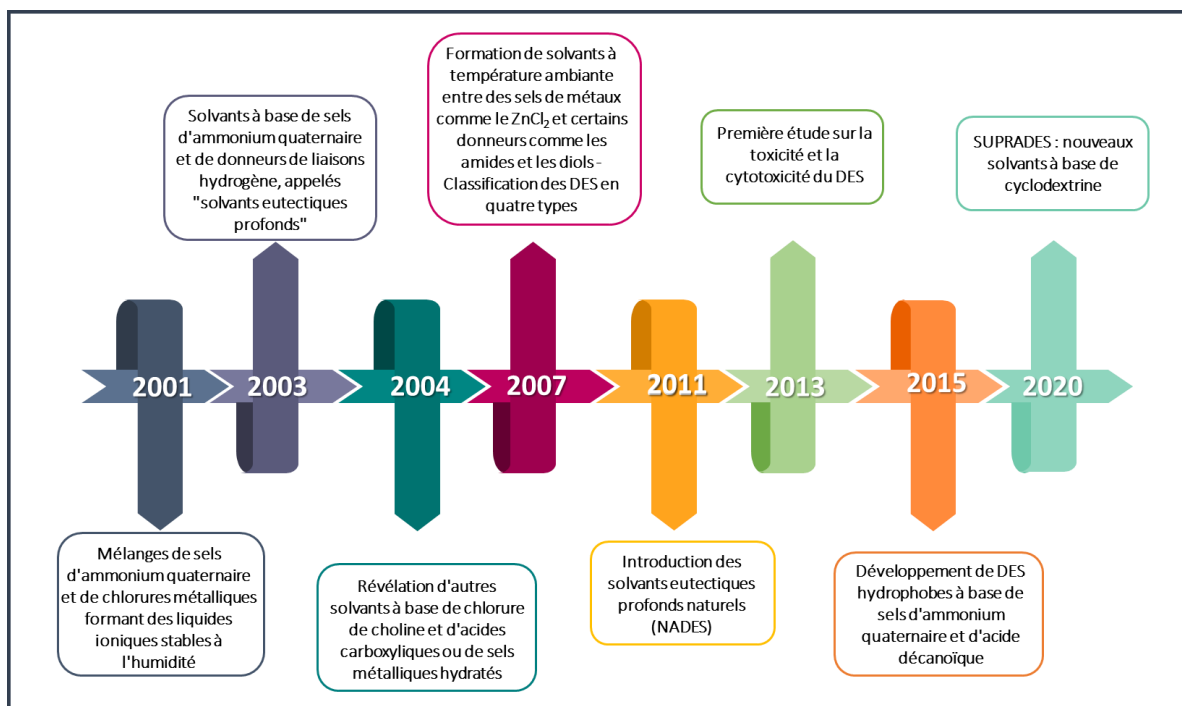


Figure 2. Les grands événements qui ont marqué le développement des solvants eutectiques profonds

### 1.3. Propriétés physico-chimiques

Outre leur faible volatilité, leur non-inflammabilité, leur faible tension de vapeur et leur stabilité chimique et thermique, les DES sont chimiquement accordables, ce qui signifie qu'ils peuvent être conçus pour des applications spécifiques étant donné la grande variété de composés formant des DES. Toutes ces propriétés ont encouragé les scientifiques à explorer les DES et à les appliquer comme une bonne alternative aux solvants conventionnels.

- Point de fusion

Comme mentionné ci-dessus, les DES ne sont pas des composés purs mais des mélanges de deux ou plusieurs composés purs. Ce système est représenté par un diagramme de phase solide-liquide, qui indique la température de fusion en fonction de la composition du mélange. Par conséquent, si nous considérons un mélange binaire de composés A et B, le point eutectique représente la composition et la température de fusion minimale à laquelle les courbes de fusion des deux composés se rencontrent (Figure 3). Les points de fusion de la plupart des DES se situent généralement entre - 69 et 149 °C (Zhang et al., 2012). Néanmoins, plusieurs autres mélanges signalés ne présentaient qu'une transition vitreuse et aucun

point de fusion n'a été détecté (Dai et al., 2013; Florindo et al., 2014; Francisco et al., 2012; Savi, Carpiné, et al., 2019; Savi, Dias, et al., 2019).

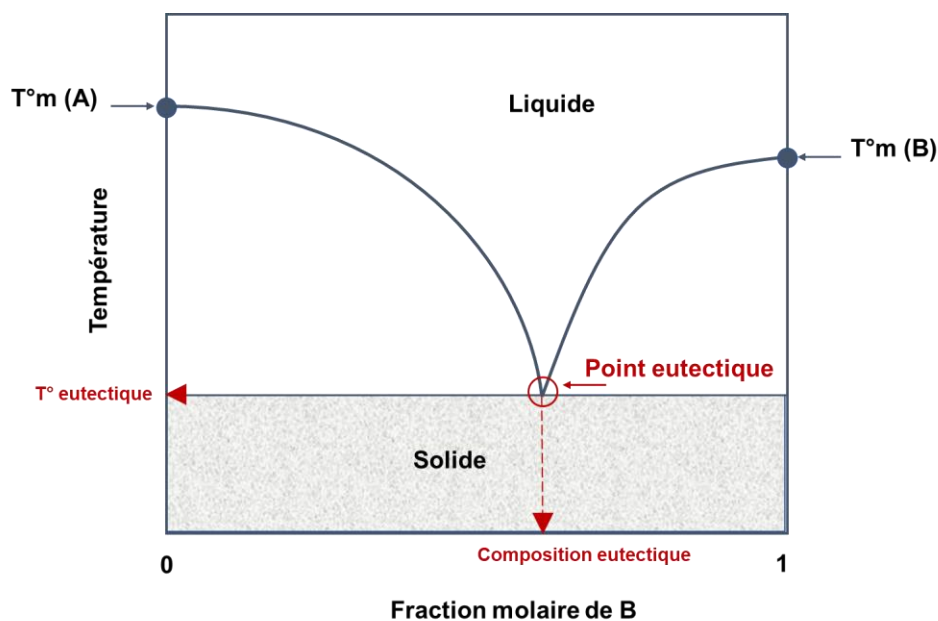


Figure 3. Diagramme de phase solide-liquide d'un mélange binaire

#### ▪ Densité et viscosité

La densité est l'une des propriétés physiques fondamentales des liquides. La plupart des DES présentent des densités plus élevées que l'eau, avec des valeurs comprises entre 1,0 et 1,3 g.cm<sup>-3</sup> à 25 °C, tandis que les DES à base de sels métalliques ont des densités comprises entre 1,3 et 1,6 g.cm<sup>-3</sup> (Tang & Row, 2013). Au contraire, des densités inférieures à celles de l'eau sont obtenues pour les eutectiques profonds hydrophobes (Florindo et al., 2019). La densité du DES diminue linéairement avec l'augmentation de la température (Cui et al., 2017; Florindo et al., 2014; Ibrahim et al., 2019; Shahbaz et al., 2012). La viscosité est une autre propriété importante et largement étudiée du DES. La plupart des DES sont très visqueux à température ambiante ( $\eta > 100$  mPa.s), ce qui est principalement attribué au réseau de liaisons hydrogène qui se produit entre les composants des DES. En outre, ils présentent une très large gamme de viscosité. En fait, le DES ChCl:EG (1:2) est connu pour avoir une très faible viscosité (37 mPa.s à 25 °C), tandis que les DES à base de sucre présentent des viscosités extrêmement importantes (12730 mPa.s pour le ChCl:sorbitol 1:1 à 30 °C et 34400 mPa. s pour 1:1 ChCl:glucose à 50 °C) et des viscosités encore plus élevées ont été enregistrées pour le DES à base de sels métalliques (85000 mPa.s pour 1:2 ChCl:chlorure de zinc à 25 °C) (Zhang et al., 2012). Cependant, de très faibles viscosités ont été enregistrées pour les DES hydrophobes à base de DL-menthol (7,61 mPa.s à 25 °C pour le 1:3 DL-menthol:acide octanoïque) (Nunes et al., 2019; Ribeiro et al., 2015). La viscosité d'un mélange eutectique est clairement affectée par la nature de ses composants (Abbott et al., 2007; D'Agostino et al., 2011), leur rapport molaire (Abbott et

al., 2007), la température (Abbott, Boothby, et al., 2004; Abbott et al., 2003, 2006; Dai et al., 2015; Kareem et al., 2010) et la teneur en eau (D'Agostino et al., 2015; Dai et al., 2015; Du et al., 2016; Florindo et al., 2014; Shah & Mjalli, 2014).

#### 1.4. Effet de l'eau

Étant donné l'omniprésence de l'eau et le caractère hygroscopique de certains DES et de leurs composés, l'absorption d'eau par les solvants eutectiques est inévitable (Du et al., 2016; Florindo et al., 2014). Alors que les traces d'eau dans les DES sont généralement considérées comme des impuretés, un très grand nombre d'études ont intentionnellement ajouté de l'eau à leurs solvants afin d'affiner leurs propriétés pour qu'ils puissent répondre aux exigences de certaines applications souhaitées et l'eau a permis, dans de nombreux cas, d'améliorer les performances des DES. D'autre part, la présence d'eau n'affecte pas seulement les propriétés physico-chimiques mais peut également mettre en danger l'intégrité des DES (El Achkar et al., 2019).

Certaines études ont proposé un passage du DES à une solution aqueuse de ses composants individuels tout en ajoutant de l'eau et d'autres ont suggéré qu'une transition du système "eau-dans-DES" à un système "DES-dans-eau" se produit à un certain niveau d'hydratation. Dans le premier système, l'eau est considérée comme un autre HBD (Hammond, Bowron, Jackson, et al., 2017; López-Salas et al., 2019; Zhekenov et al., 2017), s'intégrant ainsi dans le réseau du DES et renforçant par la suite les liaisons hydrogène qui ont lieu entre l'HBA et l'HBD à une faible teneur en eau (Hammond, Bowron, & Edler, 2017; Weng & Toner, 2018). Cependant, une dilution supplémentaire entraîne l'affaiblissement des interactions qui dominent habituellement dans la structure supramoléculaire du DES en raison de la tendance de l'eau à interagir avec les composés formant le DES. L'hydratation préférentielle des anions chlorure a été signalée dans de nombreux articles traitant de différents DES à base de ChCl comme ChCl:U, ChCl:G, ChCl:EG et ChCl:LA (Alcalde et al., 2019; Fetisov et al., 2018; Kaur et al., 2020; Kumari et al., 2018; Weng & Toner, 2018). Pourtant, en ce qui concerne le niveau d'hydratation auquel la transition se produit, les valeurs ne sont pas toujours cohérentes pour le même DES. Par exemple, le point de transition varie entre 15 et 51 wt% pour le ChCl:U (Hammond, Bowron, & Edler, 2017; Kumari et al., 2018; Posada et al., 2017; Shah & Mjalli, 2014). Il n'y a pas suffisamment d'études pour comparer les points de transition des autres DES. D'autres études doivent être menées sur d'autres DES car, bien que cette transition soit susceptible de se produire dans tous les mélanges aqueux de DES, la teneur en eau de transition dépend des types d'HBA et d'HBD ainsi que de leur rapport molaire (Gabriele et al., 2019). De plus, une compréhension approfondie de l'impact de l'eau sur la structure du DES augmentera certainement la possibilité de moduler les mélanges DES-eau en fonction des applications souhaitées.

## 2. Impact des DES sur les systèmes vivants

Malgré leurs caractéristiques attrayantes, un problème majeur lié aux DES reste à résoudre : leur sécurité. Depuis leur apparition, les DES ont toujours été présumés non toxiques en raison de la sécurité bien connue de leurs composés. Pourtant, leur toxicité et leur biodégradabilité doivent être étudiées pour les désigner comme des solvants biocompatibles. En 2013, Hayyan *et al.* ont été les premiers à s'attaquer directement à cette question en publiant une communication intitulée "Les solvants eutectiques profonds sont-ils bénins ou toxiques ? (Hayyan et al., 2013). De manière surprenante, il a été constaté que les DES à base de ChCl étudiés étaient plus cytotoxiques que leurs composants individuels envers les crevettes de saumure, mais qu'ils étaient non toxiques envers des bactéries Gram-positives et Gram-négatives. Par la suite, plusieurs études de toxicité, portant principalement sur les DES à base de ChCl et les NADES, ont été réalisées à l'égard de différents systèmes biologiques. Divers organismes ont été pris en compte pour les études de toxicité *in vitro* des DES, notamment des bactéries Gram-positives et Gram-négatives, des levures, des champignons, des plantes ainsi que des lignées cellulaires humaines, de souris et de poissons. Les études de toxicité rapportées à ce jour ne fournissent pas de réponse directe à la question de toxicité des DES. Il s'agit d'une question assez complexe et pourtant, l'examen de ces études permet de tirer de nombreuses conclusions. En fait, plusieurs facteurs peuvent affecter la toxicité globale du DES, comme le choix de l'HBD et le choix de l'HBA. De même, différentes réponses de toxicité peuvent résulter de différents organismes lorsqu'ils sont exposés aux mêmes solvants (Radošević et al., 2018).

## 3. Applications des DES

Outre les propriétés remarquables des DES, le besoin croissant de procédés respectueux de l'environnement et l'envie de remplacer les solvants organiques usuels ont conduit les chercheurs à envisager ces nouveaux solvants dans divers domaines d'application. Depuis leur découverte, les DES ont été utilisés dans la synthèse organique, la catalyse, l'électrochimie, la solubilisation et l'extraction, entre autres (Figure 4).

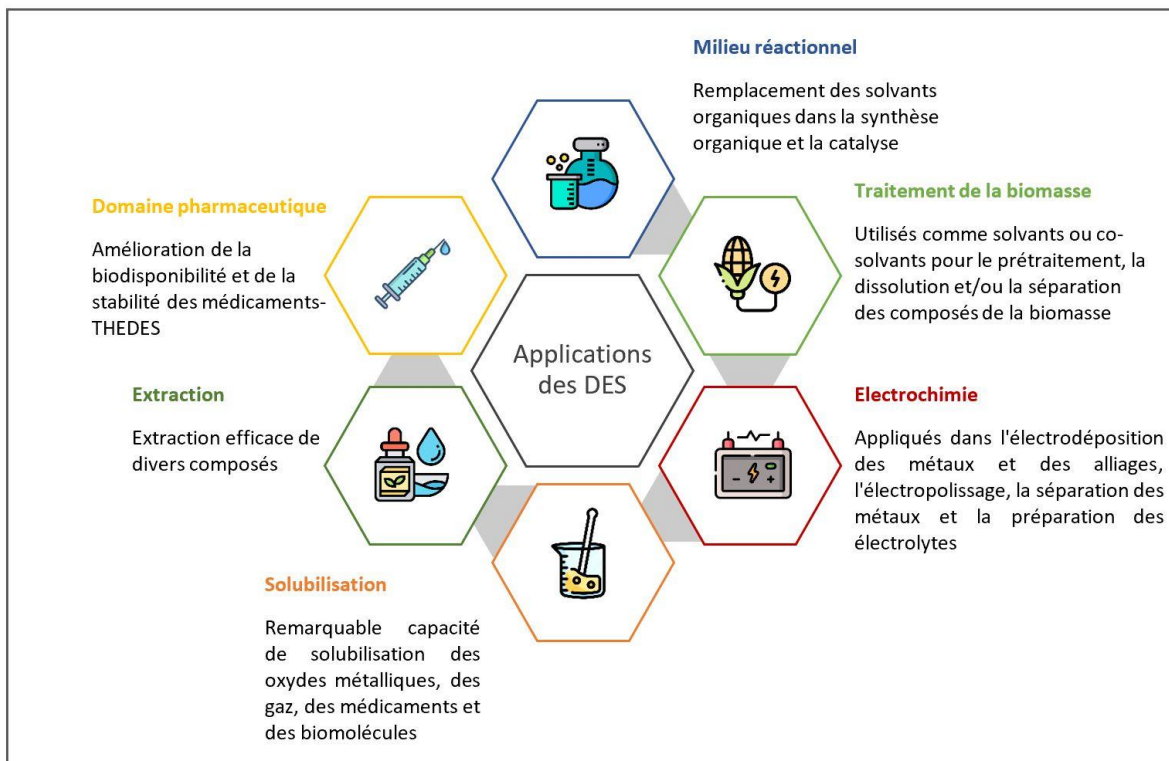


Figure 4. Aperçu des principales applications des solvants eutectiques profonds

#### 4. Combinaison des DES et des cyclodextrines

Les cyclodextrines (CD) sont des oligosaccharides cycliques naturels résultant de la dégradation enzymatique de l'amidon. Les CD natives les plus courantes comprennent 6, 7 ou 8 unités de  $\alpha$ -D-glucopyranose ( $\alpha$ -,  $\beta$ - et  $\gamma$ -CD respectivement) reliées entre elles par des liaisons glycosidiques  $\alpha$ -1,4. La conformation en chaise des unités de glucose donne naissance à des molécules en forme de cône tronqué. Ces molécules présentent une surface extérieure hydrophile caractérisée par des groupes hydroxyles primaires et secondaires positionnés sur les bords étroits et larges, respectivement, et une cavité intérieure hydrophobe marquée par des groupes C-H et des oxygènes glycosidiques (Figure 5). La  $\beta$ -CD, présente une faible solubilité dans l'eau en raison des liaisons hydrogène intramoléculaires qui ont lieu entre les groupes hydroxyles des molécules de glucose adjacentes. Par conséquent, les dérivés de la CD sont produits pour améliorer la solubilité de la CD native en remplaçant les groupes hydroxyles par d'autres fragments polaires ou apolaires. Les dérivés de CD les plus courants sont les CD hydroxypropylées, méthylées ou sulfobutylées. En raison de leur nature amphiphile, les CD sont capables d'encapsuler certaines molécules hydrophobes et de taille appropriée dans leur cavité en formant des complexes d'inclusion via des liaisons non covalentes. Cette propriété a permis aux CD d'être impliquées dans de

nombreux domaines d'application tels que agroalimentaire, pharmaceutique et cosmétique (Kfoury et al., 2016).

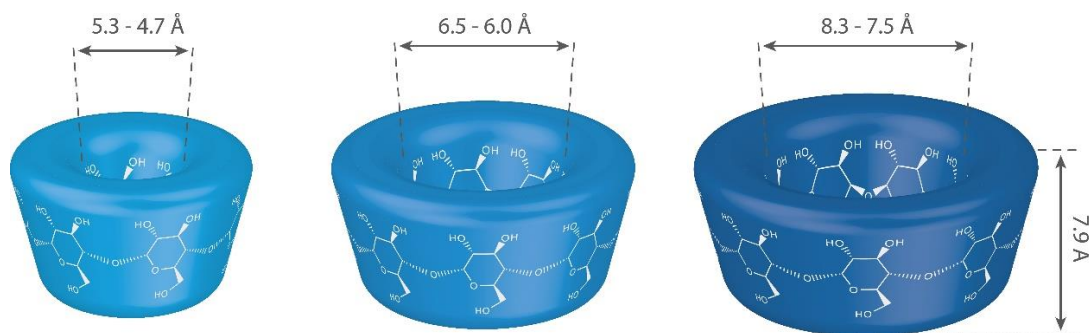


Figure 5. Illustration des trois cyclodextrines natives ( $\alpha$ -CD,  $\beta$ -CD et  $\gamma$ -CD de gauche à droite)

Il existe peu d'études ayant envisagé de combiner le concept de DES avec celui de CD. En effet, les CD ont été dissoutes dans le DES pour améliorer leur solubilité, pour étudier leurs propriétés bénéfiques et pour les explorer dans plusieurs domaines.

## 5. Auto-assemblage de molécules amphiphiles au sein des DES

L'auto-organisation des molécules amphiphiles peut être principalement entraînée par l'effet solvophobe ainsi que par la cohésion et la polarité du solvant (Arnold et al., 2015). Bien qu'encore à ses débuts, l'utilisation de DES comme solvant favorisant l'auto-assemblage présente un grand potentiel étant donné que le DES offre un environnement de liaisons hydrogène similaire à celui de l'eau (Sanchez-Fernandez et al., 2018).

Parmi les quelques études relatives à l'auto-assemblage des phospholipides dans les DES, une étude a montré, par le biais d'expériences de pénétration des solvants, que le ChCl:U peut pénétrer et solubiliser les lipides à base de phosphatidylcholine (PC) (1,2- dimyristoyl-sn-glycéro-3-phosphocholine (DMPC), 1,2-dipalmitoyl-sn- glycéro-3-phosphocholine (DPPC), 1,2-distéaroyl-sn-glycéro-3-phosphocholine (DSPC), ainsi que le phosphatidylcholine de l'oeuf ayant comme constituant principal le 1-palmitoyl-2-oleoyl-sn-glycéro-3-phosphocholine (POPC)) en l'absence d'eau. La microscopie optique polarisante a montré que le DES gonfle les lipides au-dessus de la température de transition lipidique, et qu'une phase lamellaire  $L_\alpha$  se forme spontanément, puis se transforme en vésicules avec le temps. Comme dans l'eau, la température de pénétration dans le DES augmente également avec l'augmentation de la longueur de la chaîne alkyle des lipides (Bryant et al., 2016). Le comportement des mêmes phospholipides à base de PC a été étudié dans les DES à base d'alkylammonium (HBA : chlorure d'éthylammonium, bromure d'éthylammonium, bromure de propylammonium, bromure de butylammonium et bromure de pentylammonium), cette fois en

utilisant le glycérol et l'éthylène glycol comme HBD. Les expériences de pénétration des solvants ont révélé que les phospholipides forment des phases lamellaires et génèrent spontanément des vésicules dans tous les DES testés (Bryant et al., 2017). Plus récemment, McCluskey et ses collègues ont prouvé pour la première fois la formation de monocouches de phospholipides stables à l'interface air-DES, en adoptant le DES ChCl:G et plusieurs PC et un phosphatidylglycérol comme phospholipides. Ils ont également obtenu des structures monocouches similaires à celles obtenues à l'interface air-eau (R. McCluskey et al., 2019). D'autre part, Gutiérrez *et al.* ont essayé d'incorporer des liposomes dans les DES (ChCl:U ou ChCl:thiourée) en lyophilisant un mélange de liposomes préformés (à base de DMPC) et de solutions aqueuses des composants individuels du DES (ayant une teneur en solutés de 20 wt%), après avoir prouvé que les DES peuvent être obtenus par lyophilisation des solutions aqueuses de leurs composants individuels. La microscopie confocale à fluorescence a confirmé la présence de liposomes variant entre 200 et 500 nm et la préservation de leur structure membranaire dans le DES (Gutiérrez et al., 2009).

D'autres articles ont examiné l'auto-assemblage des tensioactifs dans les DES. Le processus d'auto-assemblage des tensioactifs dépend de divers facteurs, à savoir le type du tensioactif (anionique, cationique, zwitterionique ou non ionique), la tête hydrophile, la longueur de la chaîne hydrophobe, la position de la charge et la concentration du tensioactif, ainsi que le type de DES, sa composition et sa teneur en eau. L'agrégation était, dans certains cas, plus favorable dans le DES pur ou hydraté que dans l'eau, ce qui est probablement attribué aux interactions électrostatiques supplémentaires qui ont lieu entre les composants du DES et les tensioactifs ioniques.

## II. Plan de travail

Au cours de notre étude, les DES ont d'abord été préparés en utilisant certains accepteurs de liaisons hydrogène communs comme le chlorure de choline, le bromure de tétrabutylphosphonium et le bromure de tétrabutylammonium, et des donneurs de liaisons hydrogène comme l'urée, le glycérol, l'éthylène glycol, l'acide lévulinique et l'acide décanoïque. D'autre part, de nouveaux mélanges liquides basés sur des dérivés de la  $\beta$ -cyclodextrine, agissant comme accepteurs de liaisons hydrogène, ont été décrits pour la première fois. La présence de CD pourrait donner naissance à des systèmes intéressants dotés de propriétés supramoléculaires, appelés ainsi SUPRADES. Après leur préparation, les DES et SUPRADES ont été caractérisés par la mesure de leur densité, de leur viscosité et de leur polarité. En raison de leur nouveauté, les SUPRADES ont été caractérisés par calorimétrie différentielle à balayage, analyse thermogravimétrique et études rhéologiques.

Par la suite, l'organisation des phospholipides dans les solvants a été étudiée par microscopie à force atomique et des mesures de polarité ont été effectuées à l'aide d'une sonde solvatochromique. De plus, le DES a été introduit dans la préparation des liposomes par deux méthodes conventionnelles (la méthode d'injection éthanolique et la méthode d'hydratation d'un film lipidique), en remplaçant la phase aqueuse par le DES. Les préparations résultantes ont ensuite été observées par microscopie optique et analysées par diffusion dynamique de la lumière.

Après avoir étudié le comportement des phospholipides dans les DES, nous avons examiné l'effet des DES sur les liposomes préformés, préparés par la méthode d'injection éthanolique et composés de phospholipides et de cholestérol, en utilisant la microscopie à force atomique. La première approche a consisté à exposer les liposomes adsorbés aux DES ou aux solutions aqueuses de leurs composants, tandis que la seconde approche consiste à mettre les liposomes en suspension dans les DES ou les solutions aqueuses de leurs composants, pendant différentes périodes avant leur adsorption et leur examen. De plus, l'impact de deux DES à base de chlorure de choline sur des cellules humaines de cancer du sein a été étudié en menant une combinaison d'études de cytotoxicité et de morphologie. L'effet des DES a également été comparé à l'effet de leurs composants individuels ou combinés.

Enfin, le pouvoir solubilisant des DES vis-à-vis de composés volatils, principalement le *trans*-anéthol, et des huiles essentielles associées, a été évalué par chromatographie en phase gazeuse couplée à un espace de tête. La spectroscopie de résonance magnétique nucléaire (RMN) a également été utilisée pour vérifier si la capacité des cyclodextrines à former des complexes d'inclusion était préservée dans les SUPRADES. De plus, nous avons évalué l'effet de l'eau et de certains systèmes d'encapsulation tels que les cyclodextrines, les lipides et les tensioactifs, sur la capacité de solubilisation du DES. Enfin, la libération du *trans*-anéthol à partir des solvants étudiés a été suivie par la technique d'extraction multiple de l'espace de tête.

### III. Résultats

#### 1. Préparation et caractérisation des DES

Dans la présente étude, une sélection de DES de type III a été envisagée en utilisant le chlorure de choline (ChCl), le bromure de tétrabutylphosphonium (TBPBr) et le bromure de tétrabutylammonium (TBABr) comme HBA, ainsi que l'urée (U), le glycérol (G), l'éthylène glycol (EG), l'acide lévulinique (Lev) et l'acide décanoïque (Dec) comme HBD. Le Tableau 1 présente la composition des DES étudiés qui ont été préparés en combinant l'HBA et l'HBD à un certain rapport molaire, puis en agitant et en chauffant le mélange à 60 °C jusqu'à la formation d'un liquide clair et homogène. Le chlorure de choline a été séché à 60 °C pendant 2 semaines avant d'être utilisé. La teneur en eau de tous les mélanges préparés a été déterminée à l'aide de la méthode de titrage Karl Fisher (Mettler Toledo DL31).

Tableau 1. Composition des solvants eutectiques profonds étudiés

DES	HBA	HBD	Ratio molaire HBA:HBD	Teneur en eau (%)
ChCl:U	Chlorure de choline	Urée	1:2	0.33
ChCl:G	Chlorure de choline	Glycérol	1:2	0.05
ChCl:EG	Chlorure de choline	Ethylène glycol	1:2	0.06
ChCl:Lev	Chlorure de choline	Acide lévulinique	1:2	0.05
TBPBr:Lev	Bromure de tétrabutylphosphonium	Acide lévulinique	1:6	0.04
TBABr:Dec	Bromure de tétrabutylammonium	Acide décanoïque	1:2	0.02
TBPBr:EG	Bromure de tétrabutylphosphonium	Ethylène glycol	1:2	0.01

D'autre part, les SUPRADES ont été préparés en utilisant différents dérivés de  $\beta$ -CD comme HBA, étant donné leur grand nombre de sites de liaison hydrogène. Étant des oligosaccharides cycliques naturels et possédant une importante propriété d'encapsulation, les mélanges à base de CD pourraient conduire à la formation de systèmes sûrs et intéressants. La combinaison de quatre dérivés de  $\beta$ -CD ( $\beta$ -CD hydroxypropylée (HPBCD ; degré de substitution (DS) = 4.34),  $\beta$ -CD méthylée de manière aléatoire (RAMEB ; DS = 12.9),  $\beta$ -CD faiblement méthylée (CRYSMEB ; DS = 4.9) ou sulfobutyléther- $\beta$ -CD (Captisol® ; DS = 6.5)) avec de l'acide lévulinique a été réalisée et a abouti à la formation de liquides clairs à température ambiante. Par la suite, la HPBCD ou la RAMEB a été mélangée avec différents polyalcools, tels que le glycérol, l'éthylène glycol, le 1,3-propanediol (PD) ou le 1,3-butanediol (BD) à différents rapports molaires. Les mélanges aboutissant à des liquides à température ambiante ont été retenus.

Par la suite, des mesures de densité et de viscosité de ces solvants ont été effectuées à la pression atmosphérique et à des températures comprises entre 30 et 60 °C. De même, la polarité des DES a été estimée à l'aide de la sonde solvatochromique Nile Red. Les résultats ont montré que ces propriétés dépendent de l'HBA, de l'HBD et de leur rapport molaire. Par exemple, une densité plus élevée est observée lorsqu'un groupe hydroxyle supplémentaire (1139,0 kg m<sup>-3</sup> pour le 1:40 HPBCD:1,3-PD et 1290,5 kg m<sup>-3</sup> pour le 1:40 HPBCD:G) ou une longueur de chaîne plus courte ( $\rho$  1:40 HPBCD:EG >  $\rho$  1:40 HPBCD:1,3-PD >  $\rho$  1:40 HPBCD:1,3-BD) est considérée. D'autre part, la viscosité augmente avec la longueur de la chaîne alkyle du HBD ( $\eta$  HPBCD:1,3-BD >  $\eta$  HPBCD:1,3-PD >  $\eta$  HPBCD:EG et  $\eta$  RAMEB:1,3-BD >  $\eta$  RAMEB:1,3-PD). Le choix du HBD semble aussi affecter la polarité globale des DES puisque les DES contenant de l'acide lévulinique sont les plus polaires, suivis par ceux à base de glycérol, d'éthylène glycol, d'urée, de 1,3-PD, de 1,3-BD et d'acide décanoïque. La calorimétrie différentielle à balayage et l'analyse thermogravimétrique ont prouvé que les SUPRADES présentent un état liquide et stable sur une large gamme de températures (El Achkar, Moura, et al., 2020).

## 2. Auto-assemblage des phospholipides au sein des DES

En raison de leurs propriétés uniques, les DES ont été récemment explorés comme solvants favorisant l'auto-assemblage. Leur polarité, leur cohésion et leur important réseau de liaisons hydrogène constituent des facteurs importants pour l'auto-organisation des molécules amphiphiles. Il a été signalé que les DES agissent comme solvants pour l'auto-assemblage des tensioactifs ioniques et des phospholipides. Cependant, les études portant sur le comportement des phospholipides dans le DES sont assez limitées. C'est pourquoi, dans cette section, nous avons cherché à étudier l'organisation des phospholipides dans les DES et les nouveaux systèmes à base de CD par microscopie à force atomique (AFM). L'AFM est une microscopie à haute résolution qui fournit des informations détaillées sur la surface des échantillons à l'échelle nanométrique. Ainsi, 10 mg de lipoïde E80 (80- 85% de phosphatidylcholine (PC), 7- 9,5% de phosphatidyléthanolamine, 3% de lysoPC, 0,5% de lysophosphatidyléthanolamine, 2-3% de sphingomyéline, 2% d'eau, 0,2% d'éthanol) ont été dissous dans un mélange d'eau ultra-pure (0,2 ml) et

de DES ou SUPRADES (1,8 ml) (ChCl:U, ChCl:G, ChCl:EG, ChCl:Lev, TBPBr:Lev, TBABr:Dec, TBPBr:EG, HPBCD:Lev, RAMEB:Lev ou CRYSMEB:Lev) et ont été conservés sous agitation à température ambiante. Des aliquotes ont été prélevées à 4, 24 et 48 h et déposées sur la surface du mica pour être adsorbées. Les images obtenues par l'AFM ont montré que les phospholipides ont tendance à former des bicouches lipidiques à  $t=4h$  dans les DES à base de chlorure de choline qui se transforment ensuite en vésicules lipidiques à  $t=48h$  (Eid et al., 2020). En revanche, aucune structure lipidique n'a été détectée en présence de DES à base de TBPBr ou de TBABr (TBPBr:Lev, TBPBr:EG et TBABr:Dec). Cela pourrait être dû à une dissolution complète des lipides dans les DES. De même, aucun assemblage de lipides n'a été observé dans les systèmes CD:Lev, ce qui pourrait être dû à l'emprisonnement des phospholipides dans les cavités des CD (Szente & Fenyvesi, 2016). Le choix de l'HBA a un effet majeur sur l'organisation des phospholipides dans le DES.

Afin d'étudier davantage le comportement des phospholipides dans ces systèmes, nous avons mesuré la polarité de 4 DES (ChCl:G, ChCl:EG, TBPBr:Lev et TBABr:Dec) en l'absence ou en présence de phospholipides E80, en déterminant  $\lambda_{max}$ , la longueur d'onde qui correspond à l'absorption maximale de lumière visible par la sonde solvatochromique Nile Red. Les valeurs de  $\lambda_{max}$  ont diminué après l'ajout des lipides dans ChCl:G et ChCl:EG, indiquant la transition du Nile Red vers un environnement relativement non polaire. Cette différence peut s'expliquer par l'intercalation possible de la sonde dans la bicouche lipidique des vésicules qui se sont formées dans les DES, comme cela a été détecté précédemment par la technique d'AFM. Au contraire, les valeurs de  $\lambda_{max}$  ont légèrement diminué dans le DES TBPBr:Lev et TBABr:Dec, où aucune structure lipidique n'a été observée par l'AFM.

De plus, l'auto-assemblage des phospholipides a été étudié selon une autre approche qui consiste à introduire le DES dans les méthodes de préparation des liposomes. Deux méthodes conventionnelles généralement utilisées pour la préparation des liposomes ont été considérées : la méthode d'injection éthanolique et la méthode d'hydratation du film lipidique. La méthode d'injection éthanolique, décrite en 1973 par Batzri et Korn, consiste à dissoudre les lipides dans l'éthanol, puis à injecter la solution éthanolique dans une phase aqueuse et à évaporer la phase organique, ce qui conduit à la formation de liposomes (Batzri & Korn, 1973). La méthode d'hydratation du film lipidique, également appelée méthode de Bangham, nécessite la dissolution des lipides dans une phase organique avant son évaporation qui entraînera la formation d'un film lipidique. L'hydratation ultérieure de ce film génère des liposomes (Bangham et al., 1965). La même procédure générale a été suivie ici, sauf que la phase aqueuse a été remplacée par le DES dans les deux techniques. Le lipoïde S100 (94 % de PC de soja, 3 % de lysoPC, 0,5 % de N-acyl-phosphatidyléthanolamine, 0,1 % de phosphatidyléthanolamine, 0,1 % de phosphatidylinositol, 2 % d'eau, 0,2 % d'éthanol, indice d'iode 97-107) et le cholestérol ont été utilisés à une concentration de 10 mg/mL et 5 mg/mL, respectivement. Les préparations obtenues ont ensuite été observées par microscopie optique. Des formes différentes de lipides ont été détectées dans les DES à base de ChCl par rapport aux échantillons préparés sans lipides dans les deux méthodes. Alors qu'aucune

structure lipidique n'a été détectée dans les autres DES ou SUPRADES étudiés (TBPBr:Lev, TBABr:Dec, TBPBr:EG, HPBCD:Lev, RAMEB:Lev et CRYSMEB:Lev). Ces résultats sont en quelque sorte liés aux résultats de l'AFM concernant l'organisation des phospholipides E80 dans les DES. De plus, un tensioactif non ionique, le Triton X-100 connu pour sa capacité à perturber les vésicules lipidiques en milieu aqueux, a été ajouté à une concentration de 10 % (v/v) aux préparations à base de DES. Néanmoins, des assemblages sphériques de grande taille se sont formés après l'ajout du Triton X-100 au ChCl:U, au ChCl:G et au ChCl:EG. Le tensioactif a ensuite été ajouté au DES en l'absence de lipides et les auto-assemblages sont apparus de nouveau, indiquant que le tensioactif est clairement à l'origine de leur formation (Figure 6).

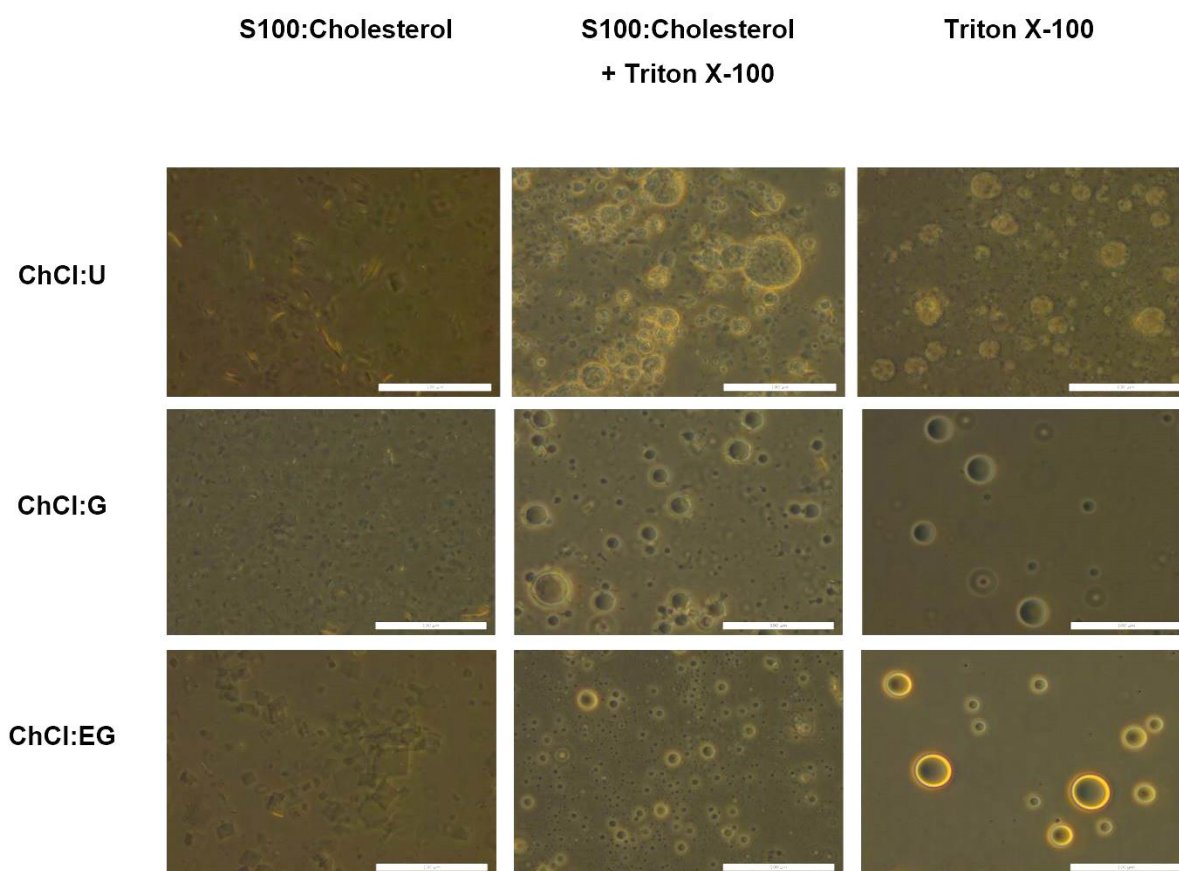


Figure 6. Méthode d'injection éthanolique à base de DES : observation de DES à base de ChCl en présence de lipides (colonne de gauche), en présence à la fois de lipides et de Triton X-100 (colonne du milieu), et en présence de Triton X-100 (colonne de droite)

### 3. Effet des DES sur les membranes synthétiques et biologiques

Après avoir examiné l'organisation des phospholipides dans les DES et après avoir prouvé la formation d'auto-assemblages dans les DES à base de ChCl, l'effet de ces DES et des solutions aqueuses de leurs constituants sur les liposomes préformés a été évalué pour la première fois par AFM. En plus des liposomes qui sont considérés comme des modèles pour les membranes biologiques, l'effet sur les cellules cancéreuses du sein humain MDA-MB-231 a également été évalué.

#### 3.1. Effet sur les liposomes préformés

Deux approches ont été envisagées pour étudier l'effet des DES sur les liposomes, qui ont été préparés par la méthode d'injection éthanolique en utilisant des phospholipides E80. La première consiste à exposer les liposomes adsorbés aux DES ou aux solutions aqueuses de leurs constituants pendant 30 min avant leur observation. Dans la seconde approche, les liposomes préformés sont mis en suspension dans les DES ou les solutions aqueuses pendant différents temps avant leur adsorption et leur observation. Lorsqu'ils sont exposés aux DES ou aux solutions aqueuses de leurs composants, les liposomes préformés conservent leurs structures bien qu'ils diminuent de taille en raison de leur déshydratation probable. Des observations similaires ont été obtenues lorsque les liposomes ont été mis en suspension dans les solutions aqueuses de composés de DES. Cependant, lorsqu'ils étaient mis en suspension dans les DES à base de ChCl, les liposomes se transformaient en bicouches lipidiques à  $t = 2$  h avant leur reconstitution en vésicules (Figure 7) (Eid et al., 2020).

#### 3.2. Effet sur les cellules humaines

Après avoir étudié l'effet des DES sur les liposomes, nous nous sommes intéressés à l'évaluation de l'impact des DES sur les cellules humaines. Comme mentionné dans la section 1.2., les DES ont toujours été considérés comme des solvants non toxiques en raison de la sécurité de leurs composants. Néanmoins, certaines études ont récemment rapporté que les DES peuvent avoir une réponse toxique différente de celle de leurs composés de départ. Dans cette section, nous avons examiné l'effet de deux des DES les plus étudiés, ChCl:U et ChCl:EG, sur MDA-MB-231, une lignée cellulaire de cancer du sein humain. De plus, l'effet du DES a été comparé à l'effet de leurs composés individuels (ChCl, urée ou éthylène glycol) ou combinés. La solution des composés combinés a été préparée en dissolvant séparément l'HBA et l'HBD dans l'eau selon le même rapport molaire HBA:HBD adopté pour le DES. Pour ce faire, une combinaison d'études de cytotoxicité et d'évaluation morphologique a été réalisée.

L'étude de cytotoxicité réalisée par le test d'exclusion du bleu de trypan a révélé que les DES sont généralement plus cytotoxiques que les solutions aqueuses de leurs composés. En outre, l'observation de la morphologie cellulaire lors de l'exposition au DES ou à la solution aqueuse des deux composés a montré un comportement différent qui peut s'expliquer par un mécanisme d'action différent. D'autre part, le choix du donneur de liaisons hydrogène peut fortement affecter la toxicité globale d'un DES, ce qui peut donner

un DES relativement inoffensif comme le ChCl:U ou un DES modérément toxique comme le ChCl:EG. Dans une autre approche, les cellules ont été incubées dans du DES pur pour la première fois et ont été suivies par microscopie optique. Les deux DES ont pu fixer les cellules dans un certain état pendant une période allant jusqu'à 12 jours, ce qui peut s'expliquer par la déshydratation des cellules suite à l'exposition au DES et la coagulation des protéines qui s'ensuit (Figure 8).

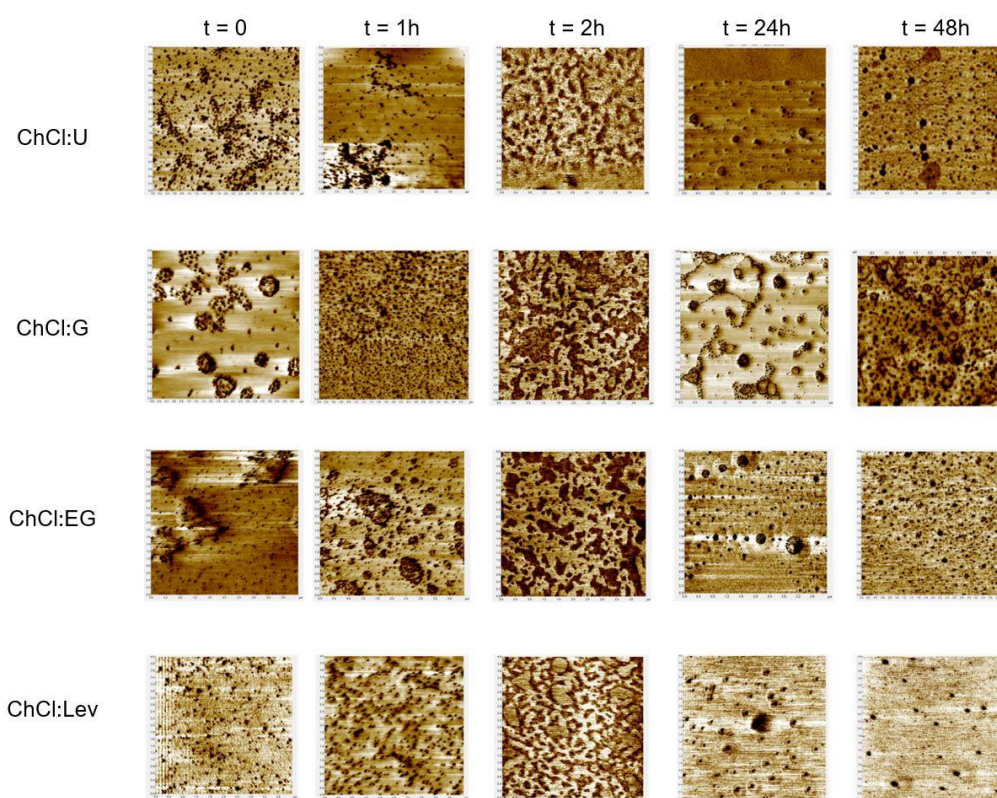


Figure 7. Images 2D de liposomes E80 ( $4 \times 4 \mu\text{m}^2$ ) en suspension dans du ChCl:U, ChCl:G, ChCl:EG ou ChCl:Lev obtenues par AFM en mode contact

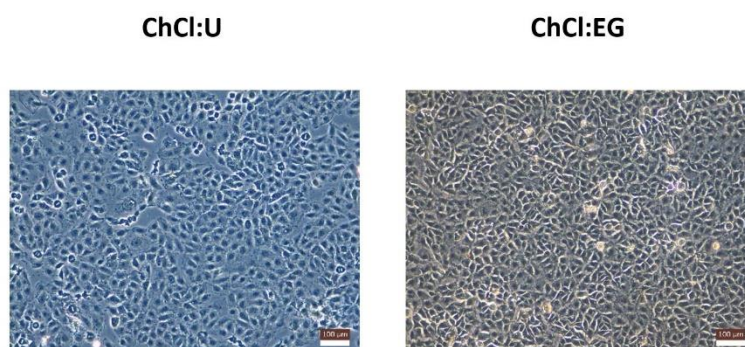


Figure 8. Observations de cellules MDA-MB-231 exposées à du DES pur pendant 12 jours

#### 4. Pouvoir solubilisant des DES vis-à-vis de composés bioactifs volatils

Dans la dernière partie de l'étude, nous avons évalué la capacité des DES à solubiliser les arômes tels que le *trans*-anéthol (AN) et la L-carvone (Carv) ainsi que des huiles essentielles. De plus, nous avons étudié l'impact de la présence d'eau ou de certains systèmes d'encapsulation comme les cyclodextrines (CD), les phospholipides et les tensioactifs sur l'efficacité de solubilisation du DES. Enfin, nous avons suivi la libération du *trans*-anéthol à partir du DES en fonction du temps.

Les études de solubilisation ont été menées par chromatographie en phase gazeuse couplée à un espace de tête (SH-GC). Dans cette technique, l'échantillon (liquide ou solide) est généralement placé dans un vial fermé et thermostaté. Par la suite, un équilibre entre la phase liquide et la phase gazeuse (appelée espace de tête) sera atteint et la concentration du composé volatil dans la phase gazeuse sera constante. Dans une deuxième étape, la phase gazeuse est analysée par chromatographie en phase gazeuse : une aliquote de l'espace de tête est transférée à la colonne (phase stationnaire) via le flux du gaz porteur (phase mobile) (Figure 9). La distribution du composé volatil entre les deux phases est représentée par un paramètre appelé coefficient de partage  $K$  qui est considéré comme le rapport de la concentration de l'analyte dans la phase gazeuse sur sa concentration dans la phase liquide. Les DES ont montré une grande capacité de solubilisation du *trans*-anéthol et de la L-carvone, traduite par une diminution importante (jusqu'à 4200 fois) du coefficient de partage  $K$  par rapport à l'eau. Le TBABr:Dec présentait la plus grande capacité de solubilisation, suivi par les DES à base de TBPBr et les DES à base de ChCl. Les SUPRADES présentaient une efficacité intermédiaire.

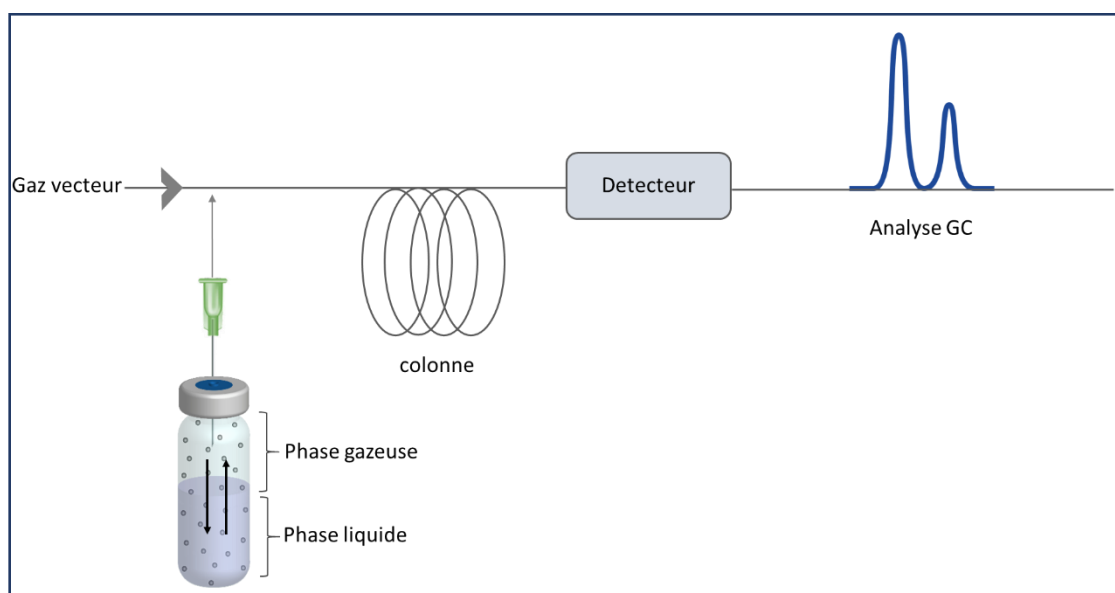


Figure 9. Principe de la chromatographie en phase gazeuse couplée à un espace de tête

De plus, tous les solvants testés ont présenté une rétention élevée des huiles essentielles d'anis étoilé et de fenouil, avec plus de 61% de rétention par rapport à l'eau. La solubilisation du *trans*-anéthol par les mélanges binaires DES-eau a diminué avec l'augmentation de la teneur en eau. De plus, une étude par RMN de RAMEB:Lev en présence de *trans*-anéthol a révélé la présence d'interactions importantes entre le composé volatil et la cavité de la CD, suggérant ainsi que la CD conservait sa capacité de complexation sous la forme de SUPRADES (El Achkar, Moufawad, et al., 2020). En outre, l'ajout de CD au ChCl:U a amélioré la solubilité du *trans*-anéthol par le DES. De même, la capacité de solubilisation du DES a été améliorée en présence des lipides ou du Triton X-100. Enfin, la technique d'extraction multiple de l'espace de tête a montré que les DES ont permis une libération contrôlée du *trans*-anéthol par rapport à l'eau (Figure 10) (El Achkar, Moura, et al., 2020).

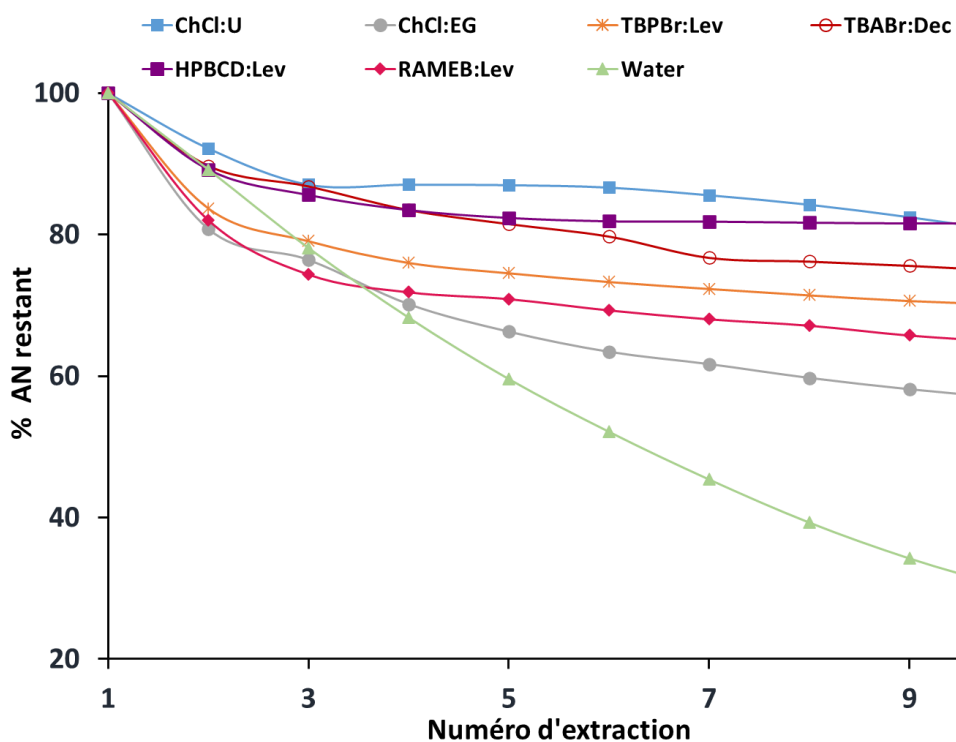


Figure 10. Libération du *trans*-anéthol à partir de l'eau ou des DES à 60°C

## Conclusion et perspectives

Cette étude visait à caractériser les solvants eutectiques profonds (DES), à explorer le comportement des liposomes et des membranes biologiques au sein de ces solvants, et à évaluer leur capacité de solubilisation envers des composés bioactifs volatils.

Dans l'ensemble, les résultats obtenus ont mis en évidence la modularité des DES et la perspective de concevoir de nouveaux solvants aux propriétés uniques comme les SUPRADES. Ils ont également révélé le comportement des phospholipides au sein du DES et le potentiel de ces solvants comme milieu pour l'auto-assemblage de molécules amphiphiles ou la préservation des liposomes. Ces découvertes ont également contribué à élucider l'impact du DES sur les membranes biologiques. Comme le prouvent les études de solubilisation, les principaux résultats de cette recherche pourraient également ouvrir la possibilité de former de nouveaux systèmes sûrs et économiques basés sur les DES pour l'encapsulation de molécules bioactives.

Sur la base de ces travaux, des investigations futures pourraient être menées afin d'élucider davantage certains des principaux résultats de cette étude. C'est pourquoi nous encourageons les considérations suivantes :

- Étudier le comportement de phase des nouveaux solvants à base de CD et de polyalcools ;
- Caractériser les structures de phospholipides formées dans les DES à base de ChCl ;
- Déterminer la concentration micellaire critique du Triton X-100 dans les DES à base de ChCl ;
- Explorer l'organisation des phospholipides à des concentrations plus élevées dans les DES à base de TBPBr et TBABr ;
- Suivre l'effet du DES à base de TBPBr et de TBABr sur les liposomes préformés ;
- Suivre la stabilité à long terme des structures auto-assemblées dans les DES ;
- Évaluer la toxicité des DES et des SUPRADES vis-à-vis d'une lignée cellulaire normale ;
- Évaluer la solubilité d'autres composés volatils dans les DES afin de comprendre le mécanisme de solubilisation ;
- Examiner la capacité de complexation des CD dans d'autres DES que le ChCl:U.

## Références bibliographiques

- Abbott, A. P., Barron, J. C., Ryder, K. S., & Wilson, D. (2007). Eutectic-based ionic liquids with metal-containing anions and cations. *Chemistry – A European Journal*, *13*(22), 6495–6501. <https://doi.org/10.1002/chem.200601738>
- Abbott, A. P., Boothby, D., Capper, G., Davies, D. L., & Rasheed, R. K. (2004). Deep eutectic solvents formed between choline chloride and carboxylic acids: Versatile alternatives to ionic liquids. *Journal of the American Chemical Society*, *126*(29), 9142–9147. <https://doi.org/10.1021/ja048266j>
- Abbott, A. P., Capper, G., Davies, D. L., Munro, H. L., Rasheed, R. K., & Tambyrajah, V. (2001). Preparation of novel, moisture-stable, Lewis-acidic ionic liquids containing quaternary ammonium salts with functional side chains. *Chemical Communications*, *19*, 2010–2011. <https://doi.org/10.1039/B106357J>
- Abbott, A. P., Capper, G., Davies, D. L., & Rasheed, R. K. (2004). Ionic liquid analogues formed from hydrated metal salts. *Chemistry – A European Journal*, *10*(15), 3769–3774. <https://doi.org/10.1002/chem.200400127>
- Abbott, A. P., Capper, G., Davies, D. L., Rasheed, R. K., & Tambyrajah, V. (2003). Novel solvent properties of choline chloride/urea mixtures. *Chemical Communications*, *1*, 70–71. <https://doi.org/10.1039/B210714G>
- Abbott, A. P., Capper, G., & Gray, S. (2006). Design of improved deep eutectic solvents using hole theory. *ChemPhysChem*, *7*(4), 803–806. <https://doi.org/10.1002/cphc.200500489>
- Alcalde, R., Gutiérrez, A., Atilhan, M., & Aparicio, S. (2019). An experimental and theoretical investigation of the physicochemical properties on choline chloride – Lactic acid based natural deep eutectic solvent (NADES). *Journal of Molecular Liquids*, *290*, 110916. <https://doi.org/10.1016/j.molliq.2019.110916>
- Anwekar, H., Patel, S., & Singhai, A. K. (2011). Liposome-as drug carriers. *International Journal of Pharmacy & Life Sciences*, *2*(7), 945–951.
- Arnold, T., Jackson, A. J., Sanchez-Fernandez, A., Magnone, D., Terry, A. E., & Edler, K. J. (2015). Surfactant behavior of sodium dodecylsulfate in deep eutectic solvent choline chloride/urea. *Langmuir*, *31*(47), 12894–12902. <https://doi.org/10.1021/acs.langmuir.5b02596>
- Bangham, A. D., Standish, M. M., & Watkins, J. C. (1965). Diffusion of univalent ions across the lamellae of swollen phospholipids. *Journal of Molecular Biology*, *13*(1), 238–252. [https://doi.org/10.1016/s0022-2836\(65\)80093-6](https://doi.org/10.1016/s0022-2836(65)80093-6)
- Batzri, S., & Korn, E. D. (1973). Single bilayer liposomes prepared without sonication. *Biochimica et Biophysica Acta (BBA) - Biomembranes*, *298*(4), 1015–1019. [https://doi.org/10.1016/0005-2736\(73\)90408-2](https://doi.org/10.1016/0005-2736(73)90408-2)
- Bryant, S. J., Atkin, R., & Warr, G. G. (2016). Spontaneous vesicle formation in a deep eutectic solvent. *Soft Matter*, *12*(6), 1645–1648. <https://doi.org/10.1039/C5SM02660A>
- Bryant, S. J., Atkin, R., & Warr, G. G. (2017). Effect of deep eutectic solvent nanostructure on phospholipid bilayer phases. *Langmuir*, *33*(27), 6878–6884. <https://doi.org/10.1021/acs.langmuir.7b01561>
- Choi, Y. H., Spronsen, J. van, Dai, Y., Verberne, M., Hollmann, F., Arends, I. W. C. E., Witkamp, G.-J., & Verpoorte, R. (2011). Are natural deep eutectic solvents the missing link in understanding cellular

- metabolism and physiology? *Plant Physiology*, *156*(4), 1701–1705.  
<https://doi.org/10.1104/pp.111.178426>
- Coutinho, J. A. P., & Pinho, S. P. (2017). Special issue on deep eutectic solvents: A foreword. *Fluid Phase Equilibria*, *448*, 1. <https://doi.org/10.1016/j.fluid.2017.06.011>
- Cui, Y., Li, C., Yin, J., Li, S., Jia, Y., & Bao, M. (2017). Design, synthesis and properties of acidic deep eutectic solvents based on choline chloride. *Journal of Molecular Liquids*, *236*, 338–343.  
<https://doi.org/10.1016/j.molliq.2017.04.052>
- D'Agostino, C., Gladden, L. F., Mantle, M. D., Abbott, A. P., Ahmed, E., I., Al-Murshedi, A. Y. M., & Harris, R. C. (2015). Molecular and ionic diffusion in aqueous – deep eutectic solvent mixtures: Probing inter-molecular interactions using PFG NMR. *Physical Chemistry Chemical Physics*, *17*(23), 15297–15304. <https://doi.org/10.1039/C5CP01493J>
- D'Agostino, C., Harris, R. C., Abbott, A. P., Gladden, L. F., & Mantle, M. D. (2011). Molecular motion and ion diffusion in choline chloride based deep eutectic solvents studied by 1H pulsed field gradient NMR spectroscopy. *Physical Chemistry Chemical Physics*, *13*(48), 21383.  
<https://doi.org/10.1039/c1cp22554e>
- Dai, Y., van Spronsen, J., Witkamp, G.-J., Verpoorte, R., & Choi, Y. H. (2013). Natural deep eutectic solvents as new potential media for green technology. *Analytica Chimica Acta*, *766*, 61–68.  
<https://doi.org/10.1016/j.aca.2012.12.019>
- Dai, Y., Witkamp, G.-J., Verpoorte, R., & Choi, Y. H. (2015). Tailoring properties of natural deep eutectic solvents with water to facilitate their applications. *Food Chemistry*, *187*, 14–19.  
<https://doi.org/10.1016/j.foodchem.2015.03.123>
- Du, C., Zhao, B., Chen, X.-B., Birbilis, N., & Yang, H. (2016). Effect of water presence on choline chloride-2urea ionic liquid and coating platings from the hydrated ionic liquid. *Scientific Reports*, *6*(1).  
<https://doi.org/10.1038/srep29225>
- Duarte, A. R. C., Ferreira, A. S. D., Barreiros, S., Cabrita, E., Reis, R. L., & Paiva, A. (2017). A comparison between pure active pharmaceutical ingredients and therapeutic deep eutectic solvents: Solubility and permeability studies. *European Journal of Pharmaceutics and Biopharmaceutics*, *114*, 296–304. <https://doi.org/10.1016/j.ejpb.2017.02.003>
- Eid, J., El Achkar, T., Fourmentin, S., Greige-Gerges, H., & Jraij, A. (2020). First investigation of liposomes behavior and phospholipids organization in choline chloride-based deep eutectic solvents by atomic force microscopy. *Journal of Molecular Liquids*, *306*, 112851.  
<https://doi.org/10.1016/j.molliq.2020.112851>
- El Achkar, T., Fourmentin, S., & Greige-Gerges, H. (2019). Deep eutectic solvents: An overview on their interactions with water and biochemical compounds. *Journal of Molecular Liquids*, *288*, 111028.  
<https://doi.org/10.1016/j.molliq.2019.111028>
- El Achkar, T., Moufawad, T., Ruellan, S., Landy, D., Greige-Gerges, H., & Fourmentin, S. (2020). Cyclodextrins: From solute to solvent. *Chemical Communications*.  
<https://doi.org/10.1039/D0CC00460J>
- El Achkar, T., Moura, L., Moufawad, T., Ruellan, S., Panda, S., Longuemart, S., Legrand, F.-X., Costa Gomes, M., Landy, D., Greige-Gerges, H., & Fourmentin, S. (2020). New generation of supramolecular mixtures: Characterization and solubilization studies. *International Journal of Pharmaceutics*, *119443*. <https://doi.org/10.1016/j.ijpharm.2020.119443>

- Fetisov, E. O., Harwood, D. B., Kuo, I.-F. W., Warrag, S. E. E., Kroon, M. C., Peters, C. J., & Siepmann, J. I. (2018). First-principles molecular dynamics study of a deep eutectic solvent: Choline chloride/urea and its mixture with water. *The Journal of Physical Chemistry B*, *122*(3), 1245–1254. <https://doi.org/10.1021/acs.jpcc.7b10422>
- Florindo, C., Branco, L. C., & Marrucho, I. M. (2019). Quest for green-solvent design: From hydrophilic to hydrophobic (deep) eutectic solvents. *ChemSusChem*, *12*(8), 1549–1559. <https://doi.org/10.1002/cssc.201900147>
- Florindo, C., Oliveira, F. S., Rebelo, L. P. N., Fernandes, A. M., & Marrucho, I. M. (2014). Insights into the synthesis and properties of deep eutectic solvents based on cholinium chloride and carboxylic acids. *ACS Sustainable Chemistry & Engineering*, *2*(10), 2416–2425. <https://doi.org/10.1021/sc500439w>
- Francisco, M., Bruinhorst, A. van den, & Kroon, M. C. (2012). New natural and renewable low transition temperature mixtures (LTTMs): Screening as solvents for lignocellulosic biomass processing. *Green Chemistry*, *14*(8), 2153–2157. <https://doi.org/10.1039/C2GC35660K>
- Gabriele, F., Chiarini, M., Germani, R., Tiecco, M., & Spreti, N. (2019). Effect of water addition on choline chloride/glycol deep eutectic solvents: Characterization of their structural and physicochemical properties. *Journal of Molecular Liquids*, *291*, 111301. <https://doi.org/10.1016/j.molliq.2019.111301>
- Gutiérrez, M. C., Ferrer, M. L., Mateo, C. R., & del Monte, F. (2009). Freeze-drying of aqueous solutions of deep eutectic solvents: A suitable approach to deep eutectic suspensions of self-assembled structures. *Langmuir*, *25*(10), 5509–5515. <https://doi.org/10.1021/la900552b>
- Hammond, O. S., Bowron, D. T., & Edler, K. J. (2017). The effect of water upon deep eutectic solvent nanostructure: An unusual transition from ionic mixture to aqueous solution. *Angewandte Chemie International Edition*, *56*(33), 9782–9785. <https://doi.org/10.1002/anie.201702486>
- Hammond, O. S., Bowron, D. T., Jackson, A. J., Arnold, T., Sanchez-Fernandez, A., Tsapatsaris, N., Garcia Sakai, V., & Edler, K. J. (2017). Resilience of malic acid natural deep eutectic solvent nanostructure to solidification and hydration. *The Journal of Physical Chemistry B*, *121*(31), 7473–7483. <https://doi.org/10.1021/acs.jpcc.7b05454>
- Hayyan, M., Hashim, M. A., Hayyan, A., Al-Saadi, M. A., AlNashef, I. M., Mirghani, M. E. S., & Saheed, O. K. (2013). Are deep eutectic solvents benign or toxic? *Chemosphere*, *90*(7), 2193–2195. <https://doi.org/10.1016/j.chemosphere.2012.11.004>
- Ibrahim, R. K., Hayyan, M., AlSaadi, M. A., Ibrahim, S., Hayyan, A., & Hashim, M. A. (2019). Physical properties of ethylene glycol-based deep eutectic solvents. *Journal of Molecular Liquids*, *276*, 794–800. <https://doi.org/10.1016/j.molliq.2018.12.032>
- Kareem, M. A., Mjalli, F. S., Hashim, M. A., & AlNashef, I. M. (2010). Phosphonium-based ionic liquids analogues and their physical properties. *Journal of Chemical & Engineering Data*, *55*(11), 4632–4637. <https://doi.org/10.1021/jc100104v>
- Kaur, S., Gupta, A., & Kashyap, H. K. (2020). How hydration affects the microscopic structural morphology in a deep eutectic solvent. *The Journal of Physical Chemistry B*, *124*(11), 2230–2237. <https://doi.org/10.1021/acs.jpcc.9b11753>

- Kfoury, M., Hădărugă, N. G., Hădărugă, D. I., & Fourmentin, S. (2016). 4—Cyclodextrins as encapsulation material for flavors and aroma. In A. M. Grumezescu (Ed.), *Encapsulations* (pp. 127–192). Academic Press. <https://doi.org/10.1016/B978-0-12-804307-3.00004-1>
- Kumari, P., Shobhna, Kaur, S., & Kashyap, H. K. (2018). Influence of hydration on the structure of reline deep eutectic solvent: A molecular dynamics study. *ACS Omega*, *3*(11), 15246–15255. <https://doi.org/10.1021/acsomega.8b02447>
- López-Salas, N., Vicent-Luna, J. M., Imberti, S., Posada, E., Roldán, M. J., Anta, J. A., Balestra, S. R. G., Madero Castro, R. M., Calero, S., Jiménez-Riobóo, R. J., Gutiérrez, M. C., Ferrer, M. L., & del Monte, F. (2019). Looking at the “water-in-deep-eutectic-solvent” system: A dilution range for high performance eutectics. *ACS Sustainable Chemistry & Engineering*, *7*(21), 17565–17573. <https://doi.org/10.1021/acssuschemeng.9b05096>
- Martins, M. A. R., Pinho, S. P., & Coutinho, J. A. P. (2019). Insights into the nature of eutectic and deep eutectic mixtures. *Journal of Solution Chemistry*, *48*(7), 962–982. <https://doi.org/10.1007/s10953-018-0793-1>
- Mbous, Y. P., Hayyan, M., Hayyan, A., Wong, W. F., Hashim, M. A., & Looi, C. Y. (2017). Applications of deep eutectic solvents in biotechnology and bioengineering—Promises and challenges. *Biotechnology Advances*, *35*(2), 105–134. <https://doi.org/10.1016/j.biotechadv.2016.11.006>
- Nunes, R. J., Saramago, B., & Marrucho, I. M. (2019). Surface tension of dl-menthol:octanoic acid eutectic mixtures. *Journal of Chemical & Engineering Data*, *64*(11), 4915–4923. <https://doi.org/10.1021/acs.jced.9b00424>
- Osch, D. J. G. P. van, Zubeir, L. F., Bruinhorst, A. van den, Rocha, M. A. A., & Kroon, M. C. (2015). Hydrophobic deep eutectic solvents as water-immiscible extractants. *Green Chemistry*, *17*(9), 4518–4521. <https://doi.org/10.1039/C5GC01451D>
- Paiva, A., Craveiro, R., Aroso, I., Martins, M., Reis, R. L., & Duarte, A. R. C. (2014). Natural deep eutectic solvents – solvents for the 21st century. *ACS Sustainable Chemistry & Engineering*, *2*(5), 1063–1071. <https://doi.org/10.1021/sc500096j>
- Posada, E., López-Salas, N., Riobóo, R. J. J., Ferrer, M. L., Gutiérrez, M. C., & Monte, F. del. (2017). Reline aqueous solutions behaving as liquid mixtures of H-bonded co-solvents: Microphase segregation and formation of co-continuous structures as indicated by Brillouin and <sup>1</sup>H NMR spectroscopies. *Physical Chemistry Chemical Physics*, *19*(26), 17103–17110. <https://doi.org/10.1039/C7CP02180A>
- Radošević, K., Čanak, I., Panić, M., Markov, K., Cvjetko Bubalo, M., Frece, J., Srček, V. G., & Redovniković, I. R. (2018). Antimicrobial, cytotoxic and antioxidative evaluation of natural deep eutectic solvents. *Environmental Science and Pollution Research*, *25*(14), 14188–14196. <https://doi.org/10.1007/s11356-018-1669-z>
- Ribeiro, B. D., Florindo, C., Iff, L. C., Coelho, M. A. Z., & Marrucho, I. M. (2015). Menthol-based eutectic mixtures: Hydrophobic low viscosity solvents. *ACS Sustainable Chemistry & Engineering*, *3*(10), 2469–2477. <https://doi.org/10.1021/acssuschemeng.5b00532>
- R. McCluskey, A., Sanchez-Fernandez, A., J. Edler, K., C. Parker, S., J. Jackson, A., A. Campbell, R., & Arnold, T. (2019). Bayesian determination of the effect of a deep eutectic solvent on the structure of lipid monolayers. *Physical Chemistry Chemical Physics*, *21*(11), 6133–6141. <https://doi.org/10.1039/C9CP00203K>

- Sanchez-Fernandez, A., L. Moody, G., C. Murfin, L., Arnold, T., J. Jackson, A., M. King, S., E. Lewis, S., & J. Edler, K. (2018). Self-assembly and surface behaviour of pure and mixed zwitterionic amphiphiles in a deep eutectic solvent. *Soft Matter*, 14(26), 5525–5536. <https://doi.org/10.1039/C8SM00755A>
- Savi, L. K., Carpiné, D., Waszczynskyj, N., Ribani, R. H., & Haminiuk, C. W. I. (2019). Influence of temperature, water content and type of organic acid on the formation, stability and properties of functional natural deep eutectic solvents. *Fluid Phase Equilibria*, 488, 40–47. <https://doi.org/10.1016/j.fluid.2019.01.025>
- Savi, L. K., Dias, M. C. G. C., Carpine, D., Waszczynskyj, N., Ribani, R. H., & Haminiuk, C. W. I. (2019). Natural deep eutectic solvents (NADES) based on citric acid and sucrose as a potential green technology: A comprehensive study of water inclusion and its effect on thermal, physical and rheological properties. *International Journal of Food Science & Technology*, 54(3), 898–907. <https://doi.org/10.1111/ijfs.14013>
- Scientific Opinion on safety and efficacy of choline chloride as a feed additive for all animal species. (2011). *EFSA Journal*, 9(9), 2353. <https://doi.org/10.2903/j.efsa.2011.2353>
- Shah, D., & Mjalli, F. S. (2014). Effect of water on the thermo-physical properties of Reline: An experimental and molecular simulation based approach. *Physical Chemistry Chemical Physics*, 16(43), 23900–23907. <https://doi.org/10.1039/C4CP02600D>
- Shahbaz, K., Baroutian, S., Mjalli, F. S., Hashim, M. A., & AlNashef, I. M. (2012). Densities of ammonium and phosphonium based deep eutectic solvents: Prediction using artificial intelligence and group contribution techniques. *Thermochimica Acta*, 527, 59–66. <https://doi.org/10.1016/j.tca.2011.10.010>
- Smith, E. L., Abbott, A. P., & Ryder, K. S. (2014). Deep eutectic solvents (DESs) and their applications. *Chemical Reviews*, 114(21), 11060–11082. <https://doi.org/10.1021/cr300162p>
- Szente, L., & Fenyvesi, É. (2016). Cyclodextrin-lipid complexes: Cavity size matters. *Structural Chemistry*, 2(28), 479–492. <https://doi.org/10.1007/s11224-016-0884-9>
- Tang, B., & Row, K. H. (2013). Recent developments in deep eutectic solvents in chemical sciences. *Monatshefte Für Chemie - Chemical Monthly*, 144(10), 1427–1454. <https://doi.org/10.1007/s00706-013-1050-3>
- Weng, L., & Toner, M. (2018). Janus-faced role of water in defining nanostructure of choline chloride/glycerol deep eutectic solvent. *Physical Chemistry Chemical Physics*, 20(35), 22455–22462. <https://doi.org/10.1039/C8CP03882A>
- Zhang, Q., De Oliveira Vigier, K., Royer, S., & Jérôme, F. (2012). Deep eutectic solvents: Syntheses, properties and applications. *Chemical Society Reviews*, 41(21), 7108–7146. <https://doi.org/10.1039/C2CS35178A>
- Zhekenov, T., Toksanbayev, N., Kazakbayeva, Z., Shah, D., & Mjalli, F. S. (2017). Formation of type III deep eutectic solvents and effect of water on their intermolecular interactions. *Fluid Phase Equilibria*, 441, 43–48. <https://doi.org/10.1016/j.fluid.2017.01.022>